Heparanase in Breast Cancer Progression and the Characterisation of Novel Heparanase Inhibitors

Submitted by

Krishnath Malindra Jayatilleke

BSc, MSc

A thesis submitted in total fulfillment

of the requirements for the degree of

Doctor of Philosophy

Department of Biochemistry and Genetics

La Trobe Institute for Molecular Science

School of Molecular Sciences

College of Science, Health and Engineering

La Trobe University

Victoria

Australia

June 2020

Table of Contents

List of Figures

List of Tables

Abstract

With its capacity to modulate the tumour microenvironment (TME) and promote the hallmarks of cancer, heparanase (HPSE) has emerged as a key mediator in the development and progression of malignant disease. HPSE overexpression has been observed in all cancers, which correlates with a poor clinical prognosis. Significant interest has therefore been focused on defining the role of HPSE within the TME and in the development of inhibitors for use in the clinic.

Employing the well-established spontaneous mammary tumour-developing PyMT-MMTV mouse model, this study explored the role of HPSE in the progression of breast cancer. The use of the HPSE-deficient PyMT-MMTVxHPSE$^{-/-}$ mice addressed the general under-utilisation of genetic ablation *in vivo* models described in the current literature. Furthermore, the tumour stroma was investigated as a critical modulator of HPSE activity within the primary tumour. The findings of this thesis indicate that although the lack of HPSE expression affected tumour angiogenesis, it plays no major role in the overall establishment, progression and metastasis of mammary tumours in the PyMT-MMTV mouse model. Additionally, novel HPSE inhibitors GW7647 and GW9578 were identified by high throughput screening of a known drug library. The *in vitro* and *in vivo* efficacy of these compounds in inhibiting the enzymatic activity of HPSE was characterised, which suggest that further optimisation of these compounds will be required for future pre-clinical studies.

This study revealed that despite the widely accepted nature of HPSE in promoting cancers, in some tumour settings, the overall role of HPSE may be redundant due to reasons yet to be elucidated. This finding, coupled with the need for more efficacious HPSE inhibitors, suggest that the precise role of HPSE within the TME and its targeting modality is yet to be comprehensively defined, creating avenues for further research.

Statement of Authorship

Except where reference is made in the text of this thesis, this thesis contains no material published elsewhere or extracted in whole or in part from a thesis accepted for the award of any other degree of diploma.

No other person's work has been used without due acknowledgement in the main text of the thesis.

This thesis has not been submitted for the award of any degree or diploma in any other tertiary institution.

All research procedures reported in the thesis were approved by the La Trobe University Animal Ethics Committee (AEC13-64, AEC15-25 and AEC16-24), the Genetic Manipulation Supervisory Committee (GMSC15-10, GMSC15-11, GMSC16-10), the La Trobe University Human Research Ethics Committee and the Australian Red Cross Blood Service Material Supply Agreement (17-01VIC-14).

Krishnath M Jayatilleke

03 June 2020

Acknowledgements

Looking back over the years of undertaking my PhD, it becomes clear to me that what seemed like a solitary pursuit would not have been possible without the support of many.

A big Thank You! to my supervisor, Professor Mark Hulett, for accepting me as your student, for allowing me the freedom to navigate, for your guidance, for placing your faith in me and most importantly, for empowering me to carve out a career path that I am passionate about. You have cultivated an admirable collaborative and supportive culture within the lab for which I am extremely grateful and of which you should be proud. Thank you to all the past and present members of the Hulett/Poon labs, especially the heparanase crew (Shaun Gaskin, Alyce Mayfosh, Alyce Forrest, Kathleen Wragg and Dr Katharine Goodall) for your support in laying the groundwork for some of the studies that were pivotal in completing this thesis. My co-supervisor, Associate Professor Belinda Parker and my PhD mentor, Professor Robyn Murphy; thank you for your guidance throughout the years in ensuring that I achieved my goals and got the most out of my studies! To the Hoogenraads who've known me since I joined the department back in 2008; Nick, thank you for convincing me to take on a PhD, one of the biggest decisions I'd made thus far, at a time when I was feeling unsure. Joan, thank you for the many coffees, chats and your support over the years. I thank Dr Erika Duan, Dr Damien Zanker, Dr Hendrika Duivenvoorden, the members of the labs of Associate Professor Belinda Parker and Professor Weisan Chen for being extremely generous with your time and advice. Thank you to the La Trobe Institute for Molecular Science for fostering a stimulating, vibrant research culture. This work was supported by a La Trobe University Postgraduate Research Scholarship, for which I am extremely thankful.

My aunt, Professor Dharshi Bopegedera, who first instilled in me an interest in science; thank you for being an inspiration and for gifting me my very first science kit when I was eight years old. I also thank Jimmy, Sandra and Bally for your company. Thank you, boys (Shaun, Rob, Stefan, Sebastien, Damo, Barney and Mo) for the laughs and the good times. Bari, thank you for your company throughout the years – well done on beating me to the PhD! Shaun, thank you for the weekly debriefs. Elva, I treasure the support that you have given me.

Finally, I thank my family who supported my move to Australia without which none of this would have been possible.

This entire body of work is dedicated to the memory of my grandparents.

Publications from this thesis

- **Krishnath M. Jayatilleke** and Mark D. Hulett, 2020. Heparanase and the hallmarks of cancer. *Journal of Translational Medicine* (submission pending at the time of writing).

- **Krishnath M. Jayatilleke**, Hendrika M. Duivenvoorden, Jenny D.Y. Chow, Gemma F. Ryan, Julie A. White, Belinda S. Parker and Mark D. Hulett, 2020. Investigating the role of heparanase in breast cancer development utilising the PyMT-MMTV murine model of mammary carcinoma. *Cancers* (submission pending at the time of writing).

Publications from other projects

- Amelia J. Johnston, Kate T. Murphy, Laura Jenkinson, David Laine, Kerstin Emmrich, Pierre Faou, Ross Weston, **Krishnath M. Jayatilleke**, Jessie Schloegel, Gert Talbo, Joanne L. Casey, Vita Levina, W. Wei-Lynn Wong, Helen Dillon, Tushar Sahay, Joan Hoogenraad, Holly Anderton, Cathrine Hall, Pascal Schneider, Maria Tanzer, Michael Foley, Andrew M. Scott, Paul Gregorevic, Spring Yingchun Liu, Linda C. Burkly, Gordon S. Lynch, John Silke and Nicholas J. Hoogenraad, 2015. Targeting of Fn14 Prevents Cancer-Induced Cachexia and Prolongs Survival. *Cell*, 162, pp 1365–1378.

- Jai Rautela, Nikola Baschuk, Clare Y. Slaney, **Krishnath M. Jayatilleke**, Kun Xiao, Bradley N. Bidwell, Erin C. Lucas, Edwin D. Hawkins, Peter Lock, Christina S. Wong, Weisan Chen, Robin L. Anderson, Paul J. Hertzog, Daniel M. Andrews, Andreas Moller and Belinda S. Parker, 2015.Loss of Host Type-I IFN Signaling Accelerates Metastasis and Impairs NK-Cell Antitumor Function in Multiple Models of Breast Cancer. *Cancer Immunology Research*, 3(11), pp 1207-1217.

- Laura E. Edgington-Mitchell, Jai Rautela, Hendrika M. Duivenvoorden, **Krishnath M. Jayatilleke**, Wouter A. van der Linden, Martijn Verdoes, Matthew Bogyo and Belinda S. Parker, 2015. Cysteine cathepsin activity suppresses osteoclastogenesis of myeloid-derived suppressor cells in breast cancer. *Oncotarget*, 6(29), pp 27008-27022.

Conferences and Presentations

- European Association for Cancer Research Conference, July 2018, Amsterdam, The Netherlands **(poster)**
- AusMedTech Conference, May 2018, Adelaide, Australia
- BioMed Link Student Research Symposium, November 2017, Melbourne, Australia **(poster)**
- La Trobe University Industry Research Showcase Event, November 2017, Melbourne, Australia **(poster)**
- La Trobe Institute for Molecular Science (LIMS) Fellows Symposium, November 2017, Melbourne, Australia **(poster)**
- AusBiotech National Conference, October 2017, Adelaide, Australia
- Victorian Comprehensive Cancer Centre (VCCC) Symposium, September 2017, Melbourne, Australia
- AusMedTech Conference, May 2017, Melbourne, Australia **(student volunteer)**
- Lorne Cancer Conference, February 2017, Lorne, Australia **(poster)**
- LIMS Fellows Symposium, November 2016, Melbourne, Australia **(poster)**
- Australian Society for Medical Research (ASMR) Symposium, April 2016, Melbourne, Australia **(awarded highly commended poster prize)**
- Lorne Cancer Conference, February 2016, Lorne, Australia **(awarded poster prize)**
- VCCC Symposium, November 2015, Melbourne, Australia **(poster)**
- Weizmann Australia Research Symposium, October 2015, Melbourne, Australia **(poster)**
- ComBio, September 2015, Melbourne, Australia **(poster)**
- Inaugural Scientific Symposium – Olivia Newton John Cancer Research Institute, April 2015, Melbourne, Australia

Awards

- LIMS Miller international travel award, July 2018
- Bruce Stone domestic travel award, February 2018
- Highly commended poster prize, ASMR Symposium, April 2016, Melbourne, Australia
- Poster prize, Lorne Cancer Conference, February 2016, Lorne, Australia
- La Trobe University PhD scholarship, 2015-2018
- This work was supported by an Australian Government Research Training Program Scholarship

Abbreviations

3D	Three-dimensional
Å	Angstrom
ºC	Degrees Celsius
µg	Microgram
µl	Microlitre
µm	Micrometre
µM	Micromolar

A	Adenine
ABC	Avidin-biotin complex
AKI	Acute kidney injury
Akt	Protein kinase-B
ANGPTL4	Angiopoietin-like 4
Arg	Arginine
ASMR	Australian Society for Medical Research
Asp	Aspartic acid
BM	Basement membrane
bp	Base pair/s
BSA	Bovine serum albumin
C	Cytosine
CAF	Cancer-associated fibroblast
CAR-T	Chimeric antigen receptor-redirected T
CCL	Chemokine (C-C motif) ligand
CD	Cluster of differentiation
cDNA	Complimentary deoxyribonucleic acid
CHAPS	3-((3-cholamidopropyl)-dimethylammonio)-1-propanesulfonate
Con-A	Concanavalin-A
COX	Cyclooxygenase
C_q	Quantification cycle
CS	Chondroitin sulphate
CSC	Cancer stem cell
CSF-1	Colony stimulating factor-1
CTC	Circulating tumour cell
CTLA	Cytotoxic T-lymphocyte-associated protein
DAB	3,3'-diaminobenzidine
DC	Dendritic cell
DCIS	Ductal carcinoma *in situ*
DMEM	Dulbecco's Modified Eagle Medium
DMG	Dimethyl glutarate
DMSO	Dimethyl sulfoxide
DNA	Deoxyribonucleic acid
ECM	Extracellular matrix
EDTA	Ethylenediaminetetraacetic acid
EGF	Epidermal growth factor
EGFR	Epidermal growth factor receptor
EGR-1	Early growth response protein-1
EMT	Epithelial-mesenchymal transition
ER	Estrogen receptor/Endoplasmic reticulum
ErbB2/Neu	Erythroblastic oncogene B/Neural tumour (derived from a rodent glioblastoma cell line)
ES	Embryonic stem

ETS	E26 transformation specific
Fabpi	Fatty acid-binding protein, intestinal
FAK	Focal adhesion kinase
FCS	Foetal calf serum
FDA	Food and Drug Administration
FGF	Fibroblast growth factor
FGFR	Fibroblast growth factor receptor
FITC	Fluorescein isothiocyanate
FRET	Fluorescence resonance energy transfer
FVB	Friend leukemia virus B (susceptible to)
Fwd	Forward
g	Gravitational force
G	Guanine/Gauge
GAG	Glycosaminoglycan
Gal	Galactose
GH-A	Glycosyl hydrolase clan-A
GlcA	D-glucuronic acid
GlcNAc	N-acetyl-D-glucosamine
GlcNS	D-glucuronic acid(β1-4)*N*-sulfoglucosamine
Gln	Glutamine
Glu	Glutamic acid
GPI	Glycophosphatidylinositol
h	Hour/s
HCC	Hepatocellular carcinoma
HER2	Human epidermal growth factor receptor-2
HGF	Hepatocyte growth factor
Hh	Hedgehog
HIF	Hypoxia-inducible factor
HLA	Human leukocyte antigen
HPC-MSC	Hypoxic preconditioning mesenchymal stem cell
HPSE	Heparanase
HS	Heparan sulphate
HSBP	Heparans sulphate-binding protein
HSPG	Heparan sulphate proteoglycan
hTERT	Human telomerase reverse transcriptase
huHPSE	Human heparanase
IARC	International agency for research on cancer
ICAM-1	Intercellular adhesion molecule-1
Ig	Immunoglobulin
IHC	Immunohistochemistry
IL	Interleukin
kb	Kilobase
kDa	Kilo Dalton
kg	Kilogram
LARTF	La Trobe University animal research and training facility
LMWH	Low molecular weight heparin
LTR	Long terminal repeat
Luc	Luciferase
Lys	Lysine
M	Molar
MBP	Major basic protein
MDSC	Myeloid-derived suppressor cell
Met	Methionine
mg	Milligram
MHC	Major histocompatibility complex
min	Minute/s

miR	Micro ribonucleic acid
mm	Millimetre
mM	Millimolar
MMP	Matrix metalloproteinase
MMTV	Mouse mammary tumour virus
mRNA	Messenger ribonucleic acid
mTOR1	Mammalian target of rapamycin-1
MTT	3-[4,5 dimethylthiazol-2-yl]-2,5 diphenyltetrazolium bromide
Myc	Myelocytomatosis oncogene
N_2	Nitrogen
NADPH	Nicotinamide adenine dinucleotide phosphate
neo^R	Neomycin resistance
NFκB	Nuclear factor kappa-light-chain-enhancer of activated B cells
ng	Nanogram
NK	Natural killer
nm	Nanometre
NS	Not significant
ORF	Open reading frame
PARP	Poly adenosine diphosphate-ribose polymerase
PBMC	Peripheral bone marrow cell
PBS	Phosphate-buffered saline
PCR	Polymerase chain reaction
PD-1	Programmed cell death protein-1
PDGF	Platelet-derived growth factor
PDL-1	Programmed cell death ligand-1
Phe	Phenylalanine
PI3K	Phosphoinositide-3-kinase
PMN	Pre-metastatic niche
PPAR	Peroxisome proliferator-activated receptor
PR	Progesterone receptor
Pro	Proline
PTEN	Phosphatase and tensin homolog
PyMT	Polyoma virus middle tumour
qPCR	Quantitative polymerase chain reaction
Ras	Rat sarcoma viral oncogene homologue
RBC	Red blood cell
Rev	Reverse
RNA	Ribonucleic acid
ROS	Reactive oxygen species
RTB	Relative tumour burden
RTK	Receptor tyrosine kinase
SD	Standard deviation
SDS	Sodium dodecyl sulphate
sec	Second/s
SEM	Standard error of the mean
siRNA	Small interfering ribonucleic acid
SMMHC	Smooth muscle myosin heavy chain
Sp1	Specificity protein-1
STAT3	Signal transducer and activator of transcription-3
STMC	Synthetic tri mannose C-C-linked dimer
T	Thymine
TAM	Tumour-associated macrophage
TCA	Tricarboxylic acid
TEM	Trans-endothelial migration
TF	Tissue factor
TGF-β	Transforming growth factor-β

TLR	Toll-like receptor
TME	Tumour microenvironment
TNAP-Cre	Tissue non-specific alkaline phosphatase-causes recombination
TNBC	Triple-negative breast cancer
TNF	Tumour necrosis factor
TR-FRET	Time-resolved fluorescence energy transfer
v/v	Volume/volume
VCCC	Victorian Comprehensive Cancer Centre
VEGF	Vascular endothelial growth factor
VINA	Vina Is Not Autodock
w/v	Weight/volume
WHO	World Health Organisation
Xyl	Xylose

“It’s a long way to the top...”

- AC/DC -

Chapter 1

Heparanase in regulating cancer progression and as an anti-cancer drug target

Part I

Heparanase in promoting the hallmarks of cancer and regulating the tumour microenvironment

1.1 Abstract

Heparanase (HPSE) is a β-D-endoglucuronidase with demonstrated roles in a variety of important physiological and pathological processes. HPSE is the only mammalian enzyme that cleaves heparan sulphate (HS) chains of heparan sulphate proteoglycans (HSPGs), a major component of the extracellular matrix (ECM). The enzymatic cleavage of HS by HPSE leads to the remodelling of the ECM whilst liberating growth factors and cytokines bound to HS. This promotes processes such as immune cell migration, inflammation, wound healing, tumour angiogenesis and metastasis. Furthermore, HPSE exhibits non-enzymatic actions in cell signalling and regulating gene expression. Essentially, all cancers examined to date have been reported to overexpress HPSE, often leading to enhanced tumour growth and metastasis with concomitant poor patient survival. This highlights an opportunity for HPSE-targeted therapies, with several HPSE inhibitors progressing through to clinical trials.

Cancer is underpinned by multiple key characteristics that have been proposed to drive malignant cell growth, termed the 'hallmarks' of cancer. HPSE contributes to a number of cancer-associated processes, with demonstrated effects across all hallmarks. Furthermore, the tumour microenvironment (TME) is well-established as playing a critical role in tumour progression and regulates many of these characteristic features.

1.2 Cancer

Cancer is a collective term describing over one hundred individual disease types. The common defining feature of all cancers is the loss of cellular regulation mechanisms through genetic changes. This leads to uncontrolled cell division, resulting in either benign or malignant neoplasms ('new-growths'). The earliest evidence of cancer was discovered in a 1.7-million-year-old hominin fossil bearing signs of osteosarcoma, suggesting that cancers pre-date human civilisation (Odes et al., 2016). The oldest case of breast cancer was discovered in an Egyptian mummy dating back to 2000 B.C (University of Granada).

Cancer is the second leading cause of death globally, following cardiovascular disease. An estimated 18.1 million new cases with 9.6 million deaths were reported in 2018 by the GLOBOCAN 2018 cancer statistics project, produced by the International agency for research on cancer (IARC), revealing a substantial increase from its 14.1 million new cases and the 8.2 million deaths reported in 2012 **(figure 1.1)** (Torre et al., 2015, Bray et al., 2018). There are numerous causes of cancer identified by the IARC, which have at times been the subject of debate. These genetic, environmental, occupational and lifestyle factors include, but are not limited to; obesity, lack of physical activity, harmful ultraviolet radiation through exposure to sunlight, tobacco use and smoking, a diet low in fibre, urban

air pollution, alcohol consumption, certain pharmaceuticals, hormones, parasitic, fungal, bacterial and viral infections, beta carotene, red meat and processed meat consumption, and changes in reproductive patterns such as lower or no parity and giving birth later in life (Blackadar, 2016). Metastasis leads to 90% of cancer-related deaths rather than the formation of a primary tumour alone (Steeg, 2016). This process will be discussed in detail later in this chapter.

Based on the recent GLOBOCAN 2018 worldwide cancer statistics, lung cancer was the most commonly diagnosed malignancy in both males and females combined, and was also the leading cause of cancer-related deaths (Bray et al., 2018). This was followed by female breast cancer, prostate cancer and colorectal cancer for incidence rates with colorectal cancer, stomach cancer and liver cancer for mortality rates **(figure 1.1)**. Males were mostly diagnosed with lung cancer followed by prostate and colorectal cancer. The leading cause of cancer-related deaths in males was lung cancer, followed by liver and stomach cancer. Amongst females, breast cancer was most prevalent, followed by colorectal and lung cancer. Most cancer-related deaths in females were due to breast cancer, followed by lung and colorectal cancers (Bray et al., 2018).

For many cancers, the incidence rate in more developed regions is two to three-fold higher compared to less developed regions (Bray et al., 2018). This can be attributed to lifestyle factors such as a Westernised diet, lack of physical activity, smoking, alcohol consumption and changes in reproductive patterns. However, the differences in mortality rates in both regions are small, partly due to a higher fatality rate in less developed countries. Infections were responsible for 2.2 million, or 15.4% of all new cases in 2012 and were more prevalent in less developed countries, highlighting the need for vaccination and screening programs (Plummer et al., 2016). Cancers are also often diagnosed late in less developed countries, leading to reduced treatment options.

In Australia, there were an estimated 144,713 new cases and 49,896 cancer-related deaths in 2019, with 150,000 new cases predicted for 2020 (Cancer Australia). The current overall risk of an individual being diagnosed with cancer by the age of 85 is 1 in 2 while that of dying from cancer is 1 in 5. Lung, colorectal, breast, prostate and pancreatic cancers account for most cancer-related deaths nationwide.

As a complex disease involving several cell and tissue types, the study of cancer has evolved from merely understanding malignant cell behaviour to adopting a more holistic approach, whilst taking into consideration the myriad of cellular and tissue components associated with malignancy. Amongst the many components associated with a tumour, the ECM plays a key role.

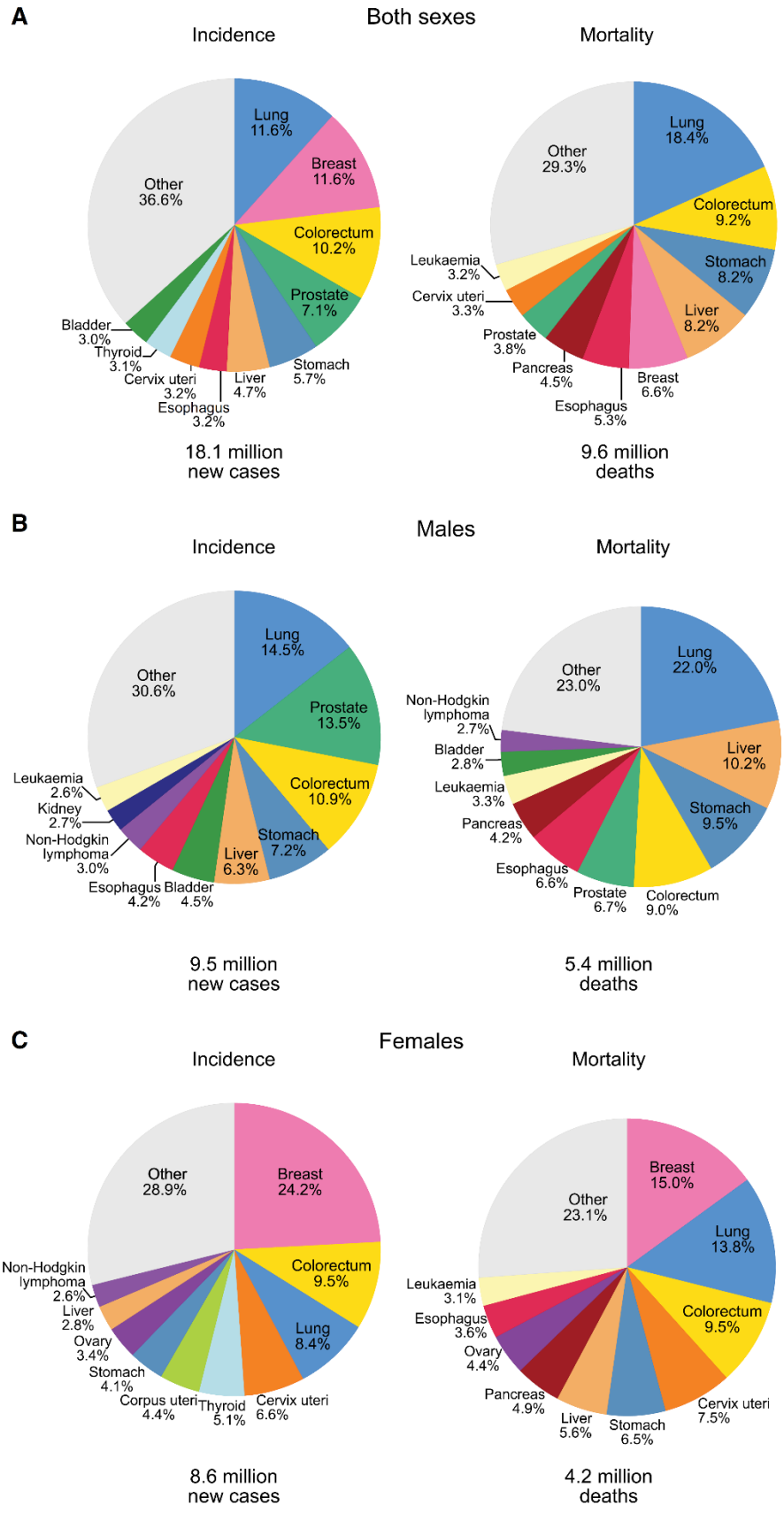

Figure 1.1 The global impact of cancer
The distribution of cases and deaths for ten of the most common cancers in 2018 for (A) both males and females (B) males alone and (C) females alone (Bray et al., 2018).

1.3 The ECM: in sickness and in health

The ECM plays critical roles in both normal physiology as well as in disease settings. Initially assumed to be a passive structural entity, key discoveries made in the 20th century redefined the ECM as an active extracellular component and as a key contributor to cellular maintenance and function (Piez, 1997). The ECM is a dynamic, non-cellular, 3D, mesh-like structure essential for tissue integrity and homeostasis which, in colloquial terms, is the 'glue' that holds cells together. It is comprised mainly of collagen, laminin and HS, key components amongst approximately 300 proteins which collectively form the 'matrisome' **(figure 1.2)** (Naba et al., 2012, Naba et al., 2016). The ECM not only exists in an interstitial form within tissues, but can also be arranged in a sheet-like manner, forming the basement membrane (BM), which underlies epithelial layers. The BM, much like the ECM, provides tissue integrity, promotes signalling and plays a vital role in development (Ramos-Lewis and Page-McCaw, 2018).

In addition to providing structural support, the ECM also interacts with surrounding cells and facilitates signalling pathways by binding and regulating the release of growth factors and cytokines. This modulates processes such as cellular migration, proliferation, adhesion, survival and differentiation (Hynes, 2009). ECM remodelling also maintains tissue homeostasis and can also contribute towards the progression of a variety of pathological conditions (Bonnans et al., 2014, Gilkes et al., 2014, Iozzo and Gubbiotti, 2018). Gene mutations of ECM components have been linked to a variety of disorders such as Marfan syndrome, Ehlers-Danlos syndrome, Dandy-Walker malformation, several myopathies and chondrodysplasias (Bateman et al., 2009, Darbro et al., 2013, Hicks et al., 2014). Abnormalities in ECM mechanoregulation involving the deposition, re-arrangement and remodelling of components leads to disorders such as hypertension (Humphrey et al., 2014, Arribas et al., 2006).

The TME is an essential regulator of cancer progression (Quail and Joyce, 2013). It is a complex arrangement of tumour cells, a number of soluble factors, immune cells, fibroblasts, pericytes, adipocytes, mesenchymal stem cells and the ECM. Although cancer-associated fibroblasts (CAFs) were considered the source of the tumour-associated ECM, it is now known that tumour cells themselves are able to produce ECM components and promote the formation of a supportive TME (Naba et al., 2014). These components collectively provide the biochemical and biophysical properties of the tumour-associated ECM that promotes growth and metastasis (Pickup et al., 2014). Aberrant levels of ECM components such as collagen-I, hyaluronan, periostin, tenascin-C and versican levels have been shown to promote various cancers (Venning et al., 2015, Alowami et al., 2003). The critical steps in metastasis rely heavily on creating a supportive

ECM, remodelling of the existing ECM and maintaining cancer cell-ECM crosstalk (Bonnans et al., 2014). Therefore, the ECM is key in promoting the hallmarks of cancer and has gathered significant interest as a key target in cancer therapy (Pickup et al., 2014). This review will focus mainly on HS, a major ECM component and the sole substrate of HPSE.

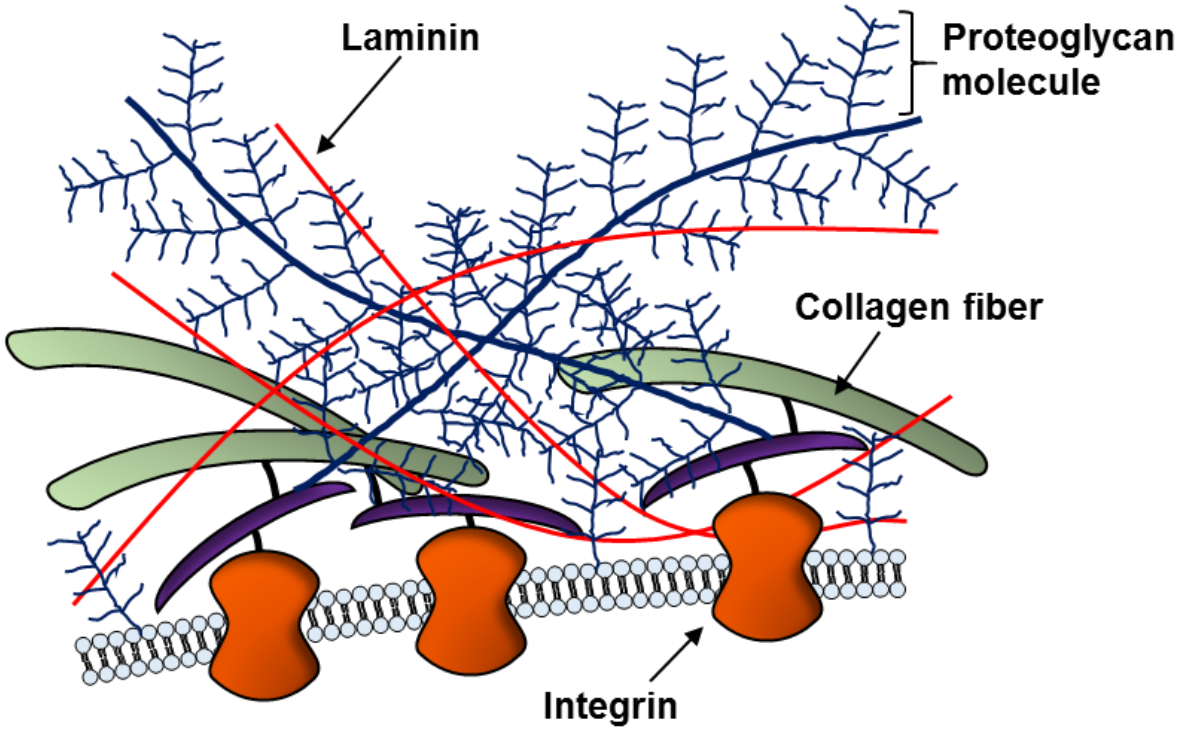

Figure 1.2 The major components of the ECM
The ECM is a complex, 3D structure, mainly comprised of laminin, collagen and proteoglycans (such as HSPGs).

1.4 HS and HSPGs

To appreciate the significance of HPSE in cancer, the structure and the multitude of functions of its substrate HS must be addressed. HS was initially described as 'heparin monosulphuric acid', a structurally-related, but less sulphated form of heparin (Jorpes and Gardell, 1948). It is a variably sulphated, anionic glycosaminoglycan (GAG) chain of repeating disaccharide units of β1-4-linked D-glucuronic acid (GlcA) and α1-4-linked N-acetyl-D-glucosamine (GlcNAc). These HS chains vary in length and typically comprise of 50-250 disaccharide units, ranging from 20-100 kDa and are bound to a protein core to form HSPGs (Sarrazin et al., 2011, Xu and Esko, 2014). A linkage tetrasaccharide comprised of GlcA-galactose-galactose-xylose (GlcA-Gal-Gal-Xyl) facilitates the attachment of the HS chain to the protein core (see section 1.8).

HS is found in all cells. Despite extensive studies, the 3D structure as well as the precise regulation mechanisms that govern the size and composition of HS remain poorly understood (Xu and Esko, 2014). The most recent hypothesis describes a multi-step process beginning in the Golgi complex where heparan, the non-sulphated precursor form of HS is first synthesised on core proteins as a chain of GlcA and GlcNAc. As heparan transits through the Golgi, it is further enzymatically modified by a series of *N*- and *O*-HS-sulphotransferases and an HS epimerase, resulting in mature chains of HS (Gallagher, 2015, Li and Kusche-Gullberg, 2016, Zhang et al., 2016c).

The anionic nature, variable sulfation levels and length of HS chains enables and regulates its interaction with several HS-binding proteins (HSBPs). HS is a reservoir for a variety of HSBPs that do not necessarily share structural similarity. These include growth factors, morphogens and cytokines such as vascular endothelial growth factor (VEGF), fibroblast growth factor (FGF), hepatocyte growth factor (HGF), epidermal growth factor (EGF), platelet derived growth factor (PDGF), transforming growth factor-beta (TGF-β), hedgehog (Hh), interleukins (IL) -5, -6, -8, -10, and tumour necrosis factor-alpha (TNF-α) (Table 1.1). In addition to its role in maintaining structural integrity of the ECM, HS plays a crucial physiological role in sequestering such molecules and regulating their availability and signalling capacity (Knelson et al., 2014, Migliorini et al., 2015, Xu and Esko, 2014, Sarrazin et al., 2011). The sequestering of ligands by HS enhances receptor activation even at low ligand concentrations (Park et al., 2000). HSBPs are protected against proteolysis by being bound to HS and their liberation facilitates the establishment of morphogen gradients during development and chemokine gradients essential for cellular recruitment. HS is also a receptor for proteases and their respective inhibitors, which regulates their distribution and activity (Sarrazin et al., 2011). Additionally, structural proteins such as collagen and fibronectin, proteins of the complement pathway, cell

HSBP	Function/s in normal physiology and cancer
Growth factors and morphogens	
VEGF	Multiple family members, most prominently VEGF-A, along with VEGF-B, -C and -D. Signal through VEGF receptors (VEGFRs) 1-3. Mediate new blood vessel formation with maintenance and remodelling of old ones during development and in adult tissue (Simons et al., 2016). Promote lymphangiogenesis during development and tumour progression (Davydova et al., 2016). In the TME, VEGF affects immune cell and fibroblast function (Goel and Mercurio, 2013).
FGF	Signals through FGF receptors (FGFRs) 1-4. Homeostatic, function in tissue repair and injury response. Regulate cell proliferation, migration and differentiation during embryonic development. Affects angiogenesis, tumour growth and cancer therapy resistance (Goetz and Mohammadi, 2013).
HGF	Signals through the c-Met receptor. Regulates cell proliferation, survival, differentiation, morphogenesis and cancer therapy resistance (Comoglio et al., 2018).
EGF	EGF receptor (EGFR) signalling promotes cell motility, proliferation and differentiation. Associated with tumour recurrence, metastasis and angiogenesis (Guo et al., 2015, Li et al., 2018).
PDGF	Exists as 4 different isoforms; PDGF-A, -B, -C and –D. Stimulates cell proliferation and migration under normal physiology. Promotes tumour proliferation, angiogenesis and tumour-associated fibroblast development (Demoulin and Essaghir, 2014).
TGF-β	Exists as 3 isoforms; TGFβ-1, -2 and -3. TGFβ signalling regulates cell growth, differentiation, motility, apoptosis, ECM production, immune responses and angiogenesis. In the TME, impacts angiogenesis, fibrosis and immune infiltration. Plays a critical role in tumour initiation, progression and metastasis (Neuzillet et al., 2015). TGF-β also acts as a tumour-suppressor.
Hh	Plays a major role in development. Hh signalling in cancer promotes proliferation, angiogenesis, epithelial-mesenchymal transition (EMT), self-renewal and the regulation of apoptosis (Gonnissen et al., 2015).
TNF-α	Induces inflammation and the downstream release of cytokines and chemokines. Although initially identified for its anti-tumour activity, TNF-α also promotes chronic inflammation and cancer cachexia (Sedger and McDermott, 2014, Porporato, 2016).
Cytokines	
IL-5	A critical factor in eosinophil differentiation and proliferation. Supports metastatic colonisation by regulating the immune microenvironment (Zaynagetdinov et al., 2015).
IL-6	Stimulates expression of Signal transducer and activator of transcription-3 (STAT3) target genes in tumour cells, promoting tumour proliferation, survival, angiogenesis, invasion and metastasis and immunosuppression (Johnson et al., 2018).
IL-8	Potent activator of neutrophils. Promotes tumour proliferation, invasion, metastasis, angiogenesis and cancer stem cell (CSC) formation (Singh et al., 2013).
IL-10	Regulator of T cell activity. Controls tumour-promoting inflammation (Oft, 2014).

Table 1.1 The multiple roles of HSBPs
The wide range of physiological and pathological functions of HSBPs which include growth factors, morphogens and cytokines.

adhesion proteins and certain blood coagulation factors exhibit HS binding, adding to its diverse role within the ECM (Tumova et al., 2000, Koda et al., 1985, Yu et al., 2005, Kallapur and Akeson, 1992, Ho et al., 1997). Furthermore, certain viruses and bacteria have evolved to exploit their HS-binding capacity to enhance pathogenicity (Bobardt et al., 2003, Shieh et al., 1992, Chen et al., 1997, Sava et al., 2009). Many cells contain structurally similar GAGs such as chondroitin sulphate (CS) and dermatan sulphate, which may bind HSBPs (Mizumoto et al., 2013). However, these interactions are generally weaker and are unaffected by the enzymatic activity of HPSE and therefore, will not be addressed in this chapter.

HSPGs are comprised of four families. The two major HSPG families are the transmembrane syndecans and the glycophosphatidylinositol (GPI)-anchored glypicans **(figure 1.3)**. Secreted forms such as perlecan, agrin and collagen-XVIII belong to the third family while serglycin, a highly-sulphated HS species residing in intracellular storage granules comprise the fourth (Li and Kusche-Gullberg, 2016). The classification and nomenclature of a wide variety of proteoglycans has been extensively reviewed (Iozzo and Schaefer, 2015).

1.4.1 Syndecans

Syndecans are a family of transmembrane proteoglycans. Mammals possess four distinct genes, and molecular phylogenetic analysis has revealed that syndecans are ancient in the animal lineage (Chakravarti and Adams, 2006). Syndecans possess a common structural organisation with distinct cytoplasmic, transmembrane and extracellular domains. The core proteins range from 20 – 45 kDa in size with a cytoplasmic domain of approximately 40 amino acids (Couchman et al., 2015). Although HS is the principle GAG found in all syndecans, syndecan-1 and -3 may additionally contain CS chains (Deepa et al., 2004). The cytoplasmic domain of syndecans interact with PDZ-domain-containing proteins such as syntenin, CASK, synectin, synbindin and Tiam-1, leading to cytoskeletal rearrangements in response to signalling as well as the promotion of ECM-cell adhesion and migration (Cheng et al., 2016, Cavalheiro et al., 2017). Apart from cytoskeletal organisation, syndecans also play a role in ECM assembly (Yang and Friedl, 2016). Syndecans further promote intercellular communication by regulating the biogenesis of exosomes (Baietti et al., 2012, Roucourt et al., 2015).

1.4.2 Glypicans

Mammals contain six glypican family members whose core proteins are GPI-anchored to the cell membrane. Mature glypican core proteins vary from 60 – 70 kDa in size, carrying 2 – 5 GAG chains (Fransson et al., 2004). Glypicans generally carry HS chains, however, glypican-5 carries both CS and HS chains (Saunders et al., 1997).

1.4.3 Secreted HSPG forms

Perlecan, agrin, and collagen-XVIII comprise the third family of HSPGs. Perlecan is one of the largest ECM proteins; human perlecan is a 4391-amino acid protein. The protein core of perlecan consists of a series of folding motifs or 'modules', facilitating its role as a long modular multi-functional protein (Farach-Carson et al., 2014). Agrin is better known for its role at the neuromuscular junction (Barik et al., 2014). Collagen-XVIII is expressed as three isoforms in various BMs and has attracted interest on account of its endostatin domain (Heljasvaara et al., 2017).

1.4.4 Serglycin

Human serglycin consists of a 158-amino acid core protein with eight serine/glycine repeats, with each serine residue a putative GAG attachment site. Serglycin was first considered as a hematopoietic proteoglycan found in intracellular secretory compartments and is expressed in all normal hematopoietic cells and hematopoietic tumour cell lines (Korpetinou et al., 2014).

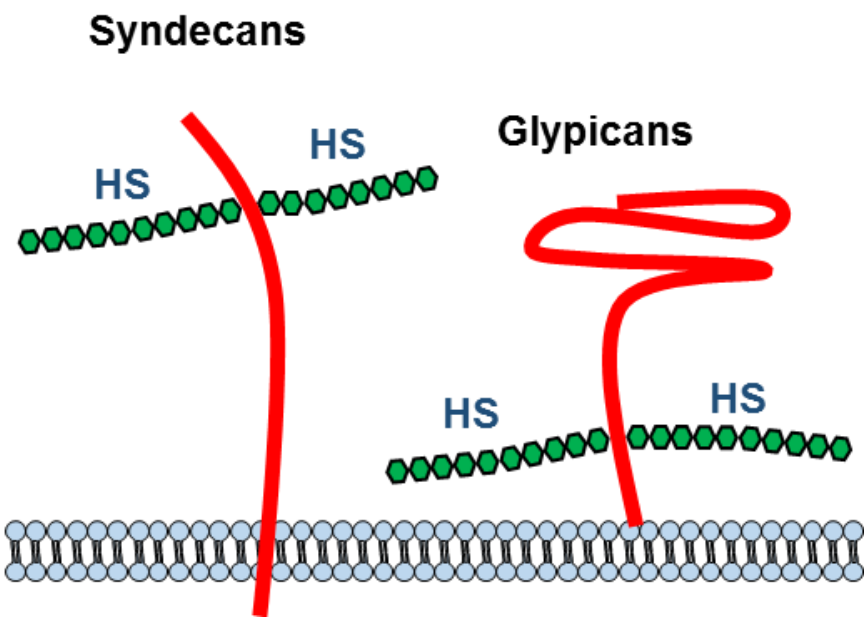

Figure 1.3 The two major families of HSPGs
HSPGs exist mainly as transmembrane syndecans or as GPI-anchored glypicans.

1.5 HPSE: a brief history – identification and characterisation

The only mammalian enzyme shown to cleave HS chains of HSPG is the β-D-endoglucuronidase, HPSE. Its identification and characterisation have a history spanning several decades. A heparin-inactivating enzyme was first described by Jaques as 'heparinase' with its purification from rabbit liver leading to its initial characterisation (Jaques and Keeri-Szanto, 1952). The isolation of 'heparinase' from a mouse mastocytoma was then described (Ogren and Lindahl, 1975). Later, an enzyme isolated from human platelets, capable of cleaving heparin and HS was described as 'heparitinase' (Oosta et al., 1982). However, heparitinase originally designated an elimination enzyme purified from *Flavobacterium heparinum* (Hovingh and Linker, 1970). The present term 'heparanase' was first coined by Nakajima upon observing the expression of a HS-degrading enzyme by metastatic B16 melanoma cells (Nakajima et al., 1984). Subsequent studies demonstrated the presence of HS-degrading enzyme from various other sources such as platelets, activated T lymphocytes, metastatic lymphoma cells, cultured endothelial cells, and normal and neoplastic murine B-lymphocytes (Yahalom et al., 1984, Naparstek et al., 1984, Bar-Ner et al., 1985, Fridman et al., 1987, Godder et al., 1991, Laskov et al., 1991).

Several factors hindered the early characterisation of HPSE, the most noteworthy being the lack of a robust activity assay (Bame, 2001). This was partly due to the hydrolase mechanism of HPSE, which was unlike bacterial lyases that cleaved heparin or HS by an eliminase mechanism (Tripathi et al., 2012). Spectrophotometric methods of assaying enzymatic activity therefore were unsuitable. The difficulty in obtaining HS prompted some to conduct assays with heparin, a highly modified version of HS (Oosta et al., 1982). However, due to fundamental structural differences in the substrates used, these assays cannot be considered physiologically relevant. Finally, the low physiological expression of HPSE presented challenges in its purification. This was however later addressed by using human platelets, a rich source of the enzyme (Freeman and Parish, 1998).

Several assays to investigate HPSE activity were developed as briefly highlighted below;

I. Gel filtration and chromatography were used to analyse radiolabelled HS fragments following HPSE cleavage (Nakajima et al., 1984, Hook et al., 1975).
II. Long HS chains were precipitated under conditions where short oligosaccharides were soluble (Oldberg et al., 1980, Graham and Underwood, 1996, Tumova and Bame, 1997).
III. Radioactivity released from immobilised heparin or HS was determined in other assays (Oosta et al., 1982, Gonzalez-Stawinski et al., 1999, Hoogewerf et al., 1995).

IV. BM with incorporated ^{35}S-HSPG was used in neutrophil ECM degradation assays (Matzner et al., 1985).

V. The retention properties of HPSE products on a labelled HS-ligand column was used to assay human platelet-derived HPSE (Freeman and Parish, 1998).

VI. Fluorescein isothiocyanate (FITC) was conjugated to bovine kidney HS followed by gel chromatography analysis of the release of FITC upon HPSE cleavage (Toyoshima and Nakajima, 1999).

VII. Finally, a time-resolved fluorescence energy transfer (TR-FRET)-based assay, where HPSE-mediated cleavage of biotin and europium-cryptate-labelled HS is measured with the addition of streptavidin-XL665 (Poon et al., 2014).

1.5.1 Cloning of human HPSE

The development of a robust method to purify and determine the enzymatic activity of HPSE from human platelets was pivotal in its characterisation and cloning. During the decades preceding its cloning, vastly different molecular weights had been reported for HPSE, ranging from 8 – 137 kDa (Oosta et al., 1982, Hoogewerf et al., 1995, Freeman and Parish, 1998). A breakthrough came with the development of a rapid quantitative assay that enabled the 1700-fold purification of human HPSE to homogeneity, demonstrating an active 50 kDa subunit with no reported activity in 8 – 10 kDa or the 137 kDa fractions, in contrast to previous observations (Freeman and Parish, 1998).

Human HPSE was first cloned in 1999 independently by two groups using (i) HPSE purified from platelets to perform N-terminal protein sequencing and oligonucleotide probe generation to screen a placental complimentary deoxyribonucleic acid (cDNA) library, and (ii) HPSE purified from placenta and a hepatoma cell line (SK-hep-1) using sequential chromatography, with the resulting peptides sequenced and the corresponding deoxyribonucleic acid (DNA) sequences identified from a placental cDNA library (Hulett et al., 1999, Vlodavsky et al., 1999). Later in the same time period, a separate study reported the cloning of HPSE from a human placental cDNA library, where the cDNA was identified via peptide sequences of purified HPSE derived from human hepatoma cells (Kussie et al., 1999).

Hulett *et al.* conducted an *in situ* trypsin digestion of a 50 kDa protein purified from platelets, resulting in ten peptides that were then amino acid-sequenced (Hulett et al., 1999). Comparison of the peptide and the N-terminal sequences revealed no homologous proteins, suggesting it was unique. This was in contrast to previous suggestions that HPSE closely resembled heat shock family-90 proteins or belonged to the connective tissue activating peptide-III family (Graham, 1994, Hoogewerf et al., 1995). Further analysis identified a clone from a human placental cDNA library, based on the amino acid

sequence. Additional database searches and library analyses revealed an open reading frame (ORF) of 1,629 bp encoding for a 543-amino acid polypeptide of a predicted mass of 65 kDa. Gel filtration studies excluded enzymatic activity of the 65 kDa 'full length' form of HPSE, and instead identified an enzymatically active 50 kDa protein, which suggested a post-translational activation process. These observations were corroborated by others (Vlodavsky et al., 1999). The enzymatically active form of HPSE is a non-covalently linked heterodimer comprising of an 8 kDa N-terminal region (Gln_{36}-Glu_{109}) and a 50 kDa C-terminal region (Lys_{158}-Ile_{543}) (Fairbanks et al., 1999). Expression of the truncated 50 kDa HPSE (Lys_{158}-Ile_{543}) failed to yield activity, indicating that the region from the N-terminus to Lys_{158} played a crucial role in the expression of a functional enzyme (Nadav et al., 2002).

HPSE orthologues from other species that have high amino acid identity with human HPSE **(figure 1.4)** have been cloned, as summarised below (Table 1.2). Furthermore, an additional gene designated *HPSE-2*, has been identified that encodes for a more distant relative of human HPSE with ~40% amino acid sequence identity (McKenzie et al., 2000). In contrast to HPSE, HPSE-2 does not have any HS-degrading activity (McKenzie et al., 2000) and instead has been shown to play an inhibitory role to its enzymatically active counterpart in a number of malignancies that has been associated with clinically favourable outcomes (Levy-Adam et al., 2010, Gross-Cohen et al., 2016). This review, however, will focus exclusively on the enzymatically active HPSE.

Species	Identity with human HPSE	Reference
Mouse	77%	(Miao et al., 2002)
Rat *(Rattus norvegicus)*	79.7%	(Hulett et al., 1999)
Cow *(Bos Taurus)*	80%	(Kizaki et al., 2003)
Chicken *(Gallus gallus)*	62%	(Goldshmidt et al., 2001)
Spalax (mole rat, *Spalax carmeli*)	85%	(Nasser et al., 2005)
Xenopus *(Xenopus tropicalis)*	57%	(Bertolesi et al., 2008)

Table 1.2 HPSE orthologues
The sequence identities of HPSE of several species with human HPSE.

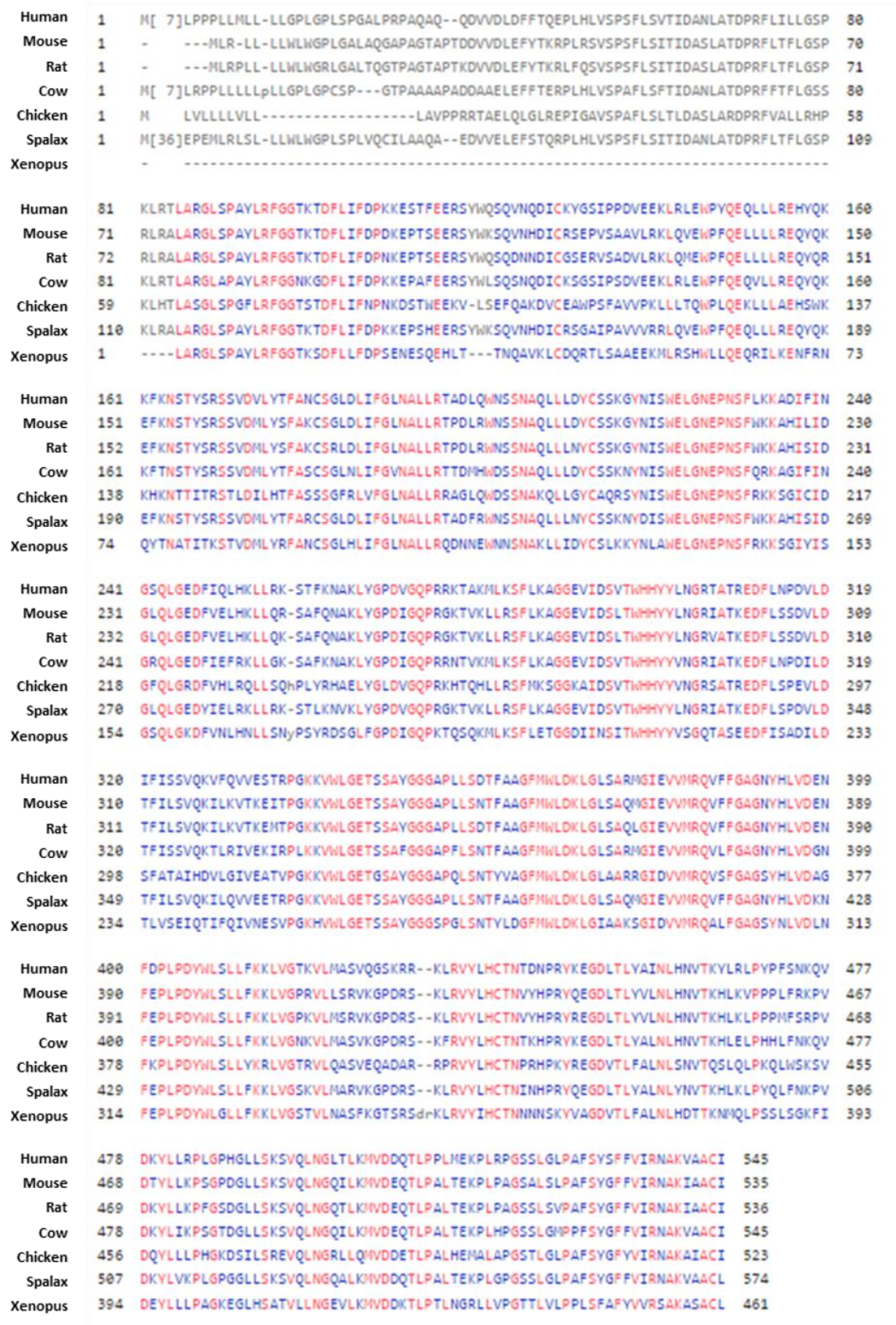

Figure 1.4 Sequence alignment of HPSE orthologues
The alignment of amino acid sequences of HPSE derived from a variety of species highlighting sequence identity (in red) with that of human HPSE.

1.6 HPSE: genomic organisation and alternate spliced transcripts

The human *HPSE* gene consists of 14 exons spanning approximately 50 kb and is located on chromosome 4q21.23, as confirmed by fluorescence *in situ* hybridisation and radiation hybrid mapping (Baker et al., 1999). The exons range in size from 48 bp (exon 7) to 1649 bp (exon 14) while the introns vary between 0.23 kb (intron 8) to 23 kb (intron 2). The second exon contains an untranslated 31 bp sequence and the start codon.

Two human HPSE transcripts encoding the same ORF for the 65 kDa protein are expressed via alternative splicing of the first and last exons (Hulett et al., 1999, Dong et al., 2000). The predicted transcript based on the cDNA cloning is the 2 kb messenger ribonucleic acid (mRNA) form (*HPSE 1b*) and was found in the placenta but not in the heart, brain, skeletal muscle, kidney, lung, liver or pancreas. The 4.4 kb mRNA form (*HPSE 1a*) was weakly detected in the placenta as well as in all other tissues. In immune tissues such as spleen, lymph node, peripheral blood leukocytes, thymus and bone marrow, both 2 and 4.4 kb transcripts were detected at similar levels. Southern blot analysis of digested genomic DNA from two donors probed with full-length human HPSE cDNA showed a simple hybridisation pattern (Hulett et al., 1999). These observations strongly suggested that both transcripts originated from a single gene. The 4.4 kb *HPSE 1a* transcript contains 14 exons and 13 introns, with a longer 3' untranslated region, while the *HPSE 1b* variant has its first and last exons spliced out (Dong et al., 2000).

Other splice variants of human HPSE have been reported. A 55 kDa variant resulting in skipping exon 5 was described which maintained the original reading frame, but lacked enzymatic activity due to the loss of 174 bp encoding for 58 amino acids, including key active site components (Nasser et al., 2007). Subcellular localisation studies in COS-7 cells demonstrated that overexpressed HPSE and its exon 5-deleted spliced variant localised to the endoplasmic reticulum (ER) independent of glycosylation (Sato et al., 2008). Spliced variants have been linked to malignancies. An additional novel spliced variant, designated T5, was identified *in silico* and following its *in vivo* validation, was shown to be upregulated in 75% of human renal cell carcinomas (Barash et al., 2010). T5 is a truncated, enzymatically inactive HPSE variant where 144 bp of intron 5 are joined with exon 4 and is endowed with pro-tumorigenic features (Barash et al., 2010, Barash et al., 2012). It is composed of only the 8 kDa subunit and the linker region but lacks the 50 kDa subunit, resulting in a 15 – 17 kDa protein, dependent upon glycosylation.

Other species have been shown to express HPSE variants as well. A variant cloned from the blind mole rat (*Spalax*), termed splice 36, which skips part of exon 3, exon 4, exon 5 and part of exon 6 was shown to inhibit HS degradation, suppress glioma tumour growth and decrease B16 mouse melanoma lung colonisation (Nasser et al., 2009). However, in

the same study, another splice variant, splice 7, resulting from the skipping of exon 7 was shown to be pro-tumorigenic, although lacking enzymatic activity. Two splice variants playing a role in early embryonic development of *Xenopus laevis* have also been described*;* a 531-amino acid long (XHpaL) variant and a short (XHpaS) variant missing 58 amino acids due to skipping exon 4 (Bertolesi et al., 2008).

The 4q21.23 location of the *HPSE* gene raises the possibility of its involvement in genetic disorders. One of six familial Parkinson's disease chromosomal localization was mapped to 4q21.23 (Polymeropoulos et al., 1996). More recently, 4q21 deletions have been linked to development disorders (Komlosi et al., 2015). However, no conclusive evidence exists for the direct involvement of the *HPSE* gene in these conditions.

1.7 HPSE: 3D structure

A model structure of human HPSE was first proposed by Hulett *et al* by identifying similarities between HPSE and several glycosyl hydrolase family members from glycosyl hydrolase clan-A (GH-A) (Hulett et al., 2000). Secondary structure predictions suggested a $(\beta/\alpha)_8$ TIM-barrel fold, with the likely proton donor and nucleophile identified as Glu_{225} and Glu_{343}, respectively. Despite significant scientific interest, the 3D structure of HPSE remained elusive for decades, until Wu *et al.* succeeded in providing the first conclusive insights (Wu et al., 2015). This was achieved by employing a baculoviral dual protein expression strategy (McKenzie et al., 2003). Expression of the 8 and 50 kDa HPSE subunits resulted in co-translational folding into mature HPSE, effectively bypassing the requirement for processing of the 65 kDa pro-HPSE form (Wu et al., 2015).

The crystal structure of human HPSE **(figure 1.5)** was resolved at 1.6-1.9 Å and consists of a substrate binding $(\beta/\alpha)_8$ TIM-barrel domain flanked by a β-sandwich domain, with Glu_{225} and Glu_{343} residues forming the catalytic region, as predicted (Hulett et al., 2000, Wu et al., 2015). The proximity of the 6 kDa linker to the $(\beta/\alpha)_8$ domain imparts steric hindrance, preventing enzymatic activity (Nardella et al., 2004). Both domains involve the 50 kDa and 8 kDa subunits, with one β-sheet contributed by the 8 kDa subunit to the β-sandwich and the first β-α-β-fold of the $(\beta/\alpha)_8$ domain. The remaining folds are contributed by the 50 kDa subunit, which also contains six putative N-glycosylation sites. Prior structural data of a GH-79 exoglucuronidase from *Acidobacterium capsulatum* and that of an *endo*-acting heparanase from *Burkholderia pseudomallei* provided crucial overview that aided in its characterisation (Bohlmann et al., 2015, Michikawa et al., 2012).

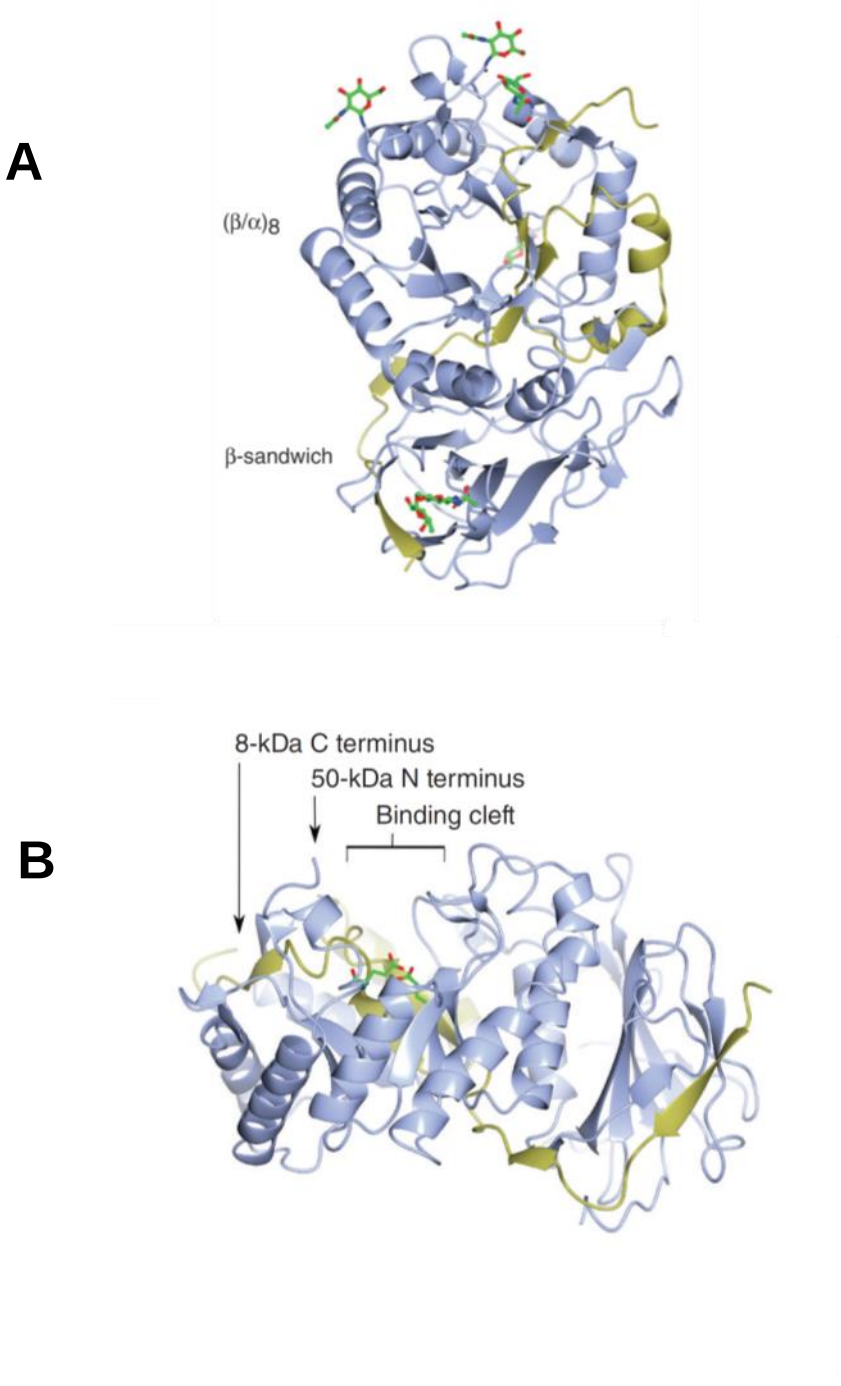

Figure 1.5 The 3D structure of human HPSE
The front view **(A)** in ribbon representation shows the 8 kDa subunit in yellow and the 50 kDa subunit in blue. The side view **(B)** of HPSE shows the binding cleft in the $(\beta/\alpha)_8$ domain which contains the catalytic residues, shown in green (Wu et al., 2015).

1.8 HPSE: substrate binding and enzymatic activity

HPSE favours acidic environments, with optimal HS-degrading activity exhibited between pH 5.0 – 6.0, with pH levels near neutral and above significantly reducing activity (Vlodavsky and Friedmann, 2001). This results in high HPSE activity in sites of inflammation and in the TME (Estrella et al., 2013, Gilat et al., 1995). The cloning of HPSE and its conservation with GH-A members, enabled the identification of residues critical for enzymatic activity (Hulett et al., 2000), as detailed above.

In an attempt to define HPSE/HS interaction, Levy-Adam *et al.* undertook site-directed mutagenesis and nuclear magnetic resonance studies (Levy-Adam et al., 2005). These studies identified the amino acid residues Lys_{158}, Lys_{159}, Phe_{160}, Lys_{161} and Asp_{162} as critical mediators of HPSE-heparin/HS interaction. Two heparin-binding domains were thus identified and mapped; Lys_{158}-Asp_{162} (KKKFKN) at the N-terminal end of the 50 kDa subunit and at Pro_{271}-Met_{278} (PRRKTAKM). A third domain containing two tandem basic amino acid clusters at Lys_{411}-Lys_{417} and Lys_{427}-Arg_{432} suggested a third potential heparin-binding domain. The domain at Lys_{158}-Asp_{171} (KKDC peptide) was shown to physically interact with HS and heparin (Levy-Adam et al., 2005). Later studies provided evidence for the interaction of the KKDC peptide with cell-surface HS, resulting in syndecan-1 and -4 clusters (Levy-Adam et al., 2008).

The substrate binding of HPSE is dependent on the sulfation patterns of HS chains (Okada et al., 2002). The enzymatic cleavage of HS chains occurs at the internal GlcA(β1-4)*N*-sulfoglucosamine (GlcNS) linkages **(figure 1.6)**. High sulfation not only directs HPSE to certain cleavage sites on HS, but the *N*-sulphate and *O*-sulphate moieties enable HPSE to pry open HS (Wu et al., 2015). HS cleavage liberates low-molecular weight HS fragments of 5 – 10 kDa. This leads to the degradation and remodelling of the ECM, resulting in the release and activation of HS-bound growth factors and cytokines (Okada et al., 2002, Wilson et al., 2014, Knelson et al., 2014). This HS-mediated signalling promotes physiological and pathological processes such as immune cell migration and activation, inflammation, angiogenesis and metastasis (Putz et al., 2017, Poon et al., 2014, Wood and Hulett, 2008, Gutter-Kapon et al., 2016, Weissmann et al., 2016, Vlodavsky and Friedmann, 2001).

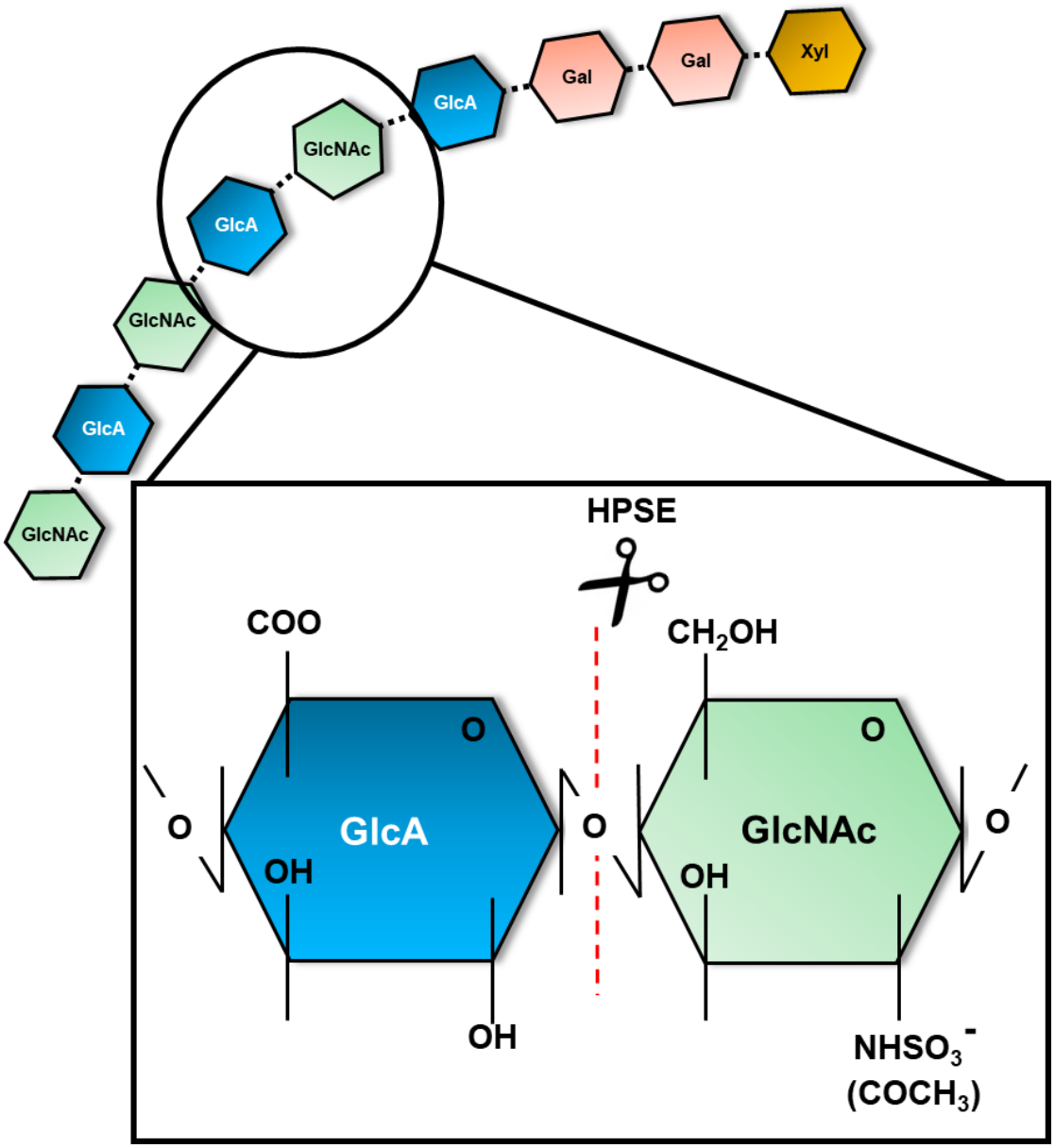

Figure 1.6 The structure of HS chains and the mode of HPSE-mediated HS cleavage
HS is a variably sulphated, anionic GAG chain of repeating disaccharide units of β1-4-linked D-glucuronic acid (GlcA) and α1-4-linked N-acetyl-D-glucosamine (GlcNAc). A GlcA-Gal-Gal-Xyl tetrasaccharide linker attaches the HS chain to its protein core. Enzymatic cleavage of HS occurs at internal GlcA(β1-4)GlcNS linkages.

1.9 HPSE: expression regulation

The expression of HPSE is tightly regulated in order to prevent non-specific tissue damage. A variety of transcription factors such as E26 transformation specific (ETS) family members, early growth response protein-1 (EGR-1), specificity protein-1 (Sp1), B-Raf kinase, NFκB and p53 are involved in regulating HPSE expression (de Mestre et al., 2003, de Mestre et al., 2007, Baraz et al., 2006, Jiang et al., 2002, Lu et al., 2003, Andela et al., 2000, Rao et al., 2010). Cloning of the *HPSE* gene promoter revealed a 3.5 kb, TATA-less, GC-rich region subjected to both positive and negative controls (Jiang et al., 2002). A minimal 0.3 kb region (-1 to -340 bp) with basal promoter activity was identified through truncation analysis to contain three Sp1 sites. The -25 to +1 bp region contains overlapping consensus EGR-1 and Sp1 binding sites (de Mestre et al., 2003). Four ETS transcription factor binding sites exist within a 598 bp region encompassing the transcription initiation site, two of which are non-functional and flank the transcription initiation site with the remaining two functional binding sites located at the 5' end (Lu et al., 2003). A cis-acting site at -391 to -164 bp with repressor activity was reported along with other repressor elements at -700 to -3,500 bp and -598 to -1089 bp (de Mestre et al., 2003).

Sp1 and ETS family member GA-binding protein was shown to collectively regulate HPSE expression in thyroid tumour cells by binding within the minimal promoter region, 0.3 kb upstream of the start site (Jiang et al., 2002). In metastatic breast cancer cells, ETS1 and ETS2 were found to regulate HPSE expression by binding to sites upstream of the 0.3 kb minimal promoter (Lu et al., 2003). Mutant *BRAF*, a potent oncogene coding for B-Raf kinase was shown to stimulate HPSE expression (Rao et al., 2010). EGR-1 was shown to be a potent inducer of HPSE transcription in activated T cells while Sp1 was also shown to bind EGR-1 consensus sequences and play a role in basal *HPSE* promoter activity (de Mestre et al., 2003). Furthermore, EGR-1 was shown to promote HPSE expression in a number of human cancers (de Mestre et al., 2005). HPSE expression was markedly reduced through NFκB signal blockade, demonstrating its role as a *HPSE* gene regulator, (Andela et al., 2000). Tumour cells exposed to hypoxic conditions were shown to upregulate HPSE in an NFκB-dependent manner (Wu et al., 2010b). *TP53*, encoding for the potent tumour suppressor p53, is the most commonly mutated gene in human cancers (Kastenhuber and Lowe, 2017, Lane and Crawford, 1979). Wild-type p53 was shown to bind to the *HPSE* promoter, effectively inhibiting its activity whereas mutant p53 failed to do so, resulting in expression (Baraz et al., 2006).

Several other biological factors function in *HPSE* gene regulation. Four estrogen response elements were found in the *HPSE* promoter region and the MCF-7 estrogen receptor (ER)-

positive human breast cancer cell line was shown to express HPSE upon estrogen treatment (Elkin et al., 2003). However, this could be due to an interplay between the ER complex and the ETS or Sp1 transcription factors rather than being directly estrogen-driven (Lincoln et al., 2003). Following these observations, a strong correlation between ER-positivity and HPSE-overexpression in breast cancer was shown, along with an estrogen-like effect of tamoxifen on HPSE expression (Cohen et al., 2007). Increased HPSE levels were observed in kidneys with diabetic nephropathy and high glucose levels were shown to promote HPSE expression via a glucose-response element in the *HPSE* promoter region (Maxhimer et al., 2005b). Finally, increased EGR-1 expression coupled with CpG hypomethylation was shown to regulate HPSE expression in prostate and bladder cancers (Ogishima et al., 2005b, Ogishima et al., 2005a). However, this is likely due to the combined effect of aberrant demethylation and the expression of related transcription factors.

1.10 HPSE: expression and processing

Human HPSE is initially expressed as a pre-pro form as a 543-amino acid polypeptide, which matures to a glycosylated 65 kDa pro-form in the ER by the removal of the N-terminal signalling peptide (Met_1-Ala_{35}) (Wu et al., 2015, Hulett et al., 2000). Initial analysis of the amino acid sequence of the active 50 kDa HPSE subunit yielded an N-terminus of KKFKXSTYSRRSVDVLY, a sequence 158 amino acids downstream of the initiation site (Hulett et al., 1999). This observation first indicated a pro-enzyme form which undergoes cleavage to produce its active form.

Pro-HPSE is then shuttled to the Golgi apparatus followed by its packaging into vesicles and secretion **(figure 1.7)**. Once secreted, pro-HPSE interacts with HSPG molecules, specifically syndecans (Gingis-Velitski et al., 2004b). This pro-HPSE-HSPG interaction promotes its cellular uptake into latent endosomes and lysosomes leading to its proteolysis mediated activation by cathepsin-L cleavage, which removes a 6 kDa linker (Ser_{110}-Gln_{157}) fragment **(figure 1.8)** (Nadav et al., 2002, Abboud-Jarrous et al., 2008). The half-life of freshly-formed HPSE was estimated to be approximately 30 h, significantly longer than that of transmembrane domain-HSPGs (2 – 6 h) and of GPI-anchored HSPGs (approximately 25 min) (Egeberg et al., 2001). The physiological expression of HPSE is limited to a few cells and tissue types such as platelets, cells and tissues of the immune system, and the placenta as described in the previous section (Vlodavsky et al., 1992, Goshen et al., 1996, Hulett et al., 1999). Klein first described the partial purification of a HS-specific endoglucuronidase from human placenta (Klein and Von Figura, 1976).

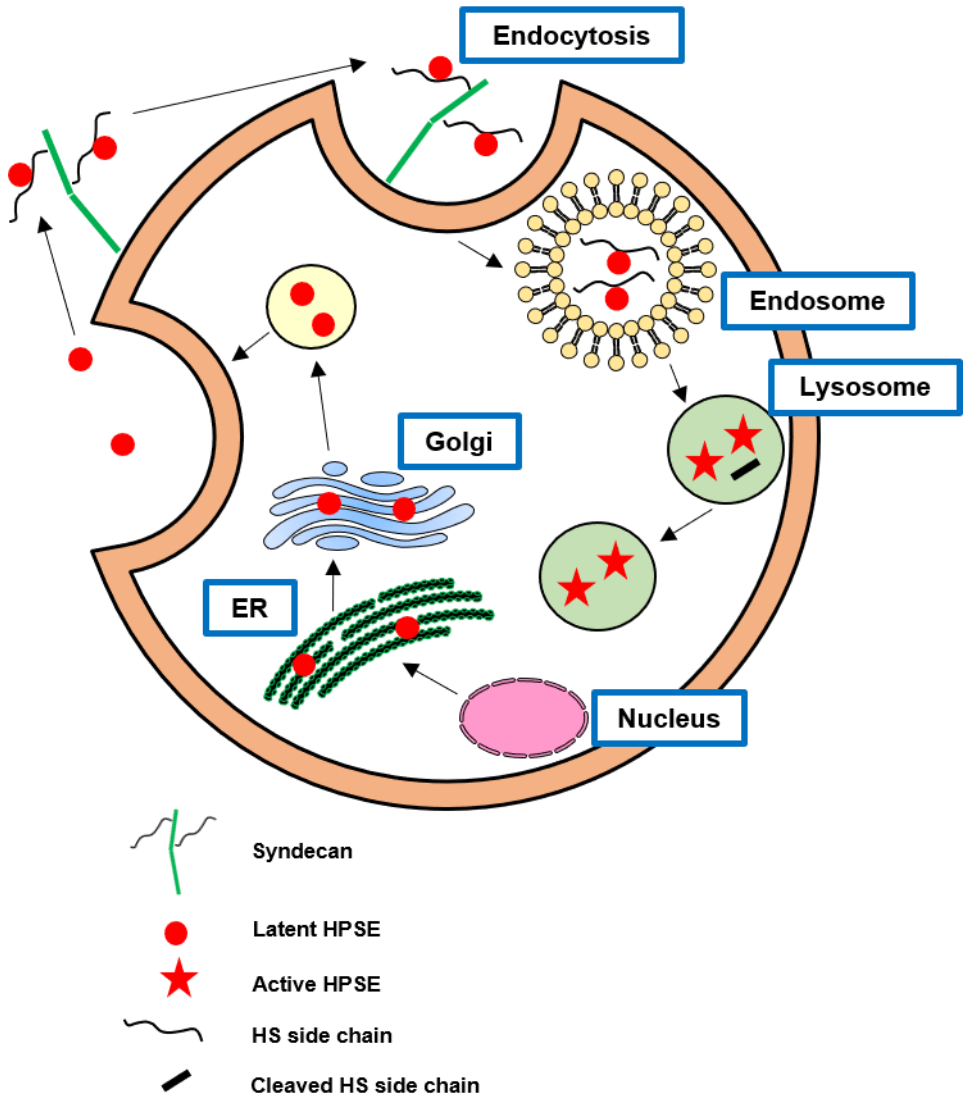

Figure 1.7 A schematic representation of the biogenesis of HPSE
HPSE is initially synthesised in its pre-pro form, which matures to its pro-form in the ER. Pro-HPSE is then shuttled to the Golgi and secreted. Secreted pro-HPSE interacts with HSPGs. The Pro-HPSE-HSPG complex undergoes endocytosis followed by cathepsin cleavage-mediated activation.

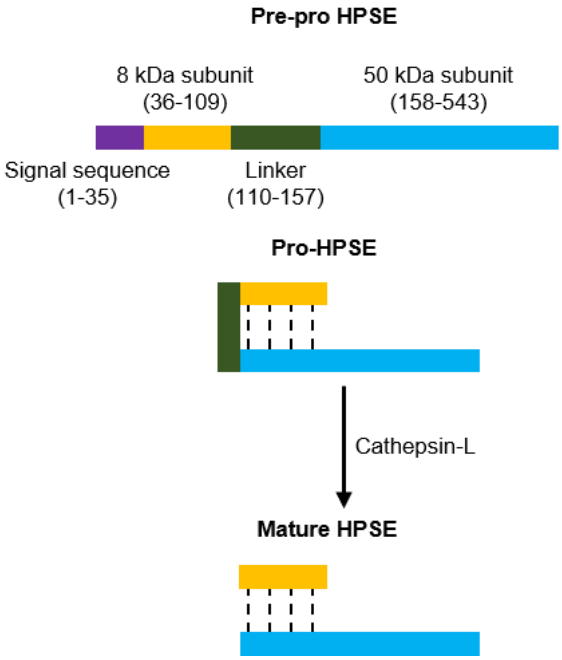

Figure 1.8 The processing of pre-pro HPSE to its mature, active form
The 543 amino acid pre-pro form of HPSE consists of a signal sequence, an 8 kDa subunit, a linker and a 50 kDa subunit. The 6 kDa linker of pro-HPSE is cleaved by cathepsin-L, leading to the active, mature form of the enzyme.

Placental HPSE is expressed mainly in trophoblasts during all stages of gestation as well as in the endothelium of the foetal capillaries (Haimov-Kochman et al., 2002, Dempsey et al., 2000). Platelets contain high levels of HPSE, which led to its initial characterisation (Oosta et al., 1982). HPSE in platelets has been shown to promote platelet adhesion and enhance coagulation activity through the upregulation of tissue factor (TF) (Nadir and Brenner, 2016, Cui et al., 2016). These non-enzymatic functions of platelet-derived HPSE play a major role in the metastatic cascade, by promoting adhesion and pro-coagulant activity, which will be discussed in detail later. Recent studies have highlighted the role of HPSE in immune cell activity. HPSE has been shown to affect several types of immune cells such as natural killer (NK) cells, neutrophils, macrophages, dendritic cells (DCs) and mast cells that mediate both acute and chronic inflammatory responses (Benhamron et al., 2012, Poon et al., 2014, Schmidt et al., 2012, Wang et al., 2011, Secchi et al., 2017a, Lerner et al., 2011, Putz et al., 2017, Gutter-Kapon et al., 2016). Furthermore, the overexpression of HPSE triggers both innate and adaptive immune responses in a mouse rheumatoid arthritis model (Digre et al., 2017). In a pivotal study, the expression of HPSE in chimeric antigen receptor-redirected T (CAR-T) cells enhanced tumour infiltration and anti-tumour activity, highlighting the potential of HPSE in cancer immunotherapy (Caruana et al., 2015). The role of HPSE in immune cells is discussed in more detail in section 1.23.5.

Dysregulated gene expression, a hallmark of cancer, leads to the overexpression of HPSE in all cancers, causing pathological ECM remodelling (Hanahan and Weinberg, 2011, Hammond et al., 2014). HPSE overexpression in cancer enhances tumour growth and metastasis, as outlined in table 1.3 (Sanderson et al., 2017). This results in a poor clinical prognosis, demonstrating the potential of HPSE as a therapeutic target (Rivara et al., 2016). HPSE also exhibits a variety of non-enzymatic functions such as regulating gene expression, promoting cell adhesion and tumour-promoting pro-coagulant activity (Nadir and Brenner, 2014, Sanderson et al., 2017). The role of HPSE in promoting the hallmarks of cancer via both enzymatic and non-enzymatic processes will be now discussed.

Cancer type	Clinical studies implicating HPSE overexpression in enhanced cancer growth/metastasis
Lung	(Cohen et al., 2008, Castelo-Branco et al., 2015, Katz et al., 2018)
Breast	(Sun et al., 2017, Vornicova et al., 2018)
Colorectal	(Nobuhisa et al., 2005a, Wu et al., 2010a)
Prostate	(Lerner et al., 2008, Stadlmann et al., 2003)
Stomach	(Liu et al., 2018, Li et al., 2015b, Sonoda et al., 2010)
Liver	(Chen et al., 2014, Liao et al., 2016a, Wang et al., 2010)
Oesophageal	(Brun et al., 2009, Han et al., 2005, Ohkawa et al., 2004a)
Cervical	(Hu et al., 2017a, Shinyo et al., 2003, Zeng et al., 2014)
Thyroid	(Matos et al., 2015, Xu et al., 2003)
Bladder	(Gohji et al., 2001b, Shafat et al., 2008, Zhao et al., 2009)

Table 1.3 HPSE is implicated in promoting the ten major human cancers
The ten major cancer types affecting humans with studies demonstrating that the expression of HPSE correlates with enhanced cancer growth/metastasis, leading to a poor clinical prognosis.

1.11 The hallmarks of cancer

The characteristic features or the 'hallmarks' of a cancer were first described by Hanahan and Weinberg in 2000 (Hanahan and Weinberg, 2000). The six classic hallmarks are sustaining proliferative signalling, evading growth suppressors, resisting cell death, enabling replicative immortality, inducing angiogenesis and activating invasion and metastasis. These are now accompanied by four newly-introduced enabling characteristics and emerging hallmarks, namely genome instability and mutation, tumour-promoting inflammation, reprogramming energy metabolism and avoiding immune destruction (Hanahan and Weinberg, 2011). By virtue of its capacity to regulate multiple pro-tumorigenic pathways, HPSE can be implicated in the promotion of each of these features **(figure 1.9)**. The remainder of this section will define in detail the role of HPSE in the hallmarks of cancer and discuss its enzymatic and non-enzymatic activity as a key player in human malignancies.

1.12 Sustaining proliferative signalling

Cell proliferation is a highly regulated physiological process, with balanced positive and negative signal transduction mechanisms. This carefully choreographed process is dysregulated in cancers, leading to uncontrolled cell proliferation; the most fundamental hallmark of cancer (Kolch et al., 2015). The progression of the cell cycle is tightly regulated by the G1/S transition, which depends on biochemical and biophysical cues arising from cellular interactions with the ECM (Xiong et al., 2013). Somatic mutations, loss in cell-ECM adhesion as well as the increased availability of growth factors through ECM remodelling promotes G1/S transition, resulting in uncontrolled cell growth. The ability of cancer cells to produce growth factors themselves and express relevant receptors, resulting in autocrine proliferative signalling, is a well-characterised phenomenon (Sporn and Roberts, 1985). Constant crosstalk between cancer cells and the stroma further results in the release of growth factors (Calon et al., 2015).

1.12.1 HPSE-driven growth factor and morphogen signalling

As previously highlighted, HS in the ECM binds to and sequesters a variety of key growth factors and morphogens in cancer settings such as FGF, HGF, VEGF, EGF, PDGF, TGF-β and Hh, regulating signal transduction through restricting their bioavailability. Remodelling of the ECM through HS cleavage by HPSE liberates these growth factors, promoting cellular proliferation, amongst several other key hallmarks of cancer (refer to table 1.1) (Knelson et al., 2014, Hynes, 2009). Growth factor-mediated receptor tyrosine kinase (RTK) signalling plays critical roles in both physiological and pathological conditions (Lemmon and Schlessinger, 2010). RTK family members are highly conserved cell-surface growth factor receptors, whose signalling pathways have garnered significant

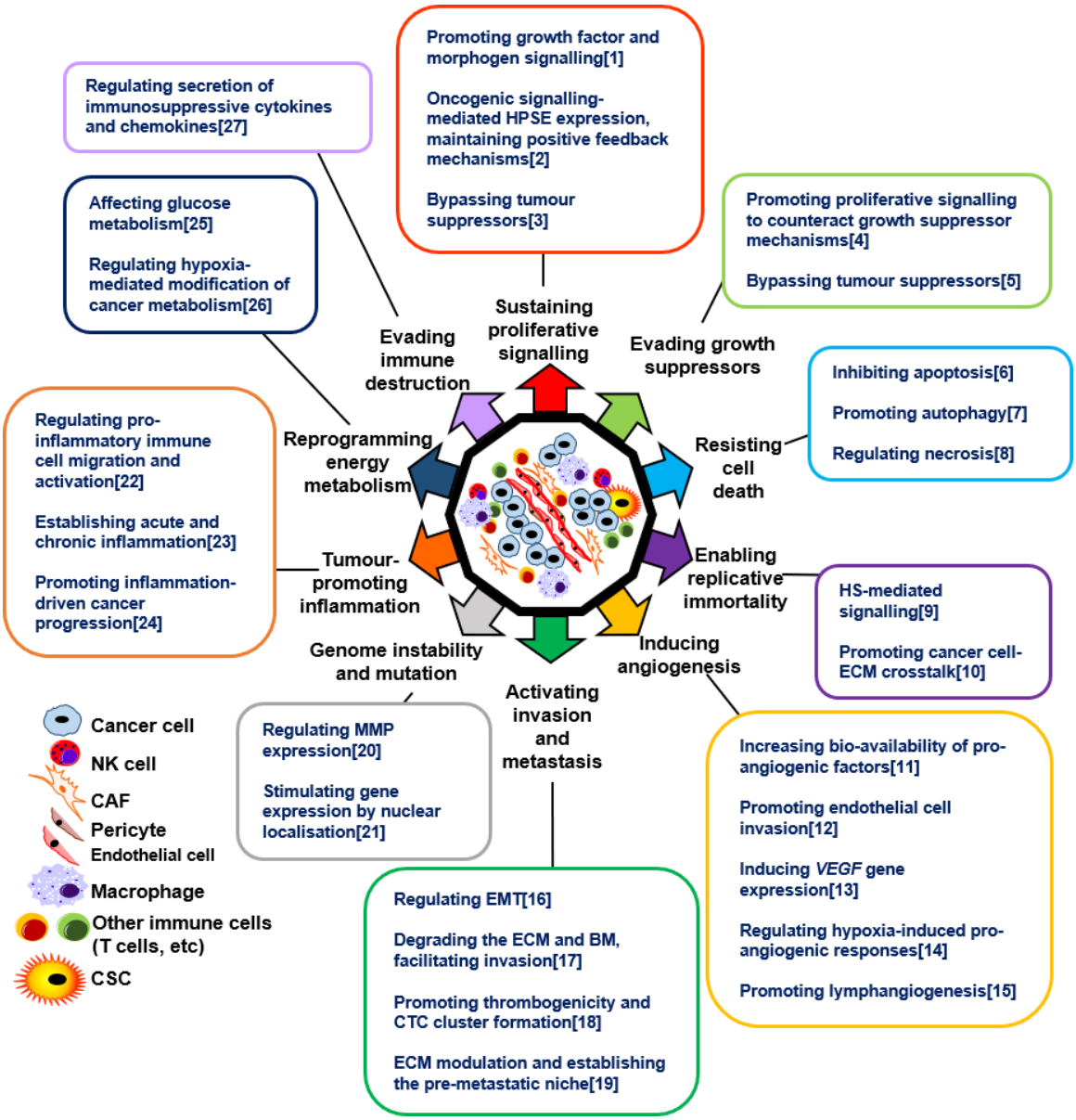

Figure 1.9 HPSE regulates all hallmarks and enabling characteristics of cancer
The enzymatic and non-enzymatic activity of HPSE directly promotes or is suggested to promote all classic and emerging hallmarks of cancer as well as all enabling characteristics. The key mechanisms of action undertaken by HPSE in facilitating each of the hallmarks and characteristic features are listed. This multi-faceted nature of HPSE thus establishes its pivotal role in the TME. Evidence is provided by the following authors.

1 (Knelson et al., 2014, Hynes, 2009, Escobar Galvis et al., 2007, Ramani et al., 2011, Hao et al., 2015, Ostapoff et al., 2013, Zetser et al., 2006, Luan et al., 2011, Wang et al., 2014, Wirstlein et al., 2013, Zhang et al., 2010, Cohen-Kaplan et al., 2008a, Malavaki et al., 2013, Troilo et al., 2016, Masola et al., 2014a, Welch et al., 1990, Batool et al., 2017)
2 (Boyango et al., 2014, Tang et al., 2016, Rao et al., 2010, Luan et al., 2011, Welch et al., 1990)
3 (Gingis-Velitski et al., 2004a, Riaz et al., 2013, Hao et al., 2015)
4 (Knelson et al., 2014, Hynes, 2009, Escobar Galvis et al., 2007, Ramani et al., 2011, Hao et al., 2015, Ostapoff et al., 2013, Zetser et al., 2006, Luan et al., 2011, Wang et al., 2014, Wirstlein et al., 2013, Zhang et al., 2010, Cohen-Kaplan et al., 2008a, Malavaki et al., 2013, Troilo et al., 2016, Masola et al., 2014a, Welch et al., 1990, Batool et al., 2017)
5 (Riaz et al., 2013, Cohen-Kaplan et al., 2012, Qu et al., 2016)
6 (Knelson et al., 2014, Cohen et al., 2006, Riaz et al., 2013, Zetser et al., 2006, Rubinfeld et al., 2011, Ostapoff et al., 2013, Joyce et al., 2005, Parangi et al., 1995)
7 (Goldshmidt et al., 2002, Shteingauz et al., 2015)
8 (Gutter-Kapon et al., 2016, Nadir and Brenner, 2016, Peled et al., 2013, Peled et al., 2016)
9 (Knelson et al., 2014, Escobar Galvis et al., 2007, Flaumenhaft et al., 1990, Jung et al., 2016b)

10 (Riaz et al., 2013)
11 (Knelson et al., 2014, Watanabe et al., 2003a, Cohen et al., 2006, Sato et al., 2004, Okawa et al., 2005, Zhang et al., 2007, Edovitsky et al., 2004, Hammond et al., 2012, Dredge et al., 2010, Parish et al., 1999)
12 (Godder et al., 1991, Purushothaman et al., 2010, Gingis-Velitski et al., 2004a)
13 (Zetser et al., 2006)
14 (Li et al., 2017b, Naomoto et al., 2007, He et al., 2004a)
15 (Tan et al., 2013, Hunter et al., 2014, Cohen-Kaplan et al., 2008b, Zhang et al., 2009)
16 (Li et al., 2016b, Masola et al., 2016, Masola et al., 2012a, Masola et al., 2012c, Strutz et al., 2002, Escobar Galvis et al., 2007, Masola et al., 2014a)
17 (Hulett et al., 1999, Vlodavsky et al., 1992, Takaoka et al., 2003, Bar-Ner et al., 1985, Bar-Ner et al., 1986, Purushothaman et al., 2008, Gonzalez-Alva et al., 2010a, Ohkawa et al., 2004a, Beckhove et al., 2005)
18 (Cui et al., 2016, Goldshmidt et al., 2003, Wei et al., 2018b, Zetser et al., 2003, Zhang et al., 2013b)
19 (Gomes et al., 2013, Roucourt et al., 2015, David and Zimmermann, 2016a, Thompson et al., 2013)
20 (Purushothaman et al., 2008, Tang et al., 2014a, Chen et al., 2012)
21 (Riaz et al., 2013, Cohen-Kaplan et al., 2012, Masola et al., 2014a, Naomoto et al., 2007, Nobuhisa et al., 2005a, Ohkawa et al., 2004a, Schubert et al., 2004a, Kobayashi et al., 2006)
22 (Naparstek et al., 1984, Vlodavsky et al., 1992, Matzner et al., 1985, Goodall et al., 2014, Poon et al., 2014, Benhamron et al., 2012, Schmidt et al., 2012, Waterman et al., 2007, Lerner et al., 2011, Edovitsky et al., 2006)
23 (Schmidt et al., 2012, Lerner et al., 2011, Waterman et al., 2007, Khamaysi et al., 2017b, Morris et al., 2015, Goldberg et al., 2014)
24 (Brun et al., 2009, Lerner et al., 2011, Gutter-Kapon et al., 2016, El-Assal et al., 2001, Koliopanos et al., 2001)
25 (Chen et al., 2004, Riaz et al., 2013, Hamoud et al., 2017, Shafat et al., 2011, Zhang et al., 2017a, Wang et al., 2012a)
26 (Li et al., 2017b, Naomoto et al., 2007, Wu et al., 2010b, Hu et al., 2012, Hu et al., 2015)
27 (Gutter-Kapon et al., 2016)

interest, owing to their functional diversity (Volinsky and Kholodenko, 2013, Bergeron et al., 2016). RTK-mediated signalling regulates cellular proliferation as well as differentiation, migration, cell cycle control, survival and metabolism. Aberrant RTK activity is linked to pathologies such as cancer, diabetes, bone disorders, arteriosclerosis, angiogenesis and inflammatory disorders. On this account, the development of RTK inhibitors has been investigated as a potential therapeutic measure for over three decades, with numerous inhibitors approved to date (Ferguson and Gray, 2018). The relationships between several key pro-proliferative HSBPs and HPSE expression are closely examined below.

FGF: The binding of FGF to HS is vital for dimerisation with and signalling through FGFR (Huang et al., 2017). The overexpression of HPSE in mouse organs and human tumours has been shown to correlate with enhanced 6-O-sulfation of HS which promoted the formation of ternary complexes with FGF-1 or -2 and FGFR (Escobar Galvis et al., 2007).

HGF: HGF-mediated c-MET signalling is observed in cancer (Pothula et al., 2016, Cascone et al., 2017). It has been demonstrated that HGF expression correlates with that of HS in cancer settings (Ramani et al., 2011). HPSE activity enhances HGF expression and signalling through syndecan shedding. It has also been shown that HGF activates phosphoinositide-3-kinase (PI3K)/protein kinase-B (Akt) and NF-κB signalling to promote HPSE in cancer cells, resulting in a poor prognosis in gastric tumours (Hao et al., 2015). This may suggest a cyclic relationship between HGF and HPSE.

VEGF: HPSE expression in the TME is directly related to the release of HS-bound VEGF (Ostapoff et al., 2013). The VEGF family members have long been known for their positive effects in angiogenesis, vascular permeability and lymphangiogenesis. However, evidence of VEGF directly targeting tumour cells through autocrine signalling to promote angiogenesis-independent processes has emerged (Goel and Mercurio, 2013). For instance, studies on neoplastic epithelial cells have demonstrated that autocrine VEGF signalling promotes cellular proliferation (Zhang et al., 2014a, Lichtenberger et al., 2010). The expression of HPSE has also been shown to promote the expression of VEGF in a Src-dependent manner (Zetser et al., 2006). Furthermore, VEGF can influence the expression levels of HPSE, demonstrating a synergy between HPSE and VEGF in cancer (Luan et al., 2011).

EGF: EGFR-mediated signalling is a potent driver of the cell cycle, enhancing proliferation and is implicated in numerous cancer settings (Wee and Wang, 2017, Gao et al., 2016, Goel et al., 2016). The EGFR family includes human-EGFR2 (HER2), of which overexpression is observed in 25-30% of all breast cancers (Mendes et al., 2015).

HPSE activates EGFR signalling through HS cleavage (Wang et al., 2014). The expression of heparin-binding EGF-like growth factor with a high affinity to HS correlates to HPSE expression, suggesting a HPSE-driven regulation of EGF expression (Wirstlein et al., 2013). Of particular interest is the observation that in brain-metastatic breast cancer, EGF induces the nucleolar localisation of HPSE, resulting in DNA topoisomerase-I modulation and enhanced proliferation (Zhang et al., 2010). Furthermore, both enzymatically active and inactive HPSE were shown to phosphorylate EGFR and enhance proliferation, which correlated with head and neck cancer progression (Cohen-Kaplan et al., 2008a).

PDGF: PDGF has potent effects in promoting tumour proliferation (Pinto et al., 2014, Bruna et al., 2007). HPSE promotes the release of HS-bound PDGF. It has also been demonstrated that PDGF mediates cell-surface HSPG expression (Malavaki et al., 2013). This suggests a positive feedback mechanism of PDGF signalling in the TME.

TGF-β: TGF-β plays a complicated role in cancer cell proliferation, initially as a tumour suppressor in early tumorigenesis through inhibiting proliferation and promoting apoptosis, to then transitioning to a tumour promoter in later stages (Bierie and Moses, 2006, Neuzillet et al., 2015). TGF-β has been shown to interact with HS, which regulates its bioavailability (Lyon et al., 1997). HS has also been shown to play a key role in TGF-β-mediated signalling (Troilo et al., 2016). Although Batool *et al.* showed that overexpressing HPSE attenuated TGF-β signalling, others have demonstrated a positive correlation and even the upregulation of HPSE expression and invasive potential upon TGF-β treatment (Welch et al., 1990, Masola et al., 2014a, Batool et al., 2017).

Hh: Binding of Hh to Patched receptors and several other type-1 membrane proteins promotes pathway activation (Lee et al., 2016). Hh-mediated signalling has been shown to correlate directly with cell cycle regulation (Duman-Scheel et al., 2002). The binding of Hh to HS followed by its release upon HPSE activity leads to increased Hh signalling and an aggressive cancer phenotype (Datta et al., 2006).

1.12.2 Oncogenic signalling incorporating HPSE and positive feedback mechanisms

A correlation of expression between HPSE and a number of oncogenes exists, which promotes tumour growth. Cellular proliferation is driven by oncogenes such as the rat sarcoma viral oncogene homologue (Ras) and the myelocytomatosis oncogene (Myc) and *BRAF*, encoding the serine/threonine-protein kinase B-raf. Ras is a binary molecular switch, alternating between an active guanidine triphosphate-bound state and an inactive guanidine diphosphate-bound state and is a potent promoter of cell proliferation (Simanshu et al., 2017). A correlation between HPSE and Ras expression was

demonstrated in driving tumorigenesis in murine models of breast and skin cancer (Boyango et al., 2014). Myc is a transcription factor which coordinates a number of biological processes (Gabay et al., 2014). Although a relationship similar to that between Ras and HPSE has not been reported for Myc, human telomerase reverse transcriptase (hTERT) was shown to correlate with Myc and HPSE expression in gastric cancer (Tang et al., 2016). The expression of hTERT plays a pivotal role in maintaining telomere length, seen in 85-90% of cancers (Schwaederle et al., 2018, Ramlee et al., 2016). Expression of Myc driven by hTERT in turn activates further hTERT transcription and HPSE expression, leading to downstream tumour-promoting enzymatic activity (Tang et al., 2016). As previously mentioned, B-Raf kinase, the product of the mutant *BRAF* oncogene upregulates HPSE expression, by *HPSE* promoter activation (Rao et al., 2010). HPSE therefore plays an integral role in oncogenic signalling.

Disrupting negative-feedback mechanisms that attenuate proliferative signalling is vital in cancer progression (Hanahan and Weinberg, 2011). As previously highlighted, the signalling by cancer-promoting growth factors is not only enhanced by HPSE activity, but growth factors such as HGF, VEGF and TGF-β in turn promote the upregulation of HPSE (Hao et al., 2015, Luan et al., 2011, Welch et al., 1990). This maintains a constant positive feedback loop which drives both HPSE expression and its resultant downstream proliferative mechanisms. The phosphatase and tensin homolog (PTEN) is a potent tumour suppressor, de-phosphorylating phosphatidylinositol-(3,4,5)-trisphosphate and counteracting PI3K/Akt activity (Lee et al., 1999). Partial or complete PTEN inactivation is associated with a large proportion of cancers and is a well-documented phenomenon (Milella et al., 2015). The non-enzymatic activity of HPSE in stimulating the PI3K/Akt pathway was demonstrated in endothelial cells (Gingis-Velitski et al., 2004a). A later observation of integrin-dependent PI3K/Akt activation following the binding of HPSE to a cell surface receptor further highlighted the non-enzymatic activity of HPSE in promoting tumour signalling (Riaz et al., 2013). Additionally, the activation of the PI3K/Akt pathway by HGF signalling was shown to stimulate the downstream expression of HPSE, promoting gastric cancer metastasis (Hao et al., 2015). These data suggest that HPSE may play a critical role in bypassing the potent PTEN-mediated tumour suppression, by directly influencing the PI3K/Akt pathway which in turn may upregulate HPSE expression.

1.13 Evading growth suppressors

HPSE-driven mechanisms overlap in their promotion of proliferative signalling as well as evading growth suppressors. A key regulator of cancerous cell growth is the *TP53*-encoded p53 tumour suppressor (Kastenhuber and Lowe, 2017, Lane and Crawford, 1979). Although HPSE plays no role in causing *TP53* gene mutations, HPSE expression is regulated by wild-type p53 binding to the *HPSE* promoter (Baraz et al., 2006). *TP53* gene mutations lead to upregulated HPSE expression, which promotes a number of HPSE-mediated growth suppressor-evasion mechanisms.

As previously mentioned, PTEN plays a potent tumour-suppressive role. The ability of HPSE to activate PI3K/Akt in a non-enzymatic manner, essentially bypassing PTEN signalling, is evidence of its ability to counter tumour-suppressive mechanisms (Riaz et al., 2013). Another, although controversial tumour suppressor is STAT3 (Zhong et al., 1994). The oncogenic potential of STAT3 has been extensively studied, with emerging experimental and clinical data demonstrating its role as a tumour suppressor (Zhang and Lai, 2014). Its tumour-suppressive role is seemingly driven by a STAT3 splice variant, STAT3β (Zhang et al., 2016a). In a study of head and neck cancer, HPSE was shown to phosphorylate STAT3, through Src and EGFR phosphorylation, leading to a poor clinical outcome (Cohen-Kaplan et al., 2012).

TGF-β plays a dual role in cancer, both as a tumour suppressor and a promoter (Neuzillet et al., 2015). In support of its tumour-suppressive role, a number of studies have demonstrated that the lack of TGF-β signalling promoted tumour growth (Lu et al., 2006, Guasch et al., 2007, Lucas et al., 2004, Forrester et al., 2005). Furthermore, SMAD family member-4, a component of the TGF-β signalling pathway, was shown to inhibit HPSE activity, adding to the tumour-suppressive role of TGF-β (Qu et al., 2016). By regulating other signalling pathways that promote tumour growth, HPSE may contribute to effectively bypassing the tumour-suppressive role of TGF-β.

1.14 Resisting cell death

1.14.1 HPSE inhibits apoptosis

Apoptosis, or programmed cell death was discovered as a fundamental biological process in maintaining tissue homeostasis (Kerr et al., 1972). This occurs in response to a number of stimuli, resulting in the activation of caspase family proteins (Nagata, 2018). Briefly, apoptosis occurs via either an extrinsic pathway in response to extracellular ligands binding to cell-surface death receptors or via an intrinsic pathway, in response to stress. These pathways congregate at the effector caspases (caspase-3 or -7), resulting in cell death.

Unlike healthy cells, cancer cells are under constant stress brought about by processes such as genomic instability and hypoxia, but have evolved means to inactivate apoptosis that is normally triggered under such conditions. Numerous studies have demonstrated the well-characterised tumour-suppressive role of apoptosis (Evan et al., 1992, Lowe et al., 2004, Fernald and Kurokawa, 2013, Parsons et al., 2013). As previously mentioned, p53 is a potent tumour suppressor (Lane and Crawford, 1979). The activation of *TP53* upon cancer-related stress stimuli and its role in promoting apoptosis of cancer cells is a well-known phenomenon (Aubrey et al., 2018). Mutant p53, found in a large proportion of human cancers, is also a promoter of HPSE expression (Baraz et al., 2006).

The anti-apoptotic role of HPSE can be attributed largely to its ability to promote and sustain tumour growth via HS-mediated signalling (Knelson et al., 2014). HPSE-promoted release of FGF has been shown to inhibit apoptosis in breast cancer cells and prolong tumour survival (Cohen et al., 2006). Basic FGF is known to inhibit caspase-3 and in turn, downregulate apoptosis (Miho et al., 1999). Additionally, the non-enzymatic activity of HPSE in activating Akt was shown to inhibit oxidative-stress and growth factor starvation-induced apoptosis (Riaz et al., 2013). HPSE further facilitates the activation of Src (Zetser et al., 2006). Activated Src has been shown to suppress apoptosis by mechanisms such as the degradation of Bik, a BH3-only protein and through the phosphorylation of the apoptosis suppressor Ku70 (Lopez et al., 2012, Morii et al., 2017).

HPSE gene silencing showed that its inactivation induces apoptosis in pituitary tumour cells with an observed increase in sub-G1 events and poly (adenosine diphosphate-ribose) polymerase (PARP) cleavage (Rubinfeld et al., 2011). The drug-mediated inhibition of HPSE has also been demonstrated to promote apoptosis in cancer cells, further validating its anti-apoptotic role. Inhibition of HPSE with PG545, a HS-mimetic, promoted apoptosis in pancreatic cancer cells (Ostapoff et al., 2013). Treatment with PI-88, another HS-mimetic, of RIP1/Tag2 transgenic mice which exhibit a multi-step

process of islet cell carcinoma showed an increase in tumour apoptosis (Parangi et al., 1995, Joyce et al., 2005).

1.14.2 HPSE mediated autophagy

Autophagy is a critical, evolutionarily-conserved process for maintaining cellular homeostasis. The discovery of lysosomes by De Duve *et al.* and of autophagy-related proteins by Oshumi *et al.* were pivotal in elucidating its role (De Duve et al., 1955, Tsukada and Ohsumi, 1993). Mammalian autophagy is a well-characterised and reviewed process with both physiological and pathological roles (Dikic and Elazar, 2018, Yu et al., 2018). Briefly, cytoplasmic contents such as macromolecules and organelles are first collected in autophagosomes. These double-membraned vesicles eventually fuse with lysosomes, leading to the degradation and recycling of intracellular material, thus maintaining cellular homeostasis. The induction of autophagy was shown to inhibit tumorigenesis, suggesting a cytoprotective role (Liang et al., 1999). However, autophagy has also been shown to promote cancer cell survival under stressful conditions and lead to chemoresistance (Degenhardt et al., 2006, Pagotto et al., 2017, Takahashi et al., 2017). HPSE was observed to reside in lysosomes in a stable form, which raised the possibility of its involvement in autophagy (Goldshmidt et al., 2002). A critical regulator of autophagy is the mammalian target of rapamycin-1 (mTOR1) (Brown et al., 1994). HPSE expression was shown to reduce mTOR1 activity, evident by the decrease of phosphorylation levels of its substrate p70S6K, which promoted autophagy, enhancing tumour growth and chemoresistance (Shteingauz et al., 2015). Shteingauz *et al.* further demonstrated that the inhibition of autophagy and HPSE resulted in reduced tumour growth, suggesting a potential therapeutic strategy. Therefore, in a rather interesting twist, the intracellular activity of HPSE is suggested to mediate tumour cell survival through promoting autophagy, a mechanism designed to maintain cellular homeostasis.

1.14.3 HPSE and necrosis

For a significant period of time, apoptosis was considered the standard form of cell death. However, Schweichel and Merker first reported the presence of three morphologically distinct types of cell death, which included not only apoptosis, but also autophagy and necrosis (Schweichel and Merker, 1973). Unlike apoptosis, necrosis was long considered to be associated with pathological cell death, trauma or injury, with characteristic plasma membrane leakage, cell and organelle swelling and limited chromatin condensation. However, with recent studies demonstrating dedicated molecular pathways regulating necrosis, this view has been revised (Chan et al., 2015).

There is no clear evidence for the direct involvement of HPSE in tumour necrosis, but HPSE has been shown to regulate TNF, a key component of necrosis. TNF is one of the

most widely-studied cytokines in the TME, initially identified to induce 'haemorrhagic-necrosis' of tumours in an endotoxin-like manner (Carswell et al., 1975, O'Malley et al., 1962). However, subsequent studies revealed TNF superfamily members as a 'double-edged sword', with potent pro-tumorigenic activity (Waters et al., 2013, Knight et al., 2000, Popivanova et al., 2008, Moore et al., 1999, Aggarwal, 2003). TNF is a central player in tumour inflammation. Tumour-associated macrophages (TAMs) produce TNF-α in a HPSE-dependent manner, promoting inflammation and tumour growth (Gutter-Kapon et al., 2016). The role of HPSE in tumour-promoting inflammation will be discussed in section 1.19.

HPSE has been shown to regulate necrosis in several other disease settings. HPSE enhances TF activity and promotes coagulation in various diseases, including cancer (Nadir and Brenner, 2016). In a study of patients with diabetic foot necrosis, HPSE-driven post-surgical pro-coagulant activity predicted a successful clinical outcome, whereas a reduction of such predicted necrosis (Peled et al., 2016). In a study of avascular necrosis of bone (osteonecrosis), an increased level of HPSE was shown to promote destruction of the femur head (Peled et al., 2013).

1.15 Enabling replicative immortality

Cancer cells by definition, are immortal. Normal cell lineages are limited in their replicative capability by cellular senescence, a non-proliferative but viable state (Hernandez-Segura et al., 2018, Hayflick and Moorhead, 1961). The expression of a wide variety of oncogenes is demonstrated to cause oncogene-induced senescence (Serrano et al., 1997, Gorgoulis and Halazonetis, 2010). Crisis, a second anti-proliferative barrier leads to cell death (Campbell, 2012, Ishikawa, 1997). Telomeres at the ends of chromosomes play a pivotal role in regulating cellular replication and the expression of telomerase by cancers enables replicative immortality (Greider and Blackburn, 1987, Blackburn and Gall, 1978, Kim et al., 1994, Arndt and MacKenzie, 2016). Although HPSE has not been reported to upregulate telomerase expression, studies in gastric cancer has shown that hTERT, a catalytic subunit of human telomerase, enhanced invasion and metastasis through the c-Myc-mediated upregulation of HPSE (Tang et al., 2016).

FGF is a key growth factor in the inhibition of cellular senescence and the promotion of cancer (Turner and Grose, 2010, Wang and Becker, 1997, Huang et al., 2017). FGF is found sequestered in the ECM by HS and as previously described, tumour-induced HPSE expression was shown to regulate HS biosynthesis and promote FGF activity, leading to enhanced tumour growth (Escobar Galvis et al., 2007). HS has also been shown to play a key role in FGF signalling by increasing the radius of diffusion of FGF (Flaumenhaft et

al., 1990). Furthermore, HS fine-tunes the FGFR signalling pathway through variable sulfation, thereby overcoming cellular senescence (Jung et al., 2016b).

The interaction between cancer cells and the ECM is also key to maintaining immortality and overcoming growth-inhibitory signals. Integrins are a major cell-ECM adhesive molecule expressed by both healthy and cancerous cells, which enables cell-ECM communication (Seguin et al., 2015). CSCs, first described in acute myeloid leukaemia, are known to play a critical role in the initiation and the maintenance of tumours (Batlle and Clevers, 2017, Bonnet and Dick, 1997). Numerous studies have shown that integrins play a key role in the maintenance of CSCs (Seguin et al., 2015). Furthermore, HS was shown to promote cell-ECM adhesion by interacting with integrins (Soares et al., 2015). Integrin-mediated cellular adhesion via αVβ3 and α5β1 was shown to promote HPSE-induced Akt phosphorylation and the induction of the pro-survival PI3K/Akt pathway (Riaz et al., 2013). This intricate relationship between HPSE, HS and integrins ensures continuous tumour growth. HPSE, therefore plays a limited but important role in enabling replicative immortality and this warrants further investigation.

1.16 Inducing angiogenesis

1.16.1 Angiogenesis

Much like healthy tissues, tumours too require nutrients, oxygen and the removal of metabolic waste and carbon dioxide. This is achieved through tumour-associated neovasculature, the result of engaging an ‘angiogenic switch’, causing quiescent vasculature to sprout new vessels continuously (Hanahan and Folkman, 1996). In addition to sustaining growth of the primary tumour, angiogenesis promotes metastasis by providing a means of escape for metastatic cancer cells (Bielenberg and Zetter, 2015). A balance exists between pro and anti-angiogenic factors, which must be tipped in favour of tumour growth (Baeriswyl and Christofori, 2009). The concept of angiogenesis has been studied for centuries, since John Hunter coined the term in 1787 (Lenzi et al., 2016). At present, tumour angiogenesis and its regulation by the TME is a very well characterised hallmark of cancer (De Palma et al., 2017b).

In 1939, Ide *et al.* reported that tumours implanted *in vivo* recruited their own capillaries, forming the basis for the notion that angiogenesis was a key process in tumour growth (Ide et al., 1939). The early 1970s were a turning point in angiogenesis research with the discovery that solid tumour growth beyond a few millimetres in diameter was dependent on angiogenesis and that tumour cells appeared to stimulate endothelial cell proliferation with angiogenic factors, which suggested a strong therapeutic potential (Folkman, 1971, Folkman, 1990). The discovery and the cloning of VEGF by Ferrera *et al.*, the purification

of a tumour-derived angiogenic factor by Shing *et al.*, the isolation of FGF independently by Böhlen *et al.* and Gospodarowicz *et al.* along with several other key discoveries of angiogenic factors made in the late 20th century, added further validity to Folkman's findings (Ferrara and Henzel, 1989, Shing et al., 1985, Gospodarowicz et al., 1984, Ribatti et al., 2000). These discoveries culminated in the finding that the administration of angiostatin, an angiogenesis inhibitor, was capable of causing *in vivo* human tumour regression in mice (O'Reilly et al., 1996).

However, in contrast to the traditional model of tumour angiogenesis, it is now known that some tumours can resort to 'alternative vascularisation' mechanisms by acquiring its vasculature from pre-existing vessels, with no endothelial cell sprouting (Döme et al., 2007). Furthermore, tumour growth lacking morphological evidences of angiogenesis has been reported (Pezzella et al., 1997). These observations, along with several others contradicting Folkman's early descriptions of angiogenesis, have raised intriguing questions on the validity of this hallmark (Dvorak, 2015). However, the pivotal role of angiogenesis in tumour growth and metastasis cannot be underestimated.

1.16.2 HPSE and angiogenesis

As previously mentioned, VEGF is a prominent HSBP (Ferrara and Henzel, 1989, Park et al., 1993). VEGF-A is the major pro-angiogenic VEGF family member, which constitutes the prime focus of this hallmark (Simons et al., 2016). A second HSBP and promoter of angiogenesis is FGF (Huang et al., 2017, Goetz and Mohammadi, 2013). Indeed, numerous studies have demonstrated that FGF is key in tumours developing resistance to VEGF inhibition and that combined anti-VEGF and anti-FGF treatments may benefit cancer patients compared to a single mode of therapy (Lieu et al., 2011). The enzymatic activity of HPSE has been shown to promote angiogenesis via activation of the VEGF and FGF signalling pathways through HS cleavage and the liberation of growth factors (Knelson et al., 2014). Numerous studies using pre-clinical disease models and patient tumour samples have demonstrated the key role of HPSE in activating the angiogenic switch and promoting this hallmark as highlighted below.

A strong correlation between expression of HPSE mRNA and microvessel density was observed in tumour samples of endometrial cancer patients, which also correlated with highly aggressive tumours (Watanabe et al., 2003b). HPSE-overexpressing MCF-7 human breast cancer cells showed increased angiogenesis *in vivo* and correlated with large tumour size (Cohen et al., 2006). Histological analysis of human colorectal cancers showed a positive correlation between HPSE expression and tumour angiogenesis (Sato et al., 2004). Endothelial cells exhibit an invasive phenotype at the onset of angiogenesis, as well as atherosclerosis and wound healing, which was shown to be mediated by HPSE

(Godder et al., 1991). HPSE expression in myeloma cells promotes syndecan-1 shedding, which promoted angiogenesis and endothelial invasion via the release of angiogenic factors (Purushothaman et al., 2010). Interestingly, Akt phosphorylation in endothelial cells was mediated by HPSE in a non-enzymatic manner which resulted in endothelial cell migration and invasion (Gingis-Velitski et al., 2004a). The small interfering ribonucleic acid (siRNA)-mediated silencing of HPSE expression resulted in the reduction of angiogenesis in an *in vivo* model of lymphoma, which prolonged survival (Edovitsky et al., 2004). A second study silencing HPSE expression in the MDA-MB-435 human breast cancer cell line demonstrated a similar effect on angiogenesis (Zhang et al., 2007). The combined effects of HPSE and cyclooxygenase-2 (COX-2) in promoting tumour angiogenesis was demonstrated in human oesophageal cancer patients, with an increased HPSE expression leading to poor survival (Okawa et al., 2005). In addition to liberating HS-bound VEGF, HPSE was shown to induce the expression of VEGF in correlation with p38 phosphorylation and Src activation, which promoted angiogenesis *in vivo* in an MDA-MB-435 xenograft model (Zetser et al., 2006). This suggests that the expression of HPSE correlates with *VEGF* gene regulation.

Several other studies have demonstrated that the inhibition of HPSE leads to the inhibition of angiogenesis, enhancing survival. Treatment with PI-88, a potent small molecule inhibitor of HPSE, inhibited angiogenesis *in vitro* and *in vivo* in a model of rat adenocarcinoma, resulting in impaired tumour growth (Parish et al., 1999). The PG500 series of HS mimetics were developed as potential HPSE inhibitors for clinical use (Dredge et al., 2010). The lead drug candidate, PG545 was shown to bind VEGF and FGF and effectively reduce angiogenesis *in vitro* and affect *in vivo* tumour development. Further pre-clinical studies with PG545 demonstrated its anti-angiogenic effects *in vivo*, resulting in increased survival (Hammond et al., 2012, Dredge et al., 2011). In addition, a low molecular weight heparin derivative was also shown to inhibit tumour angiogenesis *in vivo*, as well as λ-carrageenan, a HS-mimetic (Debergh et al., 2010, Poupard et al., 2017a). The use of HPSE inhibitors in the clinic will be discussed later in this chapter.

1.16.3 HPSE and immune cell-driven angiogenesis

The infiltration of solid tumours by immune cells is a well characterised phenomenon and has been extensively reviewed (Barnes and Amir, 2017b). Infiltrating immune cells could at times be detrimental to the tumour, but in many cases can promote its development. Numerous studies have revealed the pro-angiogenic effects of tumour-associated immune cells such as macrophages, neutrophils, myeloid-derived suppressor cells (MDSCs), mast cells, etc. (Bingle et al., 2006, Bruno et al., 2014, Chen et al., 2011, Qian and Pollard, 2010). The expression of HPSE and its role in activating and regulating the function of a

number of immune cell populations has been demonstrated (Gutter-Kapon et al., 2016, Naparstek et al., 1984, Matzner et al., 1985, Fridman et al., 1987, Vlodavsky et al., 1992, Putz et al., 2017). This raises the possibility that tumour-associated immune cells may enhance angiogenesis by virtue of their HPSE expression capacity and HPSE-mediated activation.

1.16.4 HPSE and hypoxia

Tumours rely on pre-existing vasculature and neovasculature for oxygen supply. However, due to the rapid and disorganised growth of solid tumours, the tumour generally outgrows its vasculature, resulting in hypoxia, seen mainly in its core (Goldmann, 1908). The chaotic architecture and leakiness of the tumour vasculature further contribute to hypoxia and is a well-characterised phenomenon in solid tumours (Baish and Jain, 2000, Hashizume et al., 2000). Of additional interest is the observation that abnormal solid tumour vasculature not only leads to hypoxia, but also contribute to metastasis (Cooke et al., 2012, Li et al., 2016c). Solid tumours exhibit a widely heterogeneous hypoxia pattern, with regions of variable oxygenation as well as pH levels (Helmlinger et al., 1997). The phenomenon of tumour hypoxia, the various adaptations by solid tumours to overcome oxygen starvation and the implications of hypoxia to patient survival are well-characterised (Eales et al., 2016, Wigerup et al., 2016). Cells respond to hypoxia by expressing hypoxia-inducible factors (HIFs), which promote survival (Semenza, 2012, Semenza et al., 1997). On this account, HIFs have generated much interest as cancer therapeutic targets (Semenza, 2012, Rey et al., 2017, Semenza, 2003, Semenza, 2010).

The relationship between HPSE and hypoxia is not only limited to cancer. Hypoxic conditions in postnatal development were shown to upregulate HPSE in the rat brain, resulting in hypoxia-induced neovascularisation (Navarro et al., 2008). HPSE has also been shown to be highly expressed as an adaptive mechanism in the *Spalax* mole rat, which is exposed to hypoxic stress in its underground habitat (Nasser et al., 2005). In a disease model of retinopathy of prematurity, HPSE was shown to be upregulated in response to hypoxia, leading to disease-promoting neovascularisation (Hu et al., 2012). Cancer cells exposed to hypoxic conditions were shown to upregulate HPSE expression in an NFκB-dependent manner (Wu et al., 2010b). COX-2 was shown to be a key component in HPSE-mediated HIF-1α expression, leading to increased tumour angiogenesis (Naomoto et al., 2007). Hypoxia was further shown to not only promote angiogenesis, but also to promote invasion in a HPSE-dependent manner (He et al., 2004b). HPSE was also shown to play a role in radiation resistance by upregulating the HIF-1 pathway with correlated upregulation of VEGF and FGF (Li et al., 2017a).

1.16.5 HPSE and lymphangiogenesis

Angiogenesis is a key hallmark in tumour progression; however, lymphangiogenesis also plays an important role. The lymphatic system was originally thought to play a passive role in metastasis. At present, lymphangiogenesis and the dynamic role of tumour-associated lymphatic vessels in the tumour environment and in the metastatic cascade is well-demonstrated (Stacker et al., 2014). Lymphangiogenic factors such as FGF-2, VEGF-C and VEGF-D enhance metastatic spread of tumours and have generated much clinical interest (Stacker et al., 2001, Skobe et al., 2001, Cao et al., 2012). The binding of FGF to HS has been discussed previously in this chapter. The heparin and HS-binding properties of VEGF-C and VEGF-D have been demonstrated, suggesting that the enzymatic activity of HPSE in the TME facilitates their release and subsequent activity (Yin et al., 2011, Harris et al., 2013).

The relationship between HPSE expression, lymphangiogenesis and overall tumour grade has been demonstrated in a number of studies. In a pre-clinical model of inflammation in rats, HPSE expression by neutrophils was shown to drive lymphangiogenesis via the enhanced bioavailability of VEGF-A (Tan et al., 2013). Furthermore, in clinical studies of lung, pancreatic and head and neck cancer patients, HPSE expression upregulated VEGF-C signalling and was shown to promote invasion (Hunter et al., 2013, Cohen-Kaplan et al., 2008b, Zhang et al., 2009). A relationship between COX-2 and lymphangiogenesis has also been demonstrated in a study of breast cancer patients, whereby COX-2 expression correlated with that of VEGF-C, promoting lymph node metastasis (Zhang et al., 2008). In a later study of cervical cancer patients, this relationship was more closely examined and it was demonstrated that HPSE promoted the expression of COX-2, leading to VEGF-C signalling (Zeng et al., 2014).

1.17 Activating invasion and metastasis

Undoubtedly, the most formidable hallmark of a cancer is its ability to activate invasion and metastasis, which is responsible for the majority of cancer deaths (Steeg, 2016). Owing to its clinical significance, this important hallmark has been studied in much detail. Metastasis is an extremely complex, multi-step, non-random process resulting in the dissemination of cancer cells from its origin to distant secondary sites (Lambert et al., 2017). Initially considered a late event in tumour progression, it is now evident that invasion and metastasis can occur relatively early (Linde et al., 2018). The 'seed and soil hypothesis' proposed by Stephen Paget provided an early insight into metastasis (Paget, 1889). This revealed a distinct relationship between metastatic tumour cells (seeds) and the metastatic microenvironment (soil) and described metastasis as a targeted process. Current treatment options face numerous challenges when targeting metastatic disease, which poses a major clinical challenge (Ratajczak et al., 2013).

For the purpose of this review, the metastasis of epithelial carcinomas will be considered. Cancer cells disseminate from the primary tumour by gaining invasive capabilities. This is made possible by the adoption of mesenchymal features, in a process known as 'epithelial-mesenchymal transition (EMT)' (Hay, 1995). This is driven by key transcription factors such as Snail, Slug, Zeb1 and Twist, leading to cytoskeletal reorganisation, loss of cell-cell junctions, loss of apical-basal polarity with the gain of a front-rear polarity, changes in cell shape and gene expression and acquiring the ability to degrade ECM components (Lamouille et al., 2014). Recent data suggest a 'partial-EMT' phenotype in metastatic cells, rather than a fully mesenchymal state which may enhance metastatic colonisation (George et al., 2017, Jolly et al., 2015). Several studies have shown that HPSE is able to induce EMT in disease settings such as myeloma and renal injury (Li et al., 2016a, Masola et al., 2016). Additionally, the inhibition of HPSE has been shown to block mesenchymal features both *in vitro* and *in vivo* (Li et al., 2016a). Furthermore, the sulodexide-mediated inhibition of HPSE controls EMT-driven tubular fibrosis in a diabetic nephropathy setting (Masola et al., 2012b). A key regulator of EMT is FGF, which is also a HSBP, whose signalling pathway is activated by HPSE, leading to the promotion of EMT (Strutz et al., 2002, Escobar Galvis et al., 2007). Of note is that the interplay between HPSE and syndecan-1 can induce EMT in renal tubular cells (Masola et al., 2012a). TGF-β is also a potent regulator of EMT, shown to promote renal fibrosis and cancer (Yang and Liu, 2001, Pang et al., 2015). HPSE is a demonstrated key player in TGF-β-mediated EMT, further solidifying its role in promoting this vital metastatic phenotype (Masola et al., 2014b).

Tumour cell invasion of the surrounding tissue generally occurs via 'collective-cell migration' involving a cluster of cells maintaining cell-cell adhesion but can also occur as individual cells or as a strand of single cells in 'multicellular streaming' (Friedl et al., 2012). A key rate-limiting step in the multi-step metastatic cascade is the migration of tumour cells through the ECM, which acts as a physical barrier. Indeed, the degradation of HS has been shown to be a key component in tumour cell invasion (Vlodavsky et al., 1992). A number of proteases such as members of matrix metalloproteinase (MMP), serine, aspartic and cysteine protease families are key in invasion-promoting ECM disassembly and their role in cancer promotion has been known for decades (Duffy, 1992, Duffy, 1996, Ludwig, 2005). The collective expression of ECM-degrading proteases and HPSE at the invasive tumour front enables invading cells to effectively navigate through the ECM (Bar-Ner et al., 1986, Bar-Ner et al., 1985). Furthermore, the ability of HPSE to stimulate the expression of MMP-9 through extracellular signal-regulated kinase-phosphorylation in a myeloma setting demonstrated its regulatory role in promoting invasion (Purushothaman et al., 2008). A number of clinical studies have demonstrated that the expression of HPSE at the tumour invasion front leads to poor patient prognosis, indicating a key role of HPSE in overcoming this initial rate-limiting step of the metastatic cascade (Takaoka et al., 2003, Gonzalez-Alva et al., 2010b, Ohkawa et al., 2004b, Beckhove et al., 2005). As mentioned in the previous section, tumours often experience hypoxic conditions. Recent studies have demonstrated that tumour hypoxia promotes invasion of tumour cells via a number of mechanisms such as macrophage-driven signalling, acquisition of EMT features, increasing lysyl oxidase expression, enhanced Notch and MAPK activation and the activation of the *met* proto-oncogene (Pennacchietti et al., 2003, Asnaghi et al., 2014, Azab et al., 2012, Huber et al., 2016, Kirschmann et al., 2002, Erler and Giaccia, 2006).

The expression of HPSE is not only confined to tumour cells, but to other cell types in the TME as well. In an *in vivo* model of lymphoma, the TME was shown to contribute to HPSE activity of tumour xenografts, suggesting that host cells in the TME played an active role in HPSE expression of the primary tumour (Weissmann et al., 2016). Neutralisation of HPSE activity of the TME affected primary tumour growth, indicating a bi-directional relationship between the tumour and the host with regards to HPSE expression. Furthermore, as previously mentioned, tumour-associated immune cells have been shown to express HPSE (Gutter-Kapon et al., 2016, Naparstek et al., 1984, Matzner et al., 1985, Fridman et al., 1987, Vlodavsky et al., 1992, Putz et al., 2017). It can be speculated therefore, that HPSE contributed by the host-derived cells of the TME plays a critical role in the initial invasive stage of metastasis. This will be discussed in greater detail in section 1.23.

Invading tumour cells intravasate into the circulatory system either directly (hematogenous intravasation) or via the lymphatic network (lymphatic intravasation), becoming circulating tumour cells (CTCs) (Wong and Hynes, 2006). Hematogenous intravasation involves the binding of tumour cells to endothelial cells of blood vessels which then pass through cell junctions to enter the circulation. This can be either an active or a passive process, depending on the nature and the level of tumour-associated vasculature. Lymphatic intravasation results in the invading tumour cells eventually entering the circulation through the major thoracic duct (Chiang et al., 2016). Contrary to the widely-accepted model of metastasis, however, intra-tumoural intravasation can occur independently of stromal invasion, bypassing a crucial step of the metastatic cascade (Deryugina and Kiosses, 2017). The process of intravasation is of significant interest as a rate-limiting step of the metastatic cascade. Invasion through the ECM and in particular, the BM, a more complex form of the ECM, are critical in intravasation with tumour cells employing various strategies to overcome these physical barriers (Chiang et al., 2016, Kelley et al., 2014). The role of proteases, in particular MMPs, in tumour invasion and intravasation has been demonstrated (Kim et al., 1998, Quigley and Armstrong, 1998). HPSE, with its aforementioned roles in stimulating angiogenesis and lymphangiogenesis, therefore actively participating in creating a vessel network for metastatic tumour cells and in degrading the ECM and BM, facilitating invasion followed by intravasation, is a key player in this step of the metastatic cascade.

CTCs are valuable prognostic markers, which have garnered clinical interest (Bidard et al., 2014, Krebs et al., 2014). Once in circulation, CTCs face numerous challenges such as oxidative stress, shear force and immune destruction, resulting in approximately 0.01% of CTCs capable of forming metastases (Krebs et al., 2010). To overcome some of these challenges, CTCs are coated with platelets, mediated by TF expressed on the CTC surface (Jiang et al., 2017). Platelets ‘cloak’ CTCs and form a physical barrier, which protects against shear force and masks CTCs against immune detection. The secretion of PDGF and TGF-β by platelets inhibit NK cell activity and sustain EMT pathways in CTCs (Kopp et al., 2009, Labelle et al., 2011, Palumbo et al., 2005). CTCs can also interact with neutrophils which promote tumour cell survival and extravasation (Spiegel et al., 2016). Neutrophils impart immunosuppressive functions by suppressing NK cell activity, as well as secrete MMPs, that enhance extravasation. The formation of neutrophil extracellular DNA traps designed to immobilise pathogens, trap and collect CTCs, promoting intraluminal survival (Park et al., 2016). The therapeutic potential of targeting of adhesion molecules that maintain CTC clusters has been addressed to prevent metastatic colonisation (Li and King, 2012). In addition to its enzymatic means of promoting aspects of the metastatic cascade, HPSE has been shown to promote cellular adhesion by non-

enzymatic means, with significant implications in CTC cluster formation (Goldshmidt et al., 2003). HPSE in platelets has been shown to enhance their adhesive capacity, promoting thrombogenicity, which in turn supports CTC clusters (Cui et al., 2016). The expression of HPSE in CTCs induces focal adhesion kinase (FAK) and intercellular adhesion molecule-1 (ICAM-1)-mediated adhesion and enhanced metastasis in human breast cancer cells and was also shown to affect the adhesive properties of human glioma cells (Wei et al., 2018a, Zetser et al., 2003). The brain-metastatic potential of breast cancer CTCs isolated from patients was shown to be related to HPSE expression, a key component of the 'metastatic signature' of these cells (Zhang et al., 2013a). This HPSE-mediated adhesiveness not only promotes CTC survival en route to distant metastatic sites, but also promotes extravasation and the eventual formation of the pre-metastatic niche, as will be discussed further.

Extravasation occurs with CTCs breaching the capillary wall at a distant site to form metastatic colonies, which concludes the 'metastatic cascade' (Massague and Obenauf, 2016). Despite extensive studies, the organ-specific nature of metastasis remains poorly defined. In contrast to Paget's seed and soil hypothesis, Ewing suggested metastatic colonisation to be based solely on the dynamics of circulation (Ewing, 1928). However, sufficient evidence now supports metastasis as an organ-specific event (Fidler and Nicolson, 1976). Metastatic cells undergo trans-endothelial migration (TEM) at the extravasation site by the secretion of proteins that aid in disrupting vascular integrity, such as angiopoietin-like-4 (ANGPTL4), VEGF and MMPs (Reymond et al., 2013). HPSE too, plays a key role in this process. As previously mentioned, the ability of HPSE to mediate cellular adhesion would aid in the attachment of CTCs to endothelial cells at the sites of extravasation (Lever et al., 2014, Goldshmidt et al., 2003). The sub-endothelial ECM degradation by HPSE has been shown to promote extravasation of immune cells such as mast cells, macrophages, neutrophils and CAR-T cells as well as tumour cells (Vlodavsky et al., 1992, Bashkin et al., 1990, Komatsu et al., 2008a, Parish et al., 1998, Sasaki et al., 2004).

CTC-associated platelets secrete nucleotides, which together with tumour cell-secreted chemokine (C-C motif) ligand-2 (CCL2) activate endothelial cells, rendering capillary walls permeable and promoting TEM (Schumacher et al., 2013, Wolf et al., 2012). CCL2 recruits inflammatory monocytes which may differentiate into metastasis-associated macrophages and promote metastatic seeding (Qian et al., 2011). As previously mentioned, HPSE has been shown to promote the activity of TAMs, which may also aid metastatic seeding (Gutter-Kapon et al., 2016). Contrary to the traditional metastatic cascade model, metastatic outgrowths can sometimes occur intraluminally, without the

need for extravasation (Al-Mehdi et al., 2000). Furthermore, a mechanism whereby tumour cells induce programmed necrosis (necroptosis) in endothelial cells to promote extravasation has been recently described (Strilic et al., 2016).

The malignant progression of a tumour concludes with metastatic colonisation. This depends on the receptive tissue microenvironment which can be prepared by the primary tumour, forming the 'pre-metastatic niche (PMN)' (Kaplan et al., 2005). The key contributing factors to PMN formation are tumour-secreted components, the local stromal microenvironment and tumour-mobilised bone marrow derived cells (Liu and Cao, 2016). Furthermore, infection, effects of surgery and ageing can also promote PMN formation. This creates a microenvironment that is receptive for colonisation by CTCs with characteristic features of immunosuppression, inflammation, angiogenesis, organotropism, lymphangiogenesis and reprogramming (Peinado et al., 2017). Tumour-derived exosomes have been implicated in intracellular communication in the TME as well as the pre-metastatic niche formation in a number of cancer settings (Costa-Silva et al., 2015, Peinado et al., 2012, Maia et al., 2018). Studies have shown that HPSE activates the syndecan-syntenin-ALIX exosome pathway and that it is a key regulator of tumour-derived exosomes (Roucourt et al., 2015, David and Zimmermann, 2016b, Thompson et al., 2013). Interestingly, in a study of myeloma, it was demonstrated that chemotherapy stimulated the release of exosomes containing high HPSE levels that promoted cancer progression, indicating a role of HPSE in mediating resistance to cancer therapy (Bandari et al., 2018). The formation of the pre-metastatic niche involves significant remodelling of the existing ECM, to which HPSE carried by tumour derived exosomes and produced by metastatic cells would make an important contribution (Gomes et al., 2013).

Metastatic outgrowths are highly reliant on the stromal microenvironment, similar to primary tumours (Hanahan and Coussens, 2012). Recently-arrived tumour cells may undergo dormancy, either failing to encounter a supportive stroma or experiencing suppressive cues (Sosa et al., 2014, Sosa et al., 2011). Dormant tumour cells reside in specialised niches and may acquire stem cell traits, which are a prerequisite for eventual colonisation (Plaks et al., 2015). These metastatic stem cells will initiate colonisation following a latent period, based upon the activation of signalling pathways, the tumour-initiating ability of metastatic cells and the presence of a supportive stromal microenvironment (Aguirre-Ghiso et al., 2004, Oskarsson et al., 2014, Lambert et al., 2017). The role of HPSE in the active modulation of the ECM of distant metastatic sites in order to create a supportive microenvironment is vital in colonisation, as discussed in numerous previously-mentioned studies where tumours overexpressing HPSE showed

enhanced metastasis. HPSE, through both enzymatic and non-enzymatic functions, is a key regulator of each step of the metastatic cascade.

Following the well-received definition of the six hallmarks of cancer in 2000, two enabling characteristics, namely 'genome instability and mutation' and 'tumour-promoting inflammation' as well as two emerging hallmarks of 'reprogramming energy metabolism' and 'evading immune destruction' were described (Hanahan and Weinberg, 2000, Hanahan and Weinberg, 2011). The contribution of HPSE to these emerging hallmarks of cancer will now be discussed.

1.18 Genome instability and mutation: an enabling characteristic

Genomic instability is an inherent cause of most cancers (Hanahan and Weinberg, 2011). The *TP53* gene plays a major role as the 'guardian of the genome' and its mutations are found in a majority of human malignancies (Lane, 1992). As described previously, mutant p53 is a potent mediator of HPSE expression (Baraz et al., 2006). The existence of multiple 'caretaker' and 'guardian' systems that maintain genomic stability have been described, with their defects promoting tumour development (Roth and Gellert, 2000, Kinzler and Vogelstein, 1997). An aberrant ECM has also been shown to promote genomic instability and compromise these tumour-preventative pathways.

The expression of MMPs correlates with malignant progression of nearly every cancer type. It is now evident that the role of MMPs in cancer is quite complex and not only limited to ECM remodelling but also extends to causing tumour-initiating genetic alterations (Radisky and Bissell, 2006, Xie et al., 2017). For instance, the stromal expression of stromelysin-1 was shown to promote malignant changes in transgenic mouse mammary glands in conjunction with the upregulation of MMP-3 (Sternlicht et al., 1999). MMP-3 was shown to induce the expression of Ras-related C3 botulinum toxin substrate-1, causing the increasing in reactive oxygen species (ROS), which in turn stimulated the Snail transcription factor expression, promoted EMT, caused oxidative DNA damage and led to genomic instability and malignant transformation of mouse mammary epithelial cells (Radisky et al., 2005). A similar ROS-induced tumorigenic function was suggested for MMP-9 in a mouse intestinal cancer model (Sinnamon et al., 2008). The overexpression of membrane type-1 MMP was shown to promote chromosomal instability, conferring tumorigenicity on normal cells (Golubkov et al., 2005, Golubkov et al., 2006). The expression of HPSE has been demonstrated to directly correlate with that of MMPs and indeed was shown to directly stimulate MMP-9 expression (Tang et al., 2014a, Chen et al., 2012, Purushothaman et al., 2008). By being a master regulator of MMPs, HPSE may play an indirect but critical role in achieving genomic instability through aberrant MMP expression.

As previously mentioned, HPSE bypasses the tumour-suppressive roles of several genes, such as *PTEN*, *STAT3* and *TGF-β* (Riaz et al., 2013, Cohen-Kaplan et al., 2012, Masola et al., 2014a). Although this does not translate to HPSE directly compromising genome integrity, it can be argued that bypassing crucial protective roles of such genes amounts to an indirect promotion of genetic instability. HPSE has been shown to localise to the nucleus, where it affects gene expression (Schubert et al., 2004b). This is thought to occur by passive transport, where HPSE affects gene expression through nuclear-HS cleavage and the release of proteins such as FGF and topoisomerase-1 (Kobayashi et al., 2006). Translocation of HPSE to the nucleus has been shown to promote differentiation in human and mouse cancer cell lines (Nobuhisa et al., 2005b, Nobuhisa et al., 2007). In a study of oesophageal squamous cell carcinoma patients, nuclear HPSE was shown to promote differentiation, but not proliferation (Ohkawa et al., 2004b). However, in a study of head and neck squamous cell carcinoma patients, the nuclear localisation of HPSE was shown to indicate a favourable clinical outcome, in contrast to cytoplasmic localisation (Doweck et al., 2006).

1.19 Tumour-promoting inflammation: an enabling characteristic

The phenomenon of tumour-infiltrating immune cells was briefly discussed earlier. Virchow first noticed leukocyte infiltrates within tumours and described a link between inflammation and tumour growth (Virchow, 1881). This is now a well-characterised phenomenon, with cancer-promoting inflammation described as the ‘fuel that feeds the flames’, emphasising its critical role (Balkwill and Mantovani, 2001, Crusz and Balkwill, 2015). A variety of immune cells have been shown to be intimately involved with the TME, promoting tumour progression (Barnes and Amir, 2017b, Qian and Pollard, 2010, Qian et al., 2011, Gajewski et al., 2013). On account of the similarities between the tumour stroma and the inflammatory conditions in wounds, tumours have been described as ‘wounds that do not heal’ (Dvorak, 1986). Additionally, infections have been suggested to be responsible for over 15% of malignancies, with inflammation playing a major role in infection-mediated cancer development (Elinav et al., 2013, Kuper et al., 2000). Although some infiltrating immune cells function in eliminating tumours, certain others promote tumour growth, resulting in a poor clinical outcome. This will be discussed in detail throughout this section.

1.19.1 HS/HPSE mediated immune cell migration and activation

Leukocyte migration into tissues is a well-characterised, multi-step process, which is aided by HS and HPSE (Nourshargh and Alon, 2014, Farrugia et al., 2018, Parish, 2006). Leukocytes first establish adhesive interactions with endothelial cells, leading to arrest, adhesion strengthening, crawling and the migration of cells through the vessel wall and into sites of inflammation. This process is significantly affected by the availability of

chemokines and the establishment of a chemokine gradient (Sokol and Luster, 2015, Lopez-Cotarelo et al., 2017). HS has also been shown to mediate cellular adhesion via cell-surface molecules such as integrin and selectin, in both physiological and pathological conditions (Cole et al., 1986, Lim et al., 2015, Ma and Geng, 2000, Stanley et al., 1995). The adhesion of leukocytes to the endothelial wall is thus facilitated by HS, leading to cell arrest and the initiation of infiltration (Koenig et al., 1998, Giuffrè et al., 1997). A number of pro-inflammatory chemokines bind to HS, whose activity is thus regulated (Lortat-Jacob et al., 2002, Knelson et al., 2014). HS-mediated chemokine presentation plays a critical role in leukocyte recruitment, as demonstrated in an inducible mouse model deficient for exostoses-1, a key mediator of HS synthesis (Bao et al., 2010). The enzymatic activity of HPSE enhances the liberation of HS-bound chemokines, facilitating the formation of a chemokine gradient and stimulating the recruitment of leukocytes (Zhang et al., 2014b). HPSE-cleaved HS fragments were capable of stimulating the release of pro-inflammatory cytokines such as IL-1β, IL-6, IL-8, IL-10 and TNF through the toll-like receptor (TLR)-4 pathway in human peripheral blood mononuclear cells and the release of IL-6, monocyte chemoattractant protein-1 and TNF in mouse splenocytes (Goodall et al., 2014). Fragmented HS has also been shown to activate DCs through TLR-4 stimulation, mediating an inflammatory response (Johnson et al., 2002).

The activity of HPSE in promoting the migration of leukocytes was described even prior to the cloning of the enzyme (Naparstek et al., 1984, Vlodavsky et al., 1992, Matzner et al., 1985). This observation, coupled with that of HPSE-inhibiting substances such as heparin and HS-mimetics being capable of eliciting anti-inflammatory effects, further verified the role of HPSE in a variety of inflammatory disorders (Khamaysi et al., 2017a, Parish et al., 1998, Hershkoviz et al., 1995, Morris et al., 2015). HPSE has been shown to affect several types of innate immune cells such as neutrophils, macrophages, DCs and mast cells that mediate both acute and chronic inflammatory responses (Benhamron et al., 2012, Poon et al., 2014, Schmidt et al., 2012, Wang et al., 2011, Secchi et al., 2017a, Lerner et al., 2011).

Although it was long-assumed that immune cells were the sole source of HPSE in inflammatory settings, numerous studies have demonstrated that epithelial cells also contribute to HPSE activity in conditions such as delayed-type hypersensitivity, ulcerative colitis, Crohn's disease and acute lung injury following sepsis (Schmidt et al., 2012, Waterman et al., 2007, Lerner et al., 2011, Edovitsky et al., 2006). In such conditions, HPSE was shown to be released upon the presence of inflammatory cytokines (Edovitsky et al., 2006, Lerner et al., 2011, Schmidt et al., 2012). Furthermore, the nuclear localisation of HPSE was shown to induce endothelial cell gene expression and promote inflammation

(Wang et al., 2012a). Nuclear HPSE was also shown to modify histone methylation patterns and promote an inflammatory T-cell phenotype (He et al., 2012).

1.19.2 HPSE in acute and chronic inflammation

HPSE has been implicated in acute inflammation. Neutrophils are the major mediators of acute inflammation and related tissue injury (Weiss, 1989). In contrast to this traditional view, recent studies have shed light on the role of neutrophils in mediating chronic inflammation as well (Soehnlein et al., 2017). Cerulein-induced expression of HPSE expression has been shown to increase pancreatic cytokine (TNF-α, IL-6, etc) and signalling molecules (i.e. phospho-STAT3) activity, along with enhanced pancreas oedema and inflammation marked by neutrophil infiltration, which ultimately led to acute pancreatitis (Khamaysi et al., 2017a). In addition, the sepsis-induced upregulation of HPSE within the pulmonary microvasculature leads to degradation of the endothelial glycocalyx, forming a HS-mediated chemotactic gradient, which recruits neutrophils and promotes lung tissue injury (Schmidt et al., 2012).

HPSE plays a role in chronic inflammation as well. HPSE expression was observed in the colon of irritable bowel syndrome patients during both acute and chronic disease phases (Lerner et al., 2011, Waterman et al., 2007). Interestingly, the colonic epithelial cells were shown to be a major contributor of HPSE activity (Waterman et al., 2007). These interacted with macrophages in a HPSE-mediated manner to maintain a chronic inflammatory condition, which aided the formation of a tumour-promoting microenvironment with NF-κB signalling and induction of STAT3 expression (Lerner et al., 2011). HPSE was shown to generate a vicious cycle which promoted colitis and eventual colon cancer development by stimulating macrophages, which induced the production and activation of epithelial-HPSE via TNF-α and cathepsin-L. In a mouse model of allergic pulmonary cell recruitment, the lack of HPSE expression was shown to reduce eosinophil recruitment with no effect on neutrophils, resulting in a reduced allergen-induced bronchial hyper-responsiveness (Morris et al., 2015). The same study demonstrated that lung specimens of patients with varying severity of chronic obstructive pulmonary disease showed an increase in HPSE expression. HPSE expression was also shown to promote macrophage activation, leading to TNF-α production in macrophages as well as in renal tissue and to enhance chronic inflammation associated with diabetic nephropathy (Goldberg et al., 2014). In an interesting contrast, however, overexpression of HPSE was shown to lead to aberrant neutrophil recruitment due to the HS-mediated chemokine gradient being disrupted on account of the enzymatic activity of HPSE (Massena et al., 2010).

1.19.3 HPSE in cancer-promoting inflammation

Well-characterised cases of inflammation-driven cancers include chronic gastritis developing to intestinal-type gastric carcinoma, progression of chronic hepatitis-C to hepatocellular carcinoma (HCC), pancreatitis advancing to pancreatic adenocarcinoma, progression of Barrett's oesophagus to adenocarcinoma and progression of colitis to colorectal cancer (Fitzgerald et al., 2002, Gupta et al., 2007, Guerra et al., 2011, Lowenfels et al., 1993, Chiba et al., 2012, Picardo et al., 2012). Interestingly, HPSE has been strongly implicated in the malignancy of each of these conditions. HPSE expression was shown to be activated in the early stages of initiation and progression of Barrett's oesophagus to oesophageal carcinoma (Brun et al., 2009). The progression from normal to Barrett's epithelium and then onwards to low and high-grade carcinoma and finally, adenocarcinoma, was associated with the gradual increase in HPSE activity. Patients with hepatitis-C-related HCC showed a higher level of HPSE expression, which correlated with tumour angiogenesis and invasion (El-Assal et al., 2001). In a clinical study, patient samples of chronic pancreatitis showed a high expression of HPSE, which increased further in cases of pancreatic cancer, with pancreatic cancer patients with high HPSE levels exhibiting poor post-operative survival (Koliopanos et al., 2001). Mice overexpressing HPSE showed accelerated progression of colitis to colonic tumours, with activated macrophages shown to induce HPSE expression in the colonic epithelial cells, promoting inflammation and cancer progression (Lerner et al., 2011). These findings thus suggest a strong correlation between HPSE expression, inflammation and cancer progression.

A large proportion of tumour-infiltrating immune cells are TAMs, which are key promoters of inflammation and contribute strongly to cancer progression (Aras and Zaidi, 2017, Noy and Pollard, 2014). Activated macrophages have been shown to express HPSE, aiding in ECM degradation (Savion et al., 1987). In the aforementioned study of colon cancer, a cyclic relationship between HPSE and macrophage activation was reported (Lerner et al., 2011). Colonic epithelial cells expressing HPSE and mucosal macrophages interacted to maintain a chronic inflammatory condition, which aided the formation of a tumour-promoting microenvironment with NF-κB signalling and induction of STAT3 expression. HPSE was shown to generate a vicious cycle which promoted colitis and eventual colon cancer development by stimulating macrophages, which induced the production and activation of epithelial-HPSE via TNF-α and cathepsin-L. Recently, HPSE was shown to be pivotal in the activation and function of macrophages in the TME (Gutter-Kapon et al., 2016). Using a genetic approach, mice lacking HPSE were shown to possess macrophages that expressed lower levels of cytokines such as TNF-α, IL-1β, IL-6 and IL-10. Macrophages lacking HPSE activity further showed impaired phagocytic activity and

reduced infiltrative capacity. Furthermore, these macrophages showed a significantly reduced expression of chemokine (C-X-C motif) ligand-2, which functions in attracting macrophages to sites of inflammation.

1.20 Reprogramming energy metabolism: an emerging hallmark

Cancer cells require novel metabolic means to fuel growth, which differs significantly from that of normal cells (Hanahan and Weinberg, 2011). Aberrant cancer-associated metabolism was a phenomenon first reported by Warburg (Warburg et al., 1927, Warburg, 1956b, Warburg, 1956a). Normal cells, under aerobic conditions, process glucose to pyruvate through glycolysis in the cytosol and then to carbon dioxide in the mitochondria. Under anaerobic conditions, cells switch to glycolysis. However, cancer cells reprogram their glucose metabolism by limiting energy metabolism mainly to glycolysis, with increased glucose uptake and the production of lactate; a phenomenon referred to as the 'Warburg effect' (Liberti and Locasale, 2016, Racker, 1972). The Warburg effect describes 'aerobic glycolysis', in which cancer cells preferentially employ a glycolytic energy metabolism pathway, even under aerobic conditions. Genetic studies suggested that the Warburg effect was indeed required for tumour growth, following decades of debate (Shim et al., 1998, Fantin et al., 2006). Today, cancer-associated metabolic changes can be categorised into six hallmarks as (i) deregulated glucose and amino acid uptake, (ii) using opportunistic nutrient acquisition methods, (iii) use of glycolysis/TCA cycle intermediates for biosynthesis and NADPH production, (iv) increased nitrogen demand, (v) altered metabolite-driven gene regulation and (vi) metabolic interactions with the TME (Pavlova and Thompson, 2016).

There is no reported evidence in the literature for HPSE directly promoting the Warburg effect and modulating glucose metabolism in cancer. However, HPSE expression has been shown to affect glucose metabolism in several other settings. The inhibition of HPSE in the apolipoprotein-E deficient mouse model of atherosclerosis resulted in a marked reduction of serum glucose levels (Hamoud et al., 2017). In a clinical study of type-2 diabetes mellitus patients, urine HPSE was shown to correlate with high blood glucose levels, indicating a glucose-mediated HPSE expression and secretion, with follow up *in vitro* studies showing insulin-mediated HPSE secretion by human embryonic kidney cells in culture (Shafat et al., 2011). The interesting observation of HPSE improving glucose metabolism was made in a study of transgenic HPSE overexpressing mice, with significant changes in pancreatic islet cell composition, structure, gene expression and the overall protective effect from streptozotocin-induced diabetes (Zhang et al., 2017a).

Following Warburg's observations, it was shown that tumours converted glucose or acetate into lipids and that tumour cells generate nearly all their cellular fatty acids via *de*

novo synthesis (Medes et al., 1953, Ookhtens et al., 1984). The synthesis of fatty acids in cancer and its cellular metabolism in promoting cancer cell proliferation are well-characterised phenomena (Currie et al., 2013, Röhrig and Schulze, 2016). Fatty acids were shown to upregulate HPSE expression in endothelial cells through the Sp1 site within the *HPSE* gene promoter (Chen et al., 2004). Further studies in endothelial cells showed that fatty acids caused the nuclear translocation of HPSE, leading to the regulation of genes related to glycolysis and the accumulation of lactate (Wang et al., 2012a). Lactate, once considered a glycolytic waste product, has now emerged as a fuel source and vital regulator in cancer progression (Faubert et al., 2017, Doherty and Cleveland, 2013, Feron, 2009, Thorn et al., 2009). Additionally, the activation of the PI3K signalling pathway has been shown to promote glycolysis and the Warburg effect in cancers (Hu et al., 2016, Makinoshima et al., 2015). As mentioned previously, HPSE has been shown to promote PIK3 signalling (Riaz et al., 2013). Although no direct link between HPSE expression and glycolysis in cancer is found in the literature, the above observations suggest a potential correlation in a tumour setting.

As previously mentioned, tumours experience hypoxia due to a disorganised vasculature network and have adapted survival mechanisms (Eales et al., 2016, Semenza, 2009, Semenza, 2010, Semenza, 2012). The upregulation of HIF transcription factors in response to hypoxia induces several cancer-promoting pathways, including metabolic reprogramming (Wigerup et al., 2016). HIF-1-mediated gene expression has been shown to promote the Warburg effect in cancers (Lu et al., 2002). The upregulation of HIF-1 has also been shown to actively direct the cellular energy pathway towards glycolysis (Kim et al., 2006). This has prompted the development and a phase I clinical trial of a novel glycolysis inhibitor, dichloroacetate, in patients with recurrent malignant brain tumours (Dunbar et al., 2014). The upregulation of HPSE in hypoxic conditions and the HPSE-mediated upregulation of HIFs have been well demonstrated phenomena (Wu et al., 2010b, Hu et al., 2012, Li et al., 2017a, Hu et al., 2015, Naomoto et al., 2007). These observations imply a role of HPSE in hypoxia-mediated modifications of cancer metabolism.

1.21 Evading immune destruction: an emerging hallmark

Virchow's observations of tumour-associated leukocytes provided the first evidence of immune cell infiltration and promotion of tumours (Virchow, 1881). However, subsequent studies revealed that protective immune responses played a key role in tumour suppression (Ehrlich, 1909). Later in the 20th century, the suppression of malignancy by immunosurveillance was widely appreciated, with adaptive immunity shown to play a key role (Burnet, 1957, Burnet, 1970). Today, it is known that cancer-associated immune cells can be either detrimental or beneficial to its progression, thus generating significant clinical interest (Shalapour and Karin, 2015, Grivennikov et al., 2010). These opposing roles of the immune system in either destroying cancer cells and inhibiting tumour outgrowths or in selecting for tumour cells capable of surviving in an immunocompetent host have been described in a conceptual framework termed 'cancer immunoediting' (Schreiber et al., 2011).

As previously mentioned, macrophages form a significant portion of tumour-associated immune cells and HPSE has been shown to play a key role in their activation and function (Aras and Zaidi, 2017, Gutter-Kapon et al., 2016). Macrophages have been shown to play several roles in promoting tumours, including immunosuppression (Noy and Pollard, 2014). For example, macrophages express human leukocyte antigen (HLA) molecules such as HLA-C, HLA-E and HLA-G that are capable of inhibiting NK cells and certain activated T cell subsets (Borrego et al., 1998).

The upregulation of programmed cell death protein-1 (PD-1) on activated T cells induces immune tolerance (Nishimura et al., 1999, Freeman et al., 2000). Often, the ligand for PD-1, programmed cell death ligand-1 (PD-L1) is expressed by cancer cells, aiding immune evasion (Iwai et al., 2002, Hirano et al., 2005). For these reasons, the PD-1 and PD-L1 pathway is a potent target in cancer therapy (Zou et al., 2016, Curiel et al., 2003, Strome et al., 2003). PD-1 expression by TAMs has been shown to reduce anti-tumour immunity and to promote the pro-tumorigenic M2 macrophage phenotype (Gordon et al., 2017).

Gutter-Kapon demonstrated that HPSE regulated the secretion of cytokines such as TNF-α, IL-1β, IL-10 and IL-6 by macrophages (Gutter-Kapon et al., 2016). These cytokines have been implicated in promoting an immunosuppressive tumour environment, where TNF-α promotes an immunosuppressive environment in chronic inflammation and cancer (Sade-Feldman et al., 2013, Ham et al., 2015), IL-10 induces immunosuppression in the TMEs of ovarian cancer, non-small cell lung cancer and non-Hodgkin lymphoma (Xiu et al., 2015, Vahl et al., 2017, Lamichhane et al., 2017), and an IL-6-STAT3-PD-L1 signalling pathway in HCC is mediated by CAFs promoting immunosuppression (Cheng et al., 2018).

IL-6 has been implicated in a more systemic response in a cancer cachexia model, where it was shown to reprogram host metabolism which blocked anti-tumour immunity (Flint et al., 2016). The inflammatory nature of the TME was shown to correlate with IL-1β expression, which mediates immunosuppression and enhanced cancer growth (Chien et al., 2015, Guo et al., 2016).

Macrophages also secrete chemokines that suppress $CD4^+$ and $CD8^+$ T cell function by the recruitment of regulatory T (Treg) cells. The infiltration of the TME by Treg cells is generally associated with a poor clinical prognosis (Jang et al., 2017, Shang et al., 2015). The secretion of CCL22 has been shown to recruit Treg cells to human ovarian carcinoma tumours (Curiel et al., 2004). In a study of colorectal cancer, Treg cell recruitment was mediated by TAM-secreted CCL20 (Liu et al., 2011). Other studies have shown CCL5 to be expressed by macrophages in mouse tumour models (Liou et al., 2013, Biswas et al., 2006). The involvement of HPSE in the secretion of these molecules leading to Treg recruitment therefore seems likely and warrants further investigation. These observations collectively indicate that HPSE, through activating macrophages, plays an indirect role in maintaining an immunosuppressive TME.

1.22 Consideration of the role of HPSE in future studies

With decades of research presenting evidence of the pro-tumorigenic roles of HPSE, its contribution to promoting the hallmarks of cancer cannot be downplayed. This review has attempted to comprehensively gather data generated from numerous studies to investigate the many features of this single enzyme. The ability to modify the ECM through its enzymatic activity, coupled with the ability to influence a number of cellular signalling pathways in a non-enzymatic manner, HPSE provides a clear advantage which is not found in most other TME-related enzymes. It is therefore clear that HPSE should indeed hold a prominent position in future studies addressing the hallmarks of cancer.

1.23 HPSE in the TME

1.23.1 The TME

Tumours are heterogeneous entities and are comprised of a number of different cell types, both cancerous and otherwise, collectively forming the TME (Hanahan and Coussens, 2012). This is in stark contrast to the outdated view of tumours as homogenous collections of cancer cells. The observation of tumour infiltrating leukocytes by Virchow provided early evidence that tumours were indeed comprised of components in addition to cancer cells (Balkwill and Mantovani, 2001). The composition of a tumour is further complicated by the heterogeneity amongst cancer cells themselves. This phenomenon can be explained by Darwinian evolution, where cells compete for limited resources, resulting in selection

pressure-driven genetic diversity (Cairns, 1975, Greaves, 2007, Nowell, 1976, Greaves, 2002, Greaves and Maley, 2012).

Solid tumours can be viewed as ecosystems, with a level of organisational complexity at times rivalling that of normal tissues (Pienta et al., 2008). Much like those found in the natural world, tumour ecosystems are also dynamic. Each component of this complex environment plays a key role in tumour maintenance and progression. Constant crosstalk between cancer cells and their stromal counterparts maintains a vital tumour-promoting line of communication. This interconnectedness between stromal and cancer cells as well as within stromal cells themselves have been the subject of extensive review (Quail and Joyce, 2013). Decades of studies characterising the TME have shed light on how cancers exploit their immediate surroundings to resist treatment and how the microenvironment itself may hold the key to successful therapeutic options. This section will discuss the role of HPSE in the maintenance and function of some of the major components of the TME **(figure 1.10)**.

1.23.2 Cancer cells and CSCs

Cancer cells are the fundamental building units of a tumour and carry defining genetic properties that impart oncogenic characteristics upon them (Hanahan and Weinberg, 2011). HPSE expressed by cancer cells promotes a number of key hallmark features as described in previous sections such as proliferation, inflammation, invasion and metastasis and angiogenesis. All human cancers are known to overexpress HPSE. Multiple clinical studies and patient sample analyses have demonstrated this aberrant expression as well as the correlating poor clinical prognosis in a variety of malignancies including breast, prostate, lung, pancreatic, head and neck, oral, colorectal, gastric, thyroid, liver, bladder, and cervical cancer as well as melanoma, lymphoma and leukaemia (Maxhimer et al., 2002, Sun et al., 2017, Ogishima et al., 2005a, Koliopanos et al., 2001, Kim et al., 2002, Beckhove et al., 2005, Doweck et al., 2006, Sato et al., 2004, Friedmann et al., 2000, Takaoka et al., 2003, Tang et al., 2002, Xu et al., 2003, Matos et al., 2015, El-Assal et al., 2001, Xiao et al., 2003, Shafat et al., 2008, Gohji et al., 2001a, Shinyo et al., 2003, Zeng et al., 2013, Vornicova et al., 2016, Rohloff et al., 2002, Bitan et al., 2002, Fernandes dos Santos et al., 2014, Leiser et al., 2011).

More recent observations have indicated the presence of a second subset of cancer cells within the TME, the CSCs, with the ability to give rise to new tumours (Hanahan and Weinberg, 2011). The function of stem cells in normal human tissues has been extensively studied, especially illustrated by hematopoietic stem cells (Siminovitch et al., 1963, Ng and Alexander, 2017). A pivotal observation made by Furth in demonstrating that a single mouse tumour cell possessed the ability to generate a new tumour *in vivo*, suggested that

stemness is a quality reserved not merely to healthy cells and tissues, but is also a feature of malignant disease (Furth et al., 1937). With the discovery of genetic mutations as the major cause of cancers, the clonal evolution concept was proposed by Nowell, stating that most neoplasms had a single cell of origin with tumour progression resulting from acquired genetic variability within the original clone, subsequently allowing the selection of aggressive cancer cell sublines (Nowell, 1976).

The key studies that shaped our understanding of CSCs have been reviewed elsewhere (Clevers, 2011, Batlle and Clevers, 2017). The current CSC model is based on the premises that tumour heterogeneity arises from its hierarchical organisation, driven by rare CSCs whose identity is hardwired and that CSCs are largely responsible for tumour relapse by virtue of their resistance to standard therapies (Batlle and Clevers, 2017).

Several *in vivo* studies have demonstrated the role of HPSE in normal stem cell function. HPSE was shown to affect basic hematopoietic stem and progenitor cells as well as the bone marrow environment (Spiegel et al., 2008a). Loss-of-function studies employing HPSE inhibitors demonstrated that the enzymatic activity of HPSE was key in proliferation and colony-formation efficiency of mouse bone marrow-derived mesenchymal stem cells (Cheng et al., 2014a). A growth advantage was imparted upon HPSE-overexpressing mouse embryonic stem cells, which formed larger teratomas when inoculated *in vivo* (Xiong et al., 2017). Furthermore, in a study to determine the therapeutic potential of hypoxic preconditioning mesenchymal stem cells (HPC-MSCs), mice injected with HPSE overexpressing HPC-MSCs showed enhanced blood flow recovery on account of the pro-angiogenic properties of HPSE (Hu et al., 2015). These observations suggest that HPSE may play a role in CSCs and warrants further investigation.

EMT features have been shown to play a direct role in imparting cellular stemness, with a study demonstrating the expression of EMT markers in normal mammary gland stem cells as well as mammary CSCs of both human and mouse origin (Mani et al., 2008). Furthermore, the induction of EMT in human breast cancer cells was shown to impart stem-like properties upon them (Morel et al., 2008). These and other studies have shed light on the unexpected observation that EMT programs impart stemness in both normal and neoplastic cells (Scheel and Weinberg, 2012, Sato et al., 2016). As previously mentioned, HPSE promotes EMT features in cancer cells (Li et al., 2016a, Masola et al., 2016, Masola et al., 2012b, Strutz et al., 2002, Escobar Galvis et al., 2007, Masola et al., 2012a, Masola et al., 2014a, Yang and Liu, 2001, Pang et al., 2015). This is achieved mainly through the increased availability of EMT-promoting growth factors such as FGF and TGF-β. Therefore, EMT not only aids metastatic dissemination, but may also play a key role in the generation of a reservoir of CSCs able to continuously seed tumours and

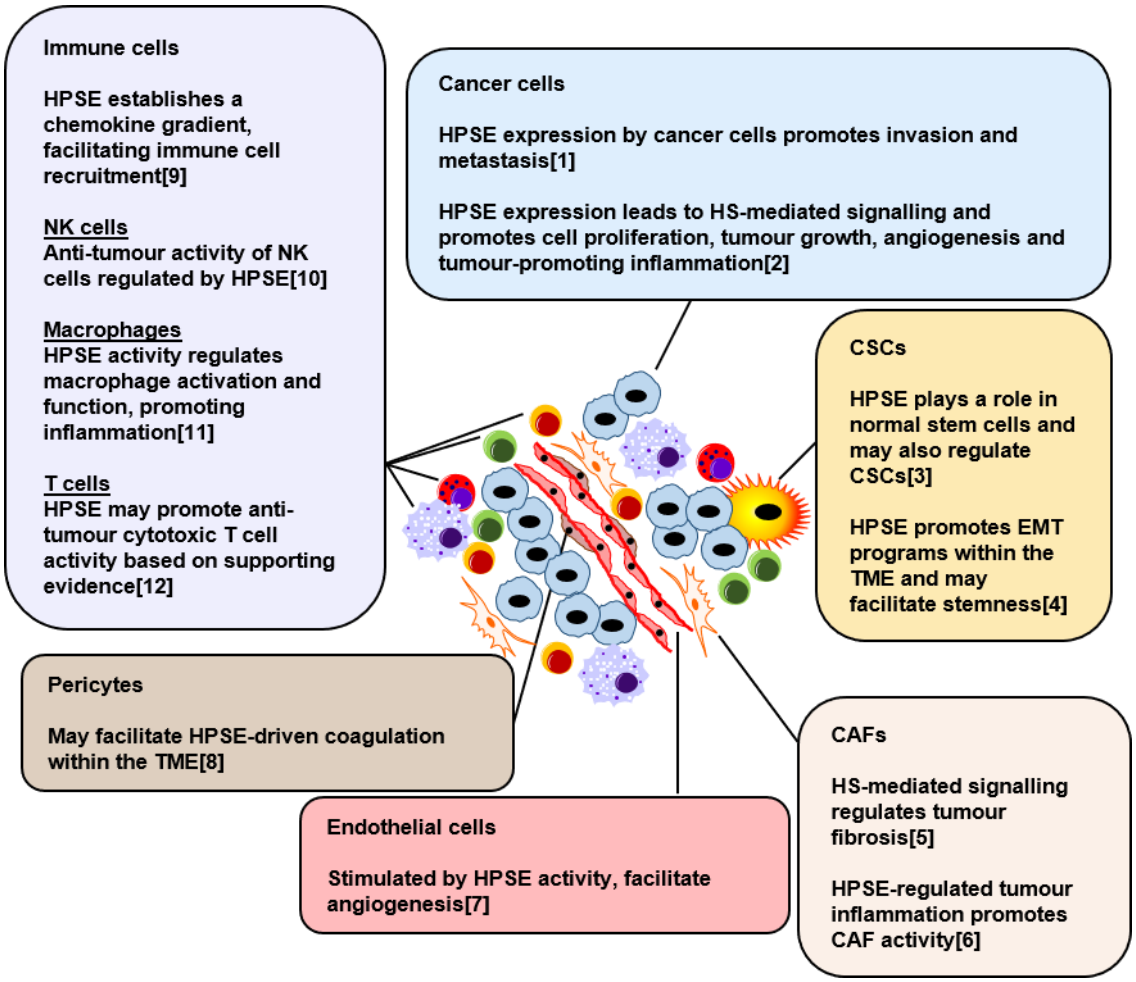

Figure 1.10 HPSE regulates multiple components within the TME
HPSE is a key regulator of a variety of cell types found within the TME. This promotes a number of pro-tumorigenic properties of these TME components as well as critical anti-tumour properties. Evidence is provided by the following authors.

1 (Maxhimer et al., 2002, Sun et al., 2017, Ogishima et al., 2005a, Koliopanos et al., 2001, Kim et al., 2002, Beckhove et al., 2005, Doweck et al., 2006, Sato et al., 2004, Friedmann et al., 2000, Takaoka et al., 2003, Tang et al., 2002, Xu et al., 2003, Matos et al., 2015, El-Assal et al., 2001, Xiao et al., 2003, Shafat et al., 2008, Gohji et al., 2001a, Shinyo et al., 2003, Zeng et al., 2013, Vornicova et al., 2016, Rohloff et al., 2002, Bitan et al., 2002, Fernandes dos Santos et al., 2014, Leiser et al., 2011)
2 (Knelson et al., 2014, Hynes, 2009, Escobar Galvis et al., 2007, Ramani et al., 2011, Hao et al., 2015, Ostapoff et al., 2013, Zetser et al., 2006, Luan et al., 2011, Wang et al., 2014, Wirstlein et al., 2013, Zhang et al., 2010, Cohen-Kaplan et al., 2008a, Malavaki et al., 2013, Troilo et al., 2016, Masola et al., 2014a, Welch et al., 1990, Batool et al., 2017)
3 (Hu et al., 2015, Spiegel et al., 2008b, Cheng et al., 2014b, Xiong et al., 2017)
4 (Li et al., 2016a, Masola et al., 2016, Masola et al., 2012b, Strutz et al., 2002, Escobar Galvis et al., 2007, Masola et al., 2012a, Masola et al., 2014a, Yang and Liu, 2001, Pang et al., 2015)
5 (Masola et al., 2014a, Lv et al., 2016a, Masola et al., 2012a, Gil et al., 2012, Secchi et al., 2017b)
6 (Gutter-Kapon et al., 2016, Erez et al., 2010a)
7 (Godder et al., 1991, Chen et al., 2004)
8 (Nadir and Brenner, 2016, Lip et al., 2002a, De Cicco, 2004, McDonald et al., 2008, Hunter et al., 2014)
9 (Naparstek et al., 1984, Vlodavsky et al., 1992, Matzner et al., 1985, Poon et al., 2014, Morris et al., 2015, Knelson et al., 2014)
10 (Putz et al., 2017)
11 (Gutter-Kapon et al., 2016)
12 (Caruana et al., 2015)

ultimately lead to therapy resistance and relapse. Although there is a lack of studies directly implicating HPSE in the generation of CSCs, this may be achieved indirectly through the promotion of EMT programs in the TME.

1.23.3 Endothelial cells and pericytes

The stromal compartment of a tumour is responsible for much of its cellular heterogeneity with endothelial cells as a key component (Hanahan and Weinberg, 2011). Endothelial cells found in the TME are fundamentally different to those found in normal, healthy tissues. For instance, these cells tend to be cytogenetically abnormal (Hida et al., 2004, Akino et al., 2009). The gene expression profile, angiogenic properties and the growth factor responses of these endothelial cells also drastically differ from those in normal tissue (Matsuda et al., 2010, Hida et al., 2008, Kurosu et al., 2011, Tsuchiya et al., 2010). Furthermore, tumour-associated endothelial cells exhibit aberrant chemotherapeutic responses, complicating disease treatment (Ohga et al., 2009, Akiyama et al., 2012, Ohga et al., 2012).

Human vascular endothelial cells were shown to produce active HPSE, released at times of cellular injury and death (Godder et al., 1991). Inflammatory cytokines such as TNF-α and IL-1β were demonstrated to promote HPSE expression in endothelial cells (Chen et al., 2004). The TME can harbour an inflammatory environment which may stimulate HPSE production by endothelial cells, causing the remodelling of the sub-endothelial matrix, thus leading to enhanced cell proliferation and angiogenesis. The enzymatic activity of HPSE mediates the crosstalk between cancer cells and endothelial cells of the TME. As described in section 1.16, HPSE promotes tumour angiogenesis through the stimulation of endothelial cells. This results in blood vessel development, tumour response to hypoxic conditions as well as lymphangiogenesis.

Pericytes, along with endothelial cells, are structural components of blood vessels and are found embedded in the microvessel BM (Ferland-McCollough et al., 2017). Although initially thought to be exclusively involved in tumour vasculature, it is now evident that pericytes play a key role in TME maintenance and regulation. Several pericyte-derived tumour types such as myopericytoma, glomus tumour and angioleiomyoma have been identified (Shen et al., 2015). Multiple studies on the role of pericytes in the TME have described their aberrant organisation with tumour-associated blood vessels, the pericyte-mediated effects on BM organisation and endothelial cell function as well as their overall effect on clinical outcome (Morikawa et al., 2002, O'Keeffe et al., 2008, Stratman et al., 2009, Franco et al., 2011, Cao et al., 2013, Reynolds et al., 2017). Targeting pericytes has been suggested as a novel therapeutic option in the treatment of cancers (Chen et al., 2017b). The diverse range of functions these previously-overlooked cells play in a

variety of pathological settings, including cancer, has been the subject of recent reviews (Ribeiro and Okamoto, 2015, Ferland-McCollough et al., 2017).

Despite the recent interest in tumour-associated pericytes, the precise role of HPSE, if any, in connection with these cells is yet to be elucidated. However, pericytes may be key in HPSE-driven coagulation in the TME. TF, crucial in the coagulation cascade, is primarily expressed by pericytes and generally not by endothelial cells (McDonald et al., 2008). HPSE has been shown to participate in the coagulation cascade as a co-factor of TF activity (Nadir and Brenner, 2016). A number of cancers have been identified to possess a pro-thrombotic state, which raises the possibility of a pericyte-initiated mechanism of tumour-promoting coagulation, aided by HPSE (De Cicco, 2004, Lip et al., 2002b). Interestingly, Hunter *et al*. reported that the deletion of HPSE in mice led to increased angiogenesis and pericyte coverage in pancreatic neuroendocrine tumours, suggesting a HPSE-dependent organisation of pericytes (Hunter et al., 2013).

1.23.4 CAFs

CAFs are a major component of the tumour stroma and their function in cancer settings has been studied extensively (Kalluri, 2016). Fibroblasts are activated in a wound healing response manner, which has led to the identification of two major cell types; (i) cells that resemble those that provide structural support within normal epithelial tissue and (ii) 'activated' fibroblasts, or myofibroblasts, expressing α-smooth muscle actin (Micallef et al., 2012). Myofibroblasts are responsible for pathological fibrosis associated with wound healing and chronic inflammation, with their high stromal cellular density correlating with a poor prognosis in cancer patients (Liu et al., 2016). The role of fibroblasts in wound healing is well characterised and is aided by their ability to produce ECM components such as proteoglycans, laminin, GAGs, collagen, glycoproteins, hyaluronic acid and HS (Kalluri, 2016, Forrest, 1983, Bainbridge, 2013). Fibroblasts are also capable of modifying the ECM through the expression of MMPs in both physiological and malignant conditions (Simian et al., 2001, Taguchi et al., 2014, Hassona et al., 2014). It is indeed this wound healing capability of fibroblasts that leads to pathologic fibrosis found in a number of organs and tissues such as eye, skin, heart, lungs, liver, kidney and pancreas (Rockey et al., 2015). Fibrosis is also a feature of solid tumours, associated with major ECM modifications in the TME, which ultimately promotes metastasis (Cox and Erler, 2014). However, the precise role of fibrosis in cancer is currently debated, with data emerging to suggest a paradoxical nature of fibrosis playing both positive and negative regulatory roles (Cox and Erler, 2016).

Pathological fibrosis is dependent on growth factor signalling (Kalluri, 2016). Clinical data has demonstrated that the inhibition of FGF, PDGF and VEGF as well as multiple tyrosine

kinases that are critical in promoting fibrosis lead to a favourable patient outcome (Richeldi et al., 2014). TGF-β is considered the master regulator of fibrosis and is potent in activated fibroblast recruitment in cancers and several other disease settings (Meng et al., 2016, Caja et al., 2018, Wei et al., 2017, Principe et al., 2016, Fuyuhiro et al., 2011). Studies on several pathological conditions have shed light on the role of HPSE in fibrosis (Lv et al., 2016b). HPSE has been shown to play a key role in the EMT transition of proximal tubular epithelial cells to myofibroblasts in renal fibrosis by regulating HS-mediated FGF signalling (Masola et al., 2012a). Additionally, HPSE has been suggested as a master regulator of TGF-β signalling, leading to the conversion of tubular cells to myofibroblasts by enhancing EMT (Masola et al., 2014a). In a mouse model of diabetes nephropathy, mice lacking HPSE experienced significantly reduced interstitial fibrosis (Gil et al., 2012). Furthermore, dysregulated paracrine and autocrine signalling has been shown to convert hepatic stellate cells into myofibroblasts, leading to liver fibrosis in a process largely mediated by macrophage-derived HPSE (Secchi et al., 2017a). Lastly, in a mouse model of pulmonary fibrosis, HPSE released by activated fibroblasts enhanced TGF-β signalling, leading to the progression of bronchiolitis obliterans syndrome (He et al., 2016).

In the TME, crosstalk between cancer cells and the CAFs is suggested to be mediated by HPSE expressed mainly by cancer cells and tumour-infiltrating immune cells. As discussed in the previous sections, the enzymatic activity of HPSE liberates a number of HS-bound growth factors, including TGF-β, FGF, PDGF and VEGF, which may directly contribute to fibroblast recruitment and activation in the TME, resulting in cancer fibrosis. The inflammatory nature of the TME can also be modified by fibroblast activity, where NF-κB signalling activation in fibroblasts leads to a tumour-promoting inflammatory signature, resulting in increased recruitment of macrophages and angiogenesis (Erez et al., 2010b). This education of fibroblasts is thought to be initially mediated by tumour-associated immune cells, mainly macrophages. As previously discussed, HPSE is a potent regulator of tumour inflammation, especially mediating TAM activity (Gutter-Kapon et al., 2016). This suggests an indirect role of HPSE in the modification of fibroblast activity in the TME through promoting immune cell recruitment and activation. An additional novel regulatory mechanism for HPSE in the TME has been suggested when primary human fibroblasts were shown to be capable of converting enzymatically inactive pre-HPSE into its active form (Nadav et al., 2002). This modulatory capability may contribute to excessive HPSE activity within the TME, enhancing tumour growth. HPSE is also highly expressed in the accompanying stromal fibroblasts in colon carcinoma metastases (Friedmann et al., 2000). This suggests a role in CAF-derived HPSE in promoting colonisation by modifying the ECM of the metastatic niche.

1.23.5 Immune cells

The role of tumour-associated immune cells in regulating the TME and promoting tumours is well characterised (Kitamura et al., 2015b, Gajewski et al., 2013, van der Woude et al., 2017). HPSE has been identified as a key mediator of immune cell recruitment and activation, whose function in the immune system has been studied for several decades (Naparstek et al., 1984, Vlodavsky et al., 1992, Matzner et al., 1985, Poon et al., 2014, Morris et al., 2015). Chemokine gradients are vital signalling pathways in the migration of immune cells to sites of inflammation and cancer (Sokol and Luster, 2015, Lopez-Cotarelo et al., 2017). HS-mediated chemokine release and activation enables the establishment of these gradients, initiated by HPSE released from cancer cells and other components of the TME (Knelson et al., 2014). Previous segments of this section have addressed these observations in detail. In a study of TAMs, HPSE was shown to regulate macrophage recruitment to tumours (Gutter-Kapon et al., 2016). Once in the tumour, macrophage-derived HPSE was shown to maintain immune cell-TME crosstalk and promote tumour growth. Based on such data, a predominantly tumour-promoting role for HPSE with respect to the tumour immune cell population can be attributed. However, recently-published data challenge this notion.

In parallel to the well-characterised phenomenon of immune cells promoting tumour growth, it is also understood that the immune system plays a critical role in preventing the establishment and the progression of a number of cancers (Chen and Mellman, 2013). With recent advances in immunotherapy, understanding the precise role of immune cells in the TME and harnessing their protective functions in combating malignancies and addressing resistance has become imperative (Rosenberg, 2014, Ribas, 2015, Sharma et al., 2017, Yang, 2015). ‘Hot’ tumours, or those rich in infiltrating T cells are considered favourable to patient outcome compared to ‘cold’ tumours, with recent clinical data demonstrating efforts to boost T cell tumour infiltration, with improved immunotherapy efficacy (Ribas et al., 2017a).

Amongst the large array of tumour-associated immune cells, NK cells have emerged as a potent safeguard against tumour and metastatic growth and is a key player in immunosurveillance (López-Soto et al., 2017). This has led to a recent interest in the promise of NK cells as a directed tumour immunotherapy method (Lowry and Zehring, 2017). In contrast to previous observations of tumour-associated immune cells promoting cancer progression in a HPSE-dependent manner, Putz *et al*. recently reported that HPSE was indeed vital in NK cell-mediated anti-tumour activity (Putz et al., 2017). It was demonstrated in a study involving human and mouse NK cells, that HPSE expression was significantly upregulated upon NK cell activation, and that mice lacking NK cell-specific

HPSE expression exhibited impaired invasion and tumour surveillance. The *in vivo* growth of tumours was also significantly enhanced with the lack of NK cell HPSE activity. Additionally, the efficacy of immunotherapy was drastically reduced in tumour-bearing mice lacking NK cell-specific HPSE. This pivotal study has shed light on a previously-unknown role of HPSE in positively influencing NK cell-mediated tumour immunosurveillance.

Cytotoxic lymphocytes, along with NK cells have also emerged as key regulators of anti-tumour immunity (Martínez-Lostao et al., 2015). This protective function has resulted in the engineering of CAR-T cells in an effort to provide targeted, highly effective cancer therapy (Newick et al., 2017). The American society of clinical oncology named CAR-T therapy the advance of the year in 2018, with an anti-CD19 therapy being approved by the food and drug administration (FDA) in 2017 for refractory B-cell acute lymphoblastic leukaemia (June et al., 2018). In a landmark study, an increase in HPSE activity in CAR-T cells was shown to significantly enhance tumour invasion and anti-tumour immunity (Caruana et al., 2015). This was aided greatly by the superior ECM-degrading capability of HPSE-overexpressing CAR-T cells, resulting in the impaired tumour growth in mouse melanoma and neuroblastoma xenograft models. Even though no direct evidence linking HPSE expression and T cells in a physiological anti-tumour setting has yet been reported, such a relationship can be strongly suggested based on these observations.

1.24 Signalling in the TME and a dual role of HPSE

Cancers are driven by complex signalling networks within the TME (Hanahan and Weinberg, 2011, Sanchez-Vega et al., 2018). This network is initiated by neoplastic cells that promotes the recruitment and activation of the cancer-associated stroma, resulting in its reprogramming to support tumour growth and metastasis. This signalling further extends to the formation of the PMN, with the ability of primary tumours to modify secondary sites in preparation for the arrival of metastatic cells.

Decades of research have unveiled multiple roles of HPSE in the development and progression of cancer as summarised earlier in this section. HPSE-mediated crosstalk amongst the various components of the TME promotes tumour maintenance and progression, which has been the subject of therapy-based research. In an effort to ameliorate the effects of HPSE, several inhibitors have progressed to human clinical trials, with many others in various stages of development (Jia and Ma, 2016, Yang et al., 2008, Dredge et al., 2010, Dredge et al., 2011, Hammond et al., 2012, Ostapoff et al., 2013, Weissmann et al., 2016, Liu et al., 2014, Lewis et al., 2008). The design and use of these will be discussed in detail later in this chapter.

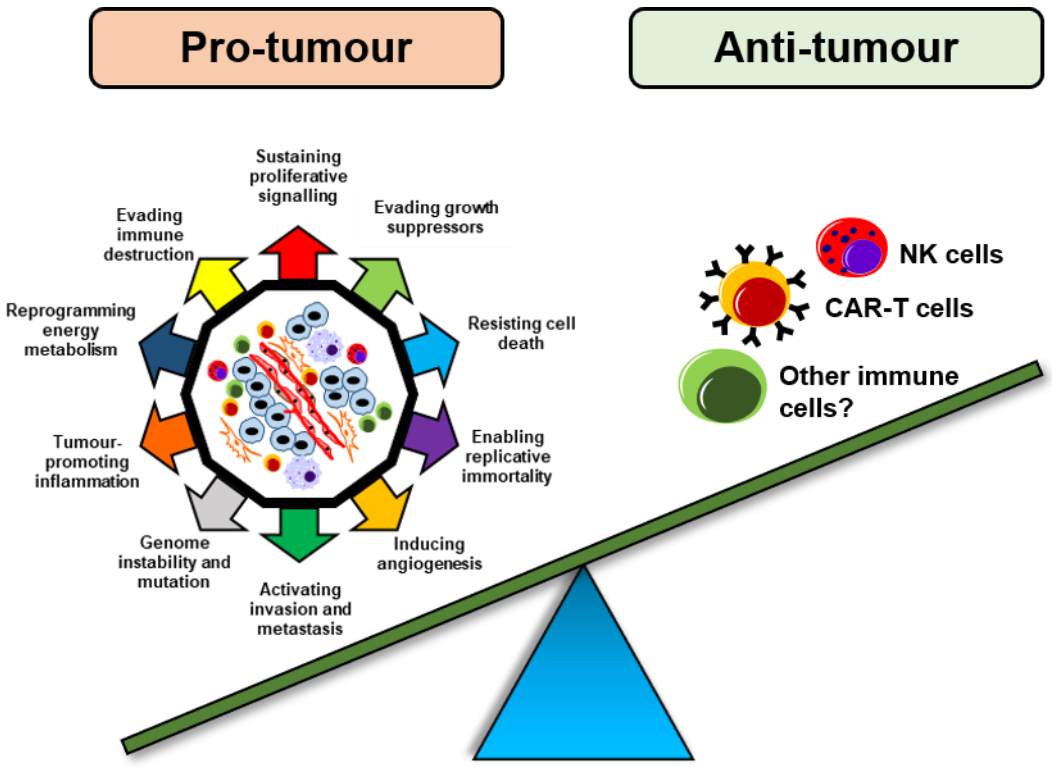

Figure 1.11 HPSE plays a dual role within the TME
The pro-tumour roles of HPSE are well characterised. However, recent data have indicated a critical anti-tumour role of HPSE within the TME. This double-edged sword nature of HPSE will prove challenging to address in the clinic.

However, recent data regarding HPSE-mediated tumour immunity has raised the possibility of a dual role of HPSE within the TME, in both promoting and inhibiting tumour growth **(figure 1.11)**. In light of the above contradictory findings, a critical question ought to be raised of whether targeting HPSE in the TME may prove detrimental or beneficial to a patient. As the complexity of the role of HPSE in cancer continues to unravel, it is now clear that a one-size-fits-all approach may not work in some, if not most tumour settings. Indeed, HPSE inhibitors may result in more harm than clinical benefit in some cancers and may explain why several human trials in the past experienced failures and have since been discontinued.

The development and first human cancer trials of MMP inhibitors provide valuable insights into the complexity of targeting TME components with proven contradictory roles. Early broad-spectrum MMP inhibitors suffered multiple failures, where their administration resulted in worsening of tumour progression by the unintended but unavoidable blocking of MMPs with anti-tumour activity and those crucial in maintaining normal physiology (Dove, 2002b, Winer et al., 2018a). This is indeed testament to the risk of indiscriminately targeting ECM-modifying enzymes in the TME, which may hold true in the case of HPSE. Much work is needed to elucidate the precise role of HPSE in a given tumour setting and

this pro and anti-tumour balance must be thoroughly addressed prior to the use of HPSE inhibitors.

The elucidation of the hallmarks of cancer has revolutionised cancer research and has successfully defined the characteristic features of the most insidious of human diseases. It is now clear that cancers are far more complex, more organised in some ways and more disorganised in other ways than originally assumed. These features result in the many challenges in the treatment of patients. Future research will continue to further dissect and define the inner workings of the TME. The ECM, long considered a passive bystander, has revealed itself as a major regulator of diseases to an extent that many pathologies, including cancer, could be considered aberrations of its normal function. ECM-modifying enzymes such as HPSE have therefore gained significant interest as therapeutic targets.

With its roles in both the maintenance of normal physiology and the promotion of several pathologies, HPSE has emerged as a 'jack-of-all-trades'. It was this notion that spurred this review as it was clear that through its multi-faceted nature, HPSE may be a potent driver of most, if not all hallmarks of cancer. Despite several decades of research, our understanding of HPSE and its many functions continues to evolve. Adding to this complexity are the recent findings demonstrating that HPSE plays a role in preventing tumours through activating cells of the innate immune system. With the current trend towards the discovery and clinical trials of novel HPSE inhibitors, this contradictory role of HPSE in cancer must be addressed.

Therefore, despite our current knowledge, much work is needed to navigate the 'grey' areas created by recent studies. HPSE may be revealed as not the previously proposed holy grail 'target' of cancer treatment, but a highly complex, unpredictable and underestimated entity of the TME.

Part II

Breast cancer

1.25 Breast cancer

1.25.1 The current landscape of breast cancer

Breast cancer has plagued human civilisation for millennia. Throughout human history, breast cancer incidences have been documented, with theories put forth by early physicians such as Hippocrates (460 BC) and Galen (200 AD) speculating on its origin and of possible treatments (Lukong, 2017). The Edwin Smith surgical papyrus and the Ebers papyrus produced in the Egyptian pyramid age (3500 – 2500 BC) contain descriptions of conditions strongly consistent with modern depictions of breast cancer (Brawanski, 2012, Hajdu, 2004). These also suggest treatment methods for cancer including, but not limited to, cautery, lead and sulphur salts, arsenic paste and knife (Hajdu, 2004). The oldest known case of breast cancer was recently discovered in an Egyptian mummy dating back to 2000 B.C., uncovered by an anthropology group led by Professor Miguel Lopez of the University of Granada (unpublished, December 2017). Several Renaissance paintings depict breast abnormalities which have now been determined as cancer (Bianucci et al., 2018). Interestingly, this period saw the pioneering of surgical techniques, eventually paving the way for 'radical mastectomy' first performed in 1894 by William Halsted which effectively revolutionised disease management (Ghossain and Ghossain, 2009). The description of the non-random nature of metastatic growth and the seed and soil hypothesis by Stephen Paget was a result of autopsies conducted on breast cancer patients (Paget, 1889).

Today, breast cancer is a major global health concern **(figure 1.12)**. It is the second most common human malignancy, the most commonly diagnosed cancer in women and the second leading cause of cancer death in women worldwide. The GLOBOCAN 2018 cancer statistics project estimated approximately 2.1 million new cases in 2018, an increase from 1.67 million diagnoses in 2012, amounting to 24.2% of all cancer cases and 15% of female cancer deaths (Torre et al., 2015, Bray et al., 2018). Female breast cancer was estimated to comprise 11.6% of all diagnosed malignancies in 2018. More developed countries account for 54.4% of global breast cancer cases and 11.6% of cancer-related mortality in 2018 (Bray et al., 2018). Countries with a low – medium human development index reported less breast cancer incidence at 31.3% with the mortality rate slightly higher at 14.9%. Even though males too develop breast cancer, these cases are significantly lower in number compared to female breast cancer, amounting to less than 1% of the total breast cancer burden (Ottini, 2014, Fentiman et al., 2006). For the purpose of this thesis, however, the malignancy in females alone will be considered.

In Australia, one in eight women will be diagnosed with breast cancer by their 85th birthday (Cancer Australia). It was estimated that in 2019, approximately 19,535 females will have

been diagnosed, comprising 14% of all new cancer cases nationwide and resulting in 3,058 deaths, or 6.2% of total cancer-related mortality. Multiple risk factors which promote breast cancer have been proposed through epidemiological studies. Early menarche or a late menopause or both will significantly increase a woman's likelihood of developing breast cancer (Britt, 2012, Collaborative Group on Hormonal Factors in Breast, 2012). Reproductive factors such as not bearing children and delaying child-bearing have historically been shown to further increase the risk of developing breast cancer by virtue of extended periods of uninterrupted reproductive cycling (Brinton et al., 1988, MacMahon et al., 1970). Additional risk factors include obesity, poor diet, physical inactivity, use of menopausal hormone therapy as well as alcohol consumption (Torre et al., 2015, Kerr et al., 2017, Bray et al., 2018). Despite the high rate of incidence, the overall prognosis for patients is generally positive, with a current 5-year survival rate of 91% reported by Cancer Australia. Studies have indicated a decline in mortality in developed nations, despite a global trend of increasing incidence rates (Ferlay et al., 2015, DeSantis et al., 2015). This decrease can be attributed to early diagnosis and the advancement in therapeutics. Some regions such as Africa, Asia and South America have reported an increased incidence of breast cancer, which may be the result of lifestyle changes and improved screening (Torre et al., 2015, Bray et al., 2018).

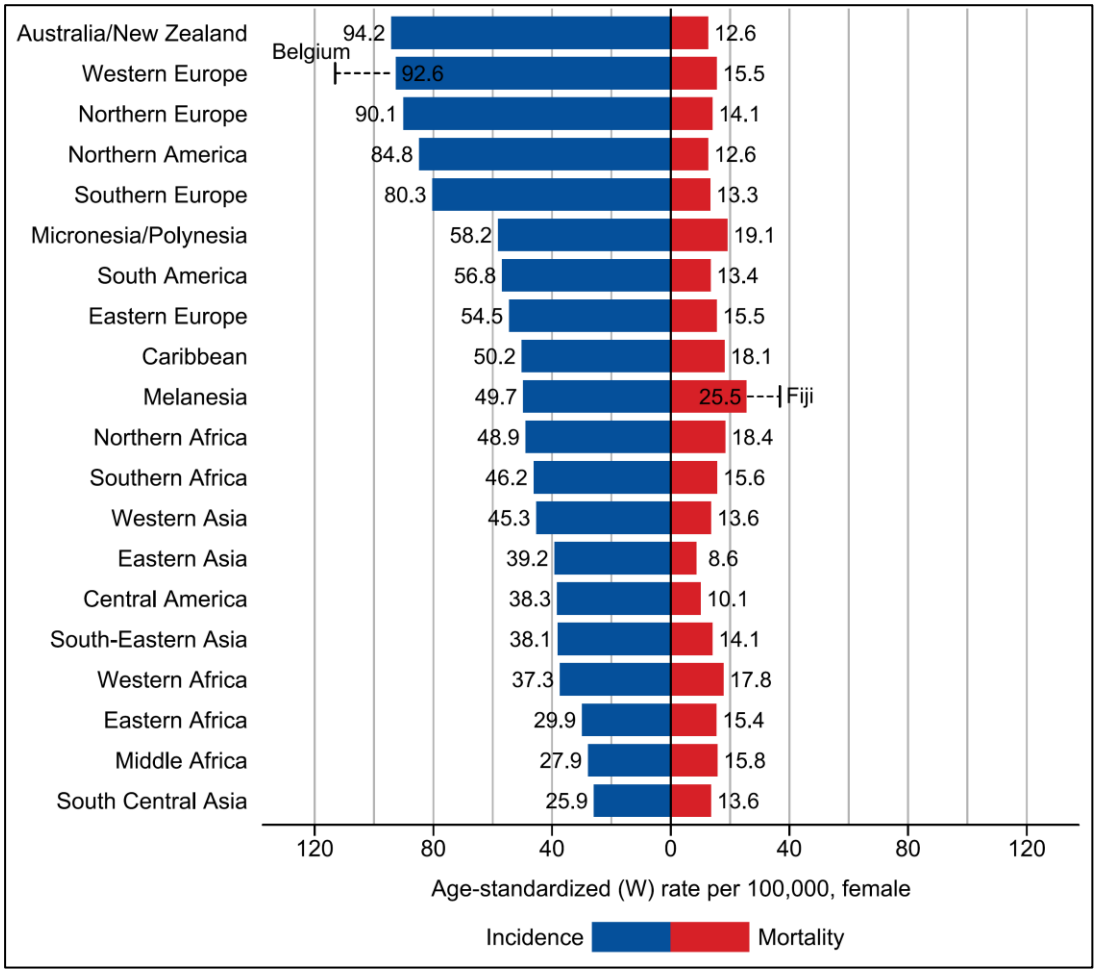

Figure 1.12 Region-specific incidence and mortality age-standardised rates of female breast cancer in 2018
Reproduced from GLOBOCAN 2018 (Bray et al., 2018).

1.25.2 Breast cancer development and progression

1.25.2.1 Normal breast structure

The female breast presents a highly complex organisation. The breast tissue extends downwards from the collarbone to the lower ribs, sternum and the armpit and houses the mammary glands, with an abundance of adipose tissue and dense connective tissue (Johnson and Cutler, 2016). These undergo changes throughout a female's lifetime, starting dramatically at puberty, during which branch formation is initiated. Constant changes of the breast structure occur during each menstrual cycle, with breasts enlarging during pregnancy and lactation. The axillary artery, several posterior intercostal arteries and the internal thoracic artery supply blood to the breast with accompanying veins along with the superficial venous plexus providing venous drainage. The breast vasculature varies during the menstrual cycle and is at its peak closer to ovulation. A complex network of lymphatics drains to the axillary and non-axillary lymph nodes. Breast lymphatics have

been considered to play a key role in metastasis (Cunnick et al., 2008, Rizwan et al., 2015). However, a study by Ullah et al. suggested that lymphatic-mediated migration may have no significant benefit to breast cancer progression (Ullah et al., 2018).

Approximately 15 – 20 glands, or 'lobes' exist within the breast, which are modified sweat glands designed to produce milk when breastfeeding. These lobes are in turn made up of numerous smaller lobules, individually embedded in a stroma of highly cellular connective tissue. These lobes and lobules are connected to the nipple via 6 – 8 mammary ducts. Based on its structural organisation, the mammary gland is categorised as branched tubulo-alveolar. The functional units of the breast are the terminal ductal lobular units, each of which consists of an intra-lobular duct and associated saccules (ductules). These saccules differentiate into acini, or alveoli, the secretory units of the breast. This ductal network has an epithelial layer which progressively thickens as it converges towards the nipple. Simple cuboidal epithelial cells line the smallest ducts while the largest contain stratified columnar epithelial cells. A BM surrounds the entire tubulo-alveolar system with myoepithelial cells found between the luminal epithelium and the BM. Luminal epithelial cells function in milk production. Myoepithelial cells secrete the BM and are found abundantly in the ducts and ductules (Ingthorsson et al., 2015). These contract to transport milk towards the nipple and maintain epithelial cell polarity. Furthermore, the myoepithelium regulates lineage segregation during development, regulates branching morphogenesis and enhances luminal cell growth and differentiation. Although true epithelial cells, the myoepithelium strongly resembles smooth muscle cells. They contain cytokeratin, smooth muscle actin, β-integrins, P-cadherin, desmosomes, hemidesmosomes and express growth factor receptors and MMPs as well as MMP inhibitors thus playing a role in ECM modification (Johnson and Cutler, 2016). Breast cancers are rarely of myoepithelial cell-origin and these cells are considered to act as a tumour suppressor, especially through maintaining the structural integrity of the duct (Duivenvoorden et al., 2017, Pandey et al., 2010, Polyak and Hu, 2005, Sternlicht et al., 1997). Breast carcinoma generally arises within the ductal network and within lobules. Although breast cancer can also arise in the connective tissue supporting the ducts and lobes, termed breast sarcoma, these account for less than 1% of all breast cancers (Yin et al., 2016, Al-Benna et al., 2010). For the purpose of this thesis, only breast carcinoma, or breast cancer of epithelial origin will be considered.

1.25.2.2 Breast cancer progression

The traditional linear model of human mammary carcinoma progression describes distinct stages of cancer development, from normal breast epithelium to hyperplasia, ductal carcinoma *in situ* (DCIS), invasive ductal carcinoma and finally metastatic disease, with each stage accompanied by discrete genetic and epigenetic profiles **(figure 1.13)**

(Rivenbark et al., 2013, Wellings and Jensen, 1973, Ma et al., 2003, Rivenbark and Coleman, 2012). Although benign breast diseases that do not lead to cancer are commonly diagnosed in women, certain features detected on a biopsy are capable of predicting the future risk of progression to malignancy (Silvera and Rohan, 2008, Dyrstad et al., 2015). These include cysts, fibrocystic disease, papillomas and fibroadenomas. Hyperplasia is the overgrowth of epithelial cells that line the ducts or lobules, with or without atypia. Atypical hyperplasia is a high-risk benign lesion of either ductal or lobular nature, whose occurrence translates to the high likelihood of developing breast cancer (Hartmann et al., 2015).

DCIS is viewed as a precursor to invasive carcinoma, with the widespread use of screening methods resulting in a rise in incidence rates (Barrio and Van Zee, 2017, Wellings and Jensen, 1973). During this stage, the malignant proliferation of ductal epithelial cells is confined to the duct, with the BM defining the structural boundary between DCIS and invasive carcinoma. The progression from DCIS to invasive carcinoma is considered to be associated with genetic changes in the cancer cells as well as changes in the DCIS-associated microenvironment (Cowell et al., 2013). Normal myoepithelial cells associated with the ducts have emerged as vital ‘gatekeepers’, effectively suppressing invasion (Duivenvoorden et al., 2017). During tumour progression, however, myoepithelial cells gradually lose this protective role, and indeed, may actively promote invasion by adopting a tumour-associated phenotype (Polyak and Hu, 2005, Lo et al., 2017). The hallmark features of DCIS-to-invasive carcinoma progression are the gradual loss of the ductal myoepithelium along with the BM and the stromal invasion of tumour cells.

Invasion of breast cancer cells into the surrounding stroma depends upon complex interactions between cancer cells and the various components of the stromal environment (Truong et al., 2016). As previously discussed, the stroma plays an active role in promoting invasion and metastasis, aided by a myriad of biochemical and biophysical cues (Khamis et al., 2012). Despite significant advances in diagnosis and cancer therapy, patients with metastatic breast cancer have reported little improvement in survival rates over the past several decades (Tevaarwerk et al., 2013). Metastatic dissemination in breast cancer has been shown to occur early in tumour formation (Hosseini et al., 2016). Clinical data gathered from patient samples has shown that metastatic breast cancer cells evolve and acquire ‘driver’ mutations as they spread, contributing to resistance and relapse (Yates et al., 2017).

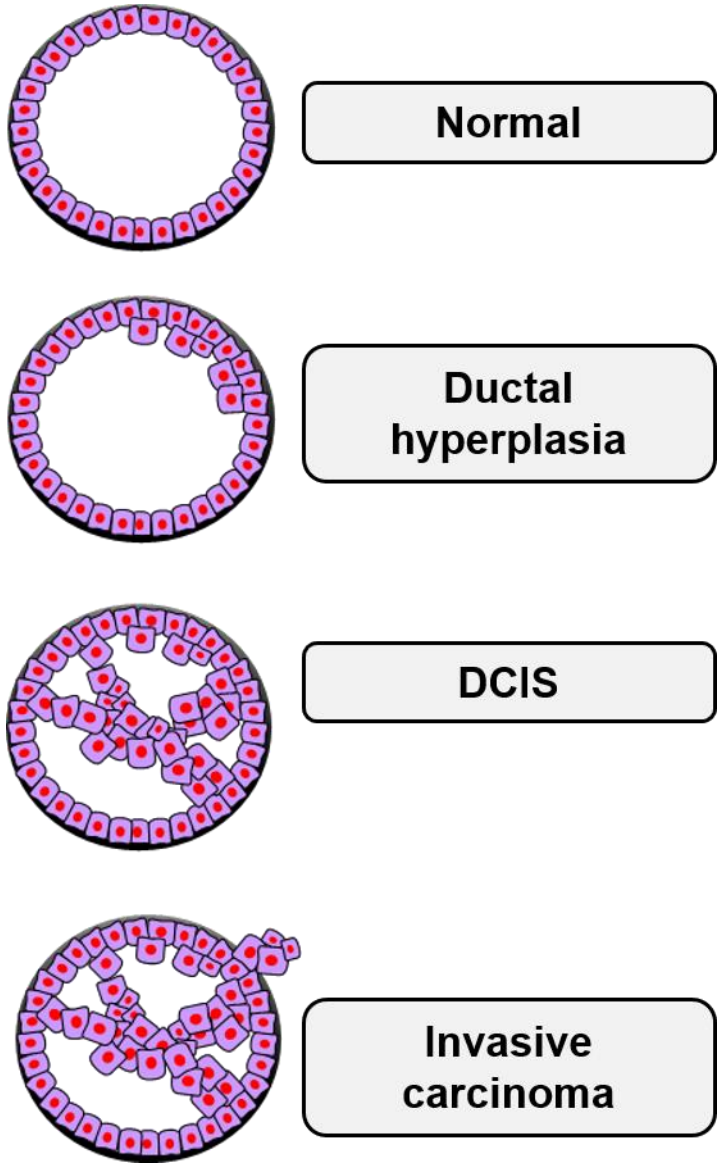

Figure 1.13 Progression of breast carcinoma
This schematic of linear cancer progression shows the progression of normal ductal epithelial cells to hyperplasia, DCIS and eventually, invasive carcinoma.

1.25.2.3 Breast cancer subtypes and treatment

Breast cancer was initially stratified to four clinically significant molecular subtypes, namely luminal-A, luminal-B, HER-2-positive and basal-like (Perou et al., 2000, Sorlie et al., 2001). However, taking into account gene copy number and expression patterns, up to ten molecular subtypes were later described (Curtis et al., 2012). Today, molecular-based classification of breast cancer has revealed a vastly complex, heterogeneous disease with multiple behavioural features and has shifted disease classification based purely on morphological description to taking into account clinical features and biomarker expression (Russnes et al., 2017). It is also likely that a single tumour may contain multiple subtypes within itself, contributing to treatment challenges (Yeo and Guan, 2017). The recently-revised breast cancer staging guidelines by the American joint committee on cancer aims to standardise diagnoses globally and has added characteristics to the

traditional TNM system to determine cancer stage (Giuliano et al., 2017). The determination of cancer stage ideally takes into account the size of the tumour and the level of invasion, whether cancer is detected in the lymph nodes and if it has indeed spread to other parts of the body beyond the breast, the level of cancer cell differentiation, ER, progesterone receptor (PR) and human epidermal HER2 status and the genomic status of the cancer based on the oncotype DX test (breastcancer.org).

Over 75% of all breast cancers express ER and/or PR with 10 – 15% expressing HER2 (Russnes et al., 2017). Of clinical significance are triple-negative breast cancers (TNBCs), devoid of ER, PR and HER2 expression, which make up 10 – 20% of all cases and present major challenges in treatment (Denkert et al., 2017, Bianchini et al., 2016). The treatment options for patients have evolved over time and depend upon molecular subtype, tumour load and metastatic burden as well as the patient's own wishes (Harbeck and Gnant, 2017).

The early diagnosis of breast cancer without metastases bodes well for the patient. Surgery and radiotherapy are used for local therapy of early breast cancer. For a systemic treatment approach, endocrine therapy and chemotherapy are administered. However, metastatic breast cancer presents major treatment challenges (Chen et al., 2017a, Redig and McAllister, 2013, Yates et al., 2017). Although breast cancers expressing the endocrine markers can be subjected to targeted therapies, TNBC varieties present fewer treatment options and instead, must be addressed mainly with a combination of surgery, radiation and chemotherapy. Advances in immunotherapy have presented novel treatment options for breast cancer (Vonderheide et al., 2017). Recently, a landmark study by Zacharakis et al. demonstrated that treating a patient with metastatic, ER-positive, HER2-negative breast cancer with the adoptive transfer of tumour-infiltrating leukocytes reactive against a panel of mutant proteins resulted in complete tumour regression (Zacharakis et al., 2018). This has renewed hope of the arrival of targeted, highly efficacious, immune-mediated therapies with a favourable clinical outcome.

1.25.3 HS and HPSE in normal breast development

The mammary ECM and BM play crucial roles in the development of the mammary gland (Fata et al., 2003, Wiseman and Werb, 2002, Nelson and Larsen, 2015). As a major component of these structures, the role of HS must be taken into account. HS plays key roles in the maintenance of normal physiology as well as in the progression of several pathological conditions, including cancer (Knelson et al., 2014). Proteoglycans, including HSPGs have been shown to be vital in normal mammary gland development (Gomes et al., 2013). The development of mammary glands rely heavily on cell-ECM interactions with

abundant experimental evidence showing the involvement of proteoglycans (Delehedde et al., 2001, Prince et al., 2002, Zako et al., 2003, Deepa et al., 2004, Hallberg et al., 2010, Xiang et al., 2001, Wiseman and Werb, 2002). Multiple ECM changes are associated with the menstrual cycle, such as fluctuating levels of proteoglycans, including HSPGs (Ferguson et al., 1992, de Lima et al., 2012). Conditional inactivation of *Ext1*, whose gene product is key in HSPG assembly was shown to affect ductal branch morphogenesis (Garner et al., 2011). Additionally, ductal branching and lobulo-alveolar formation were shown to be regulated by HS-biosynthetic enzymes (Bush et al., 2012). Furthermore, the deletion of N-deacetylase/N-sulfotransferase-1, affecting both N-acetylation and N-sulfation of HS, was shown to lead to aberrant lobulo-alveolar development (Crawford et al., 2010).

As the only enzyme to cleave HS, HPSE plays a key role in normal mammary development. The association of HPSE overexpression was shown to directly correlate with enhanced mammary gland morphogenesis in transgenic mice, suggesting a role in organ development (Zcharia et al., 2004). Mammary glands of virgin HPSE-transgenic mice showed a higher level of development compared to those of pregnant mice. Recently, it was demonstrated that mammary gland branching morphogenesis and overall mammary gland development was increased in transgenic mice with the mammary gland-targeted expression of both HPSE as well as its C-terminal domain alone, driven by the mouse mammary tumour virus (MMTV) promoter (Boyango et al., 2018). Signalling properties initiated by the C-terminal domain of HPSE was shown to promote mammary gland development, with enhanced Stat5 and Src phosphorylation. This study further demonstrated that this targeted overexpression of HPSE in mammary glands resulted in enhanced tumour growth. MMPs have been shown to regulate mammary gland development by virtue of ECM remodelling (Lee et al., 2000, Tan et al., 2014, Inman et al., 2015, Talhouk et al., 1991). As mentioned, the expression of HPSE has been shown to correlate with that of MMPs (Tang et al., 2014a, Chen et al., 2012, Purushothaman et al., 2008). This suggests that HPSE may play a role in normal mammary development through regulating MMP expression or acting in concert with MMPs. Indeed, *in vitro* 3D organotypic culturing of mammary epithelial cells as well as *in vivo* studies demonstrated that HPSE and MMP-14 reciprocally regulate each other during branching morphogenesis (Gomes et al., 2015).

The role of HS and HPSE in the development and progression of breast cancer will be discussed in detail in chapters 3 and 4 of this thesis.

Part III

HPSE as a therapeutic target and the development of HPSE inhibitors

1.26 Introduction

A range of options exist for the treatment of malignant disease, including surgery, radiation therapy, chemotherapy, immunotherapy, hormone therapy, stem cell transplants, precision medicine and targeted therapy (Schirrmacher, 2019). Amongst these, targeted therapies provide the means to disrupt disease by focusing on specific cancer-promoting pathways and molecules (Baudino, 2015). Targeted therapies generally include small molecule inhibitors and monoclonal antibodies. A great variety of these are currently in clinical use, in parallel with an active drug discovery process. These therapies have been widely reviewed and are briefly discussed herein.

Recent advances in cancer therapy through immune checkpoint blockage have been described. Most commonly, inhibiting the CTLA-4 and PD-1 pathways either in combination or alone have resulted in promising patient responses (Ribas and Wolchok, 2018). The repertoire of immunotherapy targets continues to grow, despite therapeutic limitations, with some patients not achieving a complete response (Marin-Acevedo et al., 2018). As a major hallmark of cancer, angiogenesis has remained an attractive therapeutic target. A large variety of angiogenesis inhibitors have received FDA approval and are used in disease settings including cancer (Rajabi and Mousa, 2017). As described previously, VEGF, PDGF and FGF are potent mediators of neovascularisation and are therefore key targets of a number of these inhibitors. Targeting angiogenesis in cancer, however, is not without its limitations (Moserle et al., 2014).

The process of DNA damage repair in cancer cells in response to therapy hinders treatment, therefore rendering it a potential target (Gavande et al., 2016). Small molecule inhibitors of DNA repair proteins such as the well-characterised PARP have shown efficacy at inhibiting replication of cells with mutated *BRCA1* or *BRCA2* genes, resulting in cell death (Lin and Kraus, 2017). Several other targets besides PARP such as RAD51 recombinase, MRE11 nuclease, WRN DNA helicase and RAD52 DNA repair protein have also been described (Hengel et al., 2017). Monoclonal antibodies have also emerged as potent cancer combatants over several decades (Weiner, 2015, Scott et al., 2012). These monoclonal antibodies can be conjugated to toxins or radioactive isotopes in order to deliver a lethal blow to cancer cells in a targeted manner, while minimising off-target effects. Hormone therapies target hormonally-driven cancers such as certain subtypes of breast cancer expressing ER or PR (Masoud and Pagès, 2017). As discussed previously in this chapter, the expression of hormone receptors in breast cancer patients prove clinically favourable, compared to TNBCs which are challenging.

However, targeted treatments present a range of limitations (Dagogo-Jack and Shaw, 2017, Moserle et al., 2014). Tumours constantly evolve and when subjected to therapy,

through their inherent heterogeneity, often develop resistance. In certain instances, such as in TNBCs, the lack of expression of target proteins drastically limits treatment options. It is therefore imperative that the process of drug discovery continues in the search for new targets and treatment modalities.

As it is now clear, HPSE represents an attractive therapeutic target in treating cancer as well as other diseases driven by its activity, as discussed previously (Rivara et al., 2016). The existence of HPSE as a unique enzyme is key in its choice as a target (Hulett et al., 1999, Hulett et al., 2000). Several HPSE inhibitors have been thus far described, with varying levels of *in vitro* and *in vivo* efficacy, with some progressing to clinical trials. These include HS and heparin mimetics, nucleic acid-based inhibitors, HPSE-neutralising antibodies and small molecule inhibitors (Mohamed and Coombe, 2017, Heyman and Yang, 2016, Vlodavsky et al., 2016, Jia and Ma, 2016). A number of these are discussed below, with chapter 5 of this thesis highlighting efforts to identify and characterise novel HPSE inhibitors.

1.26.1 Heparin

Heparin was investigated early as a HPSE inhibitor, due to it being closely related to HS and its ability to inhibit the ECM-degrading activity of HPSE (Shriver et al., 2012, Bar-Ner et al., 1987). However, the use of heparin in the clinic as an anti-cancer agent was limited, as it induces anti-coagulant effects and thrombocytopenia (Warkentin et al., 1995). In order to improve efficacy and reduce its off-target effects, low molecular weight heparin (LMWH) has been used as an alternative (Koopman et al., 1996, Franchini and Mannucci, 2015). Several studies have reported the clinical usage of heparin and LMWH, with varying efficacy (Klerk et al., 2005, Zhang et al., 2016b, Sanford et al., 2014, Yu et al., 2016, Niers et al., 2007). LMWH varieties such as enoxaparin, dalteparin and tinzaparin have proven effective in both *in vitro* and *in vivo* studies in a range of cancer settings (Abu Arab et al., 2011, Stevenson et al., 2005, Harvey et al., 2007, Harada et al., 2006). The ability of unfractionated heparin to inhibit HPSE and to attenuate intestinal injury in an *in vivo* model may pave the way for novel treatment options for sepsis (Chen et al., 2015). Interestingly, the capacity of HPSE to neutralise heparin has been reported, which suggests that tumours overexpressing HPSE could, in theory, develop resistance to heparin treatment (Gong et al., 2003, Nasser et al., 2006). Earlier, the pro-coagulant activity of HPSE in promoting cancer was briefly introduced (Nadir and Brenner, 2016). HPSE promotes the expression of TF, resulting in increased coagulation. Many tumours have been shown to express high levels of TF which enhances tumour growth, suggesting the involvement of the coagulation system in cancer (Versteeg et al., 2008, Bromberg et al., 1995, Wang et al., 2012b, van den Berg et al., 2012). This relationship has prompted the use of heparins

to specifically target the coagulation system (Nadir and Brenner, 2010). An ideal candidate would possess weak anti-coagulant activity and would target the beginning of the coagulation cascade. Using peptides derived from tissue factor pathway inhibitor-2, along with inhibiting the HPSE-TF interaction should be considered (Nadir and Brenner, 2018, Crispel et al., 2016).

1.26.2 PI-88 (Muparfostat)

PI-88 (Muparfostat) is the most clinically advanced of all HPSE inhibitors and is a sulphated HS-mimetic first described to inhibit tumour growth, angiogenesis and metastasis in a model of rat mammary adenocarcinoma **(figure 1.14)** (Parish et al., 1999). PI-88 inhibits the enzymatic activity of HPSE and competes with HS-binding of growth factors such as VEGF and FGF, effectively impeding angiogenesis and in turn, tumour growth and metastasis. A phosphomannan oligosaccharide mix is contained within the exopolysaccharide of the yeast species *Pichia (Hansenula) holstii* NRRL Y-2448, which formed the precursor for large-scale production of PI-88 (Yu et al., 2002). The individual components of PI-88 were later characterised by capillary electrophoresis to reveal a combination of mannose-6-phosphate (3%), monophosphorylated disaccharide (3%), monophosphorylated tetrasaccharide (28.5%), monophosphorylated pentasaccharide (59%) and monophosphorylated hexasaccharide (1%). Additionally, two other components (5.5% combined) were described, one of which corresponded to monophosphorylated trisaccharide (Yu et al., 2002). This study further investigated the anticoagulant properties reported for PI-88.

The potent *in vivo* anti-tumour activity resulted in the rapid progression of PI-88 to a phase I clinical trial of establishing a dose and toxicity profile in patients with advanced malignancies (Rosenthal et al., 2002). The interaction of PI-88 with proangiogenic factors such as FGF-1, FGF-2 and VEGF was characterised by surface plasmon resonance, with its anti-angiogenic properties forming a strong foundation for pre-clinical and clinical validation (Cochran et al., 2003, Ferro et al., 2007). Several clinical studies followed to determine the efficacy of PI-88 in malignant settings. A phase I study of PI-88 in solid tumours yielded promising results, warranting an escalation to phase II clinical trials (Basche et al., 2006). In a phase II trial of advanced melanoma patients, PI-88 resulted in overall survival and time to progression similar to chemotherapy (Lewis et al., 2008). However, the use of PI-88 in cancer treatments has resulted in several complications. In a study of PI-88 in combination with docetaxel in metastatic castrate-resistant prostate cancer, higher-than-expected febrile neutropenia was reported, suspected to be due to an interaction between the combined drugs (Khasraw et al., 2010b). The development of

dose-limiting thrombocytopenia was described in a phase I toxicity profiling study, highlighting the need for further research (Rohloff et al., 2002).

PI-88 has shown most promise in HCC. Successful phase II trials indicated significant clinical benefits of PI-88 as an adjuvant therapy to HCC patients following curative resection (Liu et al., 2009, Liu et al., 2014). It is now understood that PI-88 inhibits post-operative HCC recurrence through disrupting the HPSE surge following liver resection (Liao et al., 2016a). PI-88 is the only HPSE inhibitor to have progressed through to a phase III clinical trial and was used as an adjuvant therapy in patients with hepatitis virus-related HCC following liver resection (clinicaltrials.gov ID NCT01402908). These records indicate that the recruitment to this study was recently terminated due to interim analysis and business concerns. Disease-free survival was not significantly improved in the overall treatment group but PI-88 did prolong survival in patients with microvascular invasion, comprising 40% of all trial patients (Chen et al., 2017c). A second phase I/II trial of PI-88 in melanoma patients has not yet reported clinical outcomes at the time of writing (clinicaltrials.gov ID NCT00068172).

1.26.3 PG545 (Pixatimod)

The PG500 series, a collection of HS mimetics, were developed to target HPSE activity and angiogenesis **(figure 1.14)** (Dredge et al., 2010). Following a screening process to determine their *in vitro* efficacy, PG545, a cholestenol-sulfotetrasaccharide, was selected as the lead clinical candidate for oncology. Promising pre-clinical data indicated potent anti-angiogenic, anti-tumour growth and anti-metastatic activity, which paved the way for a phase I clinical study in patients with solid tumours (clinicaltrials.gov ID NCT01252095) (Dredge et al., 2011). However, this was terminated due to unexpected injection-site reactions. A second phase I study was established to determine the safety and tolerability of PG545, but efficacy in treating human malignancies is yet to be shown (clinicaltrials.gov ID NCT02042781). In an *in vivo* model of murine breast cancer, PG545 in combination with anti-PD-1 treatment was shown to increase tumour-specific $CD4^+$ and $CD8^+$ effector cells as well as NK cells, suggesting an immunomodulatory effect (Hammond et al., 2018).

In other recent studies, PG545 was demonstrated as an anti-lymphoma drug, involving ER stress response-induced autophagy (Weissmann et al., 2018). PG545 was shown to activate TLR-9 through elevating its ligand CpG in DCs, leading to enhanced IL-12 production, which in turn mediated NK cell activation (Brennan et al., 2016). This PG545-mediated NK cell activity was key in its anti-lymphoma effects. The expression of p21, a cyclin-dependent kinase inhibitor capable of hindering the cell cycle was shown to be downregulated by HPSE, whose inhibition with PG545 led to reduced colon polyp formation and growth *in vivo* (Singh et al., 2017). PG545 has potential applications beyond

cancer. The prophylactic HPSE-inhibitory effect of PG545 in protecting against the mosquito-borne Ross river virus was demonstrated both *in vitro* and *in vivo*, suggesting potential clinical applications (Supramaniam et al., 2018). As previously discussed, HPSE plays a role in kidney diseases. A nephroprotective role was attributed to PG545 in acute kidney injury (AKI) (Abassi et al., 2017). The pathogenesis of ischemic reperfusion-mediated AKI was attenuated through inhibiting the upregulation of HPSE as well as pro-inflammatory and pro-fibrotic mediators.

1.26.4 SST0001 (Roneparstat)

Yet another HPSE inhibitor to progress to clinical trials was SST0001, a heparin mimetic **(figure 1.14)**. Major anti-myeloma drugs were shown to upregulate the NFκB pathway, leading to HPSE upregulation as well as release into the conditioned medium *in vitro,* in tumour cells (Ramani et al., 2016a). Uptake of this soluble HPSE promoted tumour aggressiveness, which was inhibited by SST0001 treatment. Further *in vivo* studies demonstrated that SST0001 sensitizes myeloma cells to chemotherapeutic drugs through the inhibition of HPSE, which reduced relapse (Ramani et al., 2016b). In the first human trial to evaluate a HPSE inhibitor in a haematological malignancy, SST0001 was administered to multiple myeloma patients in a phase I clinical trial (clinicaltrials.gov ID NCT01764880) (Galli et al., 2018). Although an excellent safety profile was established, this study did not demonstrate a direct anti-myeloma effect of SST0001.

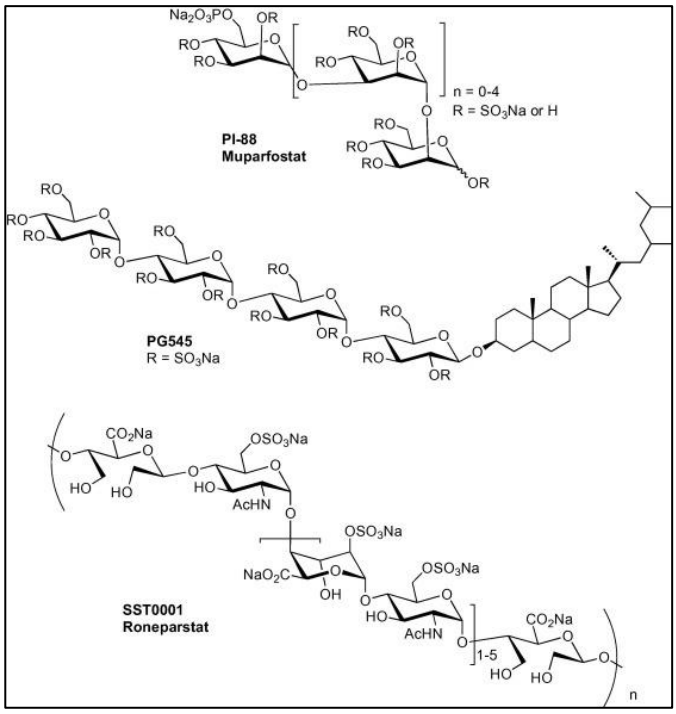

Figure 1.14 The chemical structures of PI-88, PG545 and SST0001
PI-88, PG545 and SST0001 progressed to human clinical trials (Rondanin et al., 2017).

1.26.5 M402 (Necuparanib)

An N-sulphate glycol-split modified heparin, M402 was engineered to possess reduced anti-coagulant activity while retaining HS-like binding properties to HSBPs **(figure 1.15)**. M402 treatment *in vivo* was shown to reduce angiogenesis and mouse mammary tumour metastasis (Zhou et al., 2011b). Its anti-tumour efficacy was demonstrated both as a single agent and in combination with chemotherapy. A phase I/II clinical trial of M402 in combination with nab-paclitaxel and gemcitabine in pancreatic cancer was recently terminated due to a lack of efficacy in the study population (clinicaltrials.gov ID NCT01621243).

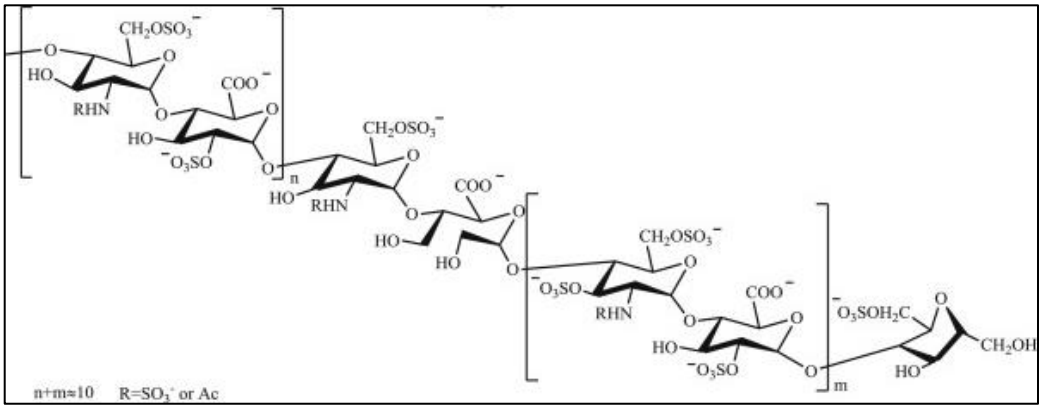

Figure 1.15 The chemical structures of M402
Adapted from Jia and Ma, 2016 (Jia and Ma, 2016).

1.26.6 Other sulphated oligosaccharides

Several other sulphated oligosaccharides have shown HPSE-inhibitory properties, although no clinical studies have yet been conducted. Chemical modification of β-1,3-glucan phycarine isolated from *Laminaria digitata*, a species of brown algae, yielded PS3 which exhibited inhibition of the enzymatic activity of human HPSE as well as bacterial heparinase II in a concentration-dependent manner (Menard et al., 2004, Schoenfeld et al., 2014). PS3 was further shown to target a range of biological functions including inflammation, in a heparin-like manner (Alban et al., 2009). The oligomannurarate sulphate JG3 was shown to bind strongly to the KKDC domain and weakly to the QPLK domain of HPSE, effectively inhibiting enzymatic activity (Zhao et al., 2006). This in turn reduced bFGF-mediated signalling in the ECM and resulted in the inhibition of angiogenesis and metastasis *in vivo*. JG3 was further shown to inhibit HPSE-mediated cell adhesion (Li et al., 2009). Novel synthetic tri-mannose C-C-linked dimers (STMCs), STMC α,β, showed potent HPSE-inhibitory activity along with the inhibition of P-selectin (Borsig et al., 2011). The highly sulphated galactans, λ-carrageenans, are isolated from red algae and have potent heparin-like properties of inhibiting HPSE enzymatic activity

and angiogenesis (Poupard et al., 2017a, Poupard et al., 2017b). A low molecular weight glycol-split λ-carrageenan was described as the major drug candidate, with virtually non-existent anti-coagulant activity which had affected a majority of heparin-like HPSE inhibitors (Poupard et al., 2017b).

1.26.7 Defibrotide

Defibrotide is a nucleic acid-based inhibitor which modulates HPSE activity **(figure 1.16)**. It is a polydisperse oligonucleotide, shown to enhance chemotherapeutic efficacy by modifying the myeloma TME (Mitsiades et al., 2009). Following promising pre-clinical data, a phase I/II clinical trial was established to determine the efficacy of defibrotide administration in combination with melphalan, prednisone and thalidomide treatment in multiple myeloma patients (Palumbo et al., 2010). The results of this trial have not yet been determined (clinicaltrials.gov ID NCT00406978).

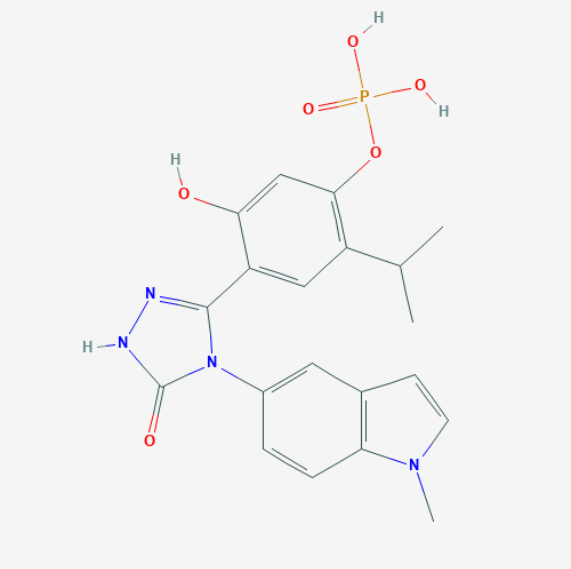

Figure 1.16 Structure of defibrotide sodium
Adapted from the National Centre for Biotechnology Information; PubChem Database; Defibrotide sodium, CID=135565962.

1.26.8 OGT2115

OGT2115 is a small molecule HPSE inhibitor, developed through high-throughput screening of a small molecule library **(figure 1.17)** (McKenzie, 2007). HPSE inhibition with OGT2115 was shown to attenuate cerebrovascular inflammation and prevent subarachnoid haemorrhage-induced neurological impairment *in vivo* (Changyaleket et al., 2017). ER stress-induced invasion and migration of human breast cancer cells was reduced with the use of heparin and OGT2115 *in vitro* (Li et al., 2013). However, no human trials have yet commenced.

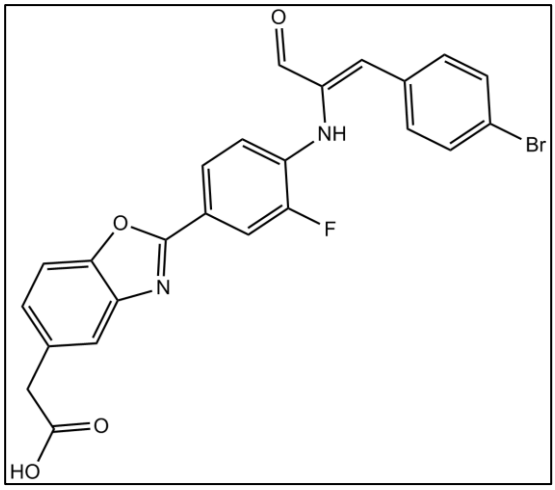

Figure 1.17 Structure of OGT2115
Adapted from ApexBio.

1.26.9 Suramin

Another small molecule inhibitor of HPSE, suramin, was first shown to inhibit cell invasion **(figure 1.18)** (Nakajima et al., 1991). This was confirmed through the study of the anti-angiogenic effects of suramin analogues *in vivo* as well as suramin-mediated inhibition of cancer cell proliferation (Marchetti et al., 2003, Li et al., 2015a). An *in vivo* study of HCC demonstrated that suramin blocked the expression of HPSE and led to prolonged survival (Tayel et al., 2014). Suramin is yet to be tested in clinical trials.

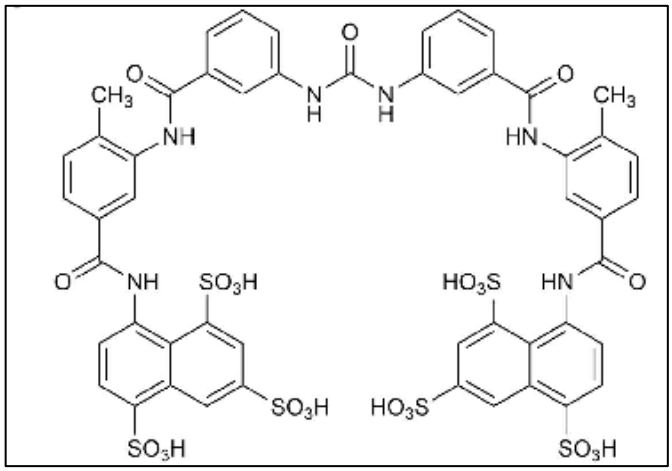

Figure 1.18 Structure of suramin
Suramin is a small molecule HPSE inhibitor (Bailly et al., 2016).

1.26.10 Other heterocyclic compounds

The carboxylic acid group, the benzoxazole ring and the isoindole-5-carboxylic acid moiety of 2,3-dihydro-1,3-dioxo-1H-isoindole-5-carboxylic acids were found to be key in inhibiting the enzymatic activity of HPSE, in a high throughout screen **(figure 1.19)** (Courtney et al., 2004). Furthermore, a series of benzoxazol-5-yl acetic acid derivatives were identified as HPSE inhibitors, possessing anti-angiogenic properties (Courtney et al., 2005). A further variety of small molecule HPSE inhibitors were described as a series of N-(4-phenyl)-benzamides (Xu et al., 2006). This study further established pharmacokinetic properties of lead compounds *in vivo*. Additionally, a series of 4-(1H-benzoimidazol-2-yl)-phenyl-ureas were investigated as potential inhibitors, with 1,3-bis-[4-(1H-benzoimidazol-2-yl)-phenyl]-urea exhibiting most promising activity (Pan et al., 2006).

Novel 1, 3-N, O-spiroheterocyclic compounds were shown to inhibit HPSE activity and result in the enhanced cytotoxicity of the anti-cancer drug nedaplatin in cervical cancer cells (Song et al., 2016). The anti-cancer effects were mediated through restoring p53 activity and downregulating the expression of h-TERT and c-Myc. DMBO (2-(2,6-difluorophenyl)-5-(4-methoxyphenyl)-1-oxa-3-azaspiro[5.5]undecane), a pyranoside mimetic, resembles the pyranosidic ring structure of HS and binds a number of growth factors and cytokines such as VEGF, EGF and TNF-α (Basappa et al., 2010). DMBO was shown to inhibit *in vitro* HPSE activity and its anti-tumour effects were demonstrated *in vivo* when in combination with heparin. A recent study involving molecular docking to identify structural features critical in HPSE inhibition led to novel benzazole derivatives with potent *in vitro* efficacy (Madia et al., 2018).

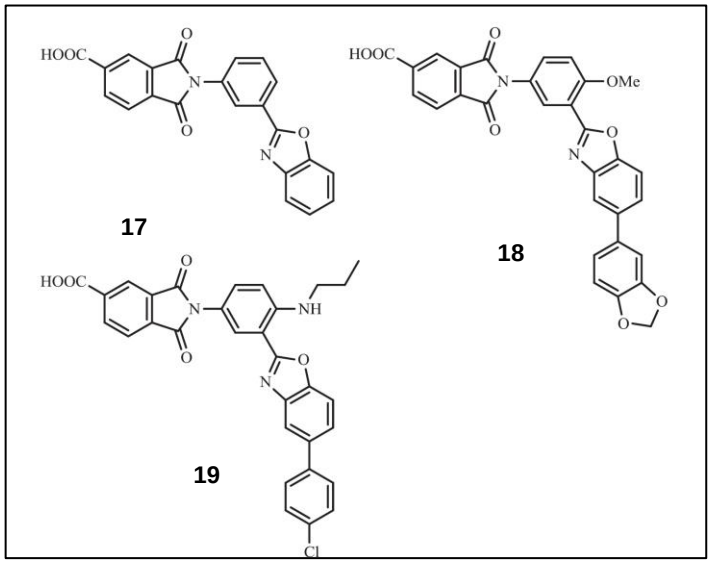

Figure 1.19 Structure of several benzoaxazoles known to inhibit HPSE
These compounds were identified through a high throughput drug screen. Compounds 17-19 exhibited potent inhibition of HPSE activity and angiogenesis (Jia and Ma, 2016).

1.26.11 Quinolines

Amodiaquines are known for their anti-malarial properties. Interestingly, these have been shown to inhibit HPSE activity **(figure 1.20)**. A subset of fourteen 4-arylaminoquinolines were selected from a set of amodiaquine analogues, based on a virtual library screen, *in silico* modelling, solubility prediction and chemical diversity analysis (Gozalbes et al., 2013).

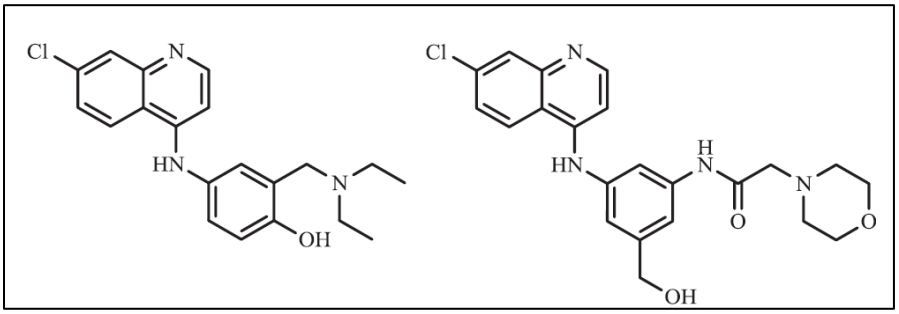

Figure 1.20 Structure of quinolones

1.26.12 Natural products

Several natural compounds with HPSE-inhibitory activity have reportedly been isolated. The eosinophil major basic protein (MBP) was the first naturally-occurring HPSE-inhibiting protein identified (Temkin et al., 2004). The presence of MBP in cellular granules suggests a protective function of eosinophils in inflammation and cancer. Trachyspic acid, a metabolic product of *Talaromyces trachyspermus*, was shown to inhibit tumour-cell HPSE, with its first total synthesis reported by Hirai *et al*. (Shiozawa et al., 1995, Hirai et al., 2003). Fungal metabolites CRM646-A and -B isolated from *Acremonium* species MT70646 demonstrated HPSE inhibition (Ko et al., 2000). Subsequent *in vitro* data suggested a potent anti-invasion effect of both compounds and total synthesis was achieved shortly afterwards (Wang et al., 2005). Based on structural information and rational drug design, (R)-3-hexadecanoyl-5-hydroxymethyltetronic acid (RK-682), isolated from *Acinomycete* strain DSM 7357 and *Streptomyces* species was shown to possess HPSE-inhibitory action (Ishida et al., 2004).

Name	Type and mode of action	Clinical trial/s	Comments
PI-88 (muparfostat)	HS mimetic, inhibits HPSE, FGF and VEGF.	Phase III, HCC (NCT01402908) Phase I/II, melanoma (NCT00068172)	Patient recruitment terminated at interim analysis. Disease-free survival was not significantly improved. No reported clinical outcomes yet.
PG545 (pixatimod)	HS mimetic, inhibits HPSE, FGF and VEGF.	Phase I, solid tumours (NCT01252095) Phase I, safety and tolerability (NCT02042781)	Terminated due to injection site reactions. No reported clinical outcomes yet.
SST0001 (Roneparstat)	Heparin mimetic, inhibits HPSE, FGF and VEGF.	Phase I, multiple myeloma (NCT01764880)	No clinical efficacy was demonstrated.
M402 (necuparanib)	Modified heparin. Inhibits HPSE, FGF and VEGF.	Phase I/II, metastatic pancreatic cancer (NCT01621243)	Terminated due to lack of efficacy.
Sulphated oligosaccharides	Various compounds, inhibit HPSE and growth factor signalling.	None	Clinical studies are yet to commence
Defibrotide	Nucleic acid-based inhibitor, downregulates HPSE expression.	Phase I/II, multiple myeloma (NCT00406978)	No reported clinical outcomes yet.
OGT2115	Small molecule inhibitor	None	Clinical studies are yet to commence
Suramin	Small molecule inhibitor	None	Clinical studies are yet to commence
Heterocyclic compounds	Molecules with a carboxylic acid group, a benzoxazole ring and an isoindole-5-carboxylic acid moiety	None	Clinical studies are yet to commence
Quinolines	Amodiaquines, bind to HPSE and inhibit activity	None	Clinical studies are yet to commence
Natural products	Inhibit HPSE activity	None	Clinical studies are yet to commence
Anti-HPSE antibodies	Inhibit HPSE activity	None	Clinical studies are yet to commence
HPSE vaccinations	Cytotoxic T cell response against HPSE peptides	None	Clinical studies are yet to commence

Table 1.4 Key HPSE inhibitors currently in development
This indicates the type of inhibitor, mode of action, the clinical trial phases which the inhibitors progressed to, along with the outcome.

1.26.13 Anti-HPSE antibodies

Recently, it was reported that the use of HPSE-neutralising antibodies resulted in attenuated lymphoma growth and metastasis in a pre-clinical study (Weissmann et al., 2016). This is the first observation of its kind and it is interesting to note that the antibodies were shown to neutralise HPSE in the TME rather than the tumour cells, which did not exhibit HPSE activity. This highlights the importance of targeting HPSE not only expressed by the primary tumour itself, but also by the components of the TME.

1.26.14 HPSE vaccinations

The overexpression of HPSE in pathological settings forms the basis for the development of vaccines for therapeutic use. A cytotoxic T cell response *in vitro* was shown to be elicited by HPSE peptides (Tang et al., 2010). Recently, a B cell multiple antigen peptide vaccine approach demonstrated a reduction in HPSE activity as well as VEGF and FGF2 expression, which resulted in reduced angiogenesis and tumour volume in a mouse HCC model (Zhang et al., 2015b). Additionally, a T cell-based vaccine demonstrated HPSE-specific anti-tumour activity both *in vitro* and *ex vivo* (Tang et al., 2014b).

1.27 Aims and nature of this thesis

As a major regulator of the ECM and a proven promoter of malignant disease, HPSE has garnered interest over the previous decades. Extensive clinical, *in vitro* and *in vivo* studies have established HPSE as a potent drug target in a number of disease settings, including cancer. All human cancers overexpress HPSE with a clear correlation demonstrated between its expression and patient survival.

Breast cancer is a major health concern amongst women worldwide with one in eight Australian women being diagnosed by their 85th birthday. Although numerous studies have demonstrated the role of HPSE in breast cancer progression, there is a lack of robust, loss-of-function *in vivo* genetic ablation models to elucidate its precise role in the mammary TME. In chapter 3 of this thesis, the well-characterised PyMT-MMTV mouse model of spontaneous mammary tumour development is used to observe tumour progression over time. To our knowledge, no other study has employed a HPSE-deficient spontaneous mouse mammary tumour model. The role of HPSE in tumour progression and metastasis in the PyMT-MMTV model is described along with the effects of HPSE in early mammary tumour establishment, which has remained largely unexplored. Interestingly, the progression of breast cancer in a HPSE-independent manner in the PyMT-MMTV mouse model was observed during the course of this study.

Chapter 4 addresses the role of the TME in modifying HPSE expression in primary mammary tumours. The stroma has emerged as an undeniable regulator of tumour growth, with HPSE-mediated crosstalk amongst the many TME components. By using HPSE-deficient C57Bl/6 mice (C57Bl/6xHPSE$^{-/-}$), this relationship is explored. Although a clear association between the stroma and tumour cells exists with respect to HPSE activity, this did not translate to overall tumour growth. The findings of this chapter echo those of the preceding chapter.

Finally, chapter 5 characterises novel, first-generation HPSE inhibitors. With the recent interest in the use of HPSE inhibitors in the clinic, this chapter provides *in vitro* and *in vivo* characterisation data of novel drug candidates.

The overall findings of chapters 3 and 4 of this thesis have been unexpected, based on published literature, which raises the possibility that HPSE in certain cancer settings may not play a major role as originally assumed. This critical observation coupled with the fact that in some settings such as in NK cell tumour immunosurveillance, HPSE has been shown to act against tumour establishment, present challenges in the use of HPSE inhibitors in the clinic.

Chapter 2

Materials and methods

2.1 Mice

2.1.1 Generation of PyMT-MMTVxHPSE$^{-/-}$ and other mouse strains

All *in vivo* animal procedures were performed in compliance with the Australian National Health and Medical Research regulations. All procedures were reviewed and approved by the La Trobe University Animal Ethics Committee. Animals were housed at the La Trobe University Animal Research and Training Facility (LARTF) with dedicated technicians appointed to allocate food, drink and bedding as needed. Mice were housed in a sterile physical containment level-2 facility with a 12 h night and day cycle, ambient temperature regulation and sterile filtered air delivered directly to individual cages.

C57Bl/6xHPSE$^{-/-}$ mice were generated as previously described **(figure 2.1)** (Poon et al., 2014). Briefly, mice with a LoxP *HPSE* gene were produced using a targeting construct incorporating exon 1 of mouse *HPSE* flanked by two LoxP sites and a neomycin resistance (*neo*^{R}) gene which enabled selection. This construct was electroporated into C57Bl/6 embryonic stem (ES) cells and screened for neomycin resistance (*neo*^{R}). Polymerase chain reaction (PCR) and Southern blot confirmed the targeting of the construct into *HPSE* by homologous recombination. Chimeric mice were produced by injecting the ES cells into wildtype albino C57Bl/6 blastocysts. These mice were bred with albino C57Bl/6 wildtype mice to result in germline transmission and *HPSE*-LoxP$^{+/-}$ mice. These *HPSE*-LoxP$^{+/-}$ mice were bred with C57Bl/6 TNAP-Cre mice to delete the exon 1 of *HPSE* and *neo*^{R}. The deletion of floxed genes was enabled by the excision during early development in primordial germ cells of TNAP-Cre mice. The resultant heterozygotes were crossed to generate C57Bl/6xHPSE$^{-/-}$ mice.

PyMT-MMTV mice are transgenic animals where the robust **p**oly**o**mavirus **m**iddle-**t**umour oncogenic antigen (PyMT) expression is driven by the MMTV promoter's long terminal repeat (LTR) regulatory sequence (Guy et al., 1992). This oncogenic expression transforms mouse cells and give rise to cancer (Lee et al., 2011, Kiefer et al., 1994, Dilworth, 2002, Schaffhausen and Roberts, 2009). To generate PyMT-MMTVxHPSE$^{-/-}$ mice, male PyMT-MMTV mice (on a C57Bl/6 genetic background, kindly provided by Associate Professor Belinda Parker) were crossed with female C57Bl/6xHPSE$^{-/-}$ mice **(figure 3.1A)**. The resultant male PyMT-MMTVxHPSE$^{+/-}$ mice were then crossed with female C57Bl/6xHPSE$^{+/-}$ mice. This gave rise to an F2 progeny of six distinct genetic backgrounds; C57Bl/6, C57Bl/6xHPSE$^{-/-}$, C57Bl/6xHPSE$^{+/}$, PyMT-MMTV, PyMT-MMTVxHPSE$^{-/-}$ and PyMT-MMTVxHPSE$^{+/-}$. Of these, animals of four genotypes were chosen for subsequent mating and experiments, namely C57Bl/6, C57Bl/6xHPSE$^{-/-}$, PyMT-MMTV and PyMT-MMTVxHPSE$^{-/-}$. For breeding purposes, male PyMT-MMTV or PyMT-MMTVxHPSE$^{-/-}$ mice were crossed with female C57Bl/6 or C57Bl/6xHPSE$^{-/-}$ mice

respectively, as required. For ethical reasons, female PyMT-MMTV and PyMT-MMTVxHPSE$^{-/-}$ mice were not used in mating as these animals would develop spontaneous mammary tumours, hindering their nursing capability.

2.1.2 Genotyping strategy

In order to maintain the mouse colony, pups were genotyped at approximately 21-days of age. Mouse ear tissue were obtained as a by-product of ear clipping identification carried out by LARTF. These clippings were digested at 95ºC in 50 mM NaOH with frequent mixing for 12-15 min. The digestion was promptly neutralised with the addition of 1/6 volumes of Tris-HCl (1.0 M, pH 8.0) per reaction. PCR was performed using GoTaq® Green master mix (M7123, Promega) in a total volume of 20 µl per primer pair. Primer pairs used are listed in table 2.1, with a fatty acid-binding protein, intestinal (Fabpi) internal control. Each individual sample obtained from an animal was subjected to four distinct PCR reactions to confirm the status of four distinct targets; PyMT-MMTV, HPSE$^{+/+}$, HPSE$^{-/-}$ and Fabpi. A final concentration of 1 µM of primer was obtained in a total reaction volume of 20 µl per sample, performed in a 96-well PCR plate (4ti-0750/TA, 4titude, supplied with PCR strip caps, 4ti-0751, 4titude). The reaction was carried out with the following temperature profile; an initial denaturation step of 95ºC for 5 min, 35 cycles of 95ºC for 30 sec, 60ºC for 30 sec, 72ºC for 25 sec, a final extension cycle of 72ºC for 10 min, followed by a holding temperature of 4ºC (T-100 thermocycler, Bio-Rad).

Target/ size	Forward (Fwd) primer (5'-3')	Reverse (Rev) primer (5'-3')
PyMT-MMTV (260 bp)	AGGAACCGGCTTCCAGGTAAGA	TTGGTGTTCCAAACCATTGCAT
HPSE$^{+/+}$ (143 bp)	GAAGAACCATTATTCATCTTGCT	CCAAGTGCCAGTCTGCAAGT
HPSE$^{-/-}$ (300 bp)	GGGATGGATGCAGGTCTTC	CAGATGGGTGCAGATTAGATAT
Fabpi (200 bp)	TGGACAGGACTGGACCTCTGCTTTCCTAGA	TAGAGCTTTCGGACATCACAGGTCATTCAG

Table 2.1 Mouse genotyping oligonucleotide primer sequences
Four primer combinations were used to determine mouse genotypes with a Fabpi internal control (See Figure 2.1).

The reaction products were loaded directly onto a 1% (w/v) agarose gel in TBE buffer [50 mM Tris base, 100 mM borate, 10 mM ethylenediaminetetraacetic acid (EDTA), pH 8.2] and subjected to electrophoresis alongside the 1 Kb Plus DNA ladder (10787018, ThermoFisher Scientific). The products were viewed and photographed with a G:BOX Chemi XL1.4 Fluorescent and Chemiluminescent imaging system (Syngene).

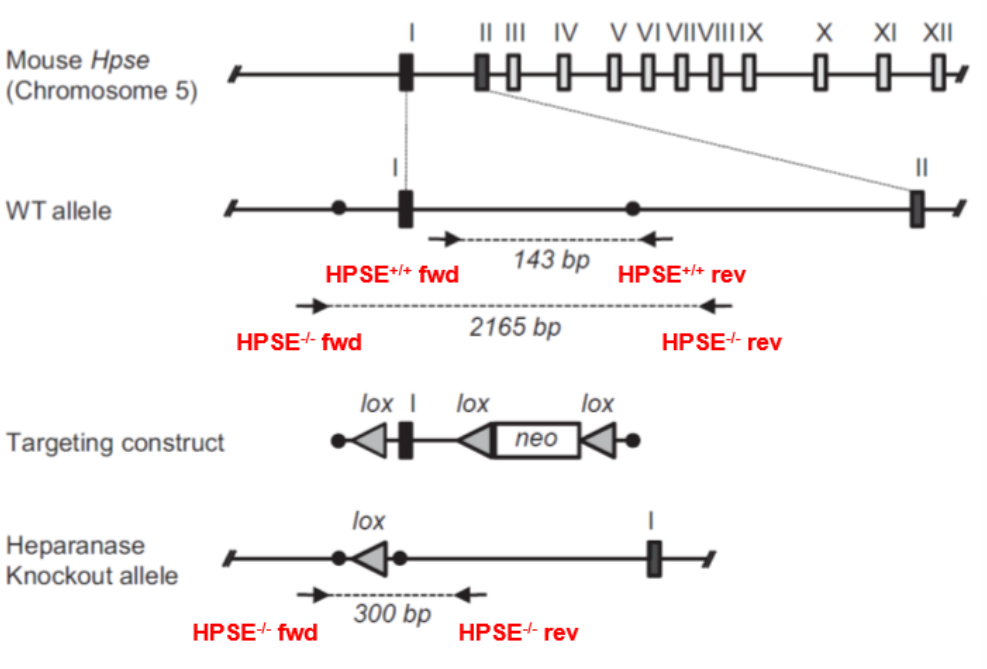

Figure 2.1 Strategy used to generate C57Bl6xHPSE$^{-/-}$ mice
The targeting construct used to introduce the *HPSE* exon-1-flanking LoxP sites and the *neo*^{R} is shown along with the binding sites for HPSE$^{+/+}$ and HPSE$^{-/-}$ primer pairs (Poon et al., 2014).

2.1.3 Dissection of mammary glands and mammary tumours of female PyMT-MMTV and PyMT-MMTVxHPSE$^{-/-}$ mice

Female PyMT-MMTV and PyMT-MMTVxHPSE$^{-/-}$ were humanely euthanised with a manual cervical dislocation. Animals were pinned in a supine position followed by performing a vertical incision from the base of the tail to the base of the neck. The skin was separated from its underlying connective tissue using a blunt dissection technique and was peeled back and away from the peritoneal cavity. The mammary glands are located on the inner surface of the skin; the cervical (1st), thoracic (2nd and 3rd) and inguinal (4th and 5th), totalling ten mammary glands per mouse. The 2nd and 3rd thoracic mammary glands are indistinct from one another and were therefore excised together as one for analysis.

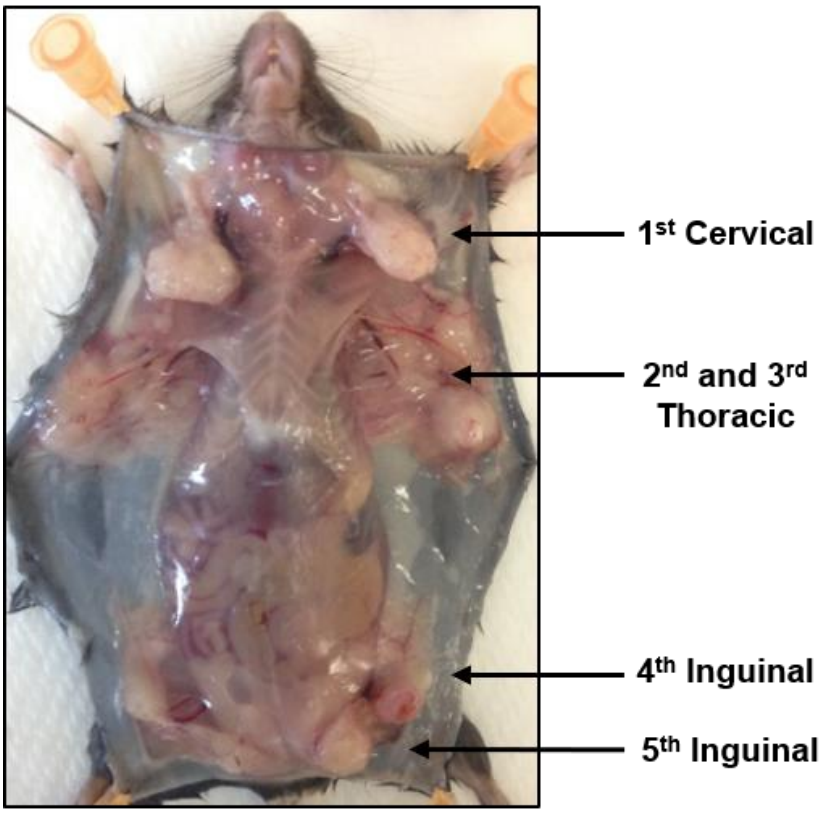

Figure 2.2 The mammary gland anatomy of a PyMT-MMTV mouse
A female PyMT-MMTV mouse bearing mammary tumours on all mammary glands is shown.

2.1.4 Mammary tumour measurements

Mouse mammary tumours were measured 2 – 3 times weekly with the use of electronic callipers and employing the formula (length x width^2)/2 mm^3. A total cumulative tumour volume of $\geq$1500 mm^3 was considered the ethical end point.

2.1.5 Orthotopic mammary tumour cell inoculation and tumour measurements

A single-cell suspension of 10^6 PyMT3 cells in sterile phosphate-buffered saline (PBS) in a total volume of 20 µl was implanted into the 4th right inguinal mammary fat pad of 8 – 12-week-old female mice under isoflurane-induced anaesthesia. Once anesthetised, the mice were connected to a nose cone for the continuous delivery of isoflurane and the 4th inguinal mammary fat pad was located by palpating. The cell suspension was injected directly into the mammary fat pad via a 27G needle (Terumo) attached to a Hamilton® gastight syringe (1705LT, Hamilton). Immediately following the injection, mice were removed from the nose cone and allowed to rapidly recover under close observation.

2.1.6 Surgical resection of induced orthotopic PyMT mammary tumours

Induced orthotopically-implanted mammary tumours were surgically resected at a volume of 500 mm^3. The animals were anaesthetised by the intraperitoneal administration of ketamine (86 mg/kg) and xylazine (17 mg/kg) using a 27G needle (Terumo) as per LARTF guidelines. Buprenorphine (0.1 mg/kg) was administered as pain relief with a 27G needle (Terumo) subcutaneously at the nape of the neck. Anaesthesia was confirmed by the complete lack of a withdrawal of a paw from an interdigital pinch. The surgical area was shaven with a pet trimmer (WAHL), cleaned and sterilised with ethanol swabs. An incision was made just below the tumour growth and the incision was widened with a blunt dissection. The tumour was separated from its underlying mammary fat pad taking extra precautions not to penetrate the peritoneum. Following the excision of the tumour, the surgical wound was closed with wound clips (7 mm Reflex Clip, RF7 KIT, Braintree Scientific Inc) or with skin sutures. The animals were closely monitored until conscious and mobile and were left to recover on a heated recovery pad for 16 h.

2.2 HPSE

2.2.1 HPSE enzymatic activity assay

A TR-FRET-based assay was employed. The substance with unknown enzymatic activity was diluted at a 1:1 ratio in buffer (20 mM Tris-HCl, 0.15 M NaCl, 0.1% CHAPS; [3-((3-cholamidopropyl)-dimethylammonio)-1-propanesulfonate, pH 5.5) followed by the addition of Biotin-HS-Eu(K) (0.7 µg/ml Biotin-HS-Eu(K), 0.2 M $NaCH_3CO_2$, pH 5.5) with the reaction incubated at 37°C for 2 h. Streptavidin-conjugated XL665 [1 µg/ml Strepavidin-XL665, 0.1 M $NaPO_4$, pH 7.5,1.2 M KF, 0.1% (w/v) BSA, 2.0 mg/ml heparin] was then added followed by an incubation in the dark for 16 h at room temperature. Using a spectrophotometer, excitation at 315 nm and emission at both 620 and 668 nm was measured. The percentage of HS degradation was calculated relative to fluorescence resonance energy transfer (FRET)-negative or positive samples (absence or presence of XL665-conjugated Streptavidin in the absence of purified HPSE).

In the screening of known and potential HPSE inhibitors, purified HPSE was pre-incubated with the inhibitor for 10 min at 37ºC prior to the addition of the substrate.

2.2.2 Purification of human HPSE from platelets and downstream validation

A modified HPSE purification procedure based on a previously described method of isolation of human HPSE from platelets was used (Freeman and Parish, 1998). Expired platelets were collected from the Australian Red Cross Blood Service (with appropriate human ethics approval) and collected by centrifuging at 1,600 *g* for 20 min at 20ºC. The pellet was then washed in saline [0.9% (w/v) sodium chloride (NaCl) in sterile PBS]

by gently distributing the pellet with a wide disposable pipette. A total of four washes were performed. The final pellet was resuspended in an appropriate volume of DMG buffer (15 mM dimethyl glutarate, pH 6.0) and stored at -80ºC until needed.

A total of 50 – 100 units of platelets were pooled for the large-scale purification of HPSE. The pooled platelets were resuspended in DMG buffer (15 mM dimethyl glutarate, pH 6.0) and subjected to three freeze-thaw cycles using liquid N_2 and a 37ºC water bath. The lysate was centrifuged at 35,000 *g* for 1 h at 4ºC. The supernatant was then collected and stored at 4ºC. The pellet was resuspended in 4 volumes of DMG buffer (15 mM dimethyl glutarate, pH 6.0) followed by three freeze-thaw cycles. The supernatant was collected by centrifugation at 35,000 *g* for 1 h at 4ºC. The resuspension of the pellet followed by a freeze-thaw cycle was performed once more and the supernatant was collected, with the pellet discarded. The collected supernatant fractions were pooled and centrifuged at 35,000 *g* for 30 min at 4ºC to remove any remaining debris. The supernatant following this clarification step was made up to contain a final concentration of 0.2% (v/v) Triton X-100 (11332481001, Roche) and 1 mM $CaCl_2$/$MnCl_2$. A concanavalin-A (con-A) sepharose 4B (17044001, GE Healthcare) column (dimensions of 1.5 cm x 5 cm) was equilibrated with one volume (20 ml) of buffer B [DMG buffer (15 mM dimethyl glutarate, pH 6.0), supplemented with 0.2% (v/v) Triton X-100 (11332481001, Roche)] at a rate of 1 ml/min with the use of a programmable pump (MINIPULS 3, Gilson) at 4ºC. The pooled supernatant was allowed to flow through the column at a rate of 1 ml/min at 4ºC. The column was then washed with 1.25 volumes of buffer B [DMG buffer (15 mM dimethyl glutarate, pH 6.0), supplemented with 0.2% (v/v) Triton X-100 (11332481001, Roche)] followed by 4 volumes of buffer A [DMG buffer (15 mM dimethyl glutarate, pH 6.0), supplemented with 0.5 M NaCl] at 4ºC. The column was then removed from 4ºC to room temperature and washed further with 2 volumes of buffer A [DMG buffer (15 mM dimethyl glutarate, pH 6.0), supplemented with 0.5 M NaCl, stored at room temperature] at a rate of 1 ml/min. The protein was eluted in 2 volumes of buffer A [DMG buffer (15 mM dimethyl glutarate, pH 6.0), supplemented with 0.5 M NaCl, stored at room temperature] further supplemented with 20% (w/v) α-methyl mannoside (M6882, Sigma-Aldrich) at a rate of 1 ml/min.

The remainder of the procedure was carried out at 4ºC. The eluted protein was added to a Zn^{2+}-chelating sepharose (GE Healthcare) column (dimensions 1 cm x 10 cm) connected in series to a blue-A agarose (GE Healthcare) column (dimensions 1 cm x 2 cm) at a rate of 1 ml/min. The columns were washed with 2.5 volumes of buffer A [DMG buffer (15 mM dimethyl glutarate, pH 6.0), supplemented with 0.5 M NaCl] followed by the blue-A agarose column being individually washed with 1 volume of Tris buffer [60 mM Tris-HCl, pH 7.2, supplemented with 10% (v/v) glycerol] containing 0.5 M NaCl. The column was then

washed again with 1 volume of Tris buffer [60 mM Tris-HCl, pH 7.2, supplemented with 10% (v/v) glycerol] containing 0.8 M NaCl. The blue-A agarose column was then connected in series to an octyl-agarose (GE Healthcare) column (dimensions 1 cm x 1.5 cm) pre-equilibrated with Tris buffer [60 mM Tris-HCl, pH 7.2, supplemented with 10% (v/v) glycerol] containing 2 M NaCl. The HPSE was eluted from the blue-A agarose column at a rate of 0.5 ml/min with 0.75 volumes of Tris buffer [60 mM Tris-HCl, pH 7.2, supplemented with 10% (v/v) glycerol] containing 2 M NaCl. The resultant purified HPSE was concentrated further by centrifugation with a centrifugal filter unit (UFC803024, Amicon® Ultra-4, Merck, with a molecular weight cut-off of 30 kDa) to approximately 1/15th of the eluted volume. This was followed by further downstream validation.

2.2.2.1 Validation of purified HPSE by gel electrophoresis

Following the purification of human HPSE, the concentration of the eluted protein was determined by a spectrophotometer (NanoDrop 1000, ThermoFisher). Loading dye (NuPAGE™ LDS sample buffer, 4X, NP0007, ThermoFisher Scientific) and denaturing agent (NuPAGE™ sample reducing agent, 20X, NP0004) were added to the protein to a total volume of 20 µl and boiled for 5 min at 95ºC. The denatured protein sample was then loaded onto a NuPAGE™ 4 – 12% Bis-Tris pre-cast protein gel (NP03335BOX, ThermoFisher Scientific) along with purified human HPSE as a control and subjected to electrophoresis. The gel was stained with Coomassie blue [0.1% (w/v) Brilliant blue R-250 (B0149, Sigma-Aldrich), 45.45% (v/v) methanol (106018, Merck), 9.09% (v/v) acetic acid (100063, Merck)] followed by treatment with a de-staining solution [7.5% (v/v) acetic acid (100063, Merck), 10% (v/v) ethanol]. The stained gels were photographed using the G:BOX Chemi XL1.4 Fluorescent and Chemiluminescent imaging system (Syngene).

2.2.2.2 Validation of purified HPSE by Western blot

Loading dye (NuPAGE™ LDS sample buffer, 4X, NP0007, ThermoFisher Scientific) and denaturing agent (NuPAGE™ sample reducing agent, 20X, NP0004) were added to the eluted HPSE to a total volume of 20 µl, boiled at 95ºC for 5 min and loaded onto a NuPAGE™ 4 – 12% Bis-Tris pre-cast protein gel (NP03335BOX, ThermoFisher Scientific) along with purified human HPSE as a control and subjected to electrophoresis. The resolved gel was transferred onto a Nitrocellulose membrane (10600001, GE Healthcare) using an XCell Sure Lock™ electrophoresis system (ThermoFisher Scientific) in NuPAGE transfer buffer (NP00061, ThermoFisher Scientific). The membrane was then blocked in 5% (w/v) skim milk in PBS for 1 h at room temperature. Incubation with the primary anti-HPSE antibody (1:500 working concentration, 2 µg/ml, rabbit polyclonal, AB85543, Abcam) was performed at 4ºC for 16 h in 5% (w/v) skim milk in 0.1% (v/v) Tween-20/PBS. The membrane was then washed in 0.1% (v/v) Tween-20/PBS, three times, with 10 min per wash. The bound primary antibody was detected by using a

secondary anti-rabbit IgG (1:2,000 working concentration, 0.5 µg/ml, donkey, NA934, GE Healthcare) in 5% (w/v) skim milk in 0.1% (v/v) Tween-20/PBS for 1 h at room temperature. Chemiluminescence detection was then performed using the Pierce ECL Western blotting substrate (32106, ThermoFisher scientific).

2.2.2.3 Validation of purified HPSE by the HPSE enzymatic activity assay

The purified HPSE was subjected to an enzymatic activity assay as described in 2.2.1

2.2.2.4 Validation of purified HPSE by mass spectrometry

Mass spectrometry analysis was performed by the La Trobe Institute for Molecular Science Proteomics facility at La Trobe University. Purified HPSE was reduced with 10 mM dithiothreitol (DTT-RO, Roche) for 1 h at 60ºC followed by alkylation with 30 mM iodoacetamide (I1149, Sigma-Aldrich) for 20 min at room temperature. Trypsin digestion was then carried out with 1 µg of trypsin for 2 h at 37ºC. The digested protein was then dried in a centrifugal evaporator (Speedvac, Thermo Scientific) followed by the analysis of the resulting peptides on an Ultraflex III Maldi-TOF-TOF-MS mass spectrometer (Bruker-Daltonics). The peptides thus recorded were analysed on a data analysis software (Bruker-Daltonics) followed by determining the identity of the proteins(s) using the Bio Tools program (Bruker-Daltonics).

2.2.3 Detection of mouse splenic HPSE by Western blot

The spleen is a rich source of HPSE. Spleens from 10 – 12-week old female PyMT-MMTV and PyMT-MMTVxHPSE$^{-/-}$ were harvested, snap-frozen in liquid N_2 and stored at -80ºC. These were then homogenized in Cytobuster™ protein extraction reagent (500 µl per spleen, 71009, Merck) using a metal bead lysing matrix (6925-050, MP bio) and with high speed disruption using a FAST-PREP-24™ instrument (SKU 116004500, MP bio). The lysate was centrifuged at 10,000 *g* for 10 min at 4ºC. A protein concentration estimation was performed as per manufacturer's instructions (Pierce™ BCA protein assay kit, 23225, ThermoFisher scientific). A total of 1.5 mg of protein content per individual spleen was incubated with 20 µl of washed con-A sepharose 4B beads (17044001, GE Healthcare) at 4ºC for 16 h with continuous rotation. The supernatant was then separated from the beads by being centrifuged at 300 *g* for 3 min at 4ºC and discarded. The beads were washed in PBS twice with centrifugation at 300 *g* for 3 min at 4ºC in between washes. Loading dye (NuPAGE™ LDS sample buffer, 4X, NP0007, ThermoFisher Scientific) and denaturing agent (NuPAGE™ sample reducing agent, 20X, NP0004) were added to the beads in a total volume of 20 µl, boiled at 95ºC for 5 min. The con-A beads were separated from the supernatant by centrifuging at 300 *g* for 3 min at room temperature. The supernatant was then loaded onto a NuPAGE™ 4 – 12% Bis-Tris pre-cast protein gel (NP03335BOX, ThermoFisher Scientific) along with purified human HPSE as a control

and subjected to electrophoresis. The resolved gel was transferred onto a Nitrocellulose membrane (10600001, GE Healthcare) using an XCell Sure Lock™ electrophoresis system (ThermoFisher Scientific) in NuPAGE transfer buffer (20X, NP00061, ThermoFisher Scientific). The membrane was then blocked in 5% (w/v) skim milk in PBS for 1 h at room temperature. Incubation with the primary anti-HPSE antibody (1:500 working concentration, 2 µg/ml, rabbit polyclonal, AB85543, Abcam) was performed at 4ºC for 16 h in 5% (w/v) skim milk in 0.1% (v/v) Tween-20/PBS. The membrane was then washed in 0.1% (v/v) Tween-20/PBS, three times, with 10 min per wash. The bound primary antibody was detected by using a secondary anti-rabbit IgG (1:2,000 working concentration, 0.5 µg/ml, donkey, NA934, GE Healthcare) in 5% (w/v) skim milk in 0.1% (v/v) Tween-20/PBS for 1 h at room temperature. Chemiluminescence detection was then performed using the SuperSignal™ West Femto reagent (34096, ThermoFisher scientific).

2.2.4 Measurement of HPSE activity of mouse splenic lysate

Animals at 10 – 12 weeks of age were euthanised with the spleen rapidly harvested and stored in ice-cold RPMI medium (11875093, ThermoFisher Scientific) supplemented with 10% (v/v) foetal calf serum (FCS, SFBSNZ, Interpath). The spleen was punctured at either end with a 23G needle and the splenic cellular content flushed out with PBS. The cells were separated from tissue debris by passing through a 70 µm strainer and collected by centrifuging at 400 *g* for 4 min at 4ºC. The cell pellet was resuspended in red blood cell (RBC) lysis buffer (155 mM NH_4Cl, 12 mM $NaHCO_3$, 0.1 mM EDTA) and incubated for 5 min at room temperature. Lysed RBCs were removed by centrifuging at 400 *g* for 4 min at 4ºC. The resulting cell pellet was lysed by resuspending in Cytobuster™ protein extraction reagent (71009, Merck, approximately 200 µl per splenocyte sample) and incubating at 4ºC. Cellular debris was then separated by centrifuging at 16,000 *g* for 10 min at 4ºC. The supernatant was collected and subjected to protein quantification as per manufacturer's instructions (Pierce™ BCA protein assay kit, 23225, ThermoFisher scientific). Equal amounts of total cellular protein were used in the HPSE enzymatic activity assay.

2.2.5 Measurement of HPSE activity of mouse mammary tumours

Excised mammary tumours were homogenised in 1% (w/v) CHAPS/DMG [CHAPS; C3023, Sigma-Aldrich. DMG; 3,3-dimethylglutaric acid, D4379, Sigma-Aldrich] using a metal bead lysing matrix (6925-050, MP bio) and with high speed disruption using a FAST-PREP-24™ instrument (SKU 116004500, MP bio). The homogenates were then subjected to three freeze/thaw cycles using liquid N_2 and a 37ºC water bath. Cellular debris was removed by centrifugation at 10,000 *g* for 10 min at 4ºC. The supernatant was collected and a protein concentration estimation was performed as per manufacturer's instructions

(Pierce™ BCA protein assay kit, 23225, ThermoFisher scientific). Equal amounts of total cellular protein (50 µg) was then subjected to the HPSE enzymatic activity assay.

2.3 Histology

2.3.1 Paraffin embedding

Excised organs and tissue were fixed in 10% neutral buffered formalin at ≥20 times the volume of the tissue for 24 h at room temperature (as required, organs such as lungs were perfused with PBS prior to being fixed in order to remove excess blood). The samples were then individually placed in cassettes (10-0114L, Grale) and processed for approximately 12 h in a tissue processor (TP1020, Leica biosystems) as follows: 70% ethanol, 1 h; 100% ethanol, 1 h; 100% ethanol, 1 h; 100% ethanol 1.5 h; 100% ethanol, 1.5 h; xylene, 1 h; xylene 1 h; xylene, 1 h; xylene, 1.5 h; paraffin wax (1151612504, Merck) (60ºC), 1 h; paraffin wax (60ºC), 1 h and paraffin wax (60ºC), 1 h. The samples were then embedded using a tissue embedding centre (EG1150, Leica) and base moulds (Tissue-Tek) and left to set at room temperature.

2.3.2 Paraffin sectioning

Paraffin blocks were sectioned with low-profile disposable blades (14035838382, Leica) to collect 4 µm-thick sections using a manual rotary microtome (RM2235, Leica). Paraffin blocks were first placed in a 37ºC histology water bath (HI1210, Leica) then transferred to wet ice for the remainder of the procedure. Between each round of sectioning, the blocks were returned promptly to wet ice to remain cold and hydrated. Tissue sections were placed on the surface of the water in the histology water bath and collected on to electrostatically charged adhesion slides (SF41296SP SuperFrost™, Thermo Scientific). The slides were then dried for 16 h in a 37ºC incubator.

2.3.3 H&E staining

H&E staining of paraffin sections were performed by incubating slides in a series of reagents using a manual staining station comprised of staining buckets (4456 and 4457, Tissue-Tek). The staining protocol was as follows: histolene (11031, Grale), 3 min; histolene, 3 min; histolene 3 min; 100% ethanol, 1 min; 100% ethanol, 1 min; 100% ethanol, 1 min; 70% ethanol, 30 sec; distilled water, 1 min; haematoxylin (MH-500, Amber Scientific), 4 min; distilled water, 1 min; distilled water, 1 min; Scotts tap water substitute (SCOT-5L, Amber Scientific), 45 sec; distilled water, 2 min; eosin (EOA1-5L, Amber Scientific), 4 min; distilled water, 15 sec; 100% ethanol, 45 sec; 100% ethanol, 45 sec; 100% ethanol, 45 sec; histolene, 3 min; histolene, 3 min and histolene, 3 min. Mounting medium (Entellan, 107960, Merck) was added on to the section prior to placing cover slips (24x50 mm, Menzel Gläser). The slides were then dried for 16 h at room temperature.

2.3.4 Immunohistochemistry (IHC)

Paraffin section slides were first de-waxed as follows: histolene (11031, Grale), 4 min; histolene, 4 min; histolene, 3 min; 100% ethanol, 1 min; 100% ethanol, 1 min; 100% ethanol, 1 min; 70% ethanol, 1 min and re-hydrated in distilled water. If required, antigen retrieval was performed in a de-cloaking chamber (DC2012, Biocare Medical) for 5 min at 5 psi and at 110ºC in sodium citrate ($Na_3C_6H_5O_7$, S1804, Sigma-Aldrich) retrieval buffer (10mM, pH 6.0). The slides were then cooled to room temperature. Endogenous peroxidase was blocked by incubating the slides in a solution of 1% (v/v) hydrogen peroxide (H_2O_2, 30%, 107209, Merck) in methanol. The sections were blocked in 3% (v/v) normal goat serum (G9023, Sigma-Aldrich) in 0.1% (v/v) Tween-20/PBS for 1 h at room temperature, in a humidified chamber. Avidin/biotin blocking was performed using a kit (AB64212, Abcam) by incubating the section in individual avidin and biotin blocking solutions for 15 min each as per manufacturer's instructions. The primary antibody was prepared in blocking solution (3% (v/v) normal goat serum (G9023, Sigma-Aldrich) in 0.1% (v/v) Tween-20/PBS), added on to the sections and incubated for 16 h at 4ºC in a humidified chamber. Slides were then washed gently in 0.1% (v/v) Tween-20/PBS three times, with 3 min per wash. The secondary antibody was added on to the sections and incubated for 1 h at room temperature in a humidified chamber. During this incubation period, the avidin-biotin-complex (ABC) solution (PK-4000, Vector Laboratories) was prepared (0.9% (v/v) solutions A and B in PBS) and incubated for 30 min at room temperature to form the ABC. The slides were washed twice in 0.1% (v/v) Tween-20/PBS followed by twice in PBS for 3 min per wash. The ABC solution was added onto the sections and incubated for 1 h at room temperature in a humidified chamber. The slides were washed twice in 0.1% (v/v) Tween-20/PBS followed by twice in PBS for 3 min per wash. The 3,3'-diaminobenzidine (DAB, SK-4100, Vector Laboratories) substrate solution was prepared as per manufacturer's instructions by adding 1 drop of buffer stock solution, 1 drop of the hydrogen peroxide (H_2O_2) solution and 2 drops of the DAB solution to 2.5 ml of Milli-Q® ultra-pure water. The DAB solution was added onto the sections and developed by observing under a light microscope until a prominent brown staining appeared. Control sections were used which lacked the primary antibody or which used an isotype control in order to detect and eliminate false-positive signals. Slides were placed in distilled water to stop the further development of the DAB stain signal. A counter-stain was performed as follows: distilled water, 1 min; haematoxylin (MH-500, Amber Scientific), 1-4 dips as required, depending on the intensity of the DAB stain; distilled water, 1 min; Scotts tap water substitute (SCOT-5L, Amber Scientific), 2 min; distilled water, 1 min; 100% ethanol,

Target	Antigen retrieval	Primary antibody	Secondary antibody
HPSE	De-cloaking chamber	Rabbit polyclonal anti-HPSE (10 µg/ml, 1:500 working concentration, AB85543, Abcam)	Biotinylated goat anti-rabbit IgG (H+L) (6 µg/ml, 1:250 working concentration, BA-1000, Vector Laboratories)
CD31	De-cloaking chamber	Rabbit polyclonal anti-CD31 (16 µg/ml, 1:50 working concentration, AB28364, Abcam)	Biotinylated goat anti-rabbit IgG (H+L) (6 µg/ml, 1:250 working concentration, BA-1000, Vector Laboratories)
Ki67	De-cloaking chamber	Rabbit polyclonal anti-Ki67 (1 µg/ml working concentration, AB15580, Abcam)	Biotinylated goat anti-rabbit IgG (H+L) (6 µg/ml, 1:250 working concentration, BA-1000, Vector Laboratories)
Smooth muscle myosin heavy chain (SMMHC)	De-cloaking chamber	Rabbit monoclonal anti-SMMHC (clone EPR5335, 1.2 µg/ml, 1:500 working concentration, AB124679, Abcam)	Biotinylated goat anti-rabbit IgG (H+L) (6 µg/ml, 1:250 working concentration, BA-1000, Vector Laboratories)
MMP-2	De-cloaking chamber	Rabbit polyclonal anti-MMP-2 (2 µg/ml working concentration, AB37150, Abcam)	Biotinylated goat anti-rabbit IgG (H+L) (6 µg/ml, 1:250 working concentration, BA-1000, Vector Laboratories)
Normal rabbit IgG (isotype control)	As required	IgG from rabbit serum (various working concentrations, 18140, Sigma-Aldrich)	Biotinylated goat anti-rabbit IgG (H+L) (6 µg/ml, 1:250 working concentration, BA-1000, Vector Laboratories)

Table 2.2 Antibodies used in IHC
Combinations of primary and secondary antibodies along with the conditions used in the detection of a variety of targets by IHC.

30 sec; 100% ethanol, 1 min; 100% ethanol, 2 min; histolene (11031, Grale), 4 min; histolene, 4 min and histolene, 4 min. The slides were then cover-slipped as described in 2.3.3. The IHC antibodies used in this thesis are listed on table 2.2.

2.3.5 Microvessel density quantification following anti-CD31 IHC

Tissue sections were made as described in 2.3.2. These were collected 100 – 200 μm apart in order to generate a more representative histology data stack per tissue sample. Photographs were taken under a light microscope.

2.3.5.1 Manual quantification of microvessels

Each image was divided into 10 – 12 grids or fields and the number of visible stained vessels were manually counted. An average vessel count per field was obtained by dividing the total number of visible microvessels counted by the number of fields employed per image.

2.3.5.2 Calculation of the %area of staining

The trainable Weka segmentation tool on the Fiji image analysis software (ImageJ) was used in the automated quantification of %area of stain. Photographs of sections were taken following IHC using a light microscope in high-quality TIF format. The colours of each image were deconvoluted using the H-DAB setting followed by selecting the DAB-specific image and auto-subtracting the background to enhance its quality. Positively stained regions of a single section were selected using the classifier tool, which was then able to automatically select similarly stained regions of all other images. Once the Weka segmentation tool had identified all positively stained regions of the image against the background, the resulting image was converted to a black and white image in order to digitally quantify particles. By creating regions of interest which enabled the elimination of non-specifically stained regions of the image, a reading of %area of stain of the selected area was obtained and used in statistical analysis.

2.3.6 Pathological grading of PyMT-MMTV and PyMT-MMTVxHPSE$^{-/-}$ mammary tumour development

Mammary glands stained with H&E were first analysed to determine the stage of mammary tumour development. Based on the appearance of the ductal structures observed on each individual section, a pathological grading of normal, hyperplasia, DCIS or invasive carcinoma was assigned to each mammary gland **(figure 2.3)**. In order to further validate the grading obtained by H&E staining, an anti-Ki67 staining was carried out to distinguish grades of hyperplasia, DCIS and invasive carcinoma from normal mammary ducts. Anti-SMMHC staining was employed to distinguish between DCIS and

invasive carcinoma. The total number of mammary glands bearing invasive carcinoma were determined and subjected to statistical analysis.

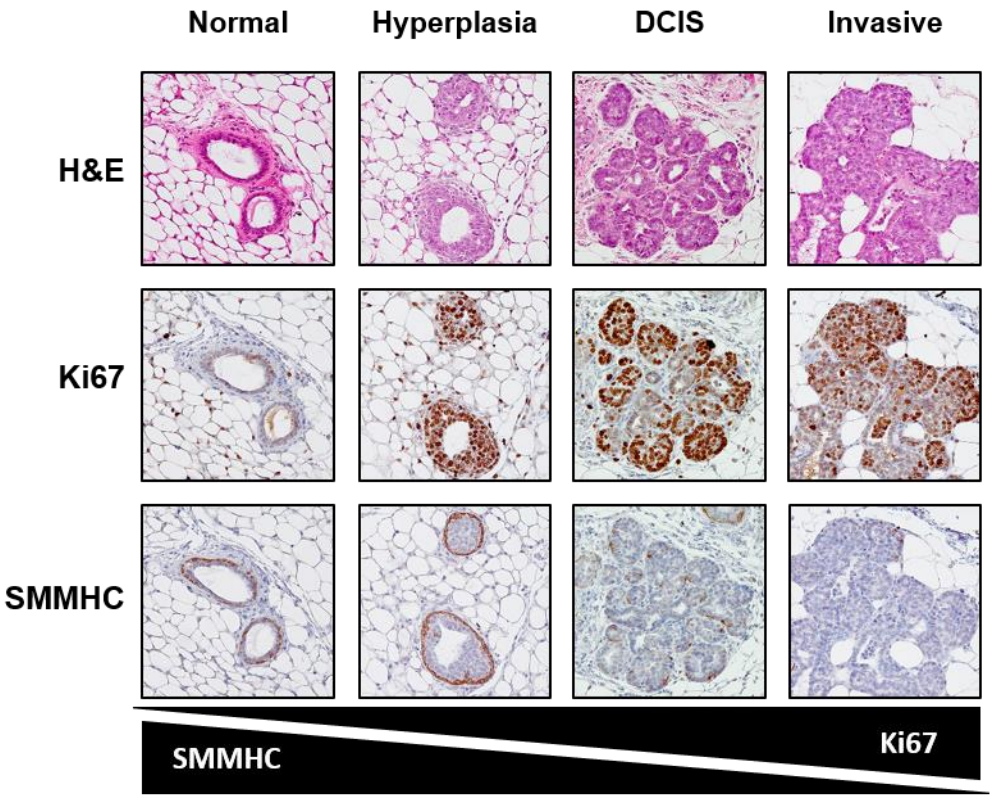

Figure 2.3 Pathological grading of mammary tumour development status of female PyMT-MMTV and PyMT-MMTVxHPSE$^{-/-}$ mice

2.3.7 H-scoring of mammary tumours

H-scoring of anti-MMP-2 stained mouse mammary gland sections bearing DCIS and invasive carcinoma lesions was carried out using the staining intensity guide **(figure 2.4)**. A score of 0 – 3 was assigned to four distinct levels of staining, from no staining to highest intensity. The percentage area of stain for each intensity level within each lesion was then visually determined. The H-score was calculated using the formula [(0 x %area of stain of score 0) + (1 x %area of stain of score 1) + (2 x %area of stain of score 2) + (3 x %area of stain of score 3)]. Statistical analysis was then carried out.

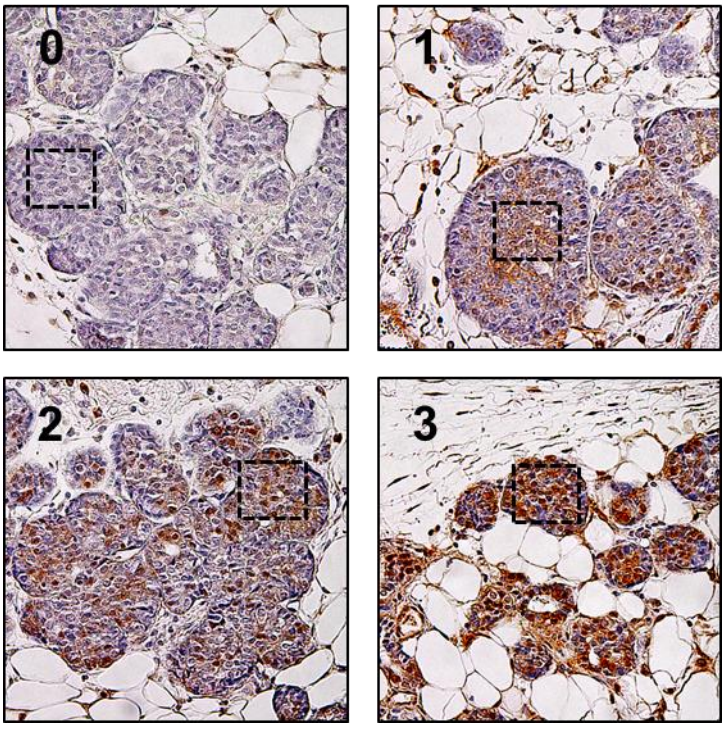

Figure 2.4 H-scoring of mammary tumour sections following IHC staining

2.3.8 Whole-mounting of mouse mammary glands

Excised mouse mammary glands were laid outstretched on a glass slide (SF41296SP SuperFrost™, Thermo Scientific) and further flattened as needed in order to avoid in-folding of the tissue. The slide with the mammary gland was then incubated in Canoy's fixative [a solution of ethanol: chloroform (102445, Merck): acetic acid (100063, Merck) in a 6:3:1 ratio, respectively] for 16 h at room temperature. The slide was then rehydrated by incubating in 70% ethanol, 15 min; 50% ethanol, 15 min; 20% ethanol, 15 min and distilled water, 5 min. The tissue was then stained in Carmine red [a solution of 0.2% (w/v) Carmine red (C1022, Sigma-Aldrich) and 0.5% (w/v) Aluminium potassium sulphate (A7167, Sigma-Aldrich), boiled for 20 min, filtered, with a crystal of Thymol (W306606, Sigma-Aldrich) added as a preservative, then stored at 4ºC] for 16 h at room temperature. The tissue was then dehydrated by incubating in 70% ethanol, 15 min; 90% ethanol, 15 min; 100% ethanol, 15 min and stored in histolene (11031, Grale) for photography under a light microscope.

2.4 Quantification of lung metastatic tumour burden by quantitative polymerase chain reaction (qPCR)

2.4.1 Phenol/chloroform extraction of genomic DNA

Mouse lungs were lysed in lysis buffer [0.1 M sodium chloride (NaCl), 0.05 M Tris-HCl (pH 7.5), 0.1 M EDTA, 1% (w/v) sodium dodecyl sulphate (SDS); a volume of at least 1 ml of lysis buffer per lung] using a metal bead lysing matrix (6925-050, MP bio) and with high speed disruption using a FAST-PREP-24™ instrument (SKU 116004500, MP bio). Proteinase-K (RPROTKSOL-RO, Roche) was added to the solution to a final concentration of 0.1 mg/ml and digested for 16 h at 50ºC. The digestion was mixed with saturated sodium chloride (NaCl, 5M) at a ratio of 1:1.5 respectively. The phenol/chloroform/isoamyl alcohol (25:24:1) solution was prepared by mixing 25 volumes of Phenol (C_6H_5OH) (P4557, Sigma-Aldrich), 24 volumes of chloroform ($CHCl_3$) (C2432, Sigma-Aldrich) and 1 volume of isoamyl alcohol [$(CH_3)_2CHCH_2CH_2OH$] (3-methlybutanol, I9392, Sigma-Aldrich) and letting the solution settle for 16 h at 4ºC. One volume of phenol/chloroform/isoamyl alcohol (25:24:1) solution was added to the lung homogenate and shaken vigorously for 15 sec. This was then centrifuged at 21,000 *g* for 5 min at room temperature. The aqueous phase was collected to a new tube. One volume of phenol/chloroform/isoamyl alcohol (25:24:1) solution was added, shaken vigorously for 15 sec and centrifuged at 21,000 *g* for 5 min at room temperature. The resulting aqueous phase was collected to a new tube and mixed vigorously for 15 sec with one volume of chloroform/isoamyl alcohol (24:1) solution [prepared by mixing 24 volumes of chloroform ($CHCl_3$) (C2432, Sigma-Aldrich) and 1 volume of isoamyl alcohol [$(CH_3)_2CHCH_2CH_2OH$]

(3-methlybutanol, I9392, Sigma-Aldrich). This solution was centrifuged at 21,000 *g* for 5 min at room temperature. The final aqueous phase was collected and mixed with a solution equivalent to 0.5 volumes of ammonium acetate ($CH_3CO_2NH_4$, A1542, Sigma-Aldrich) and 2 volumes of 100% ethanol (molecular biology grade, E7023, Sigma-Aldrich) (the solution was prepared and stored at -20ºC) in order to facilitate the precipitation of DNA. The DNA was collected by centrifugation at 21,000 *g* for 10 min at 4ºC and the pellet was washed twice in 70% ethanol [molecular biology grade, E7023, Sigma-Aldrich, prepared in nuclease-free water (B1500, New England Biolabs)] with centrifugation at 21,000 *g* for 5 min at 4ºC. The supernatant was discarded, the DNA pellet was briefly air-dried and dissolved in nuclease-free water (B1500, New England Biolabs). The purity, integrity and concentration of the DNA solution was ascertained by a spectrophotometer (NanoDrop 1000, ThermoFisher).

2.4.2 Extraction of total ribonucleic acid (RNA)

Mouse lungs were collected, snap-frozen in liquid N_2 and stored at -80ºC. The lungs were weighed and homogenised in 1 ml of TRI reagent® (RT111, Molecular Research Centre, Inc) per 100 mg of tissue using a metal bead lysing matrix (6925-050, MP bio) and with high speed disruption using a FAST-PREP-24™ instrument (SKU 116004500, MP bio). Bromoanisole (BN191, Molecular Research Centre, Inc) was added to the homogenate at a ratio of 1:20 respectively and shaken vigorously for 15 sec. The mixture was centrifuged at 12,000 *g* for 15 min at 4ºC to facilitate phase separation [protein in the lower (phenol) phase, DNA in the interphase and RNA in the upper (aqueous) phase]. The aqueous phase was extracted and mixed with 1 volume of isopropanol [$(CH_3)_2$ CHOH, molecular biology grade, 19516, Sigma-Aldrich], incubated for 10 min at room temperature, mixed vigorously on a vortex mixer and centrifuged at 12,000 *g* for 5 min at 4ºC. The supernatant was discarded and the pellet was washed with 2 volumes of 75% ethanol, mixed vigorously on a vortex mixer and centrifuged 12,000 *g* for 5 min at 4ºC. All ethanol was removed and the pellet was rehydrated and solubilised by incubating in nuclease-free water (B1500, New England Biolabs) for 5 min at room temperature. The purity, integrity and concentration of the RNA was ascertained by a spectrophotometer (NanoDrop 1000, ThermoFisher). Prior to cDNA synthesis, the purified RNA was subjected to a DNase I (M0303, New England Biolabs) digestion for 10 min at 37ºC in order to remove contaminating DNA with the reaction terminated with the addition of EDTA (pH 8.0) to a final concentration of 5 mM and incubating for 10 min at 75ºC.

2.4.3 cDNA synthesis

The synthesis of cDNA from isolated RNA was carried out using the iScript cDNA synthesis kit (170-8891, Bio-Rad), utilising a modified Moloney murine leukaemia virus-

derived reverse transcriptase with blended oligo dT and random hexamer primers. A total of 1 µg of purified RNA was subjected to cDNA synthesis as per manufacturer's recommendations, in a reaction volume of 20 µl containing 20% iScript reaction mix and 5% iScript reverse transcriptase. The cDNA synthesis was carried out in a thermocycler (T-100, Bio-Rad) using the following profile: 25ºC, 5 min; 42ºC, 30 min and a final heat inactivation at 85ºC, 5 min. The purity, integrity and concentration of the cDNA was ascertained by a spectrophotometer (NanoDrop 1000, ThermoFisher).

2.4.4 Sample preparation for qPCR

Purified DNA or cDNA was diluted to 20 ng/µl with nuclease-free water (B1500, New England Biolabs). The qPCR master reaction was prepared with a total of 120 ng of DNA and 54.7% (v/v) Sybr Green (4368702, ThermoFisher) in a total volume of 100 µl. A working solution with 0.8 µM of each primer was prepared with 46 µl of the master reaction in a total volume of 50 µl. This working solution was divided into three 15 µl fractions in a 96-well PCR plate (4ti-0750/TA, 4titude, supplied with PCR strip caps, 4ti-0751, 4titude) in order to carry out the reaction in triplicate.

2.4.5 qPCR methods

Relative tumour burden (RTB) in lungs was calculated based on the quantification cycle (C_q) for a target relative to a control/housekeeping gene. The arbitrary value of RTB was calculated using the formula below as previously described (Rautela et al., 2015).

$RTB = 10{,}000/2^{\Delta Cq}$ where $\Delta Cq = Cq$ (target gene) – Cq(control)

2.4.5.1 Quantification of lung metastatic burden of induced PyMT3 orthotopic mammary tumour-bearing and B16F10-mCherry-Luc (luciferase) tumour-bearing mice

Lung metastatic burden in PyMT3 or B16F10-mCherry-Luc tumour bearing mice was quantified by comparing the abundance of PyMT or mCherry DNA (present only in lung metastases) to *vimentin* DNA (present in all cells). Total lung genomic DNA was extracted as described in section 2.4.1. The following primers (table 2.3) were used with a qPCR cycle of an initial denaturation step of 95ºC for 10 mins, 40 cycles of 95ºC, 30 sec, 62ºC, 30 sec, 72ºC, 40 sec, then 95ºC for 1 min and a melting curve generation from 55 – 95ºC with 30 sec per 1ºC increment.

Target	Fwd primer (5' – 3')	Rev primer (5' – 3')
PyMT-MMTV	AGGAACCGGCTTCCAGGTAAGA	TTGGTGTTCCAAACCATTGCAT
mCherry	GACCACCTACAAGGCCAAGAAG	AGGTGATGTCCAACTTGATGTTGA
Vimentin	AGCTGCTAACTACCAGGACACTATTG	CGAAGGTGACGAGCCATCTC

Table 2.3 Oligonucleotide primers used in lung-metastatic burden qPCR quantification of orthotopic PyMT3 and B16F10-mCherry-Luc lung metastases-bearing mice

2.4.5.2 Quantification of lung metastatic burden of mammary tumour-bearing PyMT-MMTV mice

Total lung RNA was isolated followed by cDNA conversion as described in section 2.4.2. The following primers (table 2.4) were used with a qPCR cycle of an initial denaturation step of 95ºC for 10 mins, 40 cycles of 95ºC, 30 sec, 62ºC, 30 sec, 72ºC, 40 sec, then 95ºC for 1 min and a melting curve generation from 55 – 95ºC with 30 sec per 1ºC increment.

Target	Fwd primer (5' – 3')	Rev primer (5' – 3')
PyMT cDNA	CCAACAGATACACCCGCACAT	GGTCTTGGTCGCTTTCTGGATA
18S cDNA	GTAACCCGTTGAACCCCATT	CCATCCAATCGGTAGTAGCG

Table 2.4 Oligonucleotide primers used in lung-metastatic burden qPCR quantification of mammary tumour-bearing female PyMT-MMTV mice

2.5 Cell lines

2.5.1 PyMT3, MDA-MB-231, Phoenix-eco, B16F10 and B16F10-mCherry-Luc cells

The PyMT3, MDA-MB-231, Phoenix-eco, B16F10 and B16F10-mCherry-Luc cells were cultured in Dulbecco's modified Eagle medium [DMEM, 11995-065, Gibco, containing 4.5 mg/ml glucose, 0.11 mg/ml sodium pyruvate, supplemented additionally with 10% (v/v) FCS (SFBSNZ, Interpath) and 100 units/ml penicillin with 100 µg/ml streptomycin (15140122, Gibco)]. The cells were maintained at 37ºC with 5% CO_2 and passaged using 1 mM EDTA in PBS.

2.5.2 CHO-K1 cells

CHO-K1 cells were cultured in Ham's F-12K medium [21127022, Gibco, supplemented with 10% (v/v) FCS (SFBSNZ, Interpath) and 100 units/ml penicillin with 100 µg/ml streptomycin (15140122, Gibco, 10,000 units/ml)]. The cells were maintained at 37ºC with 5% CO_2 and passaged using 0.25% (v/v) trypsin-EDTA (25200056, Gibco). Prior to the HS surface assay, CHO-K1 cells were harvested using 0.5 mM EDTA.

2.5.3 Development of the B16F10-mCherry-Luc cell line

The Phoenix™ retrovirus producer cell line Phoenix-eco (kindly provided by Associate Professor Belinda Parker, La Trobe University) was used in the development of the B16F10-mCherry-Luc cell line. The cells were seeded in a 75 cm^2 tissue culture flask in DMEM medium [11995-065, Gibco, containing 4.5 mg/ml glucose, 0.11 mg/ml sodium pyruvate, supplemented additionally with 10% (v/v) FCS (SFBSNZ, Interpath) and 100 units/ml penicillin with 100 µg/ml streptomycin (15140122, Gibco)] and incubated at 37ºC in 5% CO_2 in order to reach 50% confluency. The retroviral expression construct pMSCV-mCherry-Luc containing the ORFs of mCherry and firefly luciferase on a pMSCV retroviral vector backbone was kindly provided by Associate Professor Belinda Parker. The cells were transfected with 30 µg of this DNA using the Lipofectamine™ 3000 reagent (L3000015, ThermoFisher) as per manufacturer's guidelines. The transfected cells were incubated for 24 h at 37ºC in 5% CO_2 in order to produce viral particles. The supernatant containing viral particles was collected, filtered through a 45 µm filter, with polybrene (TR-1003, Sigma-Aldrich) added to a final concentration of 4 µg/ml. The culture medium for Phoenix-eco cells was immediately replaced. The viral supernatant was added onto B16F10 cells [seeded at a density of $5x10^5$ cells/well in a 6-well plate in DMEM medium (Gibco) supplemented with 10% FCS, incubated for 16 h at 37ºC in 5% CO_2 to reach a confluency of 70%]. The spinfection of the cells was carried out at 750 *g* for 45 min at room temperature then promptly returned to 37ºC in 5% CO_2. This spinfection was repeated with the viral supernatants collected at 48 h and 72 h post-transfection.

The infected B16F10 cells were collected and cultured, followed by flow cytometry sorting for B16F10 cells expressing mCherry **(figure 5.16)**. These cells were cultured, followed by further sorting to achieve a cell population expressing mCherry at nearly 100%.

2.6 Flow cytometry analysis of immune cell populations

2.6.1 Isolation of mouse immune cell populations

2.6.1.1 Isolation of tumour-associated immune cells

Mice bearing orthotopic mammary tumours were euthanised and the tumour was excised, taking care to avoid collecting the inguinal lymph node. The tumour was placed in a petri dish and dissociated with scissors in a digestion solution [collagenase type-1 (1 mg/ml, 17018029, ThermoFisher scientific) and DNaseI (0.02 mg/ml, 11284932001, Roche) in RPMI medium (with 2 mg/ml D-glucose and 25 mM HEPES, 22400105, Gibco) supplemented with 2% (v/v) FCS (SFBSNZ, Interpath)]. The dissociated tumour was further digested by adding 2.5 volumes of the digestion solution and manually pipetting with a transfer pipette for 20 min at room temperature. Sterile EDTA was added to the solution to a final concentration of 12 mM and the digestion continued for a further 5 min on ice. The digested tissue was filtered through a metal wire mesh and centrifuged at 500 *g* for 5 min at 4ºC. The supernatant was discarded and the pellet was resuspended in a Ficoll®-Paque (GE17-5442-02, GE Healthcare) solution [28.6% (v/v) Ficoll®-Paque in RPMI medium (with 2 mg/ml D-glucose and 25 mM HEPES, 22400105, Gibco) supplemented with 2% (v/v) FCS (SFBSNZ, Interpath)] and a density gradient created by centrifuging at 675 *g* for 10 min at 4ºC with a minimum acceleration and deceleration setting. The supernatant containing a visible collection of cells was collected and centrifuged at 930 *g* for 5 min at 4ºC. The cell pellet was resuspended in flow cytometry buffer [sterile PBS supplemented with 2% (v/v) FCS (SFBSNZ, Interpath) and 0.2 mM EDTA]. A cell count was performed using a haemocytometer.

2.6.1.2 Isolation of mouse lung immune cells

The lungs were placed in a petri dish and dissociated with scissors in a digestion solution [collagenase type-1 (1 mg/ml, 17018029, ThermoFisher scientific) and DNaseI (0.02 mg/ml, 11284932001, Roche) in RPMI medium (with 2 mg/ml D-glucose and 25 mM HEPES, 22400105, Gibco) supplemented with 2% (v/v) FCS (SFBSNZ, Interpath)]. The dissociated tissue was further digested by adding 2.5 volumes of the digestion solution and manually pipetting with a transfer pipette for 20 min at room temperature. Sterile EDTA was added to the solution to a final concentration of 12 mM and the digestion continued for a further 5 min on ice. The digested tissue was filtered through a metal wire mesh and centrifuged at 500 *g* for 5 min at 4ºC. The resulting cell pellet was subjected to

RBC lysis by resuspending in an appropriate volume (1 – 2 ml) of RBC lysis buffer (155 mM NH_4Cl, 12 mM $NaHCO_3$, 0.1 mM EDTA) and incubating for 5 min at room temperature. The immune cells were collected by centrifugation at 500 *g* for 5 min at 4ºC. The pellet was resuspended in flow cytometry buffer [sterile PBS supplemented with 2% (v/v) FCS (SFBSNZ, Interpath) and 0.2 mM EDTA]. A cell count was performed using a haemocytometer.

2.6.1.3 Isolation of mouse splenic immune cells

Splenic cells were used in order to ensure appropriate gating and compensation of the flow cytometry protocol. The splenic immune cells were isolated and RBC lysis performed as described in section 2.2.4. The cell pellet was resuspended in flow cytometry buffer [sterile PBS supplemented with 2% (v/v) FCS (SFBSNZ, Interpath) and 0.2 mM EDTA] and a cell count was performed using a haemocytometer.

2.6.2 Flow cytometry analysis strategy

2.6.2.1 Analysis of immune cells isolated from mammary tumours and lungs of orthotopic mammary tumour-bearing mice

The immune cells isolated from the mammary tumours and lungs of C57Bl/6 and C57Bl/6xHPSE$^{-/-}$ mice bearing orthotopic PyMT3 mammary tumours were analysed using the antibodies listed on table 2.5. Compensation was performed using single-stained samples. Four distinct antibody cocktails were employed in the analysis. A total of $5x10^5$ cells were resuspended in flow cytometry buffer [sterile PBS supplemented with 2% (v/v) FCS (SFBSNZ, Interpath) and 0.2 mM EDTA] prior to a single analysis. Cells were collected by centrifugation at 500 *g* for 5 min at 4ºC. Fc receptor blocking was carried out for 10 min at 4ºC in the dark. The antibody cocktail for a given population of immune cells was then added to the cell suspension followed by an incubation for 20 min at 4ºC in the dark. The cells were then washed twice in flow cytometry buffer with centrifugation at 500 *g* for 5 min at 4ºC followed by resuspension in flow cytometry buffer. The flow cytometry was carried out using a FACSCanto™ II (Beckton Dickinson) instrument with data analysed using the FlowJo software (FlowJo LLC; gating strategy outlined in **figures 2.5 – 2.9**).

Antibody	Clone	Catalogue number/Company	Dilution
DAPI/Pacific Blue	NA	564907, BD Biosciences	1:300
Fc receptor block	2.4G2	553141, BD Biosciences	1:300
Anti-mouse CD45.2-FITC	104	109806, Biolegend	1:300
Anti-mouse CD25-PE	PC61	553866, BD Biosciences	1:300
Anti-mouse CD3-APC	17A2	565643, BD Biosciences	1:300
Anti-mouse CD69-PECy7	H1.2F3	25-0691.82, eBioscience	1:300
Anti-mouse CD4 APC-Cy7	GK1.5	552051, BD Biosciences	1:300
Anti-mouse CD8-BV510	53-6.7	560776, BD Biosciences	1:300
Anti-mouse Ly6G-PE	1A8	551461, BD Biosciences	1:300
Anti-mouse CD11c-APC	HL3	550261, BD Biosciences	1:300
Anti-mouse CD11b-PerCP5.5	M1/70	550993, BD Biosciences	1:300
Anti-mouse MHC Class II-PECy7	M5/114.15.2	4332615, eBioscience	1:600
Anti-mouse Ly6c-A780	HK1.4	4346376, eBioscience	1:300
Anti-mouse CD115-PE	T38-320	565249, BD Biosciences	1:300
Anti-mouse F4/80-PECy7	BM8	25-4801-82, eBioscience	1:300
Anti-mouse DX5(CD49b)-PE	DX5	553858, BD Biosciences	1:300
Anti-mouse NK1.1-PECy7	PK136	552878, BD Biosciences	1:300

Table 2.5 Antibodies used in quantifying tumour and lung immune cell populations of orthotopic PyMT3 tumour-bearing mice

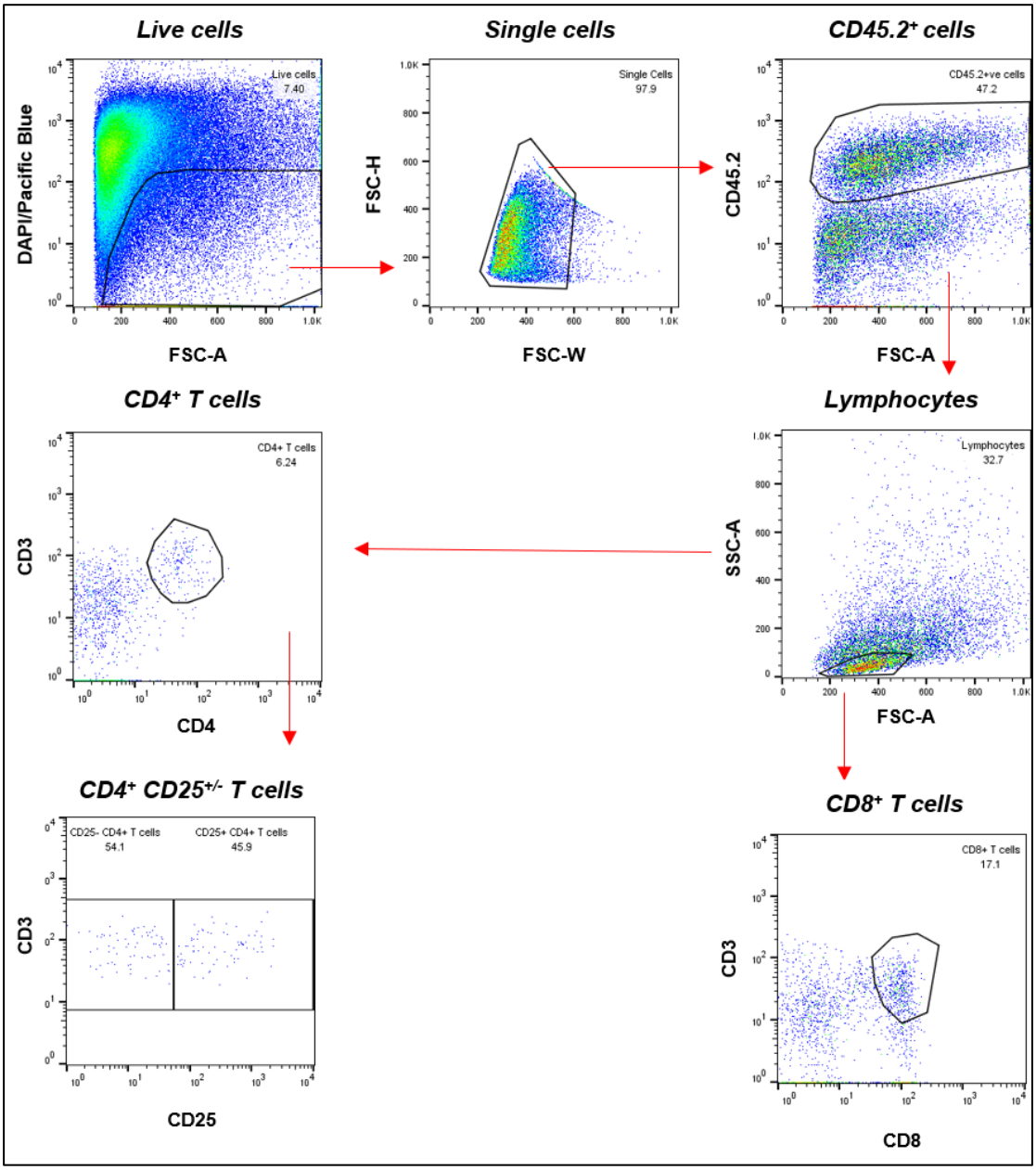

Figure 2.5 Gating strategy for orthotopic tumour T cells

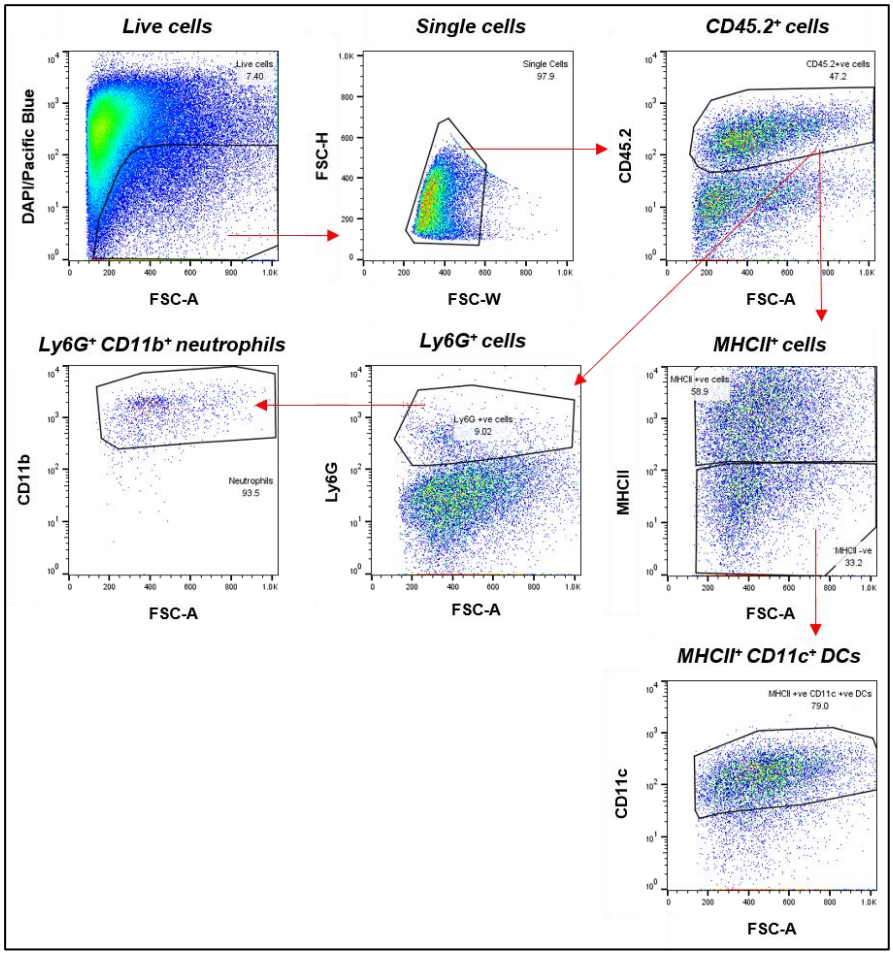

Figure 2.6 Gating strategy for orthotopic tumour neutrophils and DCs

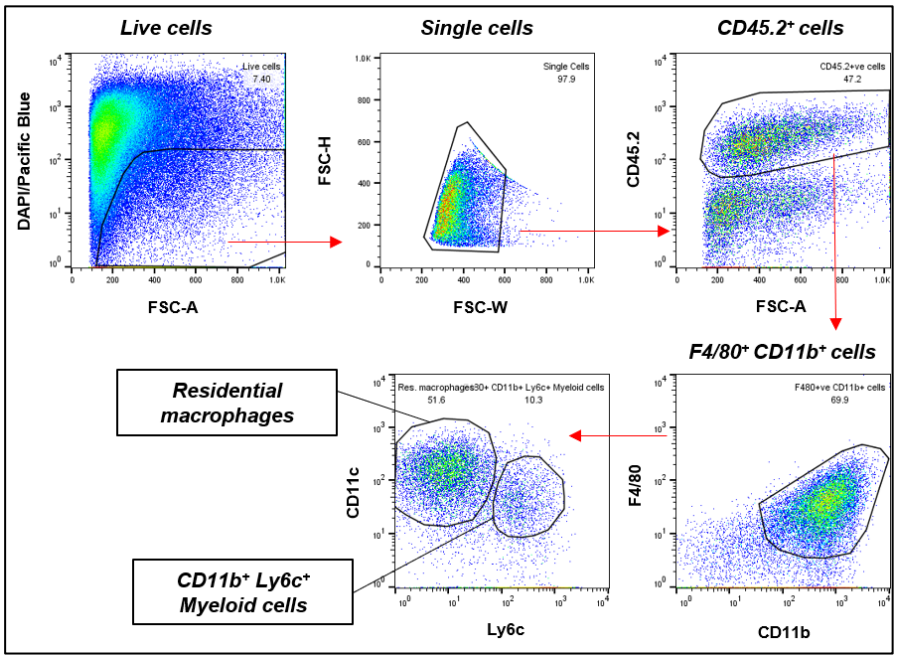

Figure 2.7 Gating strategy for orthotopic tumour residential macrophages and myeloid cells

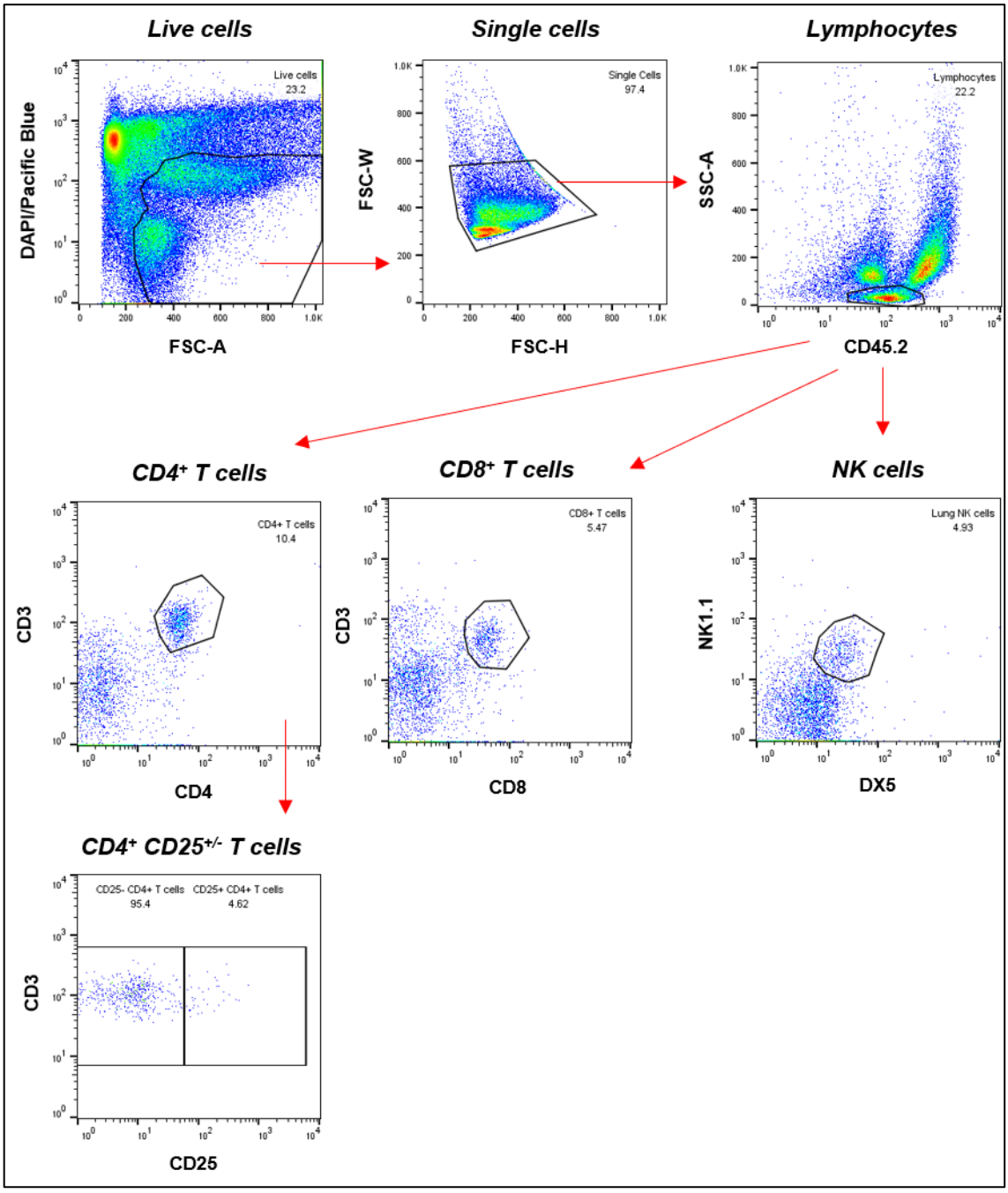

Figure 2.8 Gating strategy for lung T cells in orthotopic tumour-bearing mice

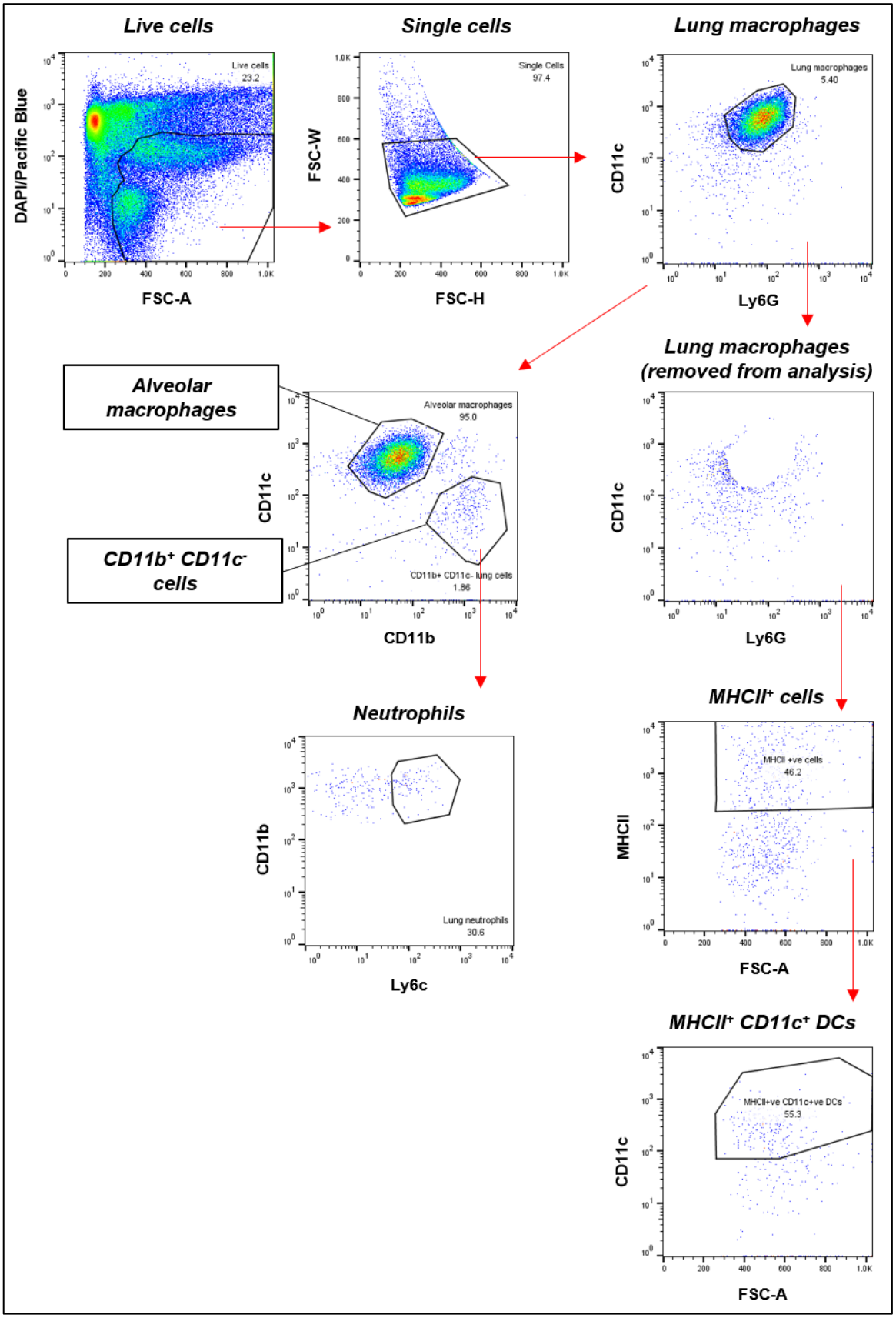

Figure 2.9 Gating strategy for lung neutrophils, alveolar macrophages and DCs in orthotopic tumour-bearing mice

2.6.2.2 Analysis of lung and spleen immune cells of mice bearing B16F10-mCherry-Luc lung metastases and treated with novel HPSE inhibitors

The immune cells isolated from the lungs and spleens of B16F10-mCherry-Luc lung metastases-bearing mice were counted, followed by the collection of $1.5x10^6$ cells for analysis at 500 *g* for 5 min at 4ºC. The cells were set up in a 96-well plate in triplicate. The supernatant was removed by centrifuging at 500 *g* for 5 min at 4ºC. The cell pellet was resuspended in the antibody cocktail followed by incubating for 20 min at 4ºC in the dark. The cell suspension was washed twice in flow cytometry buffer [sterile PBS supplemented with 2% (v/v) FCS (SFBSNZ, Interpath) and 0.2 mM EDTA] with centrifugation at 500 *g* for 5 min at 4ºC prior to resuspension in flow cytometry buffer. The staining strategy **(figures 2.10 – 2.12)** was carried out using the antibodies listed below (table 2.6) with three distinct antibody cocktails. Compensation was performed with single-stained samples. Interference with mCherry fluorescence was compensated for by using freshly isolated B16F10-mCherry-Luc cells. A CytoFLEX flow cytometer (Beckman Coulter) was used with data analysed using the FlowJo software (FlowJo LLC).

Antibody	Clone	Catalogue number/Company	Dilution
Anti-mouse NK1.1-PE	PK136	12-5941-81, eBioscience	1:200
Anti-mouse TCRβ-FITC	H57-597	11-5961-81, eBioscience	1:200
Anti-mouse NKG2D (CD314)-PECy7	CX5	25-5882-81, eBioscience	1:200
Anti-mouse CD69-APC	H1.2F3	560689, BD Biosciences	1:200
Anti-mouse CD27-APC	LG.7F9	17-0271-81, eBioscience	1:200
Anti-mouse CD11b-BV421	M1/70	562605, BD Biosciences	1:200
Anti-mouse CD4-PECy7	RM4-5	25-0042-82, eBioscience	1:200
Anti-mouse CD8-PE	53-6.7	12-0081-82, eBioscience	1:200

Table 2.6 Antibodies used in quantifying immune cell populations of B16F10-mCherry-Luc lung metastases-bearing mice

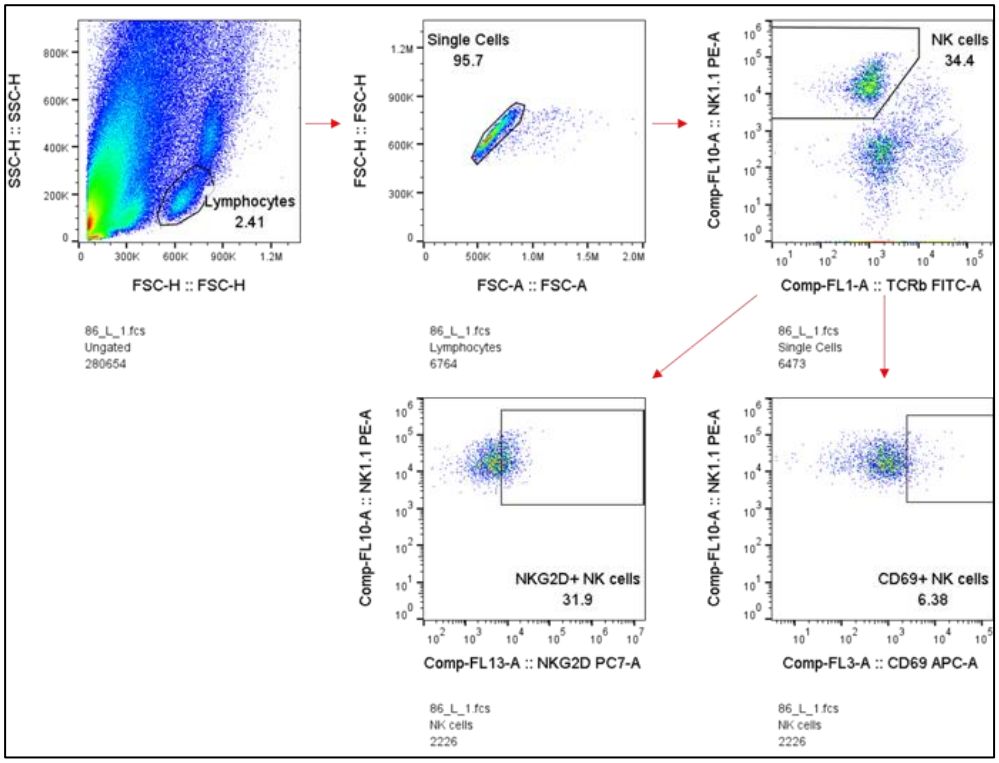

Figure 2.10 Gating strategy for NK cells, NKG2D$^+$ NK cells and CD69$^+$ NK cells of B16F10-mCherry-Luc lung metastases-bearing mice

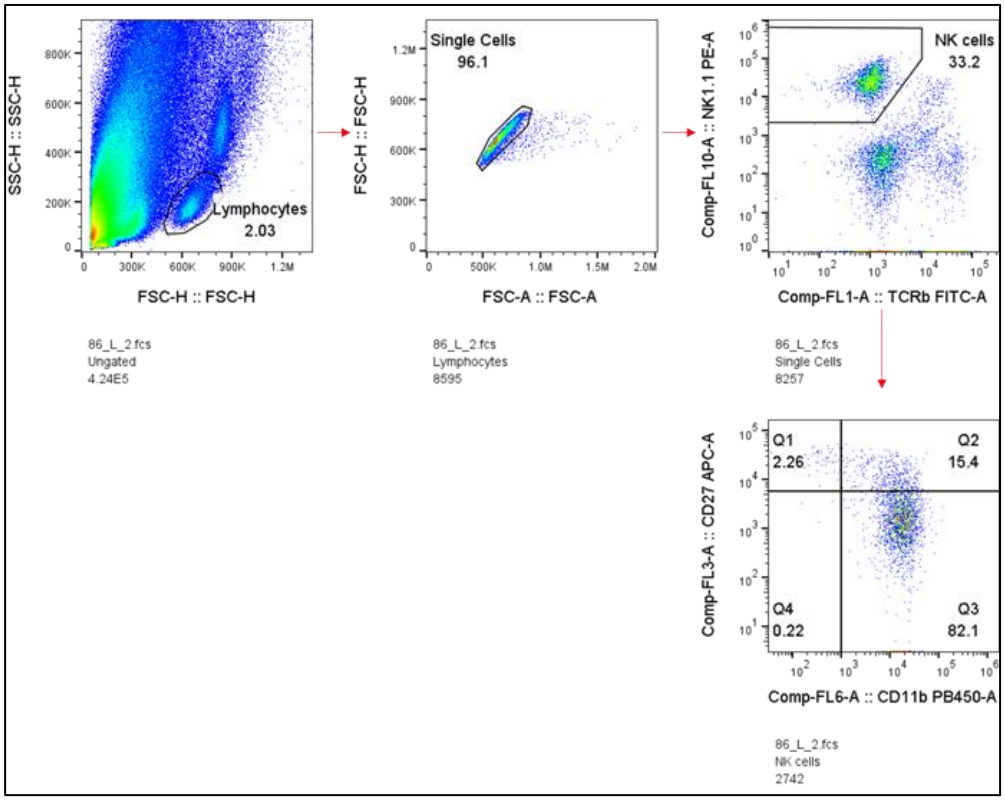

Figure 2.11 Gating strategy for NK cells, CD11b$^+$ NK cells and CD11b$^+$ CD27$^+$ NK cells of B16F10-mCherry-Luc lung metastases-bearing mice

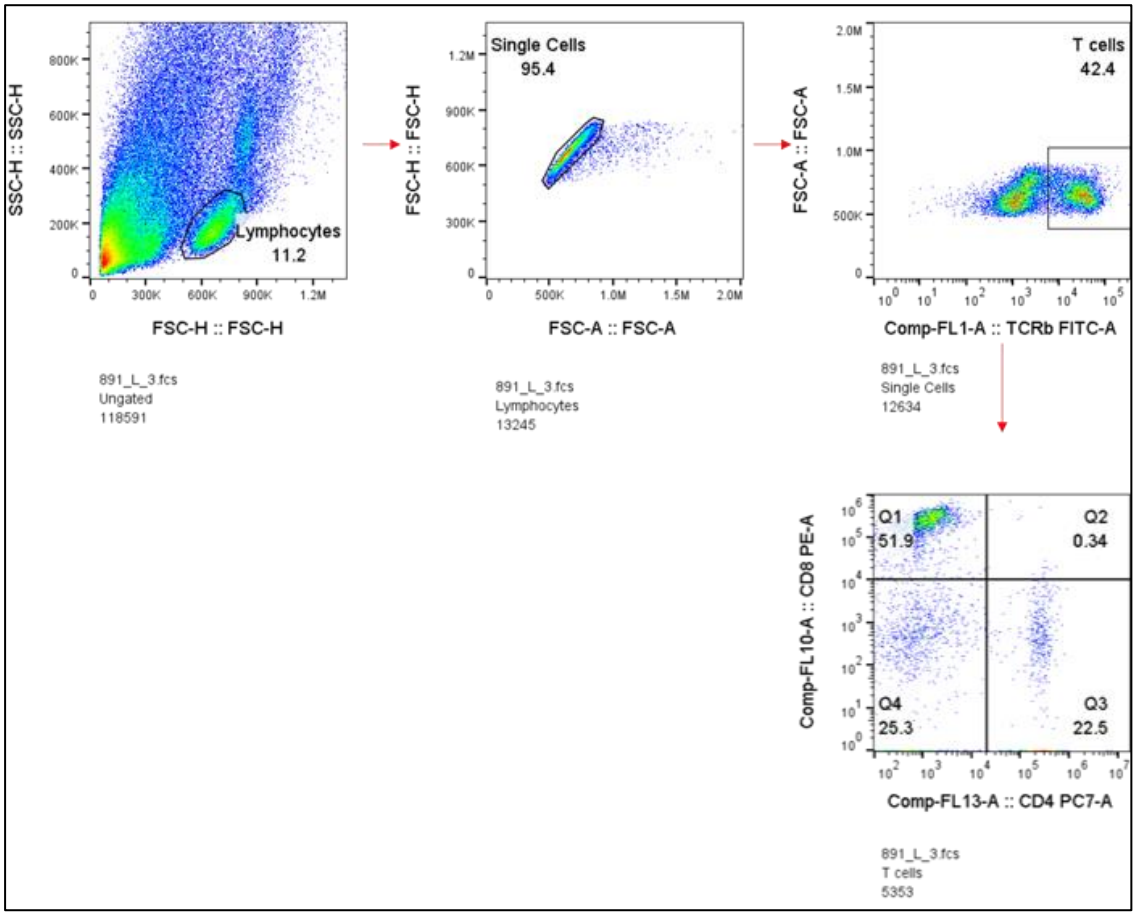

Figure 2.12 Gating strategy for lung CD4⁺ T cells and CD8⁺ T cells of B16F10-mCherry-Luc lung metastases-bearing mice

2.7 Screening for novel HPSE inhibitors

The Sigma LOPAC^{1280} drug stocks (10 mM, LO4200, Sigma-Aldrich) were diluted to 1 mM in dimethyl sulfoxide (DMSO, 41640, Sigma-Aldrich) prior to dilution in assay buffer (20 mM Tris-HCl, 0.15 M NaCl, 0.1% CHAPS, pH 5.5) to a final concentration of 10 µM of drug per reaction. The inhibition of HPSE activity was then determined using the HPSE enzymatic activity assay (2.2.1). The secondary screen of compounds which demonstrated a reduction of HPSE enzymatic activity to $\leq$40% of its basal level were re-screened for reproducibility with the 1 mM intermediate stocks.

2.7.1 Cell surface HS assay

Purified HPSE was treated with drugs of interest for 10 min at 37ºC prior to being incubated with CHO-K1 cells for 1 h at 37ºC [2x10^6 cells/ml in PBS supplemented with 0.1% (w/v) BSA]. The cells were centrifuged at 300 *g* for 5 min at room temperature and washed with PBS supplemented with 0.1% (w/v) BSA twice to remove cleaved HS. Following the washes, the cells were incubated with either anti-human HS (IgM, mouse monoclonal, clone F58-10E4, 370255, Amsbio, 1:500 working concentration) or with PBS

supplemented with 0.1% (w/v) BSA for 30 min at 4ºC. the samples were washed three times as previously, followed by treatment with a PE-conjugated anti-mouse IgM (goat, SC-3768, Santa Cruz Biotechnology, 1:100 working concentration) for 30 min at 4ºC. The cells were washed three times as previously described and resuspended in PBS supplemented with 0.1% (w/v) BSA and analysed on a flow cytometer (FACSCanto II Flow Cytometer, BD Biosciences). The data was analysed using the FlowJo software (FlowJo LLC).

2.7.2 Molecular modelling of the interaction between GW7647 and HPSE

The interaction between GW7647 and human HPSE was performed using the YASARA molecular modelling application (available at http://www.yasara.org; performed by Professor Brian Smith, La Trobe University). The VINA (Vina Is Not Autodock, developed at the Scripps research institute) approach to determine small molecule docking was employed (Trott and Olson, 2010). This is an automated program which uses the Autodock molecular mechanics force field (including electrostatics, van der Waals, desolvation, entropy, etc) to score the interaction between the ligand and the receptor. The subsequent poise prediction is controlled via a genetic algorithm.

2.7.3 Cell viability assay

$5x10^3$ MDA-MB-231 cells were seeded in serum-free DMEM (11995-065, Gibco) in a single well in a 96-well plate, allowed to adhere and treated with compounds of interest by incubating for 48 h at 37ºC and 5% CO_2. One volume of MTT (3-[4,5 dimethylthiazol-2-yl]-2,5 diphenyltetrazolium bromide, M2128, Sigma-Aldrich) was added to a final concentration of 0.5 mg/ml. A further incubation for 3 h at 37ºC and 5% CO_2 allowed the formation of formazan crystals, which were then solubilised in DMSO (41640, Sigma-Aldrich). The absorbance was measured at 570 nm. The cell viability was determined by assuming 100% viability of the untreated cells.

2.7.4 Transwell migration assay

MDA-MB-231 cells in serum-free DMEM (11995-065, Gibco) was seeded at a density of 10^5 cells/well in the upper chamber of a Transwell® cell culture insert (8 µm pore polycarbonate membrane insert, 3428, Corning), with a synthetic BM of Matrigel® (354248, Corning) at a concentration of 3.5 mg/ml reconstituted in serum-free DMEM. Prior to the addition of cells, the Matrigel® inserts were prepared by adding the solubilised Matrigel® to the inserts at 4ºC, followed by incubating the inserts for 30 min at room temperature. The solidified Matrigel® was gently washed with serum-free DMEM prior to the addition of the cell suspension. The inserts were added to wells containing DMEM supplemented with 5% (v/v) FCS (SFBSNZ, Interpath) as a chemoattractant. The cells

were incubated for 1 h at 37ºC and 5% CO_2, then treated with compounds of interest for 24 h at 37ºC and 5% CO_2. This was followed by fixing the invaded cells in 70% ethanol for 10 min and staining in 0.6% (w/v) crystal violet (C0775, Sigma-Aldrich). The crystal violet stain was dissolved in 10% (v/v) acetic acid (1.00063, Merck) with absorbance measured at 590 nm. The average fluorescence of treated samples was compared to that of the no treatment control to determine the percentage of migration.

2.7.5 *In vitro* angiogenesis assay

In order to determine the effect of known and novel HPSE inhibitors on angiogenesis, a modified *in vitro* assay based on previously published data (Brown et al., 1996) was designed. Aortas were excised from approximately 20-week old C57Bl/6 and C57Bl/6xHPSE$^{-/-}$ mice. Connective tissue was removed and the aorta was flushed free of clots in serum-free medium-199 (11150067, Gibco) supplemented with 2.5 µg/ml amphotericin B (15290018, Gibco). The aortic vessels were then sectioned finely into approximately 1 mm fragments followed by embedding in a fibrin matrix formed by the addition of thrombin [(50 units/ml, Sigma-Aldrich), 0.15 M NaCl] to fibrinogen (3 mg/ml, Sigma-Aldrich) in serum-free medium-199 (Gibco) supplemented with 5 µg/ml aprotinin (A6106, Sigma-Aldrich). Following the matrix formation, the vessel fragments were treated with compounds of interest solubilised in medium-199 (Gibco) supplemented with 20% (v/v) FCS (SFBSNZ, Interpath), 0.24 µg/ml gentamycin (15710-064, Sigma-Aldrich), 2.5 µg/ml amphotericin B (Gibco), 1 mM L-glutamine (35050061, Gibco) and 7.62 mM ε-aminocaproic acid (PHR-1224, Sigma-Aldrich). The aorta samples were then incubated for 7 days at 37ºC in 5% CO_2 with the change of treatment medium on day 4. The level of angiogenesis was determined on day 7 following the guide **(figure 5.14B)** which accounted for the number, length and the density of vessel outgrowths. The images were captured on a light microscope.

Chapter 3

Defining the role of heparanase in breast cancer progression using the PyMT-MMTV mouse model

3.1 Abstract

Breast cancer is a major health concern and is the second most common human malignancy. As a promoter of all cancers, HPSE has been widely implicated in enhancing the development and progression of breast cancer. In this chapter, the well-defined spontaneous mammary tumour-developing PyMT-MMTV mouse model is employed to investigate the role of HPSE in breast cancer, whereby HPSE-deficient PyMT-MMTV (PyMT-MMTVxHPSE$^{-/-}$) mice were generated and used to address the lack of genetic ablation models in the current literature. It was shown that despite HPSE promoting mammary tumour angiogenesis, the overall tumour progression and metastasis were HPSE-independent. HPSE was further shown to impart no effects in early mammary tumour development and no evidence of a compensatory mechanism by MMPs in response to the lack of HPSE expression in the mammary tumours was uncovered. The findings of this chapter therefore suggest that HPSE does not play a significant role in mammary tumour development in the PyMT-MMTV mouse model, which may have implications in certain clinical settings.

3.2 Introduction

As discussed in chapter 1, HS plays key roles in the progression of malignancy. The involvement of proteoglycans in malignant transformation including breast cancer, is a well-characterised phenomenon and is widely reviewed (Raman and Kuberan, 2010, Sasisekharan et al., 2002, Liu et al., 2002, Blackhall et al., 2001, Gomes et al., 2013). Even though GAGs other than HS such as CS and dermatin sulphate have been suggested to be involved in mammary gland and in turn, mammary tumour development, only HS will be considered for the purpose of this thesis (Gomes et al., 2013, Cooney et al., 2011, Weyers et al., 2012, Olsen et al., 1988).

The aforementioned features of HS as a structural as well as a physiological component of the ECM are crucial in this context. This has led to HSPGs being suggested as targets in breast cancer treatment (Koo et al., 2008). HS expression was shown to directly correlate with the aggressiveness of breast cancers in patient-derived samples and the *in vitro* inhibition of GAG-sulfation and HS species resulted in reduced cancer cell migration (Guo et al., 2007). This highlighted HS as a cancer biomarker. Gene expression analysis of patients with invasive ductal carcinoma demonstrated altered expression patterns of HSPG genes, particularly the expression and localisation of proteoglycans along with variations in sulfation levels (Fernández-Vega et al., 2013). HS was shown to enhance the response of human breast cancer cells to FGFs *in vitro*, affecting cell proliferation and migration (Nurcombe et al., 2000). More recently, *in vitro* studies employing the MCF-7 and MDA-MB-231 human breast cancer cell lines demonstrated variable expression levels

of HSPGs as well as the resulting proliferation, mobility and tumorigenicity mediated by the Wnt signalling pathway (Okolicsanyi et al., 2014).

Syndecans are a prominent variant of HSPGs (Sarrazin et al., 2011). Numerous studies have demonstrated the expression of syndecans in breast cancer. Two syndecan varieties, syndecan-1 and -4 have been demonstrated as independent indicators of breast cancer, with syndecan-1 levels correlating with tumour grade and syndecan-4 levels indicating ER and PR expression status in breast cancers (Lendorf et al., 2011). Interestingly, a previous study indicated the correlation of epithelial syndecan-1 expression with negative ER status while its stromal expression indicated a positive status (Leivonen et al., 2004). Variable syndecan-1 expression was demonstrated in malignant and non-malignant human breast samples, suggesting its correlation with the metastatic phenotype of infiltrating ductal carcinoma (Stanley et al., 1999). The expression of syndecan-1 was shown to increase in breast tumours, while that of other proteoglycans such as decorin and lumican decreased (Eshchenko et al., 2007). Syndecan-1 possesses a prognostic value in breast cancer with its IL-6-mediated role in breast cancer cell migration demonstrated *in vitro*, along with its suggested involvement in resistance to irradiation (Hassan et al., 2013). Syndecan-1 expression is not only limited to cancer cells, and its expression by stromal fibroblasts was demonstrated to promote the *in vitro* growth of MDA-MB-231 human breast cancer cells as well as *in vivo* breast tumour growth, with enhanced angiogenesis (Maeda et al., 2005, Maeda et al., 2004). The mammary fibroblast syndecan-1 expression is further suggested to be involved in tumour stroma production, regulating ECM assembly and architecture which may facilitate the migration of cancer cells (Yang et al., 2011). Additionally, the TNBC stem cell phenotype was demonstrated to be regulated by syndecan-1 expression, mainly via STAT3 signalling (Ibrahim et al., 2013, Ibrahim et al., 2017).

Other HSPG variants too, play a role in breast cancer progression. The HSPG glypican-1 overexpression was demonstrated in breast cancer which correlated with the mitogenic effects of HSBPs (Matsuda et al., 2001). Glypican-3 expression was shown to be downregulated in breast cancer, which suggests its role as a negative regulator in cancer progression (Xiang et al., 2001). The protective role of glypican-3 was again highlighted through its ability to inhibit invasion and metastasis *in vivo* (Peters et al., 2003). Mesenchymal to epithelial transition in breast cancer cells was shown to be influenced by glypican-3, indicating its potential as a therapeutic target (Castillo et al., 2016). However, an observation by Tsai et al. using microarray data suggested that glypican-3 had no prognostic value in breast cancer (Tsai et al., 2015).

As outlined earlier in this thesis, HPSE is overexpressed in essentially all cancers. A significant proportion of these studies implicate HPSE in the development and progression of breast cancer, which will now be discussed. The initial cloning of human HPSE reported a correlation of HPSE expression with the metastatic potential of rat tumour cells (Hulett et al., 1999). Complementing this observation, the highly metastatic MDA-MB-435 human breast cancer cell line was shown to express HPSE at a greater level compared to the moderately metastatic MDA-MB-231 and the weakly metastatic MCF-7 breast cancer cell lines (Vlodavsky et al., 1999). These findings provided an early insight into the role of HPSE in breast cancer. Numerous studies generating *in vitro*, *in vivo* and human data have since shed further light on the significance of HPSE in breast cancer growth, which has generated interest in its therapeutic and prognostic implications.

Early *in vivo* studies using HPSE-overexpressing MCF-7 cells demonstrated that HPSE indeed promoted tumour growth and angiogenesis, leading to larger tumours and furthermore, promoted *in vitro* cell survival (Cohen et al., 2006). Jiao *et al.* conducted DNA methylation pattern studies to define the differential regulation of HPSE expression in specific stages of breast cancer (Jiao et al., 2014). Interestingly, it was demonstrated that higher *HPSE* gene promoter methylation levels were observed in the poorly metastatic MCF-7 breast cancer cell line, while the highly aggressive MDA-MB-435 cell line exhibited much lower promoter methylation. DNA methylation levels in patient samples were further demonstrated to inversely correlate with clinical stage and accompanying HPSE expression levels. This suggests a methylation-driven regulation of HPSE expression which correlates directly with tumour aggressiveness. HPSE expression was shown to also be influenced by estrogen in both *in vitro* and *in vivo* settings, indicating its hormonal-mediated regulation in breast cancer, promoting disease progression (Elkin et al., 2003). More recently, HPSE was shown to enhance CTC clusters through the induction of FAK-1 and ICAM-1-mediated cell adhesion, resulting in enhanced breast cancer metastasis (Wei et al., 2018a).

Genetic models of mice overexpressing or lacking HPSE expression were utilised to demonstrate its role in early mammary tumorigenesis (Boyango et al., 2014). The development of breast cancer was shown to be significantly enhanced with the expression of HPSE and was further promoted with the co-expression of a mutant *H-Ras* gene. Boyango *et al*. further demonstrated that in addition to promoting mammary gland development, the MMTV regulatory element-driven expression of the C-terminal domain of HPSE also induced mammary tumour growth (Boyango et al., 2018).

Studies conducted by inhibiting the activity of HPSE have further validated its role in breast cancer. PG545, a HS-mimetic, was demonstrated to significantly reduce tumour growth

and metastasis in mice, utilising the 4T1 syngeneic breast cancer model (Hammond et al., 2012). Resistance to lapatinib in the human brain-colonising MDA-MB-231BR breast cancer cell line was attenuated through the inhibition of HPSE by SST0001 (Roneparstat) (Zhang et al., 2015d). Overexpression of extracellular superoxide dismutase was shown to inhibit HPSE expression, which in turn reduced *in vitro* breast cancer cell growth and invasion (Teoh et al., 2009). The mode of action of the plant extract elemene, a traditional Chinese anti-cancer remedy, had remained elusive for decades (Zhang et al., 2017b). Recently, by using the 4T1 murine breast cancer cells, it was demonstrated that elemene was capable of downregulating HPSE, thus imparting anti-proliferative and anti-metastatic effects. Proliferation, primary tumour growth, angiogenesis and metastasis of the highly aggressive MDA-MB-435 human breast cancer cell-derived tumours was attenuated by the use of siH1324, an siRNA acting as a *HPSE* gene-specific inhibitor (Zhang et al., 2007).

In addition to a myriad of *in vitro* and *in vivo* studies, numerous patient-derived data have explored the relationship between HPSE and breast cancer. Recently, a study of The Cancer Genome Atlas with an associated meta-analysis of available data, demonstrated that HPSE expression was upregulated in most human breast cancer specimens and was associated with larger tumours, metastasis, histological tumour grade and ultimately resulted in poor survival (Sun et al., 2017). This finding echoes those of prior studies. In a study of patient samples, HPSE expression was demonstrated to be associated with reduced HS deposition and increased metastatic potential of breast cancer (Maxhimer et al., 2002). Larger tumours were found to express higher levels of HPSE. The invasive capacity of DCIS lesions directly correlated with their expression of HPSE (Maxhimer et al., 2005a). HPSE resulted in the reduction of HS deposition in the ductal BM which contained the DCIS lesions, allowing progression to an invasive phenotype. HPSE, along with COX-2 were shown to be predictive markers of lymph node metastasis in high-grade breast tumours, further highlighting it as a predictive marker (Gawthorpe et al., 2014). The micro RNA species miR-1258 was identified to directly target HPSE and inhibit brain-metastatic breast cancer (Zhang et al., 2011). In support of HPSE-mediated breast cancer metastasis, miR-1258 levels were shown to inversely correlate with HPSE expression and activity and the overall metastatic potential of breast cancer cells. However, the expression levels of HPSE by the primary tumour and metastatic lesions do not always correlate. In a study of patient samples, a discordance in HPSE expression levels between the primary breast tumour and matched metastases was reported (Vornicova et al., 2018). This difference resulted in a poorer prognosis when compared to patients whose primary tumour and metastases showed stable HPSE expression levels.

Interestingly, peripheral blood mononuclear cells (PBMCs) of breast cancer patients showed a significantly higher level of HPSE expression when compared to healthy individuals (Theodoro et al., 2007). This was in turn shown to decrease following surgery in patients treated with neoadjuvant chemotherapy. This observation therefore suggests a tumour-inducing effect of HPSE expression in PBMCs of breast cancer patients. HPSE was shown to play a role in therapy resistance in breast cancer when tamoxifen was shown to induce HPSE expression in ER-positive breast cancer cells, thus imparting a growth advantage (Cohen et al., 2007). This was shown to occur through the recruitment of AIB1, an ER co-activator, to the *HPSE* promoter resulting in a tamoxifen-mediated agonistic effect on HPSE expression. This finding may explain the failure of tamoxifen therapy in certain breast cancer patients. This study also shed light on the ER-mediated HPSE expression as previously demonstrated through the discovery of four putative estrogen response elements within the *HPSE* gene promoter region (Elkin et al., 2003). *In vivo* studies indicated that HPSE mediates lapatinib resistance in brain-metastatic breast cancer, further suggesting its effect in overcoming cancer therapy (Zhang et al., 2015d). In a study highlighting its potential as a therapeutic target, HPSE-specific T cells were shown to exist in breast cancer patients (Sommerfeldt et al., 2006). The possibilities and challenges of the clinical use of HPSE inhibitors are discussed elsewhere in this thesis.

However, despite decades of research, much remains unknown regarding the precise role of HPSE in the establishment, early progression and metastasis of breast cancer. This is largely due to the lack of robust *in vivo* models. Many of the *in vivo* models utilised in HPSE research involve transgenic HPSE-overexpressing mice and immunodeficient mice. The use of HPSE-overexpressing mice as a comparator does not appropriately reflect the conditions found in nature and it is preferable to use a HPSE-deficient mouse model in conjunction with wild type animals for these studies. The immune system has been demonstrated to play a key role in cancer development and HPSE is now known to regulate key components of the immune system (Putz et al., 2017, Poon et al., 2014). The use of immunodeficient mice to study the effects of HPSE therefore has numerous drawbacks. Furthermore, there are no reported studies utilising a mouse model of spontaneous mammary tumour growth. All reported studies of HPSE in breast cancer have involved the *in vivo* grafting of mammary tumour cells. This does not reproduce the gradual stepwise development of breast cancer and therefore, is unsuitable to investigate the effects of HPSE throughout malignant progression. In order to address these gaps in our current knowledge, spontaneous mammary tumour-developing PyMT-MMTV mice devoid of HPSE expression (PyMT-MMTVxHPSE$^{-/-}$) were used for the study of breast cancer.

In this chapter, the development of mammary tumours in both PyMT-MMTV and PyMT-MMTVxHPSE$^{-/-}$ mice were compared over time to determine the long-term effects of HPSE in breast cancer growth in a spontaneous mammary tumour model. The effects of HPSE on several tumour growth kinetic parameters and mammary gland architecture were explored. Attempts were made to understand the expression of HPSE over time and to determine when the *HPSE* gene was 'switched on' in the mammary glands of PyMT-MMTV mice. The effect of HPSE on angiogenesis in mammary tumours as well as lung metastasis was investigated at both early and late-stage mammary tumour development. Furthermore, the role of HPSE in early mammary tumour development was studied, which had remained poorly defined. Finally, the expression of MMPs in mammary tumour lesions was studied to determine if indeed a compensatory mechanism exists in the mammary TME whereby the lack of HPSE is countered by the overexpression of MMPs as suggested by others.

3.3 Results

3.3.1 Generation of PyMT-MMTVxHPSE$^{-/-}$ mice

In order to define the role of HPSE in spontaneous murine mammary tumour development, a novel *in vivo* model was required. As mentioned, PyMT-MMTV mice provide a robust model for the study of human-like mammary tumour development. Prior to the commencement of the studies described here, the HPSE-deficient PyMT-MMTV mouse strain (PyMT-MMTVxHPSE$^{-/-}$) was developed as outlined in 2.1.1 **(figure 3.1A)**. The genotypes of animals used in these studies were confirmed as outlined in 2.1.2 **(figure 3.1B)**.

Female PyMT-MMTV and PyMT-MMTVxHPSE$^{-/-}$ mice over time developed spontaneous mammary tumours **(figure 3.1C)**. There was no visible significant difference in the growth patterns of mammary tumours between the two strains. A rare few male PyMT-MMTV and PyMT-MMTVxHPSE$^{-/-}$ mice developed mammary tumours over the course of these studies. However, the study of male breast cancer using the PyMT-MMTV model is beyond the scope of this thesis and these animals were thus discarded.

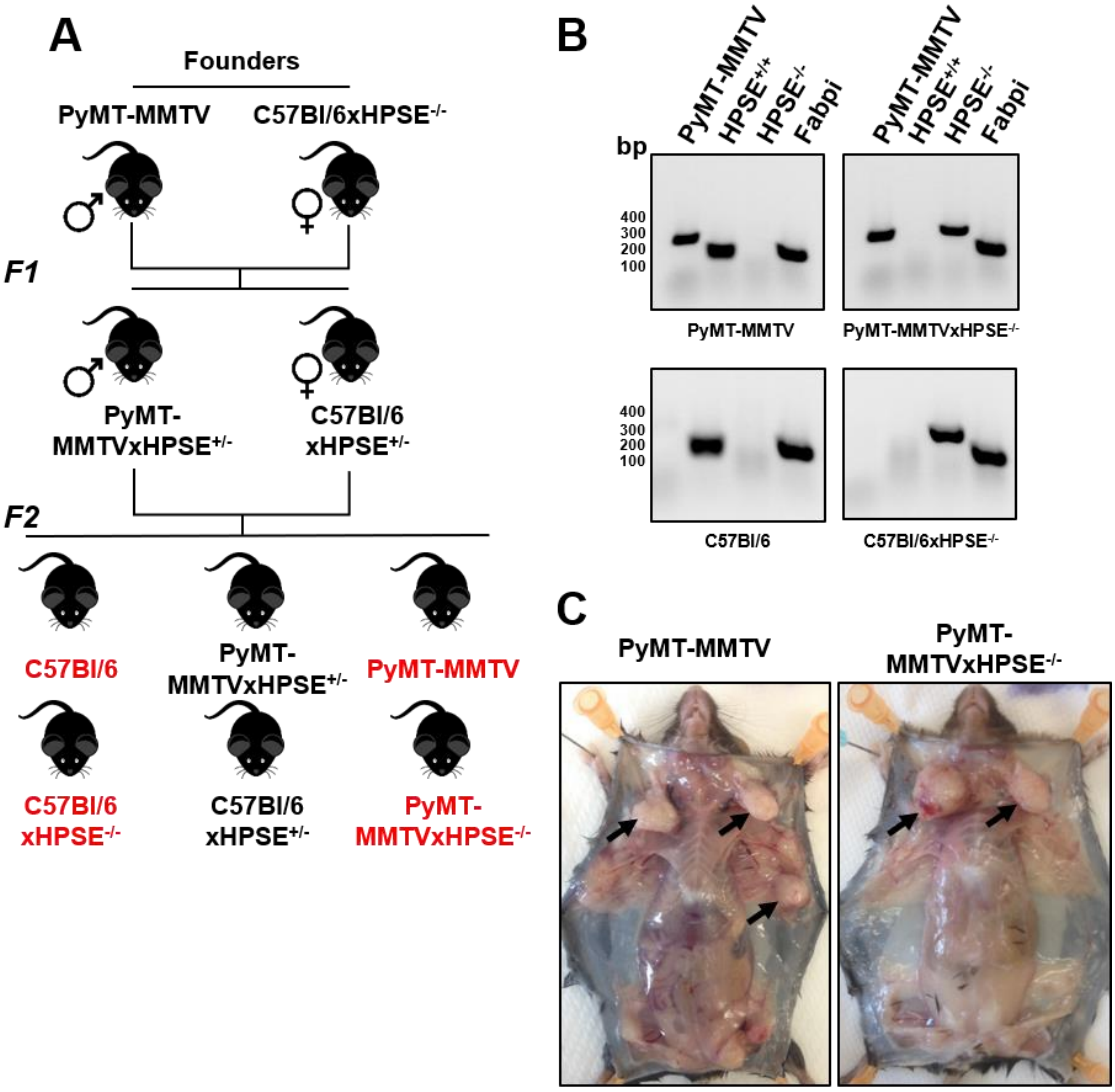

Figure 3.1 Generation of PyMT-MMTVxHPSE$^{-/-}$ mice
(A) The schematic of the breeding strategy used to generate PyMT-MMTVxHPSE$^{-/-}$ mice. The genetic backgrounds of animals resulting from the *F2* generation that were used in subsequent *in vivo* studies described in this thesis are indicated in red. **(B)** Genotypes of PyMT-MMTV, PyMT-MMTVxHPSE$^{-/-}$, C57Bl/6 and C57Bl/6xHPSE$^{-/-}$ animals were confirmed by PCR. **(C)** Representative photographs of spontaneous mammary tumour-bearing female PyMT-MMTV and PyMT-MMTVxHPSE$^{-/-}$ mice at 20-weeks of age. Both strains developed mammary tumours in a comparable manner. Visible mammary tumours are indicated by arrows.

3.3.2 Confirming the HPSE$^{-/-}$ status of mice used in this study

It was necessary to confirm the HPSE expression null status of mice used in this study. The lack of HPSE expression and activity in C57Bl/6xHPSE$^{-/-}$ mice has been previously reported (Poon et al., 2014). In order to verify the HPSE expression status of PyMT-MMTV and PyMT-MMTVxHPSE$^{-/-}$ mice, a Con-A sepharose bead pull down assay was performed on whole spleen lysates of female animals **(figure 3.2A)**. This resulted in a prominent band of approximately 45 kDa upon immunoblotting, which corresponded to the size of purified human HPSE and was present only in the spleen lysates of PyMT-MMTV mice.

It was then necessary to confirm the HPSE status of the PyMT-MMTVxHPSE$^{-/-}$ mice at an enzymatic activity level. An enzyme activity assay was performed to determine HPSE activity in whole spleen lysates of female PyMT-MMTV and PyMT-MMTVxHPSE$^{-/-}$ mice **(figure 3.2B)**. Whole spleen lysate of PyMT-MMTVxHPSE$^{-/-}$ mice exhibited a significantly lower level of HPSE activity compared to that of PyMT-MMTV mice. In order to determine the expression of HPSE in mammary tumour lesions of PyMT-MMTV and PyMT-MMTVxHPSE$^{-/-}$ mice, an anti-HPSE IHC assay was performed **(figure 3.2C)**. The 4th inguinal mammary glands were excised from animals euthanised at the ethical cumulative tumour volume end point. Tumour lesions of at least DCIS-grade within the mammary glands of PyMT-MMTV mice showed distinct regions of HPSE expression while those of PyMT-MMTVxHPSE$^{-/-}$ mice showed a lack of such. These results confirm the lack of HPSE expression in PyMT-MMTVxHPSE$^{-/-}$ mice.

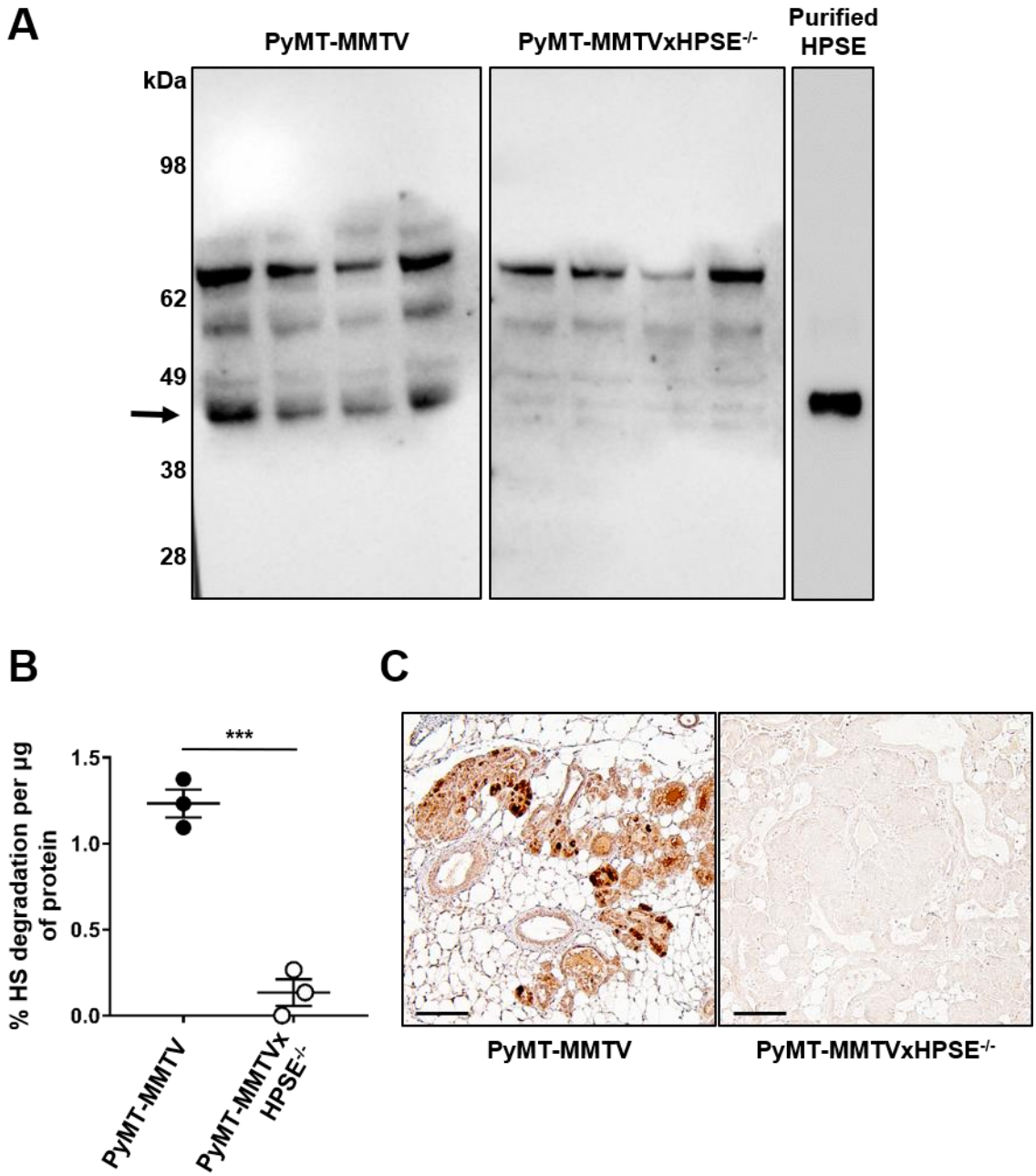

Figure 3.2 Confirmation of HPSE-null status in PyMT-MMTVxHPSE$^{-/-}$ mice
(A) Con-A-Sepharose bead pull down assay of whole spleen lysates of PyMT-MMTV and PyMT-MMTVxHPSE$^{-/-}$ mice followed by a Western blot assay indicated a prominent band of approximately 45 kDa (arrow) corresponding to enzymatically active HPSE seen only in PyMT-MMTV animals *(n* = 4). **(B)** HS degradation assay with whole spleen lysates of PyMT-MMTV and PyMT-MMTVxHPSE$^{-/-}$ mice showed a significant reduction of HPSE enzymatic activity in PyMT-MMTVxHPSE$^{-/-}$ mice (*n* = 3). **(C)** A representative image of an anti-HPSE IHC of mammary gland sections isolated from PyMT-MMTV and PyMT-MMTVx HPSE$^{-/-}$ mice shows a lack of HPSE expression within DCIS/invasive lesions of PyMT-MMTVxHPSE$^{-/-}$ mice. Scale bar = 100 µm; ***, p<0.001, unpaired t-test.

3.3.3 Evaluation of spontaneous mammary tumour growth between PyMT-MMTV and PyMT-MMTVxHPSE$^{-/-}$ mice

Based on our current knowledge of the role of HPSE in tumour growth, it was originally hypothesised that female PyMT-MMTVxHPSE$^{-/-}$ mice would exhibit a significantly less aggressive mammary tumour growth profile in contrast to female PyMT-MMTV mice. In order to investigate the influence of HPSE on spontaneous mammary tumour growth, cumulative tumour volumes of female PyMT-MMTV and PyMT-MMTVxHPSE$^{-/-}$ mice were measured from when tumours were first palpable and measurable to when the animals were euthanised at the ethical cumulative tumour volume end point **(figure 3.3A)**. Mammary tumour growth rates between female PyMT-MMTV and PyMT-MMTVxHPSE$^{-/-}$ mice were observed to be comparable. The time taken to reach the ethical cumulative tumour volume end point was also comparable between female PyMT-MMTV and PyMT-MMTVxHPSE$^{-/-}$ mice **(figure 3.3B)**. The tumour latency periods to when palpable and measurable mammary tumours were first detected were also comparable between female PyMT-MMTV and PyMT-MMTVxHPSE$^{-/-}$ mice **(figure 3.3C)**. In order to determine total mammary gland weights at the ethical end point, mammary glands were excised and weighed immediately following euthanisation. No significant difference in gross mammary gland weights was observed between female PyMT-MMTV and PyMT-MMTVxHPSE$^{-/-}$ mice **(figure 3.3D)**. In order to normalise mammary gland weight measurements, female PyMT-MMTV and PyMT-MMTVxHPSE$^{-/-}$ mice were euthanised at 20-weeks of age and total tumour weights were measured **(figure 3.3E)**. No significant difference was observed in age-matched gross mammary gland weights. These results therefore suggest that HPSE has no significant effect on the spontaneous mammary tumour development and growth kinetics in PyMT-MMTV mice.

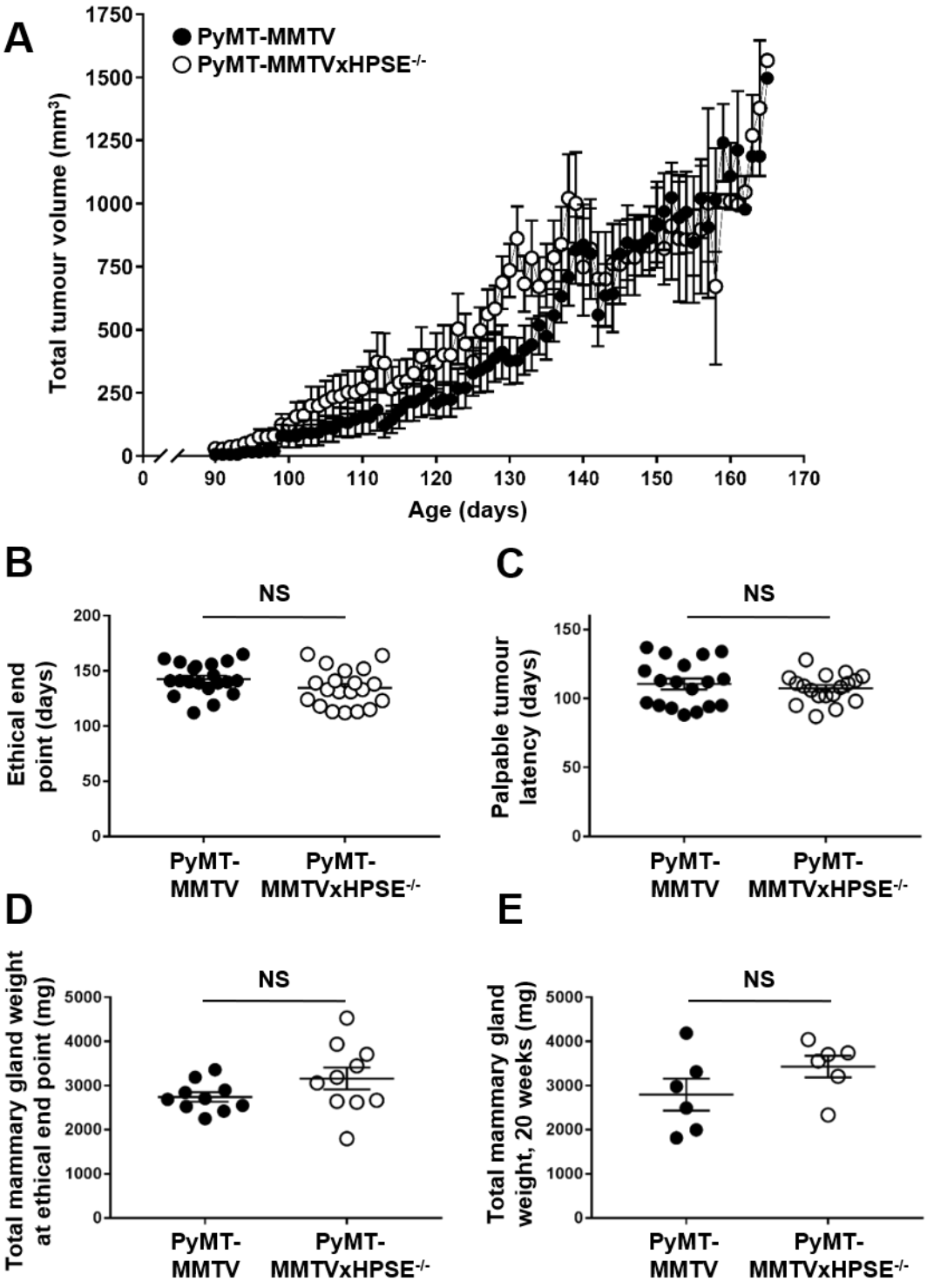

Figure 3.3 Evaluation of spontaneous mammary tumour growth between PyMT-MMTV and PyMT-MMTVxHPSE$^{-/-}$ mice

(A) Total mammary tumour growth rates between PyMT-MMTV and PyMT-MMTVxHPSE$^{-/-}$ mice were comparable; *n* = 20 per group. **(B and C)** Time to reach the ethical tumour volume end point ($\geq$1500mm^3 cumulative tumour volume) in PyMT-MMTV and PyMT-MMTVx HPSE$^{-/-}$ was comparable (*n*=20) as well as the time taken to develop palpable tumours (*n* = 18 – 20). **(D and E)** Total mammary gland weights of PyMT-MMTV and PyMT-MMTVxHPSE$^{-/-}$ at the ethical tumour volume end point (*n* = 10) as well as at 20-weeks of age (*n* = 6) were comparable. Error bars = SEM; NS, not significant; unpaired t-test.

3.3.4 The effect of HPSE on the mammary gland architecture of PyMT-MMTV mice

The effect of HPSE on the architecture of mammary glands of female PyMT-MMTV mice was then evaluated. On account of the role of HPSE in ECM remodelling, it was hypothesised that female PyMT-MMTVxHPSE$^{-/-}$ mice would exhibit a less-complex organisation of ductal branching and overall mammary gland internal architecture in comparison to PyMT-MMTV mice. The 4th inguinal mammary glands were excised at the ethical tumour volume end point, whole mounted and visually examined under magnification **(figure 3.4)**. Upon visual observation of the pattern and extent of mammary ductal branching as well as the development of alveolar buds between PyMT-MMTV and PyMT-MMTVxHPSE$^{-/-}$ mice, no significant difference was observed in the overall mammary architecture between the two strains. This result suggests that HPSE may not have a significant influence on the development of mammary glands of female PyMT-MMTV mice.

3.3.5 HPSE expression over time in PyMT-MMTV mammary glands

Although it is known that HPSE is overexpressed in breast cancer, it is not well understood precisely when during mammary tumour development this physiological change occurs (Boyango et al., 2014). An attempt was thus made to determine when significant HPSE expression first became evident during the mammary tumour progression of PyMT-MMTV mice **(figure 3.5)**. Initial H&E staining of 4th inguinal mammary glands of PyMT-MMTV mice at 4, 8, 12, 16 and 20-weeks of age confirmed tumour lesions of at least DCIS grade. This was followed by an anti-HPSE IHC, which revealed detectable levels of HPSE expression within the DCIS lesions occurring as early as 4-weeks of age and remaining consistent over time. No significant overexpression of HPSE associated with the age of the mice was observed. Therefore, these results suggest that in PyMT-MMTV mice, tumour lesion-associated HPSE expression within the mammary glands occurs early in tumour development and remains at a steady level throughout growth.

3.3.6 The influence of HPSE on angiogenesis in PyMT-MMTV mammary tumours

It is known that HPSE promotes angiogenesis in solid tumours, leading to enhanced tumour growth (Zhang et al., 2009, Ostapoff et al., 2013, Cohen et al., 2006, Naomoto et al., 2007). In order to investigate this phenomenon in PyMT-MMTV mammary tumours, an anti-CD31 IHC was performed on serial sections of mammary tumours excised at the ethical cumulative tumour volume end point **(figure 3.6A)**. Upon quantitative analysis, it was revealed that tumours excised from female PyMT-MMTVxHPSE$^{-/-}$ mice exhibited a significantly reduced level of microvessel density compared to those from PyMT-MMTV mice **(figure 3.6B)**. This result suggests that HPSE does indeed play a significant role in promoting angiogenesis in mammary tumours of PyMT-MMTV mice. It is however

interesting to note that this difference in angiogenesis did not translate to a variation in mammary tumour growth rates between female PyMT-MMTV and PyMT-MMTVxHPSE$^{-/-}$ mice.

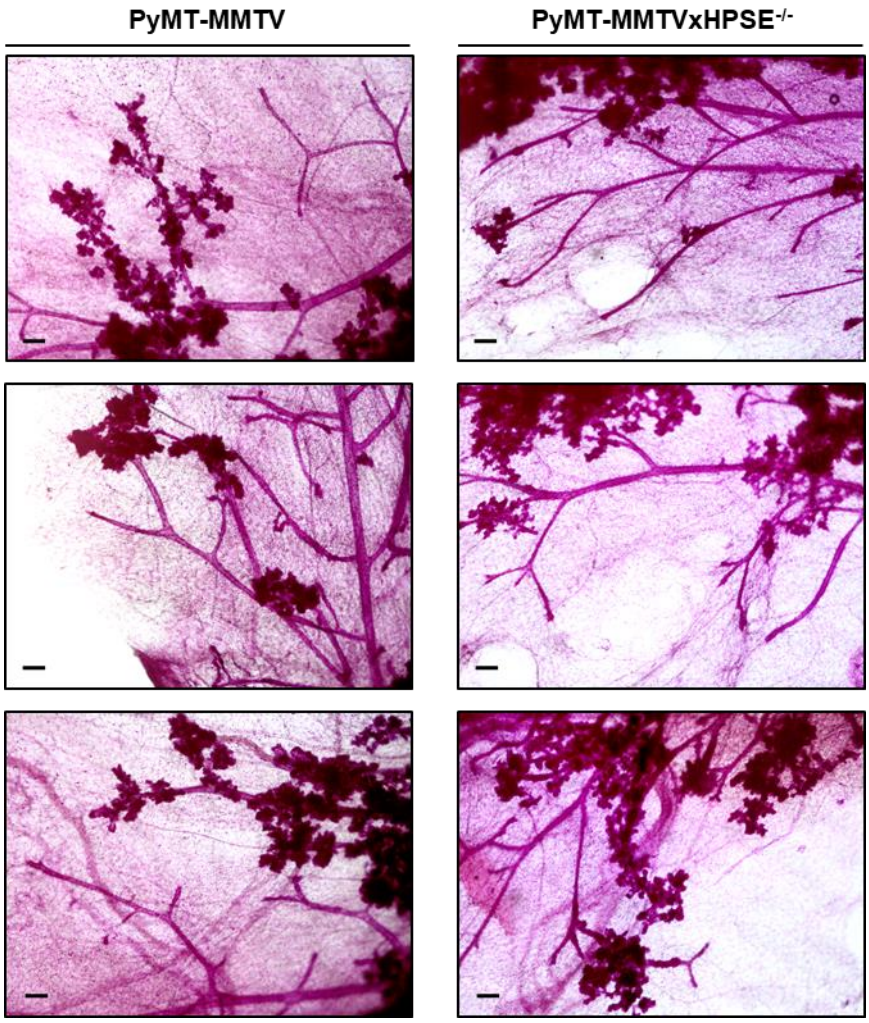

Figure 3.4 Mammary gland architecture of PyMT-MMTV and PyMT-MMTVxHPSE$^{-/-}$ mice at the ethical tumour volume end point
Whole-mounted 4th inguinal mammary glands of PyMT-MMTV and PyMT-MMTVxHPSE$^{-/-}$ mice excised at the ethical tumour volume end point appeared similar in architecture upon visual observation. Representative images of one mammary gland per mouse, *n = 3* per group. Scale bars = 50 µm.

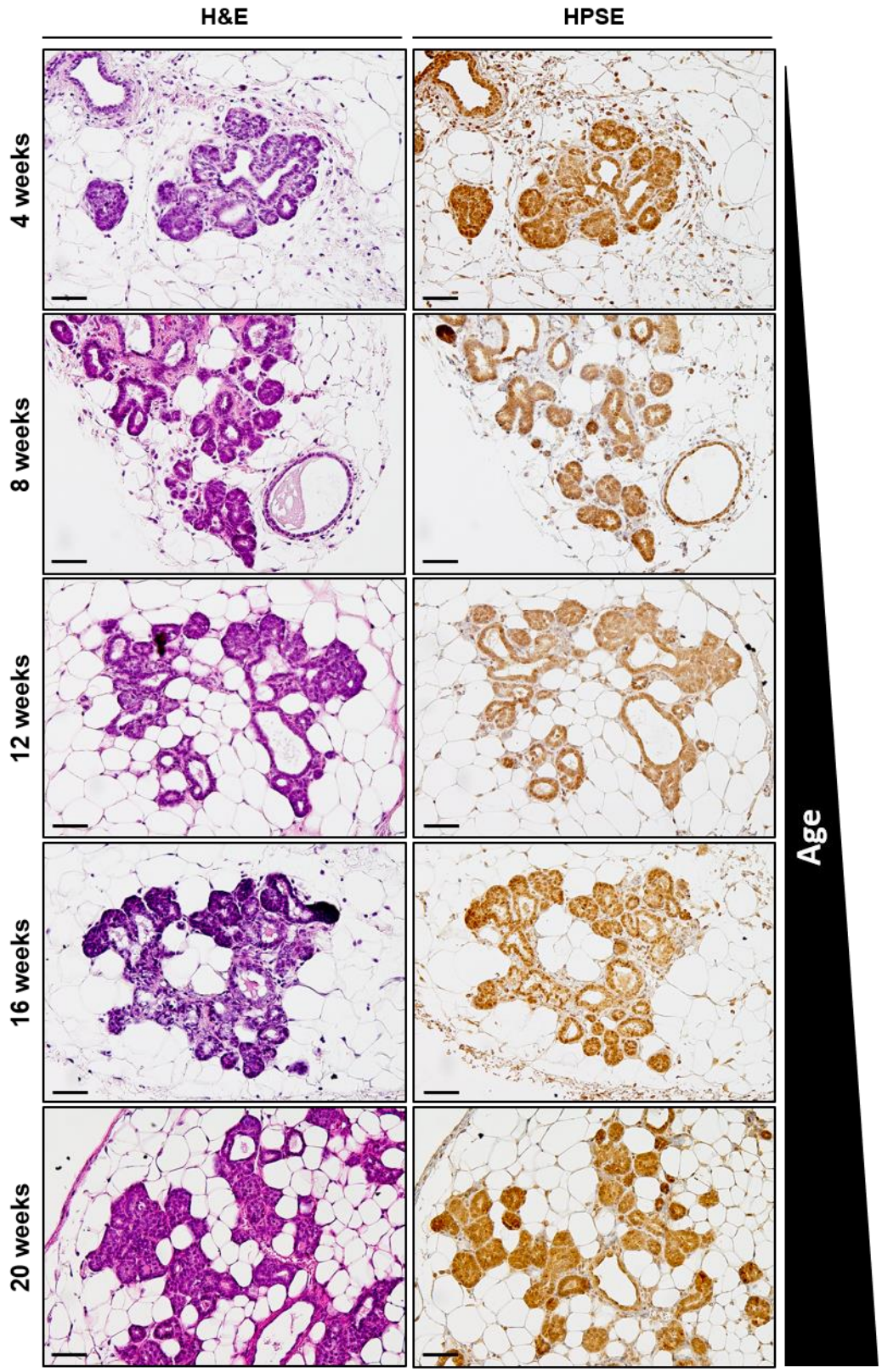

Figure 3.5 HPSE expression over time in mammary glands of PyMT-MMTV mice
Evaluation of HPSE expression by IHC in the 4th inguinal mammary glands of 4, 8, 12, 16 and 20-week old PyMT-MMTV mice bearing DCIS lesions revealed a consistent level of HPSE expression over time. Representative images of *n* = 3 per age group. Scale bar = 50 µm.

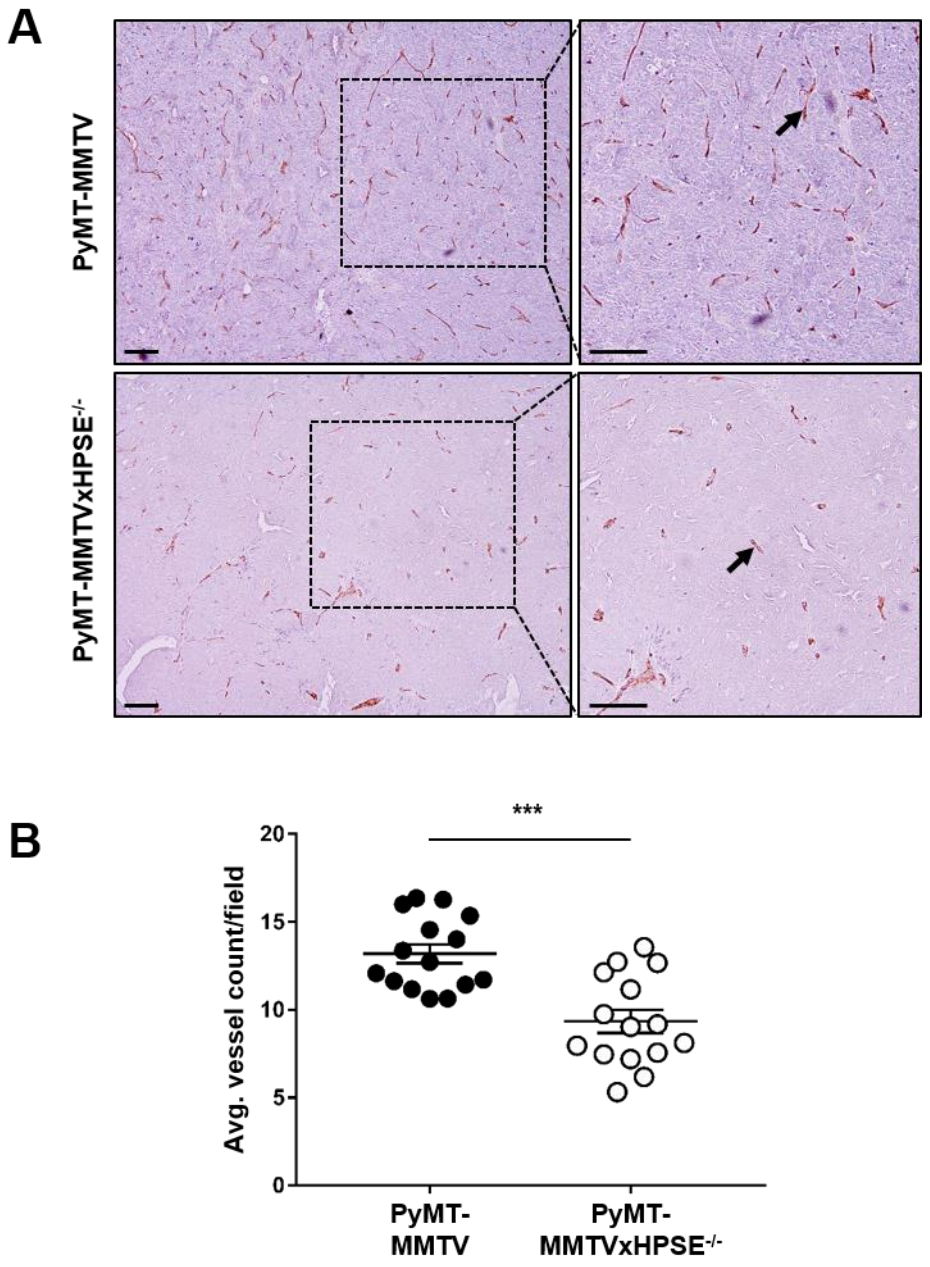

Figure 3.6 Microvessel density quantification in PyMT-MMTV and PyMT-MMTVxHPSE$^{-/-}$ mammary tumours
(A) Representative anti-CD31 IHC images of serial sections of primary mammary tumour excised from PyMT-MMTV and PyMT-MMTVxHPSE$^{-/-}$ mice. Arrows indicate microvessels positively stained for CD31. **(B)** Quantification of microvessels revealed that tumours excised from PyMT-MMTVxHPSE$^{-/-}$ mice exhibited a significantly reduced level of angiogenesis. Pooled data, *n* = 3 per group; 5 serial sections per tumour. Scale bars = 100 µm. Error bars = SEM; ***, p<0.001; unpaired t-test.

3.3.7 The influence of HPSE on angiogenesis in early PyMT-MMTV mammary tumour development

Following the observation that HPSE influences mammary tumour angiogenesis, as evident at the ethical cumulative tumour volume end point, it was decided to investigate if this phenotype was observable early in tumour development in female PyMT-MMTV and PyMT-MMTVxHPSE$^{-/-}$ mice. Serial sections of 4th inguinal mammary glands of 6-week old female PyMT-MMTV and PyMT-MMTVxHPSE$^{-/-}$ mice were subjected to an anti-CD31 IHC analysis **(figure 3.7A)**. Upon visual examination, microvessels associated with DCIS/invasive mammary tumour lesions were located. Quantitative analysis revealed there was no significant difference in vessel count between mammary gland sections of PyMT-MMTV and PyMT-MMTVxHPSE$^{-/-}$ mice **(figure 3.7B)**. This result suggests that although a positive correlation between angiogenesis and HPSE expression is evident in late-stage mammary tumours of female PyMT-MMTV mice, this phenotype does not exist in early mammary tumour development. Therefore, it is likely that HPSE-driven upregulation of angiogenesis occurs at a later stage in mammary tumour growth in female PyMT-MMTV mice.

3.3.8 The role of host HPSE in influencing metastasis of PyMT-MMTV mammary tumours

As previously described, mammary tumours in PyMT-MMTV mice result mainly in lung metastases (Guy et al., 1992). Numerous studies have demonstrated HPSE as a promoter of tumour metastasis as highlighted in the first chapter of this thesis. This therefore led to the evaluation of the role of HPSE in influencing lung metastasis in PyMT-MMTV and PyMT-MMTVxHPSE$^{-/-}$ mice to test the hypothesis that female PyMT-MMTVxHPSE$^{-/-}$ mice would exhibit significantly reduced lung metastases in contrast to PyMT-MMTV mice. To first confirm the presence of metastasis in these animals, serial lung sections were stained with H&E and visually examined for the presence of lesions **(figure 3.8A)**. This analysis revealed that both female PyMT-MMTV and PyMT-MMTVxHPSE$^{-/-}$ mice euthanised at the ethical tumour volume end point did indeed exhibit lung metastases, although only 50% of all mice of either strain presented visible lesions. A quantitative analysis of the number of metastatic lesions did not reveal a significant difference between female PyMT-MMTV and PyMT-MMTVxHPSE$^{-/-}$ mice **(figure 3.8B)**. Further quantitative analysis of the lung metastatic burden between the two strains through calculating qPCR-derived RTB confirmed the previous findings, showing no significant difference in RTB in the lungs of female PyMT-MMTV and PyMT-MMTVxHPSE$^{-/-}$ mice euthanised at the ethical tumour volume end point **(figure 3.8C)**. These results suggest that even though HPSE is known

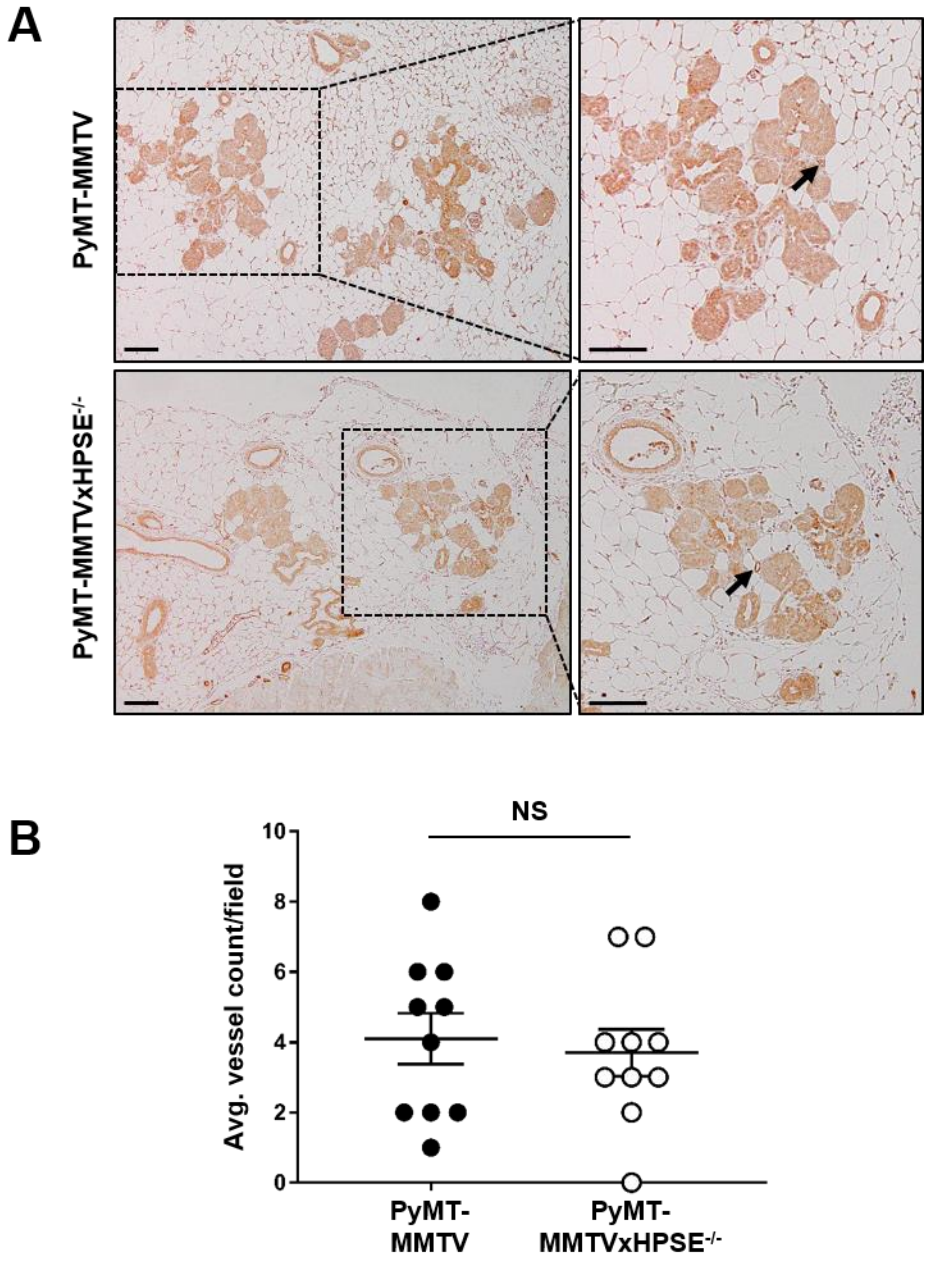

Figure 3.7 Evaluation of DCIS/invasive lesion-associated microvasculature in 6-week old PyMT-MMTV and PyMT-MMTVxHPSE$^{-/-}$ mouse mammary glands
(A) Representative anti-CD31 IHC images of DCIS/invasive lesion-bearing mammary glands of 6-week old PyMT-MMTV and PyMT-MMTVxHPSE$^{-/-}$ mice. Microvasculature positive for CD31 expression are indicated by arrows. **(B)** Visual quantification of blood vessels associated with regions of DCIS and invasive lesions revealed no significant difference in angiogenesis during early tumour development. Pooled data of *n* = 5 per group; 2 sections per mammary gland. Scale bars = 100 µm. Error bars = SEM; NS, not significant; unpaired t-test.

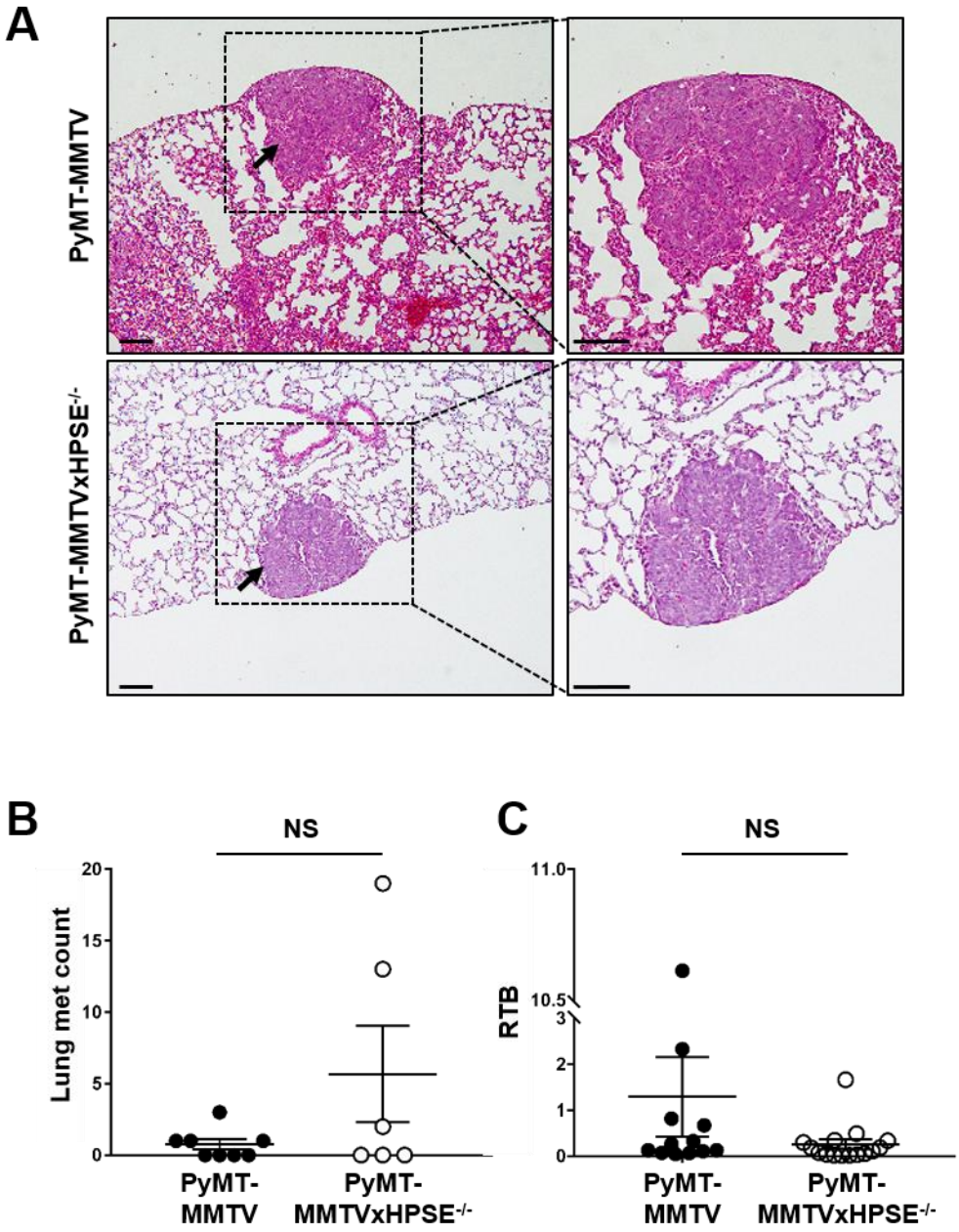

Figure 3.8 Lung metastatic burden in PyMT-MMTV and PyMT-MMTVxHPSE$^{-/-}$ mice
(A) Representative images of metastatic lesions in PyMT-MMTV and PyMT-MMTVxHPSE$^{-/-}$ female mice lungs excised at the ethical tumour volume end point; H&E stained. **(B)** Visual quantification of individual metastatic lesions in serial lung sections revealed no significant difference between PyMT-MMTV and PyMT-MMTVx HPSE$^{-/-}$ mice (n = 6 – 8). **(C)** qPCR of PyMT-MMTV and PyMT-MMTVxHPSE$^{-/-}$ mouse lungs excised at the ethical tumour volume end point revealed no significant difference in RTB (n = 12 – 15). Scale bars = 100 μm. Error bars = SEM; NS, not significant; unpaired t-test.

to promote metastasis in numerous cancer settings, HPSE in the PyMT-MMTV mouse model does not play such a role.

3.3.9 Evaluation of the role of HPSE in the early stages of mammary tumour development in the PyMT-MMTV mouse model

As discussed earlier in this chapter, it is known that HPSE promotes the development of breast cancer. However, despite extensive research, the precise role of HPSE in the early stages of mammary tumour development remains poorly defined. The spontaneous mammary tumour-developing mouse model PyMT-MMTV was therefore investigated in this context. Mammary tissue from 6-week old PyMT-MMTV and PyMT-MMTVxHPSE$^{-/-}$ mice were serially sectioned and histologically examined to reveal the pathological status of tumour lesions present in each mammary gland **(figure 3.9A)**. The presence of lesions was first determined through H&E staining, which revealed normal mammary glands or malignant grades of hyperplasia, DCIS and invasive carcinoma. Further staining with anti-Ki67 and anti-SMMHC antibodies distinguished between hyperplasia, DCIS and invasive carcinoma stages. A graphical representation shows the distribution of incidence of each major stage of breast cancer observed between all mammary glands analysed **(figure 3.9B)**. This was further expanded upon to represent the distribution between non-invasive and invasive lesions observed in each of the four mammary glands per animal analysed in this study **(figure 3.9C)**. No distinct variation in lesion grade between female PyMT-MMTV and PyMT-MMTVxHPSE$^{-/-}$ mice was observed in either of these representations. Finally, a quantitative analysis of the number of mammary glands bearing non-invasive vs invasive mammary tumour lesions between PyMT-MMTV and PyMT-MMTVxHPSE$^{-/-}$ mice was carried out by a chi-square test as previously described (Duivenvoorden et al., 2017) **(figure 3.9D)**. This revealed no significant variation in invasive lesion incidence between the two groups. Together, these data suggest that HPSE does not play a role in promoting the progression of PyMT-MMTV mammary tumours early in their development.

3.3.10 Investigating the presence of a compensatory mechanism of MMP expression in PyMT-MMTVxHPSE$^{-/-}$ mouse mammary tumour lesions

Due to the dynamic nature of the ECM, the lack of an ECM-modulatory enzyme such as HPSE is sometimes thought to be compensated for by the upregulation of other ECM remodelling enzymes such as MMPs (Zcharia et al., 2009). However, our previous data suggests otherwise (Poon et al., 2014). In order to determine the status of MMP expression within mammary gland lesions, DCIS/invasive lesions were analysed for MMP-2 expression by IHC **(figure 3.10A)**. H-score quantification of MMP-2 expression revealed no significant difference between PyMT-MMTV and PyMT-MMTVxHPSE$^{-/-}$ mice **(figure**

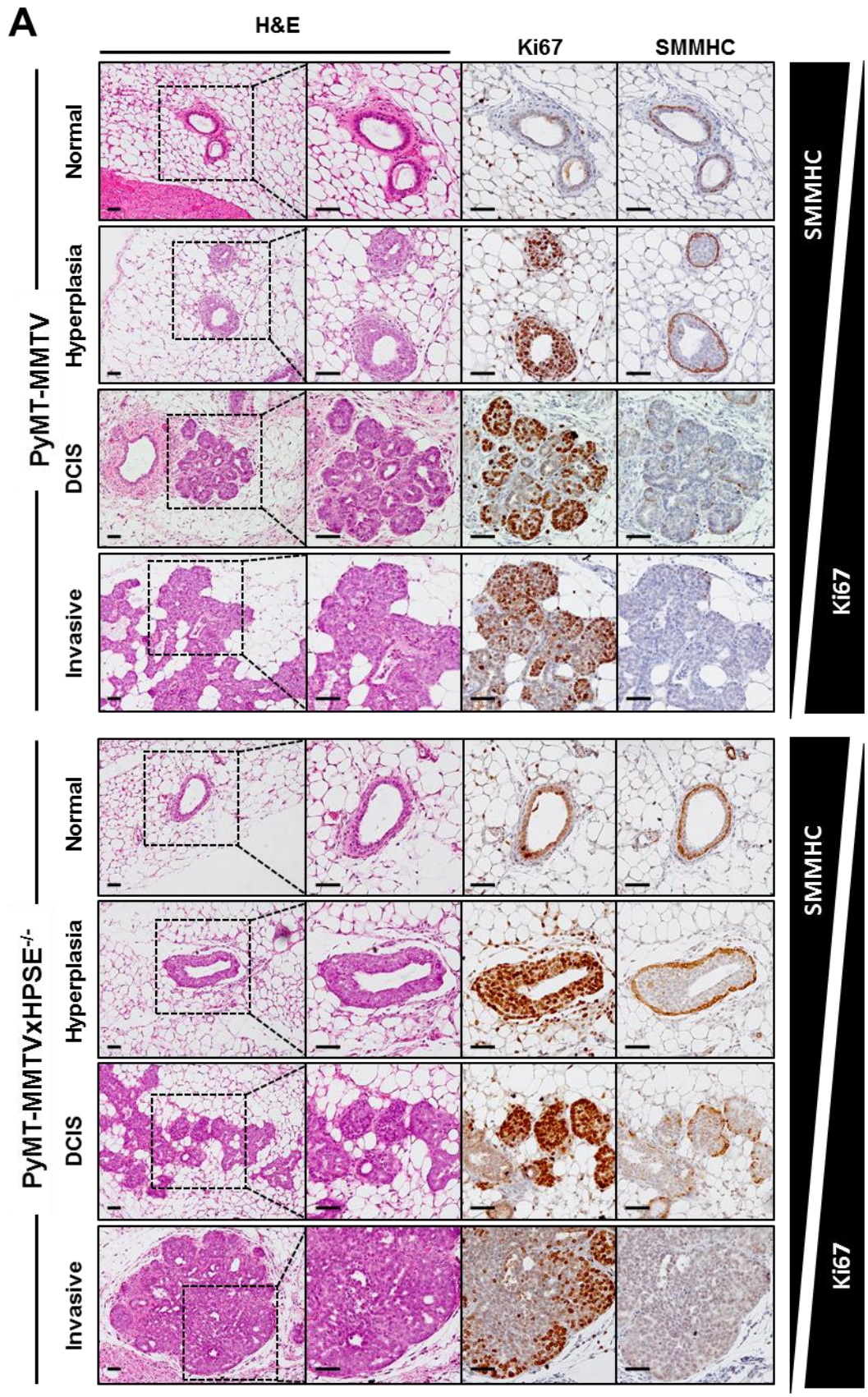
A
H&E
Ki67
SMMHC
PyMT-MMTV
Normal
Hyperplasia
DCIS
Invasive
SMMHC
Ki67
PyMT-MMTVxHPSE-/-
Normal
Hyperplasia
DCIS
Invasive
SMMHC
Ki67

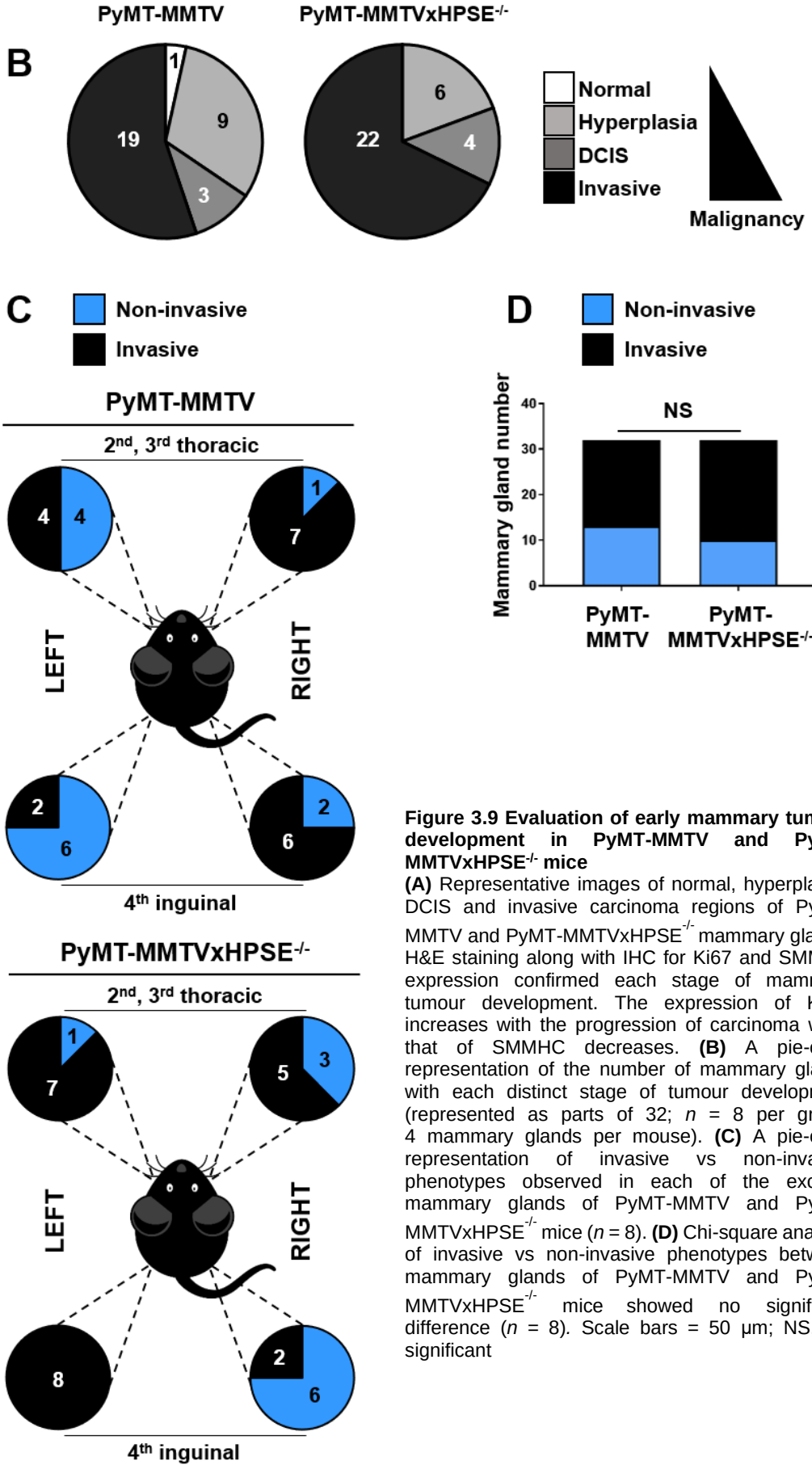

Figure 3.9 Evaluation of early mammary tumour development in PyMT-MMTV and PyMT-MMTVxHPSE$^{-/-}$ mice
(A) Representative images of normal, hyperplastic, DCIS and invasive carcinoma regions of PyMT-MMTV and PyMT-MMTVxHPSE$^{-/-}$ mammary glands. H&E staining along with IHC for Ki67 and SMMHC expression confirmed each stage of mammary tumour development. The expression of Ki-67 increases with the progression of carcinoma while that of SMMHC decreases. **(B)** A pie-chart representation of the number of mammary glands with each distinct stage of tumour development (represented as parts of 32; *n* = 8 per group, 4 mammary glands per mouse). **(C)** A pie-chart representation of invasive vs non-invasive phenotypes observed in each of the excised mammary glands of PyMT-MMTV and PyMT-MMTVxHPSE$^{-/-}$ mice (*n* = 8). **(D)** Chi-square analysis of invasive vs non-invasive phenotypes between mammary glands of PyMT-MMTV and PyMT-MMTVxHPSE$^{-/-}$ mice showed no significant difference (*n* = 8). Scale bars = 50 μm; NS, not significant

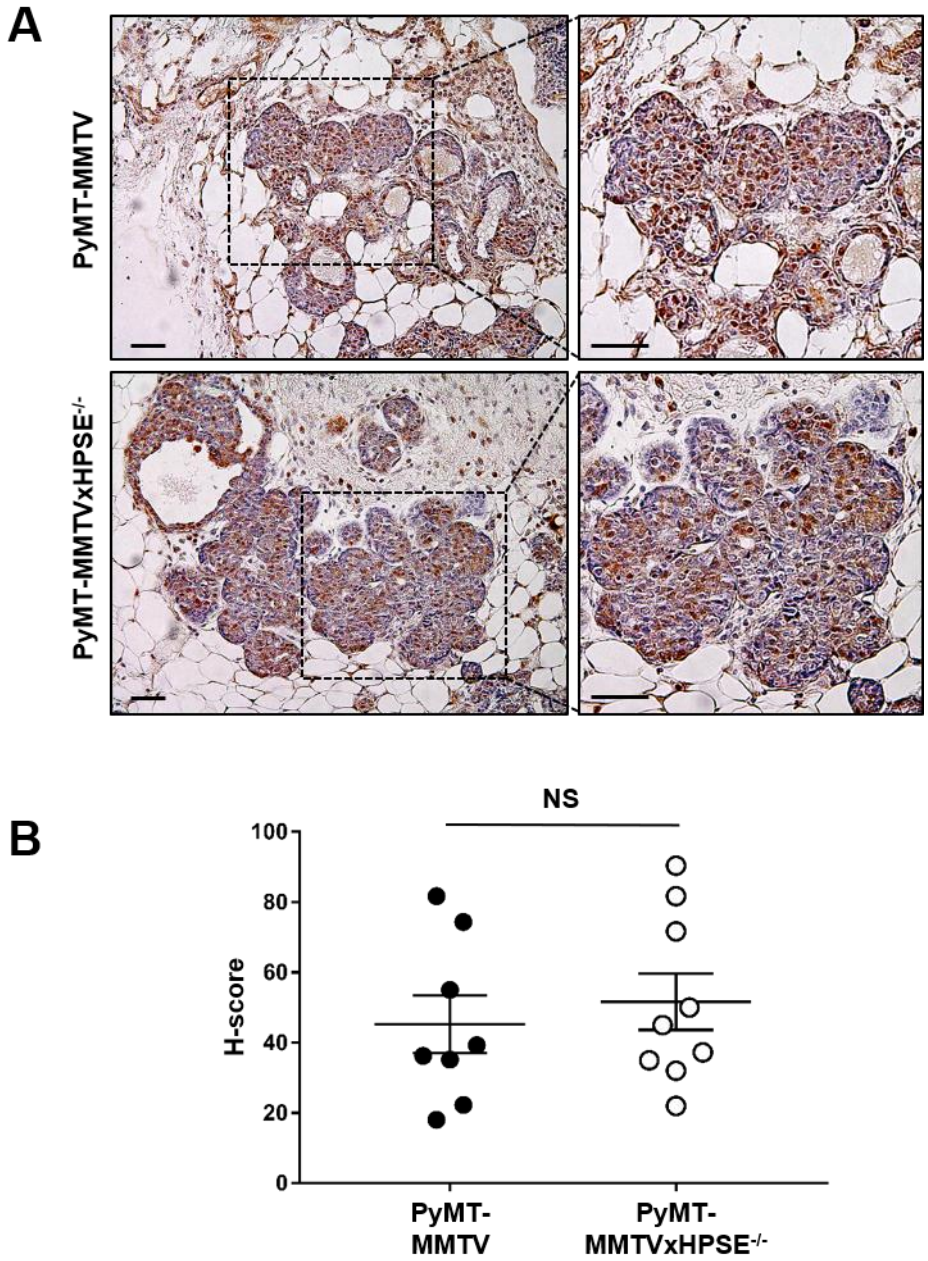

Figure 3.10 H-score quantification of MMP-2 expression in DCIS/invasive lesions of PyMT-MMTV and PyMT-MMTVxHPSE$^{-/-}$ mouse mammary glands
(A) Representative MMP-2 IHC images of serial sections of DCIS/invasive lesion-bearing mammary glands excised from 20-week old PyMT-MMTV and PyMT-MMTVxHPSE$^{-/-}$ mice. **(B)** H-score analysis revealed no significant difference in staining intensity and therefore, MMP-2 expression levels in DCIS/invasive lesions of PyMT-MMTV and PyMT-MMTVxHPSE$^{-/-}$ mice (n = 3). Scale bar = 200 μm; Error bars = SEM; NS, not significant; unpaired t-test.

3.10B).This suggests that mammary tumour-associated MMP-2 expression (and possibly the expression of other MMPs) is not influenced by the lack of HPSE in PyMT-MMTVxHPSE$^{-/-}$ mice and a previously-proposed compensatory mechanism of upregulated MMP expression does not exist in this model.

3.4 Discussion

HPSE has been suggested as a key player in breast cancer progression, as supported by extensive *in vitro* and *in vivo* data as well as numerous clinical investigations mentioned in section 3.2. A majority of cancer-related deaths are the direct result of metastasis (Steeg, 2016). Breast cancer in particular, proves potentially life-threatening in its metastatic setting in contrast to when localised to its primary site. As a key promoter of tumour growth and metastasis, HPSE has therefore garnered much attention over the past several decades in the context of breast cancer. This chapter utilised the well-defined PyMT-MMTV mouse model of spontaneous mammary tumour development in order to further define the precise role of HPSE in murine breast cancer which would in turn form a basic understanding of the human malignancy.

3.4.1 PyMT-MMTV mice as a model of human breast cancer

The study of breast cancer has involved a large variety of mouse models over several decades, whilst acknowledging that the perfect *in vivo* model does not exist (Holen et al., 2017, Saxena and Christofori, 2013). The PyMT-MMTV mouse model is a well-characterised, robust mouse model of spontaneous mammary tumour development and metastasis, which closely resembles the development of breast cancer in humans (Lin et al., 2003). Therefore, this has emerged as an ideal *in vivo* model to understand the human malignancy. These are transgenic mice where the **p**ol**y**omavirus **m**iddle-**t**umour antigen (PyMT) expression is driven by the **m**ouse **m**ammary **t**umour **v**irus (MMTV) promoter's long terminal repeat (LTR) regulatory sequence (Guy et al., 1992). The PyMT is a robust oncogenic antigen with a demonstrated capacity to transform mouse cells and give rise to cancer (Lee et al., 2011, Kiefer et al., 1994, Dilworth, 2002, Schaffhausen and Roberts, 2009). The tumour induction is through the mimicking of an activated growth factor receptor and has been demonstrated to increase cellular responsiveness to growth factors (Zhou et al., 2011a, Raptis, 1991). The development of multifocal tumours involves the activation of c-src, PI3-K and Raf-Mek-ERK signalling pathways, resulting in the malignant transformation of the mammary epithelial cells (Courtneidge and Smith, 1983, Whitman et al., 1985, Ichaso and Dilworth, 2001). At the time of derivation of these animals, a majority of mice were reported to develop lung metastases (Guy et al., 1992).

PyMT-driven mammary carcinogenesis has been shown to upregulate MMP-13 with no promotion of tumour growth (Nielsen et al., 2008). It also promotes the expression of

osteopontin, demonstrated to promote metastasis through EMT plasticity regulation (Whalen et al., 2008, Jia et al., 2016). However, no evidence yet exists for the influence of PyMT-driven carcinogenesis on HPSE expression. The MMTV-LTR contains a glucocorticoid hormone response element, resulting in a hormonal-driven regulation of protein expression (Dudley et al., 2016, Otten et al., 1988, Mink et al., 1990, Qin et al., 1999). These features result in localised, spontaneous tumour growth with associated metastasis.

Numerous studies have elucidated the malignant progression in the PyMT-MMTV model. The analysis of gene activation at each distinct stage of tumour development showed a remarkably similar gene expression pattern between both later stages and the beginning of tumour growth, shedding new light on the transcriptional dynamics of this model (Cai et al., 2017). Lin *et al*. described in detail the mammary tumour growth process in PyMT-MMTV mice (Lin et al., 2003). Here, it was reported that similar to humans, the mice exhibited morphologically distinct stages of hyperplasia, adenoma, early carcinoma and late carcinoma. The expression of biomarkers, too, was consistent with human breast cancers resulting in a poor prognosis, with the gradual loss of ER, PR as well as integrin-β1 along with the persistent expression of cyclin-D1 and ErbB2/Neu (equivalent to human HER2). Malignancy was also associated with an increased influx of leukocytes. Myoepithelial cells, critical in limiting metastasis in mammary tumours, as well as proliferation markers were recently utilised in developing a scoring matrix to distinguish normal epithelium, hyperplasia, intraepithelial neoplasia and invasive carcinoma in PyMT-MMTV mice (Duivenvoorden et al., 2018). This would enable the transition of *in vivo* findings to a clinical setting.

Several mouse strains have been derived based on the PyMT-MMTV model for the study of numerous breast cancer-related processes. These include PI3K signalling, CSF-1 driven tumorigenesis, the regulation of pulmonary metastasis of mammary carcinoma by $CD4^+$ T-cells, the role of neutrophils in supporting lung metastasis in breast cancer, the CD44-mediated metastatic invasion during breast cancer, VEGF-mediated mammary tumour growth, TGF-β signalling, urokinase-mediated breast cancer metastasis and the role of mitogen-activated protein kinase kinase kinase-1 in breast cancer metastasis (Klarenbeek et al., 2013, Lin et al., 2001, DeNardo et al., 2009, Lopez et al., 2005, Schoeffner et al., 2005, Muraoka-Cook et al., 2004, Almholt et al., 2005, Cuevas et al., 2006, Wculek and Malanchi, 2015b). Thus, the PyMT-MMTV model has established itself as an ideal tool in the study of breast cancer.

Most studies on the role of HPSE in breast cancer have been conducted using *in vivo* models incorporating HPSE overexpression, the use of isolated breast cancer cells *in vitro*

or the use of human clinical samples. No studies thus far have reported the use of an *in vivo* model of spontaneous mammary tumour development incorporating the genetic ablation of HPSE expression. This chapter aimed to address the current gap in knowledge with the use of PyMT-MMTVxHPSE$^{-/-}$ mice. Data generated from these animals were expected to shed further light on the role of HPSE in human breast cancer.

Earlier, we established the C57Bl/6xHPSE$^{-/-}$ mouse strain and demonstrated the lack of HPSE expression in these animals both at a transcription level and a protein expression level (Poon et al., 2014). However, it was necessary to also demonstrate the lack of HPSE expression localised specifically to regions of tumour lesions in the mammary glands of female PyMT-MMTVxHPSE$^{-/-}$ mice. As expected, no HPSE expression was observed within DCIS/invasive mammary tumour lesions of female PyMT-MMTVxHPSE$^{-/-}$ mice, further validating our previous findings **(figure 3.2C)**.

3.4.2 The HPSE-independent mechanism of mammary tumour progression in female PyMT-MMTVxHPSE$^{-/-}$ mice

Based on published literature, female PyMT-MMTVxHPSE$^{-/-}$ mice lacking in HPSE expression were hypothesised to develop less aggressive mammary tumours in contrast to PyMT-MMTV mice. However, results of this study suggest otherwise. Mammary tumours in both female PyMT-MMTV and PyMT-MMTVxHPSE$^{-/-}$ mice progressed in a similar manner. PyMT-MMTVxHPSE$^{-/-}$ mice mammary tumours also exhibited a similar tumour latency as those of PyMT-MMTV mice. No parameter used to evaluate mammary tumour growth suggested a disadvantage of lacking HPSE expression in these animals **(figure 3.3)**. These data therefore suggest a HPSE-independent mode of mammary tumour development in the PyMT-MMTV mouse model, which is contrary to our original hypothesis.

Recently, the MMTV-directed overexpression of HPSE in the mammary glands of mice demonstrated a HPSE-mediated promotion of mammary gland development (Boyango et al., 2018). In order to investigate the role of HPSE in the development of mammary glands of PyMT-MMTV mice in this thesis, mammary glands were examined at the ethical tumour volume end point **(figure 3.4)**. This suggested no distinct role of HPSE in mammary gland branching morphogenesis, in contrast to previously published data (Zcharia et al., 2009, Boyango et al., 2018). It should be noted, however, that the studies by Boyango *et al.* stimulated the overexpression of HPSE specifically in the mouse mammary glands and compared HPSE-transgenic mice to their wild type counterparts. A HPSE-deficient control was not employed in arriving at this conclusion. It should further be noted that mouse mammary glands undergo ovarian cycle-dependent morphological changes and its development is strongly hormonal-driven (Bocchinfuso et al., 2000, Fata et al., 2001, Chua et al., 2010). Thus, it may be crucial to consider synchronising the oestrous cycle status

of female mice used in similar studies in order to better define the role of HPSE independently of the effects of varying hormone levels.

3.4.3 Despite a lack of primary tumour growth disadvantage in PyMT-MMTVxHPSE$^{-/-}$ mice, tumour angiogenesis is affected

Angiogenesis is a key requirement for tumour progression as discussed previously, with HPSE functioning as a promoter of neovascularisation (Cohen et al., 2006). Consistent with this notion, mammary tumours excised from female PyMT-MMTVxHPSE$^{-/-}$ mice at the cumulative ethical tumour volume end point were shown to possess significantly reduced vasculature in contrast to those from PyMT-MMTV mice **(figure 3.6)**. This observation aligns with that of previous studies conducted using both *in vivo* and human clinical samples (Cohen et al., 2006, Dai et al., 2017). However, no significant variation in mammary tumour lesion-associated microvessels was observed in the early stages of PyMT-MMTV mammary tumour growth **(figure 3.7)**.

These observations suggest that HPSE is a promoter of angiogenesis in PyMT-MMTV mice, whose effects become evident at the ethical tumour volume end point. It is interesting to note that reduced angiogenesis in female PyMT-MMTVxHPSE$^{-/-}$ mice did not result in impaired mammary tumour growth. The current literature reports an increase in HPSE expression leading to increased angiogenesis that in turn correlates with an increased tumour size and growth rate in numerous cancer settings as discussed earlier. Based on the observations reported in this chapter however, it can be suggested that in the PyMT-MMTV model, a reduction in mammary tumour angiogenesis as a result of the lack of HPSE expression does not impact upon the overall tumour growth capacity. A similar relationship in human malignancies is yet to be reported. Indeed, in certain clinical settings, the use of HPSE inhibitors aimed at inhibiting tumour growth through impaired angiogenesis may not prove to be effective. This concept requires further investigation.

It should also be noted that angiogenesis is not wholly dependent on HPSE but rather enhanced through its enzymatic activity. Therefore, it is likely that the inherent capacity of a mammary tumour to generate its vasculature independently of HPSE activity is sufficient to maintain tumour growth. This likely occurs through the activity of enzymes such as MMPs, with ECM-modulating and angiogenesis-inducing capabilities (Deryugina and Quigley, 2015). It also remains to be seen if the reduction in angiogenesis in HPSE-devoid mammary tumours leads to increased hypoxia and in turn, leads to downstream HIF-mediated survival pathways, resulting in the maintenance of tumour progression (Tam et al., 2020, LaGory and Giaccia, 2016).

3.4.4 HPSE expression is detected early and remains consistent during PyMT-MMTV mammary tumour growth

The data gathered from investigating primary tumour angiogenesis in PyMT-MMTV mice further suggest that a distinct overexpression of HPSE may likely be observed at a specific and yet to be elucidated stage of PyMT-MMTV mammary tumour development. However, an attempt to pinpoint if and when an increase in mammary tumour lesion-associated HPSE expression occurred suggested that HPSE expression remains at a consistent level throughout mammary tumour development in PyMT-MMTV mice **(figure 3.5)**. The high lipid content of the mammary glands prevented the conduct of enzymatic activity assays to demonstrate the HPSE activity within these glands over time and therefore, an anti-HPSE IHC was employed. Taken together with the previous data on HPSE-driven tumour angiogenesis, these observations suggest that a distinct upregulation of HPSE expression may not occur in PyMT-MMTV mice during the course of mammary tumour development, but a consistent level of HPSE expression does activate the angiogenic switch.

3.4.5 Metastasis in PyMT-MMTV occurs independently of HPSE

Spontaneous metastasis is a key feature of the PyMT-MMTV mouse model, which further warrants its use in the understanding of breast cancer progression. The use of PyMT-MMTVxHPSE$^{-/-}$ animals therefore enabled the investigation of the influence of HPSE expression on breast cancer metastasis. PyMT-MMTV transgenic mice have been generated on a variety of genetic backgrounds which in turn has a significant impact on mammary tumour metastasis. It has been demonstrated that PyMT-MMTV mice on an FVB (indicating susceptibility to the Friend leukemia virus) background are significantly more susceptible to metastatic disease compared to those on a C57Bl/6 background (Lifsted et al., 1998). Indeed, the initial reporting of the PyMT-MMTV strain by Guy *et al*. employed FVB animals, where nearly all tumour-bearing MMTV/middle T transgenic animals developed metastases (Guy et al., 1992). However, our studies employed transgenic mice on a C57Bl/6 background. Therefore, it should be noted that only 50% of animals employed in the studies reported in this chapter exhibited histologically detectable lung metastases **(figure 3.8A)**. Follow up analysis of PyMT expression by qPCR further confirmed this observation **(figure 3.8B)**. Future studies focusing on the role of HPSE in mediating mammary tumour metastasis in PyMT-MMTV transgenic mice may benefit from using animals generated on an FVB background.

As discussed in the first chapter, tumour growth and metastasis are significantly affected by the immune system. Key components of the immune system such as NK cells have been demonstrated to be pivotal in anti-tumour immunity and additionally, be dependent on intracellular HPSE activity in order to exert cytotoxic effects (Putz et al., 2017). Based on this and other observations previously elaborated upon, a significantly higher

lung tumour burden was expected in mammary tumour-bearing female PyMT-MMTVxHPSE$^{-/-}$ mice at the ethical tumour volume end point, in contrast to PyMT-MMTV mice. However, data reported in this chapter indicate that lung metastasis in tumour-bearing female PyMT-MMTV mice remained unaffected by the lack of HPSE expression in the host tissue **(figure 3.8)**. It is possible that a difference in lung metastatic burden between mammary tumour-bearing PyMT-MMTV and PyMT-MMTVxHPSE$^{-/-}$ mice exists in the early stages of tumour growth that is not evident at the ethical tumour volume end point. However, it should be noted that due to the extremely low level of metastatic dissemination in the animals used, analysis by quantitative qPCR to determine a difference in lung RTB at an early stage prior to the ethical tumour volume end point may prove unfeasible.

3.4.6 HPSE plays no distinct role in early mammary tumour development

Attempts were made to investigate the role of HPSE in the early stages of mammary tumour development. Earlier, studies on the effects of HPSE expression on human breast cancer progression were discussed in detail. However, the current literature is focused on reports on disease in its later stages. Tumours develop gradually over time. The actions of ECM-modulating enzymes such as HPSE may have a profound impact especially in the early stages of tumour development, translating to clinically obvious effects in advanced stages of cancer. Despite this potential, no study has thus far reported on this aspect. The use of the spontaneous mammary tumour-developing PyMT-MMTV mice provided an excellent model to understand the role of HPSE in promoting early mammary tumour establishment.

A visual examination was first carried out on serial sections of mammary glands. It was important to isolate mammary glands at an age when distinct stages of tumour development would be present, without an overwhelming presence of invasive carcinoma lesions. Guidelines were adapted from studies previously conducted by Duivenvoorden *et al*. with 6-weeks of age determined as the ideal stage to observe variations in early mammary tumour establishment between female PyMT-MMTV and PyMT-MMTVx HPSE$^{-/-}$ mice (Duivenvoorden et al., 2017). Although initial H&E staining of the mammary gland sections confirmed the pathology of carcinoma or the absence of lesions to a certain degree, it was necessary to follow up with IHC confirmation **(figure 3.9A)**. This was due to the fact that subtle variations between tumour grades may not be visible upon basic-level histological examination. To distinguish normal mammary ducts from those undergoing rapid epithelial proliferation and progressed to a stage of hyperplasia, an anti-Ki67 IHC was employed. This identified epithelial cells undergoing rapid division, indicating early stages of carcinoma development. In order to distinguish between DCIS and invasive carcinoma, an anti-SMMHC IHC was employed. This in turn enabled the

identification of intact ductal walls of DCIS lesions from invasive carcinoma, which showed a severe disruption or a complete lack of ductal walls.

However, statistical analysis of the number of mammary glands exhibiting invasive carcinoma versus those that did not, suggested no significant difference in the promotion of mammary tumour invasion between female PyMT-MMTV and PyMT-MMTVxHPSE$^{-/-}$ mice at 6-weeks of age **(figure 3.9D)**. No distinct pattern in the incidence of invasive carcinoma between the different mammary glands studied was observed **(figure 3.9C)**. Neither was a significant variation between each of the four major stages of mammary tumour development observed between female PyMT-MMTV and PyMT-MMTVxHPSE$^{-/-}$ mice **(figure 3.9B)**. These results collectively suggest that HPSE imparts no effects in the early stages of mammary tumour development in PyMT-MMTV mice.

In the context of human breast cancer, this suggests that HPSE may not always promote the early establishment of disease but may play a critical role in its later stages. Although this hypothesis needs further investigation, the logistics of such a study would pose major challenges. Scientific studies are conducted on human samples collected at a clinically significant disease state and certainly not at early disease establishment, when the presence of cancer is not detectable. Therefore, the most feasible option is an animal model of spontaneous tumour development such as PyMT-MMTV, which would allow the use of animals at a pre-determined investigative time point.

3.4.7 No evidence of an MMP-mediated compensatory mechanism for the lack of HPSE expression in PyMT-MMTVxHPSE$^{-/-}$ mice

The ECM is a complex, dynamic environment as discussed in length in the first chapter (Pickup et al., 2014, Iozzo and Gubbiotti, 2018, Bonnans et al., 2014). Indeed, the multitude of ECM components with sometimes overlapping functions suggests the likelihood that the lack or inhibition of one component may be compensated for by another with a similar role within the ECM. In certain other cases, the targeted inhibition of an ECM component with the aim of curbing the severity of disease may lead to unintended side effects, as the same component could be vital in maintaining tissue homeostasis.

Previously, an upregulation of MMPs was described in HPSE-deficient mice in response to the lack of HPSE expression (Zcharia et al., 2009). This indicated a co-regulatory mechanism between MMPs and HPSE in the ECM and in particular, indicated an upregulation of MMP-2 expression in the mammary glands. These observations could lead one to the assumption that an upregulation of MMP expression in female PyMT-MMTVxHPSE$^{-/-}$ mice may explain results of the studies reported in this thesis which suggested a HPSE-independent mode of mammary carcinoma progression in the PyMT-MMTV mouse model.

However, upon the generation of the C57Bl/6xHPSE$^{-/-}$ animals that formed the founding members of the PyMT-MMTVxHPSE$^{-/-}$ mice reported in this chapter, the expression levels of a range of MMPs (MMP-2, -9, -14 and -25) in a variety of tissues were analysed (Poon et al., 2014). Here, it was reported that MMP expression levels in HPSE-deficient mice remained unchanged. In order to further elaborate on the observations by Poon et al. and to investigate if indeed an MMP-2 overexpression was present in the mammary glands of female PyMT-MMTVxHPSE$^{-/-}$ mice as described by Zcharia *et al*., an anti-MMP-2 IHC was undertaken **(figure 3.10)**. Mammary tumour lesions of DCIS/invasive grade were chosen for this purpose as the previous studies employed qPCR, which had no means of pinpointing if MMP upregulation occurred within the lesions itself. Confirming our previous findings, no significant difference in MMP-2 expression was observed in PyMT-MMTVxHPSE$^{-/-}$ mice.

3.5 Conclusion

This chapter explored the effects of HPSE on the spontaneous tumour growth of PyMT-MMTV mice and identified that the mammary tumour progression in these animals occurred in a HPSE-independent manner. Although primary tumour angiogenesis was affected by the lack of HPSE, the overall tumour burden, tumour growth rate and metastasis in mammary tumour-bearing PyMT-MMTV mice remained unperturbed. HPSE was also suggested to play no significant role during the early stages of mammary tumour development, which had remained largely undefined. Furthermore, no compensatory mechanism of MMP-2 overexpression to counter the lack of HPSE expression was observed.

Collectively, these data suggest that in some human breast cancer settings and possibly in other cancer settings too, HPSE may not always play a significant role as would be assumed based on the published literature. Coupled with recently published data demonstrating its critical anti-tumour role, the findings of this chapter suggest that HPSE may not always contribute to tumour progression. This could have significant implications in the current development and the clinical validation of HPSE inhibitors.

Chapter 4

Defining the role of heparanase in the mammary tumour microenvironment

4.1 Abstract

HPSE has been implicated as a key mediator in the development and progression of breast cancer. In this chapter, the role of the stromal components of the TME in promoting HPSE expression within the primary mammary tumour is defined by employing HPSE-deficient C57BL/6xHPSE$^{-/-}$ mice. Furthermore, the role of tumour stromal component-driven HPSE activity in regulating tumour angiogenesis, growth and metastasis is analysed. The findings of this chapter indicate that the stromal components of the mammary TME play a crucial role in promoting HPSE activity within the tumour and lead to enhanced angiogenesis. The TME-driven HPSE expression was hypothesised to originate from the migration of tumour immune cells expressing HPSE. However, this increased HPSE expression did not translate to the promotion of overall primary tumour growth and metastasis or enhanced immune cell migration.

4.2 Introduction

Mammary tumours, as other solid tumours, are heavily influenced by the TME that regulates growth and other cancer hallmarks. Numerous studies have examined this intricate relationship and have shed light on the various components of the mammary TME and their roles in tumour promotion. The roles of the various stromal cells of the TME as well as the molecular components in regulating HPSE expression, and therefore cancer progression, have been covered in detail in chapter 1. In particular, HPSE and its substrate HS have been suggested to play key roles in angiogenesis and metastasis, two key focus areas of this thesis (Gomes et al., 2013).

A correlation between angiogenesis and metastasis in invasive breast carcinoma has been clinically demonstrated (Weidner et al., 1991). Several anti-angiogenic therapies have been developed and assessed through human clinical trials in a number of malignancies, including breast cancer, with varying degrees of efficacy (Jayson et al., 2016, Miller et al., 2005, Gerber et al., 2013, Fakhrejahani and Toi, 2014, Earl et al., 2015). A large number of *in vivo* studies employing mouse models as well as human studies have indicated the role of HPSE in breast cancer angiogenesis and metastasis (highlighted in section 3.2) (Cohen et al., 2006, Zhang et al., 2007, Maxhimer et al., 2002). Elevated HPSE expression in breast cancer has been correlated with a poor clinical prognosis (Sun et al., 2017).

Immune cells make important contributions to the mammary TME and represent attractive therapeutic targets (Coussens and Pollard, 2011, Law et al., 2017). As discussed previously, immune cells are key expressers of HPSE, which is a key promoter of cell migration and activation (Gutter-Kapon et al., 2016, Putz et al., 2017, Poon et al., 2014, Morris et al., 2015, Naparstek et al., 1984, Vlodavsky et al., 1992, Matzner et al., 1985).

Therefore, it is likely that immune cells within the mammary TME contribute to the overall HPSE expression in the primary tumour. This may in turn promote HPSE-driven hallmarks of cancer such as angiogenesis and metastasis.

Several studies have described the use of transgenic HPSE-overexpressing or immunocompromised mice in investigating the role of HPSE in breast cancer (Boyango et al., 2014, Zhang et al., 2007). However, a functional immune system is critical to understanding cancer growth and metastasis as it plays a vital role in cancer progression (Vinay et al., 2015). Immunocompromised mice, therefore, will not enable the anti-tumour and/or tumour-promoting role of the immune system to be fully defined. HPSE-overexpressing mice can be limited in their physiological relevance to understanding disease. Such transgenic mice may exaggerate the effects of naturally induced overexpression of HPSE in the TME and prove the comparison to a wild type phenotype difficult. Therefore, the use of a HPSE-deficient, immunocompetent *in vivo* model is preferable for the purpose of understanding the role of the mammary TME in disease progression.

In this chapter, orthotopic tumours are induced with the use of PyMT-MMTV mouse mammary tumour-derived cells in female C57Bl/6 and C57Bl/6xHPSE$^{-/-}$ mice. With the induction of tumours using tumour cells capable of expressing HPSE *in vivo* in both C57Bl/6 and C57Bl/6xHPSE$^{-/-}$ animals, the HPSE-mediated effects of the TME components can be better defined. Additionally, the role of HPSE expressed within the mammary TME in promoting angiogenesis and lung metastasis is further studied. The use of immunocompetent animals also enabled the study of HPSE-mediated intra-tumoural immune cell migration.

4.3 Results

4.3.1 HPSE expressed by stromal cells within the TME contributes to the overall HPSE activity of mammary tumours, but does not affect tumour growth

In order to better define the role of HPSE expressed by the stromal cells within the mammary TME in affecting the growth of the primary tumour, it was necessary to first establish a model of inducible mammary tumours in female C57Bl/6 and C57Bl/6x HPSE$^{-/-}$ mice **(figure 4.1A)**. The PyMT-MMTV mammary tumour-derived cell line PyMT3 (kindly provided by Associate Professor Belinda Parker, La Trobe University) was implanted into the 4th inguinal mammary fat pads of C57Bl/6 and C57Bl/6xHPSE$^{-/-}$ female mice in order to investigate the ability of the cells to establish mammary tumours *in vivo*.

The orthotopic inoculation of PyMT3 cells into the mammary fat pad of female C57Bl/6 and C57Bl/6xHPSE$^{-/-}$ mice gave rise to solid tumours. The resulting mammary tumours of female C57Bl/6 and C57Bl/6xHPSE$^{-/-}$ mice progressed at a comparable rate and the animals were euthanised at the ethical end point of an estimated tumour volume of $\geq$1500 mm^3 **(figure 4.1B)**. Mammary tumours were excised at the ethical tumour volume end point, lysed and subjected to a HPSE enzymatic activity assay. It was thus observed that in comparison to the parental PyMT3 cell line, tumours excised from both female C57Bl/6 and C57Bl/6xHPSE$^{-/-}$ mice exhibited a significantly higher level of HPSE activity. Interestingly, mammary tumours excised from C57Bl/6 mice exhibited a significantly higher HPSE activity level compared to those excised from C57Bl/6xHPSE$^{-/-}$ mice **(figure 4.1C)**. It is therefore likely that components of the TME are active participants in promoting HPSE activity in mammary tumours either by promoting the upregulation of HPSE by the PyMT3 cells or through HPSE expressed by the TME components themselves.

4.3.2 The effect of HPSE expressed by the stromal components of the mammary TME on mammary tumour angiogenesis

Induced PyMT3 mammary tumours were excised from both female C57Bl/6 and C57Bl/6xHPSE$^{-/-}$ mice at the ethical tumour volume end point. Serial sections were analysed by anti-CD31 IHC, revealing microvessels within the tumour **(figure 4.2A)**. Quantification of the percent (%) area of CD31 stain revealed that mammary tumours excised from female C57Bl/6xHPSE$^{-/-}$ mice had a significantly reduced level of tumour angiogenesis compared to those of C57BL/6 mice **(figure 4.2B)**. This observation suggests that the HPSE expressed by the stromal cells of the TME of a mammary tumour leads to increased angiogenesis.

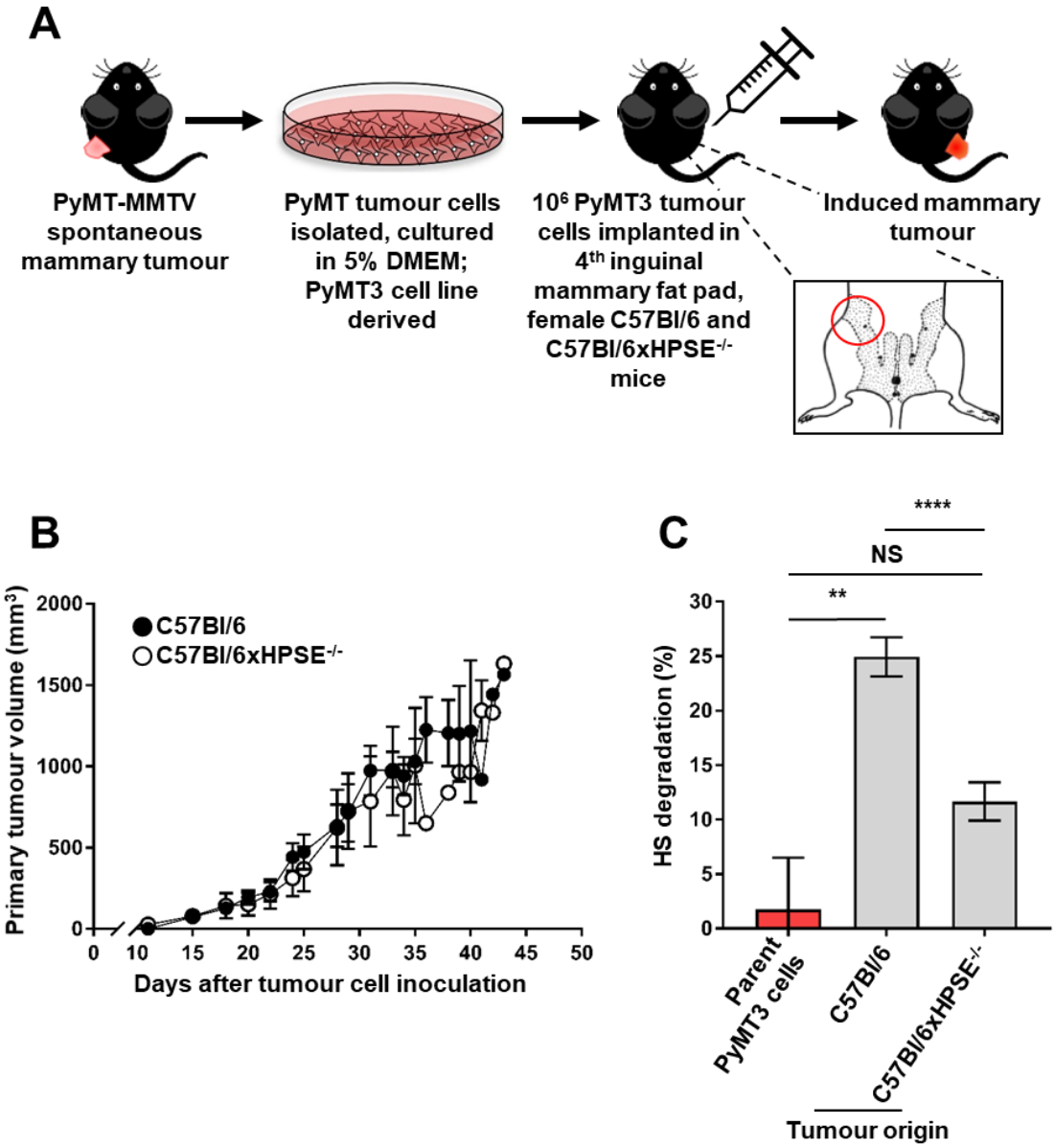

Figure 4.1 The influence of the TME on the progression and HPSE enzymatic activity of induced PyMT3 mammary tumours in C57Bl/6 and C57Bl/6xHPSE$^{-/-}$ mice

(A) A schematic representation of the study design, whereby PyMT-MMTV tumour-derived cells (PyMT3) were implanted in the 4th inguinal mammary fat pad of C57Bl/6 and C57Bl/6xHPSE$^{-/-}$ mice. **(B)** Induced PyMT3 mammary tumours progressed at a comparable rate between C57Bl/6 and C57Bl/6xHPSE$^{-/-}$ mice (n = 5); representative of one of two independent experiments **(C)** PyMT3 tumours excised at the ethical tumour volume end point from C57Bl/6 mice exhibited a significantly higher level of HPSE enzymatic activity compared to those from C57Bl/6xHPSE$^{-/-}$ mice (n = 5); representative results of one of two independent assays. Error bars = SEM; NS, not significant; **, p<0.01; ****, p<0.0001; unpaired t-test.

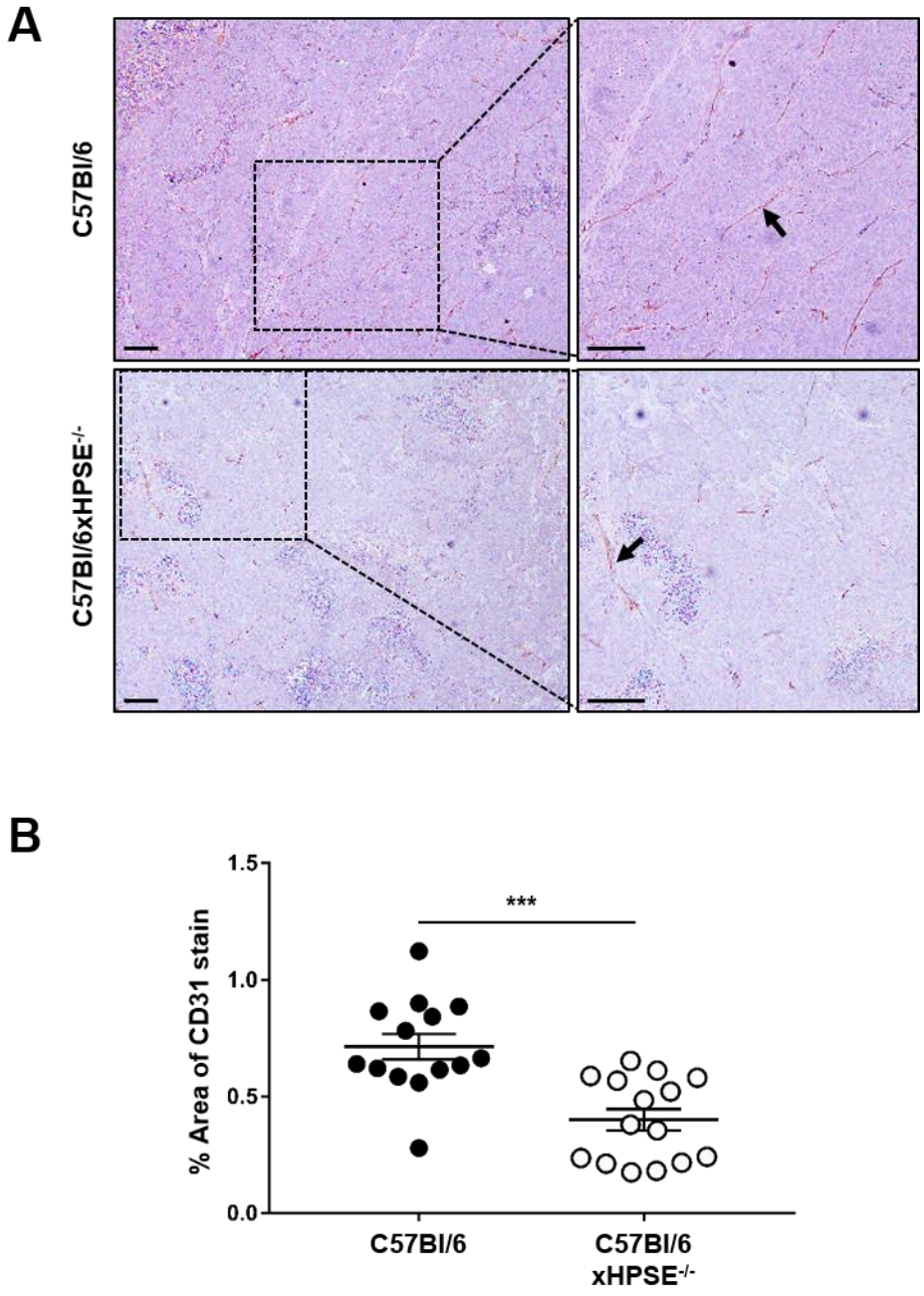

Figure 4.2 Quantification of microvessel density in induced PyMT3 mammary tumours excised from C57Bl/6 and C57Bl/6xHPSE$^{-/-}$ mice

(A) Representative anti-CD31 IHC images of serial sections of induced PyMT3 mammary tumours excised from C57Bl/6 and C57Bl/6xHPSE$^{-/-}$ mice. Arrows indicate microvessels positively stained for CD31. **(B)** Quantification of the % area of staining revealed that tumours excised from C57Bl/6xHPSE$^{-/-}$ mice exhibit significantly reduced angiogenesis. Pooled data, *n* = 5 per group; sections of 3 distinct regions analysed per tumour. Scale bars = 100 μm. Error bars = SEM; ***, p<0.001; unpaired t-test.

4.3.3 Evaluation of tumour infiltrates of induced PyMT3 mammary tumours

PyMT3 mammary tumours were excised from both female C57Bl/6 and C57Bl/6xHPSE$^{-/-}$ mice at the ethical tumour volume end point and histologically analysed in order to verify stromal cell infiltrates **(figure 4.3)**. All tumours examined showed evidence of infiltration as distinctly stained regions of a deep purple colour upon H&E staining. Based upon morphology, these clusters of infiltrates were strongly suggested to consist of immune cells. On visual examination, tumours excised from both female C57Bl/6 and C57Bl/6xHPSE$^{-/-}$ mice showed no clear difference in the degree of infiltration. This suggests that orthotopic PyMT3 mammary tumours contain infiltrating immune cells, which may contribute to elevated levels of HPSE activity as previously described. However, the intra-tumoural migration of these cells appears to not be affected by the lack of HPSE expression by the stromal components of the TME.

4.3.4 The effect of HPSE on mammary tumour-infiltrating immune cells

The significant effects of HPSE on tumour-infiltrating immune cells have been discussed (see sections 1.19 and 1.23.5). It was thus important to investigate the effect of HPSE on tumour-infiltrating immune cells in the induced mammary tumour model. Following the histological verification of tumour-infiltrating stromal cells, orthotopic PyMT3 mammary tumours excised from both female C57Bl/6 and C57Bl/6xHPSE$^{-/-}$ mice at the ethical tumour volume end point were subjected to flow cytometric analysis **(figure 4.4)**. This revealed no significant difference in total lymphocytes, CD4^{+} T cells, CD25^{+} CD4^{+} T cells, CD25^{-} CD4^{+} T cells, CD8^{+} T cells, MHCII^{+} CD11c^{+} DCs, monocytes, F4/80^{+} CD11b^{+} CD11c^{+} Ly6c^{+} myeloid cells, F4/80^{+} CD11b^{+} CD11c^{+} Ly6c^{-} residential macrophages and Ly6G^{+} CD11b^{+} neutrophils. This observation confirms the findings of section 4.3.3 and further suggests that PyMT3 mammary tumours do contain a variety of infiltrating immune cells but these remain unaffected by the lack of HPSE expressed by the stromal cells of the TME. It should be noted that tumour-infiltrating NK cells were not detected.

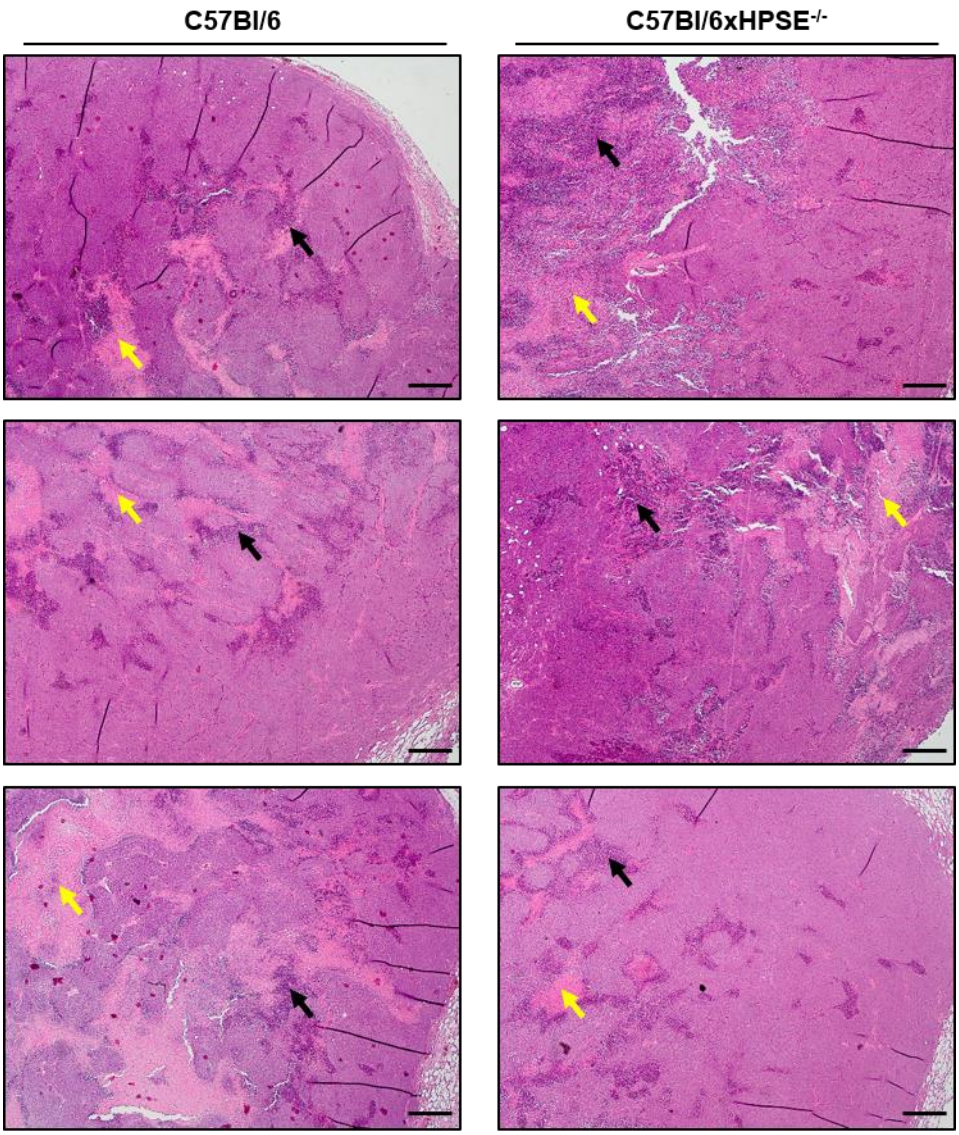

Figure 4.3 Histological analysis of induced PyMT3 mammary tumours
Representative images of H&E stained sections of induced individual PyMT3 mammary tumours excised from C57Bl/6 and C57Bl/6xHPSE$^{-/-}$ mice at the ethical tumour volume end point showed distinct regions of infiltration (indicated by black arrow). A significant level of necrotic regions was also observed (indicated by yellow arrow). Visual analysis did not reveal a significant difference in the level of infiltration between the two groups; *n* = 3 per group; sections of 3 distinct regions analysed per tumour. Scale bars = 200 μm.

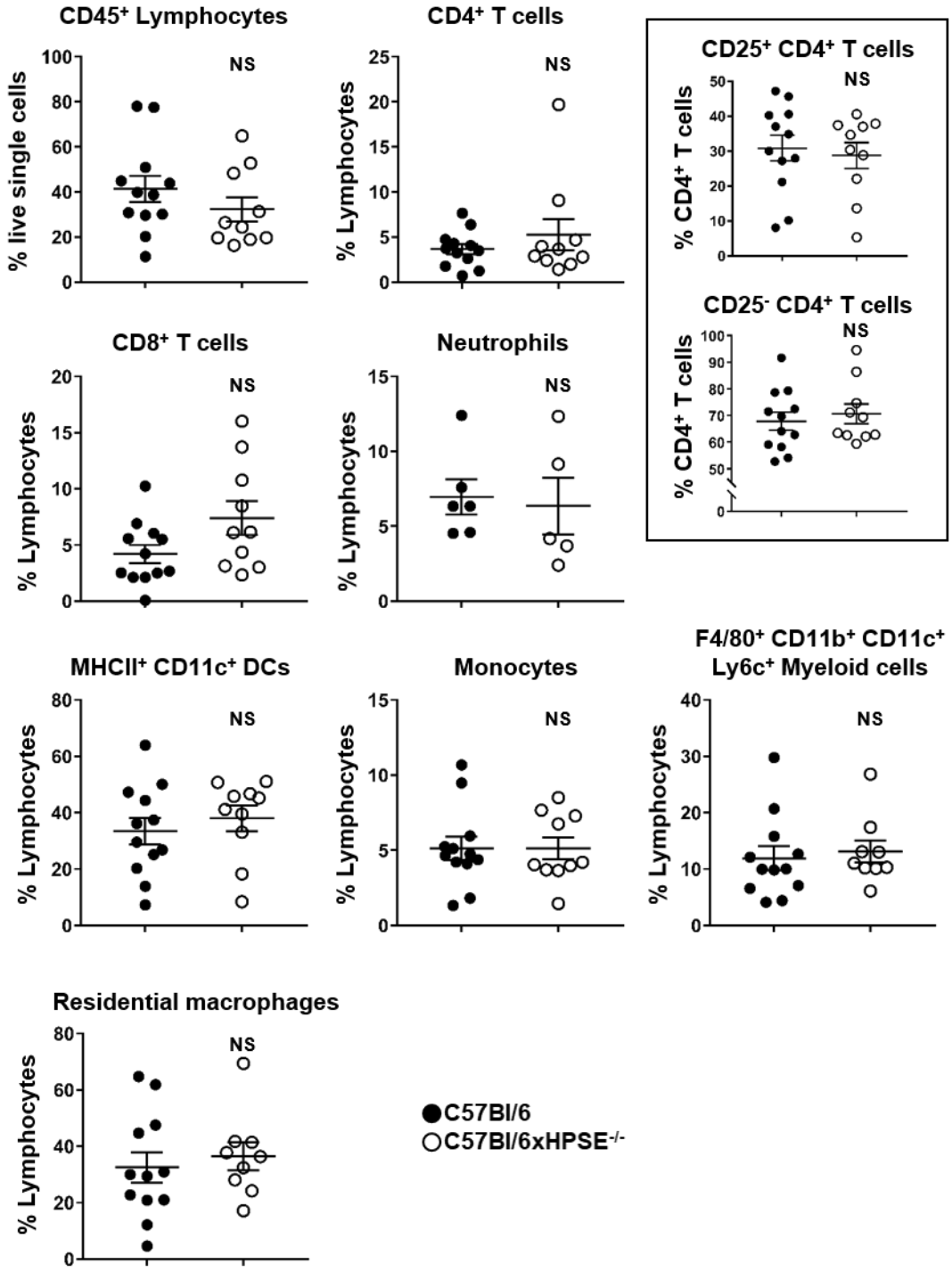

Figure 4.4 PyMT3 mammary tumour immune infiltrates analysis by flow cytometry
Analysis of induced PyMT3 mammary tumour-infiltrating immune cell populations of C57Bl/6 and C57Bl/6x HPSE$^{-/-}$ mice revealed no significant difference in immune cell content. These include total lymphocytes, CD4^{+} T cells (CD25^{+} CD4^{+} T cells and CD25^{-} CD4^{+} T cells within this population are boxed), CD8^{+} T cells, MHCII^{+} CD11c^{+} DCs, monocytes, F4/80^{+} CD11b^{+} CD11c^{+} Ly6c^{+} myeloid cells (n = 10 – 12 per group), F4/80^{+} CD11b^{+} CD11c^{+} Ly6c^{-} residential macrophages (n = 9 – 12 per group) and Ly6G^{+} CD11b^{+} neutrophils (n = 5 – 6 per group). Error bars = SEM; NS = not significant; unpaired t-test.

4.3.5 Designing a primary mammary tumour-resection model to investigate the influence of HPSE expression by the stromal cells within the TME on lung metastasis

In order to investigate the role of the mammary TME in influencing metastasis, an attempt was made to establish a primary tumour-resection model **(figure 4.5A)**. Briefly, mammary tumours were induced with the use of PyMT3 cells as described previously. These tumours were surgically resected at an estimated volume of approximately 500 mm^3 and mice were observed for subsequent signs of metastatic distress. Tumours were resected as indicated on the tumour growth curve **(figure 4.5B)**. However, in two independent experiments, it was observed that the PyMT3 induced mammary tumours resulted in a high rate of tumour regrowth, severely hindering attempts to obtain data on post-tumour resection-metastatic colonisation of the lungs. Post-surgical survival showed that only one animal per group survived with no subsequent tumour regrowth in the representative study presented here **(figure 4.5C)**. Histological examinations of the lungs of all animals was carried out for the confirmation of the presence of metastatic lesions. Only one such incidence was observed in a C57Bl/6 mouse that experienced primary tumour regrowth and was euthanised at the ethical tumour volume end point **(figure 4.5D)**. No lesions were observed in animals that survived with no primary tumour regrowth. Due to these complications, this tumour resection model was discontinued; animals were instead euthanised at the ethical tumour volume end point with subsequent analysis of lung metastasis.

4.3.6 The effect of HPSE expressed in the mammary TME on lung metastasis

The lungs are the major site of metastatic colonisation in the PyMT-MMTV mammary tumour model. Therefore, the lungs of PyMT3 mammary tumour-bearing female C57Bl/6 and C57Bl/6xHPSE$^{-/-}$ mice were examined at the ethical tumour volume end point, in order to determine if HPSE expressed by the stromal cells of the mammary TME affected the metastatic dissemination of mammary tumour cells. Initially, an H&E stain confirmed the presence of lung-metastatic lesions in these animals **(figure 4.6A)**. This was then followed by qPCR analysis to determine the RTB within the lungs, which revealed that approximately 50% of both female C57Bl/6 and C57Bl/6xHPSE$^{-/-}$ mice presented detectable metastases **(figure 4.6B)**. No significant difference in RTB was observed between the two strains. These results suggest that although the mammary TME has a significant impact on the HPSE activity and angiogenesis within the primary mammary tumour, this did not translate to enhanced metastatic progression.

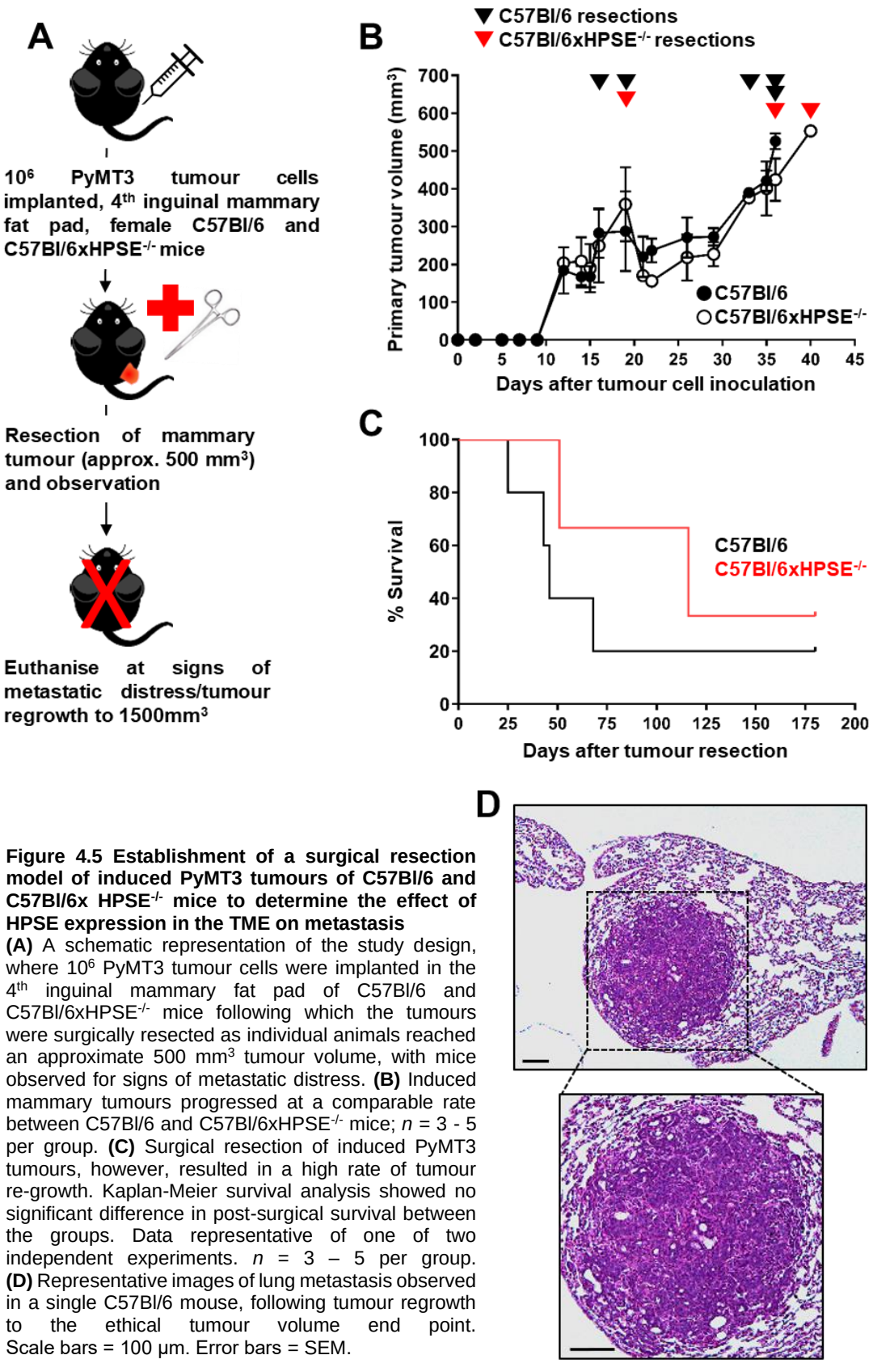

Figure 4.5 Establishment of a surgical resection model of induced PyMT3 tumours of C57Bl/6 and C57Bl/6x HPSE$^{-/-}$ mice to determine the effect of HPSE expression in the TME on metastasis
(A) A schematic representation of the study design, where 10^6 PyMT3 tumour cells were implanted in the 4th inguinal mammary fat pad of C57Bl/6 and C57Bl/6xHPSE$^{-/-}$ mice following which the tumours were surgically resected as individual animals reached an approximate 500 mm^3 tumour volume, with mice observed for signs of metastatic distress. **(B)** Induced mammary tumours progressed at a comparable rate between C57Bl/6 and C57Bl/6xHPSE$^{-/-}$ mice; *n* = 3 - 5 per group. **(C)** Surgical resection of induced PyMT3 tumours, however, resulted in a high rate of tumour re-growth. Kaplan-Meier survival analysis showed no significant difference in post-surgical survival between the groups. Data representative of one of two independent experiments. *n* = 3 – 5 per group. **(D)** Representative images of lung metastasis observed in a single C57Bl/6 mouse, following tumour regrowth to the ethical tumour volume end point. Scale bars = 100 µm. Error bars = SEM.

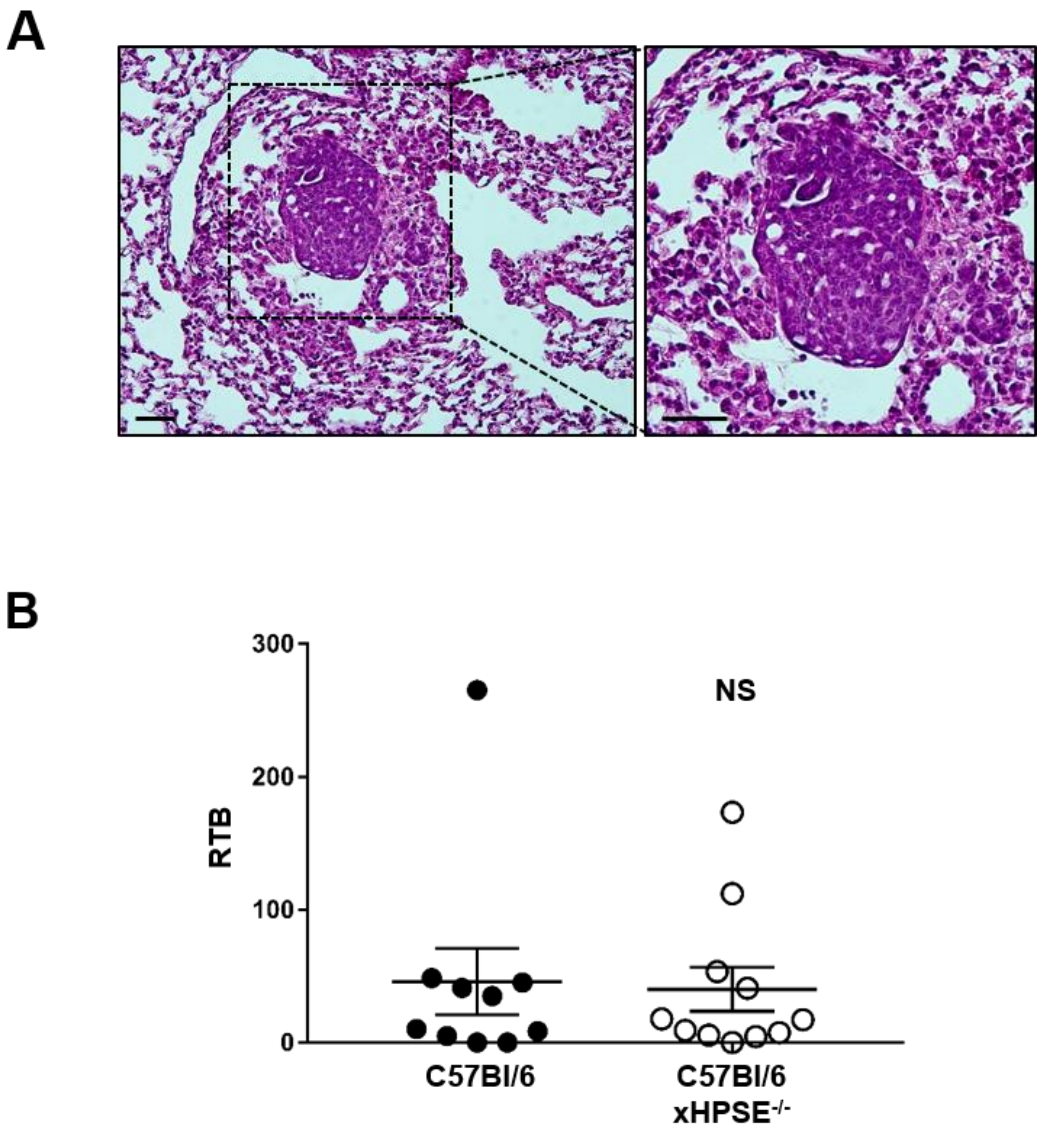

Figure 4.6 Evaluation of the effect of stromal HPSE on lung metastasis in induced PyMT3 mammary tumour-bearing C57Bl/6 and C57Bl/6xHPSE$^{-/-}$ mice at the ethical tumour volume end point
(A) A representative image of a lung-metastatic lesion of an induced PyMT3 tumour-bearing C57Bl/6 mouse at the ethical tumour volume end point of 1500 mm^3. **(B)** qPCR of C57Bl/6 and C57Bl/6xHPSE$^{-/-}$ mouse lungs excised at the ethical tumour volume end point revealed no significant difference in RTB; (n = 10 – 11). Scale bars = 100 µm. Error bars = SEM; NS = not significant; unpaired t-test.

4.3.7 Evaluation of the effect of HPSE on lung infiltrating-immune cells

Following the earlier observation of lung metastatic burden of PyMT3 mammary tumour-bearing female C57Bl/6 and C57Bl/6xHPSE$^{-/-}$ mice, the lung immune cell populations were analysed in both strains in order to determine if the lack of HPSE had an effect on the migration of immune cells to a site of metastatic colonisation **(figure 4.7)**. Flow cytometric-quantification of immune cell populations revealed no difference in total lymphocytes in the lungs of PyMT3 mammary tumour-bearing female C57Bl/6 and C57Bl/6xHPSE$^{-/-}$ mice at the ethical tumour volume end point. Further analysis revealed no difference in distinct immune cell types such as CD4^{+} T cells, CD25^{+} CD4^{+} T cells, CD25^{-} CD4^{+} T cells, CD8^{+} T cells, neutrophils, DCs and NK cells. This suggests that the migration of immune cells into the lungs of PyMT3 mammary tumour-bearing C57Bl/6 mice is unaffected by the lack of HPSE expression by the host immune system.

4.3.8 HPSE expressed by the stromal cells of the mammary TME did not affect tumour growth and metastasis in the early stages of mammary tumour development

The effect of HPSE expressed by the stromal cells of the mammary TME on the early stages of metastatic dissemination remains largely undefined. In order to first determine if metastases were detectable in early tumour growth, PyMT3 mammary tumours were induced in both female C57Bl/6 and C57Bl/6xHPSE$^{-/-}$ mice. The animals were then euthanised once the tumours reached an estimated volume of 500 – 600 mm^3. No difference in tumour growth rates were observed between female C57Bl/6 and C57Bl/6xHPSE$^{-/-}$ mice **(figure 4.8A)**. Initially, lungs of tumour-bearing mice were histologically examined for signs of metastatic lesions **(figure 4.8B)**. Histological examination of serial sections of the lungs did not reveal metastatic lesions. The RTBs of the lungs were then determined, which once again showed that a majority of lungs had no detectable metastases and that there was no significant difference in RTB between female C57Bl/6 and C57Bl/6xHPSE$^{-/-}$ mice **(figure 4.8C)**. These results suggest that HPSE expressed within the TME plays no role in metastatic dissemination of cells in the early stages of mammary tumour development.

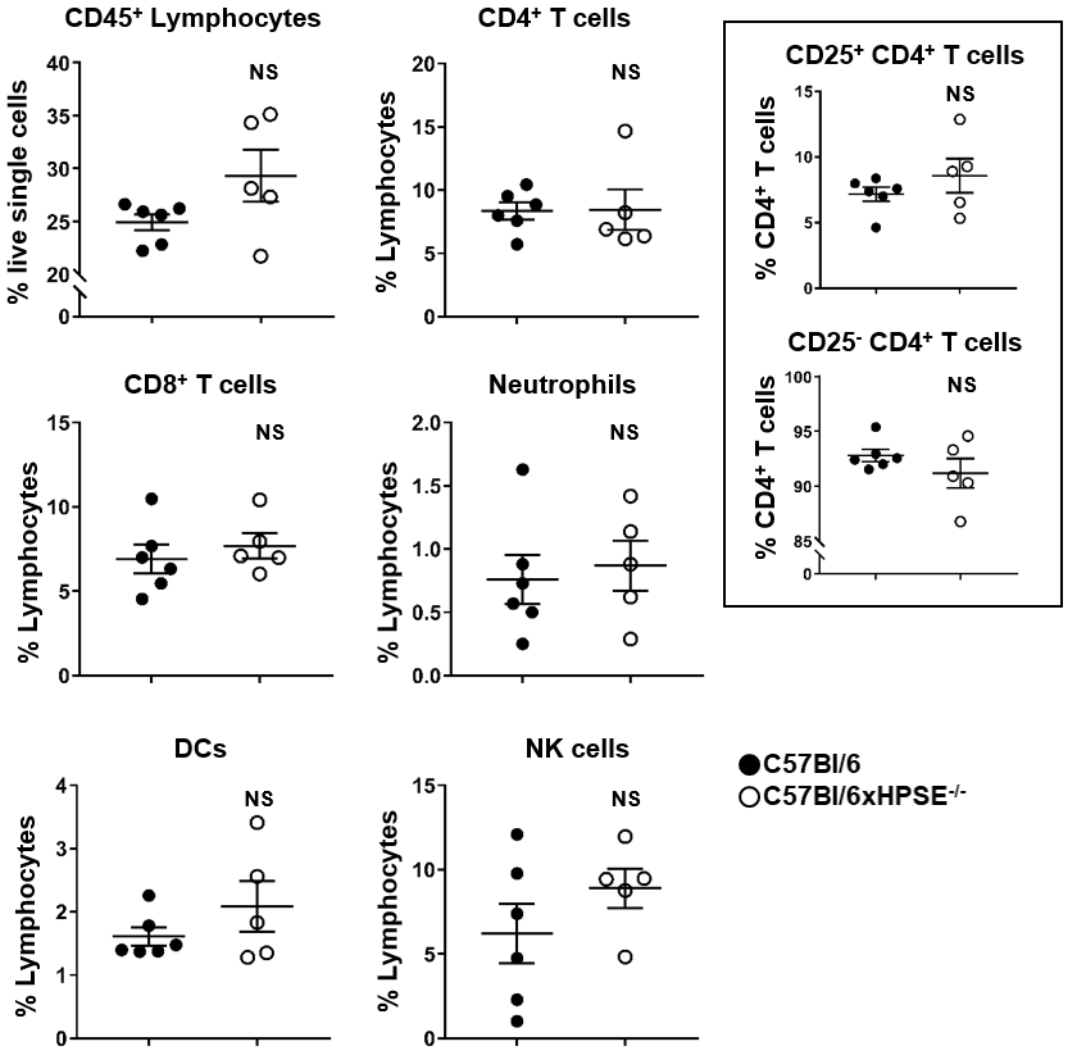

Figure 4.7 Lung immune infiltrates of PyMT3 mammary tumour-bearing mice by flow cytometry
Analysis of lung immune cell populations of induced PyMT3 mammary tumour-bearing C57Bl/6 and C57Bl/6xHPSE$^{-/-}$ mice revealed no significant difference in immune cell content. These include total lymphocytes, CD4^{+} T cells (CD25^{+} CD4^{+} T cells and CD25^{-} CD4^{+} T cells within this population are boxed), CD8^{+} T cells, neutrophils, DCs and NK cells; *n* = 5 – 6 per group; error bars = SEM; NS = not significant; unpaired t-test.

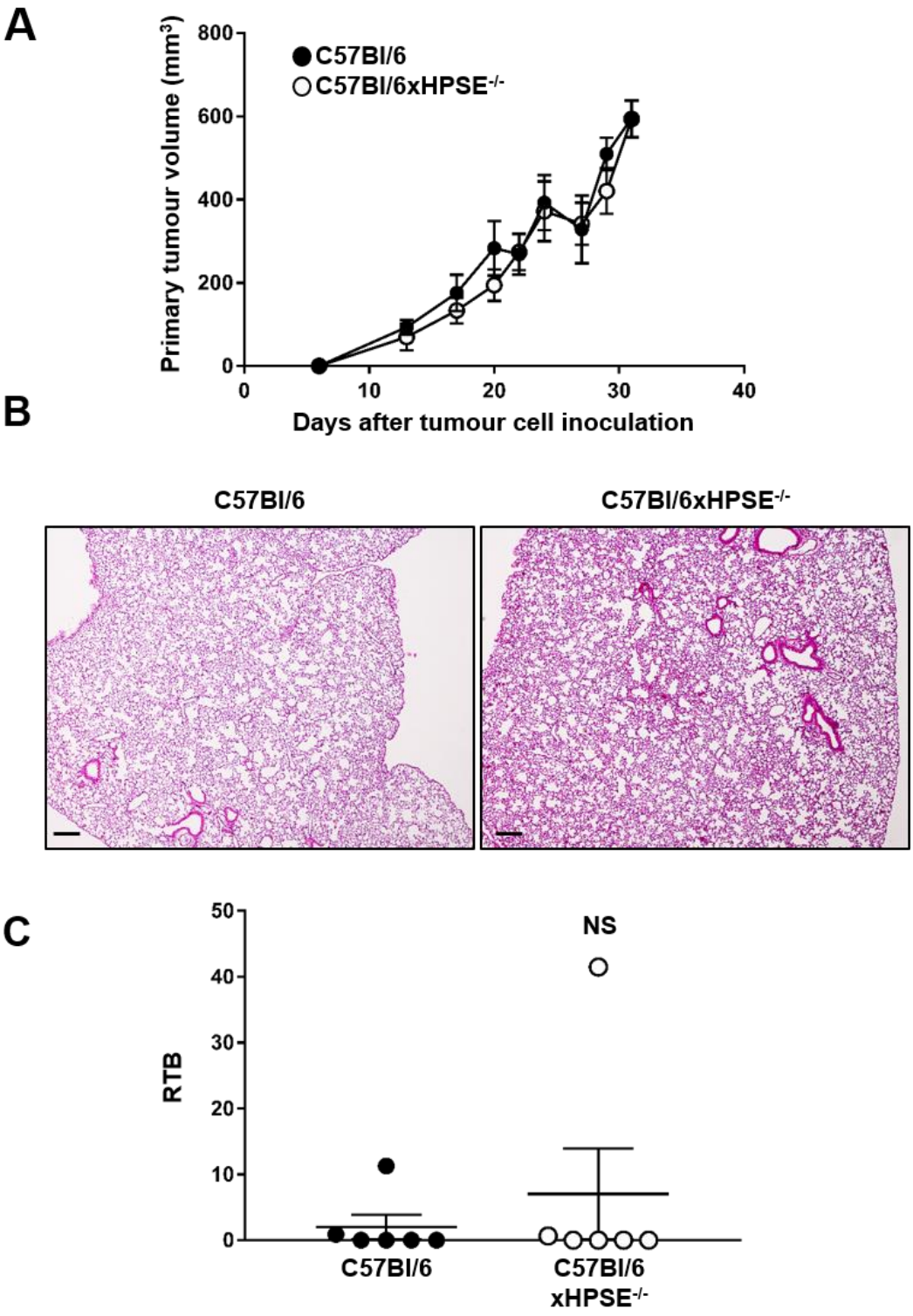

Figure 4.8 Evaluation of the effect of HPSE expressed by stromal cells in the TME on lung metastasis in induced PyMT3 mammary tumour-bearing C57Bl/6 and C57Bl/6xHPSE$^{-/-}$ mice during early tumour development

(A) Induced PyMT3 mammary tumours progressed at a comparable rate between C57Bl/6 and C57Bl/6xHPSE$^{-/-}$ mice to a volume of 500 – 600 mm^3 (n = 6). **(B)** Representative images of lung sections of induced PyMT3 tumour-bearing C57Bl/6 and C57Bl/6xHPSE$^{-/-}$ mice excised at a primary tumour volume of 500 - 600 mm^3 with no signs of metastatic lesions (n = 5). **(C)** No significant RTB was detected in the lungs of C57Bl/6 and C57Bl/6xHPSE$^{-/-}$ mice by qPCR (n = 6). Scale bar = 200 µm. Error bars = SEM; NS = not significant; unpaired t-test.

4.4 Discussion

As previously discussed, tumours are vastly complex structures comprised of a variety of cell types, collectively forming the TME (Hanahan and Coussens, 2012, Pienta et al., 2008). The TME plays a critical role in regulating tumour growth and metastatic progression. HPSE has been suggested as a key regulatory component of the TME through its enzymatic and non-enzymatic activities and thus, it is important that the precise role of HPSE within the TME be defined. This chapter investigates the role of HPSE in the TME on regulating the progression of breast cancer, which currently remains poorly defined, using an *in vivo* inducible mammary tumour model with mice of C57Bl/6 and C57Bl/6xHPSE$^{-/-}$ genetic backgrounds.

4.4.1 Establishment of an in vivo model of inducible mammary tumours

The PyMT3 cell line was provided by Associate Professor Belinda Parker (La Trobe University) and used for *in vivo* studies. A total of 10^6 PyMT3 cells were implanted in the mammary fat pads in order to overcome the extremely slow rate of tumour growth observed with the implantation of a lower number of cells as practiced with several commonly used mouse mammary tumour cell lines. Additionally, the establishment of mammary tumours by implanting PyMT3 cells orthotopically in the mammary fat pads of immunocompetent female mice was deemed more physiologically relevant to the study of tumour growth compared to the use of immunocompromised mice or the use of non-orthotopic allografts as commonly seen in other studies.

A notable difference in the establishment of induced PyMT3 mammary tumours reported in this chapter and the spontaneous PyMT-MMTV mammary tumours reported in the previous chapter is the ability of PyMT3 cell lines to express HPSE *in vitro* and *in vivo* as well as the introduction of a HPSE-expressing tumour cell line into both HPSE-expressing and HPSE-deficient mammary TMEs. Through the use of a single parental mammary tumour cell line, it was therefore possible to investigate the influence of HPSE expressed by the stromal cells of the TME on mammary tumour growth.

4.4.2 The mammary TME and/or stromal cells enhance HPSE activity within mammary tumours but do not promote tumour growth

The growth of induced PyMT3 mammary tumours was comparable between female C57Bl/6 and C57Bl/6xHPSE$^{-/-}$ mice **(figure 4.1)**. This is in contrast to previously published data using HPSE-deficient mice which demonstrated impaired tumour establishment through implanting Lewis lung carcinoma cells (Gutter-Kapon et al., 2016). However, it was observed that following the implantation of PyMT3 cells in female C57Bl/6 and C57Bl/6xHPSE$^{-/-}$ mice, the resulting mammary tumours excised exhibited a significantly higher HPSE activity level compared to the parent PyMT3 cells. Furthermore, the tumours

isolated from C57Bl/6 mice exhibited a significantly higher level of HPSE activity compared to those isolated from C57Bl/6xHPSE$^{-/-}$ mice. This suggests that once implanted and established *in vivo*, the PyMT3 tumour cells in both C57Bl/6 and C57Bl/6xHPSE$^{-/-}$ mice upregulate HPSE expression, which together with HPSE expressed by the stromal cells of the TME in the setting of the wild-type C57Bl/6 mice, likely accounted for the enhanced HPSE activity. Indeed, cellular components of the mammary TME such as immune cells would have a profound impact on the overall HPSE activity level of a solid tumour. This enhanced HPSE activity mediated by the upregulation of HPSE expression of the implanted PyMT3 cells together with the HPSE activity of the stromal components of the TME was further suggested to promote angiogenesis. It could be assumed therefore, that HPSE expression by TME components enhances HS cleavage within the tumour-associated ECM, leading to the release of pro-angiogenic factors. Future studies could isolate key components of the TME and quantitate the level of HPSE expression to determine their role in promoting the overall HPSE expression within an individual tumour. It is once more interesting to note that although the lack of HPSE within the TME led to reduced tumour angiogenesis, no growth disadvantage was observed. It could be speculated that a 'baseline level' of angiogenesis established without the influence of HPSE activity is sufficient to maintain tumour growth in this and possibly other tumour settings.

4.4.3 Effect of HPSE expression on tumour and lung immune infiltrates and metastasis

In order to investigate the degree of PyMT3 tumour infiltration dependent upon the expression of HPSE by stromal cells within the TME, a histological analysis was carried out **(figure 4.3)**. It was thus observed that mammary tumours excised from both female C57Bl/6 and C57Bl/6xHPSE$^{-/-}$ mice exhibited a substantial level of stromal infiltrates. The strong purple stain following H&E staining together with the morphological appearance suggested these as immune cells and no significant variation between the degrees of infiltration was observed between the two groups. The role of infiltrating immune cells in the primary tumour as well as in the metastatic niches has been widely studied and reviewed (Kitamura et al., 2015a, Barnes and Amir, 2017a, Janssen et al., 2017). It was therefore of interest to characterise the migration and the distinct populations of immune cells present in the primary tumour as well as the lungs and to determine the role of HPSE expressed by the stromal cells of the host TME as well as metastatic sites on their regulation.

The recruitment of immune cells to the TME and the expression of HPSE by these cells have been discussed in detail (Knelson et al., 2014, Gutter-Kapon et al., 2016, Putz et al., 2017). These findings therefore suggest that recruited immune cells are likely key

contributors to the overall HPSE expression and activity of a solid tumour. Recently, the use of the Vectra automated quantitative pathology imaging system (PerkinElmer) has yielded more reliable data on tumour-infiltrating immune cells (Brockwell et al., 2019) However, establishing this system required significant optimisation and was beyond the scope of this thesis. Therefore, a flow cytometry-based method alone was employed to determine the quantity and nature of tumour-infiltrating immune cells of female C57Bl/6 and C57Bl/6xHPSE$^{-/-}$ mice. A variety of distinct immune cell populations were thus analysed **(figure 4.4)**. However, no significant difference in the numbers of any immune cells was observed. This was in contrast to an expected reduced migration of immune cells in mammary tumour-bearing C57Bl/6xHPSE$^{-/-}$ mice on account of the lack of cellular HPSE expression, based on prior studies (Poon et al., 2014, Putz et al., 2017).

The immune cell populations investigated have been mostly demonstrated to play key roles in tumour growth and the role of HPSE in promoting the function of immune cells was discussed previously in sections 1.19 and 1.23.5. Amongst the immune components studied were CD4$^+$ T cells, T reg cells, CD8$^+$ T cells, macrophages, DCs and neutrophils. With the use of PyMT-MMTV mice, CD4$^+$ T cells have been demonstrated to regulate pulmonary metastasis in mammary carcinomas by modulating the pro-tumour characteristics of TAMs which increase the invasive capacity of malignant mammary epithelial cells (DeNardo et al., 2009). CD25$^+$ CD4$^+$ T reg cells play an immunosuppressive role in the TME and these have been shown to promote tumour growth. Indeed, highly aggressive human breast tumours present an increased level of T reg cells (Plitas et al., 2016). On the other hand, tumour infiltrating CD8$^+$ T cells have been shown to possess anti-tumour features and in some breast cancer subtypes, result in an improved patient prognosis (Egelston et al., 2017, Egelston et al., 2018). TAMs have been shown to promote tumour growth and metastasis (Mantovani, 1978, Mantovani et al., 2017). Previously, we have demonstrated that the lack of HPSE expression in mice led to reduced migration of DCs (Poon et al., 2014). DCs of various subtypes have been shown to be associated with the mammary TME (Michea et al., 2018). It was therefore of interest to quantify PyMT3 mammary tumour-associated DCs in this study to understand the influence of HPSE on DC migration. Neutrophils are promoters of tumour progression in the mammary TME as well as being key regulators of metastatic colonisation of lungs by breast cancer cells (García-Mendoza et al., 2016, Wculek and Malanchi, 2015a). Based on recent observations on the role of HPSE in promoting NK cell migration and immunosurveillance, efforts were made to investigate tumour-infiltrating NK cells of PyMT3 mammary tumours (Putz et al., 2017). However, a distinct NK cell population could not be identified by flow cytometry within the primary tumours (data not shown).

The main aim of this analysis was to gain an overview of the TME-associated immune cells in the PyMT3 mammary tumours and to determine if immune cell migration in this *in vivo* setting was indeed a HPSE-regulated process. However, as no significant difference between the groups was observed, no follow up studies were deemed necessary. It appears that HPSE expressed by the tumour cells alone or the actions of ECM-modulating enzymes such as MMPs were sufficient to maintain an influx of immune cells into the primary tumour and that the lack of HPSE expression in the immune cells themselves played no significant role in promoting intra-tumoural migration. Further studies are required to address this question.

As previously mentioned, the lungs are the major site of metastatic colonisation in the PyMT-MMTV model. Therefore, in the induced PyMT3 mammary tumour studies undertaken in this chapter, the metastatic burden within the lungs was quantified. Initially, an *in vivo* mammary tumour resection model was considered as a possible method of determining the effect of HPSE expression within the host mammary TME on lung metastasis **(figure 4.5)**. However, following surgical resection of the PyMT3 mammary tumours, most mice experienced rapid tumour regrowth, leading to euthanasia upon reaching the ethical tumour volume end point. The PyMT-MMTV mammary tumour-derived cells formed relatively diffuse tumours; this consistently led to failure in the complete removal of tumour material at the surgical site which ultimately resulted in tumour regrowth. The development of this model was further hindered by the fact that the PyMT3 tumour cell line and indeed, PyMT-MMTV tumour-derived cell lines in general, are poorly metastatic. Successful metastatic dissemination may not have occurred at a tumour volume of approximately 500 mm^3 when surgical resections were performed. This is in significant contrast to well-characterised metastatic mouse mammary tumour lines such as 4T1 and 4T1.2 used in Balb/c mice (Aslakson and Miller, 1992, Miller et al., 1983, Lelekakis et al., 1999). The exclusive use of mice on a C57Bl/6 background in these studies prevented the use of these highly metastatic cells. Furthermore, due to ethical reasons, resections could not be performed on larger mammary tumours, which may have resulted in a higher level of metastatic dissemination. The general lack of a well-characterised C57Bl/6 tumour cell line with demonstrated metastatic dissemination capacity prior to resection therefore hindered these investigations. The commonly used E0771 cell line too was shown by others to be prone to tumour regrowth upon surgical resection and to be poorly metastatic (personal communication, Associate Professor Belinda Parker, La Trobe University). Thus, the mammary tumour resection model was discontinued and mice were instead euthanised at the ethical tumour volume end point with the lung metastatic burden quantified.

The observation from these studies was that there was no significant difference in the RTB of lung metastasis between female C57Bl/6 and C57Bl/6xHPSE$^{-/-}$ mice at the ethical tumour volume end point **(figure 4.6)**. It should also be noted that the overall metastatic burden was quite low, with several animals reporting no detectable tumour cells within the lungs. As discussed, the role of the immune system in cancer growth is not only limited to the primary tumour, but also extends to the metastatic sites (Kitamura et al., 2015a, Barnes and Amir, 2017a, Janssen et al., 2017). Distinct immune cells within the lungs of mammary tumour-bearing female C57Bl/6 and C57Bl/6xHPSE$^{-/-}$ mice were therefore analysed at the ethical tumour volume end point **(figure 4.7)**. However, no significant difference was observed in infiltrating immune cells within the lungs.

The next aim was to investigate the influence of HPSE expressed within the TME on the early stages of metastasis **(figure 4.8)**. Metastatic dissemination has been shown to occur early in tumour development (Hu et al., 2017b). In order to determine the role of HPSE at this critical stage of tumour growth, the lungs of mice bearing tumours of approximately 500 – 600 mm^3 in volume were examined both histologically and by qPCR. However, no signs of metastatic colonisation were observed. It is therefore suggested that due to the poor metastatic capacity of the PyMT3 cells, the role of HPSE in the early stages of metastasis could not be assessed using this *in vivo* model. A highly metastatic C57Bl/6-compatible mammary tumour cell line is thus required for future studies.

4.5 Conclusion

This chapter aimed to define the influence of HPSE expressed within the tissues of the mammary tumour-bearing host, especially the TME, on tumour progression. It was thus demonstrated that the stromal cells of the TME indeed contribute to the HPSE expression of the primary mammary tumour, but this did not impact upon tumour growth. The HPSE expressed by the stromal cells within the TME enhanced tumour angiogenesis, which did not result in enhanced tumour growth. The migration of tumour-infiltrating immune cells was unaffected by the lack of HPSE expression within the stromal components of the TME and within the immune components themselves. Lung metastasis and the migration of lung-infiltrating immune cells were not affected by the lack of HPSE expression of stromal cells within the TME.

Although it is clear that the TME does increase HPSE expression in the primary tumour, only tumour angiogenesis appeared to be enhanced. As in the previous chapter, the potential benefits of inhibiting HPSE expression in the clinic must once again be queried based upon these findings.

Chapter 5

Identification and characterisation of novel heparanase inhibitors

5.1 Preface

The data presented in this chapter were generated in collaboration with Kathleen Wragg (Undergraduate student, Hulett laboratory), Alyce Forrest (Undergraduate student, Hulett laboratory), Alyce Mayfosh (PhD student, Hulett laboratory) and Shaun Gaskin (PhD student, Hulett laboratory).

- The initial high throughput analysis of the Sigma LOPAC^{1280} library and subsequent characterisations of novel drug candidates were performed by K. Wragg.
- The *in vitro* migration/invasion assay and the angiogenesis assay were performed by A. Forrest.
- The flow cytometry analysis of the splenic and lung immune cell populations were performed with the assistance of A. Mayfosh.
- S. Gaskin assisted in conducting the *in vivo* B16F10-mCherry-Luc lung metastasis studies.
- A. Mayfosh and S. Gaskin assisted in the purification of human HPSE.

5.2 Abstract

With its proven roles in promoting tumour progression through regulating key hallmarks of cancer, HPSE has emerged as an attractive therapeutic target. With the recent interest in the pre-clinical and clinical validation of several novel anti-HPSE drug candidates, often with no significant outcomes, this chapter explores the identification, characterisation and the preliminary pre-clinical validation of two novel HPSE inhibitors. Using HPSE purified from human platelets, a high throughput *in vitro* HPSE activity assay was established and used to screen 320 compounds of the Sigma LOPAC^{1280} library of 1280 known drugs. Using this approach, the PPAR-α agonists GW7647 and GW9578 were identified as novel HPSE inhibitors. *In silico* 3D modelling demonstrated the potential binding modality of these drugs with HPSE. The capacity of GW7647 and GW9578 to reduce tumour cell migration and angiogenesis *in vitro* is demonstrated, although interestingly, via a yet to be defined HPSE-independent mechanism. Finally, a preliminary pre-clinical study in which mice bearing B16F10 lung metastatic lesions were treated with GW7647 and GW9578 was carried out to investigate the efficacy of these novel HPSE inhibitors in inhibiting tumour metastasis *in vivo*. This, however, indicated that these compounds were ineffective at reducing metastasis. Additionally, no significant detrimental effects on immune cell populations through the use of HSPE inhibitors were observed with regards to relative cell populations within the lungs and spleen and with the maturation levels of lung and splenic NK cells. The findings of this chapter therefore identify the PPAR-α agonists GW7647 and GW9578 as novel HPSE inhibitors that warrant further development and pre-clinical validation.

5.3 Introduction

Malignant diseases have proven challenging to treat, despite decades and even centuries of study. Targeted therapies have been thrust into the spotlight by virtue of targeting a single entity that is unique and generally essential to a cancer's progression. This has provided a rational approach to drug design. This thesis has highlighted on many occasions that HPSE is upregulated in all cancers, and thus promotes key cancer hallmarks, providing an ideal therapeutic target. Many studies were initiated to discover potential drugs through various approaches such as high throughput screening of known compounds, development of synthetic inhibitors and the re-modulation of known HPSE inhibitors for better efficacy. Several pre-clinical studies yielded promising results, prompting first-in-human trials. However, as indicated previously in chapter 1, several novel inhibitors failed either in the clinical or pre-clinical stages. The reasons for this vary from lack of efficacy to adverse off-target effects. The development of HPSE inhibitors, therefore, is an ongoing process. The identification and validation of a variety of HPSE

inhibitors is discussed in detail in chapter 1. A number of more recent discoveries relevant to this chapter along with an insight into the future of anti-HPSE drug design are highlighted below.

Computational studies were employed to extract HS-HPSE interactions as a template for the design of novel HS-mimetics (Loka et al., 2017). A glycopolymer of 12 repeating disaccharide units was thus identified as a potent inhibitor which further lacked anticoagulant activity. Recently, aspirin was shown to inhibit HPSE, leading to reduced angiogenesis and metastasis *in vivo* (Dai et al., 2017). By directly binding to the catalytic Glu_{225} region of HPSE, aspirin effectively inhibited enzymatic activity, leading to downstream therapeutic effects. For the first time, patient-derived lung cancer xenografts were used to demonstrate the *in vivo* efficacy of PG545, in order to explore its potential in lung cancer, especially those that do not respond to conventional chemotherapy (Katz et al., 2018). Here, PG545 was shown to be highly effective, suggesting its possible benefits in the clinic.

Nanomedicine has made impressive strides in the use of microscopic particles to study and to treat tumours. Iron oxide nanoparticles coated with depolymerised heparin could be used in a theranostic approach, to target tumours and deliver a tumour-specific HPSE-inhibitory function (Groult et al., 2017). However, such applications are still in their infancy and are yet to progress beyond their concept phase. In another inaugural study, saccharide units were attached to a synthetic polymer backbone, resulting in glycopolymers capable of inhibiting glycosidase functions, including the enzymatic activity of HPSE (Sletten et al., 2017). Such studies highlight the importance of incorporating computational docking approaches to understanding molecular dynamics, a critical feature of drug design.

Syntatins are peptides capable of inhibiting syndecan-1 signalling, thus inhibiting angiogenesis and tumour proliferation (Rapraeger, 2013, Metwaly et al., 2018). The mechanism by which HPSE modulates syndecan-1 signalling in myeloma to promote angiogenesis and cancer cell invasion was recently elucidated (Jung et al., 2016a). By inhibiting the HPSE-induced syndecan-1 shedding, novel synstatins show potential as therapeutics against myeloma and possibly other malignancies as well. Finally, the urinary inhibitor ulinastatin was shown to inhibit HPSE activity and to maintain the pulmonary endothelial glycocalyx integrity in an *in vivo* model of acute respiratory distress syndrome (Wang et al., 2016).

This chapter describes the discovery of novel HPSE inhibitors through the screening of a library of known pharmacological compounds. These lead candidates were studied for their *in vitro* efficacy in inhibiting the enzymatic activity of HPSE, as well as their effects

on angiogenesis and tumour cell invasion. Finally, a study was established to investigate the *in vivo* efficacy of these compounds. Preliminary data presented here will form the basis of further development and characterisation of these drugs in pre-clinical studies.

5.4 Results

5.4.1 Purification of human HPSE from platelets

In order to identify novel HPSE inhibitors, the Sigma LOPAC^{1280} library of pharmacologically active compounds was screened. This relied on the availability of purified HPSE which was isolated from human platelets obtained from the Australian Red Cross. The concentration of the eluted protein was estimated at 0.45 mg/ml, followed by SDS-PAGE analysis and Coomassie staining **(figure 5.1A)** which showed a prominent band at approximately 45 kDa, suggesting the presence of the 50 kDa subunit of HPSE. Several other bands of unknown origin were also present, suggesting the purity of the eluted protein was less than 100%. The 45 kDa prominent protein band was confirmed as HPSE by Western blot with an anti-HPSE antibody with no non-specific signals observed **(figure 5.1B)**. Next, the capacity of the eluted protein to degrade HS was assessed using an *in vitro* HPSE activity assay (as described in 5.4.2). Here, 2 ng of total protein exhibited significant HS degradation capability estimated at approximately 50%, when compared to the negative control of assay buffer alone which demonstrated no activity **(figure 5.1C)**. Finally, mass spectrometric data identified this purified protein fraction conclusively as human HPSE, based on peptide fragment analysis **(figure 5.1D)**. These results indicated that enzymatically active human HPSE was successfully purified from platelets, which could be used in a series of downstream assays including attempts at identifying novel HPSE inhibitors.

Several batches of HPSE purified from human platelets were used throughout the course of this study. All batches behaved similarly with regards to their ability to degrade HS and were inhibited similarly with the use of known and novel HPSE inhibitors.

5.4.2 Validation of the *in vitro* HPSE activity assay

In order to screen the library to identify HPSE inhibitors, an *in vitro* FRET-based HPSE activity assay was utilised **(figure 5.2A)**. The reproducibility and sensitivity of this assay needed to be initially demonstrated. The assay is based on transfer of fluorescence energy dependent upon a HS substrate labelled with a europium-cryptate donor electrophore and a streptavidin-labelled XL665 acceptor electrophore remaining intact. When HPSE cleaves HS, this energy transfer is significantly reduced **(figure 5.2B)**. It was thus determined that 2 ng of HPSE demonstrated an appropriate level of HPSE activity in this assay with an ability to degrade approximately 50% of the HS substrate. This provided the

means to determine the effects of HPSE inhibitors by providing a suitable baseline level of enzymatic activity. Known HPSE inhibitors (Suramin, OGT-2115, PI-88 and heparin) were assessed in the assay to determine their effect on the enzymatic activity **(figure 5.2C)**. At 10 ng, heparin displayed the greatest inhibition, followed by PI-88 and OGT-2115. Suramin showed no inhibition at 10 or 20 ng. It is interesting to note that PI-88 appeared to display saturation at 10 ng. The potent HPSE inhibition displayed by heparin even at sub-nanogram levels led to its use in further validation of the assay **(figure 5.2D)**. Heparin was shown to have dose-dependent activity, with essentially complete inhibition reached at 5 ng or higher.

These data suggest that the *in vitro* HPSE activity assay is reproducible and sensitive and is therefore suitable to be employed in further downstream assays.

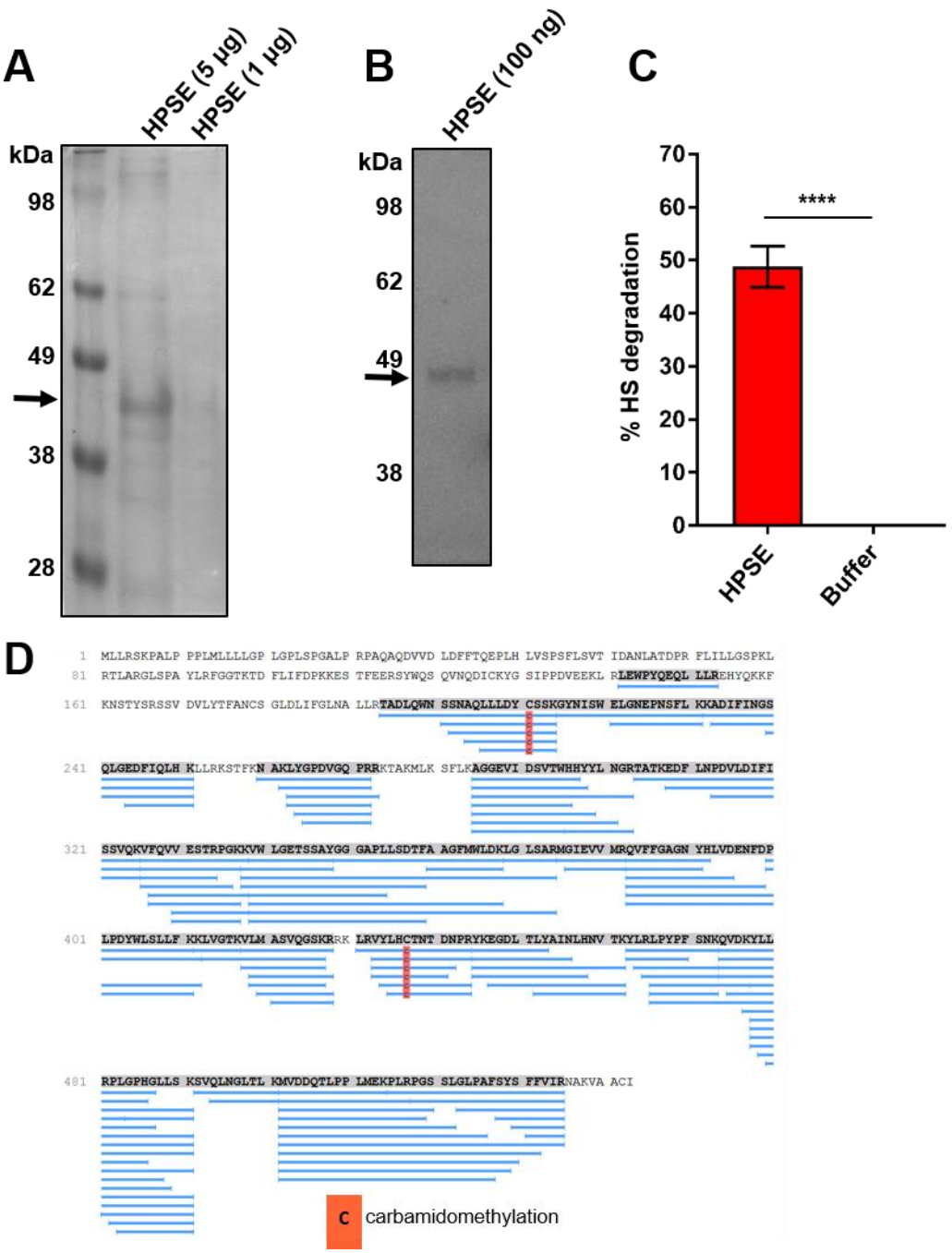

Figure 5.1 Purification of human HPSE from platelets
(A) Reducing and denaturing SDS-PAGE analysis of purification fractions of HPSE shows a distinct band of approximately 45 kDa. **(B)** Immunoblotting of purified HPSE (100 ng) detected a band of approximately 45 kDa. **(C)** Enzymatic activity assay of purified HPSE confirmed its ability to cleave HS. **(D)** Proteomic analysis of the purified protein fraction verified the isolation of HPSE. Regions of sequence identification are indicated by blue lines. Error bars = SEM; ****, $p<0.0001$; unpaired t-test.

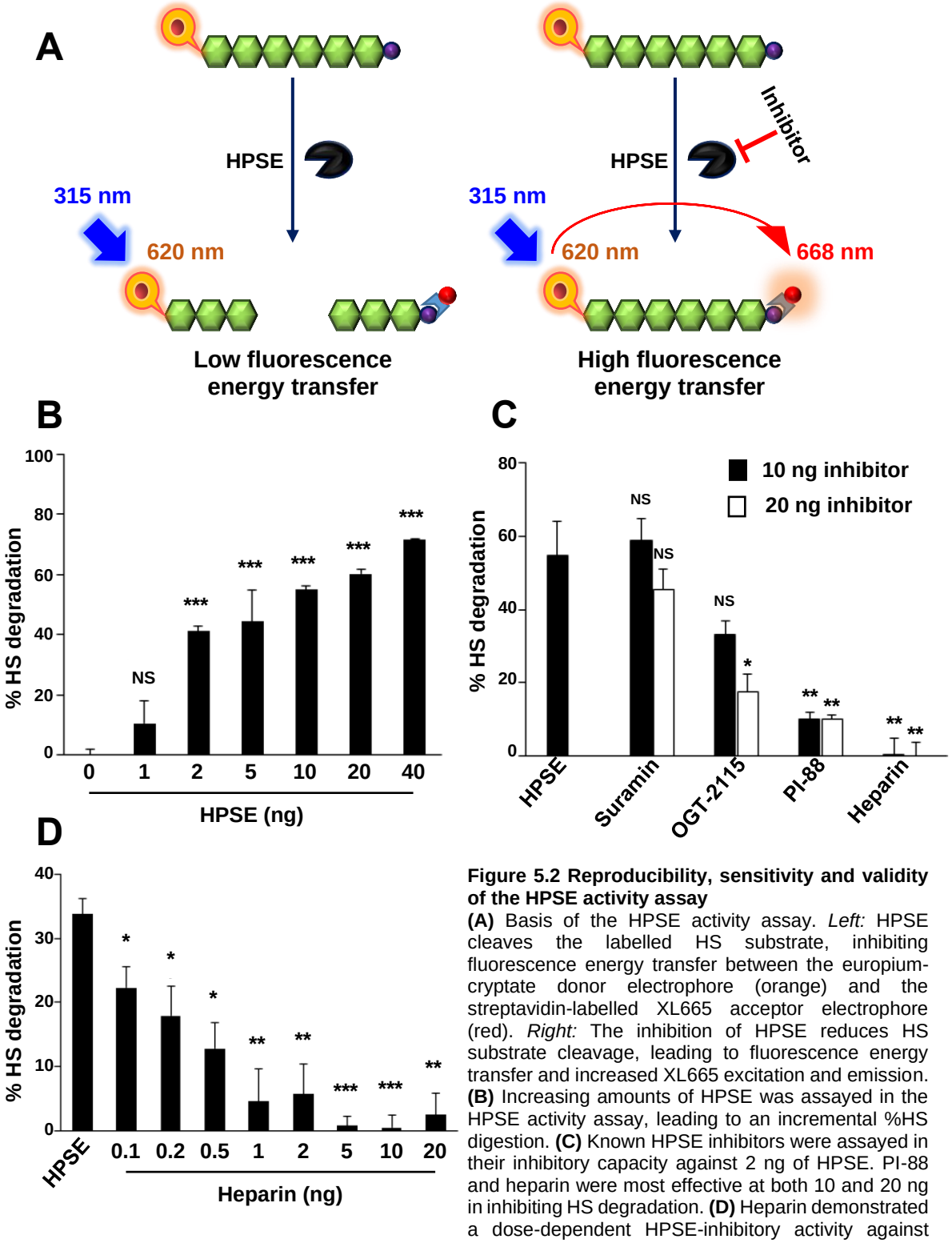

Figure 5.2 Reproducibility, sensitivity and validity of the HPSE activity assay
(A) Basis of the HPSE activity assay. *Left:* HPSE cleaves the labelled HS substrate, inhibiting fluorescence energy transfer between the europium-cryptate donor electrophore (orange) and the streptavidin-labelled XL665 acceptor electrophore (red). *Right:* The inhibition of HPSE reduces HS substrate cleavage, leading to fluorescence energy transfer and increased XL665 excitation and emission. **(B)** Increasing amounts of HPSE was assayed in the HPSE activity assay, leading to an incremental %HS digestion. **(C)** Known HPSE inhibitors were assayed in their inhibitory capacity against 2 ng of HPSE. PI-88 and heparin were most effective at both 10 and 20 ng in inhibiting HS degradation. **(D)** Heparin demonstrated a dose-dependent HPSE-inhibitory activity against 2 ng of HPSE. *n* = 3, representative data of 3 independent assays shown; Error bars = SEM; *, p<0.05; **, p<0.01; ***, p<0.001; unpaired t-test.

5.4.3 The LOPAC^{1280} library screening strategy

A high throughput screening strategy was designed to identify potential HPSE inhibitors with the use of the previously-validated HPSE activity assay **(figure 5.3A)**. Briefly, purified HPSE was pre-treated with a series of individual LOPAC^{1280} compounds at a concentration of 10 μM, followed by analysis with the FRET-based *in vitro* HPSE activity assay. This screening technique was used to analyse 320 such compounds, comprising molecules belonging to a wide range of classes from neurotransmission, apoptosis, cell cycle, G-protein coupled receptors, gene regulation, hormones, ion channels, lipids, phosphorylation, etc **(figure 5.3B)**. The overall screening strategy involved the primary screen of 320 compounds followed by a secondary screen of those compounds displaying a reduction of HPSE activity to $\leq$40% of its basal activity level **(figure 5.3C)**. This was then followed by a cell surface HS assay (an independent assay of HS-degradation involving the inhibition of degradation of cell surface HS) with the compounds identified in the secondary screen.

5.4.4 Primary screen of the LOPAC^{1280} library for novel HPSE inhibitors

Following the verification of the HPSE activity assay and the design of the LOPAC^{1280} library screening strategy, the first 320 compounds were screened simultaneously **(figures 5.4A-5.4D)**. A 10 μM concentration of the compounds was deemed appropriate for the discovery of initial hits, based on previous observations (Hughes et al., 2011). In each screen, heparin successfully inhibited HPSE activity, indicating a valid, functional screening strategy. Fifteen compounds were thus identified to inhibit HPSE enzymatic activity to $\leq$40% of the basal activity level (indicated by red arrows). These compounds were further subjected to a secondary screen to confirm reproducibility and validity.

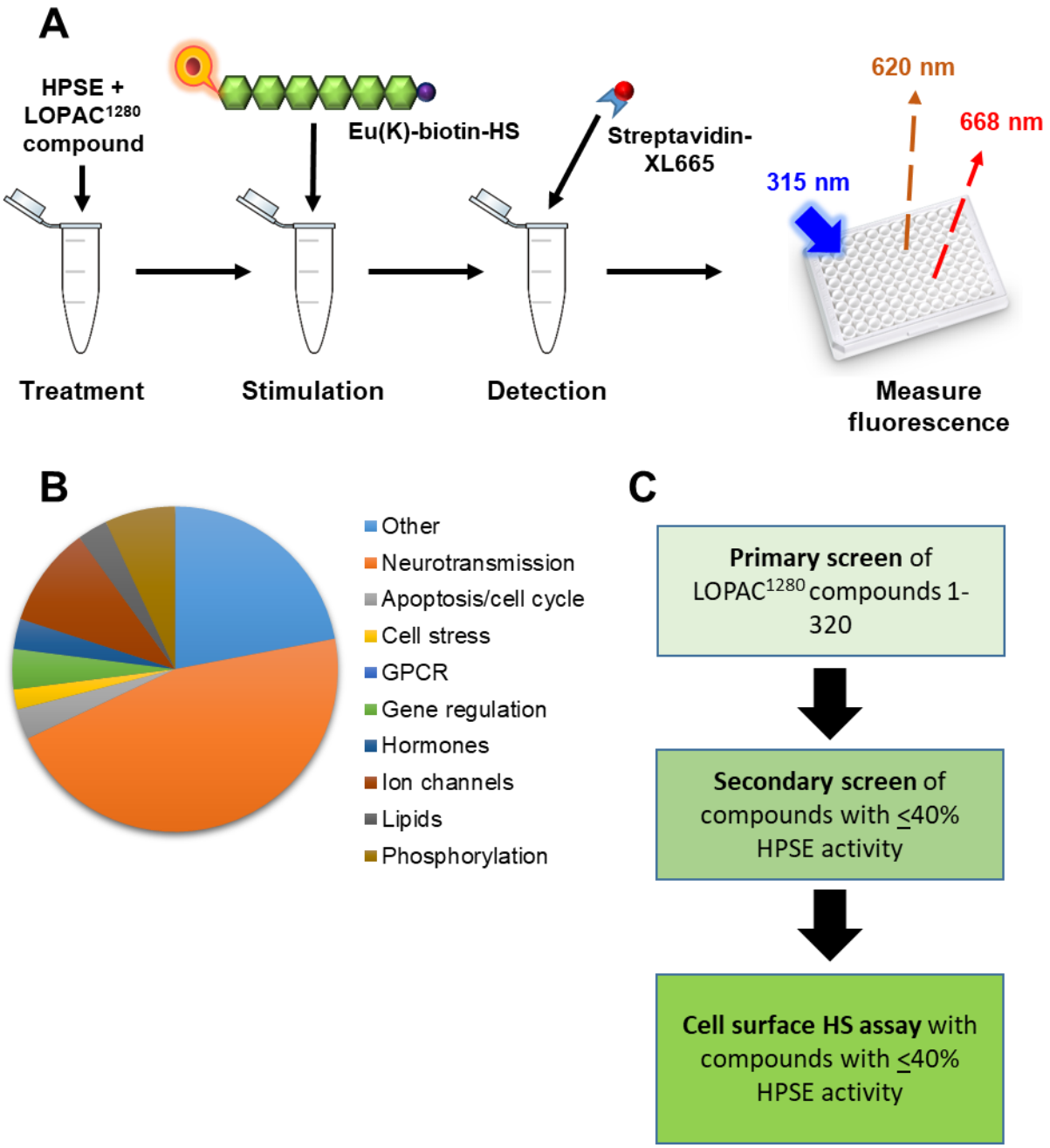

Figure 5.3 LOPAC^{1280} library screening strategy

(A) LOPAC^{1280} library screening procedure. 2 ng of HPSE was first pre-treated with 10 µM of LOPAC^{1280} library compounds. Then, the labelled HS substrate was added with the enzymatic reaction allowed to occur. HS degradation level was detected with the streptavidin-conjugated fluorophore followed by the measurement of fluorescence. **(B)** An overview of the variety of LOPAC^{1280} library compounds screened, represented by drug class. **(C)** Strategy for inhibitor identification and validation. Eu(K) = Europium cryptate.

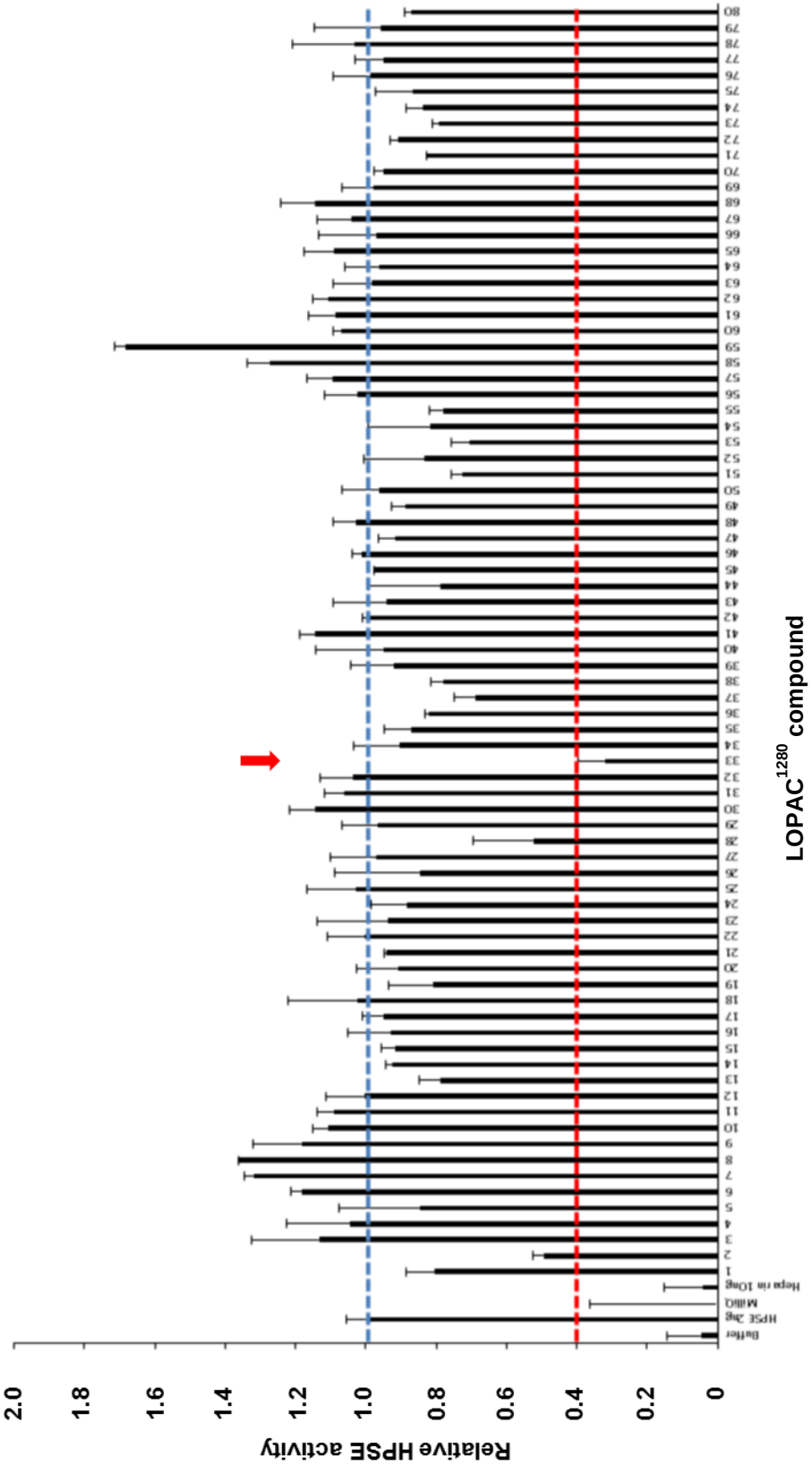

Figure 5.4A Primary screen of compounds 1-80 of the LOPAC^{1280} library
Activity relative to 2 ng of HPSE. Blue line represents untreated HPSE activity. Potential inhibitors were identified as those resulting in ≤40% HPSE activity, indicated by the red line. Data represent SD, samples in duplicate.

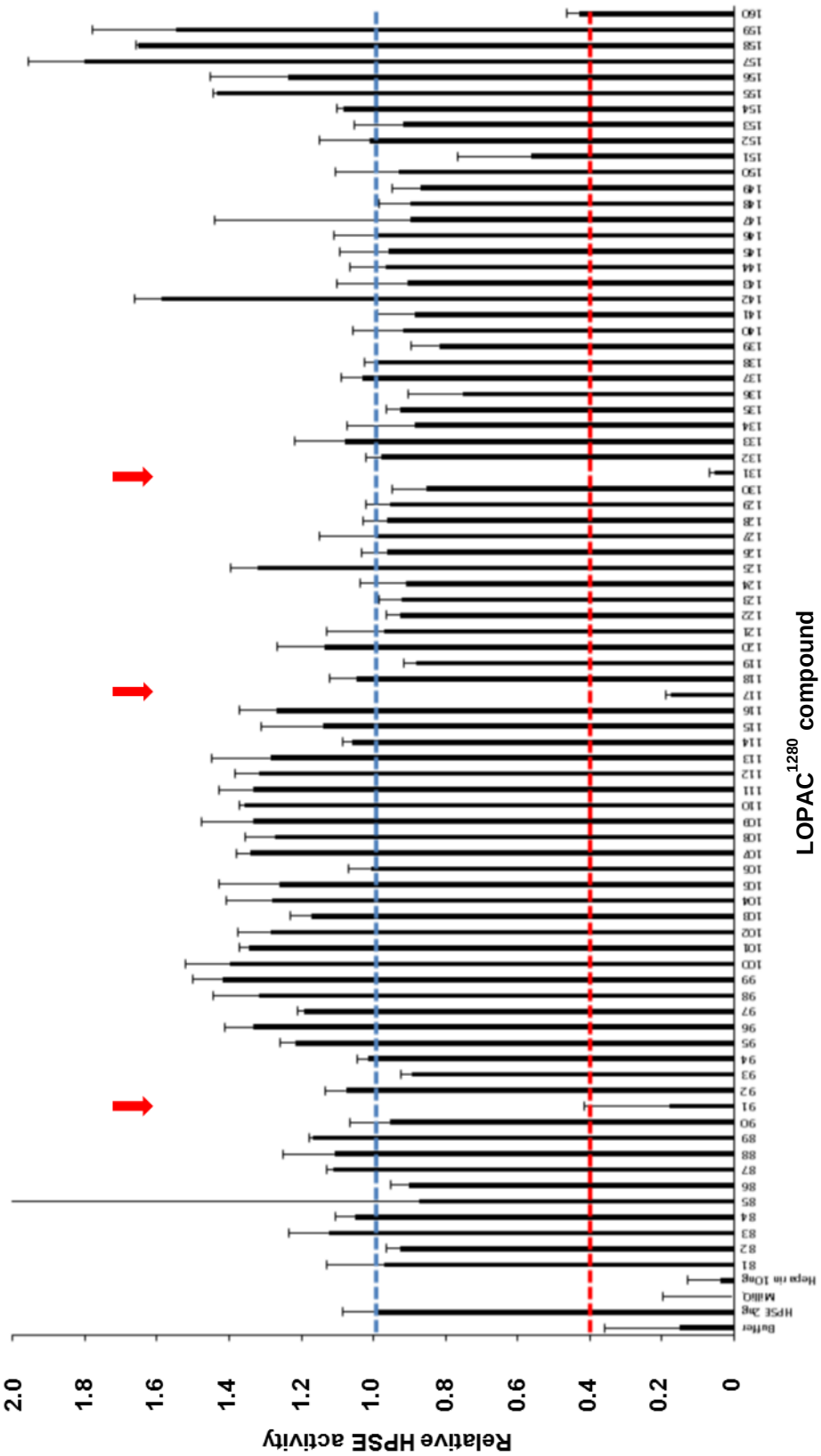

Figure 5.4B Primary screen of compounds 81-160 of the LOPAC^{1280} library
Activity relative to 2 ng of HPSE. Blue line represents untreated HPSE activity. Potential inhibitors were identified as those resulting in ≤40% HPSE activity, indicated by the red line. Data represent SD, samples in duplicate.

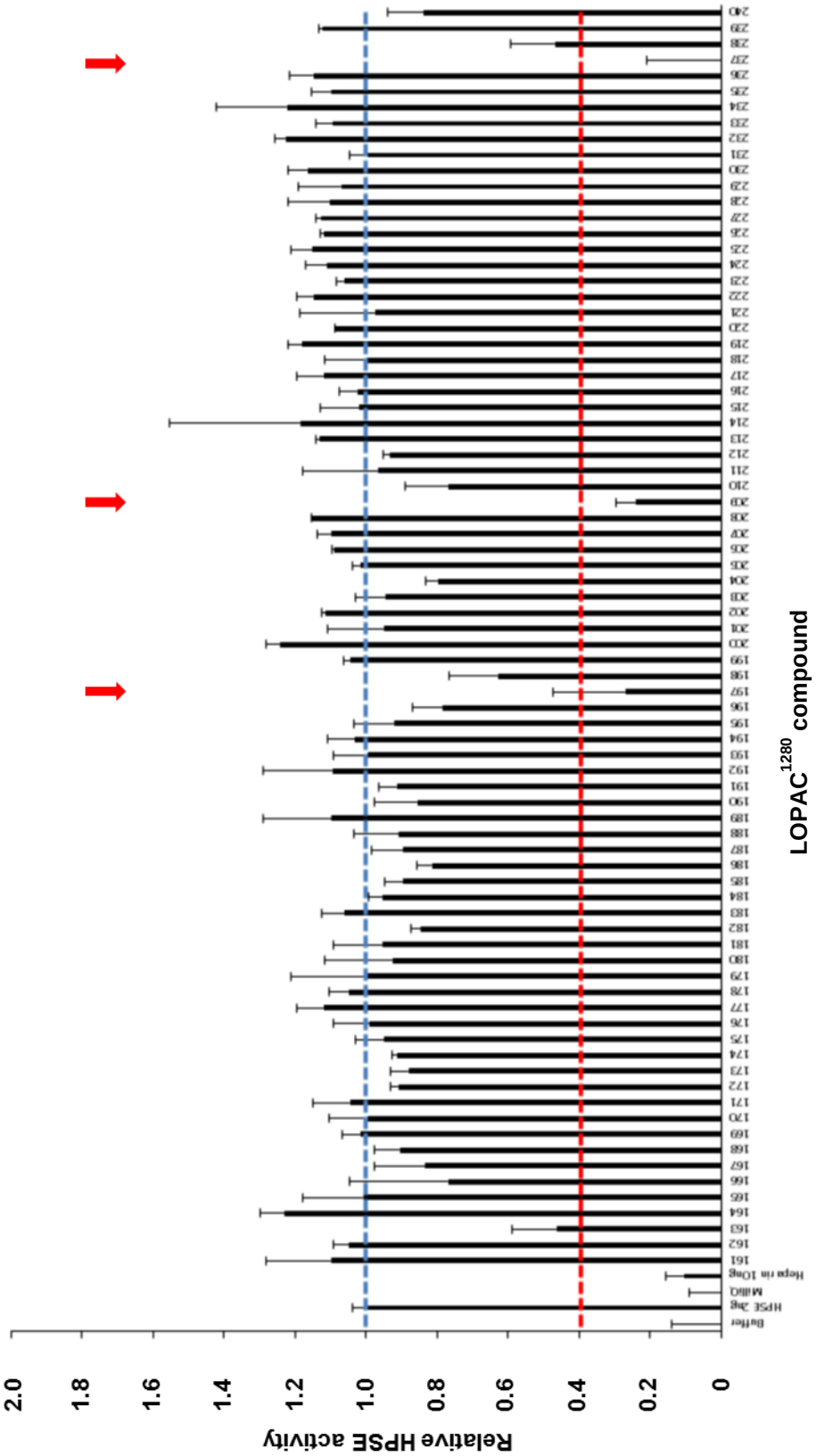

Figure 5.4C Primary screen of compounds 161-240 of the LOPAC^{1280} library
Activity relative to 2 ng of HPSE. Blue line represents untreated HPSE activity. Potential inhibitors were identified as those resulting in ≤40% HPSE activity, indicated by the red line. Data represent SD, samples in duplicate.

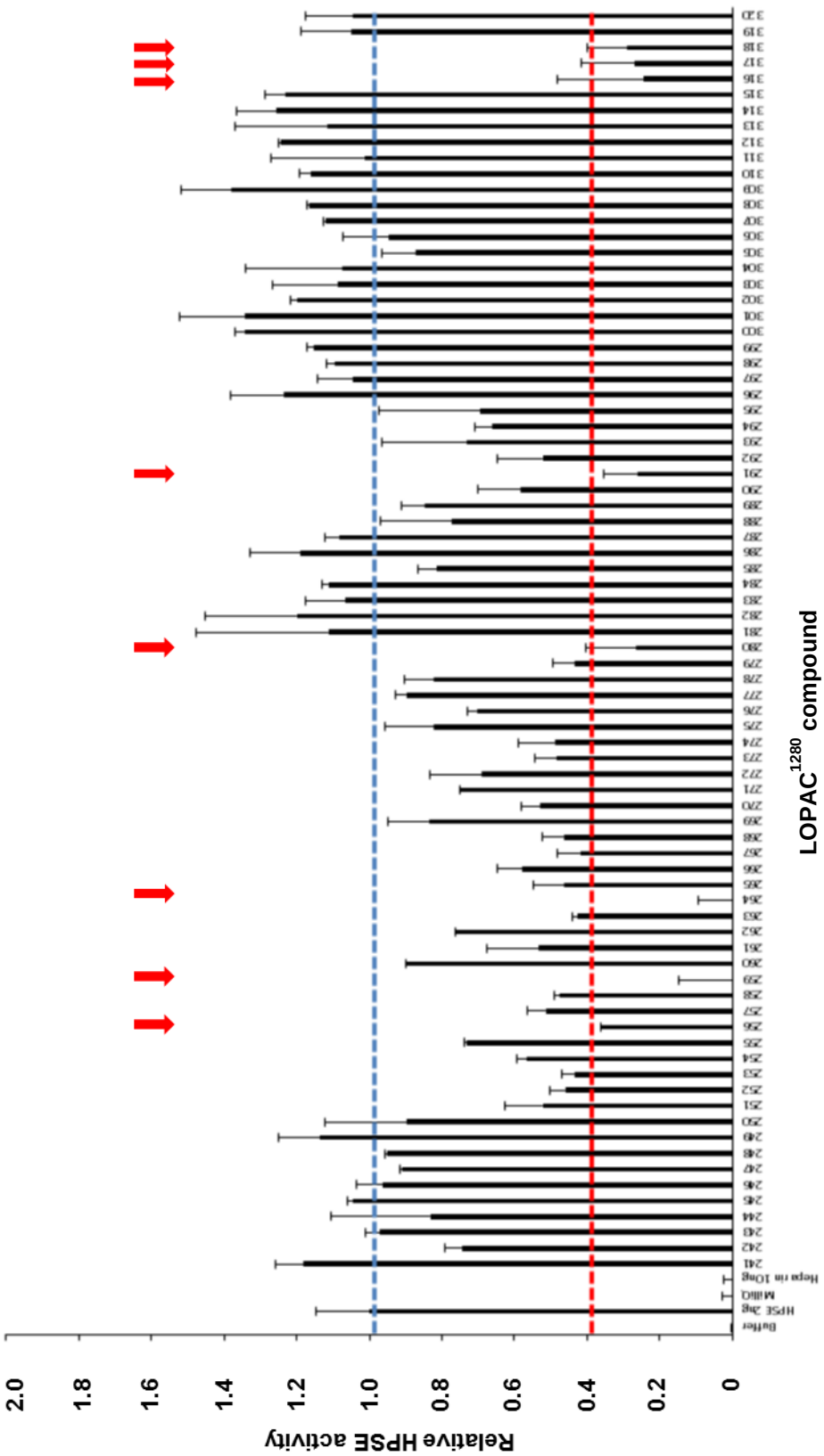

Figure 5.4D Primary screen of compounds 241-320 of the LOPAC^{1280} library
Activity relative to 2 ng of HPSE. Blue line represents untreated HPSE activity. Potential inhibitors were identified as those resulting in ≤40% HPSE activity, indicated by the red line. Data represent SD, samples in duplicate.

5.4.5 Secondary screen of candidate LOPAC^{1280} compounds displaying HPSE inhibition for further validation

The fifteen compounds identified in the primary screen of the LOPAC^{1280} library to reduce HPSE activity to $\leq$40% of its basal level were then subjected to a secondary screen to assess reproducibility **(figure 5.5)**. Interestingly, the secondary screen invalidated most compounds from further consideration, leaving only compounds 237 (GW7647, an agonist of the peroxisome proliferator activated receptor-alpha (PPAR-α)) and 264 (6-hydroxy-DOPA, a catecholamine-neurotoxin pre-cursor) for further characterisation.

5.4.6 Optimisation and validation of the cell surface HS assay

A flow cytometry-based assay to further validate GW7647 and 6-hydroxy-DOPA as HPSE inhibitors was designed. This was distinct to the HPSE activity assay and relied on the detection of the level of degradation of cell surface HS by HPSE **(figure 5.6A)**. HS levels on the surface of CHO-K1 cells were measured following treatment with HPSE. The maintenance in fluorescence was thus attributed to a reduction in HPSE enzymatic activity. Increasing levels of HPSE indicated a trend towards a reduction in PE fluorescence **(figure 5.6B)**. It was concluded that 200 ng of HPSE was sufficient for use in this assay. Approximately 40 – 55% inhibition of HPSE activity was observed for OGT-2115, PI-88 and heparin in this cell surface HS assay, reflecting those observed in the FRET-based activity assay **(figures 5.6C and 5.6D)**. Suramin displayed no significant HPSE-inhibitory effect. Furthermore, in contrast to the FRET-based activity assay, OGT-2115 displayed a higher level of HPSE inhibition compared to PI-88 and heparin. Thus, 10 ng/µl of OGT-2115 was deemed an appropriate control in this assay for the further validation of novel HPSE inhibitors.

A

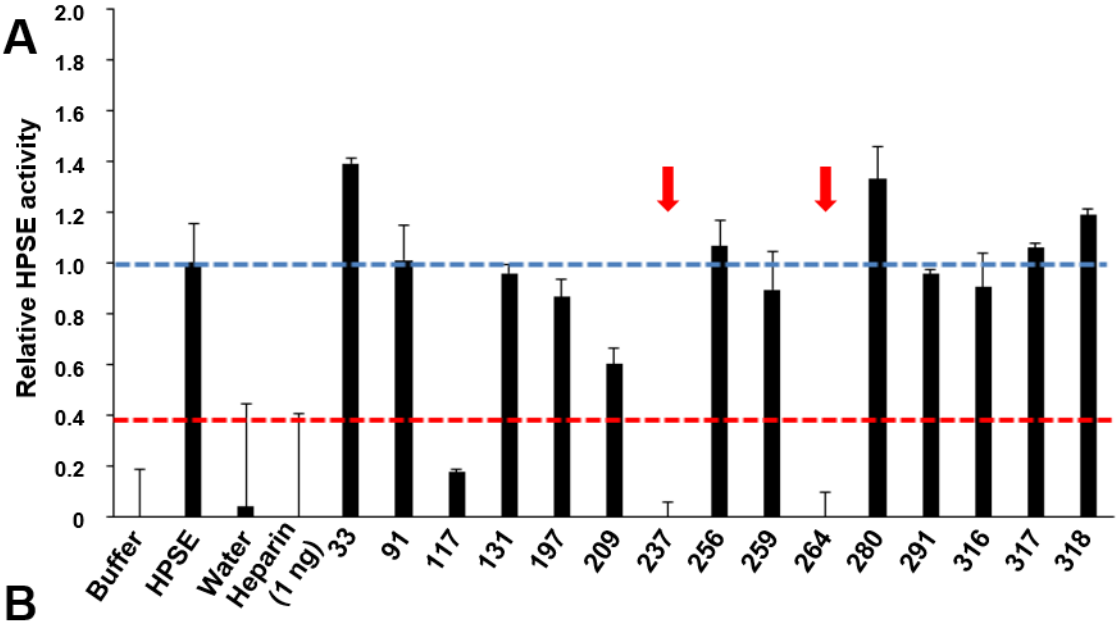

B

No.	Identity	Class	Description
33	NNGH	ECM	MMP3 inhibitor
91	Clinidipine	Ion channels	Ca2+ channel blocker
117	CGP55845 hydrochloride	Neurotransmission	GABA-B receptor antagonist
131	Domperidone	Neurotransmission	Peripheral dopamine antagonist
197	Fiduxosin hydrochloride	Neurotransmission	Adrenoreceptor antagonist
209	Forskolin	Enzyme	Activator of adenylate cyclase - antihypertensive
237	GW7647	Transcription	Selective PPARα agonist
256	Homovanillic acid	Neurotransmission	Dopamine metabolite
259	Haloperidol	Neurotransmission	Dopamine antagonist
264	6-hydroxy-DOPA	Neurotransmission	Catecholaminergic neurotoxin pre-cursor
280	Nelfinavir mesylate hydrate	Immune signalling	HIV protease inhibitor
291	SR27897 hydrate	Hormone	Cholecystokinin antagonist
316	Idarubicin	DNA metabolism	Anti-neoplastic – topoisomerase II inhibitor
317	Metolazone	Ion channel	Na+ channel inhibitor
318	GR55562 dihydrobromide	Neurotransmission	Serotonin receptor antagonist

Figure 5.5 Secondary screen of LOPAC^{1280} compounds displaying HPSE inhibition

LOPAC^{1280} library compounds with the capacity to reduce HPSE activity to ≤40% of its basal level were re-screened for reproducibility. Those which consistently demonstrated the capacity to reduce HPSE activity to ≤40% (represented by red line) were considered reproducible. Compounds 237 (GW7647) and compound 264 (6-hydroxy-DOPA) were found to consistently exhibit HPSE-inhibitory activity. Error bars = SD; samples in duplicate.

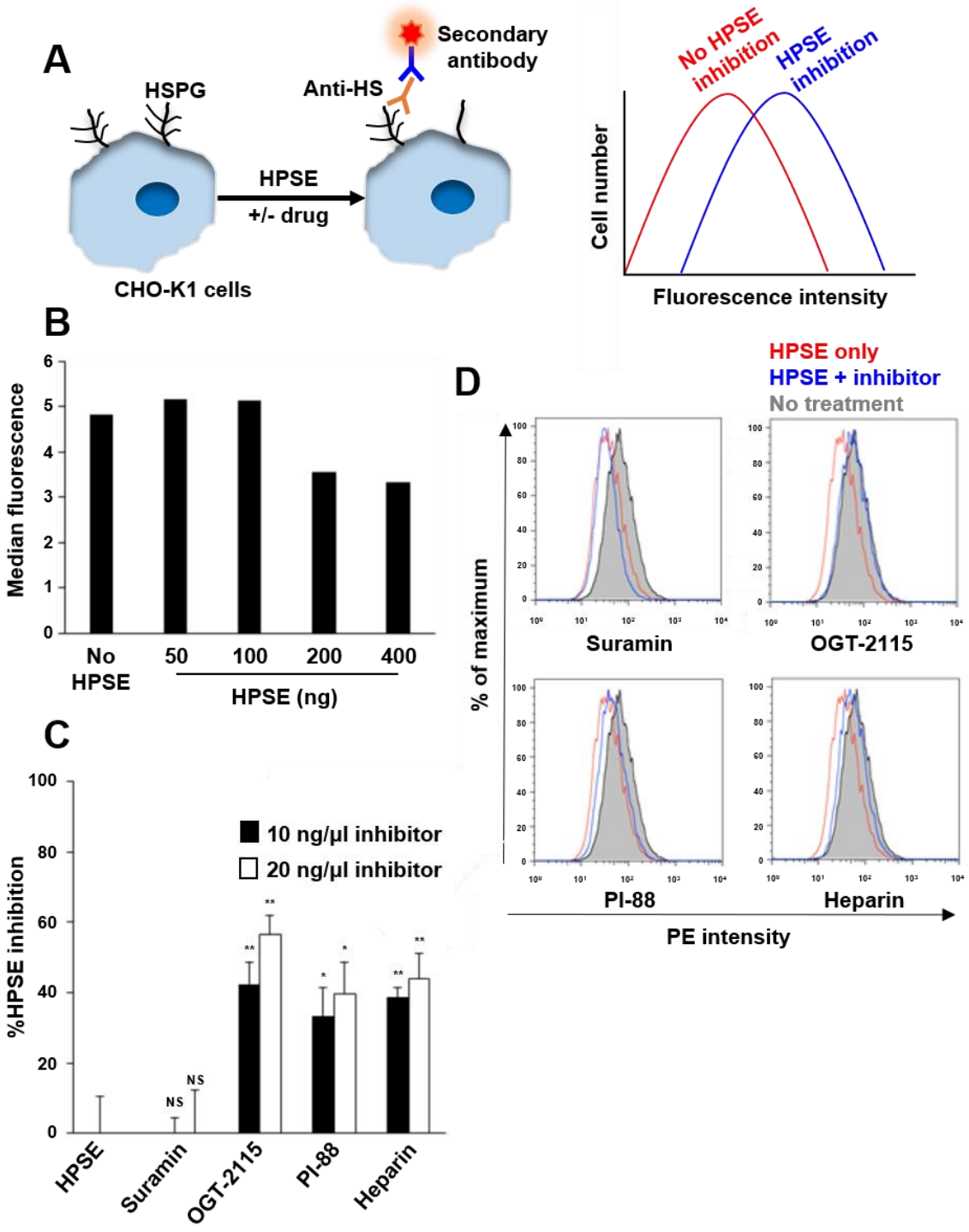

Figure 5.6 Optimisation and validation of the cell surface HS assay
(A) Cell surface HS assay. CHO-K1 cells were treated with purified HPSE and inhibitors following a pre-incubation period. Cell surface HS levels were measured with an anti-mouse HS with a secondary PE-conjugated goat anti-mouse IgM antibody. Flow cytometry was used to quantify PE fluorescence; increased fluorescence (blue) compared to HPSE only (red) indicated HPSE inhibition. **(B)** Increasing amounts of HPSE was assessed for ability to reduce PE fluorescence intensity relative to a no HPSE control in the cell surface HS assay. **(C)** Known HPSE inhibitors were validated in the cell surface HS assay. Inhibitors were screened against 2 ng of HPSE at 10 and 20 ng/µl. **(D)** Representative histograms of known HPSE inhibitors at 10 ng/µl. C; *n* = 3 (except suramin 20 ng/µl, where *n* = 2), error bars = SEM; NS, not significant; *,p<0.05; **, p<0.01; unpaired t-test.

5.4.7 Validation of novel HPSE inhibitors with the cell surface HS assay

Following the validation of the cell surface HS assay as a useful tool in further authentication of novel HPSE inhibitors, GW7647 and 6-hydroxy-DOPA were subjected to this assay **(figure 5.7A and 5.7B)**. As anticipated, OGT-2115 (10 ng/µl) inhibited HPSE cleavage of cell surface HS. GW7647 demonstrated an approximately 30% reduction of HPSE cleavage at a concentration of 10 µM. However, 6-hydroxy-DOPA at a 10 µM concentration failed to display a significant inhibitory capacity. This resulted in 6-hydroxy-DOPA no longer being considered for further validation. A titration of GW7647 in the low µM range revealed a concentration-dependent inhibitory mechanism, which further validated GW7647 as a novel HPSE inhibitor **(figure 5.7C)**.

5.4.8 Validation of GW9578, a structurally-related compound to GW7647, as a novel HPSE inhibitor

Following the demonstration that GW7647 exhibited HPSE-inhibitory activity, it was hypothesised that a structurally-related compound, GW9578, would possess a similar capability. Like GW7647, GW9578 is a PPAR-α agonist and a urea-substituted thioisobutyric acid (Brown et al., 1999). The two compounds share structural similarities; specifically, a urea substitution group and a thioisobutyric acid group **(figure 5.8A)**. This was reflected in the cell surface HS assay, with GW9578 inhibiting the cleavage of HS **(figure 5.8B)**. Both GW7647 and GW9578 inhibited the cleavage of cell surface HS in a comparable manner **(figure 5.8C)**. As expected, GW9578 showed inhibition of enzymatic activity of HPSE *in vitro*, as observed for GW7647 **(figure 5.8D)**. Both drugs thus demonstrated a drug-like, concentration-dependent manner of HPSE activity inhibition. These data suggest that the inhibition of HPSE by GW7647 and GW9578 may depend on conserved structural elements between these compounds.

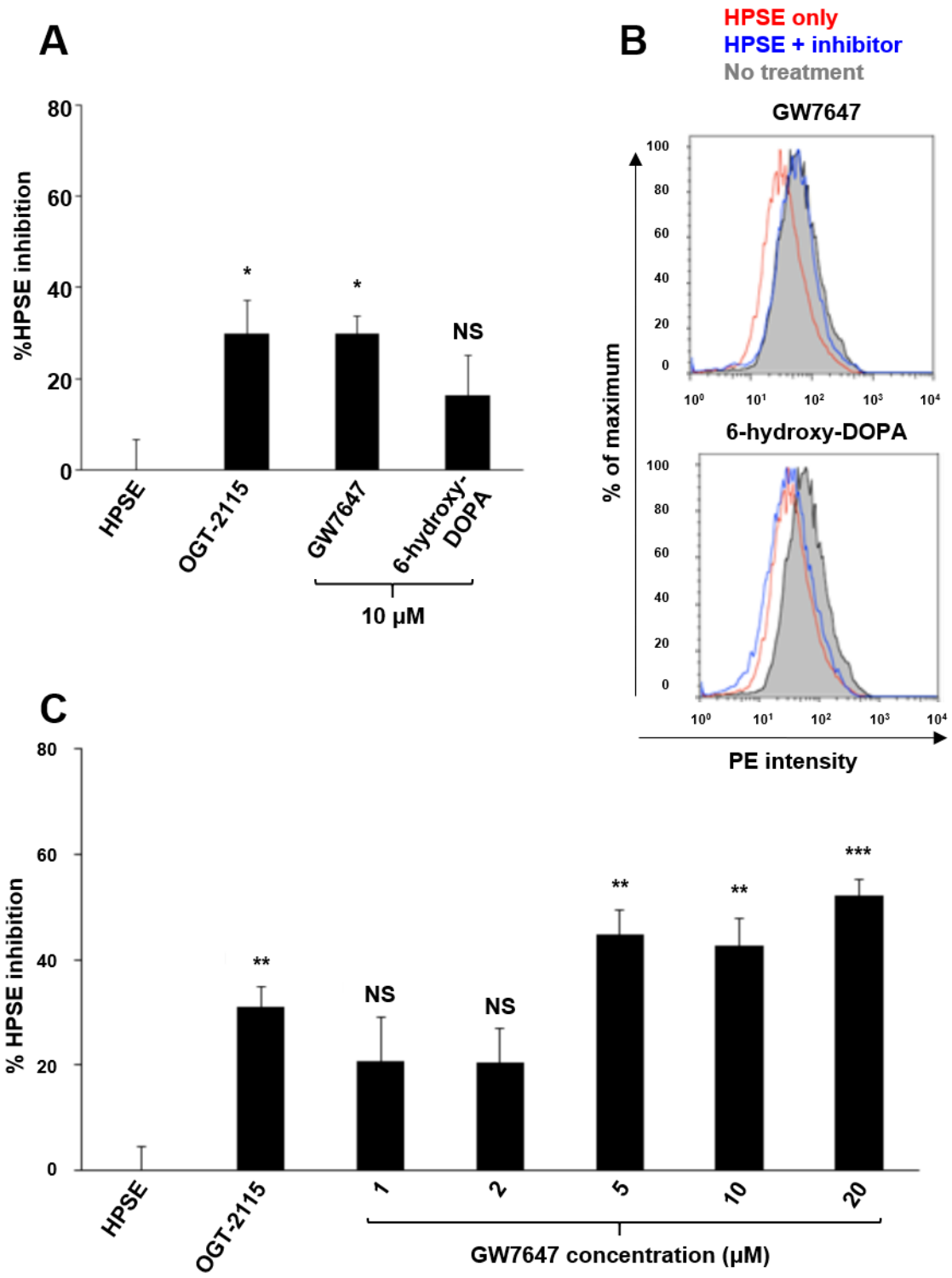

Figure 5.7 Validation of potential HPSE inhibitors in the cell surface HS assay
(A) GW7647 and 6-hydroxy-DOPA were screened in the HPSE activity assay. GW7647 exhibited HPSE activity inhibition at a 10 µM concentration against 200 ng of HPSE. However, no such activity was observed with 6-hydroxy-DOPA. OGT-2115 was used at 10 ng/µl **(B)** Representative histograms of GW7647 and 6-hydroxy-DOPA in the cell surface HS assay. **(C)** GW7647 was titrated against HPSE and exhibited a concentration-dependent HPSE-inhibitory activity. OGT-2115 was used at 10 µM. *n* = 3; error bars = SEM; *, p<0.05; **, p<0.01; ***, p<0.001; unpaired t-test.

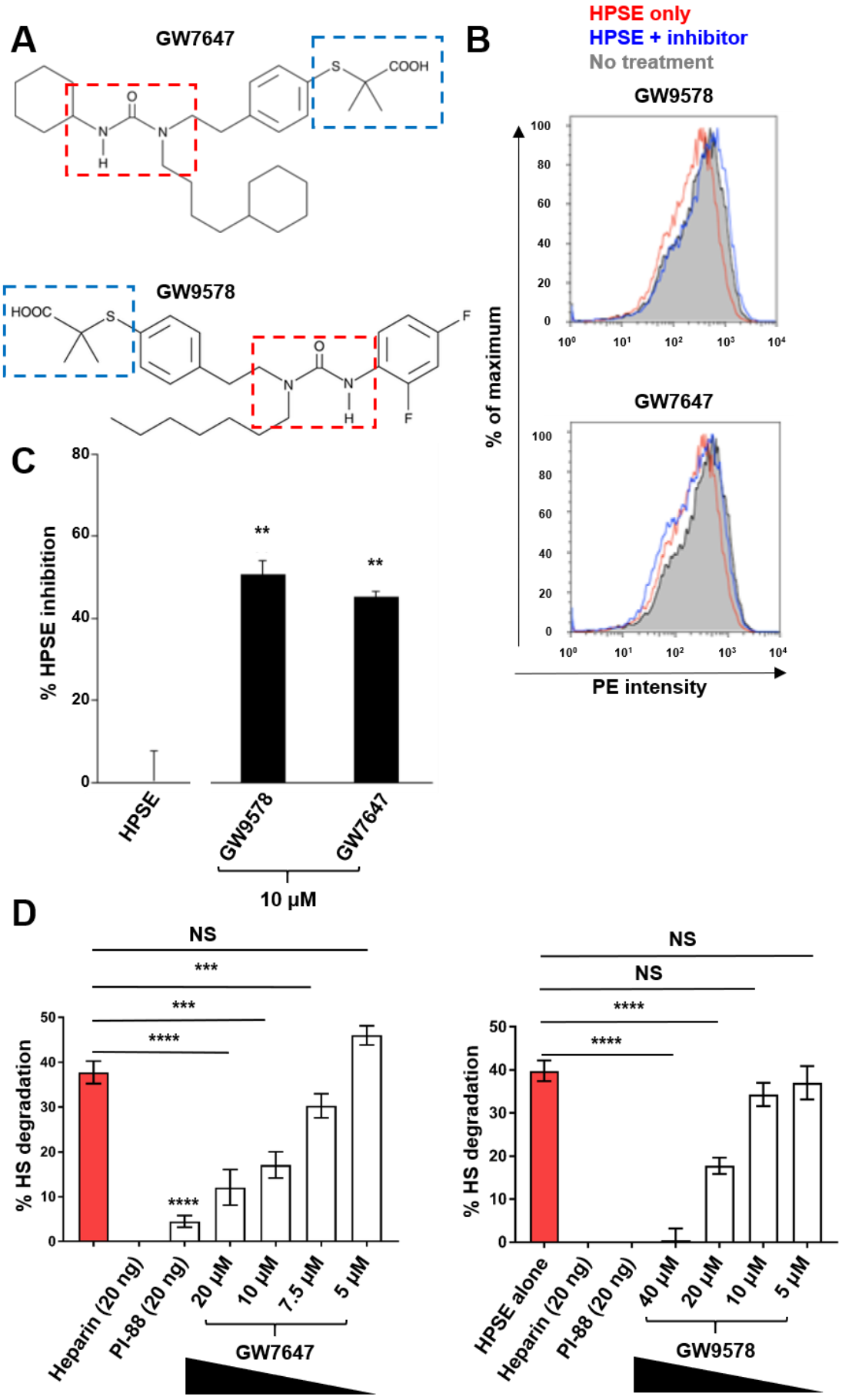

Figure 5.8 Validation of GW7647 and a structurally related compound, GW9578, as HPSE inhibitors

Figure 5.8 (A) GW7647 and GW9578 exhibit structural similarities. The urea substitution group (red) and the thioisobutyric acid group (blue) are conserved between the two compounds **(B)** Representative histograms of GW7647 and GW9578 in the cell surface HS assay demonstrated the inhibition of HS degradation at 10 µM GW9578 inhibited HPSE activity at a 10 µM concentration. **(C)** GW7647 and GW9578 inhibit the degradation of cell surface HS by inhibiting the enzymatic activity of HPSE **(D)** GW7647 and GW9578 inhibit HPSE in a drug-like, concentration-dependent manner, in the *in vitro* HPSE enzymatic activity assay. n = 3, representative data of one of three independent assays shown; error bars = SEM; NS, not significant; *, p<0.05; **, p<0.01; ***, p<0.001; ****, p<0.0001; unpaired t-test.

5.4.9 Modelling the molecular interaction between GW7647 and human HPSE

Following the *in vitro* validation of GW7647, an *in silico* modelling of the interaction between GW7647 and human HPSE was performed using the YASARA molecular modelling application (available at http://www.yasara.org; performed by Professor Brian Smith, La Trobe University). Binding energies were calculated for the binding of GW7647 to HPSE and it was suggested that GW7647 interacts with the active site of the enzyme, thus mediating the inhibition of HPSE activity **(figure 5.9)**. These data suggest that the HPSE active site interaction of GW7647 is responsible for the *in vitro* HPSE-inhibitory action described for GW7647. On account of its structural similarity to GW7647, a similar interaction could be hypothesised to exist between GW9578 and human HPSE.

5.4.10 Demonstrating the need for critical structural features for the inhibitory activity of GW7647 and GW9578

In order to demonstrate that the HPSE-inhibitory action of both GW7647 and GW9578 were dependent on structure and not on their PPAR-α agonistic capacity, a structurally-unrelated PPAR-α agonist, fenofibrate, was investigated. It was thus demonstrated that fenofibrate did not inhibit the *in vitro* activity of human HPSE as GW7647 and GW9578 **(figure 5.10A)**. The molecular structure of fenofibrate is distinct from those of GW7647 and GW9578 and lacks the structural similarities seen between these; specifically, the urea substitution group and the thioisobutyric acid group **(figure 5.10B)**. These results therefore suggest that the capacity of GW7647 and GW9578 to inhibit the enzymatic activity of HPSE is dependent upon structural features.

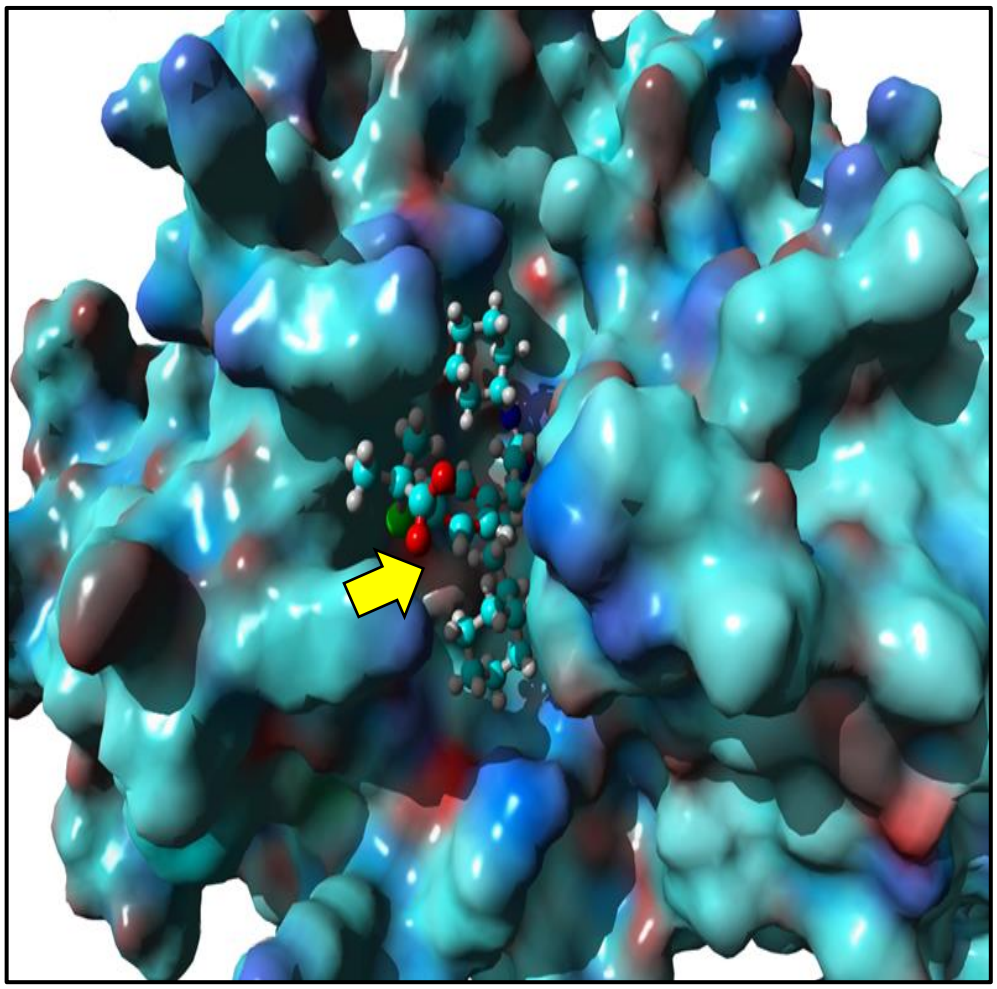

Figure 5.9 Molecular modelling of the interaction between GW7647 and HPSE
Modelling of the interaction between GW7647 and HPSE shows binding of GW7647 to the active site of HPSE. This suggests inhibition of enzymatic activity that is dependent on molecular structure.

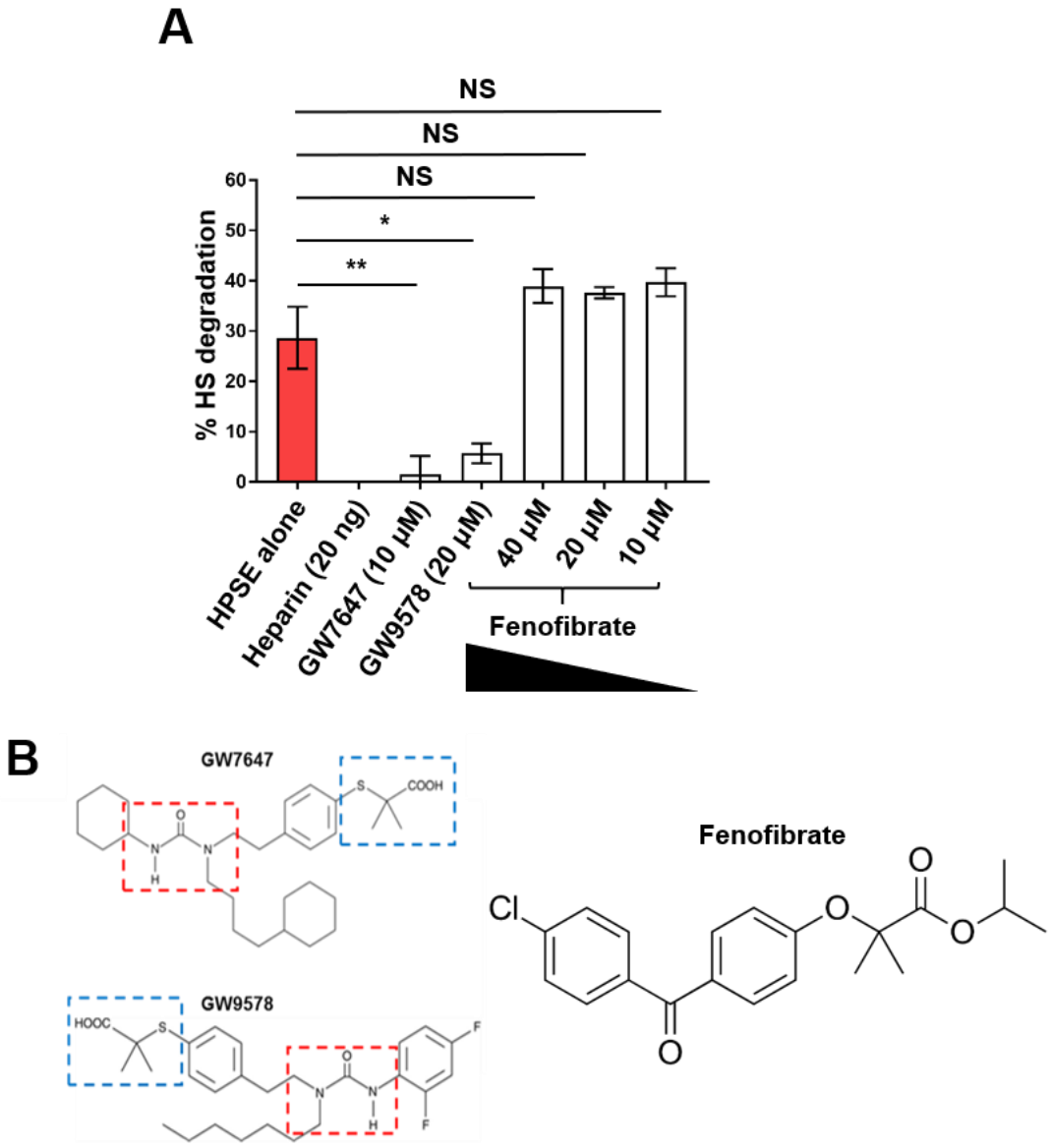

Figure 5.10 The effect of fenofibrate, a structurally unrelated PPAR-α agonist to GW7647 and GW9578, on *in vitro* HPSE enzymatic activity
(A) The PPAR-α agonist fenofibrate failed to inhibit HPSE enzymatic activity in contrast to its structurally distinct counterparts, GW7647 and GW9578. This suggests a structure-dependent inhibitory mechanism. **(B)** The molecular structures of GW7647, GW9578 and fenofibrate. GW7647 and GW9578 share common structural features as highlighted in red (urea substitution group) and blue (thioisobutyric acid group). Fenofibrate is structurally distinct to GW7647 and GW9578. *n* = 3, representative data of one of 3 independent assays shown; error bars = SEM; NS, not significant; *, p<0.05; **, p<0.01; unpaired t-test.

5.4.11 Assessing the action of MK886, a non-competitive PPAR-α inhibitor structurally distinct to GW7647 and GW9578 on the enzymatic activity of HPSE.

In order to investigate the possibility of a PPAR-α inhibitor structurally distinct to GW7647 and GW9578 interacting with and inhibiting HPSE, MK886 was employed in an *in vitro* HPSE enzymatic activity assay. MK886 is structurally distinct to both GW7647 and GW9578 **(figure 5.11A)** and has demonstrated PPAR-α inhibitory properties (Kehrer et al., 2001). As expected, GW7647 and GW9578 inhibited the enzymatic activity of HPSE in a drug-like, concentration-dependent manner **(figure 5.11B)**. Interestingly, MK886 too demonstrated the capacity to inhibit the enzymatic activity of HPSE, although not in a drug-like, nor concentration-dependent manner.

5.4.12 Optimisation of the transwell migration/invasion assay using MDA-MB-231 cells

As previously discussed, the ability of tumour cells to invade surrounding tissue and migrate through the ECM is a key hallmark of cancer (Hanahan and Weinberg, 2000, Hanahan and Weinberg, 2011). It is now well understood that HPSE is a key enzyme in cellular migration and invasion (Parish et al., 2001, Putz et al., 2017, Poon et al., 2014). In order to determine the effects of the known HPSE inhibitor heparin and novel HPSE inhibitors, namely GW7647, GW9578 and MK886, a transwell migration/invasion assay was designed using highly invasive MDA-MB-231 cells that have been demonstrated to express HPSE (Teoh et al., 2009). Furthermore, MDA-MB-231 human breast cancer cells have been demonstrated as an ideal cell line to study the migration and invasion of tumour cells (Abdelkarim et al., 2011, Wu et al., 2009, Xie et al., 2009, Paquette et al., 2011, Hsieh et al., 2013).

Initially, the effect on the viability of MDA-MB-231 cells upon treatment with inhibitors was assessed **(figure 5.12A)**. Cells were treated with heparin, GW7647, GW9578 and MK886 for 24 h in an MTT cell viability assay. Heparin did not display a significant impact on cell viability at concentrations ranging from 5 – 50 mg/ml. MK886 displayed a significant impact at 20 μM, with a 50 μM concentration reducing viability by 70%. GW7647 showed little effect at 10 and 20 μM but decreased viability by 50% at a 50 μM concentration. GW9578 did not appear to significantly affect cell viability in the concentration range assessed. Thus, a heparin concentration of 10 mg/ml and a concentration of 10 μM for GW7647, GW9578 and MK886 was chosen for subsequent studies in order to eliminate the possibility of cytotoxicity.

Next, the optimal concentration of Matrigel® was determined for use in the transwell migration/invasion assay **(figure 5.12B)**. A series of dilutions were performed of Matrigel®

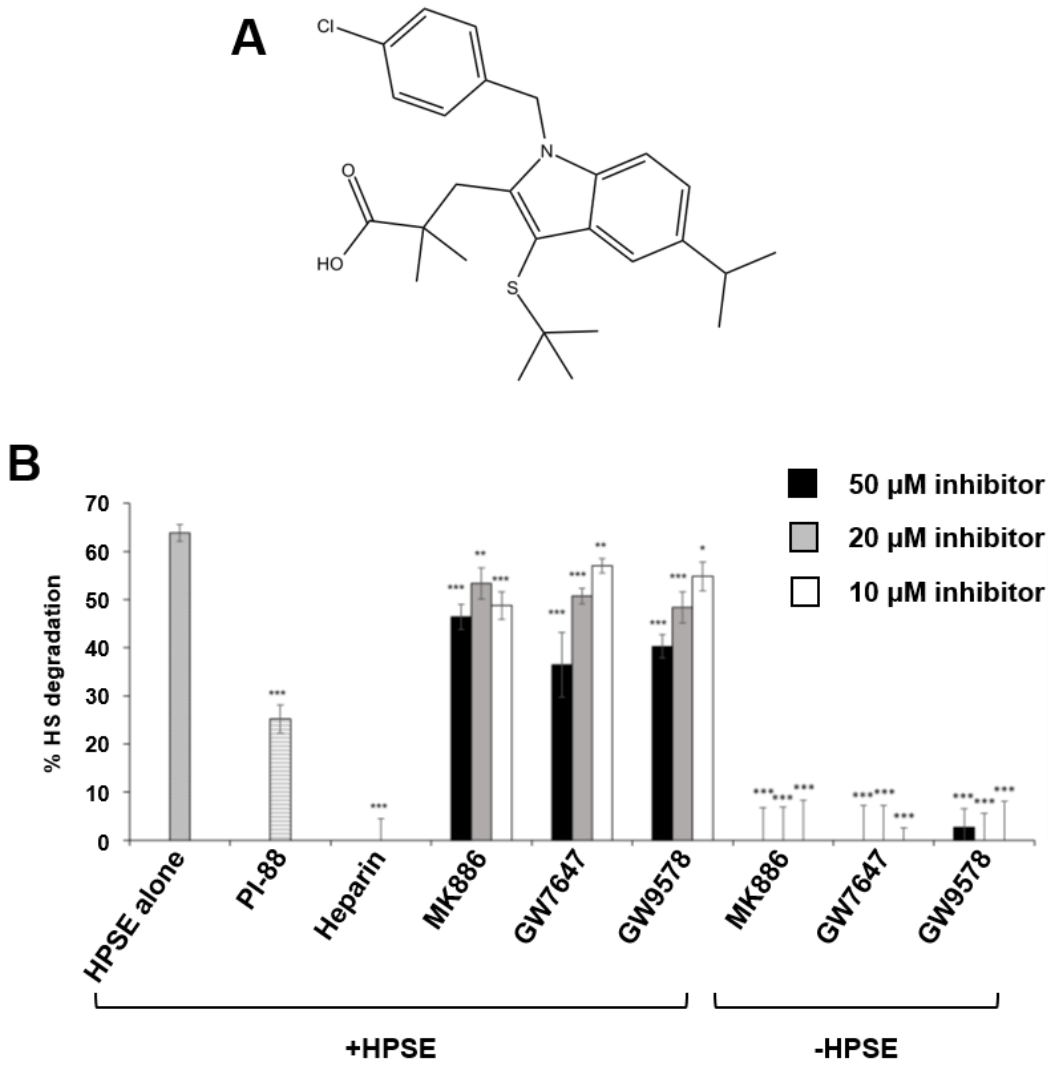

Figure 5.11 The effect of MK886, a structurally distinct, non-competitive inhibitor of PPAR- α on *in vitro* HPSE enzymatic activity
(A) The structure of MK886 is distinct from that of both GW7647 and GW9578. **(B)** MK886 demonstrated the ability to inhibit the enzymatic activity of HPSE, albeit in a non-drug-like manner. PI-88 and Heparin were used at 10 mg/ml. Statistical significance was calculated using a paired t-test in relation to the HPSE only control. *n* = 5, representative data of a single assay shown; error bars = SEM; *, p<0.05; **, p<0.01; ***, p<0.001; paired t-test.

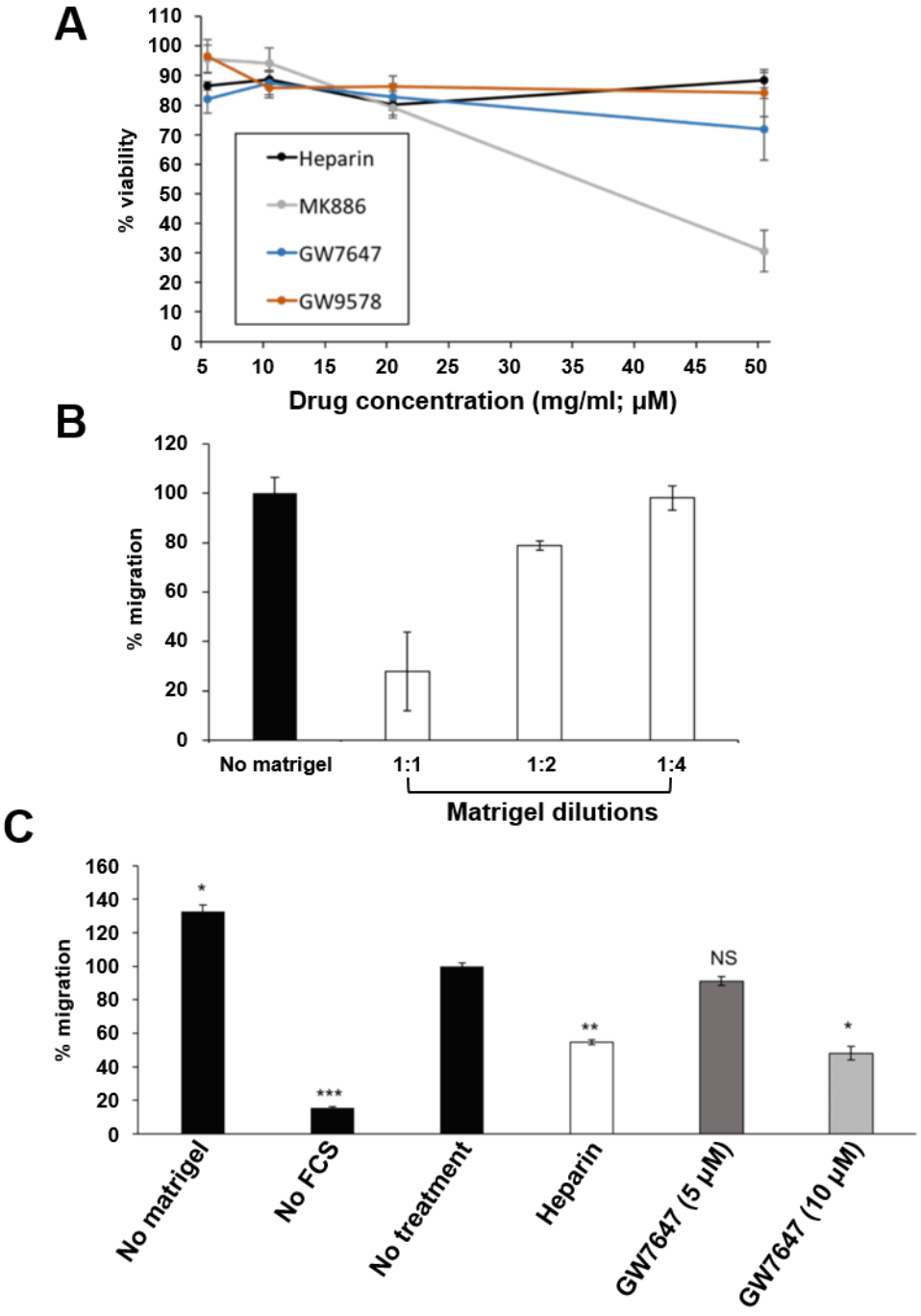

Figure 5.12 Assessing the viability of MDA-MB-231 cells on treatment with known and novel HSPE inhibitors and the optimisation of the transwell migration assay
(A) The assessment of MDA-MB-231 cell viability with the MTT viability assay. Cells were treated with varying concentrations of heparin (black; mg/ml), MK886 (grey; µM), GW7647 (blue, µM) and GW9578 (orange, µM) following which their viability and proliferative capacity were assessed *(n* = 4). **(B)** A series of Matrigel® dilutions were used to determine the optimal concentration to inhibit the migration/invasion of MDA-MB-231 cells *(n* = 2). **(C)** The optimisation of drug concentration. GW7647 was assessed at 5 and 10 µM to determine its optimal concentration in inhibiting the migration/invasion of MDA-MB-231 cells. The percentage of migrated cells were compared to the no treatment control. Statistical significance was calculated between no treatment controls and GW7647-treated cell samples using a paired t-test (*n* = 2). Error bars = SEM; *, p<0.05; **, p<0.01; ***, p<0.001.

with varying ratios of serum-free DMEM; 1:1, 1:2 and 1:4 (parts of Matrigel®: parts of serum-free DMEM, respectively). The 1:1 ratio showed a reduction in migration of 73% and the Matrigel® concentration was determined to be too high for the purpose of the assay. The 1:4 ratio showed a migration/invasion reduction of only 2% and was therefore deemed too low. The optimal Matrigel®: serum-free DMEM was thus determined to be 1:2, with a reduction in migration/invasion of 22%. This demonstrated the ability of the Matrigel® to inhibit the migration/invasion of a significant proportion of cells while allowing an appropriate number of cells to travel through, enabling quantitative analysis.

Next, as a pilot study, the concentration of GW7647 capable of affecting the migration/invasion of MDA-MB-231 cells in the transwell assay was determined **(figure 5.12C)**. GW7647 was used at concentrations of 5 and 10 μM. No significant effect was observed at 5 μM; however, a 10 μM concentration of GW7647 was shown to inhibit the migration/invasion of MDA-MB-231 cells by 52%. Heparin used at 10 mg/ml as a control demonstrated a significant reduction in migration/invasion to 60%. Thus, in subsequent experiments, GW7647, GW9578 and MK886 were used at a 10 μM concentration.

5.4.13 Assessing the action of known and novel HPSE inhibitors on the migratory/invasive capacity of MDA-MB-231 cells

Following the optimisation of the transwell migration/invasion assay of MDA-MB-231 cells, the effect of the known HPSE inhibitor heparin and novel HPSE inhibitors, namely GW7647, GW9578 and MK886, on this crucial cancer-promoting hallmark was determined. MDA-MB-231 cells were shown to produce enzymatically active HPSE as described using 50 μg of total cellular lysate with 2 ng of purified human HPSE **(figure 5.13A)**. Quantification of the migration/invasion of MDA-MB-231 cells through the Matrigel® showed that heparin significantly reduced the cellular migratory/invasive capacity **(figure 5.13B)**. This observation further validated the use of the assay in determining novel drugs capable of inhibiting cellular migration/invasion by virtue of affecting the enzymatic activity of HPSE. The control with no FCS showed low migration levels, validating FCS as an appropriate chemoattractant for MDA-MB-231 cells. Both GW7647 and GW9578 significantly inhibited the migration/invasion of MDA-MB-231 cells through the Matrigel®, in contrast to the no treatment control, with an approximately 33% and 50% reduction in cellular migration/invasion respectively. Interestingly, MK886 too showed a significant reduction of migration/invasion of MDA-MB-231 cells through the Matrigel® along with an approximately 54% reduction in migration/invasion compared to the no Matrigel® control. This suggests that this observation may not be the direct result of the inhibition of migration/invasion through the Matrigel®.

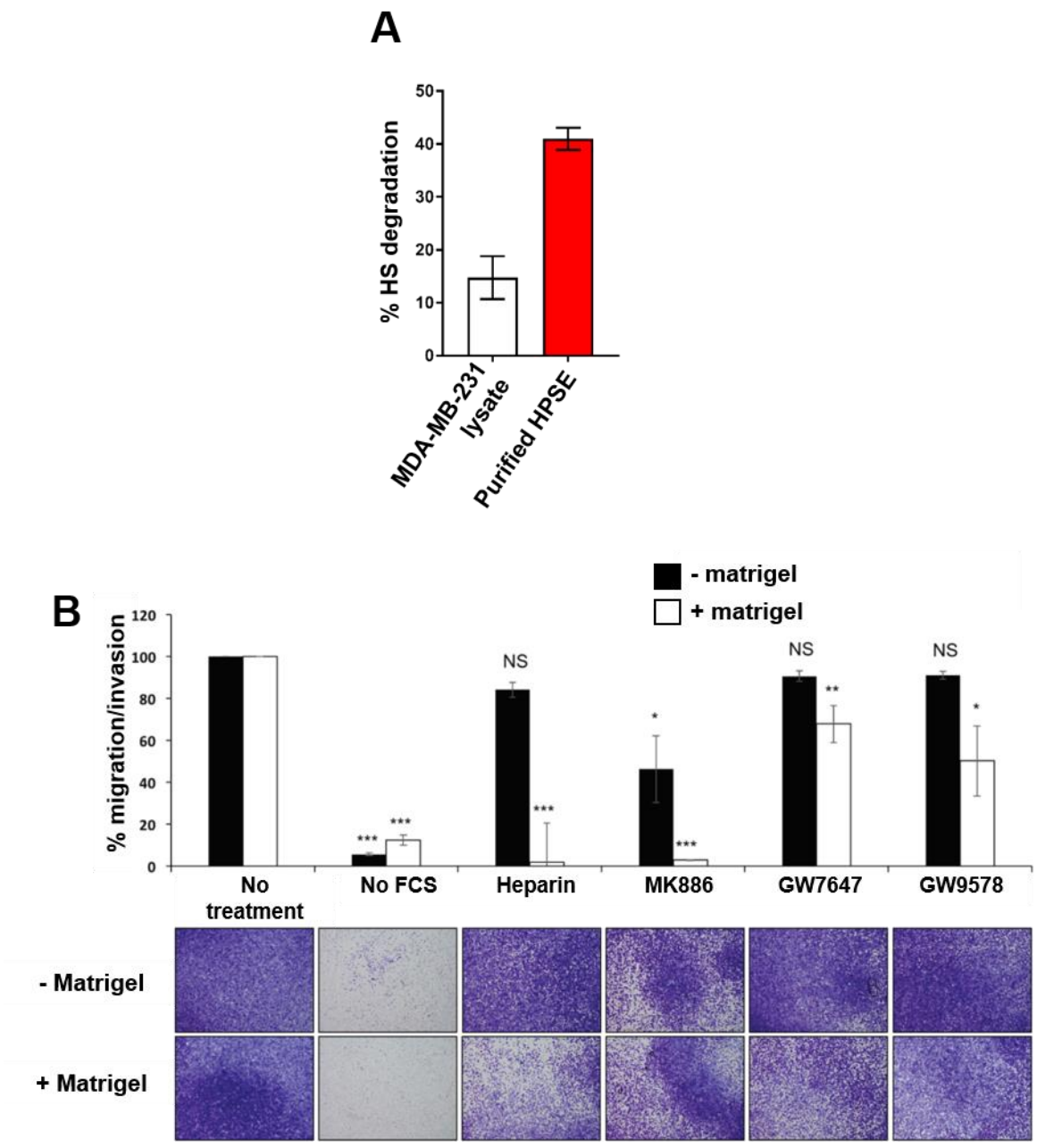

Figure 5.13 Effect of known and novel HPSE inhibitors on the migration/invasion of MDA-MB-231 cells
(A) MDA-MB-231 cells demonstrate HPSE enzymatic activity *in vitro.* **(B)** GW7647 and GW9578 inhibited the Matrigel® invasion of MDA-MB-231 cells at a concentration of 10 μM. Interestingly, MK886 also showed a reduction in cellular migration in transwells both with and without Matrigel®. Representative images of crystal violet-stained MDA-MB-231 cells are shown in the bottom panel following migration/invasion through the Matrigel® and the no Matrigel® control. A; $n = 2$, data representative of one of two independent assays with 3 technical replicates each; unpaired t-test. B; $n = 3$, representative data of one of three independent assays shown; error bars = SEM; NS, not significant; *, $p<0.05$; **, $p<0.01$; ***, $p<0.001$; statistical significance calculated between no treatment controls and drug treated samples; paired t-test.

5.4.14 Design of an assay to determine the effect of HPSE inhibitors on angiogenesis

As discussed previously, HPSE plays a well described role in angiogenesis (Knelson et al., 2014, Nadir and Brenner, 2014, Parish et al., 1999). Tumour growth and metastasis in turn are strongly promoted by HPSE through its pro-angiogenic capacity. In order to determine the role of novel HPSE inhibitors on angiogenesis, an *in vitro* assay was established. Angiogenesis assays using mouse aorta fragments *in vitro* have been previously described, which formed the basis of this study (Baker et al., 2011, Nicosia and Ottinetti, 1990). This was achieved by using sections of mouse aorta fragments embedded in a fibrin gel and exposed to a particular drug being assessed **(figure 5.14A)**. Treatment of aortic fragments was carried out with GW7647, GW9578, MK886 and heparin for 7 days. The resulting degree of vessel sprouting was assessed using a scoring matrix **(figure 5.14B)**.

5.4.15 Assessing the action of known and novel HPSE inhibitors in an *in vitro* angiogenesis assay using mouse aortas

The effect of the known HPSE inhibitor heparin and novel HPSE inhibitors, namely GW7647, GW9578 and MK886, on angiogenesis was evaluated in aortas sourced from C57Bl/6 and C57Bl/6xHPSE$^{-/-}$ mice **(figure 5.15)**. The no treatment control showed a high degree of vessel sprouting after 7 days, comparable to the DMSO control.

In aortas excised from C57Bl/6 mice, heparin significantly reduced angiogenesis **(figure 5.15A)**. Treatment with GW7647 and GW9578 also resulted in a significant reduction of vessel outgrowth. In contrast, MK886 and DMSO alone did not affect angiogenesis. Next, aortas excised from C57Bl/6xHPSE$^{-/-}$ mice were assessed to determine if the anti-angiogenic effects of the novel HPSE inhibitors observed on C57Bl/6 aortas were the result of HPSE inhibition **(figure 5.15B)**. Interestingly, treatment with GW7647, GW9578 and MK886 was shown to reduce vessel sprouting of C57Bl/6xHPSE$^{-/-}$ aortas suggesting the inhibition of angiogenesis by these compounds was occurring independently of HPSE.

Finally, when comparing the effect of the known and novel HPSE inhibitors on aortic vessel outgrowths in both C57Bl/6 and C57Bl/6xHPSE$^{-/-}$ mouse aortas, heparin significantly affected angiogenesis in vessels of C57Bl/6 mice (angiogenesis index of approximately 2.5 compared to 3.75 in the no treatment control) when compared to those of C57Bl/6xHPSE$^{-/-}$ mice (angiogenesis index of 3.5 compared to 3.75 in the no treatment control; **figure 5.15C**). No significant difference in angiogenesis was observed between C57Bl/6 and C57Bl/6xHPSE$^{-/-}$ mouse aortas treated with GW7647, GW9578 and MK886 as well as the no treatment and DMSO alone controls.

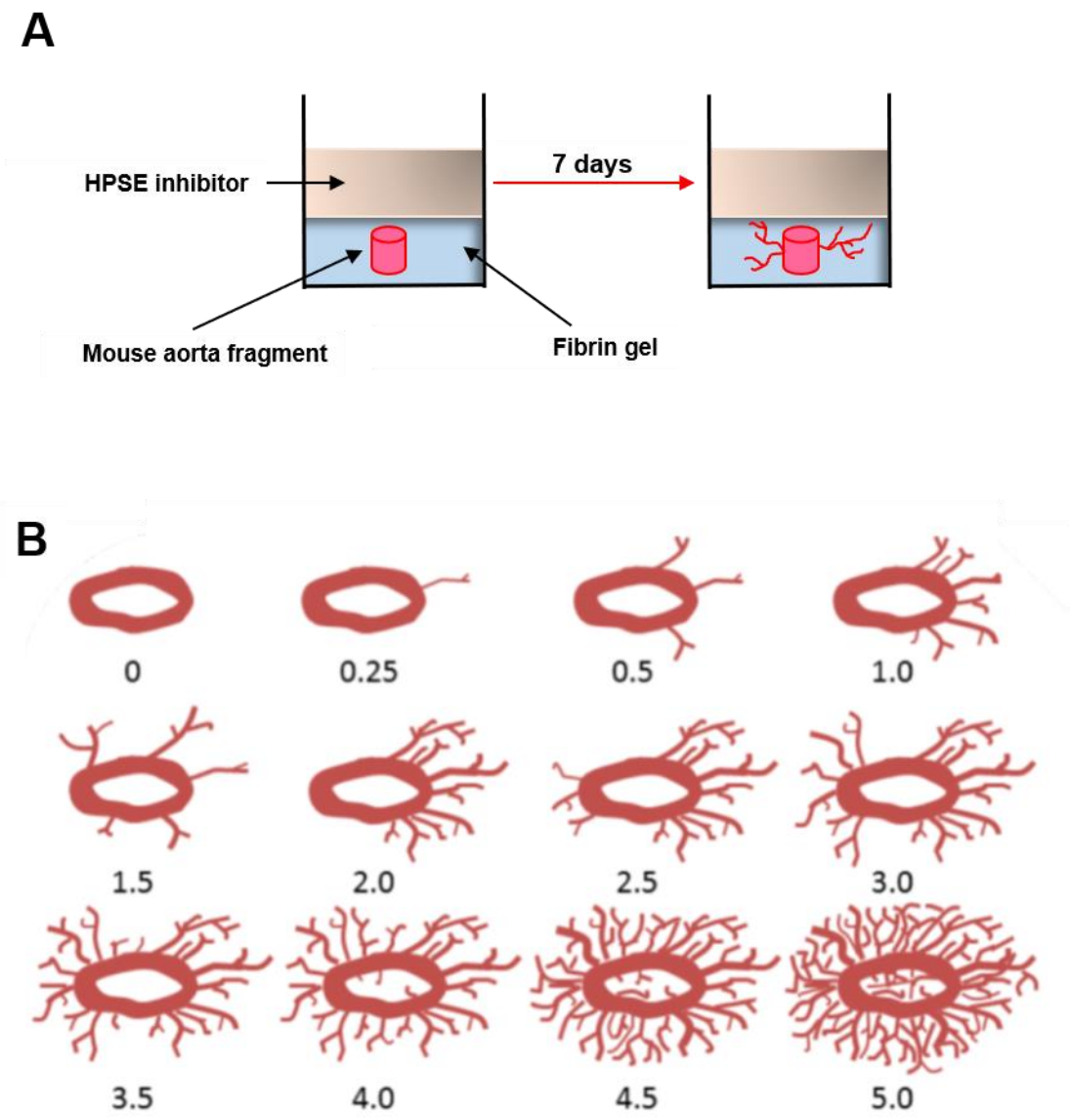

Figure 5.14 The design of the angiogenesis assay and the scoring matrix
(A) The angiogenesis assay; mouse aorta fragments were embedded in a fibrin gel and treated with HPSE inhibitors for 7 days. The resulting degree of vessel branching was then scored. **(B)** The scoring matrix employed to evaluate and quantify the level of angiogenesis seen after 7 days.

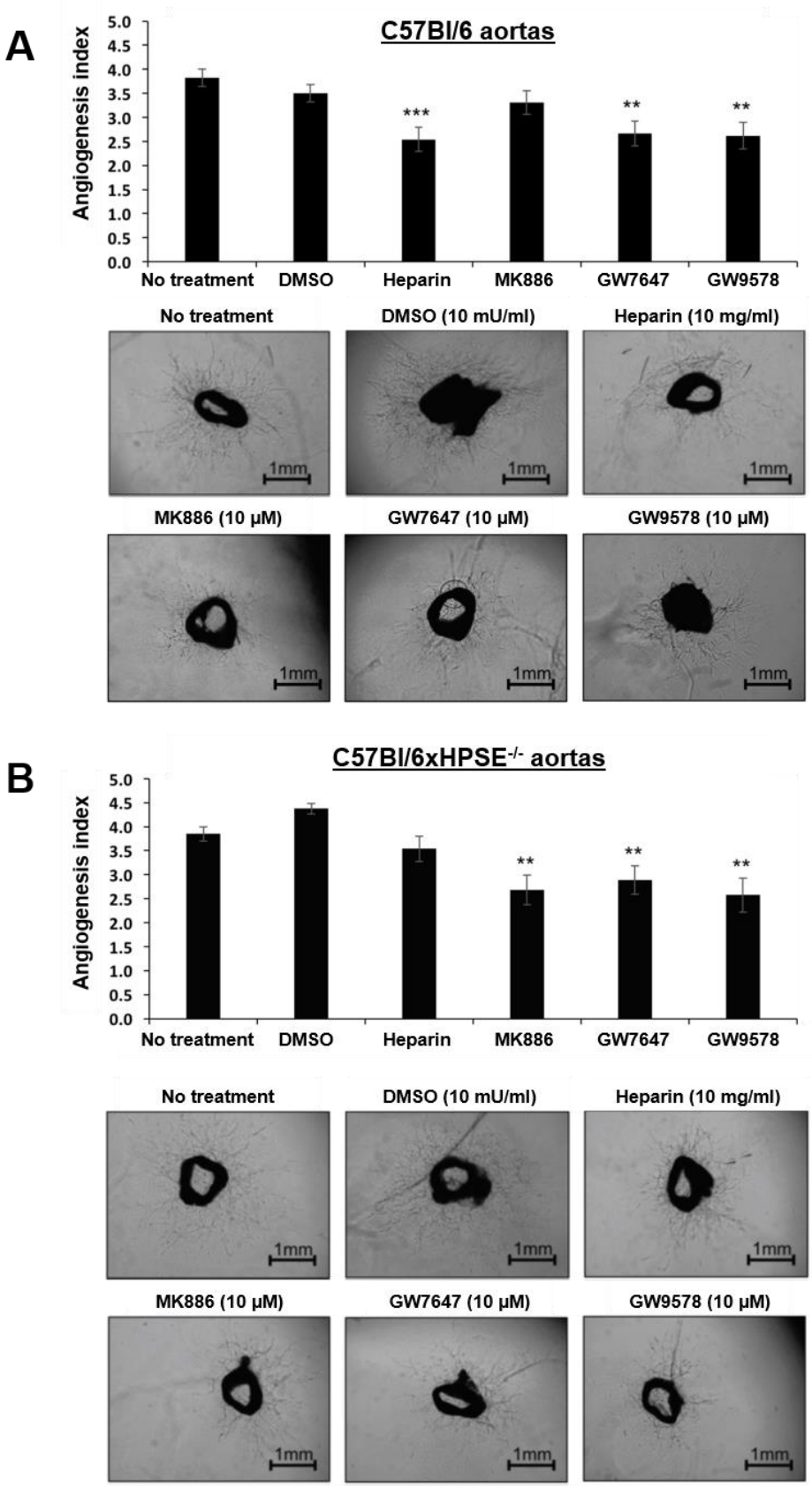

Figure 5.15 The effect of known and novel HPSE inhibitors on angiogenesis observed in aortas sourced from C57Bl/6 and C57Bl/6xHPSE$^{-/-}$ mice

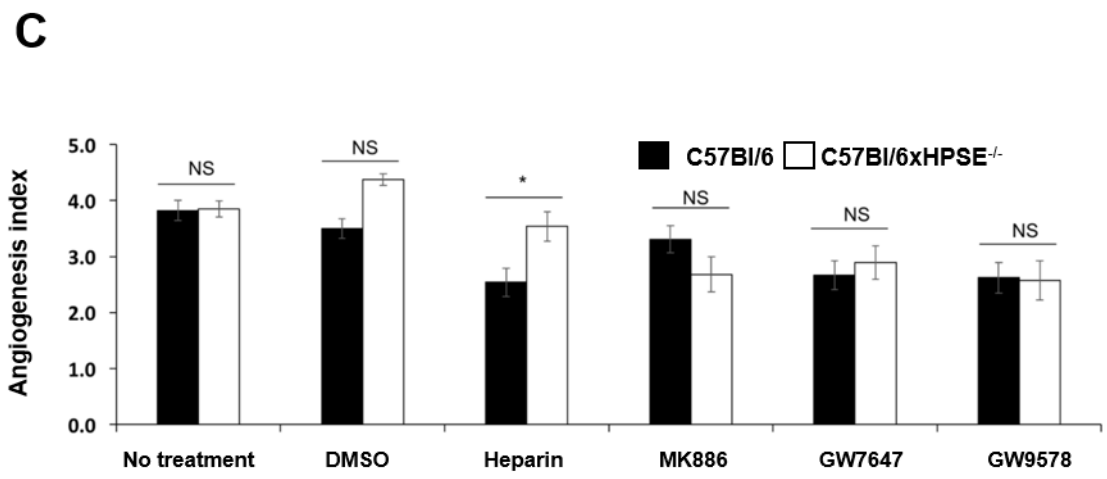

Figure 5.15 (A) A graphical representation of the effect of known and novel HPSE inhibitors on angiogenesis in aortas sourced from C57Bl/6 mice. Vessel outgrowths were normalised to the no treatment controls. Representative images are shown of aortas (from 9 – 12-week old animals) embedded in fibrin gel following a 7-day treatment. **(B)** A graphical representation of the effect of known and novel HPSE inhibitors on angiogenesis in aortas sourced from C57Bl/6xHPSE$^{-/-}$ mice. Representative images are shown of aortas (from 9 – 12-week old animals) embedded in fibrin gel following a 7-day treatment. **(C)** A concise representation of the effects of known and novel HPSE inhibitors on angiogenesis in aortas from C57Bl/6 and C57Bl/6x HPSE$^{-/-}$ mice. Vessel outgrowths were normalised to the respective no treatment controls. A, n = 4; B, n = 3; error bars = SEM; NS, not significant; *, p<0.05; **, p<0.01; ***, p<0.001; statistical significance calculated using a paired student's t-test in relation to the no treatment control.

5.4.16 The development and *in vivo* characterisation of the novel B16F10-mCherry-Luc cell line

The B16 mouse melanoma cell line has been widely used in *in vivo* tumour models, resulting in the development of several variants, including the highly-invasive B16F10 cell line (Fidler and Kripke, 1977, Overwijk and Restifo, 2001, Hart, 1979). The expression of HPSE in B16 melanoma cells has previously been described (Komatsu et al., 2008b). The B16 cell invasion model has traditionally involved the implantation of cells intravenously in mice, resulting in visible, quantifiable lesions in the lungs. This model was thus employed to assess the action of the novel HPSE inhibitors on tumour cell invasion, based on the previously described inhibition of the MDA-MB-231 migration/invasion by novel HPSE inhibitors.

First, the B16F10-mCherry-Luc cell line was generated as described in section 2.5.3. Compared to the parental B16F10 cells, the newly-developed B16F10-mCherry-Luc cell line demonstrated a significantly high level of mCherry expression by flow cytometry analysis, with fluorescence detected in over 98% of the cell population following six rounds of sorting **(figure 5.16A)**. In order to determine the capacity of this novel cell line to form lung-invasive nodules *in vivo*, 2x10^5 cells were injected intravenously, followed by IVIS *in vivo* imaging of the animals prior to lung excision **(figure 5.16B)**. This demonstrated detectable luminescence within the lungs in live animals as well as visually detectable

lesions in the lungs. The presence of mCherry DNA only within invasive colony-forming B16F10-mCherry-Luc cells in the animal provided an essential tool for downstream quantitative analysis of tumour burden. The B16F10-mCherry-Luc cells were also shown to produce enzymatically active HPSE **(figure 5.16C)**.

5.4.17 Assessing the efficacy of novel HPSE inhibitors against lung invasion by B16F10-mCherry-Luc cells

The newly-developed B16F10-mCherry-Luc cell line was used to determine the capacity of novel HPSE inhibitors GW7647 and GW9578 to inhibit lung invasion. An *in vivo* study was designed to determine the efficacy of these compounds **(figure 5.17A)**. Briefly, $2x10^5$ B16F10-mCherry-Luc cells were implanted intravenously in 10 – 12-week-old C57Bl/6 mice followed immediately by GW7647 or GW9578 (4 mg/kg) or DMSO only (0.5 – 5% v/v) treatment. The animals were administered the novel inhibitors or the DMSO alone control 3-times a week with lungs excised on day 20 for the analysis of tumour burden. The RTB thus analysed showed no significant difference between the lungs excised from the DMSO only control group and the GW7647 and GW9578 treated groups **(figure 5.17B)**. Representative images of excised lungs of each experimental group show visible tumour nodules **(figure 5.17C)**. Therefore, despite the *in vitro* data, the novel HPSE inhibitors did not show successful efficacy data *in vivo* with regards to inhibiting lung metastatic colonisation by B16F10-mCherry-Luc cells.

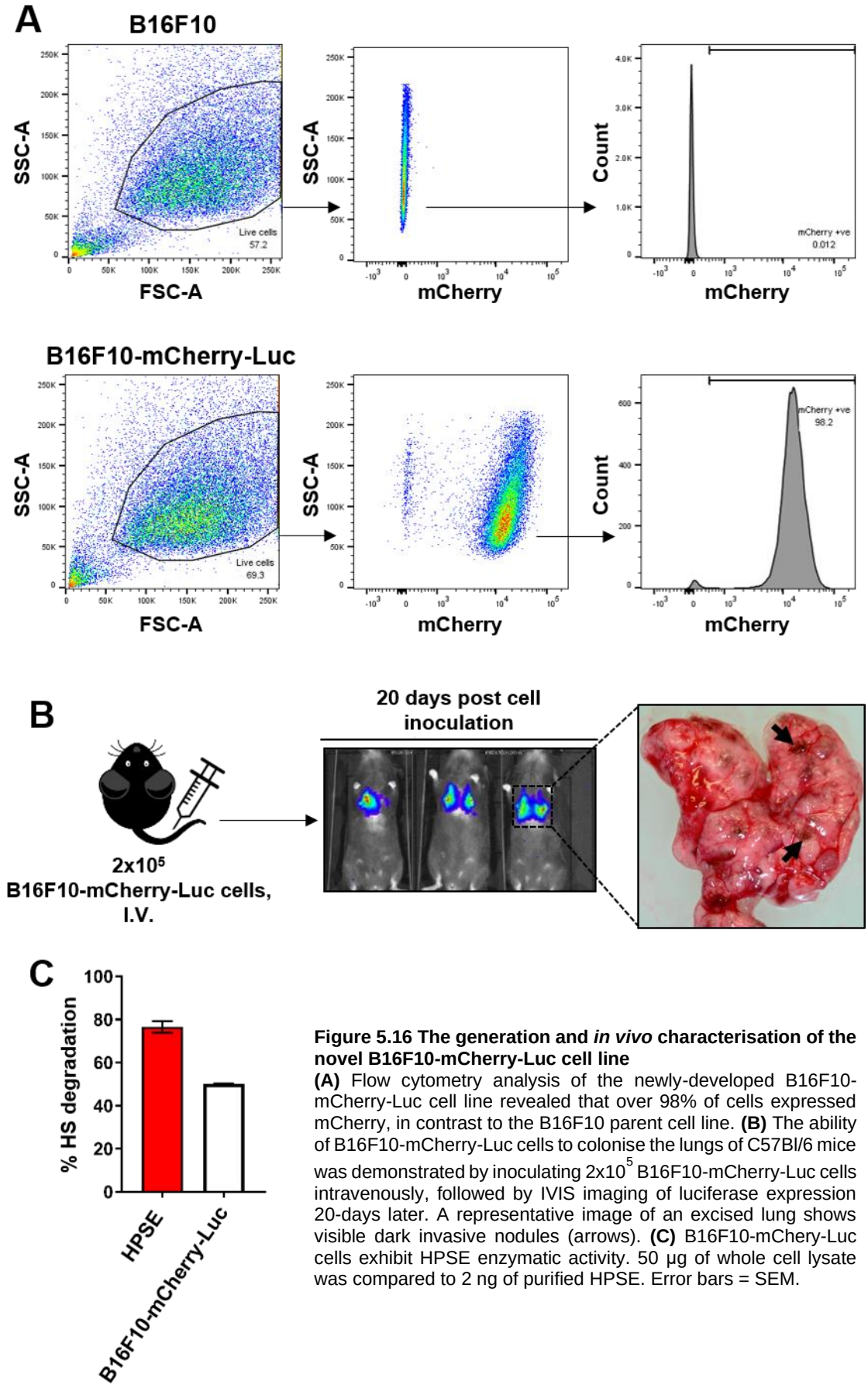

Figure 5.16 The generation and *in vivo* characterisation of the novel B16F10-mCherry-Luc cell line
(A) Flow cytometry analysis of the newly-developed B16F10-mCherry-Luc cell line revealed that over 98% of cells expressed mCherry, in contrast to the B16F10 parent cell line. **(B)** The ability of B16F10-mCherry-Luc cells to colonise the lungs of C57Bl/6 mice was demonstrated by inoculating $2x10^5$ B16F10-mCherry-Luc cells intravenously, followed by IVIS imaging of luciferase expression 20-days later. A representative image of an excised lung shows visible dark invasive nodules (arrows). **(C)** B16F10-mChery-Luc cells exhibit HPSE enzymatic activity. 50 µg of whole cell lysate was compared to 2 ng of purified HPSE. Error bars = SEM.

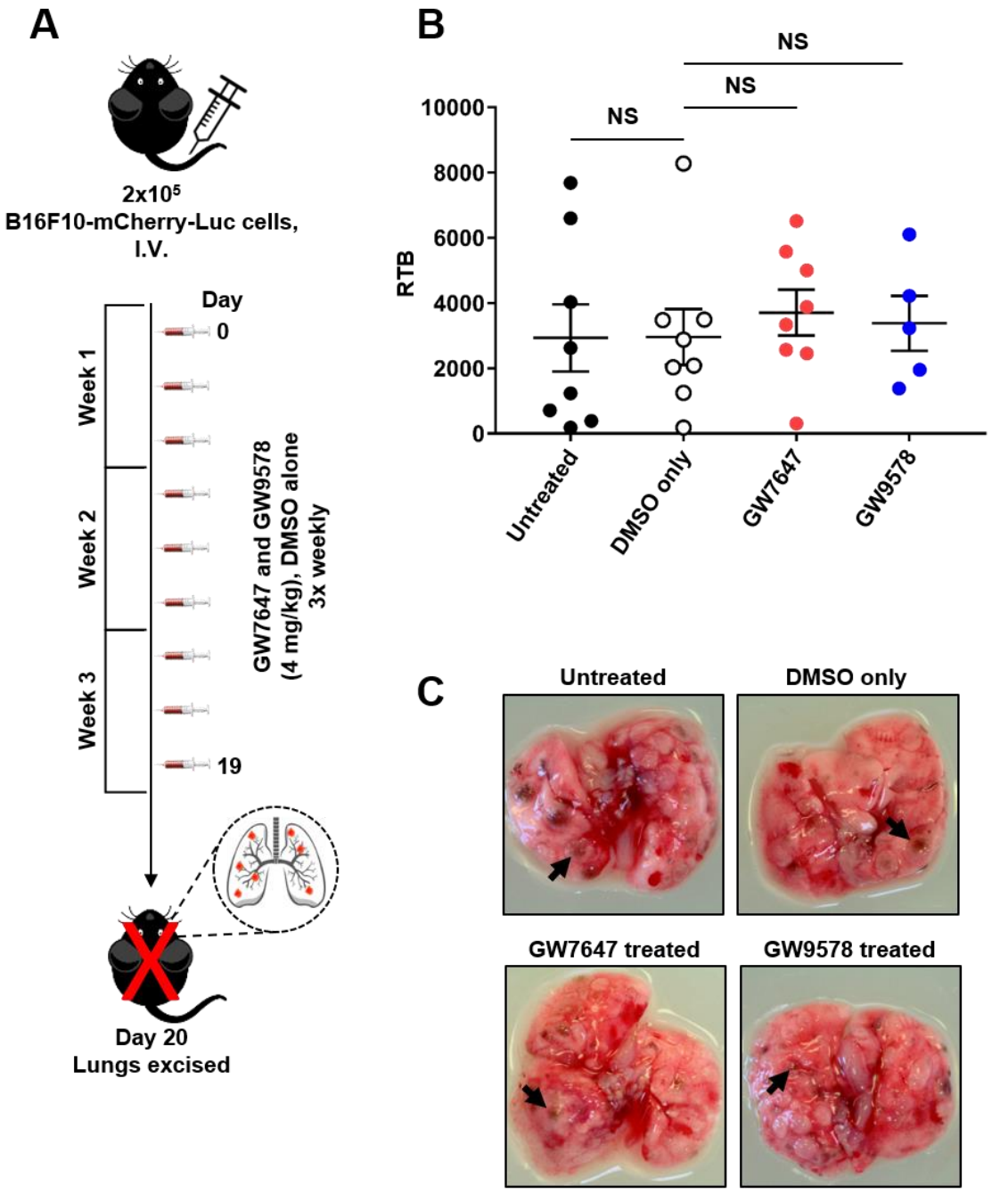

Figure 5.17 The effect of GW7647 and GW9578 treatment on mouse lung invasion by B16F10-mCherry-Luc cells

(A) A schematic representation of the study design in which 10 – 12-week old female C57Bl/6 mice were inoculated with 2x10^5 B16F10-mCherry-Luc cells intravenously and left untreated or were treated with 4 mg/kg GW7647 or 4 mg/kg GW9578 or vehicle (DMSO) only. Treatments commenced immediately at the time of cell inoculation (day 0). All animals were euthanized on day 20 and lungs were excised. **(B)** qPCR analysis of mouse lungs revealed no significant difference in RTB between groups; *n* = 5 – 8 animals per group. **(C)** Representative images of lungs bearing visible B16F10-mCherry-Luc lesions. Error bars = SEM; NS, not significant; unpaired t-test.

5.4.18 Assessing the effects of novel HPSE inhibitors on the immune cell populations within the lungs of mice bearing B16F10-mCherry-Luc cell lung-metastatic lesions

Previously, the role of HPSE in the activation and the promotion of the function of NK cells was discussed (Putz et al., 2017). The possibility of HPSE inhibitors affecting immune cells within the lungs must therefore be considered. Immune cell populations, including $CD4^+$ T cells, $CD8^+$ T cells and NK cells were thus analysed within the lungs of mice bearing B16F10-mCherry-Luc lung metastatic nodules **(figure 5.18)**. Analysis of the expression levels of CD11b and CD27 enables the differentiation of NK cells based on maturity into four distinct populations; $NKG2D^+$ NK cells, $CD69^+$ NK cells, $CD11b^+$ NK cells, $CD11b^+$ $CD27^+$ NK cells. Additionally, $CD4^+$ T cells and $CD8^+$ T cells within the lungs were also quantified. No significant difference was observed between the relative percentage of any of the immune cell types analysed in tumour-bearing mice treated with GW7647 or GW9578 and the control group treated with DMSO alone. These results suggest that the novel HPSE inhibitors did not exhibit any significant effects on the migration of $CD4^+$ and $CD8^+$ T cells nor the migration and maturation levels of NK cell populations within the lungs.

5.4.19 Assessing the effects of novel HPSE inhibitors on the splenic immune cell populations in mice bearing B16F10-mCherry-Luc cell lung metastatic lesions

Following the same hypothesis that led to the analysis of immune cell populations in the lungs of B16F10-mCherry-Luc metastatic lesion-bearing C57Bl/6 mice, a series of splenic immune cell populations of these animals were similarly investigated **(figure 5.19)**. Splenic NK cells, $NKG2D^+$ NK cells, $CD69^+$ NK cells, $CD11b^+$ NK cells, $CD11b^+$ $CD27^+$ NK cells, $CD4^+$ T cells and $CD8^+$ T cells were thus analysed by flow cytometry. No significant difference was observed between any of the immune cell types analysed in tumour-bearing mice treated with GW7647 or GW9578 and the control group treated with DMSO alone. These results suggest that the novel HPSE inhibitors did not exhibit any significant effect on the migration of $CD4^+$ and $CD8^+$ T cells nor the migration and maturation levels of NK cell populations within the spleen.

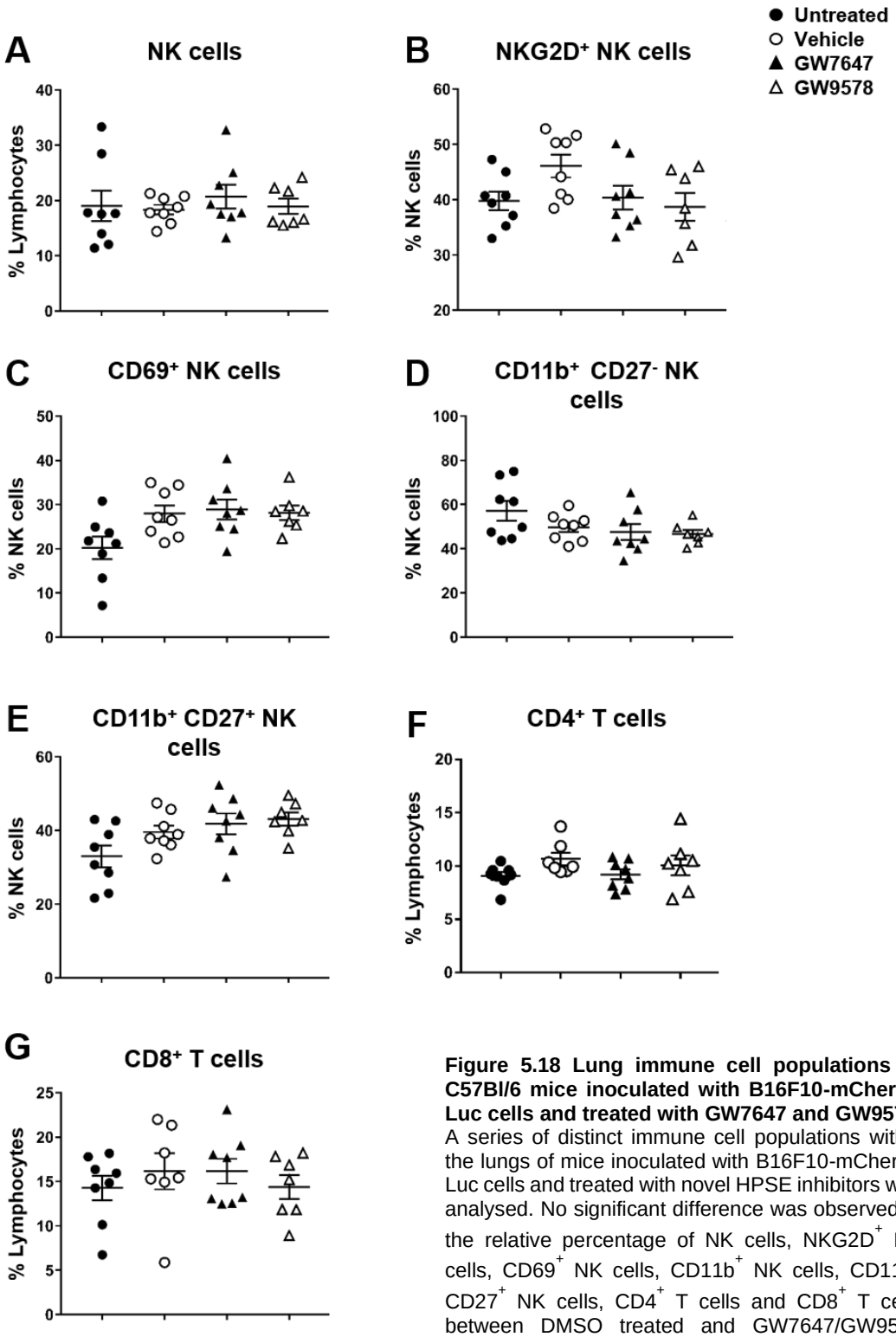

Figure 5.18 Lung immune cell populations of C57Bl/6 mice inoculated with B16F10-mCherry-Luc cells and treated with GW7647 and GW9578
A series of distinct immune cell populations within the lungs of mice inoculated with B16F10-mCherry-Luc cells and treated with novel HPSE inhibitors was analysed. No significant difference was observed in the relative percentage of NK cells, $NKG2D^+$ NK cells, $CD69^+$ NK cells, $CD11b^+$ NK cells, $CD11b^+$ $CD27^+$ NK cells, $CD4^+$ T cells and $CD8^+$ T cells between DMSO treated and GW7647/GW9578 treated animals.

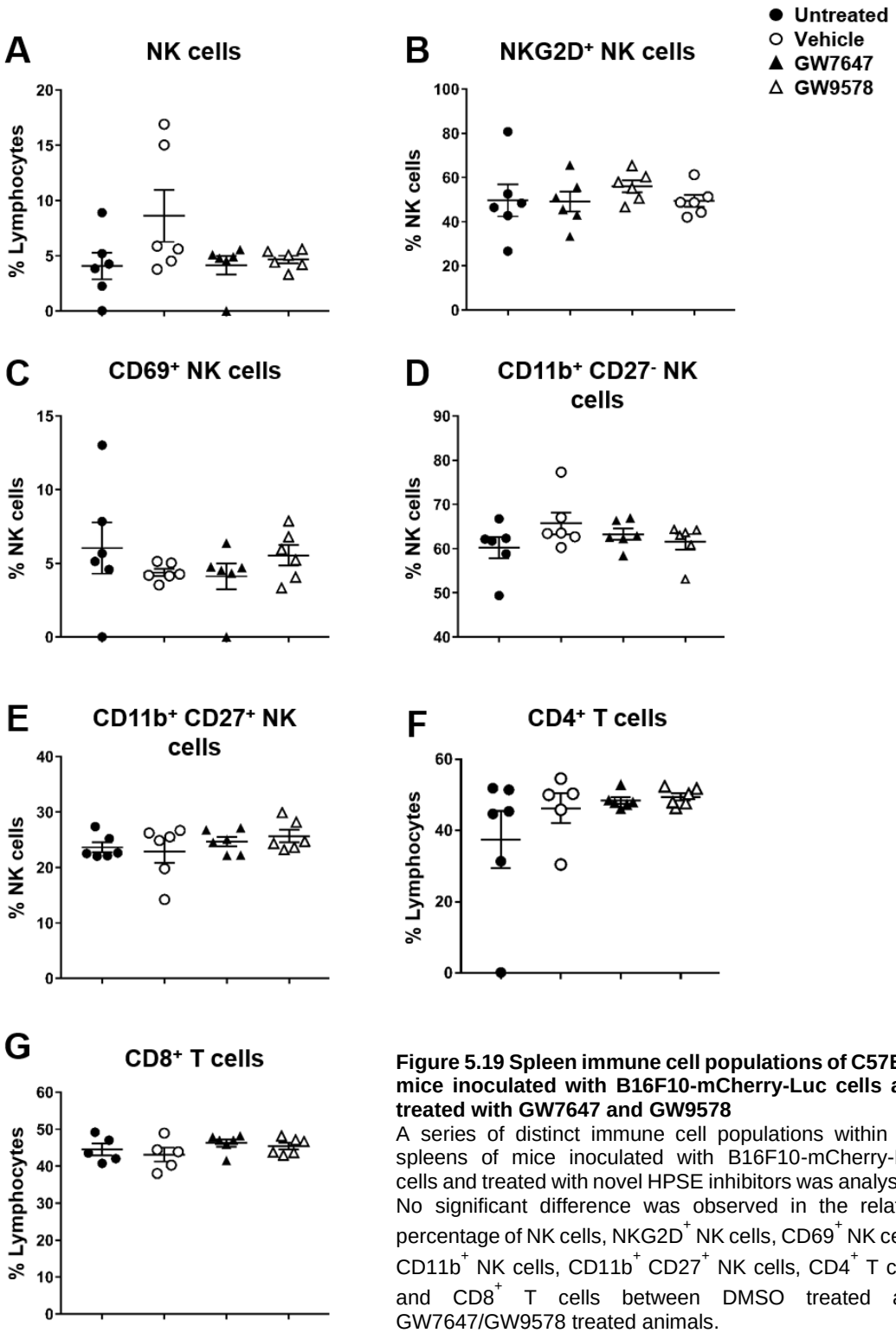

Figure 5.19 Spleen immune cell populations of C57Bl/6 mice inoculated with B16F10-mCherry-Luc cells and treated with GW7647 and GW9578

A series of distinct immune cell populations within the spleens of mice inoculated with B16F10-mCherry-Luc cells and treated with novel HPSE inhibitors was analysed. No significant difference was observed in the relative percentage of NK cells, NKG2D$^+$ NK cells, CD69$^+$ NK cells, CD11b$^+$ NK cells, CD11b$^+$ CD27$^+$ NK cells, CD4$^+$ T cells and CD8$^+$ T cells between DMSO treated and GW7647/GW9578 treated animals.

5.5 Discussion

HPSE has remained an attractive anti-cancer drug target since its initial characterisation, based on its expression as a single active form that correlates with the metastatic potential of several tumour cell types (Hulett et al., 1999, Hulett et al., 2000). Today, the targeting of HPSE has attracted widespread research efforts, with a number of drugs progressing to human trials and several others in the developmental pipeline (Mohamed and Coombe, 2017, Heyman and Yang, 2016, Vlodavsky et al., 2016, Jia and Ma, 2016). As discussed in chapter 1, HS mimetics represent the most widely-used HPSE inhibitors. However, these have been affected by a variety of off-target effects and less-than-anticipated efficacy (Khasraw et al., 2010b, Rohloff et al., 2002, Chen et al., 2017c). High throughput drug screening techniques boast advantages over conventional drug discovery methods by employing vast numbers of known and previously characterised molecules to identify novel functions (Macarron et al., 2011, Janzen, 2014). The 'repurposing' of known drugs has thus gained momentum as a fast, effective and financially viable method of drug discovery (Zheng et al., 2018, Corsello et al., 2017). Indeed, the screening of libraries of known molecules to identify potential HPSE inhibitors has previously been attempted (Pisano et al., 2014, Hammond et al., 2014). An initial series of thus identified inhibitors were described by Courtney *et al.* (Courtney et al., 2004, Courtney et al., 2005). However, the further development of these early compounds were hampered by the lack of a 3D molecular structure of HPSE (Pisano et al., 2014). Attempts at *in silico* screening for novel HPSE inhibitors was also undertaken, based on docking into a homology model of HPSE and fitting this to a pharmacophore model for known HPSE inhibitors (Gozalbes et al., 2013). The anti-malarial drug amodiaquine was thus identified followed by the preparation of a series of drug derivatives. However, these derivatives failed to demonstrate a binding affinity greater than their parent compound and no enzymatic inhibition was demonstrated. This chapter aimed to contribute to this ongoing effort by the screening of a library of known drugs to identify potential HPSE inhibitors followed by their characterisation. Here, the identification, *in vitro* characterisation and attempts at *in vivo* validation of novel HPSE inhibitors are described.

5.5.1 Establishing an in vitro HPSE activity assay

Prior to setting up a high throughput drug screen, it was essential to purify a sufficient quantity of enzymatically active HPSE, followed by establishing a robust *in vitro* assay to determine the enzymatic activity of purified HPSE. As a significant quantity of HPSE was needed for these purposes, the most commercially viable option was to purify human HPSE from platelets. As previously discussed, human platelets are a rich source of active HPSE (Hulett et al., 1999, Freeman and Parish, 1998). Platelets were sourced in bulk from the Australian Red Cross Blood Services and subjected to the HPSE purification process

described in section 2.2.2 (Freeman and Parish, 1998). Thus, enzymatically active human HPSE was purified, characterised by Western blot and mass spectrometry analysis and its activity verified by the *in vitro* HPSE enzymatic activity assay **(figure 5.1)**. Alternate expression systems were considered such as the expression and purification of human HPSE using bacterial systems (Winkler et al., 2014). HPSE, as a pro-enzyme, requires rigorous processing for its activation, post-translational glycosylation and disulphide bond formation (Simizu et al., 2004, Simizu et al., 2007). Despite its perceived ease, bacterial expression of recombinant human proteins remains challenging (Rosano and Ceccarelli, 2014). Thus, considering the processing required in expressing enzymatically active HPSE, the use of bacterial, yeast, insect or mammalian cell-expression systems were not considered and the direct purification of HPSE from human platelets was deemed the most viable, robust option. Previously published data demonstrated a high degree of purity of isolated human HPSE based on Coomassie staining (Freeman and Parish, 1998). Utilising this methodology, human HPSE was successfully purified from platelets, yielding a concentration of 0.45 mg/ml.

A number of techniques have been described for the determination of the enzymatic activity of HPSE. These include the use of high-speed gel permeation chromatography following the exposure of FITC-labelled HS to HPSE, use of radiolabelled-HS followed by HPSE digestion and analysis by chromatography and a colorimetric assay deemed suitable for kinetic analysis and inhibitor screening (Toyoshima and Nakajima, 1999, Freeman and Parish, 1997, Hammond et al., 2010). The FRET-based *in vitro* HPSE activity assay described in this thesis was borne of the need for a robust, high throughput assay for efficient screening of a large number of pharmacological compounds (Enomoto et al., 2006). The FRET-based assay demonstrated dose-dependent HPSE activity levels as well as dose-dependent inhibition of the enzymatic activity of HPSE by known HPSE inhibitors **(figure 5.2)**. Furthermore, the assay involved a simple set up and analysis of data as well as satisfying all needs expected of a high throughput screening tool.

5.5.2 Screening the LOPAC^{1280} library and the identification and characterisation of novel HPSE inhibitors

Using the high throughout HPSE activity assay, 320 compounds of the LOPAC^{1280} drug library of pharmacologically active compounds were screened **(figure 5.3)**. The compounds thus screened had a wide variety of applications. To validate hits identified in the first round of screening, a second round of screening was carried out followed by a final cell surface HS assay. This three-tiered screening method was deemed suitable to deliver robust, reliable results. The first round of screening identified 15 potential inhibitors out of the 320 compounds screened **(figures 5.4A-D)**. However, the second round of screening narrowed this to just two compounds **(figure 5.5)**.

The remainder failed to inhibit the enzymatic activity of HPSE as observed in the previous screening round. Thus, GW7647 and 6-hydroxy-DOPA progressed to the final round of screening. The two drugs that did show consistent inhibition are superior to their counterparts in inhibiting the activity of HPSE and this three-tiered validation strategy may very well identify compounds with the greatest inhibitory capacities.

The final step of the validation pathway was the cell surface HS assay, which was crucial in determining the physiological relevance of the compounds identified and to confirm the reproducibility of their inhibitory capacity **(figure 5.6)**. The cell surface HS assay thus evaluated the inhibitory capability of the drugs in a system more reflective of an *in vivo* setting. The dose-dependent reduction of cell surface HS upon titration with HPSE indicated the validity of this assay in determining the enzymatic activity of HPSE. Furthermore, this cleavage of cell surface HS was inhibited by known inhibitors of HPSE in a dose-dependent manner. It is interesting to note that compared to the FRET-based *in vitro* enzymatic activity assay, the inhibitory capacities of both heparin and PI-88 in the cell surface HS assay appeared reduced. As PI-88 is a HS-mimetic, and heparin is a highly sulphated version of HS, these molecules could be thought to possess HS-like properties in this assay (Shriver et al., 2012, Ferro et al., 2007). Indeed, heparin has been shown to bind to cell surfaces through heparin/HS-interacting proteins and to function as an intervenor in cell-cell communication (Trindade et al., 2008, Ryser et al., 1983, Xu and Dai, 2010). It is therefore possible that both PI-88 and heparin would bind to and become sequestered on the cell surface in the *in vitro* environment of the cell surface HS assay, similar to the binding exhibited by HS (Knelson et al., 2014, Sarrazin et al., 2011). Effectively, these interactions would limit the availability and physiological function of PI-88 and heparin, leading to compromised enzymatic activity inhibition observed in this assay. Thus, OGT-2115 was selected as a suitable control for further validation, as its HPSE-inhibitory activity appeared unaffected in this assay.

5.5.3 GW7647 as a novel HPSE inhibitor

Following the second round of screening of potential HPSE inhibitors, GW7647 and 6-hydroxy-DOPA emerged to demonstrate consistent, reproducible inhibitory capacity. However, 6-hydroxy-DOPA failed to inhibit HS cleavage in the cell surface HS assay **(figure 5.7)**. Thus, this compound was no longer pursued.

GW7647 further demonstrated a dose-dependent inhibition of cell surface HS cleavage, suggesting a drug-like mechanism in interacting with HPSE in this assay. The possibility that this observation may not be the direct result of GW7647 interacting with HPSE, and instead could be a result of an interference in both the enzymatic activity assay and the cell surface HS assay would be quite unlikely. One could also consider the possibility of

GW7647 interacting with HS, thus inhibiting HPSE cleavage. However, HS is largely anionic with GW7647 containing localised regions of high negative charge, which would make such as an interaction implausible. Surface plasmon resonance and isothermal titration calorimetry could be employed to determine and validate the interaction between HPSE and GW7647. These techniques could confirm binding and furthermore, determine the thermodynamic or kinetic parameters of this interaction (Huber and Mueller, 2006, Patching, 2014, Renaud et al., 2016). The inability of 6-hydroxy-DOPA to demonstrate HPSE inhibition may be due to interference within the FRET-based enzymatic activity assay. However, 6-hydroxy-DOPA possesses neurotoxic properties, which would significantly hinder its downstream *in vivo* validation (Kostrzewa, 2016). In contrast, GW7647 possesses more desirable features such as solubility and oral bio-availability (Brown et al., 2001, Yue et al., 2003). Additionally, PPAR-α agonists have been characterised to be well tolerated physiologically, supporting the further development of GW7647 (Bopst et al., 2014).

5.5.4 GW9578, a structurally-related PPAR-α agonist to GW7647, as a novel HPSE inhibitor

The PPARs are ligand-activated transcription factors of the nuclear hormone receptor superfamily comprising of PPAR-α, PPAR-β/δ and PPAR-γ subtypes (Tyagi et al., 2011). The activation of PPAR-α leads to a reduction in triglyceride levels through the regulation of genes involved in the beta-oxidation of fatty acids and is associated with energy homeostasis (van Raalte et al., 2004). Activation of PPAR-γ leads to insulin sensitisation, in turn increasing glucose metabolism and hence plays a key role in the management of type-2 diabetes (Bermudez et al., 2010). PPAR-β/δ activation leads to enhanced fatty acid metabolism along with its role as a regulator of multiple cellular functions (Wagner and Wagner, 2010). Members of the PPAR family have been implicated in the development of cancer and are thus considered potential anti-cancer drug targets (Gou et al., 2017).

The activation of PPAR-α with its ligands that include fatty acids and fibrate drugs leads to an increase in fatty acid oxidation and high density lipoprotein triglyceride levels in the serum, accompanied by a decrease in very low-density lipoprotein triglycerides (Staels et al., 2008, Pawlak et al., 2015, Wright et al., 2014). However, the biochemistry of PPAR-α remained largely undefined due to the high homology seen between the PPAR family members, despite the lipid-metabolising role of fibrates being well established (Brown et al., 1999, Wright et al., 2014). GW7647 and GW9578 were described as potent PPAR-α agonists (Brown et al., 1999, Brown et al., 2001). The modification of the fibrate head group of ureido-fibrate analogues with modified urea substituents demonstrated increased PPAR-α activity, leading to the discovery of GW9578 as a PPAR-α agonist (Brown et al., 1999). Following this observation, GW7647 was described as possessing high PPAR-α

agonistic capacity using solid-phase, parallel array synthesis to synthesise a series of urea-substituted thioisobutyric acids (Brown et al., 2001). These compounds are also structurally similar. Thus, based on the observation that GW7647 possessed HPSE-inhibitory capacity, GW9578 was assessed to determine its potential as a novel inhibitor. As expected, GW9578 displayed a similar trend in the cell surface HS assay and acted in a drug-like manner in the *in vitro* HPSE enzymatic activity assay **(figure 5.8)**.

Earlier work on the discovery of HPSE inhibitors was hindered by the lack of 3D structural information (Pisano et al., 2014). However, the crystal structure of HPSE was described recently, which could enhance future attempts at drug discovery (Wu et al., 2015). By employing an *in silico* molecular modelling tool, the docking of GW7647 to the active site of HPSE was demonstrated (figure 5.9). In conjunction with the accompanying *in vitro* data, it is possible that GW9578 too, would display a similar binding capability, based on conserved structural elements with GW7647. Further validation of the structural-dependence of the HPSE-inhibitory capacity of GW7647 and GW9578 were provided by the observation that a structurally-unrelated PPAR-α agonist, fenofibrate, did not display the capacity to inhibit HPSE in the *in vitro* enzymatic activity assay **(figure 5.10)**.

The PPAR-α antagonist, MK886, was also used in the *in vitro* enzymatic activity assay as a negative control (Mascia et al., 2011, Panlilio et al., 2012, Le Foll et al., 2013). MK886 is structurally unrelated to GW7647 and GW9578 and analysing its effects on HPSE along with the two novel inhibitors was designed to provide more insight into their inhibitory mechanism. It is interesting to note that MK886 too, exhibited HPSE-inhibitory activity, albeit in a non-drug like, dose-independent manner **(figure 5.11)**. This may be due to a possible non-drug-like interaction between MK886 and HPSE. It is also possible that the concentrations used in this assay were beyond the range within which MK886 demonstrates a dose-dependent inhibition of HPSE activity. Also, the possibility of interference within the assay with the use of MK886 cannot be excluded. However, the HPSE-inhibitory capacity of GW7647 and GW9578 were satisfactorily demonstrated *in vitro*, which deemed the progression to further validation appropriate. Further studies are needed to confirm the interaction between MK886 and HPSE and to understand the mechanism by which MK886 inhibits enzymatic activity. This could potentially be achieved through *in silico* molecular modelling, following the characterisation of the 3D structure of HPSE (Wu et al., 2015). MK886 has been demonstrated to inhibit the activity of the 5-lipooxygenase-activating protein and COX-1, leading to the suppression of platelet aggregation (Koeberle et al., 2009, Kehrer et al., 2001). Studies have shown that HPSE in platelets promotes adhesion and the formation of a protective ‘coating’ around CTCs which aids in metastasis (Nadir and Brenner, 2016, Cui et al., 2016). A search of the literature revealed no studies reporting on the HPSE-inhibitory capacity of MK886, with a

possible link between its inhibition of HPSE and reduced platelet aggregation yet to be determined.

5.5.5 Reduced cell migration/invasion by GW7647 and GW9578

A majority of cancer deaths are the direct result of metastasis rather than the primary tumour alone (Steeg, 2016). As discussed in chapter 1, this hallmark of cancer has been extensively studied due to its crucial role in cancer progression. Thus, much effort has been made in understanding how cancer cells invade their surrounding environment and to determine how to inhibit this process, leading to reduced metastasis (Lambert et al., 2017). The expression of HPSE has been implicated in the enhanced metastatic capacity of tumour cells (Weissmann et al., 2016, Yang et al., 2005, Hulett et al., 1999, Takaoka et al., 2003). The targeting of HPSE may very well in turn lead to reduced metastasis and an increased rate of survival (Weissmann et al., 2016, Dai et al., 2017, Rivara et al., 2016). Thus, the novel HPSE inhibitors GW7647 and GW9578 were assessed in their ability to inhibit cell migration/invasion using Matrigel®, a synthetic BM, in an *in vitro* cell migration/invasion assay. Matrigel® is a complex, gelatinous mixture of ECM proteins such as laminin, collagen-IV and HSPG derived from mouse tumour cells and has been extensively used to study cell growth and invasion in an *in vitro*, 3D, ECM-like environment (Orkin et al., 1977, Kleinman et al., 1982, Kleinman and Martin, 2005, Hughes et al., 2010). These properties justified its use in studying the effects of novel HPSE inhibitors in cell migration/invasion. It must also be noted that mouse and human HPSE share a high degree of sequence identity (Miao et al., 2002). This validated the use of the inhibitors in this assay which were initially screened and characterised using human HPSE.

First, it was essential to demonstrate that neither of the inhibitors had detrimental effects on the viability of the MDA-MB-231 cells used. The HPSE-expressing ability and high invasiveness of MDA-MB-231 cells were ideal properties in this assay (Teoh et al., 2009, Abdelkarim et al., 2011, Wu et al., 2009, Xie et al., 2009, Paquette et al., 2011, Hsieh et al., 2013). A concentration of 10 μM of GW7647, GW9578 and MK886 and a concentration of 10 mg/ml of heparin did not show significant detrimental effects on the viability of MDA-MB-231 cells, ensuring that any effects of the known and novel HPSE inhibitors on cell migration/invasion in the transwell assay would not be the result of cytotoxicity, but of inhibition of cellular movement through the Matrigel® layer. Treatment of MDA-MB-231 cells with heparin; a known, potent inhibitor of HPSE, demonstrated a significant reduction in cell migration/invasion. This validated the suitability of this assay in determining the effects of novel HPSE inhibitors on cell migration/invasion **(figure 5.12)**.

Interestingly, both GW7647 and GW9578 demonstrated a significant ability to reduce the invasion of MDA-MB-231 through the Matrigel® **(figure 5.13)**. GW7647 was more potent

in this regard compared to GW9578. The expression of HPSE by MDA-MB-231 cells and indeed by many cancer cells, as previously discussed, coupled with the fact that both GW7647 and GW9578 inhibited the enzymatic activity of HPSE *in vitro* as well as the reduction of cell surface HS cleavage by HPSE, collectively suggest that the reduction in the invasion of MDA-MB-231 cells through the Matrigel® seen in this assay may well be the direct result of the inhibition of HPSE by GW7647 and GW9578. However, it must be noted that MDA-MB-231 cells have been demonstrated to express PPAR-α, described as a master regulator of a number of genes, leading to a variety of downstream functions such as hepatic lipid metabolism, peroxisomal and mitochondrial fatty acid-β oxidation, hepatic lipogenesis, fatty acid uptake, metabolism of lipoprotein, glucose/glycerol, hepatic cholesterol/bile and amino acid and well as inflammation and biotransformation (Suchanek et al., 2002, Chen et al., 2017d, Rakhshandehroo et al., 2010). It could therefore by hypothesised that the effect of GW7647 and GW9578 on cell migration/invasion may be the result of the novel HPSE inhibitors interacting with PPAR-α. Indeed, the angiopoietin-like 4 (ANGPTL4) gene is a classic PPAR-α target and has been shown to be induced through PPAR-α activation (Janssen et al., 2015). ANGPTL4 has also been suggested to play a role in the crosstalk between metabolism and cancer, mediated through the PPAR signalling pathway (La Paglia et al., 2017). The expression of ANGPTL4 has been mostly linked to enhanced angiogenesis in a number of physiological and pathological conditions, but a study published by Okochi-Takada *et al*. suggested that ANGPTL4 may possess anti-angiogenic properties and may act as a secreted tumour suppressor (Le Jan et al., 2003, Babapoor-Farrokhran et al., 2015, Mousavizadeh et al., 2016, Okochi-Takada et al., 2014). Furthermore, ANGPTL4 has been linked to metastasis and has thus demonstrated a number of roles in human malignancies (Izraely et al., 2017, Tanaka et al., 2015, Liao et al., 2016b, Tan et al., 2012). The inhibition of HIF-1-mediated expression of ANGPTL4 in MDA-MB-231 cells has been shown to reduce metastasis (Zhang et al., 2012). It is therefore interesting to observe that the use of PPAR-α agonists in the transwell migration/invasion assay inhibited cell invasion, seemingly contrary to published observations, if indeed the use of GW7647 and GW9578 in the assay led to an upregulation of ANGPTL4 through PPAR-α activation. This phenomenon warrants further investigation with the use of HPSE-deficient MDA-MB-231 cells to determine if the novel HPSE inhibitors did indeed affect cell invasion through Matrigel® via the inhibition of the enzymatic activity of HPSE or with the use of PPAR-α-deficient MDA-MB-231 cells to determine if the effects seen here involved the interaction of GW7647 and GW9578 with PPAR-α and/or its derivatives.

The use of the Matrigel® in the transwell migration/invasion assay served the vital purpose of differentiating between cell migration and cell invasion, which are two fundamentally

distinct processes (Stuelten et al., 2018, Welch, 2015). In this assay, FCS served as the chemoattractant for MDA-MB-231 cells incubated in a medium devoid of FCS. The Matrigel® barrier between the cells and the medium supplemented with FCS served as an ECM-equivalent through which the MDA-MB-231 cells were required to actively invade. MK886 treatment significantly reduced the movement of MDA-MB-231 cells through the Matrigel® membrane as well as in the negative control, which lacked Matrigel®. Therefore, the inhibitory effect displayed by MK886 can be suggested to be the result of inhibiting cell migration, not active invasion.

5.5.6 Reduced angiogenesis upon treatment with GW7647 and GW9578

As previously discussed, angiogenesis is a key hallmark of cancer (Hanahan and Weinberg, 2000, Hanahan and Weinberg, 2011). Angiogenesis has been demonstrated to be a vital regulator of tumour growth and metastasis and thus has been the focus of anti-cancer drug development (Folkman, 1971, Bielenberg and Zetter, 2015). The relationship between HPSE expression and angiogenesis has been studied extensively and it has been demonstrated that HPSE expression correlates with the growth and metastatic potential of cancer, as a result of enhanced angiogenesis (Marchetti et al., 2003, Cohen et al., 2006, Nadir and Brenner, 2014, Dai et al., 2017). This has led to several HPSE inhibitors being assessed in the clinic for their anti-angiogenic properties (Ferro et al., 2007, Dredge et al., 2010, Dredge et al., 2011, Ostapoff et al., 2013). In our attempts at isolating novel HPSE inhibitors, it was important that the effect of these compounds on angiogenesis was investigated.

First, a suitable *in vitro* assay was required, and a mouse aortic ring assay was thus selected **(figure 5.14)**. This assay has been demonstrated as an ideal alternative to other *in vitro* assays, with *ex vivo*, 3D studies on a mouse aorta made with developing microvessels. These microvessels undergo key features of angiogenesis on a comparable timescale to that seen in an *in vivo* setting (Baker et al., 2011, Nicosia and Ottinetti, 1990). Aortas from C57Bl/6 and C57Bl/6xHPSE$^{-/-}$ mice were used to determine if anti-angiogenic effects seen, if any, were due to the direct inhibition of the enzymatic activity of HPSE.

The study of aortas excised from C57Bl/6 mice treated with heparin displayed a markedly reduced level of angiogenesis **(figure 5.15)**. Previous studies have reported on the effects of heparin on angiogenesis, with mixed results. Angiogenesis assays using human placenta reportedly showed no inhibition of angiogenesis upon treatment with heparin (Parish et al., 1999). An earlier study on mast cells described that heparin released by mast cells enhanced angiogenesis and led to an increase in the migration of capillary endothelial cells (Folkman et al., 1983). Heparin was further shown to downregulate microRNA-10b in human microvascular endothelial cells, effectively inhibiting

angiogenesis (Shen et al., 2011). Adding to this complex nature of the role of heparin in regulating angiogenesis is the observation that low and high molecular weight fractions of heparin have opposing functions in angiogenesis, with the former inhibiting and the latter stimulating angiogenesis respectively (Norrby, 1993, Debergh et al., 2010). However, based on the ability of heparin to significantly reduce the enzymatic activity of HPSE using *in vitro* activity assays, heparin was expected to reduce angiogenesis, which was indeed observed. GW7647 and GW9578 too displayed a significant ability to reduce angiogenesis *in vitro*, adding further validation to their use as HPSE inhibitors with beneficial downstream effects. Heparin did not show the capacity to reduce angiogenesis in aortas excised from C57Bl/6xHPSE$^{-/-}$ mice, suggesting that the previously observed heparin-mediated inhibition of angiogenesis was indeed likely via the inhibition of the enzymatic activity of HPSE. However, GW7647 and GW9578 treatment led to a reduction in angiogenesis in C57Bl/6xHPSE$^{-/-}$ mouse aortas, suggesting that the anti-angiogenic properties observed may not have been through the inhibition of HPSE. Furthermore, MK886 displayed a reduction in angiogenesis in C57Bl/6xHPSE$^{-/-}$ mouse aortas, which was not observed in C57Bl/6 samples. This unanticipated observation may be due to the downstream effects of MK886 on cellular pathways normally influenced by HPSE that may be redundant in the presence of HPSE expression, but not so in its absence and this remains to be elucidated.

The observation that GW7647 and GW9578 reduced angiogenesis in both C57Bl/6 and C57Bl/6xHPSE$^{-/-}$ mouse aortas to a comparable degree suggests that while both drugs do affect angiogenesis, this may not be directly due to the inhibition of HPSE. Tumour angiogenesis is a vastly complex biological process, as previously discussed and is regulated by a wide variety of factors (De Palma et al., 2017a). It is possible that GW7647 and GW9578 may be interacting with pro-angiogenic factors, thereby indirectly affecting angiogenesis (Simons et al., 2016, Goetz and Mohammadi, 2013). An alternative explanation could be provided by the fact that GW7647 and GW9578 are PPAR-α agonists, leading to the activation of a number of PPAR-α-regulated genes that are known to possess a wide variety of functions as previously described (Suchanek et al., 2002, Chen et al., 2017d, Rakhshandehroo et al., 2010). Fenofibrate, a PPAR-α agonist that is structurally distinct to GW7647 and GW9578 was shown to inhibit angiogenesis *in vitro* and *in vivo* in a study of atherosclerosis (Varet et al., 2003). However, a later study demonstrated that the activation of PPAR-α promoted angiogenesis (Rizvi et al., 2013). As discussed, ANGPTL4 is regulated by PPAR-α with seemingly conflicting roles in angiogenesis (Le Jan et al., 2003, Babapoor-Farrokhran et al., 2015, Mousavizadeh et al., 2016, Okochi-Takada et al., 2014). Although the role of PPAR-α in angiogenesis remains controversial, it can be suggested that the downstream effects of a possible interaction

with GW7647 and GW9578 with PPAR-α may have led to impaired angiogenesis observed in these studies. In conclusion, GW7647 and GW9578 do not appear to reduce angiogenesis in a HPSE inhibition-mediated manner, highlighting that at least in this model, HPSE may not be critical for angiogenesis. These observations further highlight a level of redundancy in angiogenesis as it is clearly regulated by multiple pathways, as can be expected from a physiological process that is vital to tissue maintenance. Thus, the targeting of angiogenesis through the inhibition of HPSE must consider the high level of redundancy built into this process through evolution, resulting in compensatory mechanisms for when one pathway is inhibited. The incorporation of ANGPTL4-null and PPAR-α-null mouse aortas could assist in elucidating their role in similar assays in future studies.

5.5.7 The effect of GW7647 and GW9578 on tumour cell invasion in vivo

Following the results observed *in vitro* with the use of GW7647 and GW9578, an *in vivo* study was designed to assess the effects of these novel HPSE inhibitors in a pathological setting. The HPSE-expressing B16 mouse melanoma cell line has been extensively used in *in vivo* tumour models (Fidler and Kripke, 1977, Overwijk and Restifo, 2001, Hart, 1979, Komatsu et al., 2008b). Previous data have shown that treatment with PI-88 significantly reduced lung metastasis in a rat adenocarcinoma model (Parish et al., 1999). Additionally, the novel HPSE inhibitor, compound 7a, inhibited lung metastasis by approximately 50% in mice implanted with B16-BL6 melanoma cells intravenously (Pan et al., 2006). The HPSE inhibitor suramin was shown to affect the invasion of B16 cells *in vitro* (Nakajima et al., 1991). Thus, our investigations focused on elucidating the *in vivo* efficacy of these compounds in a B16F10 mouse melanoma-lung metastasis model.

First, a suitable cell line was required. The traditional B16F10 mouse melanoma-lung metastasis model has relied upon visual quantification of metastatic nodules on the lungs following the implantation of cells into the tail vein (Menon et al., 1995). However, this approach does not allow *in vivo* imaging of live animals to verify tumour growth nor provide a qPCR-compatible target for downstream tumour burden quantification. Therefore, B16F10 cells were modified to express the fluorescent mCherry protein which would aid in sorting mCherry-expressing cells and luciferase, which would aid in live imaging. A flow cytometry cell sort was carried out on retroviral-infected B16F10 cells to positively select a highly mCherry-expressing cell population. This process was repeated six times, following which a large majority (98.2%) of cells were found to express mCherry **(figure 5.16)**. Subsequent *in vivo* implantation of the newly-generated B16F10-mCherry-Luc cells showed successful colonisation of the lungs of mice with visible metastatic lesions on the organ following excision. Furthermore, the B16F10-mCherry-Luc cells were shown to express HPSE.

Following the successful characterisation of this novel B16F10-mCherry-Luc cell line, an *in vivo* study to investigate the effects of GW7647 and GW9578 on lung metastasis was designed. No similar studies have been reported in the published literature, which prompted the design of an *in vivo* model based on previously observed results with the use of HPSE inhibitors and the use of GW7647 and GW9578 in mouse models (Parish et al., 1999). The use of these compounds in mice at concentrations between 3 – 5 mg/kg have been reported in studies investigating their role in a range of conditions such as ischemia/reperfusion injury, Alzheimer's disease and insulin sensitivity (Guerre-Millo et al., 2000, D'Agostino et al., 2012, Yue et al., 2003). Furthermore, both compounds were dissolved in DMSO, which restricted the amount that could be administered to an animal in a single dose, on the advice of the La Trobe University animal ethics committee. Therefore, a final dose of 4 mg/kg was administered per animal in order to maintain the final concentration of DMSO at a physiologically safe range of 0.5 – 5% (v/v). Based on the studies by Parish *et al.*, the initial dose was administered immediately following the intravenous implantation of B16F10-mCherry-Luc cells (Parish et al., 1999). This was followed by 3 doses per week for 3 weeks. In the initial *in vivo* characterisation study conducted with the novel B16F10-mCherry-Luc cell line, the mice exhibited distinct lung metastatic nodules 20-days following cell inoculation. Therefore, in order to terminate the study prior to the animals exhibiting metastatic distress, the animals were euthanised on day-20. Upon the analysis of the RTB, it was observed that GW7647 and GW9578 had no effect on lung metastasis **(figure 5.17)**.

It must be noted, however, that this was a pilot study with limited published data available to use in aiding its design. It must also be appreciated that drug discovery is a complex, vastly expensive and time-consuming process with an extremely high failure rate, driven partly by the failure of lead compounds to demonstrate *in vivo* efficacy (Kraljevic et al., 2004, Issa et al., 2017, Calcoen et al., 2015, Dickson and Gagnon, 2004, Paul et al., 2010). One strategy to reduce the significant costs of research and development of novel small molecule drugs is to re-purpose known drugs (Swamidass, 2011, Xue et al., 2018). The intent to screen the LOPAC^{1280} library for potential HPSE inhibitors was borne of this concept. The potent *in vitro* effects exhibited by GW7647 and GW9578 were anticipated to yield promising preliminary data, although statistically, the likelihood of such an observation is generally low. These studies were hindered by a large number of factors which could be addressed in future attempts at optimisation. The low solubility of GW7647 and GW9578 requiring suspension in DMSO, a toxic compound, drastically reduced the amount of either compound that could be administered to an animal. These molecules could therefore be chemically redesigned to be soluble in an aqueous solvent. The optimal route and frequency of administration of these drugs for a similar study need further

investigation, with the possibility of an intravenous route of drug delivery explored. Furthermore, an osmotic pump designed for continuous delivery of drugs could also be used (Lu et al., 2015, Tauer et al., 2013, Sanchez-Mendoza et al., 2016). With a significantly high failure rate of novel drugs progressing from *in vitro* characterisation to *in vivo* validation, the results seen in this study are not wholly unexpected. However, further optimisation as outlined may improve their *in vivo* efficacy.

Next, it was necessary to determine if the novel HPSE inhibitors displayed an inhibitory role upon immune cells in the animals. As discussed, HPSE plays a key role in regulating immune cell recruitment and activation (Naparstek et al., 1984, Vlodavsky et al., 1992, Matzner et al., 1985, Poon et al., 2014). Most recently, a landmark study demonstrated that NK cells relied upon HPSE expression in order to impart anti-tumour functions (Putz et al., 2017). This, along with previous observations of the role of HPSE in the immune system suggests that its expression may be a vital component to the ability of immune cells to keep infection and tumour growth at bay. Therefore, the effect of GW7647 and GW9578 on immune cell populations in both the lungs and spleen of mice bearing B16F10-mCherry-Luc lung metastases was investigated **(figures 5.18 and 5.19)**.

A special emphasis was placed upon NK cell populations in this analysis. NKG2D is an NK cell activating receptor, providing NK cell activating signals and co-stimulatory T cell signalling (Zhang et al., 2015a, Yabe et al., 1993, Lopez-Soto et al., 2015). CD69 too, has been demonstrated to be an NK cell activation marker (Borrego et al., 1999, Cibrián and Sánchez-Madrid, 2017). NK cells can be categorised into four distinct populations, based on maturation stage as indicated by the expression of CD11b and CD27 markers (Chiossone et al., 2009, Fu et al., 2014). This maturation progresses from $CD11b^-$ $CD27^-$ to $CD11b^-$ $CD27^+$ to $CD11b^+$ $CD27^+$ and finally to $CD11b^+$ $CD27^-$ NK cells. Analysis of the expression levels of CD11b and CD27 therefore enabled the determination of the maturity stages of NK cells present in the lungs and spleen. As previously described, the tumour infiltration by T cells is a key predictive feature of clinical outcomes in cancer (Ribas et al., 2017b, Martinez-Lostao et al., 2015). Studies have shown that $CD4^+$ and $CD8^+$ T cells play critical roles in anti-tumour immunity (Kim and Cantor, 2014, Durgeau et al., 2018). The aforementioned role of HPSE in regulating immune cell infiltration prompted the analysis of $CD4^+$ and $CD8^+$ T cells in the lungs and spleen of metastases-bearing mice (Naparstek et al., 1984, Vlodavsky et al., 1992, Poon et al., 2014, Goodall et al., 2014, Matzner et al., 1985). However, none of the distinct lung and spleen immune cell populations analysed in this study suggested an effect imparted by GW7647 and GW9578 upon immune cell activation and infiltration. As discussed in chapter 1, HPSE may play a dual role in cancer progression, both promoting tumour growth as well as regulating anti-tumour immunity. It is therefore critical that the development of novel HPSE inhibitors

considers the possibility that the intent to inhibit the activity of HPSE expressed within the primary TME may impair anti-tumour immunity. The results reported here do not support an anti-tumour role of GW7647 and GW9578 nor suggest a detrimental effect on key immune cell populations within the lungs, the site of tumour growth. Key immune cell populations within the spleen were also unaffected. In order to develop these molecules with the aim of conducting pre-clinical validation studies, their anti-tumour properties must be further investigated and possibly enhanced through modifications to their chemical structure.

5.6 Conclusion and future directions

The efforts to develop anti-cancer drugs have yielded promising results whilst revealing the complexity and the dynamic nature of the TME, in which HPSE plays a key role. HPSE has and still remains an attractive target in cancer treatment, purely due to its ability to promote key hallmarks of cancer and has resulted in a number of drug candidates progressing through the multiple phases of clinical development. However, due to the widespread lack of efficacy and off-target effects of a majority of these lead compounds, there exists a need for improved efficacy, specificity and safer drug candidates. The re-purposing of existing drugs has emerged as a more feasible option to address the arduous nature of drug design. This chapter describes lead anti-HPSE compounds identified through a high throughput screen of a library of known drugs. Through a variety of *in vitro* assays, GW7647 and GW9578 have proven to be inhibitors of the enzymatic activity of HPSE. Through their HPSE-inhibitory capacity, these compounds inhibited *in vitro* cell migration/invasion, a key HPSE-driven process in the metastatic cascade. However, the perceived inhibition of angiogenesis was demonstrated to occur not through the inhibition of HPSE, but via a mechanism yet to be elucidated. These observations thus strongly emphasise the need to incorporate HPSE-null controls in the future pre-clinical development of novel inhibitors which could yield insights into the extremely complex physiological nature of the TME. Preliminary attempts did not demonstrate the *in vivo* anti-metastatic efficacy of GW7647 and GW9578. However, it is important to note that significant further development of these compounds will be required for future *in vivo* validation attempts. The dual nature of HPSE in the TME must also be considered in future pre-clinical development in order to investigate the effects imparted upon key anti-tumour immune cell populations by novel anti-HPSE compounds. Navigation through these confounding features driven by HPSE will require a more thorough understanding of its role in the TME and indeed, in each specific cancer setting.

Chapter 6

Concluding remarks

6.1 Introduction

Cancer is a leading cause of morbidity and mortality globally, with incidence rates expected to rise with an ageing population and lifestyle changes (Bray et al., 2018). This has led to the in-depth investigations of TME components which promote the development and the progression of cancers. Over the decades since its cloning, HPSE has emerged as a modulator of the TME and a key promoter of the hallmarks of cancer (Hulett et al., 1999, Knelson et al., 2014). A wide variety of studies spanning major human malignancies have implicated HPSE in all cancers, indicating its overexpression within the TME correlates with a poor clinical prognosis (as described in Chapter 1).

Amongst the multitude of malignant disease varieties, breast cancer imparts a significant impact both within Australia and globally. Numerous studies have implicated HPSE in promoting the development and progression of breast cancer (Wei et al., 2018b, Boyango et al., 2014, Cohen et al., 2006). However, a general lack of robust, *in vivo* HPSE-ablation models has hindered the accurate definition of its role within the breast TME. In order to address this current gap in the literature, chapter 3 utilised the well-characterised PyMT-MMTV model of spontaneous murine mammary tumour development to define the role of HPSE within the mammary TME and in the development and progression of breast cancer.

Tumours are a diverse collection of cell types with stromal components shown to play a key role in tumour development (Hanahan and Weinberg, 2011). Chapter 4 outlines the use of HPSE-deficient C57Bl/6xHPSE$^{-/-}$ mice in order to define the role played by the stromal components of the mammary TME in promoting tumour-HPSE activity and the broader effects on overall tumour growth.

Compounding the complexity of addressing the role of HPSE in promoting cancer is the widespread failure of novel HPSE inhibitors at various pre-clinical and clinical trial stages as discussed earlier in this thesis. With cancer therapeutic strategies moving towards a more targeted approach, HPSE has emerged as an attractive candidate (Rivara et al., 2016). However, on account of the aforementioned complexities in successful drug targeting, a clinically available anti-HPSE drug has continued to remain elusive. In order to establish more effective HPSE inhibitors, chapter 5 employed high throughput drug screening to identify two compounds that were characterised *in vitro* and *in vivo*.

This chapter will highlight the key findings of this thesis and their significance in the context of broader clinical implications.

6.2 The role of HPSE in mammary tumour progression

6.2.1 HPSE does not promote mammary tumour progression in the PyMT-MMTV model

Chapter 3 focused on the use of the HPSE-deficient spontaneous mammary tumour-developing PyMT-MMTVxHPSE$^{-/-}$ mice to define the role of HPSE in the development and progression of breast cancer. The PyMT-MMTV model proved the most suitable candidate for the purpose of this study as it closely resembles its counterpart human malignancy (Lin et al., 2003). With the use of this model, it was thus demonstrated that HPSE does not play a critical role in mammary tumour development and progression in the PyMT-MMTV model.

This is in significant contrast to other previously mentioned studies that strongly implicate HPSE in the development of cancer with the use of *in vivo* models. However, the studies described in this thesis differ to much of the published literature, in that a spontaneous mammary tumour-developing model was employed with tumours developing and progressing through all major stages of breast cancer with or without the influence of HPSE. Being pathologically comparable to the human malignancy, it is a significantly more robust model to investigate breast cancer in contrast to the use of (i) *in vitro* systems, (ii) tumour-derived cell lines in order to induce tumours, or (iii) the use of HPSE-overexpressing transgenic mouse models. Through employing PyMT-MMTVxHPSE$^{-/-}$ mice in parallel with PyMT-MMTV mice, it was possible to clearly distinguish the role of HPSE in the stepwise development of mammary tumours in these animals. Furthermore, the PyMT-MMTVxHPSE$^{-/-}$ / PyMT-MMTV system would enable the identification of any physiological or pathological compensatory mechanisms in response to the lack of HPSE expression. Importantly, as immunocompetent animals were used in these studies, the role of an intact immune system during tumour development and progression was also taken into account.

The intriguing finding that HPSE does not play a major role in PyMT-MMTV murine mammary tumour development highlights that the function of HPSE within the mammary TME may be redundant or more complex than previously hypothesised. Despite a reduction in tumour angiogenesis through the lack of HPSE expression, metastatic dissemination was unaffected in PyMT-MMTV animals. This observation confounds the hypothesis based on studies of HPSE activity within the TME made over the years which associated HPSE expression with enhanced angiogenesis and in turn, associated angiogenesis with metastatic dissemination (Knelson et al., 2014, Nadir and Brenner, 2014, Pisano et al., 2014). To the best of our knowledge, no similar observations to that in this thesis have been reported in the published literature. The role of HPSE in the critical

early mammary tumour development stage which has thus far been ill-defined was investigated and was not shown to be significant. The lack of HPSE activity within the ECM/TME leading to compensatory actions by other ECM-modulating enzymes such as MMPs has been demonstrated previously (Zcharia et al., 2009). Interestingly, other studies have reported contrasting observations (Poon et al., 2014). The findings reported in this thesis were consistent with the observations of Poon *et al.* with no findings to indicate that the lack of HPSE was compensated for by MMP-2.

6.2.2 Stromal components regulate HPSE activity within the primary mammary TME but do not affect overall tumour development and progression

Following the observations in chapter 3 which indicated that HPSE may, in certain settings, not play a key role in the development of mammary tumours, the role of stromal components in modulating the HPSE activity within the mammary TME was investigated. The studies outlined in chapter 4 utilised C57Bl/6 and C57Bl/6xHPSE$^{-/-}$ mice to address this question. The findings herein indicated that the stroma upregulates HPSE activity. Increased HPSE activity is in turn suggested to promote tumour angiogenesis. HPSE-driven angiogenesis has been demonstrated to play a key role in enhancing tumour growth and to facilitate metastatic dissemination (Knelson et al., 2014). However, as evident in the studies conducted in this thesis, HPSE activity regulated by the stromal components of the mammary TME did not influence the overall growth and metastasis of the primary mammary tumours; an observation that contradicts what is widely reported in the literature. Additionally, tumour-infiltrating immune cells were also investigated in respect to their migratory capacity influenced by HPSE. The promotion of migration, activation and function of a variety of immune cells by HPSE has been reported in the literature which prompted this analysis (Putz et al., 2017, Gutter-Kapon et al., 2016, Goodall et al., 2014, Poon et al., 2014). However, the immune cell populations in the mammary tumour-bearing mice investigated in this thesis were not influenced by stromal HPSE activity.

6.3 The identification and characterisation of novel HPSE inhibitors

In order to address the current need for novel, efficacious HPSE inhibitors, chapter 5 involved the high throughput screening of a library of known compounds to identify lead drug candidates. This yielded promising results with GW7647 and GW9578, two PPAR-α agonists identified to possess HPSE-inhibitory activity. These were verified through *in vitro* validation and were additionally shown to possess anti-angiogenic properties. Interestingly, the anti-angiogenic capacity of these compounds was suggested to be independent of HPSE inhibition. Furthermore, GW7647 and GW9578 were shown to inhibit the invasion of the metastatic MDA-MB-231 cell line *in vitro*, indicating potential anti-

metastatic properties. However, this too was suggested to occur via a HPSE-independent manner, with the exact nature of anti-invasive mechanism of these compounds yet to be defined. In an attempt to investigate the *in vivo* efficacy of these compounds in inhibiting metastasis, a study was carried out utilising a newly-designed B16F10-mCherry-Luc cell line. However, these preliminary findings did not indicate that GW7647 and GW9578 imparted an anti-metastatic effect *in vivo*. Additionally, there was no indication of these compounds imparting an effect on infiltrating immune cells.

6.4 The significance of the findings of this thesis and future directions

The rising need for efficacious cancer therapeutics is coupled with the constant unravelling of the complex nature of the TME highlighted in recent studies, adding fuel to the fire of highly targeted anti-cancer approaches (Pickup et al., 2014). HPSE has remained in the crosshairs of anti-cancer therapeutics since its cloning over two decades ago (Hulett et al., 1999, Vlodavsky et al., 1999). The implication of a key role for HPSE in essentially all cancers by promoting multiple hallmarks (described in chapter 1) has further focused a spotlight on HPSE as a promising therapeutic target. The studies undertaken in this thesis were designed in consideration of the above, along with acknowledging that defining the true role of HPSE in the TME is far from being accomplished.

Chapters 3 and 4 of this thesis specifically focused on the role of HPSE in breast cancer. The findings raise the possibility that in certain breast cancer settings, HPSE may not play a significant role and indeed, its role may be redundant due to reasons yet to be elucidated. The clinical implications of these findings are yet to be seen and it must be emphasised that the findings are limited to a specific cancer setting in a select *in vivo* model. However, owing to the robust, human-like pathological nature of breast cancer progression of the PyMT-MMTV model, as demonstrated by its prominent position within the literature, these findings are likely to be impactful (Lin et al., 2003). Future studies could employ HPSE-overexpressing PyMT-MMTV mice in parallel with both PyMT-MMTV and PyMT-MMTVxHPSE$^{-/-}$ mice to determine if the overexpression of HPSE has an effect on the mammary tumour development of these animals.

This raises the additional possibility that these findings may also apply to other cancer settings in the context of HPSE. A vast majority of studies in the current literature do not employ *in vivo* models of spontaneous tumour development. This is largely due to the lack of availability of such models (Gómez-Cuadrado et al., 2017). This significantly impacts the ability to conduct observations on the true nature and role of TME components throughout the stepwise tumour development process. Tumours develop gradually over time, progressing through multiple stages of pathology prior to becoming malignant (Hanahan and Weinberg, 2011, Hanahan and Weinberg, 2000). The use of spontaneous

tumour-developing *in vivo* models provides the observer with the opportunity to conduct long-term observations as opposed to inducing tumours with cell lines cultivated *in vitro*. Although xenograft tumour models do provide significant merit, their limitations must be acknowledged when the intricate interplay of TME components are the subject of investigation (Gómez-Cuadrado et al., 2017).

Confounding this further is the general limited or lack of use of HPSE-deficient *in vivo* models in conducting studies on the role of HPSE in malignant disease settings, including studies on breast cancer (Zhang et al., 2017c, Zhang et al., 2017b, Wei et al., 2018b, Zhang et al., 2015c). The use of transgenic HPSE-overexpressing *in vivo* and *in vitro* models in direct comparison with wildtype counterparts may not provide as robust results as the use of HPSE-deficient models in parallel with their wildtype counterparts. The use of a HPSE-deficient phenotype would take into account any potential physiological or pathological mechanisms to compensate for the lack of HPSE. Additionally, HPSE-overexpressing transgenic phenotypes would likely result in the exaggeration of the role of HPSE to an extent which would prove the interpretation of its pathophysiological role difficult. The focus of this thesis therefore was to address the above gaps in the current knowledge. Prior to investigating the role of HPSE in other cancer settings and expanding further on breast cancer, it is important that the use of well-characterised HPSE-deficient *in vivo* models of spontaneous tumour development be employed, if feasible.

Chapter 5 of this thesis described novel compounds with demonstrated *in vitro* HPSE-inhibitory capabilities. As described, a majority of HPSE inhibitors developed thus far have failed in clinical and pre-clinical testing due to a lack of efficacy or significant side effects (Rohloff et al., 2002, Khasraw et al., 2010a). Employing high throughput screening, GW7647 and GW9578 were identified as potent HPSE inhibitors with demonstrated *in vitro* efficacy. However, much optimisation of the capacity of these compounds to inhibit HPSE within the complex TME setting will be required prior to any successful pre-clinical or clinical validation. The limited *in vivo* studies conducted in this thesis did not indicate the ability of these compounds to inhibit tumour growth and metastasis. However, this was limited to a single delivery technique and no modification to the design of the compound itself was performed. Future studies will be required to investigate the optimal mode of delivery and dosage of these compounds in a variety of tumour settings in order to provide a conclusion. It is also possible that the compounds may require modifications to their chemical makeup itself in order to enhance delivery and solubility as well as improving the specificity and activity in targeting HPSE. The recent solving of the 3D structure of HPSE will undoubtedly aid in constructing the optimal design of HPSE-targeting small molecules (Wu et al., 2015).

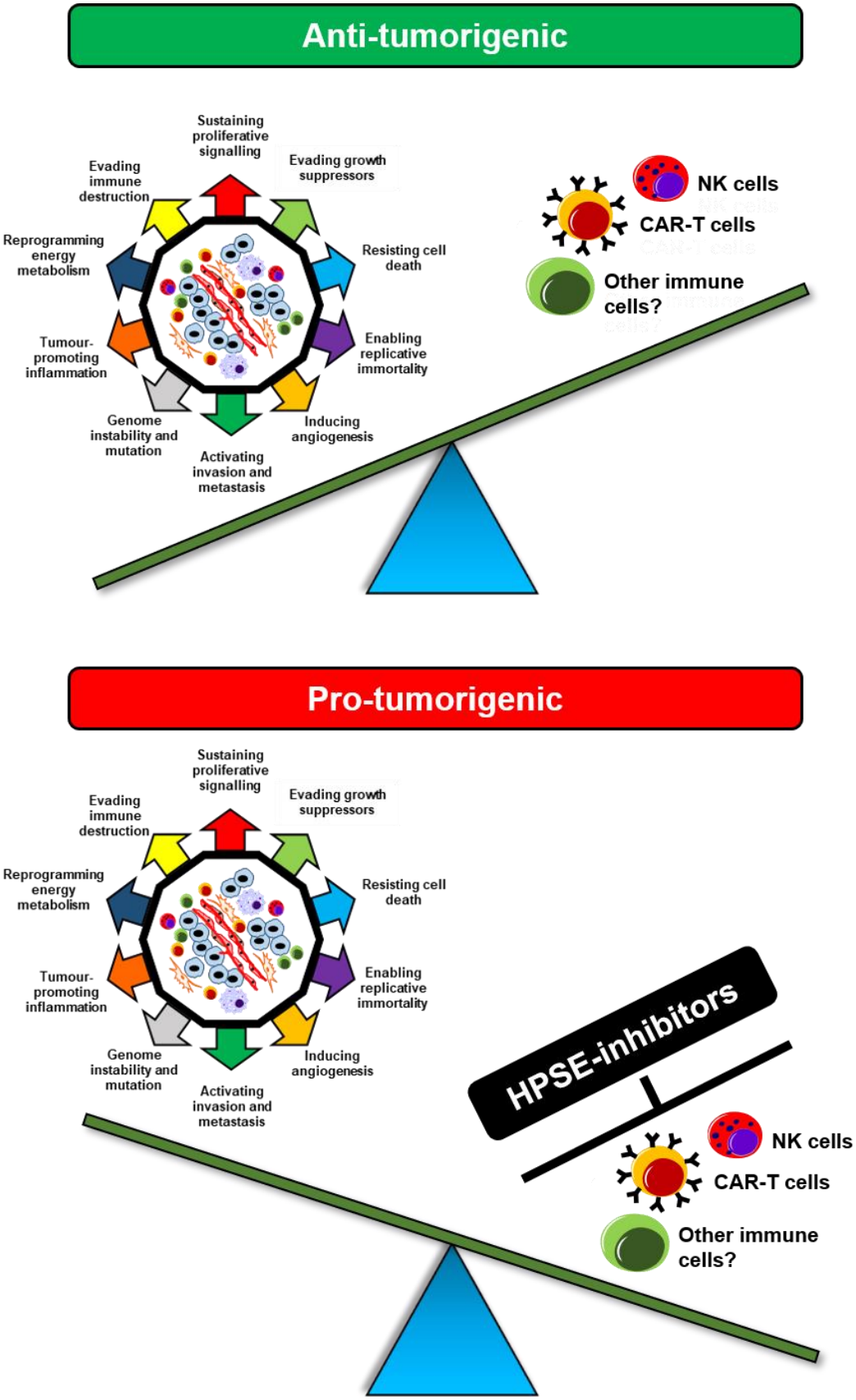

Figure 6.1 The use of HPSE inhibitors may promote cancer progression
The indiscriminate targeting of HPSE within the TME may inadvertently promote the hallmarks of cancer by inhibiting key anti-tumour immune system components, thereby favouring pro-tumorigenic conditions.

The timing of the administration of HPSE inhibitors in the clinic may play a critical role. As discussed in previous chapters, metastasis can occur early in tumour development (Linde et al., 2018). Tumour angiogenesis must also be established early in tumour development (Folkman, 1971, Folkman, 1990). It remains to be seen if HPSE inhibitors may prove advantageous if administered early in tumour development.

Finally, the 'double-edged' nature of HPSE within the TME must be carefully considered when designing HPSE-targeted therapeutics. As described on numerous occasions in this thesis, recent studies have indicated that HPSE is critical in maintaining the function of the components of the immune system (Poon et al., 2014, Putz et al., 2017). Amongst these components are NK cells which are vital in tumour immunosurveillance (Lopez-Soto et al., 2015). With regards to the balance between the pro-tumorigenic hallmarks of cancer and the anti-tumour components of the immune system, the indiscriminate targeting of HPSE within the TME may tip the balance in favour of promoting the hallmarks of cancer **(figure 6.1)**.

It is therefore vital that future studies dissect and define the precise role of HPSE within the TME in each tumour setting, as individual cancer types and tumour settings are vastly different from each other. The dual role of HPSE adds a significant layer of complexity to this task, but in order to minimise or prevent undesirable off-target effects seen in the past through the indiscriminatory targeting of MMPs, such detailed studies are necessary (Winer et al., 2018b, Dove, 2002a). These considerations will pave the way for multiple avenues of future research, as will each new discovery on the complicated nature of HPSE and its role in tumour progression.

In conclusion, it must be emphasised that unlike many other aspects of cancer and its components, the role of HPSE as defined over the past two decades is not black and white but in fact, is many shades of grey.

References

ABASSI, Z., HAMOUD, S., HASSAN, A., KHAMAYSI, I., NATIV, O., HEYMAN, S. N., MUHAMMAD, R. S., ILAN, N., SINGH, P., HAMMOND, E., ZAZA, G., LUPO, A., ONISTO, M., BELLIN, G., MASOLA, V., VLODAVSKY, I. & GAMBARO, G. 2017. Involvement of heparanase in the pathogenesis of acute kidney injury: nephroprotective effect of PG545. *Oncotarget,* 8**,** 34191-34204.

ABBOUD-JARROUS, G., ATZMON, R., PERETZ, T., PALERMO, C., GADEA, B. B., JOYCE, J. A. & VLODAVSKY, I. 2008. Cathepsin L is responsible for processing and activation of proheparanase through multiple cleavages of a linker segment. *J Biol Chem,* 283**,** 18167-76.

ABDELKARIM, M., VINTONENKO, N., STARZEC, A., ROBLES, A., AUBERT, J., MARTIN, M.-L., MOURAH, S., PODGORNIAK, M.-P., RODRIGUES-FERREIRA, S., NAHMIAS, C., COURAUD, P.-O., DOLIGER, C., SAINTE-CATHERINE, O., PEYRI, N., CHEN, L., MARIAU, J., ETIENNE, M., PERRET, G.-Y., CREPIN, M., POYET, J.-L., KHATIB, A.-M. & DI BENEDETTO, M. 2011. Invading Basement Membrane Matrix Is Sufficient for MDA-MB-231 Breast Cancer Cells to Develop a Stable In Vivo Metastatic Phenotype. *PLOS ONE,* 6**,** e23334.

ABU ARAB, W., KOTB, R., SIROIS, M. & ROUSSEAU, E. 2011. Concentration- and time-dependent effects of enoxaparin on human adenocarcinomic epithelial cell line A549 proliferation in vitro. *Can J Physiol Pharmacol,* 89**,** 705-11.

AGGARWAL, B. B. 2003. Signalling pathways of the TNF superfamily: a double-edged sword. *Nat Rev Immunol,* 3**,** 745-56.

AGUIRRE-GHISO, J. A., OSSOWSKI, L. & ROSENBAUM, S. K. 2004. Green fluorescent protein tagging of extracellular signal-regulated kinase and p38 pathways reveals novel dynamics of pathway activation during primary and metastatic growth. *Cancer Res,* 64**,** 7336-45.

AKINO, T., HIDA, K., HIDA, Y., TSUCHIYA, K., FREEDMAN, D., MURAKI, C., OHGA, N., MATSUDA, K., AKIYAMA, K., HARABAYASHI, T., SHINOHARA, N., NONOMURA, K., KLAGSBRUN, M. & SHINDOH, M. 2009. Cytogenetic abnormalities of tumor-associated endothelial cells in human malignant tumors. *Am J Pathol,* 175**,** 2657-67.

AKIYAMA, K., OHGA, N., HIDA, Y., KAWAMOTO, T., SADAMOTO, Y., ISHIKAWA, S., MAISHI, N., AKINO, T., KONDOH, M., MATSUDA, A., INOUE, N., SHINDOH, M. & HIDA, K. 2012. Tumor endothelial cells acquire drug resistance by MDR1 up-regulation via VEGF signaling in tumor microenvironment. *Am J Pathol,* 180**,** 1283-93.

AL-BENNA, S., POGGEMANN, K., STEINAU, H. U. & STEINSTRAESSER, L. 2010. Diagnosis and management of primary breast sarcoma. *Breast Cancer Res Treat,* 122**,** 619-26.

AL-MEHDI, A. B., TOZAWA, K., FISHER, A. B., SHIENTAG, L., LEE, A. & MUSCHEL, R. J. 2000. Intravascular origin of metastasis from the proliferation of endothelium-attached tumor cells: a new model for metastasis. *Nat Med,* 6**,** 100-2.

ALBAN, S., LUDWIG, R. J., BENDAS, G., SCHÖN, M. P., OOSTINGH, G. J., RADEKE, H. H., FRITZSCHE, J., PFEILSCHIFTER, J., KAUFMANN, R. & BOEHNCKE, W.-H. 2009. PS3, A Semisynthetic β-1,3-Glucan Sulfate, Diminishes Contact Hypersensitivity Responses Through Inhibition of L- and P-Selectin Functions. *Journal of Investigative Dermatology,* 129**,** 1192-1202.

ALMHOLT, K., LUND, L. R., RYGAARD, J., NIELSEN, B. S., DANO, K., ROMER, J. & JOHNSEN, M. 2005. Reduced metastasis of transgenic mammary cancer in urokinase-deficient mice. *Int J Cancer,* 113**,** 525-32.

ALOWAMI, S., TROUP, S., AL-HADDAD, S., KIRKPATRICK, I. & WATSON, P. H. 2003. Mammographic density is related to stroma and stromal proteoglycan expression. *Breast Cancer Res,* 5**,** R129-35.

ANDELA, V. B., SCHWARZ, E. M., PUZAS, J. E., O'KEEFE, R. J. & ROSIER, R. N. 2000. Tumor metastasis and the reciprocal regulation of prometastatic and antimetastatic factors by nuclear factor kappaB. *Cancer Res,* 60**,** 6557-62.

ARAS, S. & ZAIDI, M. R. 2017. TAMeless traitors: macrophages in cancer progression and metastasis. *British Journal Of Cancer,* 117**,** 1583.

ARNDT, G. M. & MACKENZIE, K. L. 2016. New prospects for targeting telomerase beyond the telomere. *Nat Rev Cancer,* 16**,** 508-24.

ARRIBAS, S. M., HINEK, A. & GONZALEZ, M. C. 2006. Elastic fibres and vascular structure in hypertension. *Pharmacol Ther,* 111**,** 771-91.

ASLAKSON, C. J. & MILLER, F. R. 1992. Selective events in the metastatic process defined by analysis of the sequential dissemination of subpopulations of a mouse mammary tumor. *Cancer Res,* 52**,** 1399-405.

ASNAGHI, L., LIN, M. H., LIM, K. S., LIM, K. J., TRIPATHY, A., WENDEBORN, M., MERBS, S. L., HANDA, J. T., SODHI, A., BAR, E. E. & EBERHART, C. G. 2014. Hypoxia promotes uveal melanoma invasion through enhanced Notch and MAPK activation. *PLoS One,* 9**,** e105372.

AUBREY, B. J., KELLY, G. L., JANIC, A., HEROLD, M. J. & STRASSER, A. 2018. How does p53 induce apoptosis and how does this relate to p53-mediated tumour suppression? *Cell Death and Differentiation,* 25**,** 104-113.

AZAB, A. K., HU, J., QUANG, P., AZAB, F., PITSILLIDES, C., AWWAD, R., THOMPSON, B., MAISO, P., SUN, J. D., HART, C. P., ROCCARO, A. M., SACCO, A., NGO, H. T., LIN, C. P., KUNG, A. L., CARRASCO, R. D., VANDERKERKEN, K. & GHOBRIAL, I. M. 2012. Hypoxia promotes dissemination of multiple myeloma through acquisition of epithelial to mesenchymal transition-like features. *Blood,* 119**,** 5782-94.

BABAPOOR-FARROKHRAN, S., JEE, K., PUCHNER, B., HASSAN, S. J., XIN, X., RODRIGUES, M., KASHIWABUCHI, F., MA, T., HU, K., DESHPANDE, M., DAOUD, Y., SOLOMON, S., WENICK, A., LUTTY, G. A., SEMENZA, G. L., MONTANER, S. & SODHI, A. 2015. Angiopoietin-like 4 is a potent angiogenic

factor and a novel therapeutic target for patients with proliferative diabetic retinopathy. *Proc Natl Acad Sci U S A,* 112**,** E3030-9.

BAERISWYL, V. & CHRISTOFORI, G. 2009. The angiogenic switch in carcinogenesis. *Semin Cancer Biol,* 19**,** 329-37.

BAIETTI, M. F., ZHANG, Z., MORTIER, E., MELCHIOR, A., DEGEEST, G., GEERAERTS, A., IVARSSON, Y., DEPOORTERE, F., COOMANS, C., VERMEIREN, E., ZIMMERMANN, P. & DAVID, G. 2012. Syndecan-syntenin-ALIX regulates the biogenesis of exosomes. *Nat Cell Biol,* 14**,** 677-85.

BAILLY, B., DIRR, L., EL-DEEB, I. M., ALTMEYER, R., GUILLON, P. & VON ITZSTEIN, M. 2016. A dual drug regimen synergistically blocks human parainfluenza virus infection. *Sci Rep,* 6**,** 24138.

BAINBRIDGE, P. 2013. Wound healing and the role of fibroblasts. *J Wound Care,* 22**,** 407-8, 410-12.

BAISH, J. W. & JAIN, R. K. 2000. Fractals and cancer. *Cancer Res,* 60**,** 3683-8.

BAKER, E., CRAWFORD, J., SUTHERLAND, G. R., FREEMAN, C., PARISH, C. R. & HULETT, M. D. 1999. Human HPA endoglycosidase heparanase. Map position 4q21.3. *Chromosome Res,* 7**,** 319.

BAKER, M., ROBINSON, S. D., LECHERTIER, T., BARBER, P. R., TAVORA, B., D'AMICO, G., JONES, D. T., VOJNOVIC, B. & HODIVALA-DILKE, K. 2011. Use of the mouse aortic ring assay to study angiogenesis. *Nature Protocols,* 7**,** 89.

BALKWILL, F. & MANTOVANI, A. 2001. Inflammation and cancer: back to Virchow? *Lancet,* 357**,** 539-45.

BAME, K. J. 2001. Heparanases: endoglycosidases that degrade heparan sulfate proteoglycans. *Glycobiology,* 11**,** 91R-98R.

BANDARI, S. K., PURUSHOTHAMAN, A., RAMANI, V. C., BRINKLEY, G. J., CHANDRASHEKAR, D. S., VARAMBALLY, S., MOBLEY, J. A., ZHANG, Y., BROWN, E. E., VLODAVSKY, I. & SANDERSON, R. D. 2018. Chemotherapy induces secretion of exosomes loaded with heparanase that degrades extracellular matrix and impacts tumor and host cell behavior. *Matrix Biology,* 65**,** 104-118.

BAO, X., MOSEMAN, E. A., SAITO, H., PETRYANIK, B., THIRIOT, A., HATAKEYAMA, S., ITO, Y., KAWASHIMA, H., YAMAGUCHI, Y., LOWE, J. B., VON ANDRIAN, U. H. & FUKUDA, M. 2010. Endothelial Heparan Sulfate Controls Chemokine Presentation in Recruitment of Lymphocytes and Dendritic Cells to Lymph Nodes. *Immunity,* 33**,** 817-829.

BAR-NER, M., ELDOR, A., WASSERMAN, L., MATZNER, Y., COHEN, I. R., FUKS, Z. & VLODAVSKY, I. 1987. Inhibition of heparanase-mediated degradation of extracellular matrix heparan sulfate by non-anticoagulant heparin species. *Blood,* 70**,** 551-7.

BAR-NER, M., KRAMER, M. D., SCHIRRMACHER, V., ISHAI-MICHAELI, R., FUKS, Z. & VLODAVSKY, I. 1985. Sequential degradation of heparan sulfate in the subendothelial extracellular matrix by highly metastatic lymphoma cells. *Int J Cancer,* 35**,** 483-91.

BAR-NER, M., MAYER, M., SCHIRRMACHER, V. & VLODAVSKY, I. 1986. Involvement of both heparanase and plasminogen activator in lymphoma cell-mediated degradation of heparan sulfate in the subendothelial extracellular matrix. *J Cell Physiol,* 128**,** 299-306.

BARASH, U., ARVATZ, G., FARFARA, R., NARODITSKY, I., DOWECK, I., FELD, S., BEN-IZHAK, O., ILAN, N., NATIV, O. & VLODAVSKY, I. 2012. Clinical significance of heparanase splice variant (t5) in renal cell carcinoma: evaluation by a novel t5-specific monoclonal antibody. *PLoS One,* 7**,** e51494.

BARASH, U., COHEN-KAPLAN, V., ARVATZ, G., GINGIS-VELITSKI, S., LEVY-ADAM, F., NATIV, O., SHEMESH, R., AYALON-SOFER, M., ILAN, N. & VLODAVSKY, I. 2010. A novel human heparanase splice variant, T5, endowed with protumorigenic characteristics. *FASEB J,* 24**,** 1239-48.

BARAZ, L., HAUPT, Y., ELKIN, M., PERETZ, T. & VLODAVSKY, I. 2006. Tumor suppressor p53 regulates heparanase gene expression. *Oncogene,* 25**,** 3939-47.

BARIK, A., ZHANG, B., SOHAL, G. S., XIONG, W. C. & MEI, L. 2014. Crosstalk between Agrin and Wnt signaling pathways in development of vertebrate neuromuscular junction. *Dev Neurobiol,* 74**,** 828-38.

BARNES, T. A. & AMIR, E. 2017a. HYPE or HOPE: the prognostic value of infiltrating immune cells in cancer. *British journal of cancer,* 117**,** 451-460.

BARNES, T. A. & AMIR, E. 2017b. HYPE or HOPE: the prognostic value of infiltrating immune cells in cancer. *British Journal Of Cancer,* 117**,** 451.

BARRIO, A. V. & VAN ZEE, K. J. 2017. Controversies in the Treatment of Ductal Carcinoma in Situ. *Annu Rev Med,* 68**,** 197-211.

BASAPPA, MURUGAN, S., KAVITHA, C. V., PURUSHOTHAMAN, A., NEVIN, K. G., SUGAHARA, K. & RANGAPPA, K. S. 2010. A small oxazine compound as an anti-tumor agent: A novel pyranoside mimetic that binds to VEGF, HB-EGF, and TNF-α. *Cancer Letters,* 297**,** 231-243.

BASCHE, M., GUSTAFSON, D. L., HOLDEN, S. N., O'BRYANT, C. L., GORE, L., WITTA, S., SCHULTZ, M. K., MORROW, M., LEVIN, A., CREESE, B. R., KANGAS, M., ROBERTS, K., NGUYEN, T., DAVIS, K., ADDISON, R. S., MOORE, J. C. & ECKHARDT, S. G. 2006. A Phase I Biological and Pharmacologic Study of the Heparanase Inhibitor PI-88 in Patients with Advanced Solid Tumors. *Clinical Cancer Research,* 12**,** 5471-5480.

BASHKIN, P., RAZIN, E., ELDOR, A. & VLODAVSKY, I. 1990. Degranulating mast cells secrete an endoglycosidase that degrades heparan sulfate in subendothelial extracellular matrix. *Blood,* 75**,** 2204-12.

BATEMAN, J. F., BOOT-HANDFORD, R. P. & LAMANDE, S. R. 2009. Genetic diseases of connective tissues: cellular and extracellular effects of ECM mutations. *Nat Rev Genet,* 10**,** 173-83.

BATLLE, E. & CLEVERS, H. 2017. Cancer stem cells revisited. *Nat Med,* 23**,** 1124-1134.

BATOOL, T., FANG, J., BARASH, U., MOUSTAKAS, A., VLODAVSKY, I. & LI, J. P. 2017. Overexpression of heparanase attenuated TGF-beta-stimulated signaling in tumor cells. *FEBS Open Bio,* 7**,** 405-413.

BAUDINO, T. 2015. Targeted Cancer Therapy: The Next Generation of Cancer Treatment. *Current Drug Discovery Technologies,* 12**,** 3-20.

BECKHOVE, P., HELMKE, B. M., ZIOUTA, Y., BUCUR, M., DORNER, W., MOGLER, C., DYCKHOFF, G. & HEROLD-MENDE, C. 2005. Heparanase expression at the invasion front of human head and neck cancers and correlation with poor prognosis. *Clin Cancer Res,* 11**,** 2899-906.

BENHAMRON, S., REINER, I., ZCHARIA, E., ATALLAH, M., GRAU, A., VLODAVSKY, I. & MEVORACH, D. 2012. Dissociation between mature phenotype and impaired transmigration in dendritic cells from heparanase-deficient mice. *PLoS One,* 7**,** e35602.

BERGERON, J. J., DI GUGLIELMO, G. M., DAHAN, S., DOMINGUEZ, M. & POSNER, B. I. 2016. Spatial and Temporal Regulation of Receptor Tyrosine Kinase Activation and Intracellular Signal Transduction. *Annu Rev Biochem,* 85**,** 573-97.

BERMUDEZ, V., FINOL, F., PARRA, N., PARRA, M., PEREZ, A., PENARANDA, L., VILCHEZ, D., ROJAS, J., ARRAIZ, N. & VELASCO, M. 2010. PPAR-gamma agonists and their role in type 2 diabetes mellitus management. *Am J Ther,* 17**,** 274-83.

BERTOLESI, G. E., MICHAIEL, G. & MCFARLANE, S. 2008. Two heparanase splicing variants with distinct properties are necessary in early Xenopus development. *J Biol Chem,* 283**,** 16004-16.

BIANCHINI, G., BALKO, J. M., MAYER, I. A., SANDERS, M. E. & GIANNI, L. 2016. Triple-negative breast cancer: challenges and opportunities of a heterogeneous disease. *Nature Reviews Clinical Oncology,* 13**,** 674.

BIANUCCI, R., PERCIACCANTE, A., CHARLIER, P., APPENZELLER, O. & LIPPI, D. 2018. Earliest evidence of malignant breast cancer in Renaissance paintings. *Lancet Oncol,* 19**,** 166-167.

BIDARD, F. C., PEETERS, D. J., FEHM, T., NOLE, F., GISBERT-CRIADO, R., MAVROUDIS, D., GRISANTI, S., GENERALI, D., GARCIA-SAENZ, J. A., STEBBING, J., CALDAS, C., GAZZANIGA, P., MANSO, L., ZAMARCHI, R., DE LASCOITI, A. F., DE MATTOS-ARRUDA, L., IGNATIADIS, M., LEBOFSKY, R., VAN LAERE, S. J., MEIER-STIEGEN, F., SANDRI, M. T., VIDAL-MARTINEZ, J., POLITAKI, E., CONSOLI, F., BOTTINI, A., DIAZ-RUBIO, E., KRELL, J., DAWSON, S. J., RAIMONDI, C., RUTTEN, A., JANNI, W., MUNZONE, E.,

CARANANA, V., AGELAKI, S., ALMICI, C., DIRIX, L., SOLOMAYER, E. F., ZORZINO, L., JOHANNES, H., REIS-FILHO, J. S., PANTEL, K., PIERGA, J. Y. & MICHIELS, S. 2014. Clinical validity of circulating tumour cells in patients with metastatic breast cancer: a pooled analysis of individual patient data. *Lancet Oncol,* 15**,** 406-14.

BIELENBERG, D. R. & ZETTER, B. R. 2015. The Contribution of Angiogenesis to the Process of Metastasis. *Cancer journal (Sudbury, Mass.),* 21**,** 267-273.

BIERIE, B. & MOSES, H. L. 2006. Tumour microenvironment: TGFbeta: the molecular Jekyll and Hyde of cancer. *Nat Rev Cancer,* 6**,** 506-20.

BINGLE, L., LEWIS, C. E., CORKE, K. P., REED, M. W. & BROWN, N. J. 2006. Macrophages promote angiogenesis in human breast tumour spheroids in vivo. *Br J Cancer,* 94**,** 101-7.

BISWAS, S. K., GANGI, L., PAUL, S., SCHIOPPA, T., SACCANI, A., SIRONI, M., BOTTAZZI, B., DONI, A., VINCENZO, B., PASQUALINI, F., VAGO, L., NEBULONI, M., MANTOVANI, A. & SICA, A. 2006. A distinct and unique transcriptional program expressed by tumor-associated macrophages (defective NF-kappaB and enhanced IRF-3/STAT1 activation). *Blood,* 107**,** 2112-22.

BITAN, M., POLLIACK, A., ZECCHINA, G., NAGLER, A., FRIEDMANN, Y., NADAV, L., DEUTSCH, V., PECKER, I., ELDOR, A., VLODAVSKY, I. & KATZ, B. Z. 2002. Heparanase expression in human leukemias is restricted to acute myeloid leukemias. *Exp Hematol,* 30**,** 34-41.

BLACKADAR, C. B. 2016. Historical review of the causes of cancer. *World J Clin Oncol,* 7**,** 54-86.

BLACKBURN, E. H. & GALL, J. G. 1978. A tandemly repeated sequence at the termini of the extrachromosomal ribosomal RNA genes in Tetrahymena. *J Mol Biol,* 120**,** 33-53.

BLACKHALL, F. H., MERRY, C. L., DAVIES, E. J. & JAYSON, G. C. 2001. Heparan sulfate proteoglycans and cancer. *Br J Cancer,* 85**,** 1094-8.

BOBARDT, M. D., SAPHIRE, A. C., HUNG, H. C., YU, X., VAN DER SCHUEREN, B., ZHANG, Z., DAVID, G. & GALLAY, P. A. 2003. Syndecan captures, protects, and transmits HIV to T lymphocytes. *Immunity,* 18**,** 27-39.

BOCCHINFUSO, W. P., LINDZEY, J. K., HEWITT, S. C., CLARK, J. A., MYERS, P. H., COOPER, R. & KORACH, K. S. 2000. Induction of Mammary Gland Development in Estrogen Receptor-α Knockout Mice. *Endocrinology,* 141**,** 2982-2994.

BOHLMANN, L., TREDWELL, G. D., YU, X., CHANG, C. W., HASELHORST, T., WINGER, M., DYASON, J. C., THOMSON, R. J., TIRALONGO, J., BEACHAM, I. R., BLANCHARD, H. & VON ITZSTEIN, M. 2015. Functional and structural characterization of a heparanase. *Nat Chem Biol,* 11**,** 955-7.

BONNANS, C., CHOU, J. & WERB, Z. 2014. Remodelling the extracellular matrix in development and disease. *Nat Rev Mol Cell Biol,* 15**,** 786-801.

BONNET, D. & DICK, J. E. 1997. Human acute myeloid leukemia is organized as a hierarchy that originates from a primitive hematopoietic cell. *Nat Med,* 3**,** 730-7.

BOPST, M., BORTOLINI, M., WRIGHT, M. B. & TADAYYON, M. 2014. Minireview: Challenges and Opportunities in Development of PPAR Agonists. *Molecular Endocrinology,* 28**,** 1756-1768.

BORREGO, F., ROBERTSON, M. J., RITZ, J., PENA, J. & SOLANA, R. 1999. CD69 is a stimulatory receptor for natural killer cell and its cytotoxic effect is blocked by CD94 inhibitory receptor. *Immunology,* 97**,** 159-65.

BORREGO, F., ULBRECHT, M., WEISS, E. H., COLIGAN, J. E. & BROOKS, A. G. 1998. Recognition of human histocompatibility leukocyte antigen (HLA)-E complexed with HLA class I signal sequence-derived peptides by CD94/NKG2 confers protection from natural killer cell-mediated lysis. *J Exp Med,* 187**,** 813-8.

BORSIG, L., VLODAVSKY, I., ISHAI-MICHAELI, R., TORRI, G. & VISMARA, E. 2011. Sulfated Hexasaccharides Attenuate Metastasis by Inhibition of P-selectin and Heparanase. *Neoplasia,* 13**,** 445-452.

BOYANGO, I., BARASH, U., FUX, L., NARODITSKY, I., ILAN, N. & VLODAVSKY, I. 2018. Targeting heparanase to the mammary epithelium enhances mammary gland development and promotes tumor growth and metastasis. *Matrix Biology,* 65**,** 91-103.

BOYANGO, I., BARASH, U., NARODITSKY, I., LI, J. P., HAMMOND, E., ILAN, N. & VLODAVSKY, I. 2014. Heparanase cooperates with Ras to drive breast and skin tumorigenesis. *Cancer Res,* 74**,** 4504-14.

BRAWANSKI, A. 2012. On the myth of the Edwin Smith papyrus: is it magic or science? *Acta Neurochir (Wien),* 154**,** 2285-91.

BRAY, F., FERLAY, J., SOERJOMATARAM, I., SIEGEL, R. L., TORRE, L. A. & JEMAL, A. 2018. Global cancer statistics 2018: GLOBOCAN estimates of incidence and mortality worldwide for 36 cancers in 185 countries. *CA: A Cancer Journal for Clinicians,* 68**,** 394-424.

BRENNAN, T. V., LIN, L., BRANDSTADTER, J. D., RENDELL, V. R., DREDGE, K., HUANG, X. & YANG, Y. 2016. Heparan sulfate mimetic PG545-mediated antilymphoma effects require TLR9-dependent NK cell activation. *J Clin Invest,* 126**,** 207-19.

BRINTON, L. A., SCHAIRER, C., HOOVER, R. N. & FRAUMENI, J. F., JR. 1988. Menstrual factors and risk of breast cancer. *Cancer Invest,* 6**,** 245-54.

BRITT, K. 2012. Menarche, menopause, and breast cancer risk. *Lancet Oncol,* 13**,** 1071-2.

BROCKWELL, N. K., RAUTELA, J., OWEN, K. L., GEARING, L. J., DEB, S., HARVEY, K., SPURLING, A., ZANKER, D., CHAN, C.-L., CUMMING, H. E., DENG, N., ZAKHOUR, J. M., DUIVENVOORDEN, H. M., ROBINSON, T., HARRIS, M., WHITE, M., FOX, J., OOI, C., KUMAR, B., THOMSON, J., POTASZ, N., SWARBRICK, A., HERTZOG, P. J., MOLLOY, T. J., TOOLE, S. O., GANJU, V. & PARKER, B. S. 2019. Tumor inherent interferon regulators as biomarkers of long-term chemotherapeutic response in TNBC. *npj Precision Oncology,* 3**,** 21.

BROMBERG, M. E., KONIGSBERG, W. H., MADISON, J. F., PAWASHE, A. & GAREN, A. 1995. Tissue factor promotes melanoma metastasis by a pathway independent of blood coagulation. *Proc Natl Acad Sci U S A,* 92**,** 8205-9.

BROWN, E. J., ALBERS, M. W., SHIN, T. B., ICHIKAWA, K., KEITH, C. T., LANE, W. S. & SCHREIBER, S. L. 1994. A mammalian protein targeted by G1-arresting rapamycin-receptor complex. *Nature,* 369**,** 756-8.

BROWN, K. J., MAYNES, S. F., BEZOS, A., MAGUIRE, D. J., FORD, M. D. & PARISH, C. R. 1996. A novel in vitro assay for human angiogenesis. *Lab Invest,* 75**,** 539-55.

BROWN, P. J., STUART, L. W., HURLEY, K. P., LEWIS, M. C., WINEGAR, D. A., WILSON, J. G., WILKISON, W. O., ITTOOP, O. R. & WILLSON, T. M. 2001. Identification of a subtype selective human PPARα agonist through parallel-array synthesis. *Bioorganic & Medicinal Chemistry Letters,* 11**,** 1225-1227.

BROWN, P. J., WINEGAR, D. A., PLUNKET, K. D., MOORE, L. B., LEWIS, M. C., WILSON, J. G., SUNDSETH, S. S., KOBLE, C. S., WU, Z., CHAPMAN, J. M., LEHMANN, J. M., KLIEWER, S. A. & WILLSON, T. M. 1999. A Ureido-Thioisobutyric Acid (GW9578) Is a Subtype-Selective PPARα Agonist with Potent Lipid-Lowering Activity. *Journal of Medicinal Chemistry,* 42**,** 3785-3788.

BRUN, R., NARODITSKY, I., WATERMAN, M., BEN-IZHAK, O., GROISMAN, G., ILAN, N. & VLODAVSKY, I. 2009. Heparanase expression by Barrett's epithelium and during esophageal carcinoma progression. *Mod Pathol,* 22**,** 1548-54.

BRUNA, A., DARKEN, R. S., ROJO, F., OCANA, A., PENUELAS, S., ARIAS, A., PARIS, R., TORTOSA, A., MORA, J., BASELGA, J. & SEOANE, J. 2007. High TGFbeta-Smad activity confers poor prognosis in glioma patients and promotes cell proliferation depending on the methylation of the PDGF-B gene. *Cancer Cell,* 11**,** 147-60.

BRUNO, A., PAGANI, A., PULZE, L., ALBINI, A., DALLAGLIO, K., NOONAN, D. M. & MORTARA, L. 2014. Orchestration of Angiogenesis by Immune Cells. *Frontiers in Oncology,* 4**,** 131.

BURNET, F. M. 1970. The concept of immunological surveillance. *Prog Exp Tumor Res,* 13**,** 1-27.

BURNET, M. 1957. Cancer: a biological approach. III. Viruses associated with neoplastic conditions. IV. Practical applications. *Br Med J,* 1**,** 841-7.

BUSH, K. T., CRAWFORD, B. E., GARNER, O. B., NIGAM, K. B., ESKO, J. D. & NIGAM, S. K. 2012. N-sulfation of heparan sulfate regulates early branching events in the developing mammary gland. *J Biol Chem,* 287**,** 42064-70.

CAI, Y., NOGALES-CADENAS, R., ZHANG, Q., LIN, J. R., ZHANG, W., O'BRIEN, K., MONTAGNA, C. & ZHANG, Z. D. 2017. Transcriptomic dynamics of breast cancer progression in the MMTV-PyMT mouse model. *BMC Genomics,* 18**,** 185.

CAIRNS, J. 1975. Mutation selection and the natural history of cancer. *Nature,* 255**,** 197-200.

CAJA, L., DITURI, F., MANCARELLA, S., CABALLERO-DIAZ, D., MOUSTAKAS, A., GIANNELLI, G. & FABREGAT, I. 2018. TGF-beta and the Tissue Microenvironment: Relevance in Fibrosis and Cancer. *Int J Mol Sci,* 19.

CALCOEN, D., ELIAS, L. & YU, X. 2015. What does it take to produce a breakthrough drug? *Nature Reviews Drug Discovery,* 14**,** 161.

CALON, A., LONARDO, E., BERENGUER-LLERGO, A., ESPINET, E., HERNANDO-MOMBLONA, X., IGLESIAS, M., SEVILLANO, M., PALOMO-PONCE, S., TAURIELLO, D. V., BYROM, D., CORTINA, C., MORRAL, C., BARCELO, C., TOSI, S., RIERA, A., ATTOLINI, C. S., ROSSELL, D., SANCHO, E. & BATLLE, E. 2015. Stromal gene expression defines poor-prognosis subtypes in colorectal cancer. *Nat Genet,* 47**,** 320-9.

CAMPBELL, P. J. 2012. Telomeres and cancer: from crisis to stability to crisis to stability. *Cell,* 148**,** 633-5.

CAO, R., JI, H., FENG, N., ZHANG, Y., YANG, X., ANDERSSON, P., SUN, Y., TRITSARIS, K., HANSEN, A. J., DISSING, S. & CAO, Y. 2012. Collaborative interplay between FGF-2 and VEGF-C promotes lymphangiogenesis and metastasis. *Proc Natl Acad Sci U S A,* 109**,** 15894-9.

CAO, Y., ZHANG, Z. L., ZHOU, M., ELSON, P., RINI, B., AYDIN, H., FEENSTRA, K., TAN, M. H., BERGHUIS, B., TABBEY, R., RESAU, J. H., ZHOU, F. J., TEH, B. T. & QIAN, C. N. 2013. Pericyte coverage of differentiated vessels inside tumor vasculature is an independent unfavorable prognostic factor for patients with clear cell renal cell carcinoma. *Cancer,* 119**,** 313-24.

CARSWELL, E. A., OLD, L. J., KASSEL, R. L., GREEN, S., FIORE, N. & WILLIAMSON, B. 1975. An endotoxin-induced serum factor that causes necrosis of tumors. *Proc Natl Acad Sci U S A,* 72**,** 3666-70.

CARUANA, I., SAVOLDO, B., HOYOS, V., WEBER, G., LIU, H., KIM, E. S., ITTMANN, M. M., MARCHETTI, D. & DOTTI, G. 2015. Heparanase promotes tumor infiltration and antitumor activity of CAR-redirected T lymphocytes. *Nat Med,* 21**,** 524-9.

CASCONE, T., XU, L., LIN, H. Y., LIU, W., TRAN, H. T., LIU, Y., HOWELLS, K., HADDAD, V., HANRAHAN, E., NILSSON, M. B., CORTEZ, M. A., GIRI, U., KADARA, H., SAIGAL, B., PARK, Y. Y., PENG, W., LEE, J. S., RYAN, A. J., JUERGENSMEIER, J. M., HERBST, R. S., WANG, J., LANGLEY, R. R., WISTUBA, II, LEE, J. J. &

HEYMACH, J. V. 2017. The HGF/c-MET Pathway Is a Driver and Biomarker of VEGFR-inhibitor Resistance and Vascular Remodeling in Non-Small Cell Lung Cancer. *Clin Cancer Res,* 23**,** 5489-5501.

CASTELO-BRANCO, M., SOUZA, H., PASCHOAL, M., PAVÃO, M. & RUMJANEK, V. 2015. Tumor-associated macrophages and heparanase in lung cancer microenvironment. (TUM6P.970). *The Journal of Immunology,* 194**,** 141.18.

CASTILLO, L. F., TASCÓN, R., HUVELLE, M. A. L., NOVACK, G., LLORENS, M. C., DOS SANTOS, A. F., SHORTREDE, J., CABANILLAS, A. M., JOFFÉ, E. B. D. K., LABRIOLA, L. & PETERS, M. G. 2016. Glypican-3 induces a mesenchymal to epithelial transition in human breast cancer cells. *Oncotarget,* 7**,** 60133-60154.

CAVALHEIRO, R. P., LIMA, M. A., JARROUGE-BOUCAS, T. R., VIANA, G. M., LOPES, C. C., COULSON-THOMAS, V. J., DREYFUSS, J. L., YATES, E. A., TERSARIOL, I. L. S. & NADER, H. B. 2017. Coupling of vinculin to F-actin demands Syndecan-4 proteoglycan. *Matrix Biol,* 63**,** 23-37.

CHAKRAVARTI, R. & ADAMS, J. C. 2006. Comparative genomics of the syndecans defines an ancestral genomic context associated with matrilins in vertebrates. *BMC Genomics,* 7**,** 83.

CHAN, F. K., LUZ, N. F. & MORIWAKI, K. 2015. Programmed necrosis in the cross talk of cell death and inflammation. *Annu Rev Immunol,* 33**,** 79-106.

CHANGYALEKET, B., CHONG, Z. Z., DULL, R. O., NANEGRUNGSUNK, D. & XU, H. 2017. Heparanase promotes neuroinflammatory response during subarachnoid hemorrhage in rats. *J Neuroinflammation,* 14**,** 137.

CHEN, B., CHEN, X. P., WU, M. S., CUI, W. & ZHONG, M. 2014. Expressions of heparanase and upstream stimulatory factor in hepatocellular carcinoma. *Eur J Med Res,* 19**,** 45.

CHEN, DANIEL S. & MELLMAN, I. 2013. Oncology Meets Immunology: The Cancer-Immunity Cycle. *Immunity,* 39**,** 1-10.

CHEN, G., WANG, D., VIKRAMADITHYAN, R., YAGYU, H., SAXENA, U., PILLARISETTI, S. & GOLDBERG, I. J. 2004. Inflammatory cytokines and fatty acids regulate endothelial cell heparanase expression. *Biochemistry,* 43**,** 4971-7.

CHEN, M.-T., SUN, H.-F., ZHAO, Y., FU, W.-Y., YANG, L.-P., GAO, S.-P., LI, L.-D., JIANG, H.-L. & JIN, W. 2017a. Comparison of patterns and prognosis among distant metastatic breast cancer patients by age groups: a SEER population-based analysis. *Scientific Reports,* 7**,** 9254.

CHEN, M., LEI, X., SHI, C., HUANG, M., LI, X., WU, B., LI, Z., HAN, W., DU, B., HU, J., NIE, Q., MAI, W., MA, N., XU, N., ZHANG, X., FAN, C., HONG, A., XIA, M., LUO, L., MA, A., LI, H., YU, Q., CHEN, H., ZHANG, D. & YE, W. 2017b. Pericyte-targeting prodrug overcomes tumor resistance to vascular disrupting agents. *J Clin Invest,* 127**,** 3689-3701.

CHEN, P., HUANG, Y., BONG, R., DING, Y., SONG, N., WANG, X., SONG, X. & LUO, Y. 2011. Tumor-associated macrophages promote angiogenesis and melanoma growth via adrenomedullin in a paracrine and autocrine manner. *Clin Cancer Res,* 17**,** 7230-9.

CHEN, P. J., LEE, P. H., HAN, K. H., FAN, J., CHEUNG, T. T., HU, R. H., PAIK, S. W., LEE, W. C., CHAU, G. Y., JENG, L. B., WANG, H. J., CHOI, J. Y., CHEN, C. L., CHO, M., HO, M. C., WU, C. C., LEE, K. S., MAO, Y., HU, F. C. & LAI, K. L. 2017c. 624PDA phase III trial of muparfostat (PI-88) as adjuvant therapy in patients with hepatitis virus related hepatocellular carcinoma (HV-HCC) after resection. *Annals of Oncology,* 28**,** mdx369.008-mdx369.008.

CHEN, S., ZHANG, X., SUN, Y., HU, Z., LU, S. & MA, X. 2015. Unfractionated heparin attenuates intestinal injury in mouse model of sepsis by inhibiting heparanase. *Int J Clin Exp Pathol,* 8**,** 4903-12.

CHEN, Y., CHEN, Y., HUANG, L. & YU, J. 2012. Evaluation of heparanase and matrix metalloproteinase-9 in patients with cutaneous malignant melanoma. *J Dermatol,* 39**,** 339-43.

CHEN, Y., MAGUIRE, T., HILEMAN, R. E., FROMM, J. R., ESKO, J. D., LINHARDT, R. J. & MARKS, R. M. 1997. Dengue virus infectivity depends on envelope protein binding to target cell heparan sulfate. *Nat Med,* 3**,** 866-71.

CHEN, Y., WANG, Y., HUANG, Y., ZENG, H., HU, B., GUAN, L., ZHANG, H., YU, A. M., JOHNSON, C. H., GONZALEZ, F. J., HUANG, M. & BI, H. 2017d. PPARalpha regulates tumor cell proliferation and senescence via a novel target gene carnitine palmitoyltransferase 1C. *Carcinogenesis,* 38**,** 474-483.

CHENG, B., MONTMASSON, M., TERRADOT, L. & ROUSSELLE, P. 2016. Syndecans as Cell Surface Receptors in Cancer Biology. A Focus on their Interaction with PDZ Domain Proteins. *Front Pharmacol,* 7**,** 10.

CHENG, C.-C., LEE, Y.-H., LIN, S.-P., HUANGFU, W.-C. & LIU, I. H. 2014a. Cell-autonomous heparanase modulates self-renewal and migration in bone marrow-derived mesenchymal stem cells. *Journal of Biomedical Science,* 21**,** 21-21.

CHENG, C. C., LEE, Y. H., LIN, S. P., HUANGFU, W. C. & LIU, I. H. 2014b. Cell-autonomous heparanase modulates self-renewal and migration in bone marrow-derived mesenchymal stem cells. *J Biomed Sci,* 21**,** 21.

CHENG, Y., LI, H., DENG, Y., TAI, Y., ZENG, K., ZHANG, Y., LIU, W., ZHANG, Q. & YANG, Y. 2018. Cancer-associated fibroblasts induce PDL1+ neutrophils through the IL6-STAT3 pathway that foster immune suppression in hepatocellular carcinoma. *Cell Death & Disease,* 9**,** 422.

CHIANG, S. P., CABRERA, R. M. & SEGALL, J. E. 2016. Tumor cell intravasation. *Am J Physiol Cell Physiol,* 311**,** C1-C14.

CHIBA, T., MARUSAWA, H. & USHIJIMA, T. 2012. Inflammation-associated cancer development in digestive organs: mechanisms and roles for genetic and epigenetic modulation. *Gastroenterology,* 143**,** 550-563.

CHIEN, C. H., LEE, M. J., LIOU, H. C., LIOU, H. H. & FU, W. M. 2015. Local immunosuppressive microenvironment enhances migration of melanoma cells to lungs in DJ-1 knockout mice. *PLoS One,* 10**,** e0115827.

CHIOSSONE, L., CHAIX, J., FUSERI, N., ROTH, C., VIVIER, E. & WALZER, T. 2009. Maturation of mouse NK cells is a 4-stage developmental program. *Blood,* 113**,** 5488-96.

CHUA, A. C., HODSON, L. J., MOLDENHAUER, L. M., ROBERTSON, S. A. & INGMAN, W. V. 2010. Dual roles for macrophages in ovarian cycle-associated development and remodelling of the mammary gland epithelium. *Development,* 137**,** 4229-38.

CIBRIÁN, D. & SÁNCHEZ-MADRID, F. 2017. CD69: from activation marker to metabolic gatekeeper. *European Journal of Immunology,* 47**,** 946-953.

CLEVERS, H. 2011. The cancer stem cell: premises, promises and challenges. *Nature Medicine,* 17**,** 313.

COCHRAN, S., LI, C., FAIRWEATHER, J. K., KETT, W. C., COOMBE, D. R. & FERRO, V. 2003. Probing the interactions of phosphosulfomannans with angiogenic growth factors by surface plasmon resonance. *J Med Chem,* 46**,** 4601-8.

COHEN-KAPLAN, V., DOWECK, I., NARODITSKY, I., VLODAVSKY, I. & ILAN, N. 2008a. Heparanase augments epidermal growth factor receptor phosphorylation: correlation with head and neck tumor progression. *Cancer Res,* 68**,** 10077-85.

COHEN-KAPLAN, V., JRBASHYAN, J., YANIR, Y., NARODITSKY, I., BEN-IZHAK, O., ILAN, N., DOWECK, I. & VLODAVSKY, I. 2012. Heparanase induces signal transducer and activator of transcription (STAT) protein phosphorylation: preclinical and clinical significance in head and neck cancer. *J Biol Chem,* 287**,** 6668-78.

COHEN-KAPLAN, V., NARODITSKY, I., ZETSER, A., ILAN, N., VLODAVSKY, I. & DOWECK, I. 2008b. Heparanase induces VEGF C and facilitates tumor lymphangiogenesis. *Int J Cancer,* 123**,** 2566-73.

COHEN, E., DOWECK, I., NARODITSKY, I., BEN-IZHAK, O., KREMER, R., BEST, L. A., VLODAVSKY, I. & ILAN, N. 2008. Heparanase is overexpressed in lung cancer and correlates inversely with patient survival. *Cancer,* 113**,** 1004-11.

COHEN, I., MALY, B., SIMON, I., MEIROVITZ, A., PIKARSKY, E., ZCHARIA, E., PERETZ, T., VLODAVSKY, I. & ELKIN, M. 2007. Tamoxifen induces heparanase expression in estrogen receptor-positive breast cancer. *Clin Cancer Res,* 13**,** 4069-77.

COHEN, I., PAPPO, O., ELKIN, M., SAN, T., BAR-SHAVIT, R., HAZAN, R., PERETZ, T., VLODAVSKY, I. & ABRAMOVITCH, R. 2006. Heparanase promotes growth, angiogenesis and survival of primary breast tumors. *Int J Cancer,* 118**,** 1609-17.

COLE, G. J., LOEWY, A. & GLASER, L. 1986. Neuronal cell–cell adhesion depends on interactions of N-CAM with heparin-like molecules. *Nature,* 320**,** 445.

COLLABORATIVE GROUP ON HORMONAL FACTORS IN BREAST, C. 2012. Menarche, menopause, and breast cancer risk: individual participant meta-analysis, including 118 964 women with breast cancer from 117 epidemiological studies. *Lancet Oncol,* 13**,** 1141-51.

COMOGLIO, P. M., TRUSOLINO, L. & BOCCACCIO, C. 2018. Known and novel roles of the MET oncogene in cancer: a coherent approach to targeted therapy. *Nat Rev Cancer*.

COOKE, VESSELINA G., LEBLEU, VALERIE S., KESKIN, D., KHAN, Z., O'CONNELL, JOYCE T., TENG, Y., DUNCAN, MICHAEL B., XIE, L., MAEDA, G., VONG, S., SUGIMOTO, H., ROCHA, RAFAEL M., DAMASCENA, A., BRENTANI, RICARDO R. & KALLURI, R. 2012. Pericyte Depletion Results in Hypoxia-Associated Epithelial-to-Mesenchymal Transition and Metastasis Mediated by Met Signaling Pathway. *Cancer Cell,* 21**,** 66-81.

COONEY, C. A., JOUSHEGHANY, F., YAO-BORENGASSER, A., PHANAVANH, B., GOMES, T., KIEBER-EMMONS, A. M., SIEGEL, E. R., SUVA, L. J., FERRONE, S., KIEBER-EMMONS, T. & MONZAVI-KARBASSI, B. 2011. Chondroitin sulfates play a major role in breast cancer metastasis: a role for CSPG4 and CHST11gene expression in forming surface P-selectin ligands in aggressive breast cancer cells. *Breast Cancer Research,* 13**,** R58.

CORSELLO, S. M., BITTKER, J. A., LIU, Z., GOULD, J., MCCARREN, P., HIRSCHMAN, J. E., JOHNSTON, S. E., VRCIC, A., WONG, B., KHAN, M., ASIEDU, J., NARAYAN, R., MADER, C. C., SUBRAMANIAN, A. & GOLUB, T. R. 2017. The Drug Repurposing Hub: a next-generation drug library and information resource. *Nature medicine,* 23**,** 405-408.

COSTA-SILVA, B., AIELLO, N. M., OCEAN, A. J., SINGH, S., ZHANG, H., THAKUR, B. K., BECKER, A., HOSHINO, A., MARK, M. T., MOLINA, H., XIANG, J., ZHANG, T., THEILEN, T.-M., GARCÍA-SANTOS, G., WILLIAMS, C., ARARSO, Y., HUANG, Y., RODRIGUES, G., SHEN, T.-L., LABORI, K. J., LOTHE, I. M. B., KURE, E. H., HERNANDEZ, J., DOUSSOT, A., EBBESEN, S. H., GRANDGENETT, P. M., HOLLINGSWORTH, M. A., JAIN, M., MALLYA, K., BATRA, S. K., JARNAGIN, W. R., SCHWARTZ, R. E., MATEI, I., PEINADO, H., STANGER, B. Z., BROMBERG, J. & LYDEN, D. C. 2015. Pancreatic cancer exosomes initiate pre-metastatic niche formation in the liver. *Nature cell biology,* 17**,** 816-826.

COUCHMAN, J. R., GOPAL, S., LIM, H. C., NORGAARD, S. & MULTHAUPT, H. A. 2015. Fell-Muir Lecture: Syndecans: from peripheral coreceptors to mainstream regulators of cell behaviour. *Int J Exp Pathol,* 96**,** 1-10.

COURTNEIDGE, S. A. & SMITH, A. E. 1983. Polyoma virus transforming protein associates with the product of the c-src cellular gene. *Nature,* 303**,** 435-9.

COURTNEY, S. M., HAY, P. A., BUCK, R. T., COLVILLE, C. S., PHILLIPS, D. J., SCOPES, D. I., POLLARD, F. C., PAGE, M. J., BENNETT, J. M., HIRCOCK, M. L., MCKENZIE, E. A., BHAMAN, M., FELIX, R., STUBBERFIELD, C. R. & TURNER, P. R. 2005. Furanyl-1,3-thiazol-2-yl and benzoxazol-5-yl acetic acid derivatives: novel classes of heparanase inhibitor. *Bioorg Med Chem Lett,* 15**,** 2295-9.

COURTNEY, S. M., HAY, P. A., BUCK, R. T., COLVILLE, C. S., PORTER, D. W., SCOPES, D. I. C., POLLARD, F. C., PAGE, M. J., BENNETT, J. M., HIRCOCK, M. L., MCKENZIE, E. A., STUBBERFIELD, C. R. & TURNER, P. R. 2004. 2,3-Dihydro-1,3-dioxo-1H-isoindole-5-carboxylic acid derivatives: a novel class of small molecule heparanase inhibitors. *Bioorganic & Medicinal Chemistry Letters,* 14**,** 3269-3273.

COUSSENS, L. M. & POLLARD, J. W. 2011. Leukocytes in Mammary Development and Cancer. *Cold Spring Harbor Perspectives in Biology,* 3**,** a003285.

COWELL, C. F., WEIGELT, B., SAKR, R. A., NG, C. K. Y., HICKS, J., KING, T. A. & REIS-FILHO, J. S. 2013. Progression from ductal carcinoma in situ to invasive breast cancer: Revisited. *Molecular Oncology,* 7**,** 859-869.

COX, T. R. & ERLER, J. T. 2014. Molecular pathways: connecting fibrosis and solid tumor metastasis. *Clin Cancer Res,* 20**,** 3637-43.

COX, T. R. & ERLER, J. T. 2016. Fibrosis and Cancer: Partners in Crime or Opposing Forces? *Trends Cancer,* 2**,** 279-282.

CRAWFORD, B. E., GARNER, O. B., BISHOP, J. R., ZHANG, D. Y., BUSH, K. T., NIGAM, S. K. & ESKO, J. D. 2010. Loss of the heparan sulfate sulfotransferase, Ndst1, in mammary epithelial cells selectively blocks lobuloalveolar development in mice. *PLoS One,* 5**,** e10691.

CRISPEL, Y., AXELMAN, E., TATOUR, M., KOGAN, I., NEVO, N., BRENNER, B. & NADIR, Y. 2016. Peptides inhibiting heparanase procoagulant activity significantly reduce tumour growth and vascularisation in a mouse model. *Thromb Haemost,* 116**,** 669-78.

CRUSZ, S. M. & BALKWILL, F. R. 2015. Inflammation and cancer: advances and new agents. *Nat Rev Clin Oncol,* 12**,** 584-96.

CUEVAS, B. D., WINTER-VANN, A. M., JOHNSON, N. L. & JOHNSON, G. L. 2006. MEKK1 controls matrix degradation and tumor cell dissemination during metastasis of polyoma middle-T driven mammary cancer. *Oncogene,* 25**,** 4998-5010.

CUI, H., TAN, Y. X., OSTERHOLM, C., ZHANG, X., HEDIN, U., VLODAVSKY, I. & LI, J. P. 2016. Heparanase expression upregulates platelet adhesion activity and thrombogenicity. *Oncotarget,* 7**,** 39486-39496.

CUNNICK, G. H., JIANG, W. G., DOUGLAS-JONES, T., WATKINS, G., GOMEZ, K. F., MORGAN, M. J., SUBRAMANIAN, A., MOKBEL, K. & MANSEL, R. E. 2008.

Lymphangiogenesis and lymph node metastasis in breast cancer. *Molecular Cancer,* 7**,** 23.

CURIEL, T. J., COUKOS, G., ZOU, L., ALVAREZ, X., CHENG, P., MOTTRAM, P., EVDEMON-HOGAN, M., CONEJO-GARCIA, J. R., ZHANG, L., BUROW, M., ZHU, Y., WEI, S., KRYCZEK, I., DANIEL, B., GORDON, A., MYERS, L., LACKNER, A., DISIS, M. L., KNUTSON, K. L., CHEN, L. & ZOU, W. 2004. Specific recruitment of regulatory T cells in ovarian carcinoma fosters immune privilege and predicts reduced survival. *Nat Med,* 10**,** 942-9.

CURIEL, T. J., WEI, S., DONG, H., ALVAREZ, X., CHENG, P., MOTTRAM, P., KRZYSIEK, R., KNUTSON, K. L., DANIEL, B., ZIMMERMANN, M. C., DAVID, O., BUROW, M., GORDON, A., DHURANDHAR, N., MYERS, L., BERGGREN, R., HEMMINKI, A., ALVAREZ, R. D., EMILIE, D., CURIEL, D. T., CHEN, L. & ZOU, W. 2003. Blockade of B7-H1 improves myeloid dendritic cell-mediated antitumor immunity. *Nat Med,* 9**,** 562-7.

CURRIE, E., SCHULZE, A., ZECHNER, R., WALTHER, TOBIAS C. & FARESE, ROBERT V., JR. 2013. Cellular Fatty Acid Metabolism and Cancer. *Cell Metabolism,* 18**,** 153-161.

CURTIS, C., SHAH, S. P., CHIN, S. F., TURASHVILI, G., RUEDA, O. M., DUNNING, M. J., SPEED, D., LYNCH, A. G., SAMARAJIWA, S., YUAN, Y., GRAF, S., HA, G., HAFFARI, G., BASHASHATI, A., RUSSELL, R., MCKINNEY, S., LANGEROD, A., GREEN, A., PROVENZANO, E., WISHART, G., PINDER, S., WATSON, P., MARKOWETZ, F., MURPHY, L., ELLIS, I., PURUSHOTHAM, A., BORRESEN-DALE, A. L., BRENTON, J. D., TAVARE, S., CALDAS, C. & APARICIO, S. 2012. The genomic and transcriptomic architecture of 2,000 breast tumours reveals novel subgroups. *Nature,* 486**,** 346-52.

D'AGOSTINO, G., RUSSO, R., AVAGLIANO, C., CRISTIANO, C., MELI, R. & CALIGNANO, A. 2012. Palmitoylethanolamide protects against the amyloid-β25-35-induced learning and memory impairment in mice, an experimental model of Alzheimer disease. *Neuropsychopharmacology : official publication of the American College of Neuropsychopharmacology,* 37**,** 1784-1792.

DAGOGO-JACK, I. & SHAW, A. T. 2017. Tumour heterogeneity and resistance to cancer therapies. *Nature Reviews Clinical Oncology,* 15**,** 81.

DAI, X. Y., YAN, J., FU, X., PAN, Q., SUN, D., XU, Y., WANG, J., NIE, L., TONG, L. J., SHEN, A., ZHENG, M., HUANG, M., TAN, M., LIU, H., HUANG, X., DING, J. & GENG, M. 2017. Aspirin inhibits cancer metastasis and angiogenesis via targeting heparanase. *Clin Cancer Res*.

DARBRO, B. W., MAHAJAN, V. B., GAKHAR, L., SKEIE, J. M., CAMPBELL, E., WU, S., BING, X., MILLEN, K. J., DOBYNS, W. B., KESSLER, J. A., JALALI, A., CREMER, J., SEGRE, A., MANAK, J. R., ALDINGER, K. A., SUZUKI, S., NATSUME, N., ONO, M., HAI, H. D., VIET, L. T., LODDO, S., VALENTE, E. M., BERNARDINI, L., GHONGE, N., FERGUSON, P. J. & BASSUK, A. G. 2013. Mutations in extracellular matrix genes NID1 and LAMC1 cause autosomal dominant Dandy-Walker malformation and occipital cephaloceles. *Human mutation,* 34**,** 1075-1079.

DATTA, S., PIERCE, M. & DATTA, M. W. 2006. Perlecan signaling: helping hedgehog stimulate prostate cancer growth. *Int J Biochem Cell Biol,* 38**,** 1855-61.

DAVID, G. & ZIMMERMANN, P. 2016a. Heparanase tailors syndecan for exosome production. *Mol Cell Oncol,* 3**,** e1047556.

DAVID, G. & ZIMMERMANN, P. 2016b. Heparanase tailors syndecan for exosome production. *Molecular & Cellular Oncology,* 3**,** e1047556.

DAVYDOVA, N., HARRIS, N. C., ROUFAIL, S., PAQUET-FIFIELD, S., ISHAQ, M., STRELTSOV, V. A., WILLIAMS, S. P., KARNEZIS, T., STACKER, S. A. & ACHEN, M. G. 2016. Differential Receptor Binding and Regulatory Mechanisms for the Lymphangiogenic Growth Factors Vascular Endothelial Growth Factor (VEGF)-C and -D. *J Biol Chem,* 291**,** 27265-27278.

DE CICCO, M. 2004. The prothrombotic state in cancer: pathogenic mechanisms. *Crit Rev Oncol Hematol,* 50**,** 187-96.

DE DUVE, C., PRESSMAN, B. C., GIANETTO, R., WATTIAUX, R. & APPELMANS, F. 1955. Tissue fractionation studies. 6. Intracellular distribution patterns of enzymes in rat-liver tissue. *Biochem J,* 60**,** 604-17.

DE LIMA, C. R., DOS SANTOS, J. D. A., NAZÁRIO, A. C. P. & MICHELACCI, Y. M. 2012. Changes in glycosaminoglycans and proteoglycans of normal breast and fibroadenoma during the menstrual cycle. *Biochimica et Biophysica Acta (BBA) - General Subjects,* 1820**,** 1009-1019.

DE MESTRE, A. M., KHACHIGIAN, L. M., SANTIAGO, F. S., STAYKOVA, M. A. & HULETT, M. D. 2003. Regulation of inducible heparanase gene transcription in activated T cells by early growth response 1. *J Biol Chem,* 278**,** 50377-85.

DE MESTRE, A. M., RAO, S., HORNBY, J. R., SOE-HTWE, T., KHACHIGIAN, L. M. & HULETT, M. D. 2005. Early growth response gene 1 (EGR1) regulates heparanase gene transcription in tumor cells. *J Biol Chem,* 280**,** 35136-47.

DE MESTRE, A. M., SOE-HTWE, T., SUTCLIFFE, E. L., RAO, S., PAGLER, E. B., HORNBY, J. R. & HULETT, M. D. 2007. Regulation of mouse Heparanase gene expression in T lymphocytes and tumor cells. *Immunol Cell Biol,* 85**,** 205-14.

DE PALMA, M., BIZIATO, D. & PETROVA, T. V. 2017a. Microenvironmental regulation of tumour angiogenesis. *Nature Reviews Cancer,* 17**,** 457.

DE PALMA, M., BIZIATO, D. & PETROVA, T. V. 2017b. Microenvironmental regulation of tumour angiogenesis. *Nat Rev Cancer,* 17**,** 457-474.

DEBERGH, I., VAN DAMME, N., PATTYN, P., PEETERS, M. & CEELEN, W. P. 2010. The low-molecular-weight heparin, nadroparin, inhibits tumour angiogenesis in a rodent dorsal skinfold chamber model. *British Journal Of Cancer,* 102**,** 837.

DEEPA, S. S., YAMADA, S., ZAKO, M., GOLDBERGER, O. & SUGAHARA, K. 2004. Chondroitin sulfate chains on syndecan-1 and syndecan-4 from normal murine mammary gland epithelial cells are structurally and functionally distinct and cooperate with heparan sulfate chains to bind growth factors. A novel function to control binding of midkine, pleiotrophin, and basic fibroblast growth factor. *J Biol Chem,* 279**,** 37368-76.

DEGENHARDT, K., MATHEW, R., BEAUDOIN, B., BRAY, K., ANDERSON, D., CHEN, G., MUKHERJEE, C., SHI, Y., GELINAS, C., FAN, Y., NELSON, D. A., JIN, S. & WHITE, E. 2006. Autophagy promotes tumor cell survival and restricts necrosis, inflammation, and tumorigenesis. *Cancer Cell,* 10**,** 51-64.

DELEHEDDE, M., LYON, M., SERGEANT, N., RAHMOUNE, H. & FERNIG, D. G. 2001. Proteoglycans: pericellular and cell surface multireceptors that integrate external stimuli in the mammary gland. *J Mammary Gland Biol Neoplasia,* 6**,** 253-73.

DEMOULIN, J. B. & ESSAGHIR, A. 2014. PDGF receptor signaling networks in normal and cancer cells. *Cytokine Growth Factor Rev,* 25**,** 273-83.

DEMPSEY, L. A., PLUMMER, T. B., COOMBES, S. L. & PLATT, J. L. 2000. Heparanase expression in invasive trophoblasts and acute vascular damage. *Glycobiology,* 10**,** 467-75.

DENARDO, D. G., BARRETO, J. B., ANDREU, P., VASQUEZ, L., TAWFIK, D., KOLHATKAR, N. & COUSSENS, L. M. 2009. CD4(+) T cells regulate pulmonary metastasis of mammary carcinomas by enhancing protumor properties of macrophages. *Cancer Cell,* 16**,** 91-102.

DENKERT, C., LIEDTKE, C., TUTT, A. & VON MINCKWITZ, G. 2017. Molecular alterations in triple-negative breast cancer-the road to new treatment strategies. *Lancet,* 389**,** 2430-2442.

DERYUGINA, E. I. & KIOSSES, W. B. 2017. Intratumoral Cancer Cell Intravasation Can Occur Independent of Invasion into the Adjacent Stroma. *Cell Rep,* 19**,** 601-616.

DERYUGINA, E. I. & QUIGLEY, J. P. 2015. Tumor Angiogenesis: MMP-Mediated Induction of Intravasation- and Metastasis-Sustaining Neovasculature. *Matrix biology : journal of the International Society for Matrix Biology,* 44-46**,** 94-112.

DESANTIS, C. E., BRAY, F., FERLAY, J., LORTET-TIEULENT, J., ANDERSON, B. O. & JEMAL, A. 2015. International Variation in Female Breast Cancer Incidence and Mortality Rates. *Cancer Epidemiol Biomarkers Prev,* 24**,** 1495-506.

DICKSON, M. & GAGNON, J. P. 2004. Key factors in the rising cost of new drug discovery and development. *Nat Rev Drug Discov,* 3**,** 417-29.

DIGRE, A., SINGH, K., ABRINK, M., REIJMERS, R. M., SANDLER, S., VLODAVSKY, I. & LI, J. P. 2017. Overexpression of heparanase enhances T lymphocyte activities and intensifies the inflammatory response in a model of murine rheumatoid arthritis. *Sci Rep,* 7**,** 46229.

DIKIC, I. & ELAZAR, Z. 2018. Mechanism and medical implications of mammalian autophagy. *Nat Rev Mol Cell Biol*.

DILWORTH, S. M. 2002. Polyoma virus middle T antigen and its role in identifying cancer-related molecules. *Nature Reviews Cancer,* 2**,** 951.

DOHERTY, J. R. & CLEVELAND, J. L. 2013. Targeting lactate metabolism for cancer therapeutics. *J Clin Invest,* 123**,** 3685-92.

DÖME, B., HENDRIX, M. J. C., PAKU, S., TÓVÁRI, J. & TÍMÁR, J. 2007. Alternative Vascularization Mechanisms in Cancer: Pathology and Therapeutic Implications. *The American Journal of Pathology,* 170**,** 1-15.

DONG, J., KUKULA, A. K., TOYOSHIMA, M. & NAKAJIMA, M. 2000. Genomic organization and chromosome localization of the newly identified human heparanase gene. *Gene,* 253**,** 171-8.

DOVE, A. 2002a. MMP inhibitors: glimmers of hope amidst clinical failures. *Nat Med,* 8**,** 95.

DOVE, A. 2002b. MMP inhibitors: Glimmers of hope amidst clinical failures. *Nature Medicine,* 8**,** 95.

DOWECK, I., KAPLAN-COHEN, V., NARODITSKY, I., SABO, E., ILAN, N. & VLODAVSKY, I. 2006. Heparanase Localization and Expression by Head and Neck Cancer: Correlation with Tumor Progression and Patient Survival. *Neoplasia (New York, N.Y.),* 8**,** 1055-1061.

DREDGE, K., HAMMOND, E., DAVIS, K., LI, C. P., LIU, L., JOHNSTONE, K., HANDLEY, P., WIMMER, N., GONDA, T. J., GAUTAM, A., FERRO, V. & BYTHEWAY, I. 2010. The PG500 series: novel heparan sulfate mimetics as potent angiogenesis and heparanase inhibitors for cancer therapy. *Invest New Drugs,* 28**,** 276-83.

DREDGE, K., HAMMOND, E., HANDLEY, P., GONDA, T. J., SMITH, M. T., VINCENT, C., BRANDT, R., FERRO, V. & BYTHEWAY, I. 2011. PG545, a dual heparanase and angiogenesis inhibitor, induces potent anti-tumour and anti-metastatic efficacy in preclinical models. *Br J Cancer,* 104**,** 635-42.

DUDLEY, J. P., GOLOVKINA, T. V. & ROSS, S. R. 2016. Lessons Learned from Mouse Mammary Tumor Virus in Animal Models. *ILAR Journal,* 57**,** 12-23.

DUFFY, M. J. 1992. The role of proteolytic enzymes in cancer invasion and metastasis. *Clinical & Experimental Metastasis,* 10**,** 145-155.

DUFFY, M. J. 1996. Proteases as prognostic markers in cancer. *Clin Cancer Res,* 2**,** 613-8.

DUIVENVOORDEN, H. M., RAUTELA, J., EDGINGTON-MITCHELL, L. E., SPURLING, A., GREENING, D. W., NOWELL, C. J., MOLLOY, T. J., ROBBINS, E., BROCKWELL, N. K., LEE, C. S., CHEN, M., HOLLIDAY, A., SELINGER, C. I., HU,

M., BRITT, K. L., STROUD, D. A., BOGYO, M., MOLLER, A., POLYAK, K., SLOANE, B. F., O'TOOLE, S. A. & PARKER, B. S. 2017. Myoepithelial cell-specific expression of stefin A as a suppressor of early breast cancer invasion. *J Pathol,* 243**,** 496-509.

DUIVENVOORDEN, H. M., SPURLING, A., O'TOOLE, S. A. & PARKER, B. S. 2018. Discriminating the earliest stages of mammary carcinoma using myoepithelial and proliferative markers. *PLOS ONE,* 13**,** e0201370.

DUMAN-SCHEEL, M., WENG, L., XIN, S. & DU, W. 2002. Hedgehog regulates cell growth and proliferation by inducing Cyclin D and Cyclin E. *Nature,* 417**,** 299-304.

DUNBAR, E. M., COATS, B. S., SHROADS, A. L., LANGAEE, T., LEW, A., FORDER, J. R., SHUSTER, J. J., WAGNER, D. A. & STACPOOLE, P. W. 2014. Phase 1 trial of dichloroacetate (DCA) in adults with recurrent malignant brain tumors. *Invest New Drugs,* 32**,** 452-64.

DURGEAU, A., VIRK, Y., CORGNAC, S. & MAMI-CHOUAIB, F. 2018. Recent Advances in Targeting CD8 T-Cell Immunity for More Effective Cancer Immunotherapy. *Frontiers in immunology,* 9**,** 14-14.

DVORAK, H. F. 1986. Tumors: wounds that do not heal. Similarities between tumor stroma generation and wound healing. *N Engl J Med,* 315**,** 1650-9.

DVORAK, H. F. 2015. Tumor Stroma, Tumor Blood Vessels, and Antiangiogenesis Therapy. *Cancer J,* 21**,** 237-43.

DYRSTAD, S. W., YAN, Y., FOWLER, A. M. & COLDITZ, G. A. 2015. Breast cancer risk associated with benign breast disease: systematic review and meta-analysis. *Breast Cancer Res Treat,* 149**,** 569-75.

EALES, K. L., HOLLINSHEAD, K. E. R. & TENNANT, D. A. 2016. Hypoxia and metabolic adaptation of cancer cells. *Oncogenesis,* 5**,** e190.

EARL, H. M., HILLER, L., DUNN, J. A., BLENKINSOP, C., GRYBOWICZ, L., VALLIER, A. L., ABRAHAM, J., THOMAS, J., PROVENZANO, E., HUGHES-DAVIES, L., GOUNARIS, I., MCADAM, K., CHAN, S., AHMAD, R., HICKISH, T., HOUSTON, S., REA, D., BARTLETT, J., CALDAS, C., CAMERON, D. A. & HAYWARD, L. 2015. Efficacy of neoadjuvant bevacizumab added to docetaxel followed by fluorouracil, epirubicin, and cyclophosphamide, for women with HER2-negative early breast cancer (ARTemis): an open-label, randomised, phase 3 trial. *Lancet Oncol,* 16**,** 656-66.

EDOVITSKY, E., ELKIN, M., ZCHARIA, E., PERETZ, T. & VLODAVSKY, I. 2004. Heparanase gene silencing, tumor invasiveness, angiogenesis, and metastasis. *J Natl Cancer Inst,* 96**,** 1219-30.

EDOVITSKY, E., LERNER, I., ZCHARIA, E., PERETZ, T., VLODAVSKY, I. & ELKIN, M. 2006. Role of endothelial heparanase in delayed-type hypersensitivity. *Blood,* 107**,** 3609-16.

EGEBERG, M., KJEKEN, R., KOLSET, S. O., BERG, T. & PRYDZ, K. 2001. Internalization and stepwise degradation of heparan sulfate proteoglycans in rat hepatocytes. *Biochim Biophys Acta,* 1541**,** 135-49.

EGELSTON, C., SRINIVASAN, G., AVALOS, C., HUANG, Y., ROSARIO, A., WANG, R., JIMENEZ, G., SIMONS, D. L., YOST, S., YUAN, Y. & LEE, P. P. 2017. CD8+ tissue resident memory T cells are associated with good prognosis in breast cancer patients. *The Journal of Immunology,* 198**,** 196.11-196.11.

EGELSTON, C. A., AVALOS, C., TU, T. Y., SIMONS, D. L., JIMENEZ, G., JUNG, J. Y., MELSTROM, L., MARGOLIN, K., YIM, J. H., KRUPER, L., MORTIMER, J. & LEE, P. P. 2018. Human breast tumor-infiltrating CD8+ T cells retain polyfunctionality despite PD-1 expression. *Nature Communications,* 9**,** 4297.

EHRLICH, P. 1909. Über den jetzigen Stand der Chemotherapie. *Berichte der deutschen chemischen Gesellschaft,* 42.

EL-ASSAL, O. N., YAMANOI, A., ONO, T., KOHNO, H. & NAGASUE, N. 2001. The clinicopathological significance of heparanase and basic fibroblast growth factor expressions in hepatocellular carcinoma. *Clin Cancer Res,* 7**,** 1299-305.

ELINAV, E., NOWARSKI, R., A THAISS, C., HU, B., JIN, C. & FLAVELL, R. 2013. *Inflammation-induced cancer: Crosstalk between tumours, immune cells and microorganisms*.

ELKIN, M., COHEN, I., ZCHARIA, E., ORGEL, A., GUATTA-RANGINI, Z., PERETZ, T., VLODAVSKY, I. & KLEINMAN, H. K. 2003. Regulation of heparanase gene expression by estrogen in breast cancer. *Cancer Res,* 63**,** 8821-6.

ENOMOTO, K., OKAMOTO, H., NUMATA, Y. & TAKEMOTO, H. 2006. A simple and rapid assay for heparanase activity using homogeneous time-resolved fluorescence. *Journal of Pharmaceutical and Biomedical Analysis,* 41**,** 912-917.

EREZ, N., TRUITT, M., OLSON, P., ARRON, S. T. & HANAHAN, D. 2010a. Cancer-Associated Fibroblasts Are Activated in Incipient Neoplasia to Orchestrate Tumor-Promoting Inflammation in an NF-kappaB-Dependent Manner. *Cancer Cell,* 17**,** 135-47.

EREZ, N., TRUITT, M., OLSON, P. & HANAHAN, D. 2010b. Cancer-Associated Fibroblasts Are Activated in Incipient Neoplasia to Orchestrate Tumor-Promoting Inflammation in an NF-κB-Dependent Manner. *Cancer Cell,* 17**,** 135-147.

ERLER, J. T. & GIACCIA, A. J. 2006. Lysyl oxidase mediates hypoxic control of metastasis. *Cancer Res,* 66**,** 10238-41.

ESCOBAR GALVIS, M. L., JIA, J., ZHANG, X., JASTREBOVA, N., SPILLMANN, D., GOTTFRIDSSON, E., VAN KUPPEVELT, T. H., ZCHARIA, E., VLODAVSKY, I., LINDAHL, U. & LI, J. P. 2007. Transgenic or tumor-induced expression of heparanase upregulates sulfation of heparan sulfate. *Nat Chem Biol,* 3**,** 773-8.

ESHCHENKO, T. Y., RYKOVA, V. I., CHERNAKOV, A. E., SIDOROV, S. V. & GRIGORIEVA, E. V. 2007. Expression of different proteoglycans in human breast tumors. *Biochemistry (Moscow),* 72**,** 1016-1020.

ESTRELLA, V., CHEN, T., LLOYD, M., WOJTKOWIAK, J., CORNNELL, H. H., IBRAHIM-HASHIM, A., BAILEY, K., BALAGURUNATHAN, Y., ROTHBERG, J. M., SLOANE, B. F., JOHNSON, J., GATENBY, R. A. & GILLIES, R. J. 2013. Acidity generated by the tumor microenvironment drives local invasion. *Cancer Res,* 73**,** 1524-35.

EVAN, G. I., WYLLIE, A. H., GILBERT, C. S., LITTLEWOOD, T. D., LAND, H., BROOKS, M., WATERS, C. M., PENN, L. Z. & HANCOCK, D. C. 1992. Induction of apoptosis in fibroblasts by c-myc protein. *Cell,* 69**,** 119-28.

EWING, J. 1928. Neoplastic diseases. A treatise on tumors. *Am J Med Sci.* W. B. Saunders Co. Ltd.

FAIRBANKS, M. B., MILDNER, A. M., LEONE, J. W., CAVEY, G. S., MATHEWS, W. R., DRONG, R. F., SLIGHTOM, J. L., BIENKOWSKI, M. J., SMITH, C. W., BANNOW, C. A. & HEINRIKSON, R. L. 1999. Processing of the human heparanase precursor and evidence that the active enzyme is a heterodimer. *J Biol Chem,* 274**,** 29587-90.

FAKHREJAHANI, E. & TOI, M. 2014. Antiangiogenesis therapy for breast cancer: an update and perspectives from clinical trials. *Jpn J Clin Oncol,* 44**,** 197-207.

FANTIN, V. R., ST-PIERRE, J. & LEDER, P. 2006. Attenuation of LDH-A expression uncovers a link between glycolysis, mitochondrial physiology, and tumor maintenance. *Cancer Cell,* 9**,** 425-34.

FARACH-CARSON, M. C., WARREN, C. R., HARRINGTON, D. A. & CARSON, D. D. 2014. Border patrol: insights into the unique role of perlecan/heparan sulfate proteoglycan 2 at cell and tissue borders. *Matrix Biol,* 34**,** 64-79.

FARRUGIA, B. L., LORD, M. S., MELROSE, J. & WHITELOCK, J. M. 2018. The Role of Heparan Sulfate in Inflammation, and the Development of Biomimetics as Anti-Inflammatory Strategies. *J Histochem Cytochem,* 66**,** 321-336.

FATA, J. E., CHAUDHARY, V. & KHOKHA, R. 2001. Cellular Turnover in the Mammary Gland Is Correlated with Systemic Levels of Progesterone and Not 17β-Estradiol During the Estrous Cycle1. *Biology of Reproduction,* 65**,** 680-688.

FATA, J. E., WERB, Z. & BISSELL, M. J. 2003. Regulation of mammary gland branching morphogenesis by the extracellular matrix and its remodeling enzymes. *Breast Cancer Research,* 6**,** 1.

FAUBERT, B., LI, K. Y., CAI, L., HENSLEY, C. T., KIM, J., ZACHARIAS, L. G., YANG, C., DO, Q. N., DOUCETTE, S., BURGUETE, D., LI, H., HUET, G., YUAN, Q., WIGAL, T., BUTT, Y., NI, M., TORREALBA, J., OLIVER, D., LENKINSKI, R. E., MALLOY, C. R., WACHSMANN, J. W., YOUNG, J. D., KERNSTINE, K. & DEBERARDINIS, R. J. 2017. Lactate Metabolism in Human Lung Tumors. *Cell,* 171**,** 358-371 e9.

FENTIMAN, I. S., FOURQUET, A. & HORTOBAGYI, G. N. 2006. Male breast cancer. *Lancet,* 367**,** 595-604.

FERGUSON, F. M. & GRAY, N. S. 2018. Kinase inhibitors: the road ahead. *Nat Rev Drug Discov,* 17**,** 353-377.

FERGUSON, J. E., SCHOR, A. M., HOWELL, A. & FERGUSON, M. W. 1992. Changes in the extracellular matrix of the normal human breast during the menstrual cycle. *Cell Tissue Res,* 268**,** 167-77.

FERLAND-MCCOLLOUGH, D., SLATER, S., RICHARD, J., RENI, C. & MANGIALARDI, G. 2017. Pericytes, an overlooked player in vascular pathobiology. *Pharmacology & Therapeutics,* 171**,** 30-42.

FERLAY, J., SOERJOMATARAM, I., DIKSHIT, R., ESER, S., MATHERS, C., REBELO, M., PARKIN, D. M., FORMAN, D. & BRAY, F. 2015. Cancer incidence and mortality worldwide: sources, methods and major patterns in GLOBOCAN 2012. *Int J Cancer,* 136**,** E359-86.

FERNALD, K. & KUROKAWA, M. 2013. Evading apoptosis in cancer. *Trends Cell Biol,* 23**,** 620-33.

FERNANDES DOS SANTOS, T. C., GOMES, A. M., PASCHOAL, M. E., STELLING, M. P., RUMJANEK, V. M., JUNIOR ADO, R., VALIANTE, P. M., MADI, K., PEREIRA DE SOUZA, H. S., PAVAO, M. S. & CASTELO-BRANCO, M. T. 2014. Heparanase expression and localization in different types of human lung cancer. *Biochim Biophys Acta,* 1840**,** 2599-608.

FERNÁNDEZ-VEGA, I., GARCÍA, O., CRESPO, A., CASTAÑÓN, S., MENÉNDEZ, P., ASTUDILLO, A. & QUIRÓS, L. M. 2013. Specific genes involved in synthesis and editing of heparan sulfate proteoglycans show altered expression patterns in breast cancer. *BMC Cancer,* 13**,** 24.

FERON, O. 2009. Pyruvate into lactate and back: from the Warburg effect to symbiotic energy fuel exchange in cancer cells. *Radiother Oncol,* 92**,** 329-33.

FERRARA, N. & HENZEL, W. J. 1989. Pituitary follicular cells secrete a novel heparin-binding growth factor specific for vascular endothelial cells. *Biochemical and Biophysical Research Communications,* 161**,** 851-858.

FERRO, V., DREDGE, K., LIU, L., HAMMOND, E., BYTHEWAY, I., LI, C., JOHNSTONE, K., KAROLI, T., DAVIS, K., COPEMAN, E. & GAUTAM, A. 2007. PI-88 and novel heparan sulfate mimetics inhibit angiogenesis. *Semin Thromb Hemost,* 33**,** 557-68.

FIDLER, I. J. & KRIPKE, M. L. 1977. Metastasis results from preexisting variant cells within a malignant tumor. *Science,* 197**,** 893.

FIDLER, I. J. & NICOLSON, G. L. 1976. Organ selectivity for implantation survival and growth of B16 melanoma variant tumor lines. *J Natl Cancer Inst,* 57**,** 1199-202.

FITZGERALD, R. C., ABDALLA, S., ONWUEGBUSI, B. A., SIRIEIX, P., SAEED, I. T., BURNHAM, W. R. & FARTHING, M. J. 2002. Inflammatory gradient in Barrett's oesophagus: implications for disease complications. *Gut,* 51**,** 316-22.

FLAUMENHAFT, R., MOSCATELLI, D. & RIFKIN, D. B. 1990. Heparin and heparan sulfate increase the radius of diffusion and action of basic fibroblast growth factor. *J Cell Biol,* 111**,** 1651-9.

FLINT, T. R., JANOWITZ, T., CONNELL, C. M., ROBERTS, E. W., DENTON, A. E., COLL, A. P., JODRELL, D. I. & FEARON, D. T. 2016. Tumor-Induced IL-6 Reprograms Host Metabolism to Suppress Anti-tumor Immunity. *Cell Metab,* 24**,** 672-684.

FOLKMAN, J. 1971. Tumor angiogenesis: therapeutic implications. *N Engl J Med,* 285**,** 1182-6.

FOLKMAN, J. 1990. What is the evidence that tumors are angiogenesis dependent? *J Natl Cancer Inst,* 82**,** 4-6.

FOLKMAN, J., TAYLOR, S. & SPILLBERG, C. 1983. The role of heparin in angiogenesis. *Ciba Found Symp,* 100**,** 132-49.

FORREST, L. 1983. Current concepts in soft connective tissue wound healing. *Br J Surg,* 70**,** 133-40.

FORRESTER, E., CHYTIL, A., BIERIE, B., AAKRE, M., GORSKA, A. E., SHARIF-AFSHAR, A. R., MULLER, W. J. & MOSES, H. L. 2005. Effect of conditional knockout of the type II TGF-beta receptor gene in mammary epithelia on mammary gland development and polyomavirus middle T antigen induced tumor formation and metastasis. *Cancer Res,* 65**,** 2296-302.

FRANCHINI, M. & MANNUCCI, P. M. 2015. Low-molecular-weight heparins and cancer: focus on antitumoral effect. *Ann Med,* 47**,** 116-21.

FRANCO, M., ROSWALL, P., CORTEZ, E., HANAHAN, D. & PIETRAS, K. 2011. Pericytes promote endothelial cell survival through induction of autocrine VEGF-A signaling and Bcl-w expression. *Blood,* 118**,** 2906-17.

FRANSSON, L. A., BELTING, M., CHENG, F., JONSSON, M., MANI, K. & SANDGREN, S. 2004. Novel aspects of glypican glycobiology. *Cell Mol Life Sci,* 61**,** 1016-24.

FREEMAN, C. & PARISH, C. R. 1997. A rapid quantitative assay for the detection of mammalian heparanase activity. *Biochem J,* 325 (Pt 1)**,** 229-37.

FREEMAN, C. & PARISH, C. R. 1998. Human platelet heparanase: purification, characterization and catalytic activity. *Biochem J,* 330 (Pt 3)**,** 1341-50.

FREEMAN, G. J., LONG, A. J., IWAI, Y., BOURQUE, K., CHERNOVA, T., NISHIMURA, H., FITZ, L. J., MALENKOVICH, N., OKAZAKI, T., BYRNE, M. C., HORTON, H. F., FOUSER, L., CARTER, L., LING, V., BOWMAN, M. R., CARRENO, B. M., COLLINS, M., WOOD, C. R. & HONJO, T. 2000. Engagement of the PD-1

immunoinhibitory receptor by a novel B7 family member leads to negative regulation of lymphocyte activation. *J Exp Med,* 192**,** 1027-34.

FRIDMAN, R., LIDER, O., NAPARSTEK, Y., FUKS, Z., VLODAVSKY, I. & COHEN, I. R. 1987. Soluble antigen induces T lymphocytes to secrete an endoglycosidase that degrades the heparan sulfate moiety of subendothelial extracellular matrix. *J Cell Physiol,* 130**,** 85-92.

FRIEDL, P., LOCKER, J., SAHAI, E. & SEGALL, J. E. 2012. Classifying collective cancer cell invasion. *Nat Cell Biol,* 14**,** 777-83.

FRIEDMANN, Y., VLODAVSKY, I., AINGORN, H., AVIV, A., PERETZ, T., PECKER, I. & PAPPO, O. 2000. Expression of heparanase in normal, dysplastic, and neoplastic human colonic mucosa and stroma. Evidence for its role in colonic tumorigenesis. *Am J Pathol,* 157**,** 1167-75.

FU, B., TIAN, Z. & WEI, H. 2014. Subsets of human natural killer cells and their regulatory effects. *Immunology,* 141**,** 483-489.

FURTH, J., KAHN, M. C. & BREEDIS, C. 1937. The Transmission of Leukemia of Mice with a Single Cell. *The American Journal of Cancer,* 31**,** 276-282.

FUYUHIRO, Y., YASHIRO, M., NODA, S., KASHIWAGI, S., MATSUOKA, J., DOI, Y., KATO, Y., HASEGAWA, T., SAWADA, T. & HIRAKAWA, K. 2011. Upregulation of cancer-associated myofibroblasts by TGF-β from scirrhous gastric carcinoma cells. *British Journal Of Cancer,* 105**,** 996.

GABAY, M., LI, Y. & FELSHER, D. W. 2014. MYC activation is a hallmark of cancer initiation and maintenance. *Cold Spring Harb Perspect Med,* 4.

GAJEWSKI, T. F., SCHREIBER, H. & FU, Y.-X. 2013. Innate and adaptive immune cells in the tumor microenvironment. *Nature Immunology,* 14**,** 1014.

GALLAGHER, J. 2015. Fell-Muir Lecture: Heparan sulphate and the art of cell regulation: a polymer chain conducts the protein orchestra. *Int J Exp Pathol,* 96**,** 203-31.

GALLI, M., CHATTERJEE, M., GRASSO, M., SPECCHIA, G., MAGEN, H., EINSELE, H., CELEGHINI, I., BARBIERI, P., PAOLETTI, D., PACE, S., SANDERSON, R. D., RAMBALDI, A. & NAGLER, A. 2018. Phase I study of the heparanase inhibitor Roneparstat: an innovative approach for multiple myeloma therapy. *Haematologica*.

GAO, S. P., CHANG, Q., MAO, N., DALY, L. A., VOGEL, R., CHAN, T., LIU, S. H., BOURNAZOU, E., SCHORI, E., ZHANG, H., BREWER, M. R., PAO, W., MORRIS, L., LADANYI, M., ARCILA, M., MANOVA-TODOROVA, K., DE STANCHINA, E., NORTON, L., LEVINE, R. L., ALTAN-BONNET, G., SOLIT, D., ZINDA, M., HUSZAR, D., LYDEN, D. & BROMBERG, J. F. 2016. JAK2 inhibition sensitizes resistant EGFR-mutant lung adenocarcinoma to tyrosine kinase inhibitors. *Sci Signal,* 9**,** ra33.

GARCÍA-MENDOZA, M. G., INMAN, D. R., PONIK, S. M., JEFFERY, J. J., SHEERAR, D. S., VAN DOORN, R. R. & KEELY, P. J. 2016. Neutrophils drive accelerated tumor progression in the collagen-dense mammary tumor microenvironment. *Breast Cancer Research,* 18**,** 49.

GARNER, O. B., BUSH, K. T., NIGAM, K. B., YAMAGUCHI, Y., XU, D., ESKO, J. D. & NIGAM, S. K. 2011. Stage-dependent regulation of mammary ductal branching by heparan sulfate and HGF-cMet signaling. *Dev Biol,* 355**,** 394-403.

GAVANDE, N. S., VANDERVERE-CAROZZA, P. S., HINSHAW, H. D., JALAL, S. I., SEARS, C. R., PAWELCZAK, K. S. & TURCHI, J. J. 2016. DNA repair targeted therapy: The past or future of cancer treatment? *Pharmacology & Therapeutics,* 160**,** 65-83.

GAWTHORPE, S., BROWN, J. E., ARIF, M., NIGHTINGALE, P., NEVILL, A. & CARMICHAEL, A. R. 2014. Heparanase and COX-2 expression as predictors of lymph node metastasis in large, high-grade breast tumors. *Anticancer Res,* 34**,** 2797-800.

GEORGE, J. T., JOLLY, M. K., XU, S., SOMARELLI, J. A. & LEVINE, H. 2017. Survival Outcomes in Cancer Patients Predicted by a Partial EMT Gene Expression Scoring Metric. *Cancer Res,* 77**,** 6415-6428.

GERBER, B., LOIBL, S., EIDTMANN, H., REZAI, M., FASCHING, P. A., TESCH, H., EGGEMANN, H., SCHRADER, I., KITTEL, K., HANUSCH, C., KREIENBERG, R., SOLBACH, C., JACKISCH, C., KUNZ, G., BLOHMER, J. U., HUOBER, J., HAUSCHILD, M., NEKLJUDOVA, V., UNTCH, M. & VON MINCKWITZ, G. 2013. Neoadjuvant bevacizumab and anthracycline-taxane-based chemotherapy in 678 triple-negative primary breast cancers; results from the geparquinto study (GBG 44). *Ann Oncol,* 24**,** 2978-84.

GHOSSAIN, A. & GHOSSAIN, M. A. 2009. History of mastectomy before and after Halsted. *J Med Liban,* 57**,** 65-71.

GIL, N., GOLDBERG, R., NEUMAN, T., GARSEN, M., ZCHARIA, E., RUBINSTEIN, A. M., VAN KUPPEVELT, T., MEIROVITZ, A., PISANO, C., LI, J. P., VAN DER VLAG, J., VLODAVSKY, I. & ELKIN, M. 2012. Heparanase is essential for the development of diabetic nephropathy in mice. *Diabetes,* 61**,** 208-16.

GILAT, D., HERSHKOVIZ, R., GOLDKORN, I., CAHALON, L., KORNER, G., VLODAVSKY, I. & LIDER, O. 1995. Molecular behavior adapts to context: heparanase functions as an extracellular matrix-degrading enzyme or as a T cell adhesion molecule, depending on the local pH. *J Exp Med,* 181**,** 1929-34.

GILKES, D. M., SEMENZA, G. L. & WIRTZ, D. 2014. Hypoxia and the extracellular matrix: drivers of tumour metastasis. *Nat Rev Cancer,* 14**,** 430-9.

GINGIS-VELITSKI, S., ZETSER, A., FLUGELMAN, M. Y., VLODAVSKY, I. & ILAN, N. 2004a. Heparanase induces endothelial cell migration via protein kinase B/Akt activation. *J Biol Chem,* 279**,** 23536-41.

GINGIS-VELITSKI, S., ZETSER, A., KAPLAN, V., BEN-ZAKEN, O., COHEN, E., LEVY-ADAM, F., BASHENKO, Y., FLUGELMAN, M. Y., VLODAVSKY, I. & ILAN, N. 2004b. Heparanase uptake is mediated by cell membrane heparan sulfate proteoglycans. *J Biol Chem,* 279**,** 44084-92.

GIUFFRÈ, L., CORDEY, A.-S., MONAI, N., TARDY, Y., SCHAPIRA, M. & SPERTINI, O. 1997. Monocyte adhesion to activated aortic endothelium: role of L-selectin and heparan sulfate proteoglycans. *The Journal of cell biology,* 136**,** 945-956.

GIULIANO, A. E., CONNOLLY, J. L., EDGE, S. B., MITTENDORF, E. A., RUGO, H. S., SOLIN, L. J., WEAVER, D. L., WINCHESTER, D. J. & HORTOBAGYI, G. N. 2017. Breast Cancer-Major changes in the American Joint Committee on Cancer eighth edition cancer staging manual. *CA Cancer J Clin,* 67**,** 290-303.

GODDER, K., VLODAVSKY, I., ELDOR, A., WEKSLER, B. B., HAIMOVITZ-FREIDMAN, A. & FUKS, Z. 1991. Heparanase activity in cultured endothelial cells. *J Cell Physiol,* 148**,** 274-80.

GOEL, H. L. & MERCURIO, A. M. 2013. VEGF targets the tumour cell. *Nat Rev Cancer,* 13**,** 871-82.

GOEL, S., WANG, Q., WATT, A. C., TOLANEY, S. M., DILLON, D. A., LI, W., RAMM, S., PALMER, A. C., YUZUGULLU, H., VARADAN, V., TUCK, D., HARRIS, L. N., WONG, K. K., LIU, X. S., SICINSKI, P., WINER, E. P., KROP, I. E. & ZHAO, J. J. 2016. Overcoming Therapeutic Resistance in HER2-Positive Breast Cancers with CDK4/6 Inhibitors. *Cancer Cell,* 29**,** 255-269.

GOETZ, R. & MOHAMMADI, M. 2013. Exploring mechanisms of FGF signalling through the lens of structural biology. *Nat Rev Mol Cell Biol,* 14**,** 166-80.

GOHJI, K., OKAMOTO, M., KITAZAWA, S., TOYOSHIMA, M., DONG, J., KATSUOKA, Y. & NAKAJIMA, M. 2001a. HEPARANASE PROTEIN AND GENE EXPRESSION IN BLADDER CANCER. *The Journal of Urology,* 166**,** 1286-1290.

GOHJI, K., OKAMOTO, M., KITAZAWA, S., TOYOSHIMA, M., DONG, J., KATSUOKA, Y. & NAKAJIMA, M. 2001b. Heparanase protein and gene expression in bladder cancer. *J Urol,* 166**,** 1286-90.

GOLDBERG, R., RUBINSTEIN, A. M., GIL, N., HERMANO, E., LI, J. P., VAN DER VLAG, J., ATZMON, R., MEIROVITZ, A. & ELKIN, M. 2014. Role of heparanase-driven inflammatory cascade in pathogenesis of diabetic nephropathy. *Diabetes,* 63**,** 4302-13.

GOLDMANN, E. 1908. The Growth of Malignant Disease in Man and the Lower Animals, with special reference to the Vascular System. *Proceedings of the Royal Society of Medicine,* 1**,** 1-13.

GOLDSHMIDT, O., NADAV, L., AINGORN, H., IRIT, C., FEINSTEIN, N., ILAN, N., ZAMIR, E., GEIGER, B., VLODAVSKY, I. & KATZ, B. Z. 2002. Human heparanase is localized within lysosomes in a stable form. *Exp Cell Res,* 281**,** 50-62.

GOLDSHMIDT, O., ZCHARIA, E., AINGORN, H., GUATTA-RANGINI, Z., ATZMON, R., MICHAL, I., PECKER, I., MITRANI, E. & VLODAVSKY, I. 2001. Expression pattern and secretion of human and chicken heparanase are determined by their signal peptide sequence. *J Biol Chem,* 276**,** 29178-87.

GOLDSHMIDT, O., ZCHARIA, E., COHEN, M., AINGORN, H., COHEN, I., NADAV, L., KATZ, B. Z., GEIGER, B. & VLODAVSKY, I. 2003. Heparanase mediates cell adhesion independent of its enzymatic activity. *FASEB J,* 17**,** 1015-25.

GOLUBKOV, V. S., BOYD, S., SAVINOV, A. Y., CHEKANOV, A. V., OSTERMAN, A. L., REMACLE, A., ROZANOV, D. V., DOXSEY, S. J. & STRONGIN, A. Y. 2005. Membrane type-1 matrix metalloproteinase (MT1-MMP) exhibits an important intracellular cleavage function and causes chromosome instability. *Journal of Biological Chemistry,* 280**,** 25079-25086.

GOLUBKOV, V. S., CHEKANOV, A. V., SAVINOV, A. Y., ROZANOV, D. V., GOLUBKOVA, N. V. & STRONGIN, A. Y. 2006. Membrane type-1 matrix metalloproteinase confers aneuploidy and tumorigenicity on mammary epithelial cells. *Cancer research,* 66**,** 10460-10465.

GOMES, A. M., BHAT, R., CORREIA, A. L., MOTT, J. D., ILAN, N., VLODAVSKY, I., PAVAO, M. S. & BISSELL, M. 2015. Mammary Branching Morphogenesis Requires Reciprocal Signaling by Heparanase and MMP-14. *J Cell Biochem,* 116**,** 1668-79.

GOMES, A. M., STELLING, M. P. & PAVAO, M. S. 2013. Heparan sulfate and heparanase as modulators of breast cancer progression. *Biomed Res Int,* 2013**,** 852093.

GÓMEZ-CUADRADO, L., TRACEY, N., MA, R., QIAN, B. & BRUNTON, V. G. 2017. Mouse models of metastasis: progress and prospects. *Disease models & mechanisms,* 10**,** 1061-1074.

GONG, F., JEMTH, P., ESCOBAR GALVIS, M. L., VLODAVSKY, I., HORNER, A., LINDAHL, U. & LI, J. P. 2003. Processing of macromolecular heparin by heparanase. *J Biol Chem,* 278**,** 35152-8.

GONNISSEN, A., ISEBAERT, S. & HAUSTERMANS, K. 2015. Targeting the Hedgehog signaling pathway in cancer: beyond Smoothened. *Oncotarget,* 6**,** 13899-913.

GONZALEZ-ALVA, P., KIKUCHI, K., MIYAZAKI, Y., OKAMOTO, E., OKU, Y., TSUCHIYA, H., NOGUCHI, Y., SAKASHITA, H., IDE, F. & KUSAMA, K. 2010a. Expression of heparanase: a possible role in invasiveness and aggressive clinical behavior of ameloblastomas. *J Oral Sci,* 52**,** 39-47.

GONZALEZ-ALVA, P., KIKUCHI, K., MIYAZAKI, Y., OKAMOTO, E., OKU, Y., TSUCHIYA, H., NOGUCHI, Y., SAKASHITA, H., IDE, F. & KUSAMA, K. 2010b. Expression of heparanase: a possible role in invasiveness and aggressive clinical behavior of ameloblastomas. *Journal of Oral Science,* 52**,** 39-47.

GONZALEZ-STAWINSKI, G. V., PARKER, W., HOLZKNECHT, Z. E., HUBER, N. S. & PLATT, J. L. 1999. Partial sequence of human platelet heparitinase and evidence of its ability to polymerize. *Biochim Biophys Acta,* 1429**,** 431-8.

GOODALL, K. J., POON, I. K., PHIPPS, S. & HULETT, M. D. 2014. Soluble heparan sulfate fragments generated by heparanase trigger the release of pro-inflammatory cytokines through TLR-4. *PLoS One,* 9**,** e109596.

GORDON, S. R., MAUTE, R. L., DULKEN, B. W., HUTTER, G., GEORGE, B. M., MCCRACKEN, M. N., GUPTA, R., TSAI, J. M., SINHA, R., COREY, D., RING, A. M., CONNOLLY, A. J. & WEISSMAN, I. L. 2017. PD-1 expression by tumour-associated macrophages inhibits phagocytosis and tumour immunity. *Nature,* 545**,** 495.

GORGOULIS, V. G. & HALAZONETIS, T. D. 2010. Oncogene-induced senescence: the bright and dark side of the response. *Curr Opin Cell Biol,* 22**,** 816-27.

GOSHEN, R., HOCHBERG, A. A., KORNER, G., LEVY, E., ISHAI-MICHAELI, R., ELKIN, M., DE GROOT, N. & VLODAVSKY, I. 1996. Purification and characterization of placental heparanase and its expression by cultured cytotrophoblasts. *Mol Hum Reprod,* 2**,** 679-84.

GOSPODAROWICZ, D., CHENG, J., LUI, G. M., BAIRD, A. & BOHLENT, P. 1984. Isolation of brain fibroblast growth factor by heparin-Sepharose affinity chromatography: identity with pituitary fibroblast growth factor. *Proc Natl Acad Sci U S A,* 81**,** 6963-7.

GOU, Q., GONG, X., JIN, J., SHI, J. & HOU, Y. 2017. Peroxisome proliferator-activated receptors (PPARs) are potential drug targets for cancer therapy. *Oncotarget,* 8**,** 60704-60709.

GOZALBES, R., MOSULÉN, S., ORTÍ, L., RODRÍGUEZ-DÍAZ, J., CARBAJO, R. J., MELNYK, P. & PINEDA-LUCENA, A. 2013. Hit identification of novel heparanase inhibitors by structure- and ligand-based approaches. *Bioorganic & Medicinal Chemistry,* 21**,** 1944-1951.

GRAHAM, L. D. 1994. Tumour rejection antigens of the hsp90 family (gp96) closely resemble tumour-associated heparanase enzymes. *Biochem J,* 301 (Pt 3)**,** 917-8.

GRAHAM, L. D. & UNDERWOOD, P. A. 1996. Comparison of the heparanase enzymes from mouse melanoma cells, mouse macrophages, and human platelets. *Biochem Mol Biol Int,* 39**,** 563-71.

GREAVES, M. 2002. Cancer causation: the Darwinian downside of past success? *The Lancet Oncology,* 3**,** 244-251.

GREAVES, M. 2007. Darwinian medicine: a case for cancer. *Nat Rev Cancer,* 7**,** 213-21.

GREAVES, M. & MALEY, C. C. 2012. Clonal evolution in cancer. *Nature,* 481**,** 306.

GREIDER, C. W. & BLACKBURN, E. H. 1987. The telomere terminal transferase of Tetrahymena is a ribonucleoprotein enzyme with two kinds of primer specificity. *Cell,* 51**,** 887-98.

GRIVENNIKOV, S. I., GRETEN, F. R. & KARIN, M. 2010. Immunity, Inflammation, and Cancer. *Cell,* 140**,** 883-899.

GROSS-COHEN, M., FELD, S., DOWECK, I., NEUFELD, G., HASSON, P., ARVATZ, G., BARASH, U., NARODITSKY, I., ILAN, N. & VLODAVSKY, I. 2016. Heparanase 2 Attenuates Head and Neck Tumor Vascularity and Growth. *Cancer Res,* 76**,** 2791-801.

GROULT, H., POUPARD, N., HERRANZ, F., CONFORTO, E., BRIDIAU, N., SANNIER, F., BORDENAVE, S., PIOT, J. M., RUIZ-CABELLO, J., FRUITIER-ARNAUDIN, I. & MAUGARD, T. 2017. Family of Bioactive Heparin-Coated Iron Oxide Nanoparticles with Positive Contrast in Magnetic Resonance Imaging for Specific Biomedical Applications. *Biomacromolecules,* 18**,** 3156-3167.

GUASCH, G., SCHOBER, M., PASOLLI, H. A., CONN, E. B., POLAK, L. & FUCHS, E. 2007. Loss of TGFbeta signaling destabilizes homeostasis and promotes squamous cell carcinomas in stratified epithelia. *Cancer Cell,* 12**,** 313-27.

GUERRA, C., COLLADO, M., NAVAS, C., SCHUHMACHER, ALBERTO J., HERNÁNDEZ-PORRAS, I., CAÑAMERO, M., RODRIGUEZ-JUSTO, M., SERRANO, M. & BARBACID, M. 2011. Pancreatitis-Induced Inflammation Contributes to Pancreatic Cancer by Inhibiting Oncogene-Induced Senescence. *Cancer Cell,* 19**,** 728-739.

GUERRE-MILLO, M., GERVOIS, P., RASPE, E., MADSEN, L., POULAIN, P., DERUDAS, B., HERBERT, J. M., WINEGAR, D. A., WILLSON, T. M., FRUCHART, J. C., BERGE, R. K. & STAELS, B. 2000. Peroxisome proliferator-activated receptor alpha activators improve insulin sensitivity and reduce adiposity. *J Biol Chem,* 275**,** 16638-42.

GUO, B., FU, S., ZHANG, J., LIU, B. & LI, Z. 2016. Targeting inflammasome/IL-1 pathways for cancer immunotherapy. *Scientific Reports,* 6**,** 36107.

GUO, C. H., KOO, C. Y., BAY, B. H., TAN, P. H. & YIP, G. W. 2007. Comparison of the effects of differentially sulphated bovine kidney- and porcine intestine-derived heparan sulphate on breast carcinoma cellular behaviour. *Int J Oncol,* 31**,** 1415-23.

GUO, G., GONG, K., WOHLFELD, B., HATANPAA, K. J., ZHAO, D. & HABIB, A. A. 2015. Ligand-Independent EGFR Signaling. *Cancer Res,* 75**,** 3436-41.

GUPTA, R. B., HARPAZ, N., ITZKOWITZ, S., HOSSAIN, S., MATULA, S., KORNBLUTH, A., BODIAN, C. & ULLMAN, T. 2007. Histologic inflammation is a risk factor for progression to colorectal neoplasia in ulcerative colitis: a cohort study. *Gastroenterology,* 133**,** 1099-105; quiz 1340-1.

GUTTER-KAPON, L., ALISHEKEVITZ, D., SHAKED, Y., LI, J. P., ARONHEIM, A., ILAN, N. & VLODAVSKY, I. 2016. Heparanase is required for activation and function of macrophages. *Proc Natl Acad Sci U S A,* 113**,** E7808-E7817.

GUY, C. T., CARDIFF, R. D. & MULLER, W. J. 1992. Induction of mammary tumors by expression of polyomavirus middle T oncogene: a transgenic mouse model for metastatic disease. *Mol Cell Biol,* 12**,** 954-61.

HAIMOV-KOCHMAN, R., FRIEDMANN, Y., PRUS, D., GOLDMAN-WOHL, D. S., GREENFIELD, C., ANTEBY, E. Y., AVIV, A., VLODAVSKY, I. & YAGEL, S. 2002. Localization of heparanase in normal and pathological human placenta. *Mol Hum Reprod,* 8**,** 566-73.

HAJDU, S. I. 2004. Greco-Roman thought about cancer. *Cancer,* 100**,** 2048-51.

HALLBERG, G., ANDERSSON, E., NAESSEN, T. & ORDEBERG, G. E. 2010. The expression of syndecan-1, syndecan-4 and decorin in healthy human breast tissue during the menstrual cycle. *Reprod Biol Endocrinol,* 8**,** 35.

HAM, B., WANG, N., D'COSTA, Z., FERNANDEZ, M. C., BOURDEAU, F., AUGUSTE, P., ILLEMANN, M., EEFSEN, R. L., HOYER-HANSEN, G., VAINER, B., EVRARD, M., GAO, Z. H. & BRODT, P. 2015. TNF Receptor-2 Facilitates an Immunosuppressive Microenvironment in the Liver to Promote the Colonization and Growth of Hepatic Metastases. *Cancer Res,* 75**,** 5235-47.

HAMMOND, E., BRANDT, R. & DREDGE, K. 2012. PG545, a heparan sulfate mimetic, reduces heparanase expression in vivo, blocks spontaneous metastases and enhances overall survival in the 4T1 breast carcinoma model. *PLoS One,* 7**,** e52175.

HAMMOND, E., HAYNES, N. M., CULLINANE, C., BRENNAN, T. V., BAMPTON, D., HANDLEY, P., KAROLI, T., LANKSHEER, F., LIN, L., YANG, Y. & DREDGE, K. 2018. Immunomodulatory activities of pixatimod: emerging nonclinical and clinical data, and its potential utility in combination with PD-1 inhibitors. *Journal for ImmunoTherapy of Cancer,* 6**,** 54.

HAMMOND, E., KHURANA, A., SHRIDHAR, V. & DREDGE, K. 2014. The Role of Heparanase and Sulfatases in the Modification of Heparan Sulfate Proteoglycans within the Tumor Microenvironment and Opportunities for Novel Cancer Therapeutics. *Front Oncol,* 4**,** 195.

HAMMOND, E., LI, C. P. & FERRO, V. 2010. Development of a colorimetric assay for heparanase activity suitable for kinetic analysis and inhibitor screening. *Analytical Biochemistry,* 396**,** 112-116.

HAMOUD, S., SHEKH MUHAMMAD, R., ABU-SALEH, N., HASSAN, A., ZOHAR, Y. & HAYEK, T. 2017. Heparanase Inhibition Reduces Glucose Levels, Blood Pressure, and Oxidative Stress in Apolipoprotein E Knockout Mice. *Biomed Res Int,* 2017**,** 7357495.

HAN, B., LIU, J., MA, M. J. & ZHAO, L. 2005. Clinicopathological significance of heparanase and basic fibroblast growth factor expression in human esophageal cancer. *World J Gastroenterol,* 11**,** 2188-92.

HANAHAN, D. & COUSSENS, L. M. 2012. Accessories to the crime: functions of cells recruited to the tumor microenvironment. *Cancer Cell,* 21**,** 309-22.

HANAHAN, D. & FOLKMAN, J. 1996. Patterns and emerging mechanisms of the angiogenic switch during tumorigenesis. *Cell,* 86**,** 353-64.

HANAHAN, D. & WEINBERG, R. A. 2000. The hallmarks of cancer. *Cell,* 100**,** 57-70.

HANAHAN, D. & WEINBERG, R. A. 2011. Hallmarks of cancer: the next generation. *Cell,* 144**,** 646-74.

HAO, N. B., TANG, B., WANG, G. Z., XIE, R., HU, C. J., WANG, S. M., WU, Y. Y., LIU, E., XIE, X. & YANG, S. M. 2015. Hepatocyte growth factor (HGF) upregulates heparanase expression via the PI3K/Akt/NF-kappaB signaling pathway for gastric cancer metastasis. *Cancer Lett,* 361**,** 57-66.

HARADA, N., OKAJIMA, K. & UCHIBA, M. 2006. Dalteparin, a low molecular weight heparin, attenuates inflammatory responses and reduces ischemia-reperfusion-induced liver injury in rats. *Crit Care Med,* 34**,** 1883-91.

HARBECK, N. & GNANT, M. 2017. Breast cancer. *Lancet,* 389**,** 1134-1150.

HARRIS, N. C., DAVYDOVA, N., ROUFAIL, S., PAQUET-FIFIELD, S., PAAVONEN, K., KARNEZIS, T., ZHANG, Y.-F., SATO, T., ROTHACKER, J., NICE, E. C., STACKER, S. A. & ACHEN, M. G. 2013. The Propeptides of VEGF-D Determine Heparin Binding, Receptor Heterodimerization, and Effects on Tumor Biology. *The Journal of Biological Chemistry,* 288**,** 8176-8186.

HART, I. R. 1979. The selection and characterization of an invasive variant of the B16 melanoma. *Am J Pathol,* 97**,** 587-600.

HARTMANN, L. C., DEGNIM, A. C., SANTEN, R. J., DUPONT, W. D. & GHOSH, K. 2015. Atypical hyperplasia of the breast--risk assessment and management options. *N Engl J Med,* 372**,** 78-89.

HARVEY, J. R., MELLOR, P., ELDALY, H., LENNARD, T. W., KIRBY, J. A. & ALI, S. 2007. Inhibition of CXCR4-mediated breast cancer metastasis: a potential role for heparinoids? *Clin Cancer Res,* 13**,** 1562-70.

HASHIZUME, H., BALUK, P., MORIKAWA, S., MCLEAN, J. W., THURSTON, G., ROBERGE, S., JAIN, R. K. & MCDONALD, D. M. 2000. Openings between Defective Endothelial Cells Explain Tumor Vessel Leakiness. *The American Journal of Pathology,* 156**,** 1363-1380.

HASSAN, H., GREVE, B., PAVAO, M. S., KIESEL, L., IBRAHIM, S. A. & GOTTE, M. 2013. Syndecan-1 modulates beta-integrin-dependent and interleukin-6-dependent

functions in breast cancer cell adhesion, migration, and resistance to irradiation. *Febs j,* 280**,** 2216-27.

HASSONA, Y., CIRILLO, N., HEESOM, K., PARKINSON, E. K. & PRIME, S. S. 2014. Senescent cancer-associated fibroblasts secrete active MMP-2 that promotes keratinocyte dis-cohesion and invasion. *British Journal Of Cancer,* 111**,** 1230.

HAY, E. D. 1995. An overview of epithelio-mesenchymal transformation. *Acta Anat (Basel),* 154**,** 8-20.

HAYFLICK, L. & MOORHEAD, P. S. 1961. The serial cultivation of human diploid cell strains. *Exp Cell Res,* 25**,** 585-621.

HE, L., SUN, F., WANG, Y., ZHU, J., FANG, J., ZHANG, S., YU, Q., GONG, Q., REN, B., XIANG, X., CHEN, Z., NING, Q., HU, J., YANG, P. & WANG, C. Y. 2016. HMGB1 exacerbates bronchiolitis obliterans syndrome via RAGE/NF-kappaB/HPSE signaling to enhance latent TGF-beta release from ECM. *Am J Transl Res,* 8**,** 1971-84.

HE, X., BRENCHLEY, P. E., JAYSON, G. C., HAMPSON, L., DAVIES, J. & HAMPSON, I. N. 2004a. Hypoxia increases heparanase-dependent tumor cell invasion, which can be inhibited by antiheparanase antibodies. *Cancer Res,* 64**,** 3928-33.

HE, X., BRENCHLEY, P. E. C., JAYSON, G. C., HAMPSON, L., DAVIES, J. & HAMPSON, I. N. 2004b. Hypoxia Increases Heparanase-Dependent Tumor Cell Invasion, Which Can Be Inhibited by Antiheparanase Antibodies. *Cancer Research,* 64**,** 3928-3933.

HE, Y. Q., SUTCLIFFE, E. L., BUNTING, K. L., LI, J., GOODALL, K. J., POON, I. K., HULETT, M. D., FREEMAN, C., ZAFAR, A., MCINNES, R. L., TAYA, T., PARISH, C. R. & RAO, S. 2012. The endoglycosidase heparanase enters the nucleus of T lymphocytes and modulates H3 methylation at actively transcribed genes via the interplay with key chromatin modifying enzymes. *Transcription,* 3**,** 130-45.

HELJASVAARA, R., AIKIO, M., RUOTSALAINEN, H. & PIHLAJANIEMI, T. 2017. Collagen XVIII in tissue homeostasis and dysregulation - Lessons learned from model organisms and human patients. *Matrix Biol,* 57-58**,** 55-75.

HELMLINGER, G., YUAN, F., DELLIAN, M. & JAIN, R. K. 1997. Interstitial pH and pO2 gradients in solid tumors in vivo: High-resolution measurements reveal a lack of correlation. *Nature Medicine,* 3**,** 177.

HENGEL, S. R., SPIES, M. A. & SPIES, M. 2017. Small-Molecule Inhibitors Targeting DNA Repair and DNA Repair Deficiency in Research and Cancer Therapy. *Cell Chemical Biology,* 24**,** 1101-1119.

HERNANDEZ-SEGURA, A., NEHME, J. & DEMARIA, M. 2018. Hallmarks of Cellular Senescence. *Trends Cell Biol,* 28**,** 436-453.

HERSHKOVIZ, R., MOR, F., MIAO, H. Q., VLODAVSKY, I. & LIDER, O. 1995. Differential effects of polysulfated polysaccharide on experimental encephalomyelitis,

proliferation of autoimmune T cells, and inhibition of heparanase activity. *J Autoimmun,* 8**,** 741-50.

HEYMAN, B. & YANG, Y. 2016. Mechanisms of heparanase inhibitors in cancer therapy. *Exp Hematol,* 44**,** 1002-1012.

HICKS, D., FARSANI, G. T., LAVAL, S., COLLINS, J., SARKOZY, A., MARTONI, E., SHAH, A., ZOU, Y., KOCH, M., BONNEMANN, C. G., ROBERTS, M., LOCHMULLER, H., BUSHBY, K. & STRAUB, V. 2014. Mutations in the collagen XII gene define a new form of extracellular matrix-related myopathy. *Hum Mol Genet,* 23**,** 2353-63.

HIDA, K., HIDA, Y., AMIN, D. N., FLINT, A. F., PANIGRAHY, D., MORTON, C. C. & KLAGSBRUN, M. 2004. Tumor-associated endothelial cells with cytogenetic abnormalities. *Cancer Res,* 64**,** 8249-55.

HIDA, K., HIDA, Y. & SHINDOH, M. 2008. Understanding tumor endothelial cell abnormalities to develop ideal anti-angiogenic therapies. *Cancer Sci,* 99**,** 459-66.

HIRAI, K., OOI, H., ESUMI, T., IWABUCHI, Y. & HATAKEYAMA, S. 2003. Total synthesis of (+/-)-trachyspic acid and determination of the relative configuration. *Org Lett,* 5**,** 857-9.

HIRANO, F., KANEKO, K., TAMURA, H., DONG, H., WANG, S., ICHIKAWA, M., RIETZ, C., FLIES, D. B., LAU, J. S., ZHU, G., TAMADA, K. & CHEN, L. 2005. Blockade of B7-H1 and PD-1 by monoclonal antibodies potentiates cancer therapeutic immunity. *Cancer Res,* 65**,** 1089-96.

HO, G., BROZE, G. J., JR. & SCHWARTZ, A. L. 1997. Role of heparan sulfate proteoglycans in the uptake and degradation of tissue factor pathway inhibitor-coagulation factor Xa complexes. *J Biol Chem,* 272**,** 16838-44.

HOLEN, I., SPEIRS, V., MORRISSEY, B. & BLYTH, K. 2017. In vivo models in breast cancer research: progress, challenges and future directions. *Disease Models & Mechanisms,* 10**,** 359-371.

HOOGEWERF, A. J., LEONE, J. W., REARDON, I. M., HOWE, W. J., ASA, D., HEINRIKSON, R. L. & LEDBETTER, S. R. 1995. CXC chemokines connective tissue activating peptide-III and neutrophil activating peptide-2 are heparin/heparan sulfate-degrading enzymes. *J Biol Chem,* 270**,** 3268-77.

HOOK, M., WASTESON, A. & OLDBERG, A. 1975. A heparan sulfate-degrading endoglycosidase from rat liver tissue. *Biochem Biophys Res Commun,* 67**,** 1422-8.

HOSSEINI, H., OBRADOVIĆ, M. M. S., HOFFMANN, M., HARPER, K. L., SOSA, M. S., WERNER-KLEIN, M., NANDURI, L. K., WERNO, C., EHRL, C., MANECK, M., PATWARY, N., HAUNSCHILD, G., GUŽVIĆ, M., REIMELT, C., GRAUVOGL, M., EICHNER, N., WEBER, F., HARTKOPF, A. D., TARAN, F.-A., BRUCKER, S. Y., FEHM, T., RACK, B., BUCHHOLZ, S., SPANG, R., MEISTER, G., AGUIRRE-

GHISO, J. A. & KLEIN, C. A. 2016. Early dissemination seeds metastasis in breast cancer. *Nature,* 540**,** 552.

HOVINGH, P. & LINKER, A. 1970. The enzymatic degradation of heparin and heparitin sulfate. 3. Purification of a heparitinase and a heparinase from flavobacteria. *J Biol Chem,* 245**,** 6170-5.

HSIEH, C.-Y., TSAI, P.-C., CHU, C.-L., CHANG, F.-R., CHANG, L.-S., WU, Y.-C. & LIN, S.-R. 2013. Brazilein suppresses migration and invasion of MDA-MB-231 breast cancer cells. *Chemico-Biological Interactions,* 204**,** 105-115.

HU, B., WANG, Q., SHI, Y., LU, S., QU, H., WANG, L. & CUI, J. 2017a. Significance of heparanase in metastatic lymph nodes of cervical squamous cell cancer. *Oncol Lett,* 13**,** 3219-3224.

HU, H., JUVEKAR, A., LYSSIOTIS, COSTAS A., LIEN, EVAN C., ALBECK, JOHN G., OH, D., VARMA, G., HUNG, YIN P., ULLAS, S., LAURING, J., SETH, P., LUNDQUIST, MARK R., TOLAN, DEAN R., GRANT, AARON K., NEEDLEMAN, DANIEL J., ASARA, JOHN M., CANTLEY, LEWIS C. & WULF, GERBURG M. 2016. Phosphoinositide 3-Kinase Regulates Glycolysis through Mobilization of Aldolase from the Actin Cytoskeleton. *Cell,* 164**,** 433-446.

HU, J., SONG, X., HE, Y. Q., FREEMAN, C., PARISH, C. R., YUAN, L., YU, H. & TANG, S. 2012. Heparanase and vascular endothelial growth factor expression is increased in hypoxia-induced retinal neovascularization. *Invest Ophthalmol Vis Sci,* 53**,** 6810-7.

HU, X., ZHANG, L., JIN, J., ZHU, W., XU, Y., WU, Y., WANG, Y., CHEN, H., WEBSTER, K. A., CHEN, H., YU, H. & WANG, J. 2015. Heparanase released from mesenchymal stem cells activates integrin beta1/HIF-2alpha/Flk-1 signaling and promotes endothelial cell migration and angiogenesis. *Stem Cells,* 33**,** 1850-1862.

HU, Y., YU, X., XU, G. & LIU, S. 2017b. Metastasis: an early event in cancer progression. *Journal of Cancer Research and Clinical Oncology,* 143**,** 745-757.

HUANG, Z., TAN, Y., GU, J., LIU, Y., SONG, L., NIU, J., ZHAO, L., SRINIVASAN, L., LIN, Q., DENG, J., LI, Y., CONKLIN, D. J., NEUBERT, T. A., CAI, L., LI, X. & MOHAMMADI, M. 2017. Uncoupling the Mitogenic and Metabolic Functions of FGF1 by Tuning FGF1-FGF Receptor Dimer Stability. *Cell Rep,* 20**,** 1717-1728.

HUBER, R., MEIER, B., OTSUKA, A., FENINI, G., SATOH, T., GEHRKE, S., WIDMER, D., LEVESQUE, M. P., MANGANA, J., KERL, K., GEBHARDT, C., FUJII, H., NAKASHIMA, C., NONOMURA, Y., KABASHIMA, K., DUMMER, R., CONTASSOT, E. & FRENCH, L. E. 2016. Tumour hypoxia promotes melanoma growth and metastasis via High Mobility Group Box-1 and M2-like macrophages. *Sci Rep,* 6**,** 29914.

HUBER, W. & MUELLER, F. 2006. Biomolecular interaction analysis in drug discovery using surface plasmon resonance technology. *Curr Pharm Des,* 12**,** 3999-4021.

HUGHES, C. S., POSTOVIT, L. M. & LAJOIE, G. A. 2010. Matrigel: a complex protein mixture required for optimal growth of cell culture. *Proteomics,* 10**,** 1886-90.

HUGHES, J. P., REES, S., KALINDJIAN, S. B. & PHILPOTT, K. L. 2011. Principles of early drug discovery. *Br J Pharmacol,* 162**,** 1239-49.

HULETT, M. D., FREEMAN, C., HAMDORF, B. J., BAKER, R. T., HARRIS, M. J. & PARISH, C. R. 1999. Cloning of mammalian heparanase, an important enzyme in tumor invasion and metastasis. *Nat Med,* 5**,** 803-9.

HULETT, M. D., HORNBY, J. R., OHMS, S. J., ZUEGG, J., FREEMAN, C., GREADY, J. E. & PARISH, C. R. 2000. Identification of active-site residues of the pro-metastatic endoglycosidase heparanase. *Biochemistry,* 39**,** 15659-67.

HUMPHREY, J. D., DUFRESNE, E. R. & SCHWARTZ, M. A. 2014. Mechanotransduction and extracellular matrix homeostasis. *Nat Rev Mol Cell Biol,* 15**,** 802-12.

HUNTER, K. E., PALERMO, C., KESTER, J. C., SIMPSON, K., LI, J. P., TANG, L. H., KLIMSTRA, D. S., VLODAVSKY, I. & JOYCE, J. A. 2013. Heparanase promotes lymphangiogenesis and tumor invasion in pancreatic neuroendocrine tumors. *Oncogene,* 33**,** 1799.

HUNTER, K. E., PALERMO, C., KESTER, J. C., SIMPSON, K., LI, J. P., TANG, L. H., KLIMSTRA, D. S., VLODAVSKY, I. & JOYCE, J. A. 2014. Heparanase promotes lymphangiogenesis and tumor invasion in pancreatic neuroendocrine tumors. *Oncogene,* 33**,** 1799-808.

HYNES, R. O. 2009. The extracellular matrix: not just pretty fibrils. *Science,* 326**,** 1216-9.

IBRAHIM, S. A., GADALLA, R., EL-GHONAIMY, E. A., SAMIR, O., MOHAMED, H. T., HASSAN, H., GREVE, B., EL-SHINAWI, M., MOHAMED, M. M. & GÖTTE, M. 2017. Syndecan-1 is a novel molecular marker for triple negative inflammatory breast cancer and modulates the cancer stem cell phenotype via the IL-6/STAT3, Notch and EGFR signaling pathways. *Molecular Cancer,* 16**,** 57.

IBRAHIM, S. A., HASSAN, H., VILARDO, L., KUMAR, S. K., KUMAR, A. V., KELSCH, R., SCHNEIDER, C., KIESEL, L., EICH, H. T., ZUCCHI, I., REINBOLD, R., GREVE, B. & GOTTE, M. 2013. Syndecan-1 (CD138) modulates triple-negative breast cancer stem cell properties via regulation of LRP-6 and IL-6-mediated STAT3 signaling. *PLoS One,* 8**,** e85737.

ICHASO, N. & DILWORTH, S. M. 2001. Cell transformation by the middle T-antigen of polyoma virus. *Oncogene,* 20**,** 7908-16.

IDE, A. G., BAKER, N. H. & WARREN, S. L. 1939. Vascularization of the Brown Pearce rabbit epithelioma transplant as seen in the transparent ear chamber. *Am. J. Roentgenol,* 42**,** 891-899.

INGTHORSSON, S., HILMARSDOTTIR, B., KRICKER, J., MAGNUSSON, M. K. & GUDJONSSON, T. 2015. Context-Dependent Function of Myoepithelial Cells in Breast Morphogenesis and Neoplasia. *Curr Mol Biol Rep,* 1**,** 168-174.

INMAN, J. L., ROBERTSON, C., MOTT, J. D. & BISSELL, M. J. 2015. Mammary gland development: cell fate specification, stem cells and the microenvironment. *Development,* 142**,** 1028-1042.

IOZZO, R. V. & GUBBIOTTI, M. A. 2018. Extracellular matrix: The driving force of mammalian diseases. *Matrix Biol*.

IOZZO, R. V. & SCHAEFER, L. 2015. Proteoglycan form and function: A comprehensive nomenclature of proteoglycans. *Matrix Biol,* 42**,** 11-55.

ISHIDA, K., HIRAI, G., MURAKAMI, K., TERUYA, T., SIMIZU, S., SODEOKA, M. & OSADA, H. 2004. Structure-based design of a selective heparanase inhibitor as an antimetastatic agent. *Mol Cancer Ther,* 3**,** 1069-77.

ISHIKAWA, F. 1997. Telomere crisis, the driving force in cancer cell evolution. *Biochem Biophys Res Commun,* 230**,** 1-6.

ISSA, N. T., WATHIEU, H., OJO, A., BYERS, S. W. & DAKSHANAMURTHY, S. 2017. Drug Metabolism in Preclinical Drug Development: A Survey of the Discovery Process, Toxicology, and Computational Tools. *Current drug metabolism,* 18**,** 556-565.

IWAI, Y., ISHIDA, M., TANAKA, Y., OKAZAKI, T., HONJO, T. & MINATO, N. 2002. Involvement of PD-L1 on tumor cells in the escape from host immune system and tumor immunotherapy by PD-L1 blockade. *Proc Natl Acad Sci U S A,* 99**,** 12293-7.

IZRAELY, S., BEN-MENACHEM, S., SAGI-ASSIF, O., MESHEL, T., MARZESE, D. M., OHE, S., ZUBRILOV, I., PASMANIK-CHOR, M., HOON, D. S. B. & WITZ, I. P. 2017. ANGPTL4 promotes the progression of cutaneous melanoma to brain metastasis. *Oncotarget,* 8**,** 75778-75796.

JANG, J.-E., HAJDU, C. H., LIOT, C., MILLER, G., DUSTIN, M. L. & BAR-SAGI, D. 2017. Crosstalk between Regulatory T Cells and Tumor-Associated Dendritic Cells Negates Anti-tumor Immunity in Pancreatic Cancer. *Cell Reports,* 20**,** 558-571.

JANSSEN, A. W. F., BETZEL, B., STOOPEN, G., BERENDS, F. J., JANSSEN, I. M., PEIJNENBURG, A. A. & KERSTEN, S. 2015. The impact of PPARα activation on whole genome gene expression in human precision cut liver slices. *BMC genomics,* 16**,** 760-760.

JANSSEN, L. M. E., RAMSAY, E. E., LOGSDON, C. D. & OVERWIJK, W. W. 2017. The immune system in cancer metastasis: friend or foe? *Journal for immunotherapy of cancer,* 5**,** 79-79.

JANZEN, WILLIAM P. 2014. Screening Technologies for Small Molecule Discovery: The State of the Art. *Chemistry & Biology,* 21**,** 1162-1170.

JAQUES, L. B. & KEERI-SZANTO, E. 1952. Heparinase. II. Distribution of enzyme in various tissues and its action on natural heparins and certain synthetic anticoagulants. *Can J Med Sci,* 30**,** 353-9.

JAYSON, G. C., KERBEL, R., ELLIS, L. M. & HARRIS, A. L. 2016. Antiangiogenic therapy in oncology: current status and future directions. *Lancet,* 388**,** 518-29.

JIA, L. & MA, S. 2016. Recent advances in the discovery of heparanase inhibitors as anti-cancer agents. *European Journal of Medicinal Chemistry,* 121**,** 209-220.

JIA, R., LIANG, Y., CHEN, R., LIU, G., WANG, H., TANG, M., ZHOU, X., WANG, H., YANG, Y., WEI, H., LI, B., SONG, Y. & ZHAO, J. 2016. Osteopontin facilitates tumor metastasis by regulating epithelial–mesenchymal plasticity. *Cell Death & Disease,* 7**,** e2564.

JIANG, P., KUMAR, A., PARRILLO, J. E., DEMPSEY, L. A., PLATT, J. L., PRINZ, R. A. & XU, X. 2002. Cloning and characterization of the human heparanase-1 (HPR1) gene promoter: role of GA-binding protein and Sp1 in regulating HPR1 basal promoter activity. *J Biol Chem,* 277**,** 8989-98.

JIANG, X., WONG, K. H. K., KHANKHEL, A. H., ZEINALI, M., REATEGUI, E., PHILLIPS, M. J., LUO, X., ACETO, N., FACHIN, F., HOANG, A. N., KIM, W., JENSEN, A. E., SEQUIST, L. V., MAHESWARAN, S., HABER, D. A., STOTT, S. L. & TONER, M. 2017. Microfluidic isolation of platelet-covered circulating tumor cells. *Lab Chip,* 17**,** 3498-3503.

JIAO, F., BAI, S. Y., MA, Y., YAN, Z. H., YUE, Z., YU, Y., WANG, X. & WANG, J. 2014. DNA methylation of heparanase promoter influences its expression and associated with the progression of human breast cancer. *PLoS One,* 9**,** e92190.

JOHNSON, D. E., O'KEEFE, R. A. & GRANDIS, J. R. 2018. Targeting the IL-6/JAK/STAT3 signalling axis in cancer. *Nat Rev Clin Oncol,* 15**,** 234-248.

JOHNSON, G. B., BRUNN, G. J., KODAIRA, Y. & PLATT, J. L. 2002. Receptor-mediated monitoring of tissue well-being via detection of soluble heparan sulfate by Toll-like receptor 4. *J Immunol,* 168**,** 5233-9.

JOHNSON, M. C. & CUTLER, M. L. 2016. Anatomy and Physiology of the Breast. *In:* JATOI, I. & RODY, A. (eds.) *Management of Breast Diseases.* Cham: Springer International Publishing.

JOLLY, M. K., BOARETO, M., HUANG, B., JIA, D., LU, M., BEN-JACOB, E., ONUCHIC, J. N. & LEVINE, H. 2015. Implications of the Hybrid Epithelial/Mesenchymal Phenotype in Metastasis. *Front Oncol,* 5**,** 155.

JORPES, J. E. & GARDELL, S. 1948. On heparin monosulfuric acid. *J Biol Chem,* 176**,** 267-76.

JOYCE, J. A., FREEMAN, C., MEYER-MORSE, N., PARISH, C. R. & HANAHAN, D. 2005. A functional heparan sulfate mimetic implicates both heparanase and heparan sulfate in tumor angiogenesis and invasion in a mouse model of multistage cancer. *Oncogene,* 24**,** 4037-51.

JUNE, C. H., O'CONNOR, R. S., KAWALEKAR, O. U., GHASSEMI, S. & MILONE, M. C. 2018. CAR T cell immunotherapy for human cancer. *Science,* 359**,** 1361-1365.

JUNG, O., TRAPP-STAMBORSKI, V., PURUSHOTHAMAN, A., JIN, H., WANG, H., SANDERSON, R. D. & RAPRAEGER, A. C. 2016a. Heparanase-induced shedding of syndecan-1/CD138 in myeloma and endothelial cells activates VEGFR2 and an invasive phenotype: prevention by novel synstatins. *Oncogenesis,* 5**,** e202.

JUNG, S. H., LEE, H. C., YU, D. M., KIM, B. C., PARK, S. M., LEE, Y. S., PARK, H. J., KO, Y. G. & LEE, J. S. 2016b. Heparan sulfation is essential for the prevention of cellular senescence. *Cell Death Differ,* 23**,** 417-29.

KALLAPUR, S. G. & AKESON, R. A. 1992. The neural cell adhesion molecule (NCAM) heparin binding domain binds to cell surface heparan sulfate proteoglycans. *J Neurosci Res,* 33**,** 538-48.

KALLURI, R. 2016. The biology and function of fibroblasts in cancer. *Nat Rev Cancer,* 16**,** 582-98.

KAPLAN, R. N., RIBA, R. D., ZACHAROULIS, S., BRAMLEY, A. H., VINCENT, L., COSTA, C., MACDONALD, D. D., JIN, D. K., SHIDO, K., KERNS, S. A., ZHU, Z., HICKLIN, D., WU, Y., PORT, J. L., ALTORKI, N., PORT, E. R., RUGGERO, D., SHMELKOV, S. V., JENSEN, K. K., RAFII, S. & LYDEN, D. 2005. VEGFR1-positive haematopoietic bone marrow progenitors initiate the pre-metastatic niche. *Nature,* 438**,** 820-7.

KASTENHUBER, E. R. & LOWE, S. W. 2017. Putting p53 in Context. *Cell,* 170**,** 1062-1078.

KATZ, A., BARASH, U., BOYANGO, I., FELD, S., ZOHAR, Y., HAMMOND, E., ILAN, N., KREMER, R. & VLODAVSKY, I. 2018. Patient derived xenografts (PDX) predict an effective heparanase-based therapy for lung cancer. *Oncotarget,* 9**,** 19294-19306.

KEHRER, J. P., BISWAL, S. S., LA, E., THUILLIER, P., DATTA, K., FISCHER, S. M. & VANDEN HEUVEL, J. P. 2001. Inhibition of peroxisome-proliferator-activated receptor (PPAR)alpha by MK886. *Biochem J,* 356**,** 899-906.

KELLEY, L. C., LOHMER, L. L., HAGEDORN, E. J. & SHERWOOD, D. R. 2014. Traversing the basement membrane in vivo: a diversity of strategies. *J Cell Biol,* 204**,** 291-302.

KERR, J., ANDERSON, C. & LIPPMAN, S. M. 2017. Physical activity, sedentary behaviour, diet, and cancer: an update and emerging new evidence. *Lancet Oncol,* 18**,** e457-e471.

KERR, J. F., WYLLIE, A. H. & CURRIE, A. R. 1972. Apoptosis: a basic biological phenomenon with wide-ranging implications in tissue kinetics. *Br J Cancer,* 26**,** 239-57.

KHAMAYSI, I., SINGH, P., NASSER, S., AWAD, H., CHOWERS, Y., SABO, E., HAMMOND, E., GRALNEK, I., MINKOV, I., NOSEDA, A., ILAN, N., VLODAVSKY,

I. & ABASSI, Z. 2017a. The Role of Heparanase in the Pathogenesis of Acute Pancreatitis: A Potential Therapeutic Target. *Scientific Reports,* 7**,** 715.

KHAMAYSI, I., SINGH, P., NASSER, S., AWAD, H., CHOWERS, Y., SABO, E., HAMMOND, E., GRALNEK, I., MINKOV, I., NOSEDA, A., ILAN, N., VLODAVSKY, I. & ABASSI, Z. 2017b. The Role of Heparanase in the Pathogenesis of Acute Pancreatitis: A Potential Therapeutic Target. *Sci Rep,* 7**,** 715.

KHAMIS, Z. I., SAHAB, Z. J. & SANG, Q. X. 2012. Active roles of tumor stroma in breast cancer metastasis. *Int J Breast Cancer,* 2012**,** 574025.

KHASRAW, M., PAVLAKIS, N., MCCOWATT, S., UNDERHILL, C., BEGBIE, S., DE SOUZA, P., BOYCE, A., PARNIS, F., LIM, V., HARVIE, R. & MARX, G. 2010a. Multicentre phase I/II study of PI-88, a heparanase inhibitor in combination with docetaxel in patients with metastatic castrate-resistant prostate cancer. *Ann Oncol,* 21**,** 1302-7.

KHASRAW, M., PAVLAKIS, N., MCCOWATT, S., UNDERHILL, C., BEGBIE, S., DE SOUZA, P., BOYCE, A., PARNIS, F., LIM, V., HARVIE, R. & MARX, G. 2010b. Multicentre phase I/II study of PI-88, a heparanase inhibitor in combination with docetaxel in patients with metastatic castrate-resistant prostate cancer. *Annals of Oncology,* 21**,** 1302-1307.

KIEFER, F., ANHAUSER, I., SORIANO, P., AGUZZI, A., COURTNEIDGE, S. A. & WAGNER, E. F. 1994. Endothelial cell transformation by polyomavirus middle T antigen in mice lacking Src-related kinases. *Curr Biol,* 4**,** 100-9.

KIM, A. W., XU, X., HOLLINGER, E. F., GATTUSO, P., GODELLAS, C. V. & PRINZ, R. A. 2002. Human heparanase-1 gene expression in pancreatic adenocarcinoma. *J Gastrointest Surg,* 6**,** 167-72.

KIM, H. J. & CANTOR, H. 2014. CD4 T-cell subsets and tumor immunity: the helpful and the not-so-helpful. *Cancer Immunol Res,* 2**,** 91-8.

KIM, J., YU, W., KOVALSKI, K. & OSSOWSKI, L. 1998. Requirement for specific proteases in cancer cell intravasation as revealed by a novel semiquantitative PCR-based assay. *Cell,* 94**,** 353-62.

KIM, J. W., TCHERNYSHYOV, I., SEMENZA, G. L. & DANG, C. V. 2006. HIF-1-mediated expression of pyruvate dehydrogenase kinase: a metabolic switch required for cellular adaptation to hypoxia. *Cell Metab,* 3**,** 177-85.

KIM, N. W., PIATYSZEK, M. A., PROWSE, K. R., HARLEY, C. B., WEST, M. D., HO, P. L., COVIELLO, G. M., WRIGHT, W. E., WEINRICH, S. L. & SHAY, J. W. 1994. Specific association of human telomerase activity with immortal cells and cancer. *Science,* 266**,** 2011-5.

KINZLER, K. W. & VOGELSTEIN, B. 1997. Gatekeepers and caretakers. *Nature,* 386**,** 761.

KIRSCHMANN, D. A., SEFTOR, E. A., FONG, S. F., NIEVA, D. R., SULLIVAN, C. M., EDWARDS, E. M., SOMMER, P., CSISZAR, K. & HENDRIX, M. J. 2002. A molecular role for lysyl oxidase in breast cancer invasion. *Cancer Res,* 62**,** 4478-83.

KITAMURA, T., QIAN, B.-Z. & POLLARD, J. W. 2015a. Immune cell promotion of metastasis. *Nature reviews. Immunology,* 15**,** 73-86.

KITAMURA, T., QIAN, B. Z. & POLLARD, J. W. 2015b. Immune cell promotion of metastasis. *Nat Rev Immunol,* 15**,** 73-86.

KIZAKI, K., YAMADA, O., NAKANO, H., TAKAHASHI, T., YAMAUCHI, N., IMAI, K. & HASHIZUME, K. 2003. Cloning and localization of heparanase in bovine placenta. *Placenta,* 24**,** 424-30.

KLARENBEEK, S., VAN MILTENBURG, M. H. & JONKERS, J. 2013. Genetically engineered mouse models of PI3K signaling in breast cancer. *Mol Oncol,* 7**,** 146-64.

KLEIN, U. & VON FIGURA, K. 1976. Partial purification and characterization of heparan sulfate specific endoglucuronidase. *Biochem Biophys Res Commun,* 73**,** 569-76.

KLEINMAN, H. K. & MARTIN, G. R. 2005. Matrigel: basement membrane matrix with biological activity. *Semin Cancer Biol,* 15**,** 378-86.

KLEINMAN, H. K., MCGARVEY, M. L., LIOTTA, L. A., ROBEY, P. G., TRYGGVASON, K. & MARTIN, G. R. 1982. Isolation and characterization of type IV procollagen, laminin, and heparan sulfate proteoglycan from the EHS sarcoma. *Biochemistry,* 21**,** 6188-93.

KLERK, C. P., SMORENBURG, S. M., OTTEN, H. M., LENSING, A. W., PRINS, M. H., PIOVELLA, F., PRANDONI, P., BOS, M. M., RICHEL, D. J., VAN TIENHOVEN, G. & BULLER, H. R. 2005. The effect of low molecular weight heparin on survival in patients with advanced malignancy. *J Clin Oncol,* 23**,** 2130-5.

KNELSON, E. H., NEE, J. C. & BLOBE, G. C. 2014. Heparan sulfate signaling in cancer. *Trends Biochem Sci,* 39**,** 277-88.

KNIGHT, B., YEOH, G. C., HUSK, K. L., LY, T., ABRAHAM, L. J., YU, C., RHIM, J. A. & FAUSTO, N. 2000. Impaired preneoplastic changes and liver tumor formation in tumor necrosis factor receptor type 1 knockout mice. *J Exp Med,* 192**,** 1809-18.

KO, H. R., KIM, B. Y., OH, W. K., KANG, D. O., LEE, H. S., KOSHINO, H., OSADA, H., MHEEN, T. I. & AHN, J. S. 2000. CRM646-A and -B, novel fungal metabolites that inhibit heparinase. *J Antibiot (Tokyo),* 53**,** 211-4.

KOBAYASHI, M., NAOMOTO, Y., NOBUHISA, T., OKAWA, T., TAKAOKA, M., SHIRAKAWA, Y., YAMATSUJI, T., MATSUOKA, J., MIZUSHIMA, T., MATSUURA, H., NAKAJIMA, M., NAKAGAWA, H., RUSTGI, A. & TANAKA, N. 2006. Heparanase regulates esophageal keratinocyte differentiation through nuclear translocation and heparan sulfate cleavage. *Differentiation,* 74**,** 235-43.

KODA, J. E., RAPRAEGER, A. & BERNFIELD, M. 1985. Heparan sulfate proteoglycans from mouse mammary epithelial cells. Cell surface proteoglycan as a receptor for interstitial collagens. *J Biol Chem,* 260**,** 8157-62.

KOEBERLE, A., SIEMONEIT, U., NORTHOFF, H., HOFMANN, B., SCHNEIDER, G. & WERZ, O. 2009. MK-886, an inhibitor of the 5-lipoxygenase-activating protein, inhibits cyclooxygenase-1 activity and suppresses platelet aggregation. *Eur J Pharmacol,* 608**,** 84-90.

KOENIG, A., NORGARD-SUMNICHT, K., LINHARDT, R. & VARKI, A. 1998. Differential interactions of heparin and heparan sulfate glycosaminoglycans with the selectins. Implications for the use of unfractionated and low molecular weight heparins as therapeutic agents. *The Journal of clinical investigation,* 101**,** 877-889.

KOLCH, W., HALASZ, M., GRANOVSKAYA, M. & KHOLODENKO, B. N. 2015. The dynamic control of signal transduction networks in cancer cells. *Nat Rev Cancer,* 15**,** 515-27.

KOLIOPANOS, A., FRIESS, H., KLEEFF, J., SHI, X., LIAO, Q., PECKER, I., VLODAVSKY, I., ZIMMERMANN, A. & BUCHLER, M. W. 2001. Heparanase expression in primary and metastatic pancreatic cancer. *Cancer Res,* 61**,** 4655-9.

KOMATSU, N., WAKI, M., SUE, M., TOKUDA, C., KASAOKA, T., NAKAJIMA, M., HIGASHI, N. & IRIMURA, T. 2008a. Heparanase expression in B16 melanoma cells and peripheral blood neutrophils before and after extravasation detected by novel anti-mouse heparanase monoclonal antibodies. *Journal of Immunological Methods,* 331**,** 82-93.

KOMATSU, N., WAKI, M., SUE, M., TOKUDA, C., KASAOKA, T., NAKAJIMA, M., HIGASHI, N. & IRIMURA, T. 2008b. Heparanase expression in B16 melanoma cells and peripheral blood neutrophils before and after extravasation detected by novel anti-mouse heparanase monoclonal antibodies. *J Immunol Methods,* 331**,** 82-93.

KOMLOSI, K., DUGA, B., HADZSIEV, K., CZAKO, M., KOSZTOLANYI, G., FOGARASI, A. & MELEGH, B. 2015. Phenotypic variability in a Hungarian patient with the 4q21 microdeletion syndrome. *Mol Cytogenet,* 8**,** 16.

KOO, C. Y., SEN, Y. P., BAY, B. H. & YIP, G. W. 2008. Targeting heparan sulfate proteoglycans in breast cancer treatment. *Recent Pat Anticancer Drug Discov,* 3**,** 151-8.

KOOPMAN, M. M., PRANDONI, P., PIOVELLA, F., OCKELFORD, P. A., BRANDJES, D. P., VAN DER MEER, J., GALLUS, A. S., SIMONNEAU, G., CHESTERMAN, C. H. & PRINS, M. H. 1996. Treatment of venous thrombosis with intravenous unfractionated heparin administered in the hospital as compared with subcutaneous low-molecular-weight heparin administered at home. The Tasman Study Group. *N Engl J Med,* 334**,** 682-7.

KOPP, H. G., PLACKE, T. & SALIH, H. R. 2009. Platelet-derived transforming growth factor-beta down-regulates NKG2D thereby inhibiting natural killer cell antitumor reactivity. *Cancer Res,* 69**,** 7775-83.

KORPETINOU, A., SKANDALIS, S. S., LABROPOULOU, V. T., SMIRLAKI, G., NOULAS, A., KARAMANOS, N. K. & THEOCHARIS, A. D. 2014. Serglycin: at the crossroad of inflammation and malignancy. *Front Oncol,* 3**,** 327.

KOSTRZEWA, R. M. 2016. Perinatal Lesioning and Lifelong Effects of the Noradrenergic Neurotoxin 6-Hydroxydopa. *Curr Top Behav Neurosci,* 29**,** 43-50.

KRALJEVIC, S., STAMBROOK, P. J. & PAVELIC, K. 2004. Accelerating drug discovery. *EMBO reports,* 5**,** 837-842.

KREBS, M. G., HOU, J. M., WARD, T. H., BLACKHALL, F. H. & DIVE, C. 2010. Circulating tumour cells: their utility in cancer management and predicting outcomes. *Ther Adv Med Oncol,* 2**,** 351-65.

KREBS, M. G., METCALF, R. L., CARTER, L., BRADY, G., BLACKHALL, F. H. & DIVE, C. 2014. Molecular analysis of circulating tumour cells-biology and biomarkers. *Nat Rev Clin Oncol,* 11**,** 129-44.

KUPER, H., ADAMI, H. O. & TRICHOPOULOS, D. 2000. Infections as a major preventable cause of human cancer. *J Intern Med,* 248**,** 171-83.

KUROSU, T., OHGA, N., HIDA, Y., MAISHI, N., AKIYAMA, K., KAKUGUCHI, W., KUROSHIMA, T., KONDO, M., AKINO, T., TOTSUKA, Y., SHINDOH, M., HIGASHINO, F. & HIDA, K. 2011. HuR keeps an angiogenic switch on by stabilising mRNA of VEGF and COX-2 in tumour endothelium. *Br J Cancer,* 104**,** 819-29.

KUSSIE, P. H., HULMES, J. D., LUDWIG, D. L., PATEL, S., NAVARRO, E. C., SEDDON, A. P., GIORGIO, N. A. & BOHLEN, P. 1999. Cloning and functional expression of a human heparanase gene. *Biochem Biophys Res Commun,* 261**,** 183-7.

LA PAGLIA, L., LISTÌ, A., CARUSO, S., AMODEO, V., PASSIGLIA, F., BAZAN, V. & FANALE, D. 2017. Potential Role of ANGPTL4 in the Cross Talk between Metabolism and Cancer through PPAR Signaling Pathway. *PPAR research,* 2017**,** 8187235-8187235.

LABELLE, M., BEGUM, S. & HYNES, R. O. 2011. Direct signaling between platelets and cancer cells induces an epithelial-mesenchymal-like transition and promotes metastasis. *Cancer Cell,* 20**,** 576-90.

LAGORY, E. L. & GIACCIA, A. J. 2016. The ever-expanding role of HIF in tumour and stromal biology. *Nature cell biology,* 18**,** 356-365.

LAMBERT, A. W., PATTABIRAMAN, D. R. & WEINBERG, R. A. 2017. Emerging Biological Principles of Metastasis. *Cell,* 168**,** 670-691.

LAMICHHANE, P., KARYAMPUDI, L., SHREEDER, B., KREMPSKI, J., BAHR, D., DAUM, J., KALLI, K. R., GOODE, E. L., BLOCK, M. S., CANNON, M. J. & KNUTSON, K. L. 2017. IL10 Release upon PD-1 Blockade Sustains Immunosuppression in Ovarian Cancer. *Cancer Res,* 77**,** 6667-6678.

LAMOUILLE, S., XU, J. & DERYNCK, R. 2014. Molecular mechanisms of epithelial-mesenchymal transition. *Nat Rev Mol Cell Biol,* 15**,** 178-96.

LANE, D. P. 1992. p53, guardian of the genome. *Nature,* 358**,** 15-6.

LANE, D. P. & CRAWFORD, L. V. 1979. T antigen is bound to a host protein in SV40-transformed cells. *Nature,* 278.

LASKOV, R., MICHAELI, R. I., SHARIR, H., YEFENOF, E. & VLODAVSKY, I. 1991. Production of heparanase by normal and neoplastic murine B-lymphocytes. *Int J Cancer,* 47**,** 92-8.

LAW, A. M. K., LIM, E., ORMANDY, C. J. & GALLEGO-ORTEGA, D. 2017. The innate and adaptive infiltrating immune systems as targets for breast cancer immunotherapy. *Endocrine-Related Cancer,* 24**,** R123-R144.

LE FOLL, B., DI CIANO, P., PANLILIO, L. V., GOLDBERG, S. R. & CICCOCIOPPO, R. 2013. Peroxisome proliferator-activated receptor (PPAR) agonists as promising new medications for drug addiction: preclinical evidence. *Current drug targets,* 14**,** 768-776.

LE JAN, S., AMY, C., CAZES, A., MONNOT, C., LAMANDÉ, N., FAVIER, J., PHILIPPE, J., SIBONY, M., GASC, J.-M., CORVOL, P. & GERMAIN, S. 2003. Angiopoietin-like 4 is a proangiogenic factor produced during ischemia and in conventional renal cell carcinoma. *The American journal of pathology,* 162**,** 1521-1528.

LEE, J. O., YANG, H., GEORGESCU, M. M., DI CRISTOFANO, A., MAEHAMA, T., SHI, Y., DIXON, J. E., PANDOLFI, P. & PAVLETICH, N. P. 1999. Crystal structure of the PTEN tumor suppressor: implications for its phosphoinositide phosphatase activity and membrane association. *Cell,* 99**,** 323-34.

LEE, P.-P. H., HWANG, J.-J., MURPHY, G. & IP, M. M. 2000. Functional Significance of MMP-9 in Tumor Necrosis Factor-Induced Proliferation and Branching Morphogenesis of Mammary Epithelial Cells*. *Endocrinology,* 141**,** 3764-3773.

LEE, R. T., ZHAO, Z. & INGHAM, P. W. 2016. Hedgehog signalling. *Development,* 143**,** 367-72.

LEE, S. H., JIA, S., ZHU, Y., UTERMARK, T., SIGNORETTI, S., LODA, M., SCHAFFHAUSEN, B. & ROBERTS, T. M. 2011. Transgenic Expression of Polyomavirus Middle T Antigen in the Mouse Prostate Gives Rise to Carcinoma. *Journal of Virology,* 85**,** 5581-5592.

LEISER, Y., ABU-EL-NAAJ, I., SABO, E., AKRISH, S., ILAN, N., BEN-IZHAK, O., PELED, M. & VLODAVSKY, I. 2011. Prognostic value of heparanase expression and cellular localization in oral cancer. *Head Neck,* 33**,** 871-7.

LEIVONEN, M., LUNDIN, J., NORDLING, S., VON BOGUSLAWSKI, K. & HAGLUND, C. 2004. Prognostic value of syndecan-1 expression in breast cancer. *Oncology,* 67**,** 11-8.

LELEKAKIS, M., MOSELEY, J. M., MARTIN, T. J., HARDS, D., WILLIAMS, E., HO, P., LOWEN, D., JAVNI, J., MILLER, F. R., SLAVIN, J. & ANDERSON, R. L. 1999. A novel orthotopic model of breast cancer metastasis to bone. *Clin Exp Metastasis,* 17**,** 163-70.

LEMMON, M. A. & SCHLESSINGER, J. 2010. Cell signaling by receptor tyrosine kinases. *Cell,* 141**,** 1117-34.

LENDORF, M. E., MANON-JENSEN, T., KRONQVIST, P., MULTHAUPT, H. A. B. & COUCHMAN, J. R. 2011. Syndecan-1 and Syndecan-4 Are Independent Indicators in Breast Carcinoma. *Journal of Histochemistry and Cytochemistry,* 59**,** 615-629.

LENZI, P., BOCCI, G. & NATALE, G. 2016. John Hunter and the origin of the term "angiogenesis". *Angiogenesis,* 19**,** 255-6.

LERNER, I., BARAZ, L., PIKARSKY, E., MEIROVITZ, A., EDOVITSKY, E., PERETZ, T., VLODAVSKY, I. & ELKIN, M. 2008. Function of heparanase in prostate tumorigenesis: potential for therapy. *Clin Cancer Res,* 14**,** 668-76.

LERNER, I., HERMANO, E., ZCHARIA, E., RODKIN, D., BULVIK, R., DOVINER, V., RUBINSTEIN, A. M., ISHAI-MICHAELI, R., ATZMON, R., SHERMAN, Y., MEIROVITZ, A., PERETZ, T., VLODAVSKY, I. & ELKIN, M. 2011. Heparanase powers a chronic inflammatory circuit that promotes colitis-associated tumorigenesis in mice. *J Clin Invest,* 121**,** 1709-21.

LEVER, R., ROSE, M. J., MCKENZIE, E. A. & PAGE, C. P. 2014. Heparanase induces inflammatory cell recruitment in vivo by promoting adhesion to vascular endothelium. *Am J Physiol Cell Physiol,* 306**,** C1184-90.

LEVY-ADAM, F., ABBOUD-JARROUS, G., GUERRINI, M., BECCATI, D., VLODAVSKY, I. & ILAN, N. 2005. Identification and characterization of heparin/heparan sulfate binding domains of the endoglycosidase heparanase. *J Biol Chem,* 280**,** 20457-66.

LEVY-ADAM, F., FELD, S., COHEN-KAPLAN, V., SHTEINGAUZ, A., GROSS, M., ARVATZ, G., NARODITSKY, I., ILAN, N., DOWECK, I. & VLODAVSKY, I. 2010. Heparanase 2 interacts with heparan sulfate with high affinity and inhibits heparanase activity. *J Biol Chem,* 285**,** 28010-9.

LEVY-ADAM, F., FELD, S., SUSS-TOBY, E., VLODAVSKY, I. & ILAN, N. 2008. Heparanase facilitates cell adhesion and spreading by clustering of cell surface heparan sulfate proteoglycans. *PLoS One,* 3**,** e2319.

LEWIS, K. D., ROBINSON, W. A., MILLWARD, M. J., POWELL, A., PRICE, T. J., THOMSON, D. B., WALPOLE, E. T., HAYDON, A. M., CREESE, B. R., ROBERTS, K. L., ZALCBERG, J. R. & GONZALEZ, R. 2008. A phase II study of the heparanase inhibitor PI-88 in patients with advanced melanoma. *Invest New Drugs,* 26**,** 89-94.

LI, H., HUANG, Y., JIANG, D. Q., CUI, L. Z., HE, Z., WANG, C., ZHANG, Z. W., ZHU, H. L., DING, Y. M., LI, L. F., LI, Q., JIN, H. J. & QIAN, Q. J. 2018. Antitumor activity of EGFR-specific CAR T cells against non-small-cell lung cancer cells in vitro and in mice. *Cell Death Dis,* 9**,** 177.

LI, H., LI, H., QU, H., ZHAO, M., YUAN, B., CAO, M. & CUI, J. 2015a. Suramin inhibits cell proliferation in ovarian and cervical cancer by downregulating heparanase expression. *Cancer Cell Int,* 15**,** 52.

LI, H. L., GU, J., WU, J. J., MA, C. L., YANG, Y. L., WANG, H. P., WANG, J., WANG, Y., CHEN, C. & WU, H. Y. 2015b. Heparanase mRNA and Protein Expression Correlates with Clinicopathologic Features of Gastric Cancer Patients: a Meta-analysis. *Asian Pac J Cancer Prev,* 16**,** 8653-8.

LI, J. & KING, M. R. 2012. Adhesion receptors as therapeutic targets for circulating tumor cells. *Front Oncol,* 2**,** 79.

LI, J., MENG, X., HU, J., ZHANG, Y., DANG, Y., WEI, L. & SHI, M. 2017a. Heparanase promotes radiation resistance of cervical cancer by upregulating hypoxia inducible factor 1. *American Journal of Cancer Research,* 7**,** 234-244.

LI, J., MENG, X., HU, J., ZHANG, Y., DANG, Y., WEI, L. & SHI, M. 2017b. Heparanase promotes radiation resistance of cervical cancer by upregulating hypoxia inducible factor 1. *Am J Cancer Res,* 7**,** 234-244.

LI, J., PAN, Q., ROWAN, P. D., TROTTER, T. N., PEKER, D., REGAL, K. M., JAVED, A., SUVA, L. J. & YANG, Y. 2016a. Heparanase promotes myeloma progression by inducing mesenchymal features and motility of myeloma cells. *Oncotarget,* 7**,** 11299-11309.

LI, J., PAN, Q., ROWAN, P. D., TROTTER, T. N., PEKER, D., REGAL, K. M., JAVED, A., SUVA, L. J. & YANG, Y. 2016b. Heparanase promotes myeloma progression by inducing mesenchymal features and motility of myeloma cells. *Oncotarget,* 7**,** 11299-309.

LI, J. P. & KUSCHE-GULLBERG, M. 2016. Heparan Sulfate: Biosynthesis, Structure, and Function. *Int Rev Cell Mol Biol,* 325**,** 215-73.

LI, Q.-N., LIU, H.-Y., XIN, X.-L., PAN, Q.-M., WANG, L., ZHANG, J., CHEN, Q., GENG, M.-Y. & DING, J. 2009. Marine-derived oligosaccharide sulfate (JG3) suppresses heparanase-driven cell adhesion events in heparanase over-expressing CHO-K1 cells. *Acta Pharmacologica Sinica,* 30**,** 1033.

LI, X., PADHAN, N., SJÖSTRÖM, E. O., ROCHE, F. P., TESTINI, C., HONKURA, N., SÁINZ-JASPEADO, M., GORDON, E., BENTLEY, K., PHILIPPIDES, A., TOLMACHEV, V., DEJANA, E., STAN, R. V., VESTWEBER, D., BALLMER-HOFER, K., BETSHOLTZ, C., PIETRAS, K., JANSSON, L. & CLAESSON-WELSH, L. 2016c. VEGFR2 pY949 signalling regulates adherens junction integrity and metastatic spread. *Nature Communications,* 7**,** 11017.

LI, Y., LIU, H., HUANG, Y. Y., PU, L. J., ZHANG, X. D., JIANG, C. C. & JIANG, Z. W. 2013. Suppression of endoplasmic reticulum stress-induced invasion and migration of breast cancer cells through the downregulation of heparanase. *Int J Mol Med,* 31**,** 1234-42.

LIANG, X. H., JACKSON, S., SEAMAN, M., BROWN, K., KEMPKES, B., HIBSHOOSH, H. & LEVINE, B. 1999. Induction of autophagy and inhibition of tumorigenesis by beclin 1. *Nature,* 402**,** 672-6.

LIAO, B. Y., WANG, Z., HU, J., LIU, W. F., SHEN, Z. Z., ZHANG, X., YU, L., FAN, J. & ZHOU, J. 2016a. PI-88 inhibits postoperative recurrence of hepatocellular carcinoma via disrupting the surge of heparanase after liver resection. *Tumour Biol,* 37**,** 2987-98.

LIAO, Y. H., CHIANG, K. H., SHIEH, J. M., HUANG, C. R., SHEN, C. J., HUANG, W. C. & CHEN, B. K. 2016b. Epidermal growth factor-induced ANGPTL4 enhances anoikis resistance and tumour metastasis in head and neck squamous cell carcinoma. *Oncogene,* 36**,** 2228.

LIBERTI, M. V. & LOCASALE, J. W. 2016. The Warburg Effect: How Does it Benefit Cancer Cells? *Trends Biochem Sci,* 41**,** 211-218.

LICHTENBERGER, B. M., TAN, P. K., NIEDERLEITHNER, H., FERRARA, N., PETZELBAUER, P. & SIBILIA, M. 2010. Autocrine VEGF signaling synergizes with EGFR in tumor cells to promote epithelial cancer development. *Cell,* 140**,** 268-79.

LIEU, C., HEYMACH, J., OVERMAN, M., TRAN, H. & KOPETZ, S. 2011. Beyond VEGF: Inhibition of the Fibroblast Growth Factor Pathway and Anti-Angiogenesis. *Clinical cancer research : an official journal of the American Association for Cancer Research,* 17**,** 6130-6139.

LIFSTED, T., LE VOYER, T., WILLIAMS, M., MULLER, W., KLEIN-SZANTO, A., BUETOW, K. H. & HUNTER, K. W. 1998. Identification of inbred mouse strains harboring genetic modifiers of mammary tumor age of onset and metastatic progression. *Int J Cancer,* 77**,** 640-4.

LIM, H. C., MULTHAUPT, H. A. & COUCHMAN, J. R. 2015. Cell surface heparan sulfate proteoglycans control adhesion and invasion of breast carcinoma cells. *Mol Cancer,* 14**,** 15.

LIN, E. Y., JONES, J. G., LI, P., ZHU, L., WHITNEY, K. D., MULLER, W. J. & POLLARD, J. W. 2003. Progression to malignancy in the polyoma middle T oncoprotein mouse breast cancer model provides a reliable model for human diseases. *Am J Pathol,* 163**,** 2113-26.

LIN, E. Y., NGUYEN, A. V., RUSSELL, R. G. & POLLARD, J. W. 2001. Colony-stimulating factor 1 promotes progression of mammary tumors to malignancy. *J Exp Med,* 193**,** 727-40.

LIN, K. Y. & KRAUS, W. L. 2017. PARP Inhibitors for Cancer Therapy. *Cell,* 169**,** 183.

LINCOLN, D. W., 2ND, PHILLIPS, P. G. & BOVE, K. 2003. Estrogen-induced Ets-1 promotes capillary formation in an in vitro tumor angiogenesis model. *Breast Cancer Res Treat,* 78**,** 167-78.

LINDE, N., CASANOVA-ACEBES, M., SOSA, M. S., MORTHA, A., RAHMAN, A., FARIAS, E., HARPER, K., TARDIO, E., REYES TORRES, I., JONES, J., CONDEELIS, J., MERAD, M. & AGUIRRE-GHISO, J. A. 2018. Macrophages orchestrate breast cancer early dissemination and metastasis. *Nat Commun,* 9**,** 21.

LIOU, G. Y., DOPPLER, H., NECELA, B., KRISHNA, M., CRAWFORD, H. C., RAIMONDO, M. & STORZ, P. 2013. Macrophage-secreted cytokines drive pancreatic acinar-to-ductal metaplasia through NF-kappaB and MMPs. *J Cell Biol,* 202**,** 563-77.

LIP, G. Y., CHIN, B. S. & BLANN, A. D. 2002a. Cancer and the prothrombotic state. *Lancet Oncol,* 3**,** 27-34.

LIP, G. Y. H., CHIN, B. S. P. & BLANN, A. D. 2002b. Cancer and the prothrombotic state. *The Lancet Oncology,* 3**,** 27-34.

LIU, C.-J., CHANG, J., LEE, P.-H., LIN, D.-Y., WU, C.-C., JENG, L.-B., LIN, Y.-J., MOK, K.-T., LEE, W.-C., YEH, H.-Z., HO, M.-C., YANG, S.-S., YANG, M.-D., YU, M.-C., HU, R.-H., PENG, C.-Y., LAI, K.-L., CHANG, S. S.-C. & CHEN, P.-J. 2014. Adjuvant heparanase inhibitor PI-88 therapy for hepatocellular carcinoma recurrence. *World Journal of Gastroenterology : WJG,* 20**,** 11384-11393.

LIU, C. J., LEE, P. H., LIN, D. Y., WU, C. C., JENG, L. B., LIN, P. W., MOK, K. T., LEE, W. C., YEH, H. Z., HO, M. C., YANG, S. S., LEE, C. C., YU, M. C., HU, R. H., PENG, C. Y., LAI, K. L., CHANG, S. S. & CHEN, P. J. 2009. Heparanase inhibitor PI-88 as adjuvant therapy for hepatocellular carcinoma after curative resection: a randomized phase II trial for safety and optimal dosage. *J Hepatol,* 50**,** 958-68.

LIU, D., SHRIVER, Z., QI, Y., VENKATARAMAN, G. & SASISEKHARAN, R. 2002. Dynamic regulation of tumor growth and metastasis by heparan sulfate glycosaminoglycans. *Semin Thromb Hemost,* 28**,** 67-78.

LIU, J., ZHANG, N., LI, Q., ZHANG, W., KE, F., LENG, Q., WANG, H., CHEN, J. & WANG, H. 2011. Tumor-associated macrophages recruit CCR6+ regulatory T cells and promote the development of colorectal cancer via enhancing CCL20 production in mice. *PLoS One,* 6**,** e19495.

LIU, L., LIU, L., YAO, H. H., ZHU, Z. Q., NING, Z. L. & HUANG, Q. 2016. Stromal Myofibroblasts Are Associated with Poor Prognosis in Solid Cancers: A Meta-Analysis of Published Studies. *PLoS One,* 11**,** e0159947.

LIU, L. P., SHENG, X. P., SHUAI, T. K., ZHAO, Y. X., LI, B. & LI, Y. M. 2018. Helicobacter pylori promotes invasion and metastasis of gastric cancer by enhancing heparanase expression. *World J Gastroenterol,* 24**,** 4565-4577.

LIU, Y. & CAO, X. 2016. Characteristics and Significance of the Pre-metastatic Niche. *Cancer Cell,* 30**,** 668-681.

LO, P. K., ZHANG, Y., YAO, Y., WOLFSON, B., YU, J., HAN, S. Y., DURU, N. & ZHOU, Q. 2017. Tumor-associated myoepithelial cells promote the invasive progression of ductal carcinoma in situ through activation of TGFbeta signaling. *J Biol Chem,* 292**,** 11466-11484.

LOKA, R. S., YU, F., SLETTEN, E. T. & NGUYEN, H. M. 2017. Design, synthesis, and evaluation of heparan sulfate mimicking glycopolymers for inhibiting heparanase activity. *Chem Commun (Camb),* 53**,** 9163-9166.

LOPEZ-COTARELO, P., GOMEZ-MOREIRA, C., CRIADO-GARCIA, O., SANCHEZ, L. & RODRIGUEZ-FERNANDEZ, J. L. 2017. Beyond Chemoattraction: Multifunctionality of Chemokine Receptors in Leukocytes. *Trends Immunol,* 38**,** 927-941.

LÓPEZ-SOTO, A., GONZALEZ, S., SMYTH, M. J. & GALLUZZI, L. 2017. Control of Metastasis by NK Cells. *Cancer Cell,* 32**,** 135-154.

LOPEZ-SOTO, A., HUERGO-ZAPICO, L., ACEBES-HUERTA, A., VILLA-ALVAREZ, M. & GONZALEZ, S. 2015. NKG2D signaling in cancer immunosurveillance. *Int J Cancer,* 136**,** 1741-50.

LOPEZ, J., HESLING, C., PRUDENT, J., POPGEORGIEV, N., GADET, R., MIKAELIAN, I., RIMOKH, R., GILLET, G. & GONZALO, P. 2012. Src tyrosine kinase inhibits apoptosis through the Erk1/2- dependent degradation of the death accelerator Bik. *Cell Death Differ,* 19**,** 1459-69.

LOPEZ, J. I., CAMENISCH, T. D., STEVENS, M. V., SANDS, B. J., MCDONALD, J. & SCHROEDER, J. A. 2005. CD44 attenuates metastatic invasion during breast cancer progression. *Cancer Res,* 65**,** 6755-63.

LORTAT-JACOB, H., GROSDIDIER, A. & IMBERTY, A. 2002. Structural diversity of heparan sulfate binding domains in chemokines. *Proc Natl Acad Sci U S A,* 99**,** 1229-34.

LOWE, S. W., CEPERO, E. & EVAN, G. 2004. Intrinsic tumour suppression. *Nature,* 432**,** 307-15.

LOWENFELS, A. B., MAISONNEUVE, P., CAVALLINI, G., AMMANN, R. W., LANKISCH, P. G., ANDERSEN, J. R., DIMAGNO, E. P., ANDREN-SANDBERG, A. & DOMELLOF, L. 1993. Pancreatitis and the risk of pancreatic cancer. International Pancreatitis Study Group. *N Engl J Med,* 328**,** 1433-7.

LOWRY, L. E. & ZEHRING, W. A. 2017. Potentiation of Natural Killer Cells for Cancer Immunotherapy: A Review of Literature. *Frontiers in Immunology,* 8**,** 1061.

LU, H., FORBES, R. A. & VERMA, A. 2002. Hypoxia-inducible factor 1 activation by aerobic glycolysis implicates the Warburg effect in carcinogenesis. *J Biol Chem,* 277**,** 23111-5.

LU, H., HOWATT, D. A., BALAKRISHNAN, A., MOORLEGHEN, J. J., RATERI, D. L., CASSIS, L. A. & DAUGHERTY, A. 2015. Subcutaneous Angiotensin II Infusion using Osmotic Pumps Induces Aortic Aneurysms in Mice. *Journal of visualized experiments : JoVE***,** 53191.

LU, S. L., HERRINGTON, H., REH, D., WEBER, S., BORNSTEIN, S., WANG, D., LI, A. G., TANG, C. F., SIDDIQUI, Y., NORD, J., ANDERSEN, P., CORLESS, C. L. & WANG, X. J. 2006. Loss of transforming growth factor-beta type II receptor promotes metastatic head-and-neck squamous cell carcinoma. *Genes Dev,* 20**,** 1331-42.

LU, W. C., LIU, Y. N., KANG, B. B. & CHEN, J. H. 2003. Trans-activation of heparanase promoter by ETS transcription factors. *Oncogene,* 22**,** 919-23.

LUAN, Q., SUN, J., LI, C., ZHANG, G., LV, Y., WANG, G., LI, C., MA, C. & GAO, T. 2011. Mutual enhancement between heparanase and vascular endothelial growth factor: a novel mechanism for melanoma progression. *Cancer Lett,* 308**,** 100-11.

LUCAS, P. J., MCNEIL, N., HILGENFELD, E., CHOUDHURY, B., KIM, S. J., ECKHAUS, M. A., RIED, T. & GRESS, R. E. 2004. Transforming growth factor-beta pathway serves as a primary tumor suppressor in CD8+ T cell tumorigenesis. *Cancer Res,* 64**,** 6524-9.

LUDWIG, T. 2005. Local proteolytic activity in tumor cell invasion and metastasis. *Bioessays,* 27**,** 1181-91.

LUKONG, K. E. 2017. Understanding breast cancer – The long and winding road. *BBA Clinical,* 7**,** 64-77.

LV, Q., ZENG, J. & HE, L. 2016a. The advancements of heparanase in fibrosis. *Int J Mol Epidemiol Genet,* 7**,** 137-140.

LV, Q., ZENG, J. & HE, L. 2016b. The advancements of heparanase in fibrosis. *International Journal of Molecular Epidemiology and Genetics,* 7**,** 137-140.

LYON, M., RUSHTON, G. & GALLAGHER, J. T. 1997. The interaction of the transforming growth factor-betas with heparin/heparan sulfate is isoform-specific. *J Biol Chem,* 272**,** 18000-6.

MA, X.-J., SALUNGA, R., TUGGLE, J. T., GAUDET, J., ENRIGHT, E., MCQUARY, P., PAYETTE, T., PISTONE, M., STECKER, K., ZHANG, B. M., ZHOU, Y.-X., VARNHOLT, H., SMITH, B., GADD, M., CHATFIELD, E., KESSLER, J., BAER, T. M., ERLANDER, M. G. & SGROI, D. C. 2003. Gene expression profiles of human breast cancer progression. *Proceedings of the National Academy of Sciences,* 100**,** 5974-5979.

MA, Y. Q. & GENG, J. G. 2000. Heparan sulfate-like proteoglycans mediate adhesion of human malignant melanoma A375 cells to P-selectin under flow. *J Immunol,* 165**,** 558-65.

MACARRON, R., BANKS, M. N., BOJANIC, D., BURNS, D. J., CIROVIC, D. A., GARYANTES, T., GREEN, D. V. S., HERTZBERG, R. P., JANZEN, W. P., PASLAY, J. W., SCHOPFER, U. & SITTAMPALAM, G. S. 2011. Impact of high-throughput screening in biomedical research. *Nature Reviews Drug Discovery,* 10**,** 188.

MACMAHON, B., COLE, P., LIN, T. M., LOWE, C. R., MIRRA, A. P., RAVNIHAR, B., SALBER, E. J., VALAORAS, V. G. & YUASA, S. 1970. Age at first birth and breast cancer risk. *Bull World Health Organ,* 43**,** 209-21.

MADIA, V. N., MESSORE, A., PESCATORI, L., SACCOLITI, F., TUDINO, V., DE LEO, A., BORTOLAMI, M., SCIPIONE, L., COSTI, R., RIVARA, S., SCALVINI, L., MOR, M., FERRARA, F. F., PAVONI, E., ROSCILLI, G., CASSINELLI, G., MILAZZO, F. M., BATTISTUZZI, G., DI SANTO, R. & GIANNINI, G. 2018. Novel Benzazole Derivatives Endowed with Potent Antiheparanase Activity. *J Med Chem,* 61**,** 6918-6936.

MAEDA, T., ALEXANDER, C. M. & FRIEDL, A. 2004. Induction of Syndecan-1 Expression in Stromal Fibroblasts Promotes Proliferation of Human Breast Cancer Cells. *Cancer Research,* 64**,** 612-621.

MAEDA, T., DESOUKY, J. & FRIEDL, A. 2005. Syndecan-1 expression by stromal fibroblasts promotes breast carcinoma growth in vivo and stimulates tumor angiogenesis. *Oncogene,* 25**,** 1408.

MAIA, J., CAJA, S., STRANO MORAES, M. C., COUTO, N. & COSTA-SILVA, B. 2018. Exosome-Based Cell-Cell Communication in the Tumor Microenvironment. *Front Cell Dev Biol,* 6**,** 18.

MAKINOSHIMA, H., TAKITA, M., SARUWATARI, K., UMEMURA, S., OBATA, Y., ISHII, G., MATSUMOTO, S., SUGIYAMA, E., OCHIAI, A., ABE, R., GOTO, K., ESUMI, H. & TSUCHIHARA, K. 2015. Signaling through the Phosphatidylinositol 3-Kinase (PI3K)/Mammalian Target of Rapamycin (mTOR) Axis Is Responsible for Aerobic Glycolysis mediated by Glucose Transporter in Epidermal Growth Factor Receptor (EGFR)-mutated Lung Adenocarcinoma. *J Biol Chem,* 290**,** 17495-504.

MALAVAKI, C. J., ROUSSIDIS, A. E., GIALELI, C., KLETSAS, D., TSEGENIDIS, T., THEOCHARIS, A. D., TZANAKAKIS, G. N. & KARAMANOS, N. K. 2013. Imatinib as a key inhibitor of the platelet-derived growth factor receptor mediated expression of cell surface heparan sulfate proteoglycans and functional properties of breast cancer cells. *FEBS J,* 280**,** 2477-89.

MANI, S. A., GUO, W., LIAO, M.-J., EATON, E. N., AYYANAN, A., ZHOU, A. Y., BROOKS, M., REINHARD, F., ZHANG, C. C., SHIPITSIN, M., CAMPBELL, L. L., POLYAK, K., BRISKEN, C., YANG, J. & WEINBERG, R. A. 2008. The Epithelial-Mesenchymal Transition Generates Cells with Properties of Stem Cells. *Cell,* 133**,** 704-715.

MANTOVANI, A. 1978. Effects on in vitro tumor growth of murine macrophages isolated from sarcoma lines differing in immunogenicity and metastasizing capacity. *Int J Cancer,* 22**,** 741-6.

MANTOVANI, A., MARCHESI, F., MALESCI, A., LAGHI, L. & ALLAVENA, P. 2017. Tumour-associated macrophages as treatment targets in oncology. *Nature Reviews Clinical Oncology,* 14**,** 399.

MARCHETTI, D., REILAND, J., ERWIN, B. & ROY, M. 2003. Inhibition of heparanase activity and heparanase-induced angiogenesis by suramin analogues. *Int J Cancer,* 104**,** 167-74.

MARIN-ACEVEDO, J. A., SOYANO, A. E., DHOLARIA, B., KNUTSON, K. L. & LOU, Y. 2018. Cancer immunotherapy beyond immune checkpoint inhibitors. *Journal of Hematology & Oncology,* 11**,** 8.

MARTINEZ-LOSTAO, L., ANEL, A. & PARDO, J. 2015. How Do Cytotoxic Lymphocytes Kill Cancer Cells? *Clin Cancer Res,* 21**,** 5047-56.

MARTÍNEZ-LOSTAO, L., ANEL, A. & PARDO, J. 2015. How Do Cytotoxic Lymphocytes Kill Cancer Cells? *Clinical Cancer Research,* 21**,** 5047-5056.

MASCIA, P., PISTIS, M., JUSTINOVA, Z., PANLILIO, L. V., LUCHICCHI, A., LECCA, S., SCHERMA, M., FRATTA, W., FADDA, P., BARNES, C., REDHI, G. H., YASAR, S., LE FOLL, B., TANDA, G., PIOMELLI, D. & GOLDBERG, S. R. 2011. Blockade of nicotine reward and reinstatement by activation of alpha-type peroxisome proliferator-activated receptors. *Biol Psychiatry,* 69**,** 633-41.

MASOLA, V., GAMBARO, G., TIBALDI, E., BRUNATI, A. M., GASTALDELLO, A., D'ANGELO, A., ONISTO, M. & LUPO, A. 2012a. Heparanase and syndecan-1 interplay orchestrates fibroblast growth factor-2-induced epithelial-mesenchymal transition in renal tubular cells. *J Biol Chem,* 287**,** 1478-88.

MASOLA, V., ONISTO, M., ZAZA, G., LUPO, A. & GAMBARO, G. 2012b. A new mechanism of action of sulodexide in diabetic nephropathy: inhibits heparanase-1 and prevents FGF-2-induced renal epithelial-mesenchymal transition. *Journal of Translational Medicine,* 10**,** 213.

MASOLA, V., ONISTO, M., ZAZA, G., LUPO, A. & GAMBARO, G. 2012c. A new mechanism of action of sulodexide in diabetic nephropathy: inhibits heparanase-1 and prevents FGF-2-induced renal epithelial-mesenchymal transition. *J Transl Med,* 10**,** 213.

MASOLA, V., ZAZA, G., GAMBARO, G., ONISTO, M., BELLIN, G., VISCHINI, G., KHAMAYSI, I., HASSAN, A., HAMOUD, S., NATIV, O., HEYMAN, S. N., LUPO, A., VLODAVSKY, I. & ABASSI, Z. 2016. Heparanase: A Potential New Factor Involved in the Renal Epithelial Mesenchymal Transition (EMT) Induced by Ischemia/Reperfusion (I/R) Injury. *PLoS One,* 11**,** e0160074.

MASOLA, V., ZAZA, G., SECCHI, M. F., GAMBARO, G., LUPO, A. & ONISTO, M. 2014a. Heparanase is a key player in renal fibrosis by regulating TGF-beta expression and activity. *Biochim Biophys Acta,* 1843**,** 2122-8.

MASOLA, V., ZAZA, G., SECCHI, M. F., GAMBARO, G., LUPO, A. & ONISTO, M. 2014b. Heparanase is a key player in renal fibrosis by regulating TGF-β expression and

activity. *Biochimica et Biophysica Acta (BBA) - Molecular Cell Research,* 1843**,** 2122-2128.

MASOUD, V. & PAGÈS, G. 2017. Targeted therapies in breast cancer: New challenges to fight against resistance. *World Journal of Clinical Oncology,* 8**,** 120-134.

MASSAGUE, J. & OBENAUF, A. C. 2016. Metastatic colonization by circulating tumour cells. *Nature,* 529**,** 298-306.

MASSENA, S., CHRISTOFFERSSON, G., HJERTSTROM, E., ZCHARIA, E., VLODAVSKY, I., AUSMEES, N., ROLNY, C., LI, J. P. & PHILLIPSON, M. 2010. A chemotactic gradient sequestered on endothelial heparan sulfate induces directional intraluminal crawling of neutrophils. *Blood,* 116**,** 1924-31.

MATOS, L. L., SUAREZ, E. R., THEODORO, T. R., TRUFELLI, D. C., MELO, C. M., GARCIA, L. F., OLIVEIRA, O. C., MATOS, M. G., KANDA, J. L., NADER, H. B., MARTINS, J. R. & PINHAL, M. A. 2015. The Profile of Heparanase Expression Distinguishes Differentiated Thyroid Carcinoma from Benign Neoplasms. *PLoS One,* 10**,** e0141139.

MATSUDA, K., MARUYAMA, H., GUO, F., KLEEFF, J., ITAKURA, J., MATSUMOTO, Y., LANDER, A. D. & KORC, M. 2001. Glypican-1 is overexpressed in human breast cancer and modulates the mitogenic effects of multiple heparin-binding growth factors in breast cancer cells. *Cancer Res,* 61**,** 5562-9.

MATSUDA, K., OHGA, N., HIDA, Y., MURAKI, C., TSUCHIYA, K., KUROSU, T., AKINO, T., SHIH, S. C., TOTSUKA, Y., KLAGSBRUN, M., SHINDOH, M. & HIDA, K. 2010. Isolated tumor endothelial cells maintain specific character during long-term culture. *Biochem Biophys Res Commun,* 394**,** 947-54.

MATZNER, Y., BAR-NER, M., YAHALOM, J., ISHAI-MICHAELI, R., FUKS, Z. & VLODAVSKY, I. 1985. Degradation of heparan sulfate in the subendothelial extracellular matrix by a readily released heparanase from human neutrophils. Possible role in invasion through basement membranes. *J Clin Invest,* 76**,** 1306-13.

MAXHIMER, J. B., PESCE, C. E., STEWART, R. A., GATTUSO, P., PRINZ, R. A. & XU, X. 2005a. Ductal carcinoma in situ of the breast and heparanase-1 expression: A molecular explanation for more aggressive subtypes. *Journal of the American College of Surgeons,* 200**,** 328-335.

MAXHIMER, J. B., QUIROS, R. M., STEWART, R., DOWLATSHAHI, K., GATTUSO, P., FAN, M., PRINZ, R. A. & XU, X. 2002. Heparanase-1 expression is associated with the metastatic potential of breast cancer. *Surgery,* 132**,** 326-333.

MAXHIMER, J. B., SOMENEK, M., RAO, G., PESCE, C. E., BALDWIN, D., JR., GATTUSO, P., SCHWARTZ, M. M., LEWIS, E. J., PRINZ, R. A. & XU, X. 2005b. Heparanase-1 gene expression and regulation by high glucose in renal epithelial cells: a potential role in the pathogenesis of proteinuria in diabetic patients. *Diabetes,* 54**,** 2172-8.

MCDONALD, A. G., YANG, K., ROBERTS, H. R., MONROE, D. M. & HOFFMAN, M. 2008. Perivascular tissue factor is down-regulated following cutaneous wounding: implications for bleeding in hemophilia. *Blood,* 111**,** 2046-8.

MCKENZIE, E., TYSON, K., STAMPS, A., SMITH, P., TURNER, P., BARRY, R., HIRCOCK, M., PATEL, S., BARRY, E., STUBBERFIELD, C., TERRETT, J. & PAGE, M. 2000. Cloning and expression profiling of Hpa2, a novel mammalian heparanase family member. *Biochem Biophys Res Commun,* 276**,** 1170-7.

MCKENZIE, E., YOUNG, K., HIRCOCK, M., BENNETT, J., BHAMAN, M., FELIX, R., TURNER, P., STAMPS, A., MCMILLAN, D., SAVILLE, G., NG, S., MASON, S., SNELL, D., SCHOFIELD, D., GONG, H., TOWNSEND, R., GALLAGHER, J., PAGE, M., PAREKH, R. & STUBBERFIELD, C. 2003. Biochemical characterization of the active heterodimer form of human heparanase (Hpa1) protein expressed in insect cells. *Biochem J,* 373**,** 423-35.

MCKENZIE, E. A. 2007. Heparanase: a target for drug discovery in cancer and inflammation. *British Journal of Pharmacology,* 151**,** 1-14.

MEDES, G., THOMAS, A. & WEINHOUSE, S. 1953. Metabolism of neoplastic tissue. IV. A study of lipid synthesis in neoplastic tissue slices in vitro. *Cancer Res,* 13**,** 27-9.

MENARD, R., ALBAN, S., DE RUFFRAY, P., JAMOIS, F., FRANZ, G., FRITIG, B., YVIN, J. C. & KAUFFMANN, S. 2004. Beta-1,3 glucan sulfate, but not beta-1,3 glucan, induces the salicylic acid signaling pathway in tobacco and Arabidopsis. *Plant Cell,* 16**,** 3020-32.

MENDES, D., ALVES, C., AFONSO, N., CARDOSO, F., PASSOS-COELHO, J. L., COSTA, L., ANDRADE, S. & BATEL-MARQUES, F. 2015. The benefit of HER2-targeted therapies on overall survival of patients with metastatic HER2-positive breast cancer--a systematic review. *Breast Cancer Res,* 17**,** 140.

MENG, X. M., NIKOLIC-PATERSON, D. J. & LAN, H. Y. 2016. TGF-beta: the master regulator of fibrosis. *Nat Rev Nephrol,* 12**,** 325-38.

MENON, L. G., KUTTAN, R. & KUTTAN, G. 1995. Inhibition of lung metastasis in mice induced by B16F10 melanoma cells by polyphenolic compounds. *Cancer Letters,* 95**,** 221-225.

METWALY, H. A., EL-GAYAR, A. M. & EL-SHISHTAWY, M. M. 2018. Inhibition of the signaling pathway of syndecan-1 by synstatin: A promising anti-integrin inhibitor of angiogenesis and proliferation in HCC in rats. *Arch Biochem Biophys,* 652**,** 50-58.

MIAO, H. Q., NAVARRO, E., PATEL, S., SARGENT, D., KOO, H., WAN, H., PLATA, A., ZHOU, Q., LUDWIG, D., BOHLEN, P. & KUSSIE, P. 2002. Cloning, expression, and purification of mouse heparanase. *Protein Expr Purif,* 26**,** 425-31.

MICALLEF, L., VEDRENNE, N., BILLET, F., COULOMB, B., DARBY, I. A. & DESMOULIERE, A. 2012. The myofibroblast, multiple origins for major roles in normal and pathological tissue repair. *Fibrogenesis Tissue Repair,* 5**,** S5.

MICHEA, P., NOËL, F., ZAKINE, E., CZERWINSKA, U., SIRVEN, P., ABOUZID, O., GOUDOT, C., SCHOLER-DAHIREL, A., VINCENT-SALOMON, A., REYAL, F., AMIGORENA, S., GUILLOT-DELOST, M., SEGURA, E. & SOUMELIS, V. 2018. Adjustment of dendritic cells to the breast-cancer microenvironment is subset specific. *Nature Immunology,* 19**,** 885-897.

MICHIKAWA, M., ICHINOSE, H., MOMMA, M., BIELY, P., JONGKEES, S., YOSHIDA, M., KOTAKE, T., TSUMURAYA, Y., WITHERS, S. G., FUJIMOTO, Z. & KANEKO, S. 2012. Structural and biochemical characterization of glycoside hydrolase family 79 beta-glucuronidase from Acidobacterium capsulatum. *J Biol Chem,* 287**,** 14069-77.

MIGLIORINI, E., THAKAR, D., KUHNLE, J., SADIR, R., DYER, D. P., LI, Y., SUN, C., VOLKMAN, B. F., HANDEL, T. M., COCHE-GUERENTE, L., FERNIG, D. G., LORTAT-JACOB, H. & RICHTER, R. P. 2015. Cytokines and growth factors cross-link heparan sulfate. *Open Biol,* 5.

MIHO, Y., KOUROKU, Y., FUJITA, E., MUKASA, T., URASE, K., KASAHARA, T., ISOAI, A., MOMOI, M. Y. & MOMOI, T. 1999. bFGF inhibits the activation of caspase-3 and apoptosis of P19 embryonal carcinoma cells during neuronal differentiation. *Cell Death Differ,* 6**,** 463-70.

MILELLA, M., FALCONE, I., CONCIATORI, F., CESTA INCANI, U., DEL CURATOLO, A., INZERILLI, N., NUZZO, C. M., VACCARO, V., VARI, S., COGNETTI, F. & CIUFFREDA, L. 2015. PTEN: Multiple Functions in Human Malignant Tumors. *Front Oncol,* 5**,** 24.

MILLER, F. R., MILLER, B. E. & HEPPNER, G. H. 1983. Characterization of metastatic heterogeneity among subpopulations of a single mouse mammary tumor: heterogeneity in phenotypic stability. *Invasion Metastasis,* 3**,** 22-31.

MILLER, K. D., CHAP, L. I., HOLMES, F. A., COBLEIGH, M. A., MARCOM, P. K., FEHRENBACHER, L., DICKLER, M., OVERMOYER, B. A., REIMANN, J. D., SING, A. P., LANGMUIR, V. & RUGO, H. S. 2005. Randomized phase III trial of capecitabine compared with bevacizumab plus capecitabine in patients with previously treated metastatic breast cancer. *J Clin Oncol,* 23**,** 792-9.

MINK, S., PONTA, H. & CATO, A. C. 1990. The long terminal repeat region of the mouse mammary tumour virus contains multiple regulatory elements. *Nucleic Acids Research,* 18**,** 2017-2024.

MITSIADES, C. S., ROULEAU, C., ECHART, C., MENON, K., TEICHER, B., DISTASO, M., PALUMBO, A., BOCCADORO, M., ANDERSON, K. C., IACOBELLI, M. & RICHARDSON, P. G. 2009. Preclinical studies in support of defibrotide for the treatment of multiple myeloma and other neoplasias. *Clin Cancer Res,* 15**,** 1210-21.

MIZUMOTO, S., FONGMOON, D. & SUGAHARA, K. 2013. Interaction of chondroitin sulfate and dermatan sulfate from various biological sources with heparin-binding growth factors and cytokines. *Glycoconj J,* 30**,** 619-32.

MOHAMED, S. & COOMBE, D. R. 2017. Heparin Mimetics: Their Therapeutic Potential. *Pharmaceuticals (Basel),* 10.

MOORE, R. J., OWENS, D. M., STAMP, G., ARNOTT, C., BURKE, F., EAST, N., HOLDSWORTH, H., TURNER, L., ROLLINS, B., PASPARAKIS, M., KOLLIAS, G. & BALKWILL, F. 1999. Mice deficient in tumor necrosis factor-alpha are resistant to skin carcinogenesis. *Nat Med,* 5**,** 828-31.

MOREL, A. P., LIEVRE, M., THOMAS, C., HINKAL, G., ANSIEAU, S. & PUISIEUX, A. 2008. Generation of breast cancer stem cells through epithelial-mesenchymal transition. *PLoS One,* 3**,** e2888.

MORII, M., KUBOTA, S., HONDA, T., YUKI, R., MORINAGA, T., KUGA, T., TOMONAGA, T., YAMAGUCHI, N. & YAMAGUCHI, N. 2017. Src Acts as an Effector for Ku70-dependent Suppression of Apoptosis through Phosphorylation of Ku70 at Tyr-530. *J Biol Chem,* 292**,** 1648-1665.

MORIKAWA, S., BALUK, P., KAIDOH, T., HASKELL, A., JAIN, R. K. & MCDONALD, D. M. 2002. Abnormalities in pericytes on blood vessels and endothelial sprouts in tumors. *Am J Pathol,* 160**,** 985-1000.

MORRIS, A., WANG, B., WAERN, I., VENKATASAMY, R., PAGE, C., SCHMIDT, E. P., WERNERSSON, S., LI, J. P. & SPINA, D. 2015. The role of heparanase in pulmonary cell recruitment in response to an allergic but not non-allergic stimulus. *PLoS One,* 10**,** e0127032.

MOSERLE, L., JIMÉNEZ-VALERIO, G. & CASANOVAS, O. 2014. Antiangiogenic Therapies: Going beyond Their Limits. *Cancer Discovery,* 4**,** 31-41.

MOUSAVIZADEH, R., SCOTT, A., LU, A., ARDEKANI, G. S., BEHZAD, H., LUNDGREEN, K., GHAFFARI, M., MCCORMACK, R. G. & DURONIO, V. 2016. Angiopoietin-like 4 promotes angiogenesis in the tendon and is increased in cyclically loaded tendon fibroblasts. *The Journal of physiology,* 594**,** 2971-2983.

MURAOKA-COOK, R. S., KUROKAWA, H., KOH, Y., FORBES, J. T., ROEBUCK, L. R., BARCELLOS-HOFF, M. H., MOODY, S. E., CHODOSH, L. A. & ARTEAGA, C. L. 2004. Conditional overexpression of active transforming growth factor beta1 in vivo accelerates metastases of transgenic mammary tumors. *Cancer Res,* 64**,** 9002-11.

NABA, A., CLAUSER, K. R., DING, H., WHITTAKER, C. A., CARR, S. A. & HYNES, R. O. 2016. The extracellular matrix: Tools and insights for the "omics" era. *Matrix Biol,* 49**,** 10-24.

NABA, A., CLAUSER, K. R., HOERSCH, S., LIU, H., CARR, S. A. & HYNES, R. O. 2012. The matrisome: in silico definition and in vivo characterization by proteomics of normal and tumor extracellular matrices. *Mol Cell Proteomics,* 11**,** M111 014647.

NABA, A., CLAUSER, K. R., LAMAR, J. M., CARR, S. A. & HYNES, R. O. 2014. Extracellular matrix signatures of human mammary carcinoma identify novel metastasis promoters. *Elife,* 3**,** e01308.

NADAV, L., ELDOR, A., YACOBY-ZEEVI, O., ZAMIR, E., PECKER, I., ILAN, N., GEIGER, B., VLODAVSKY, I. & KATZ, B. Z. 2002. Activation, processing and trafficking of extracellular heparanase by primary human fibroblasts. *J Cell Sci,* 115**,** 2179-87.

NADIR, Y. & BRENNER, B. 2010. Heparanase procoagulant effects and inhibition by heparins. *Thrombosis Research,* 125**,** S72-S76.

NADIR, Y. & BRENNER, B. 2014. Heparanase multiple effects in cancer. *Thromb Res,* 133 Suppl 2**,** S90-4.

NADIR, Y. & BRENNER, B. 2016. Heparanase procoagulant activity in cancer progression. *Thromb Res,* 140 Suppl 1**,** S44-8.

NADIR, Y. & BRENNER, B. 2018. Novel strategies of coagulation inhibition for reducing tumor growth and angiogenesis. *Thromb Res,* 164 Suppl 1**,** S153-s156.

NAGATA, S. 2018. Apoptosis and Clearance of Apoptotic Cells. *Annu Rev Immunol,* 36**,** 489-517.

NAKAJIMA, M., DECHAVIGNY, A., JOHNSON, C. E., HAMADA, J., STEIN, C. A. & NICOLSON, G. L. 1991. Suramin. A potent inhibitor of melanoma heparanase and invasion. *J Biol Chem,* 266**,** 9661-6.

NAKAJIMA, M., IRIMURA, T., DI FERRANTE, N. & NICOLSON, G. L. 1984. Metastatic melanoma cell heparanase. Characterization of heparan sulfate degradation fragments produced by B16 melanoma endoglucuronidase. *J Biol Chem,* 259**,** 2283-90.

NAOMOTO, Y., GUNDUZ, M., TAKAOKA, M., OKAWA, T., GUNDUZ, E., NOBUHISA, T., KOBAYASHI, M., SHIRAKAWA, Y., YAMATSUJI, T., SONODA, R., MATSUOKA, J. & TANAKA, N. 2007. Heparanase promotes angiogenesis through Cox-2 and HIF1alpha. *Med Hypotheses,* 68**,** 162-5.

NAPARSTEK, Y., COHEN, I. R., FUKS, Z. & VLODAVSKY, I. 1984. Activated T lymphocytes produce a matrix-degrading heparan sulphate endoglycosidase. *Nature,* 310**,** 241-4.

NARDELLA, C., LAHM, A., PALLAORO, M., BRUNETTI, M., VANNINI, A. & STEINKUHLER, C. 2004. Mechanism of activation of human heparanase investigated by protein engineering. *Biochemistry,* 43**,** 1862-73.

NASSER, N. J., AVIVI, A., SHAFAT, I., EDOVITSKY, E., ZCHARIA, E., ILAN, N., VLODAVSKY, I. & NEVO, E. 2009. Alternatively spliced Spalax heparanase inhibits extracellular matrix degradation, tumor growth, and metastasis. *Proc Natl Acad Sci U S A,* 106**,** 2253-8.

NASSER, N. J., AVIVI, A., SHUSHY, M., VLODAVSKY, I. & NEVO, E. 2007. Cloning, expression, and characterization of an alternatively spliced variant of human heparanase. *Biochem Biophys Res Commun,* 354**,** 33-8.

NASSER, N. J., NEVO, E., SHAFAT, I., ILAN, N., VLODAVSKY, I. & AVIVI, A. 2005. Adaptive evolution of heparanase in hypoxia-tolerant Spalax: gene cloning and identification of a unique splice variant. *Proc Natl Acad Sci U S A,* 102**,** 15161-6.

NASSER, N. J., SARIG, G., BRENNER, B., NEVO, E., GOLDSHMIDT, O., ZCHARIA, E., LI, J. P. & VLODAVSKY, I. 2006. Heparanase neutralizes the anticoagulation properties of heparin and low-molecular-weight heparin. *J Thromb Haemost,* 4**,** 560-5.

NAVARRO, F. P., FARES, R. P., SANCHEZ, P. E., NADAM, J., GEORGES, B., MOULIN, C., MORALES, A., PEQUIGNOT, J. M. & BEZIN, L. 2008. Brain heparanase expression is up-regulated during postnatal development and hypoxia-induced neovascularization in adult rats. *J Neurochem,* 105**,** 34-45.

NELSON, D. A. & LARSEN, M. 2015. Heterotypic Control of Basement Membrane Dynamics During Branching Morphogenesis. *Developmental biology,* 401**,** 103-109.

NEUZILLET, C., TIJERAS-RABALLAND, A., COHEN, R., CROS, J., FAIVRE, S., RAYMOND, E. & DE GRAMONT, A. 2015. Targeting the TGFbeta pathway for cancer therapy. *Pharmacol Ther,* 147**,** 22-31.

NEWICK, K., O'BRIEN, S., MOON, E. & ALBELDA, S. M. 2017. CAR T Cell Therapy for Solid Tumors. *Annu Rev Med,* 68**,** 139-152.

NG, A. P. & ALEXANDER, W. S. 2017. Haematopoietic stem cells: past, present and future. *Cell Death Discovery,* 3**,** 17002.

NICOSIA, R. F. & OTTINETTI, A. 1990. Growth of microvessels in serum-free matrix culture of rat aorta. A quantitative assay of angiogenesis in vitro. *Lab Invest,* 63**,** 115-22.

NIELSEN, B. S., EGEBLAD, M., RANK, F., ASKAUTRUD, H. A., PENNINGTON, C. J., PEDERSEN, T. X., CHRISTENSEN, I. J., EDWARDS, D. R., WERB, Z. & LUND, L. R. 2008. Matrix Metalloproteinase 13 Is Induced in Fibroblasts in Polyomavirus Middle T Antigen-Driven Mammary Carcinoma without Influencing Tumor Progression. *PLOS ONE,* 3**,** e2959.

NIERS, T. M., KLERK, C. P., DINISIO, M., VAN NOORDEN, C. J., BULLER, H. R., REITSMA, P. H. & RICHEL, D. J. 2007. Mechanisms of heparin induced anti-cancer activity in experimental cancer models. *Crit Rev Oncol Hematol,* 61**,** 195-207.

NISHIMURA, H., NOSE, M., HIAI, H., MINATO, N. & HONJO, T. 1999. Development of Lupus-like Autoimmune Diseases by Disruption of the PD-1 Gene Encoding an ITIM Motif-Carrying Immunoreceptor. *Immunity,* 11**,** 141-151.

NOBUHISA, T., NAOMOTO, Y., OHKAWA, T., TAKAOKA, M., ONO, R., MURATA, T., GUNDUZ, M., SHIRAKAWA, Y., YAMATSUJI, T., HAISA, M., MATSUOKA, J., TSUJIGIWA, H., NAGATSUKA, H., NAKAJIMA, M. & TANAKA, N. 2005a.

Heparanase expression correlates with malignant potential in human colon cancer. *J Cancer Res Clin Oncol,* 131**,** 229-37.

NOBUHISA, T., NAOMOTO, Y., OKAWA, T., TAKAOKA, M., GUNDUZ, M., MOTOKI, T., NAGATSUKA, H., TSUJIGIWA, H., SHIRAKAWA, Y., YAMATSUJI, T., HAISA, M., MATSUOKA, J., KUREBAYASHI, J., NAKAJIMA, M., TANIGUCHI, S., SAGARA, J., DONG, J. & TANAKA, N. 2007. Translocation of heparanase into nucleus results in cell differentiation. *Cancer Sci,* 98**,** 535-40.

NOBUHISA, T., NAOMOTO, Y., TAKAOKA, M., TABUCHI, Y., OOKAWA, K., KITAMOTO, D., GUNDUZ, E., GUNDUZ, M., NAGATSUKA, H., HAISA, M., MATSUOKA, J., NAKAJIMA, M. & TANAKA, N. 2005b. Emergence of nuclear heparanase induces differentiation of human mammary cancer cells. *Biochemical and Biophysical Research Communications,* 331**,** 175-180.

NORRBY, K. 1993. Heparin and angiogenesis: a low-molecular-weight fraction inhibits and a high-molecular-weight fraction stimulates angiogenesis systemically. *Haemostasis,* 23 Suppl 1**,** 141-9.

NOURSHARGH, S. & ALON, R. 2014. Leukocyte Migration into Inflamed Tissues. *Immunity,* 41**,** 694-707.

NOWELL, P. C. 1976. The clonal evolution of tumor cell populations. *Science,* 194**,** 23-8.

NOY, R. & POLLARD, J. W. 2014. Tumor-associated macrophages: from mechanisms to therapy. *Immunity,* 41**,** 49-61.

NURCOMBE, V., SMART, C. E., CHIPPERFIELD, H., COOL, S. M., BOILLY, B. & HONDERMARCK, H. 2000. The proliferative and migratory activities of breast cancer cells can be differentially regulated by heparan sulfates. *J Biol Chem,* 275**,** 30009-18.

O'KEEFFE, M. B., DEVLIN, A. H., BURNS, A. J., GARDINER, T. A., LOGAN, I. D., HIRST, D. G. & MCKEOWN, S. R. 2008. Investigation of pericytes, hypoxia, and vascularity in bladder tumors: association with clinical outcomes. *Oncol Res,* 17**,** 93-101.

O'MALLEY, W. E., ACHINSTEIN, B. & SHEAR, M. J. 1962. Action of Bacterial Polysaccharide on Tumors. II. Damage of Sarcoma 37 by Serum of Mice Treated With Serratia Marcescens Polysaccharide, and Induced Tolerance. *JNCI: Journal of the National Cancer Institute,* 29**,** 1169-1175.

O'REILLY, M. S., HOLMGREN, L., CHEN, C. & FOLKMAN, J. 1996. Angiostatin induces and sustains dormancy of human primary tumors in mice. *Nat Med,* 2**,** 689-92.

ODES, E. J., RANDOLPH-QUINNEY, P. S., STEYN, M., THROCKMORTON, Z., SMILG, J. S., ZIPFEL, B., AUGUSTINE, T. N., BEER, F. D., HOFFMAN, J. W., FRANKLIN, R. D. & BERGER, L. R. 2016. Earliest hominin cancer: 1.7-million-year old osteosarcoma from Swartkrans Cave, South Africa. *South African Journal of Science* 112.

OFT, M. 2014. IL-10: master switch from tumor-promoting inflammation to antitumor immunity. *Cancer Immunol Res,* 2**,** 194-9.

OGISHIMA, T., SHIINA, H., BREAULT, J. E., TABATABAI, L., BASSETT, W. W., ENOKIDA, H., LI, L. C., KAWAKAMI, T., URAKAMI, S., RIBEIRO-FILHO, L. A., TERASHIMA, M., FUJIME, M., IGAWA, M. & DAHIYA, R. 2005a. Increased heparanase expression is caused by promoter hypomethylation and up-regulation of transcriptional factor early growth response-1 in human prostate cancer. *Clin Cancer Res,* 11**,** 1028-36.

OGISHIMA, T., SHIINA, H., BREAULT, J. E., TERASHIMA, M., HONDA, S., ENOKIDA, H., URAKAMI, S., TOKIZANE, T., KAWAKAMI, T., RIBEIRO-FILHO, L. A., FUJIME, M., KANE, C. J., CARROLL, P. R., IGAWA, M. & DAHIYA, R. 2005b. Promoter CpG hypomethylation and transcription factor EGR1 hyperactivate heparanase expression in bladder cancer. *Oncogene,* 24**,** 6765-72.

OGREN, S. & LINDAHL, U. 1975. Cleavage of macromolecular heparin by an enzyme from mouse mastocytoma. *J Biol Chem,* 250**,** 2690-7.

OHGA, N., HIDA, K., HIDA, Y., MURAKI, C., TSUCHIYA, K., MATSUDA, K., OHIRO, Y., TOTSUKA, Y. & SHINDOH, M. 2009. Inhibitory effects of epigallocatechin-3 gallate, a polyphenol in green tea, on tumor-associated endothelial cells and endothelial progenitor cells. *Cancer Sci,* 100**,** 1963-70.

OHGA, N., ISHIKAWA, S., MAISHI, N., AKIYAMA, K., HIDA, Y., KAWAMOTO, T., SADAMOTO, Y., OSAWA, T., YAMAMOTO, K., KONDOH, M., OHMURA, H., SHINOHARA, N., NONOMURA, K., SHINDOH, M. & HIDA, K. 2012. Heterogeneity of tumor endothelial cells: comparison between tumor endothelial cells isolated from high- and low-metastatic tumors. *Am J Pathol,* 180**,** 1294-307.

OHKAWA, T., NAOMOTO, Y., TAKAOKA, M., NOBUHISA, T., NOMA, K., MOTOKI, T., MURATA, T., UETSUKA, H., KOBAYASHI, M., SHIRAKAWA, Y., YAMATSUJI, T., MATSUBARA, N., MATSUOKA, J., HAISA, M., GUNDUZ, M., TSUJIGIWA, H., NAGATSUKA, H., HOSOKAWA, M., NAKAJIMA, M. & TANAKA, N. 2004a. Localization of heparanase in esophageal cancer cells: respective roles in prognosis and differentiation. *Lab Invest,* 84**,** 1289-304.

OHKAWA, T., NAOMOTO, Y., TAKAOKA, M., NOBUHISA, T., NOMA, K., MOTOKI, T., MURATA, T., UETSUKA, H., KOBAYASHI, M., SHIRAKAWA, Y., YAMATSUJI, T., MATSUBARA, N., MATSUOKA, J., HAISA, M., GUNDUZ, M., TSUJIGIWA, H., NAGATSUKA, H., HOSOKAWA, M., NAKAJIMA, M. & TANAKA, N. 2004b. Localization of heparanase in esophageal cancer cells: respective roles in prognosis and differentiation. *Laboratory Investigation,* 84**,** 1289.

OKADA, Y., YAMADA, S., TOYOSHIMA, M., DONG, J., NAKAJIMA, M. & SUGAHARA, K. 2002. Structural recognition by recombinant human heparanase that plays critical roles in tumor metastasis. Hierarchical sulfate groups with different effects and the essential target disulfated trisaccharide sequence. *J Biol Chem,* 277**,** 42488-95.

OKAWA, T., NAOMOTO, Y., NOBUHISA, T., TAKAOKA, M., MOTOKI, T., SHIRAKAWA, Y., YAMATSUJI, T., INOUE, H., OUCHIDA, M., GUNDUZ, M., NAKAJIMA, M. &

TANAKA, N. 2005. Heparanase is involved in angiogenesis in esophageal cancer through induction of cyclooxygenase-2. *Clin Cancer Res,* 11**,** 7995-8005.

OKOCHI-TAKADA, E., HATTORI, N., TSUKAMOTO, T., MIYAMOTO, K., ANDO, T., ITO, S., YAMAMURA, Y., WAKABAYASHI, M., NOBEYAMA, Y. & USHIJIMA, T. 2014. ANGPTL4 is a secreted tumor suppressor that inhibits angiogenesis. *Oncogene,* 33**,** 2273-8.

OKOLICSANYI, R. K., VAN WIJNEN, A. J., COOL, S. M., STEIN, G. S., GRIFFITHS, L. R. & HAUPT, L. M. 2014. Heparan sulfate proteoglycans and human breast cancer epithelial cell tumorigenicity. *J Cell Biochem,* 115**,** 967-76.

OLDBERG, A., HELDIN, C. H., WASTESON, A., BUSCH, C. & HOOK, M. 1980. Characterization of a platelet endoglycosidase degrading heparin-like polysaccharides. *Biochemistry,* 19**,** 5755-62.

OLSEN, E. B., TRIER, K., ELDOV, K. & AMMITZBOLL, T. 1988. Glycosaminoglycans in human breast cancer. *Acta Obstet Gynecol Scand,* 67**,** 539-42.

OOKHTENS, M., KANNAN, R., LYON, I. & BAKER, N. 1984. Liver and adipose tissue contributions to newly formed fatty acids in an ascites tumor. *Am J Physiol,* 247**,** R146-53.

OOSTA, G. M., FAVREAU, L. V., BEELER, D. L. & ROSENBERG, R. D. 1982. Purification and properties of human platelet heparitinase. *J Biol Chem,* 257**,** 11249-55.

ORKIN, R. W., GEHRON, P., MCGOODWIN, E. B., MARTIN, G. R., VALENTINE, T. & SWARM, R. 1977. A murine tumor producing a matrix of basement membrane. *J Exp Med,* 145**,** 204-20.

OSKARSSON, T., BATLLE, E. & MASSAGUE, J. 2014. Metastatic stem cells: sources, niches, and vital pathways. *Cell Stem Cell,* 14**,** 306-21.

OSTAPOFF, K. T., AWASTHI, N., CENIK, B. K., HINZ, S., DREDGE, K., SCHWARZ, R. E. & BREKKEN, R. A. 2013. PG545, an angiogenesis and heparanase inhibitor, reduces primary tumor growth and metastasis in experimental pancreatic cancer. *Mol Cancer Ther,* 12**,** 1190-201.

OTTEN, A. D., SANDERS, M. M. & MCKNIGHT, G. S. 1988. The MMTV LTR promoter is induced by progesterone and dihydrotestosterone but not by estrogen. *Mol Endocrinol,* 2**,** 143-7.

OTTINI, L. 2014. Male breast cancer: a rare disease that might uncover underlying pathways of breast cancer. *Nature Reviews Cancer,* 14**,** 643.

OVERWIJK, W. W. & RESTIFO, N. P. 2001. B16 as a mouse model for human melanoma. *Current protocols in immunology,* Chapter 20**,** Unit-20.1.

PAGET, S. 1889. The distribution of secondary growths in cancer of the breast. *Lancet,* 1**,** 99-101.

PAGOTTO, A., PILOTTO, G., MAZZOLDI, E. L., NICOLETTO, M. O., FREZZINI, S., PASTO, A. & AMADORI, A. 2017. Autophagy inhibition reduces chemoresistance and tumorigenic potential of human ovarian cancer stem cells. *Cell Death Dis,* 8**,** e2943.

PALUMBO, A., LAROCCA, A., GENUARDI, M., KOTWICA, K., GAY, F., ROSSI, D., BENEVOLO, G., MAGAROTTO, V., CAVALLO, F., BRINGHEN, S., RUS, C., MASINI, L., IACOBELLI, M., GAIDANO, G., MITSIADES, C., ANDERSON, K., BOCCADORO, M. & RICHARDSON, P. 2010. Melphalan, prednisone, thalidomide and defibrotide in relapsed/refractory multiple myeloma: results of a multicenter phase I/II trial. *Haematologica,* 95**,** 1144-9.

PALUMBO, J. S., TALMAGE, K. E., MASSARI, J. V., LA JEUNESSE, C. M., FLICK, M. J., KOMBRINCK, K. W., JIROUSKOVA, M. & DEGEN, J. L. 2005. Platelets and fibrin(ogen) increase metastatic potential by impeding natural killer cell-mediated elimination of tumor cells. *Blood,* 105**,** 178-85.

PAN, W., MIAO, H.-Q., XU, Y.-J., NAVARRO, E. C., TONRA, J. R., CORCORAN, E., LAHIJI, A., KUSSIE, P., KISELYOV, A. S., WONG, W. C. & LIU, H. 2006. 1-[4-(1H-Benzoimidazol-2-yl)-phenyl]-3-[4-(1H-benzoimidazol-2-yl)-phenyl]-urea derivatives as small molecule heparanase inhibitors. *Bioorganic & Medicinal Chemistry Letters,* 16**,** 409-412.

PANDEY, P. R., SAIDOU, J. & WATABE, K. 2010. Role of myoepithelial cells in breast tumor progression. *Frontiers in bioscience : a journal and virtual library,* 15**,** 226-236.

PANG, M. F., GEORGOUDAKI, A. M., LAMBUT, L., JOHANSSON, J., TABOR, V., HAGIKURA, K., JIN, Y., JANSSON, M., ALEXANDER, J. S., NELSON, C. M., JAKOBSSON, L., BETSHOLTZ, C., SUND, M., KARLSSON, M. C. I. & FUXE, J. 2015. TGF-β1-induced EMT promotes targeted migration of breast cancer cells through the lymphatic system by the activation of CCR7/CCL21-mediated chemotaxis. *Oncogene,* 35**,** 748.

PANLILIO, L. V., JUSTINOVA, Z., MASCIA, P., PISTIS, M., LUCHICCHI, A., LECCA, S., BARNES, C., REDHI, G. H., ADAIR, J., HEISHMAN, S. J., YASAR, S., ALICZKI, M., HALLER, J. & GOLDBERG, S. R. 2012. Novel use of a lipid-lowering fibrate medication to prevent nicotine reward and relapse: preclinical findings. *Neuropsychopharmacology,* 37**,** 1838-47.

PAQUETTE, B., THERRIAULT, H., DESMARAIS, G., WAGNER, R., ROYER, R. & BUJOLD, R. 2011. Radiation-enhancement of MDA-MB-231 breast cancer cell invasion prevented by a cyclooxygenase-2 inhibitor. *British Journal Of Cancer,* 105**,** 534.

PARANGI, S., DIETRICH, W., CHRISTOFORI, G., LANDER, E. S. & HANAHAN, D. 1995. Tumor suppressor loci on mouse chromosomes 9 and 16 are lost at distinct stages of tumorigenesis in a transgenic model of islet cell carcinoma. *Cancer Res,* 55**,** 6071-6.

PARISH, C. R. 2006. The role of heparan sulphate in inflammation. *Nature Reviews Immunology,* 6**,** 633.

PARISH, C. R., FREEMAN, C., BROWN, K. J., FRANCIS, D. J. & COWDEN, W. B. 1999. Identification of sulfated oligosaccharide-based inhibitors of tumor growth and metastasis using novel in vitro assays for angiogenesis and heparanase activity. *Cancer Res,* 59**,** 3433-41.

PARISH, C. R., FREEMAN, C. & HULETT, M. D. 2001. Heparanase: a key enzyme involved in cell invasion. *Biochim Biophys Acta,* 1471**,** M99-108.

PARISH, C. R., HINDMARSH, E. J., BARTLETT, M. R., STAYKOVA, M. A., COWDEN, W. B. & WILLENBORG, D. O. 1998. Treatment of central nervous system inflammation with inhibitors of basement membrane degradation. *Immunol Cell Biol,* 76**,** 104-13.

PARK, J., WYSOCKI, R. W., AMOOZGAR, Z., MAIORINO, L., FEIN, M. R., JORNS, J., SCHOTT, A. F., KINUGASA-KATAYAMA, Y., LEE, Y., WON, N. H., NAKASONE, E. S., HEARN, S. A., KUTTNER, V., QIU, J., ALMEIDA, A. S., PERURENA, N., KESSENBROCK, K., GOLDBERG, M. S. & EGEBLAD, M. 2016. Cancer cells induce metastasis-supporting neutrophil extracellular DNA traps. *Sci Transl Med,* 8**,** 361ra138.

PARK, J. E., KELLER, G. A. & FERRARA, N. 1993. The vascular endothelial growth factor (VEGF) isoforms: differential deposition into the subepithelial extracellular matrix and bioactivity of extracellular matrix-bound VEGF. *Mol Biol Cell,* 4**,** 1317-26.

PARK, P. W., REIZES, O. & BERNFIELD, M. 2000. Cell surface heparan sulfate proteoglycans: selective regulators of ligand-receptor encounters. *J Biol Chem,* 275**,** 29923-6.

PARSONS, M. J., MCCORMICK, L., JANKE, L., HOWARD, A., BOUCHIER-HAYES, L. & GREEN, D. R. 2013. Genetic deletion of caspase-2 accelerates MMTV/c-neu-driven mammary carcinogenesis in mice. *Cell Death Differ,* 20**,** 1174-82.

PATCHING, S. G. 2014. Surface plasmon resonance spectroscopy for characterisation of membrane protein–ligand interactions and its potential for drug discovery. *Biochimica et Biophysica Acta (BBA) - Biomembranes,* 1838**,** 43-55.

PAUL, S. M., MYTELKA, D. S., DUNWIDDIE, C. T., PERSINGER, C. C., MUNOS, B. H., LINDBORG, S. R. & SCHACHT, A. L. 2010. How to improve R&D productivity: the pharmaceutical industry's grand challenge. *Nat Rev Drug Discov,* 9**,** 203-14.

PAVLOVA, N. N. & THOMPSON, C. B. 2016. The Emerging Hallmarks of Cancer Metabolism. *Cell Metab,* 23**,** 27-47.

PAWLAK, M., LEFEBVRE, P. & STAELS, B. 2015. Molecular mechanism of PPARα action and its impact on lipid metabolism, inflammation and fibrosis in non-alcoholic fatty liver disease. *Journal of Hepatology,* 62**,** 720-733.

PEINADO, H., ALEČKOVIĆ, M., LAVOTSHKIN, S., MATEI, I., COSTA-SILVA, B., MORENO-BUENO, G., HERGUETA-REDONDO, M., WILLIAMS, C., GARCÍA-SANTOS, G., GHAJAR, C. M., NITADORI-HOSHINO, A., HOFFMAN, C., BADAL, K., GARCIA, B. A., CALLAHAN, M. K., YUAN, J., MARTINS, V. R., SKOG, J.,

KAPLAN, R. N., BRADY, M. S., WOLCHOK, J. D., CHAPMAN, P. B., KANG, Y., BROMBERG, J. & LYDEN, D. 2012. Melanoma exosomes educate bone marrow progenitor cells toward a pro-metastatic phenotype through MET. *Nature Medicine,* 18**,** 883.

PEINADO, H., ZHANG, H., MATEI, I. R., COSTA-SILVA, B., HOSHINO, A., RODRIGUES, G., PSAILA, B., KAPLAN, R. N., BROMBERG, J. F., KANG, Y., BISSELL, M. J., COX, T. R., GIACCIA, A. J., ERLER, J. T., HIRATSUKA, S., GHAJAR, C. M. & LYDEN, D. 2017. Pre-metastatic niches: organ-specific homes for metastases. *Nat Rev Cancer,* 17**,** 302-317.

PELED, E., DAVIS, M., AXELMAN, E., NORMAN, D. & NADIR, Y. 2013. Heparanase role in the treatment of avascular necrosis of femur head. *Thromb Res,* 131**,** 94-8.

PELED, E., MELAMED, E., PORTAL, T. B., AXELMAN, E., NORMAN, D., BRENNER, B. & NADIR, Y. 2016. Heparanase procoagulant activity as a predictor of wound necrosis following diabetic foot amputation. *Thromb Res,* 139**,** 148-53.

PENNACCHIETTI, S., MICHIELI, P., GALLUZZO, M., MAZZONE, M., GIORDANO, S. & COMOGLIO, P. M. 2003. Hypoxia promotes invasive growth by transcriptional activation of the met protooncogene. *Cancer Cell,* 3**,** 347-61.

PEROU, C. M., SORLIE, T., EISEN, M. B., VAN DE RIJN, M., JEFFREY, S. S., REES, C. A., POLLACK, J. R., ROSS, D. T., JOHNSEN, H., AKSLEN, L. A., FLUGE, O., PERGAMENSCHIKOV, A., WILLIAMS, C., ZHU, S. X., LONNING, P. E., BORRESEN-DALE, A. L., BROWN, P. O. & BOTSTEIN, D. 2000. Molecular portraits of human breast tumours. *Nature,* 406**,** 747-52.

PETERS, M. G., FARIAS, E., COLOMBO, L., FILMUS, J., PURICELLI, L. & BAL DE KIER JOFFE, E. 2003. Inhibition of invasion and metastasis by glypican-3 in a syngeneic breast cancer model. *Breast Cancer Res Treat,* 80**,** 221-32.

PEZZELLA, F., PASTORINO, U., TAGLIABUE, E., ANDREOLA, S., SOZZI, G., GASPARINI, G., MENARD, S., GATTER, K. C., HARRIS, A. L., FOX, S., BUYSE, M., PILOTTI, S., PIEROTTI, M. & RILKE, F. 1997. Non-small-cell lung carcinoma tumor growth without morphological evidence of neo-angiogenesis. *Am J Pathol,* 151**,** 1417-23.

PICARDO, S. L., MAHER, S. G., O'SULLIVAN, J. N. & REYNOLDS, J. V. 2012. Barrett's to oesophageal cancer sequence: a model of inflammatory-driven upper gastrointestinal cancer. *Dig Surg,* 29**,** 251-60.

PICKUP, M. W., MOUW, J. K. & WEAVER, V. M. 2014. The extracellular matrix modulates the hallmarks of cancer. *EMBO Rep,* 15**,** 1243-53.

PIENTA, K. J., MCGREGOR, N., AXELROD, R. & AXELROD, D. E. 2008. Ecological therapy for cancer: defining tumors using an ecosystem paradigm suggests new opportunities for novel cancer treatments. *Transl Oncol,* 1**,** 158-64.

PIEZ, K. A. 1997. History of extracellular matrix: a personal view. *Matrix Biol,* 16**,** 85-92.

PINTO, M. P., DYE, W. W., JACOBSEN, B. M. & HORWITZ, K. B. 2014. Malignant stroma increases luminal breast cancer cell proliferation and angiogenesis through platelet-derived growth factor signaling. *BMC Cancer,* 14**,** 735.

PISANO, C., VLODAVSKY, I., ILAN, N. & ZUNINO, F. 2014. The potential of heparanase as a therapeutic target in cancer. *Biochem Pharmacol,* 89**,** 12-9.

PLAKS, V., KONG, N. & WERB, Z. 2015. The cancer stem cell niche: how essential is the niche in regulating stemness of tumor cells? *Cell Stem Cell,* 16**,** 225-38.

PLITAS, G., KONOPACKI, C., WU, K., BOS, P. D., MORROW, M., PUTINTSEVA, E. V., CHUDAKOV, D. M. & RUDENSKY, A. Y. 2016. Regulatory T Cells Exhibit Distinct Features in Human Breast Cancer. *Immunity,* 45**,** 1122-1134.

PLUMMER, M., DE MARTEL, C., VIGNAT, J., FERLAY, J., BRAY, F. & FRANCESCHI, S. 2016. Global burden of cancers attributable to infections in 2012: a synthetic analysis. *Lancet Glob Health,* 4**,** e609-16.

POLYAK, K. & HU, M. 2005. Do myoepithelial cells hold the key for breast tumor progression? *J Mammary Gland Biol Neoplasia,* 10**,** 231-47.

POLYMEROPOULOS, M. H., HIGGINS, J. J., GOLBE, L. I., JOHNSON, W. G., IDE, S. E., DI IORIO, G., SANGES, G., STENROOS, E. S., PHO, L. T., SCHAFFER, A. A., LAZZARINI, A. M., NUSSBAUM, R. L. & DUVOISIN, R. C. 1996. Mapping of a gene for Parkinson's disease to chromosome 4q21-q23. *Science,* 274**,** 1197-9.

POON, I. K., GOODALL, K. J., PHIPPS, S., CHOW, J. D., PAGLER, E. B., ANDREWS, D. M., CONLAN, C. L., RYAN, G. F., WHITE, J. A., WONG, M. K., HORAN, C., MATTHAEI, K. I., SMYTH, M. J. & HULETT, M. D. 2014. Mice deficient in heparanase exhibit impaired dendritic cell migration and reduced airway inflammation. *Eur J Immunol,* 44**,** 1016-30.

POPIVANOVA, B. K., KITAMURA, K., WU, Y., KONDO, T., KAGAYA, T., KANEKO, S., OSHIMA, M., FUJII, C. & MUKAIDA, N. 2008. Blocking TNF-alpha in mice reduces colorectal carcinogenesis associated with chronic colitis. *J Clin Invest,* 118**,** 560-70.

PORPORATO, P. E. 2016. Understanding cachexia as a cancer metabolism syndrome. *Oncogenesis,* 5**,** e200.

POTHULA, S. P., XU, Z., GOLDSTEIN, D., BIANKIN, A. V., PIROLA, R. C., WILSON, J. S. & APTE, M. V. 2016. Hepatocyte growth factor inhibition: a novel therapeutic approach in pancreatic cancer. *Br J Cancer,* 114**,** 269-80.

POUPARD, N., BADAROU, P., FASANI, F., GROULT, H., BRIDIAU, N., SANNIER, F., BORDENAVE-JUCHEREAU, S., KIEDA, C., PIOT, J.-M., GRILLON, C., FRUITIER-ARNAUDIN, I. & MAUGARD, T. 2017a. Assessment of Heparanase-Mediated Angiogenesis Using Microvascular Endothelial Cells: Identification of λ-Carrageenan Derivative as a Potent Anti Angiogenic Agent. *Marine Drugs,* 15**,** 134.

POUPARD, N., GROULT, H., BODIN, J., BRIDIAU, N., BORDENAVE-JUCHEREAU, S., SANNIER, F., PIOT, J. M., FRUITIER-ARNAUDIN, I. & MAUGARD, T. 2017b. Production of heparin and lambda-carrageenan anti-heparanase derivatives using a combination of physicochemical depolymerization and glycol splitting. *Carbohydr Polym,* 166**,** 156-165.

PRINCE, J. M., KLINOWSKA, T. C. M., MARSHMAN, E., LOWE, E. T., MAYER, U., MINER, J., ABERDAM, D., VESTWEBER, D., GUSTERSON, B. & STREULI, C. H. 2002. Cell–matrix interactions during development and apoptosis of the mouse mammary gland in vivo. *Developmental Dynamics,* 223**,** 497-516.

PRINCIPE, D. R., DECANT, B., MASCARINAS, E., WAYNE, E. A., DIAZ, A. M., AKAGI, N., HWANG, R., PASCHE, B., DAWSON, D. W., FANG, D., BENTREM, D. J., MUNSHI, H. G., JUNG, B. & GRIPPO, P. J. 2016. TGFbeta Signaling in the Pancreatic Tumor Microenvironment Promotes Fibrosis and Immune Evasion to Facilitate Tumorigenesis. *Cancer Res,* 76**,** 2525-39.

PURUSHOTHAMAN, A., CHEN, L., YANG, Y. & SANDERSON, R. D. 2008. Heparanase stimulation of protease expression implicates it as a master regulator of the aggressive tumor phenotype in myeloma. *J Biol Chem,* 283**,** 32628-36.

PURUSHOTHAMAN, A., UYAMA, T., KOBAYASHI, F., YAMADA, S., SUGAHARA, K., RAPRAEGER, A. C. & SANDERSON, R. D. 2010. Heparanase-enhanced shedding of syndecan-1 by myeloma cells promotes endothelial invasion and angiogenesis. *Blood,* 115**,** 2449-57.

PUTZ, E. M., MAYFOSH, A. J., KOS, K., BARKAUSKAS, D. S., NAKAMURA, K., TOWN, L., GOODALL, K. J., YEE, D. Y., POON, I. K., BASCHUK, N., SOUZA-FONSECA-GUIMARAES, F., HULETT, M. D. & SMYTH, M. J. 2017. NK cell heparanase controls tumor invasion and immune surveillance. *J Clin Invest,* 127**,** 2777-2788.

QIAN, B.-Z. & POLLARD, J. W. 2010. Macrophage Diversity Enhances Tumor Progression and Metastasis. *Cell,* 141**,** 39-51.

QIAN, B. Z., LI, J., ZHANG, H., KITAMURA, T., ZHANG, J., CAMPION, L. R., KAISER, E. A., SNYDER, L. A. & POLLARD, J. W. 2011. CCL2 recruits inflammatory monocytes to facilitate breast-tumour metastasis. *Nature,* 475**,** 222-5.

QIN, W., GOLOVKINA, T. V., PENG, T., NEPOMNASCHY, I., BUGGIANO, V., PIAZZON, I. & ROSS, S. R. 1999. Mammary Gland Expression of Mouse Mammary Tumor Virus Is Regulated by a Novel Element in the Long Terminal Repeat. *Journal of Virology,* 73**,** 368-376.

QU, H., ZHENG, L., JIAO, W., MEI, H., LI, D., SONG, H., FANG, E., WANG, X., LI, S., HUANG, K. & TONG, Q. 2016. Smad4 suppresses the tumorigenesis and aggressiveness of neuroblastoma through repressing the expression of heparanase. *Sci Rep,* 6**,** 32628.

QUAIL, D. F. & JOYCE, J. A. 2013. Microenvironmental regulation of tumor progression and metastasis. *Nat Med,* 19**,** 1423-37.

QUIGLEY, J. P. & ARMSTRONG, P. B. 1998. Tumor Cell Intravasation Alu-cidated: The Chick Embryo Opens the Window. *Cell,* 94**,** 281-284.

RACKER, E. 1972. Bioenergetics and the problem of tumor growth. *Am Sci,* 60**,** 56-63.

RADISKY, D. C. & BISSELL, M. J. 2006. Matrix metalloproteinase-induced genomic instability. *Current opinion in genetics & development,* 16**,** 45-50.

RADISKY, D. C., LEVY, D. D., LITTLEPAGE, L. E., LIU, H., NELSON, C. M., FATA, J. E., LEAKE, D., GODDEN, E. L., ALBERTSON, D. G., ANGELA NIETO, M., WERB, Z. & BISSELL, M. J. 2005. Rac1b and reactive oxygen species mediate MMP-3-induced EMT and genomic instability. *Nature,* 436**,** 123.

RAJABI, M. & MOUSA, S. A. 2017. The Role of Angiogenesis in Cancer Treatment. *Biomedicines,* 5**,** 34.

RAKHSHANDEHROO, M., KNOCH, B., MULLER, M. & KERSTEN, S. 2010. Peroxisome proliferator-activated receptor alpha target genes. *PPAR Res,* 2010.

RAMAN, K. & KUBERAN, B. 2010. Chemical Tumor Biology of Heparan Sulfate Proteoglycans. *Current chemical biology,* 4**,** 20-31.

RAMANI, V. C., VLODAVSKY, I., NG, M., ZHANG, Y., BARBIERI, P., NOSEDA, A. & SANDERSON, R. D. 2016a. Chemotherapy induces expression and release of heparanase leading to changes associated with an aggressive tumor phenotype. *Matrix Biol,* 55**,** 22-34.

RAMANI, V. C., YANG, Y., REN, Y., NAN, L. & SANDERSON, R. D. 2011. Heparanase plays a dual role in driving hepatocyte growth factor (HGF) signaling by enhancing HGF expression and activity. *J Biol Chem,* 286**,** 6490-9.

RAMANI, V. C., ZHAN, F., HE, J., BARBIERI, P., NOSEDA, A., TRICOT, G. & SANDERSON, R. D. 2016b. Targeting heparanase overcomes chemoresistance and diminishes relapse in myeloma. *Oncotarget,* 7**,** 1598-607.

RAMLEE, M. K., WANG, J., TOH, W. X. & LI, S. 2016. Transcription Regulation of the Human Telomerase Reverse Transcriptase (hTERT) Gene. *Genes (Basel),* 7.

RAMOS-LEWIS, W. & PAGE-MCCAW, A. 2018. Basement membrane mechanics shape development: Lesson from the fly. *Matrix Biol*.

RAO, G., LIU, D., XING, M., TAULER, J., PRINZ, R. A. & XU, X. 2010. Induction of heparanase-1 expression by mutant B-Raf kinase: role of GA binding protein in heparanase-1 promoter activation. *Neoplasia,* 12**,** 946-56.

RAPRAEGER, A. C. 2013. Synstatin: a selective inhibitor of the syndecan-1-coupled IGF1R-αvβ3 integrin complex in tumorigenesis and angiogenesis. *The FEBS journal,* 280**,** 2207-2215.

RAPTIS, L. 1991. Polyomavirus middle tumor antigen increases responsiveness to growth factors. *J Virol,* 65**,** 2691-4.

RATAJCZAK, M. Z., JADCZYK, T., SCHNEIDER, G., KAKAR, S. S. & KUCIA, M. 2013. Induction of a tumor-metastasis-receptive microenvironment as an unwanted and underestimated side effect of treatment by chemotherapy or radiotherapy. *J Ovarian Res,* 6**,** 95.

RAUTELA, J., BASCHUK, N., SLANEY, C. Y., JAYATILLEKE, K. M., XIAO, K., BIDWELL, B. N., LUCAS, E. C., HAWKINS, E. D., LOCK, P., WONG, C. S., CHEN, W., ANDERSON, R. L., HERTZOG, P. J., ANDREWS, D. M., MOLLER, A. & PARKER, B. S. 2015. Loss of Host Type-I IFN Signaling Accelerates Metastasis and Impairs NK-cell Antitumor Function in Multiple Models of Breast Cancer. *Cancer Immunol Res,* 3**,** 1207-17.

REDIG, A. J. & MCALLISTER, S. S. 2013. Breast cancer as a systemic disease: a view of metastasis. *Journal of Internal Medicine,* 274**,** 113-126.

RENAUD, J.-P., CHUNG, C.-W., DANIELSON, U. H., EGNER, U., HENNIG, M., HUBBARD, R. E. & NAR, H. 2016. Biophysics in drug discovery: impact, challenges and opportunities. *Nature Reviews Drug Discovery,* 15**,** 679.

REY, S., SCHITO, L., WOUTERS, B. G., ELIASOF, S. & KERBEL, R. S. 2017. Targeting Hypoxia-Inducible Factors for Antiangiogenic Cancer Therapy. *Trends Cancer,* 3**,** 529-541.

REYMOND, N., D'AGUA, B. B. & RIDLEY, A. J. 2013. Crossing the endothelial barrier during metastasis. *Nat Rev Cancer,* 13**,** 858-70.

REYNOLDS, L. E., D'AMICO, G., LECHERTIER, T., PAPACHRISTODOULOU, A., MUNOZ-FELIX, J. M., DE ARCANGELIS, A., BAKER, M., SERRELS, B. & HODIVALA-DILKE, K. M. 2017. Dual role of pericyte alpha6beta1-integrin in tumour blood vessels. *J Cell Sci,* 130**,** 1583-1595.

RIAZ, A., ILAN, N., VLODAVSKY, I., LI, J. P. & JOHANSSON, S. 2013. Characterization of heparanase-induced phosphatidylinositol 3-kinase-AKT activation and its integrin dependence. *J Biol Chem,* 288**,** 12366-75.

RIBAS, A. 2015. Releasing the Brakes on Cancer Immunotherapy. *N Engl J Med,* 373**,** 1490-2.

RIBAS, A., DUMMER, R., PUZANOV, I., VANDERWALDE, A., ANDTBACKA, R. H. I., MICHIELIN, O., OLSZANSKI, A. J., MALVEHY, J., CEBON, J., FERNANDEZ, E., KIRKWOOD, J. M., GAJEWSKI, T. F., CHEN, L., GORSKI, K. S., ANDERSON, A. A., DIEDE, S. J., LASSMAN, M. E., GANSERT, J., HODI, F. S. & LONG, G. V. 2017a. Oncolytic Virotherapy Promotes Intratumoral T Cell Infiltration and Improves Anti-PD-1 Immunotherapy. *Cell,* 170**,** 1109-1119.e10.

RIBAS, A., DUMMER, R., PUZANOV, I., VANDERWALDE, A., ANDTBACKA, R. H. I., MICHIELIN, O., OLSZANSKI, A. J., MALVEHY, J., CEBON, J., FERNANDEZ, E., KIRKWOOD, J. M., GAJEWSKI, T. F., CHEN, L., GORSKI, K. S., ANDERSON, A.

A., DIEDE, S. J., LASSMAN, M. E., GANSERT, J., HODI, F. S. & LONG, G. V. 2017b. Oncolytic Virotherapy Promotes Intratumoral T Cell Infiltration and Improves Anti-PD-1 Immunotherapy. *Cell,* 170**,** 1109-1119 e10.

RIBAS, A. & WOLCHOK, J. D. 2018. Cancer immunotherapy using checkpoint blockade. *Science,* 359**,** 1350-1355.

RIBATTI, D., VACCA, A. & PRESTA, M. 2000. The discovery of angiogenic factors:: A historical review. *General Pharmacology: The Vascular System,* 35**,** 227-231.

RIBEIRO, A. L. & OKAMOTO, O. K. 2015. Combined effects of pericytes in the tumor microenvironment. *Stem Cells Int,* 2015**,** 868475.

RICHELDI, L., DU BOIS, R. M., RAGHU, G., AZUMA, A., BROWN, K. K., COSTABEL, U., COTTIN, V., FLAHERTY, K. R., HANSELL, D. M., INOUE, Y., KIM, D. S., KOLB, M., NICHOLSON, A. G., NOBLE, P. W., SELMAN, M., TANIGUCHI, H., BRUN, M., LE MAULF, F., GIRARD, M., STOWASSER, S., SCHLENKER-HERCEG, R., DISSE, B. & COLLARD, H. R. 2014. Efficacy and safety of nintedanib in idiopathic pulmonary fibrosis. *N Engl J Med,* 370**,** 2071-82.

RIVARA, S., MILAZZO, F. M. & GIANNINI, G. 2016. Heparanase: a rainbow pharmacological target associated to multiple pathologies including rare diseases. *Future Med Chem,* 8**,** 647-80.

RIVENBARK, A. G. & COLEMAN, W. B. 2012. Field cancerization in mammary carcinogenesis — Implications for prevention and treatment of breast cancer. *Experimental and Molecular Pathology,* 93**,** 391-398.

RIVENBARK, A. G., O'CONNOR, S. M. & COLEMAN, W. B. 2013. Molecular and Cellular Heterogeneity in Breast Cancer. *The American Journal of Pathology,* 183**,** 1113-1124.

RIZVI, Y. Q., MEHTA, C. S. & OYEKAN, A. 2013. Interactions of PPAR-alpha and adenosine receptors in hypoxia-induced angiogenesis. *Vascular pharmacology,* 59**,** 144-151.

RIZWAN, A., BULTE, C., KALAICHELVAN, A., CHENG, M., KRISHNAMACHARY, B., BHUJWALLA, Z. M., JIANG, L. & GLUNDE, K. 2015. Metastatic breast cancer cells in lymph nodes increase nodal collagen density. *Scientific Reports,* 5**,** 10002.

ROCKEY, D. C., BELL, P. D. & HILL, J. A. 2015. Fibrosis--A Common Pathway to Organ Injury and Failure. *N Engl J Med,* 373**,** 96.

ROHLOFF, J., ZINKE, J., SCHOPPMEYER, K., TANNAPFEL, A., WITZIGMANN, H., MOSSNER, J., WITTEKIND, C. & CACA, K. 2002. Heparanase expression is a prognostic indicator for postoperative survival in pancreatic adenocarcinoma. *Br J Cancer,* 86**,** 1270-5.

RÖHRIG, F. & SCHULZE, A. 2016. The multifaceted roles of fatty acid synthesis in cancer. *Nature Reviews Cancer,* 16**,** 732.

RONDANIN, R., FOCHI, S., BARUCHELLO, R., BERNARDI, T., OLIVA, P., SEMERARO, F., SIMONI, D. & GIANNINI, G. 2017. Arylamidonaphtalene sulfonate compounds as a novel class of heparanase inhibitors. *Bioorganic & Medicinal Chemistry Letters,* 27**,** 4421-4425.

ROSANO, G. L. & CECCARELLI, E. A. 2014. Recombinant protein expression in Escherichia coli: advances and challenges. *Front Microbiol,* 5**,** 172.

ROSENBERG, S. A. 2014. Entering the mainstream of cancer treatment. *Nature Reviews Clinical Oncology,* 11**,** 630.

ROSENTHAL, M. A., RISCHIN, D., MCARTHUR, G., RIBBONS, K., CHONG, B., FAREED, J., TONER, G., GREEN, M. D. & BASSER, R. L. 2002. Treatment with the novel anti-angiogenic agent PI-88 is associated with immune-mediated thrombocytopenia. *Annals of Oncology,* 13**,** 770-776.

ROTH, D. B. & GELLERT, M. 2000. New guardians of the genome. *Nature,* 404**,** 823.

ROUCOURT, B., MEEUSSEN, S., BAO, J., ZIMMERMANN, P. & DAVID, G. 2015. Heparanase activates the syndecan-syntenin-ALIX exosome pathway. *Cell Res,* 25**,** 412-28.

RUBINFELD, H., COHEN-KAPLAN, V., NASS, D., ILAN, N., MEISEL, S., COHEN, Z. R., HADANI, M., VLODAVSKY, I. & SHIMON, I. 2011. Heparanase is highly expressed and regulates proliferation in GH-secreting pituitary tumor cells. *Endocrinology,* 152**,** 4562-70.

RUSSNES, H. G., LINGJAERDE, O. C., BORRESEN-DALE, A. L. & CALDAS, C. 2017. Breast Cancer Molecular Stratification: From Intrinsic Subtypes to Integrative Clusters. *Am J Pathol,* 187**,** 2152-2162.

RYSER, H. J., MORAD, N. & SHEN, W. C. 1983. Heparin interaction with cultured cells: possible role of fibronectin in uncoupling surface binding and endocytosis. *Cell Biol Int Rep,* 7**,** 923-30.

SADE-FELDMAN, M., KANTERMAN, J., ISH-SHALOM, E., ELNEKAVE, M., HORWITZ, E. & BANIYASH, M. 2013. Tumor Necrosis Factor-α Blocks Differentiation and Enhances Suppressive Activity of Immature Myeloid Cells during Chronic Inflammation. *Immunity,* 38**,** 541-554.

SANCHEZ-MENDOZA, E. H., CARBALLO, J., LONGART, M., HERMANN, D. M. & DOEPPNER, T. R. 2016. Implantation of Miniosmotic Pumps and Delivery of Tract Tracers to Study Brain Reorganization in Pathophysiological Conditions. *Journal of visualized experiments : JoVE***,** e52932-e52932.

SANCHEZ-VEGA, F., MINA, M., ARMENIA, J., CHATILA, W. K., LUNA, A., LA, K. C., DIMITRIADOY, S., LIU, D. L., KANTHETI, H. S., SAGHAFINIA, S., CHAKRAVARTY, D., DAIAN, F., GAO, Q., BAILEY, M. H., LIANG, W.-W., FOLTZ, S. M., SHMULEVICH, I., DING, L., HEINS, Z., OCHOA, A., GROSS, B., GAO, J., ZHANG, H., KUNDRA, R., KANDOTH, C., BAHCECI, I., DERVISHI, L., DOGRUSOZ, U., ZHOU, W., SHEN, H., LAIRD, P. W., WAY, G. P., GREENE, C.

S., LIANG, H., XIAO, Y., WANG, C., IAVARONE, A., BERGER, A. H., BIVONA, T. G., LAZAR, A. J., HAMMER, G. D., GIORDANO, T., KWONG, L. N., MCARTHUR, G., HUANG, C., TWARD, A. D., FREDERICK, M. J., MCCORMICK, F., MEYERSON, M., CAESAR-JOHNSON, S. J., DEMCHOK, J. A., FELAU, I., KASAPI, M., FERGUSON, M. L., HUTTER, C. M., SOFIA, H. J., TARNUZZER, R., WANG, Z., YANG, L., ZENKLUSEN, J. C., ZHANG, J., CHUDAMANI, S., LIU, J., LOLLA, L., NARESH, R., PIHL, T., SUN, Q., WAN, Y., WU, Y., CHO, J., DEFREITAS, T., FRAZER, S., GEHLENBORG, N., GETZ, G., HEIMAN, D. I., KIM, J., LAWRENCE, M. S., LIN, P., MEIER, S., NOBLE, M. S., SAKSENA, G., VOET, D., ZHANG, H., BERNARD, B., CHAMBWE, N., DHANKANI, V., KNIJNENBURG, T., KRAMER, R., LEINONEN, K., LIU, Y., MILLER, M., REYNOLDS, S., SHMULEVICH, I., THORSSON, V., ZHANG, W., AKBANI, R., BROOM, B. M., HEGDE, A. M., JU, Z., KANCHI, R. S., et al. 2018. Oncogenic Signaling Pathways in The Cancer Genome Atlas. *Cell,* 173**,** 321-337.e10.

SANDERSON, R. D., ELKIN, M., RAPRAEGER, A. C., ILAN, N. & VLODAVSKY, I. 2017. Heparanase regulation of cancer, autophagy and inflammation: new mechanisms and targets for therapy. *FEBS J,* 284**,** 42-55.

SANFORD, D., NAIDU, A., ALIZADEH, N. & LAZO-LANGNER, A. 2014. The effect of low molecular weight heparin on survival in cancer patients: an updated systematic review and meta-analysis of randomized trials. *J Thromb Haemost,* 12**,** 1076-85.

SARRAZIN, S., LAMANNA, W. C. & ESKO, J. D. 2011. Heparan sulfate proteoglycans. *Cold Spring Harb Perspect Biol,* 3.

SASAKI, N., HIGASHI, N., TAKA, T., NAKAJIMA, M. & IRIMURA, T. 2004. Cell surface localization of heparanase on macrophages regulates degradation of extracellular matrix heparan sulfate. *J Immunol,* 172**,** 3830-5.

SASISEKHARAN, R., SHRIVER, Z., VENKATARAMAN, G. & NARAYANASAMI, U. 2002. Roles of heparan-sulphate glycosaminoglycans in cancer. *Nature Reviews Cancer,* 2**,** 521.

SATO, M., AMEMIYA, K., HAYAKAWA, S. & MUNAKATA, H. 2008. Subcellular localization of human heparanase and its alternative splice variant in COS-7 cells. *Cell Biochem Funct,* 26**,** 676-83.

SATO, R., SEMBA, T., SAYA, H. & ARIMA, Y. 2016. Concise Review: Stem Cells and Epithelial-Mesenchymal Transition in Cancer: Biological Implications and Therapeutic Targets. *Stem Cells,* 34**,** 1997-2007.

SATO, T., YAMAGUCHI, A., GOI, T., HIRONO, Y., TAKEUCHI, K., KATAYAMA, K. & MATSUKAWA, S. 2004. Heparanase expression in human colorectal cancer and its relationship to tumor angiogenesis, hematogenous metastasis, and prognosis. *J Surg Oncol,* 87**,** 174-81.

SAUNDERS, S., PAINE-SAUNDERS, S. & LANDER, A. D. 1997. Expression of the cell surface proteoglycan glypican-5 is developmentally regulated in kidney, limb, and brain. *Dev Biol,* 190**,** 78-93.

SAVA, I. G., ZHANG, F., TOMA, I., THEILACKER, C., LI, B., BAUMERT, T. F., HOLST, O., LINHARDT, R. J. & HUEBNER, J. 2009. Novel interactions of glycosaminoglycans and bacterial glycolipids mediate binding of enterococci to human cells. *J Biol Chem,* 284**,** 18194-201.

SAVION, N., DISATNIK, M. H. & NEVO, Z. 1987. Murine macrophage heparanase: inhibition and comparison with metastatic tumor cells. *J Cell Physiol,* 130**,** 77-84.

SAXENA, M. & CHRISTOFORI, G. 2013. Rebuilding cancer metastasis in the mouse. *Molecular Oncology,* 7**,** 283-296.

SCHAFFHAUSEN, B. S. & ROBERTS, T. M. 2009. Lessons from polyoma middle T antigen on signaling and transformation: A DNA tumor virus contribution to the war on cancer. *Virology,* 384**,** 304-316.

SCHEEL, C. & WEINBERG, R. A. 2012. Cancer stem cells and epithelial–mesenchymal transition: Concepts and molecular links. *Seminars in Cancer Biology,* 22**,** 396-403.

SCHIRRMACHER, V. 2019. From chemotherapy to biological therapy: A review of novel concepts to reduce the side effects of systemic cancer treatment (Review). *International journal of oncology,* 54**,** 407-419.

SCHMIDT, E. P., YANG, Y., JANSSEN, W. J., GANDJEVA, A., PEREZ, M. J., BARTHEL, L., ZEMANS, R. L., BOWMAN, J. C., KOYANAGI, D. E., YUNT, Z. X., SMITH, L. P., CHENG, S. S., OVERDIER, K. H., THOMPSON, K. R., GERACI, M. W., DOUGLAS, I. S., PEARSE, D. B. & TUDER, R. M. 2012. The pulmonary endothelial glycocalyx regulates neutrophil adhesion and lung injury during experimental sepsis. *Nat Med,* 18**,** 1217-23.

SCHOEFFNER, D. J., MATHENY, S. L., AKAHANE, T., FACTOR, V., BERRY, A., MERLINO, G. & THORGEIRSSON, U. P. 2005. VEGF contributes to mammary tumor growth in transgenic mice through paracrine and autocrine mechanisms. *Lab Invest,* 85**,** 608-23.

SCHOENFELD, A.-K., VIERFUß, S., LÜHN, S. & ALBAN, S. 2014. Testing of potential glycan-based heparanase inhibitors in a fluorescence activity assay using either bacterial heparinase II or human heparanase. *Journal of Pharmaceutical and Biomedical Analysis,* 95**,** 130-138.

SCHREIBER, R. D., OLD, L. J. & SMYTH, M. J. 2011. Cancer immunoediting: integrating immunity's roles in cancer suppression and promotion. *Science,* 331**,** 1565-70.

SCHUBERT, S. Y., ILAN, N., SHUSHY, M., BEN-IZHAK, O., VLODAVSKY, I. & GOLDSHMIDT, O. 2004a. Human heparanase nuclear localization and enzymatic activity. *Lab Invest,* 84**,** 535-44.

SCHUBERT, S. Y., ILAN, N., SHUSHY, M., BEN-IZHAK, O., VLODAVSKY, I. & GOLDSHMIDT, O. 2004b. Human heparanase nuclear localization and enzymatic activity. *Laboratory Investigation,* 84**,** 535.

SCHUMACHER, D., STRILIC, B., SIVARAJ, K. K., WETTSCHURECK, N. & OFFERMANNS, S. 2013. Platelet-derived nucleotides promote tumor-cell transendothelial migration and metastasis via P2Y2 receptor. *Cancer Cell,* 24**,** 130-7.

SCHWAEDERLE, M., KRISHNAMURTHY, N., DANIELS, G. A., PICCIONI, D. E., KESARI, S., FANTA, P. T., SCHWAB, R. B., PATEL, S. P., PARKER, B. A. & KURZROCK, R. 2018. Telomerase reverse transcriptase promoter alterations across cancer types as detected by next-generation sequencing: A clinical and molecular analysis of 423 patients. *Cancer,* 124**,** 1288-1296.

SCHWEICHEL, J. U. & MERKER, H. J. 1973. The morphology of various types of cell death in prenatal tissues. *Teratology,* 7**,** 253-66.

SCOTT, A. M., WOLCHOK, J. D. & OLD, L. J. 2012. Antibody therapy of cancer. *Nature Reviews Cancer,* 12**,** 278.

SECCHI, M. F., CRESCENZI, M., MASOLA, V., RUSSO, F. P., FLOREANI, A. & ONISTO, M. 2017a. Heparanase and macrophage interplay in the onset of liver fibrosis. *Scientific Reports,* 7**,** 14956.

SECCHI, M. F., CRESCENZI, M., MASOLA, V., RUSSO, F. P., FLOREANI, A. & ONISTO, M. 2017b. Heparanase and macrophage interplay in the onset of liver fibrosis. *Sci Rep,* 7**,** 14956.

SEDGER, L. M. & MCDERMOTT, M. F. 2014. TNF and TNF-receptors: From mediators of cell death and inflammation to therapeutic giants - past, present and future. *Cytokine Growth Factor Rev,* 25**,** 453-72.

SEGUIN, L., DESGROSELLIER, J. S., WEIS, S. M. & CHERESH, D. A. 2015. Integrins and cancer: regulators of cancer stemness, metastasis, and drug resistance. *Trends Cell Biol,* 25**,** 234-40.

SEMENZA, G. L. 2003. Targeting HIF-1 for cancer therapy. *Nature Reviews Cancer,* 3**,** 721.

SEMENZA, G. L. 2009. Defining the role of hypoxia-inducible factor 1 in cancer biology and therapeutics. *Oncogene,* 29**,** 625.

SEMENZA, G. L. 2010. HIF-1: upstream and downstream of cancer metabolism. *Current Opinion in Genetics & Development,* 20**,** 51-56.

SEMENZA, GREGG L. 2012. Hypoxia-Inducible Factors in Physiology and Medicine. *Cell,* 148**,** 399-408.

SEMENZA, G. L., AGANI, F., BOOTH, G., FORSYTHE, J., IYER, N., JIANG, B.-H., LEUNG, S., ROE, R., WIENER, C. & YU, A. 1997. Structural and functional analysis of hypoxia-inducible factor 1. *Kidney International,* 51**,** 553-555.

SERRANO, M., LIN, A. W., MCCURRACH, M. E., BEACH, D. & LOWE, S. W. 1997. Oncogenic ras provokes premature cell senescence associated with accumulation of p53 and p16INK4a. *Cell,* 88**,** 593-602.

SHAFAT, I., ILAN, N., ZOABI, S., VLODAVSKY, I. & NAKHOUL, F. 2011. Heparanase levels are elevated in the urine and plasma of type 2 diabetes patients and associate with blood glucose levels. *PLoS One,* 6**,** e17312.

SHAFAT, I., PODE, D., PERETZ, T., ILAN, N., VLODAVSKY, I. & BENJAMIN, N. 2008. Clinical Significance of Urine Heparanase in Bladder Cancer Progression. *Neoplasia,* 10**,** 125-130.

SHALAPOUR, S. & KARIN, M. 2015. Immunity, inflammation, and cancer: an eternal fight between good and evil. *The Journal of Clinical Investigation,* 125**,** 3347-3355.

SHANG, B., LIU, Y., JIANG, S.-J. & LIU, Y. 2015. Prognostic value of tumor-infiltrating FoxP3+ regulatory T cells in cancers: a systematic review and meta-analysis. *Scientific Reports,* 5**,** 15179.

SHARMA, P., HU-LIESKOVAN, S., WARGO, J. A. & RIBAS, A. 2017. Primary, Adaptive, and Acquired Resistance to Cancer Immunotherapy. *Cell,* 168**,** 707-723.

SHEN, J., SHRESTHA, S., YEN, Y. H., ASATRIAN, G., MRAVIC, M., SOO, C., TING, K., DRY, S. M., PEAULT, B. & JAMES, A. W. 2015. Pericyte Antigens in Perivascular Soft Tissue Tumors. *Int J Surg Pathol,* 23**,** 638-48.

SHEN, X., FANG, J., LV, X., PEI, Z., WANG, Y., JIANG, S. & DING, K. 2011. Heparin impairs angiogenesis through inhibition of microRNA-10b. *J Biol Chem,* 286**,** 26616-27.

SHIEH, M. T., WUDUNN, D., MONTGOMERY, R. I., ESKO, J. D. & SPEAR, P. G. 1992. Cell surface receptors for herpes simplex virus are heparan sulfate proteoglycans. *J Cell Biol,* 116**,** 1273-81.

SHIM, H., CHUN, Y. S., LEWIS, B. C. & DANG, C. V. 1998. A unique glucose-dependent apoptotic pathway induced by c-Myc. *Proc Natl Acad Sci U S A,* 95**,** 1511-6.

SHING, Y., FOLKMAN, J., HAUDENSCHILD, C., LUND, D., CRUM, R. & KLAGSBRUN, M. 1985. Angiogenesis is stimulated by a tumor-derived endothelial cell growth factor. *J Cell Biochem,* 29**,** 275-87.

SHINYO, Y., KODAMA, J., HONGO, A., YOSHINOUCHI, M. & HIRAMATSU, Y. 2003. Heparanase expression is an independent prognostic factor in patients with invasive cervical cancer. *Ann Oncol,* 14**,** 1505-10.

SHIOZAWA, H., TAKAHASHI, M., TAKATSU, T., KINOSHITA, T., TANZAWA, K., HOSOYA, T., FURUYA, K., TAKAHASHI, S., FURIHATA, K. & SETO, H. 1995. Trachyspic acid, a new metabolite produced by Talaromyces trachyspermus, that inhibits tumor cell heparanase: taxonomy of the producing strain, fermentation, isolation, structural elucidation, and biological activity. *J Antibiot (Tokyo),* 48**,** 357-62.

SHRIVER, Z., CAPILA, I., VENKATARAMAN, G. & SASISEKHARAN, R. 2012. Heparin and heparan sulfate: analyzing structure and microheterogeneity. *Handbook of experimental pharmacology***,** 159-176.

SHTEINGAUZ, A., BOYANGO, I., NARODITSKY, I., HAMMOND, E., GRUBER, M., DOWECK, I., ILAN, N. & VLODAVSKY, I. 2015. Heparanase Enhances Tumor Growth and Chemoresistance by Promoting Autophagy. *Cancer Res,* 75**,** 3946-57.

SILVERA, S. A. & ROHAN, T. E. 2008. Benign proliferative epithelial disorders of the breast: a review of the epidemiologic evidence. *Breast Cancer Res Treat,* 110**,** 397-409.

SIMANSHU, D. K., NISSLEY, D. V. & MCCORMICK, F. 2017. RAS Proteins and Their Regulators in Human Disease. *Cell,* 170**,** 17-33.

SIMIAN, M., HIRAI, Y., NAVRE, M., WERB, Z., LOCHTER, A. & BISSELL, M. J. 2001. The interplay of matrix metalloproteinases, morphogens and growth factors is necessary for branching of mammary epithelial cells. *Development,* 128**,** 3117-31.

SIMINOVITCH, L., MCCULLOCH, E. A. & TILL, J. E. 1963. THE DISTRIBUTION OF COLONY-FORMING CELLS AMONG SPLEEN COLONIES. *J Cell Comp Physiol,* 62**,** 327-36.

SIMIZU, S., ISHIDA, K., WIERZBA, M. K. & OSADA, H. 2004. Secretion of heparanase protein is regulated by glycosylation in human tumor cell lines. *J Biol Chem,* 279**,** 2697-703.

SIMIZU, S., SUZUKI, T., MUROI, M., LAI, N. S., TAKAGI, S., DOHMAE, N. & OSADA, H. 2007. Involvement of disulfide bond formation in the activation of heparanase. *Cancer Res,* 67**,** 7841-9.

SIMONS, M., GORDON, E. & CLAESSON-WELSH, L. 2016. Mechanisms and regulation of endothelial VEGF receptor signalling. *Nat Rev Mol Cell Biol,* 17**,** 611-25.

SINGH, J. K., SIMOES, B. M., HOWELL, S. J., FARNIE, G. & CLARKE, R. B. 2013. Recent advances reveal IL-8 signaling as a potential key to targeting breast cancer stem cells. *Breast Cancer Res,* 15**,** 210.

SINGH, P., BLATT, A., FELD, S., ZOHAR, Y., SAADI, E., BARKI-HARRINGTON, L., HAMMOND, E., ILAN, N., VLODAVSKY, I., CHOWERS, Y. & HALF, E. 2017. The Heparanase Inhibitor PG545 Attenuates Colon Cancer Initiation and Growth, Associating with Increased p21 Expression. *Neoplasia,* 19**,** 175-184.

SINNAMON, M. J., CARTER, K. J., FINGLETON, B. & MATRISIAN, L. M. 2008. MMP-9 contributes to intestinal tumourigenesis in the APC-Min mouse. *International journal of experimental pathology,* 89**,** 466-475.

SKOBE, M., HAWIGHORST, T., JACKSON, D. G., PREVO, R., JANES, L., VELASCO, P., RICCARDI, L., ALITALO, K., CLAFFEY, K. & DETMAR, M. 2001. Induction of tumor lymphangiogenesis by VEGF-C promotes breast cancer metastasis. *Nat Med,* 7**,** 192-8.

SLETTEN, E. T., LOKA, R. S., YU, F. & NGUYEN, H. M. 2017. Glycosidase Inhibition by Multivalent Presentation of Heparan Sulfate Saccharides on Bottlebrush Polymers. *Biomacromolecules,* 18**,** 3387-3399.

SOARES, M. A., TEIXEIRA, F. C., FONTES, M., AREAS, A. L., LEAL, M. G., PAVAO, M. S. & STELLING, M. P. 2015. Heparan Sulfate Proteoglycans May Promote or Inhibit Cancer Progression by Interacting with Integrins and Affecting Cell Migration. *Biomed Res Int,* 2015**,** 453801.

SOEHNLEIN, O., STEFFENS, S., HIDALGO, A. & WEBER, C. 2017. Neutrophils as protagonists and targets in chronic inflammation. *Nature Reviews Immunology,* 17**,** 248.

SOKOL, C. L. & LUSTER, A. D. 2015. The Chemokine System in Innate Immunity. *Cold Spring Harbor Perspectives in Biology,* 7**,** a016303.

SOMMERFELDT, N., BECKHOVE, P., GE, Y., SCHÜTZ, F., CHOI, C., BUCUR, M., DOMSCHKE, C., SOHN, C., SCHNEEWEIS, A., ROM, J., POLLMANN, D., LEUCHT, D., VLODAVSKY, I. & SCHIRRMACHER, V. 2006. Heparanase: A New Metastasis-Associated Antigen Recognized in Breast Cancer Patients by Spontaneously Induced Memory T Lymphocytes. *Cancer Research,* 66**,** 7716-7723.

SONG, Y., HU, B., QU, H., WANG, L., ZHANG, Y., TAO, J. & CUI, J. 2016. Novel 1, 3-N, O-Spiroheterocyclic compounds inhibit heparanase activity and enhance nedaplatin-induced cytotoxicity in cervical cancer cells. *Oncotarget,* 7**,** 36154-36167.

SONODA, R., NAOMOTO, Y., SHIRAKAWA, Y., FUJIWARA, Y., YAMATSUJI, T., NOMA, K., TANABE, S., TAKAOKA, M., GUNDUZ, M., TSUJIGIWA, H., NAGATSUKA, H., OHARA, N., YOSHINO, T., TAKUBO, K., VIETH, M. & TANAKA, N. 2010. Preferential up-regulation of heparanase and cyclooxygenase-2 in carcinogenesis of Barrett's oesophagus and intestinal-type gastric carcinoma. *Histopathology,* 57**,** 90-100.

SORLIE, T., PEROU, C. M., TIBSHIRANI, R., AAS, T., GEISLER, S., JOHNSEN, H., HASTIE, T., EISEN, M. B., VAN DE RIJN, M., JEFFREY, S. S., THORSEN, T., QUIST, H., MATESE, J. C., BROWN, P. O., BOTSTEIN, D., LONNING, P. E. & BORRESEN-DALE, A. L. 2001. Gene expression patterns of breast carcinomas distinguish tumor subclasses with clinical implications. *Proc Natl Acad Sci U S A,* 98**,** 10869-74.

SOSA, M. S., AVIVAR-VALDERAS, A., BRAGADO, P., WEN, H. C. & AGUIRRE-GHISO, J. A. 2011. ERK1/2 and p38alpha/beta signaling in tumor cell quiescence: opportunities to control dormant residual disease. *Clin Cancer Res,* 17**,** 5850-7.

SOSA, M. S., BRAGADO, P. & AGUIRRE-GHISO, J. A. 2014. Mechanisms of disseminated cancer cell dormancy: an awakening field. *Nat Rev Cancer,* 14**,** 611-22.

SPIEGEL, A., BROOKS, M. W., HOUSHYAR, S., REINHARDT, F., ARDOLINO, M., FESSLER, E., CHEN, M. B., KRALL, J. A., DECOCK, J., ZERVANTONAKIS, I. K.,

IANNELLO, A., IWAMOTO, Y., CORTEZ-RETAMOZO, V., KAMM, R. D., PITTET, M. J., RAULET, D. H. & WEINBERG, R. A. 2016. Neutrophils Suppress Intraluminal NK Cell-Mediated Tumor Cell Clearance and Enhance Extravasation of Disseminated Carcinoma Cells. *Cancer Discov,* 6**,** 630-49.

SPIEGEL, A., ZCHARIA, E., VAGIMA, Y., ITKIN, T., KALINKOVICH, A., DAR, A., KOLLET, O., NETZER, N., GOLAN, K., SHAFAT, I., ILAN, N., NAGLER, A., VLODAVSKY, I. & LAPIDOT, T. 2008a. Heparanase regulates retention and proliferation of primitive Sca-1(+)/c-Kit(+)/Lin(−) cells via modulation of the bone marrow microenvironment. *Blood,* 111**,** 4934-4943.

SPIEGEL, A., ZCHARIA, E., VAGIMA, Y., ITKIN, T., KALINKOVICH, A., DAR, A., KOLLET, O., NETZER, N., GOLAN, K., SHAFAT, I., ILAN, N., NAGLER, A., VLODAVSKY, I. & LAPIDOT, T. 2008b. Heparanase regulates retention and proliferation of primitive Sca-1+/c-Kit+/Lin- cells via modulation of the bone marrow microenvironment. *Blood,* 111**,** 4934-43.

SPORN, M. B. & ROBERTS, A. B. 1985. Autocrine growth factors and cancer. *Nature,* 313**,** 745-7.

STACKER, S. A., CAESAR, C., BALDWIN, M. E., THORNTON, G. E., WILLIAMS, R. A., PREVO, R., JACKSON, D. G., NISHIKAWA, S., KUBO, H. & ACHEN, M. G. 2001. VEGF-D promotes the metastatic spread of tumor cells via the lymphatics. *Nat Med,* 7**,** 186-91.

STACKER, S. A., WILLIAMS, S. P., KARNEZIS, T., SHAYAN, R., FOX, S. B. & ACHEN, M. G. 2014. Lymphangiogenesis and lymphatic vessel remodelling in cancer. *Nature Reviews Cancer,* 14**,** 159.

STADLMANN, S., MOSER, P. L., POLLHEIMER, J., STEINER, P., KRUGMANN, J., DIRNHOFER, S., MIKUZ, G., MARGREITER, R. & AMBERGER, A. 2003. Heparanase-1 gene expression in normal, hyperplastic and neoplastic prostatic tissue. *Eur J Cancer,* 39**,** 2229-33.

STAELS, B., MAES, M. & ZAMBON, A. 2008. Fibrates and future PPARalpha agonists in the treatment of cardiovascular disease. *Nat Clin Pract Cardiovasc Med,* 5**,** 542-53.

STANLEY, M. J., LIEBERSBACH, B. F., LIU, W., ANHALT, D. J. & SANDERSON, R. D. 1995. Heparan sulfate-mediated cell aggregation. Syndecans-1 and -4 mediate intercellular adhesion following their transfection into human B lymphoid cells. *J Biol Chem,* 270**,** 5077-83.

STANLEY, M. J., STANLEY, M. W., SANDERSON, R. D. & ZERA, R. 1999. Syndecan-1 expression is induced in the stroma of infiltrating breast carcinoma. *Am J Clin Pathol,* 112**,** 377-83.

STEEG, P. S. 2016. Targeting metastasis. *Nat Rev Cancer,* 16**,** 201-18.

STERNLICHT, M. D., KEDESHIAN, P., SHAO, Z. M., SAFARIANS, S. & BARSKY, S. H. 1997. The human myoepithelial cell is a natural tumor suppressor. *Clinical Cancer Research,* 3**,** 1949-1958.

STERNLICHT, M. D., LOCHTER, A., SYMPSON, C. J., HUEY, B., ROUGIER, J.-P., GRAY, J. W., PINKEL, D., BISSELL, M. J. & WERB, Z. 1999. The Stromal Proteinase MMP3/Stromelysin-1 Promotes Mammary Carcinogenesis. *Cell,* 98**,** 137-146.

STEVENSON, J. L., CHOI, S. H. & VARKI, A. 2005. Differential metastasis inhibition by clinically relevant levels of heparins--correlation with selectin inhibition, not antithrombotic activity. *Clin Cancer Res,* 11**,** 7003-11.

STRATMAN, A. N., MALOTTE, K. M., MAHAN, R. D., DAVIS, M. J. & DAVIS, G. E. 2009. Pericyte recruitment during vasculogenic tube assembly stimulates endothelial basement membrane matrix formation. *Blood,* 114**,** 5091-101.

STRILIC, B., YANG, L., ALBARRAN-JUAREZ, J., WACHSMUTH, L., HAN, K., MULLER, U. C., PASPARAKIS, M. & OFFERMANNS, S. 2016. Tumour-cell-induced endothelial cell necroptosis via death receptor 6 promotes metastasis. *Nature,* 536**,** 215-8.

STROME, S. E., DONG, H., TAMURA, H., VOSS, S. G., FLIES, D. B., TAMADA, K., SALOMAO, D., CHEVILLE, J., HIRANO, F., LIN, W., KASPERBAUER, J. L., BALLMAN, K. V. & CHEN, L. 2003. B7-H1 blockade augments adoptive T-cell immunotherapy for squamous cell carcinoma. *Cancer Res,* 63**,** 6501-5.

STRUTZ, F., ZEISBERG, M., ZIYADEH, F. N., YANG, C. Q., KALLURI, R., MULLER, G. A. & NEILSON, E. G. 2002. Role of basic fibroblast growth factor-2 in epithelial-mesenchymal transformation. *Kidney Int,* 61**,** 1714-28.

STUELTEN, C. H., PARENT, C. A. & MONTELL, D. J. 2018. Cell motility in cancer invasion and metastasis: insights from simple model organisms. *Nature Reviews Cancer,* 18**,** 296.

SUCHANEK, K. M., MAY, F. J., ROBINSON, J. A., LEE, W. J., HOLMAN, N. A., MONTEITH, G. R. & ROBERTS-THOMSON, S. J. 2002. Peroxisome proliferator-activated receptor alpha in the human breast cancer cell lines MCF-7 and MDA-MB-231. *Mol Carcinog,* 34**,** 165-71.

SUN, X., ZHANG, G., NIAN, J., YU, M., CHEN, S., ZHANG, Y., YANG, G., YANG, L., CHENG, P., YAN, C., MA, Y., MENG, H., WANG, X. & LI, J. P. 2017. Elevated heparanase expression is associated with poor prognosis in breast cancer: a study based on systematic review and TCGA data. *Oncotarget,* 8**,** 43521-43535.

SUPRAMANIAM, A., LIU, X., FERRO, V. & HERRERO, L. J. 2018. Prophylactic Antiheparanase Activity by PG545 Is Antiviral In Vitro and Protects against Ross River Virus Disease in Mice. *Antimicrob Agents Chemother,* 62.

SWAMIDASS, S. J. 2011. Mining small-molecule screens to repurpose drugs. *Briefings in Bioinformatics,* 12**,** 327-335.

TAGUCHI, A., KAWANA, K., TOMIO, K., YAMASHITA, A., ISOBE, Y., NAGASAKA, K., KOGA, K., INOUE, T., NISHIDA, H., KOJIMA, S., ADACHI, K., MATSUMOTO, Y., ARIMOTO, T., WADA-HIRAIKE, O., ODA, K., KANG, J. X., ARAI, H., ARITA, M., OSUGA, Y. & FUJII, T. 2014. Matrix metalloproteinase (MMP)-9 in cancer-associated fibroblasts (CAFs) is suppressed by omega-3 polyunsaturated fatty acids in vitro and in vivo. *PLoS One,* 9**,** e89605.

TAKAHASHI, H., INOUE, J., SAKAGUCHI, K., TAKAGI, M., MIZUTANI, S. & INAZAWA, J. 2017. Autophagy is required for cell survival under L-asparaginase-induced metabolic stress in acute lymphoblastic leukemia cells. *Oncogene,* 36**,** 4267-4276.

TAKAOKA, M., NAOMOTO, Y., OHKAWA, T., UETSUKA, H., SHIRAKAWA, Y., UNO, F., FUJIWARA, T., GUNDUZ, M., NAGATSUKA, H., NAKAJIMA, M., TANAKA, N. & HAISA, M. 2003. Heparanase expression correlates with invasion and poor prognosis in gastric cancers. *Lab Invest,* 83**,** 613-22.

TALHOUK, R. S., CHIN, J. R., UNEMORI, E. N., WERB, Z. & BISSELL, M. J. 1991. Proteinases of the mammary gland: developmental regulation in vivo and vectorial secretion in culture. *Development,* 112**,** 439-449.

TAM, S. Y., WU, V. W. C. & LAW, H. K. W. 2020. Hypoxia-Induced Epithelial-Mesenchymal Transition in Cancers: HIF-1α and Beyond. *Frontiers in Oncology,* 10.

TAN, J., BUACHE, E., ALPY, F., DAGUENET, E., TOMASETTO, C. L., REN, G. S. & RIO, M. C. 2014. Stromal matrix metalloproteinase-11 is involved in the mammary gland postnatal development. *Oncogene,* 33**,** 4050-9.

TAN, K. W., CHONG, S. Z., WONG, F. H., EVRARD, M., TAN, S. M., KEEBLE, J., KEMENY, D. M., NG, L. G., ABASTADO, J. P. & ANGELI, V. 2013. Neutrophils contribute to inflammatory lymphangiogenesis by increasing VEGF-A bioavailability and secreting VEGF-D. *Blood,* 122**,** 3666-77.

TAN, M. J., TEO, Z., SNG, M. K., ZHU, P. & TAN, N. S. 2012. Emerging roles of angiopoietin-like 4 in human cancer. *Mol Cancer Res,* 10**,** 677-88.

TANAKA, J., IRIE, T., YAMAMOTO, G., YASUHARA, R., ISOBE, T., HOKAZONO, C., TACHIKAWA, T., KOHNO, Y. & MISHIMA, K. 2015. ANGPTL4 regulates the metastatic potential of oral squamous cell carcinoma. *J Oral Pathol Med,* 44**,** 126-33.

TANG, B., XIE, R., QIN, Y., XIAO, Y. F., YONG, X., ZHENG, L., DONG, H. & YANG, S. M. 2016. Human telomerase reverse transcriptase (hTERT) promotes gastric cancer invasion through cooperating with c-Myc to upregulate heparanase expression. *Oncotarget,* 7**,** 11364-79.

TANG, D., PIAO, Y., ZHAO, S., MU, X., LI, S., MA, W., SONG, Y., WANG, J., ZHAO, W. & ZHANG, Q. 2014a. Expression and correlation of matrix metalloproteinase-9 and heparanase in patients with breast cancer. *Med Oncol,* 31**,** 26.

TANG, W., NAKAMURA, Y., TSUJIMOTO, M., SATO, M., WANG, X., KUROZUMI, K., NAKAHARA, M., NAKAO, K., NAKAMURA, M., MORI, I. & KAKUDO, K. 2002. Heparanase: a key enzyme in invasion and metastasis of gastric carcinoma. *Mod Pathol,* 15**,** 593-8.

TANG, X. D., GUO, S. L., WANG, G. Z., LI, N., WU, Y. Y., FANG, D. C., FAN, Y. H. & YANG, S. M. 2014b. In vitro and ex vivo evaluation of a multi-epitope heparinase vaccine for various malignancies. *Cancer Sci,* 105**,** 9-17.

TANG, X. D., LIANG, G. P., LI, C., WAN, Y., CHEN, T., CHEN, L., YU, S. T., XIONG, Z., FANG, D. C., WANG, G. Z. & YANG, S. M. 2010. Cytotoxic T lymphocyte epitopes from human heparanase can elicit a potent anti-tumor immune response in mice. *Cancer Immunol Immunother,* 59**,** 1041-7.

TAUER, J. T., HOFBAUER, L. C., JUNG, R., ERBEN, R. G. & SUTTORP, M. 2013. Micro-osmotic pumps for continuous release of the tyrosine kinase inhibitor bosutinib in juvenile rats and its impact on bone growth. *Medical science monitor basic research,* 19**,** 274-278.

TAYEL, A., ABD EL GALIL, K. H., EBRAHIM, M. A., IBRAHIM, A. S., EL-GAYAR, A. M. & AL-GAYYAR, M. M. 2014. Suramin inhibits hepatic tissue damage in hepatocellular carcinoma through deactivation of heparanase enzyme. *Eur J Pharmacol,* 728**,** 151-60.

TEMKIN, V., AINGORN, H., PUXEDDU, I., GOLDSHMIDT, O., ZCHARIA, E., GLEICH, G. J., VLODAVSKY, I. & LEVI-SCHAFFER, F. 2004. Eosinophil major basic protein: first identified natural heparanase-inhibiting protein. *Journal of Allergy and Clinical Immunology,* 113**,** 703-709.

TEOH, M. L. T., FITZGERALD, M. P., OBERLEY, L. W. & DOMANN, F. E. 2009. Overexpression of Extracellular Superoxide Dismutase Attenuates Heparanase Expression and Inhibits Breast Carcinoma Cell Growth and Invasion. *Cancer Research,* 69**,** 6355-6363.

TEVAARWERK, A. J., GRAY, R. J., SCHNEIDER, B. P., SMITH, M. L., WAGNER, L. I., FETTING, J. H., DAVIDSON, N., GOLDSTEIN, L. J., MILLER, K. D. & SPARANO, J. A. 2013. Survival in patients with metastatic recurrent breast cancer after adjuvant chemotherapy: little evidence of improvement over the past 30 years. *Cancer,* 119**,** 1140-8.

THEODORO, T. R., DE MATOS, L. L., LAMBIASI SANT ANNA, A. V., FONSECA, F. L. A., SEMEDO, P., MARTINS, L. C., NADER, H. B., DEL GIGLIO, A. & DA SILVA PINHAL, M. A. 2007. Heparanase Expression in Circulating Lymphocytes of Breast Cancer Patients Depends on the Presence of the Primary Tumor and/or Systemic Metastasis. *Neoplasia,* 9**,** 504-510.

THOMPSON, C. A., PURUSHOTHAMAN, A., RAMANI, V. C., VLODAVSKY, I. & SANDERSON, R. D. 2013. Heparanase regulates secretion, composition, and function of tumor cell-derived exosomes. *J Biol Chem,* 288**,** 10093-9.

THORN, C. C., FREEMAN, T. C., SCOTT, N., GUILLOU, P. J. & JAYNE, D. G. 2009. Laser microdissection expression profiling of marginal edges of colorectal tumours

reveals evidence of increased lactate metabolism in the aggressive phenotype. *Gut,* 58**,** 404-12.

TORRE, L. A., BRAY, F., SIEGEL, R. L., FERLAY, J., LORTET-TIEULENT, J. & JEMAL, A. 2015. Global cancer statistics, 2012. *CA Cancer J Clin,* 65**,** 87-108.

TOYOSHIMA, M. & NAKAJIMA, M. 1999. Human heparanase. Purification, characterization, cloning, and expression. *J Biol Chem,* 274**,** 24153-60.

TRINDADE, E. S., OLIVER, C., JAMUR, M. C., ROCHA, H. A., FRANCO, C. R., BOUCAS, R. I., JARROUGE, T. R., PINHAL, M. A., TERSARIOL, I. L., GOUVEA, T. C., DIETRICH, C. P. & NADER, H. B. 2008. The binding of heparin to the extracellular matrix of endothelial cells up-regulates the synthesis of an antithrombotic heparan sulfate proteoglycan. *J Cell Physiol,* 217**,** 328-37.

TRIPATHI, C. K., BANGA, J. & MISHRA, V. 2012. Microbial heparin/heparan sulphate lyases: potential and applications. *Appl Microbiol Biotechnol,* 94**,** 307-21.

TROILO, H., STEER, R., COLLINS, R. F., KIELTY, C. M. & BALDOCK, C. 2016. Independent multimerization of Latent TGFbeta Binding Protein-1 stabilized by cross-linking and enhanced by heparan sulfate. *Sci Rep,* 6**,** 34347.

TROTT, O. & OLSON, A. J. 2010. AutoDock Vina: improving the speed and accuracy of docking with a new scoring function, efficient optimization, and multithreading. *J Comput Chem,* 31**,** 455-61.

TRUONG, D., PULEO, J., LLAVE, A., MOUNEIMNE, G., KAMM, R. D. & NIKKHAH, M. 2016. Breast Cancer Cell Invasion into a Three Dimensional Tumor-Stroma Microenvironment. *Scientific Reports,* 6**,** 34094.

TSAI, C.-H., SU, W.-T., SHEEN-CHEN, S.-M., LIANG, J.-L., HSU, H.-W., CHEN, W.-T., HUANG, E.-Y., HUANG, C.-C., RAU, K.-M. & TANG, R.-P. 2015. Glypican-3 Expression in Breast Cancer. *Journal of Cancer Research and Practice,* 2**,** 285-292.

TSUCHIYA, K., HIDA, K., HIDA, Y., MURAKI, C., OHGA, N., AKINO, T., KONDO, T., MISEKI, T., NAKAGAWA, K., SHINDOH, M., HARABAYASHI, T., SHINOHARA, N., NONOMURA, K. & KOBAYASHI, M. 2010. Adrenomedullin antagonist suppresses tumor formation in renal cell carcinoma through inhibitory effects on tumor endothelial cells and endothelial progenitor mobilization. *Int J Oncol,* 36**,** 1379-86.

TSUKADA, M. & OHSUMI, Y. 1993. Isolation and characterization of autophagy-defective mutants of Saccharomyces cerevisiae. *FEBS Lett,* 333**,** 169-74.

TUMOVA, S. & BAME, K. J. 1997. The interaction between basic fibroblast growth factor and heparan sulfate can prevent the in vitro degradation of the glycosaminoglycan by Chinese hamster ovary cell heparanases. *J Biol Chem,* 272**,** 9078-85.

TUMOVA, S., WOODS, A. & COUCHMAN, J. R. 2000. Heparan sulfate chains from glypican and syndecans bind the Hep II domain of fibronectin similarly despite minor structural differences. *J Biol Chem,* 275**,** 9410-7.

TURNER, N. & GROSE, R. 2010. Fibroblast growth factor signalling: from development to cancer. *Nat Rev Cancer,* 10**,** 116-29.

TYAGI, S., GUPTA, P., SAINI, A. S., KAUSHAL, C. & SHARMA, S. 2011. The peroxisome proliferator-activated receptor: A family of nuclear receptors role in various diseases. *Journal of advanced pharmaceutical technology & research,* 2**,** 236-240.

ULLAH, I., KARTHIK, G.-M., ALKODSI, A., KJÄLLQUIST, U., STÅLHAMMAR, G., LÖVROT, J., MARTINEZ, N.-F., LAGERGREN, J., HAUTANIEMI, S., HARTMAN, J. & BERGH, J. 2018. Evolutionary history of metastatic breast cancer reveals minimal seeding from axillary lymph nodes. *The Journal of Clinical Investigation,* 128**,** 1355-1370.

VAHL, J. M., FRIEDRICH, J., MITTLER, S., TRUMP, S., HEIM, L., KACHLER, K., BALABKO, L., FUHRICH, N., GEPPERT, C.-I., TRUFA, D. I., SOPEL, N., RIEKER, R., SIRBU, H. & FINOTTO, S. 2017. Interleukin-10-regulated tumour tolerance in non-small cell lung cancer. *British Journal Of Cancer,* 117**,** 1644.

VAN DEN BERG, Y. W., OSANTO, S., REITSMA, P. H. & VERSTEEG, H. H. 2012. The relationship between tissue factor and cancer progression: insights from bench and bedside. *Blood,* 119**,** 924.

VAN DER WOUDE, L. L., GORRIS, M. A. J., HALILOVIC, A., FIGDOR, C. G. & DE VRIES, I. J. M. 2017. Migrating into the Tumor: a Roadmap for T Cells. *Trends in Cancer,* 3**,** 797-808.

VAN RAALTE, D. H., LI, M., PRITCHARD, P. H. & WASAN, K. M. 2004. Peroxisome proliferator-activated receptor (PPAR)-alpha: a pharmacological target with a promising future. *Pharm Res,* 21**,** 1531-8.

VARET, J., VINCENT, L., MIRSHAHI, P., PILLE, J. V., LEGRAND, E., OPOLON, P., MISHAL, Z., SORIA, J., LI, H. & SORIA, C. 2003. Fenofibrate inhibits angiogenesis in vitro and in vivo. *Cellular and Molecular Life Sciences CMLS,* 60**,** 810-819.

VENNING, F. A., WULLKOPF, L. & ERLER, J. T. 2015. Targeting ECM Disrupts Cancer Progression. *Front Oncol,* 5**,** 224.

VERSTEEG, H. H., SCHAFFNER, F., KERVER, M., PETERSEN, H. H., AHAMED, J., FELDING-HABERMANN, B., TAKADA, Y., MUELLER, B. M. & RUF, W. 2008. Inhibition of tissue factor signaling suppresses tumor growth. *Blood,* 111**,** 190.

VINAY, D. S., RYAN, E. P., PAWELEC, G., TALIB, W. H., STAGG, J., ELKORD, E., LICHTOR, T., DECKER, W. K., WHELAN, R. L., KUMARA, H. M. C. S., SIGNORI, E., HONOKI, K., GEORGAKILAS, A. G., AMIN, A., HELFERICH, W. G., BOOSANI, C. S., GUHA, G., CIRIOLO, M. R., CHEN, S., MOHAMMED, S. I., AZMI, A. S., KEITH, W. N., BILSLAND, A., BHAKTA, D., HALICKA, D., FUJII, H., AQUILANO, K., ASHRAF, S. S., NOWSHEEN, S., YANG, X., CHOI, B. K. &

KWON, B. S. 2015. Immune evasion in cancer: Mechanistic basis and therapeutic strategies. *Seminars in Cancer Biology,* 35**,** S185-S198.

VIRCHOW, R. 1881. An Address on the Value of Pathological Experiments. *British Medical Journal,* 2**,** 198-203.

VLODAVSKY, I., ELDOR, A., HAIMOVITZ-FRIEDMAN, A., MATZNER, Y., ISHAI-MICHAELI, R., LIDER, O., NAPARSTEK, Y., COHEN, I. R. & FUKS, Z. 1992. Expression of heparanase by platelets and circulating cells of the immune system: possible involvement in diapedesis and extravasation. *Invasion Metastasis,* 12**,** 112-27.

VLODAVSKY, I. & FRIEDMANN, Y. 2001. Molecular properties and involvement of heparanase in cancer metastasis and angiogenesis. *J Clin Invest,* 108**,** 341-7.

VLODAVSKY, I., FRIEDMANN, Y., ELKIN, M., AINGORN, H., ATZMON, R., ISHAI-MICHAELI, R., BITAN, M., PAPPO, O., PERETZ, T., MICHAL, I., SPECTOR, L. & PECKER, I. 1999. Mammalian heparanase: gene cloning, expression and function in tumor progression and metastasis. *Nat Med,* 5**,** 793-802.

VLODAVSKY, I., SINGH, P., BOYANGO, I., GUTTER-KAPON, L., ELKIN, M., SANDERSON, R. D. & ILAN, N. 2016. Heparanase: From basic research to therapeutic applications in cancer and inflammation. *Drug Resist Updat,* 29**,** 54-75.

VOLINSKY, N. & KHOLODENKO, B. N. 2013. Complexity of receptor tyrosine kinase signal processing. *Cold Spring Harb Perspect Biol,* 5**,** a009043.

VONDERHEIDE, R. H., DOMCHEK, S. M. & CLARK, A. S. 2017. Immunotherapy for breast cancer: what are we missing? *Clinical cancer research : an official journal of the American Association for Cancer Research,* 23**,** 2640-2646.

VORNICOVA, O., BOYANGO, I., FELD, S., NARODITSKY, I., KAZARIN, O., ZOHAR, Y., TIRAM, Y., ILAN, N., BEN-IZHAK, O., VLODAVSKY, I. & BAR-SELA, G. 2016. The prognostic significance of heparanase expression in metastatic melanoma. *Oncotarget,* 7**,** 74678-74685.

VORNICOVA, O., NARODITSKY, I., BOYANGO, I., SHACHAR, S. S., MASHIACH, T., ILAN, N., VLODAVSKY, I. & BAR-SELA, G. 2018. Prognostic significance of heparanase expression in primary and metastatic breast carcinoma. *Oncotarget,* 9**,** 6238-6244.

WAGNER, K. D. & WAGNER, N. 2010. Peroxisome proliferator-activated receptor beta/delta (PPARbeta/delta) acts as regulator of metabolism linked to multiple cellular functions. *Pharmacol Ther,* 125**,** 423-35.

WANG, B., JIA, J., ZHANG, X., ZCHARIA, E., VLODAVSKY, I., PEJLER, G. & LI, J.-P. 2011. Heparanase affects secretory granule homeostasis of murine mast cells through degrading heparin. *Journal of Allergy and Clinical Immunology,* 128**,** 1310-1317.e8.

WANG, F., WANG, Y., ZHANG, D., PUTHANVEETIL, P., JOHNSON, J. D. & RODRIGUES, B. 2012a. Fatty acid-induced nuclear translocation of heparanase uncouples glucose metabolism in endothelial cells. *Arterioscler Thromb Vasc Biol,* 32**,** 406-14.

WANG, G. B., ZHOU, X. Y. & WANG, X. Q. 2010. Relationship between serum heparanase and microscopic venous invasion in patients with hepatocellular carcinoma. *Am J Clin Pathol,* 134**,** 242-8.

WANG, J.-G., GEDDINGS, J. E., ALEMAN, M. M., CARDENAS, J. C., CHANTRATHAMMACHART, P., WILLIAMS, J. C., KIRCHHOFER, D., BOGDANOV, V. Y., BACH, R. R., RAK, J., CHURCH, F. C., WOLBERG, A. S., PAWLINSKI, R., KEY, N. S., YEH, J. J. & MACKMAN, N. 2012b. Tumor-derived tissue factor activates coagulation and enhances thrombosis in a mouse xenograft model of human pancreatic cancer. *Blood,* 119**,** 5543.

WANG, L., HUANG, X., KONG, G., XU, H., LI, J., HAO, D., WANG, T., HAN, S., HAN, C., SUN, Y., LIU, X. & WANG, X. 2016. Ulinastatin attenuates pulmonary endothelial glycocalyx damage and inhibits endothelial heparanase activity in LPS-induced ARDS. *Biochemical and Biophysical Research Communications,* 478**,** 669-675.

WANG, P., ZHANG, Z. & YU, B. 2005. Total Synthesis of CRM646-A and -B, Two Fungal Glucuronides with Potent Heparinase Inhibition Activities. *The Journal of Organic Chemistry,* 70**,** 8884-8889.

WANG, X., ZUO, D., CHEN, Y., LI, W., LIU, R., HE, Y., REN, L., ZHOU, L., DENG, T., WANG, X., YING, G. & BA, Y. 2014. Shed Syndecan-1 is involved in chemotherapy resistance via the EGFR pathway in colorectal cancer. *Br J Cancer,* 111**,** 1965-76.

WANG, Y. & BECKER, D. 1997. Antisense targeting of basic fibroblast growth factor and fibroblast growth factor receptor-1 in human melanomas blocks intratumoral angiogenesis and tumor growth. *Nat Med,* 3**,** 887-93.

WARBURG, O. 1956a. On respiratory impairment in cancer cells. *Science,* 124**,** 269-70.

WARBURG, O. 1956b. On the origin of cancer cells. *Science,* 123**,** 309-14.

WARBURG, O., WIND, F. & NEGELEIN, E. 1927. The Metabolism of Tumors in the Body. *J Gen Physiol,* 8**,** 519-30.

WARKENTIN, T. E., LEVINE, M. N., HIRSH, J., HORSEWOOD, P., ROBERTS, R. S., GENT, M. & KELTON, J. G. 1995. Heparin-induced thrombocytopenia in patients treated with low-molecular-weight heparin or unfractionated heparin. *N Engl J Med,* 332**,** 1330-5.

WATANABE, M., AOKI, Y., KASE, H. & TANAKA, K. 2003a. Heparanase expression and angiogenesis in endometrial cancer. *Gynecol Obstet Invest,* 56**,** 77-82.

WATANABE, M., AOKI, Y., KASE, H. & TANAKA, K. 2003b. Heparanase Expression and Angiogenesis in Endometrial Cancer. *Gynecologic and Obstetric Investigation,* 56**,** 77-82.

WATERMAN, M., BEN-IZHAK, O., ELIAKIM, R., GROISMAN, G., VLODAVSKY, I. & ILAN, N. 2007. Heparanase upregulation by colonic epithelium in inflammatory bowel disease. *Mod Pathol,* 20**,** 8-14.

WATERS, J. P., POBER, J. S. & BRADLEY, J. R. 2013. Tumour necrosis factor and cancer. *J Pathol,* 230**,** 241-8.

WCULEK, S. K. & MALANCHI, I. 2015a. Neutrophils support lung colonization of metastasis-initiating breast cancer cells. *Nature,* 528**,** 413-7.

WCULEK, S. K. & MALANCHI, I. 2015b. Neutrophils support lung colonization of metastasis-initiating breast cancer cells. *Nature,* 528**,** 413.

WEE, P. & WANG, Z. 2017. Epidermal Growth Factor Receptor Cell Proliferation Signaling Pathways. *Cancers (Basel),* 9.

WEI, R. R., SUN, D. N., YANG, H., YAN, J., ZHANG, X., ZHENG, X. L., FU, X. H., GENG, M. Y., HUANG, X. & DING, J. 2018a. CTC clusters induced by heparanase enhance breast cancer metastasis. *Acta Pharmacol Sin*.

WEI, R. R., SUN, D. N., YANG, H., YAN, J., ZHANG, X., ZHENG, X. L., FU, X. H., GENG, M. Y., HUANG, X. & DING, J. 2018b. CTC clusters induced by heparanase enhance breast cancer metastasis. *Acta Pharmacol Sin,* 39**,** 1326-1337.

WEI, Y., KIM, T. J., PENG, D. H., DUAN, D., GIBBONS, D. L., YAMAUCHI, M., JACKSON, J. R., LE SAUX, C. J., CALHOUN, C., PETERS, J., DERYNCK, R., BACKES, B. J. & CHAPMAN, H. A. 2017. Fibroblast-specific inhibition of TGF-beta1 signaling attenuates lung and tumor fibrosis. *J Clin Invest,* 127**,** 3675-3688.

WEIDNER, N., SEMPLE, J. P., WELCH, W. R. & FOLKMAN, J. 1991. Tumor angiogenesis and metastasis--correlation in invasive breast carcinoma. *N Engl J Med,* 324**,** 1-8.

WEINER, G. J. 2015. Building better monoclonal antibody-based therapeutics. *Nature Reviews Cancer,* 15**,** 361.

WEISS, S. J. 1989. Tissue destruction by neutrophils. *N Engl J Med,* 320**,** 365-76.

WEISSMANN, M., ARVATZ, G., HOROWITZ, N., FELD, S., NARODITSKY, I., ZHANG, Y., NG, M., HAMMOND, E., NEVO, E., VLODAVSKY, I. & ILAN, N. 2016. Heparanase-neutralizing antibodies attenuate lymphoma tumor growth and metastasis. *Proc Natl Acad Sci U S A,* 113**,** 704-9.

WEISSMANN, M., BHATTACHARYA, U., FELD, S., HAMMOND, E., ILAN, N. & VLODAVSKY, I. 2018. The heparanase inhibitor PG545 is a potent anti-lymphoma drug: Mode of action. *Matrix Biol*.

WELCH, D. R., FABRA, A. & NAKAJIMA, M. 1990. Transforming growth factor beta stimulates mammary adenocarcinoma cell invasion and metastatic potential. *Proc Natl Acad Sci U S A,* 87**,** 7678-82.

WELCH, M. D. 2015. Cell migration, freshly squeezed. *Cell,* 160**,** 581-582.

WELLINGS, S. R. & JENSEN, H. M. 1973. On the origin and progression of ductal carcinoma in the human breast. *J Natl Cancer Inst,* 50**,** 1111-8.

WEYERS, A., YANG, B., YOON, D. S., PARK, J.-H., ZHANG, F., LEE, K. B. & LINHARDT, R. J. 2012. A Structural Analysis of Glycosaminoglycans from Lethal and Nonlethal Breast Cancer Tissues: Toward a Novel Class of Theragnostics for Personalized Medicine in Oncology? *OMICS : a Journal of Integrative Biology,* 16**,** 79-89.

WHALEN, K. A., WEBER, G. F., BENJAMIN, T. L. & SCHAFFHAUSEN, B. S. 2008. Polyomavirus Middle T Antigen Induces the Transcription of Osteopontin, a Gene Important for the Migration of Transformed Cells. *Journal of Virology,* 82**,** 4946-4954.

WHITMAN, M., KAPLAN, D. R., SCHAFFHAUSEN, B., CANTLEY, L. & ROBERTS, T. M. 1985. Association of phosphatidylinositol kinase activity with polyoma middle-T competent for transformation. *Nature,* 315**,** 239-42.

WIGERUP, C., PÅHLMAN, S. & BEXELL, D. 2016. Therapeutic targeting of hypoxia and hypoxia-inducible factors in cancer. *Pharmacology & Therapeutics,* 164**,** 152-169.

WILSON, J. C., LALOO, A. E., SINGH, S. & FERRO, V. 2014. 1H NMR spectroscopic studies establish that heparanase is a retaining glycosidase. *Biochem Biophys Res Commun,* 443**,** 185-8.

WINER, A., ADAMS, S. & MIGNATTI, P. 2018a. Matrix Metalloproteinase Inhibitors in Cancer Therapy: Turning Past Failures Into Future Successes. *Molecular Cancer Therapeutics,* 17**,** 1147-1155.

WINER, A., ADAMS, S. & MIGNATTI, P. 2018b. Matrix Metalloproteinase Inhibitors in Cancer Therapy: Turning Past Failures Into Future Successes. *Mol Cancer Ther,* 17**,** 1147-1155.

WINKLER, S., SCHWEIGER, D., WEI, Z., RAJKOVIC, E. & KUNGL, A. J. 2014. Bacterial expression and functional reconstitution of human heparanase. *Carbohydrate Research,* 389**,** 72-77.

WIRSTLEIN, P. K., MIKOLAJCZYK, M. & SKRZYPCZAK, J. 2013. Correlation of the expression of heparanase and heparin-binding EGF-like growth factor in the implantation window of nonconceptual cycle endometrium. *Folia Histochem Cytobiol,* 51**,** 127-34.

WISEMAN, B. S. & WERB, Z. 2002. Stromal Effects on Mammary Gland Development and Breast Cancer. *Science,* 296**,** 1046-1049.

WOLF, M. J., HOOS, A., BAUER, J., BOETTCHER, S., KNUST, M., WEBER, A., SIMONAVICIUS, N., SCHNEIDER, C., LANG, M., STURZL, M., CRONER, R. S., KONRAD, A., MANZ, M. G., MOCH, H., AGUZZI, A., VAN LOO, G., PASPARAKIS, M., PRINZ, M., BORSIG, L. & HEIKENWALDER, M. 2012. Endothelial CCR2

signaling induced by colon carcinoma cells enables extravasation via the JAK2-Stat5 and p38MAPK pathway. *Cancer Cell,* 22**,** 91-105.

WONG, S. Y. & HYNES, R. O. 2006. Lymphatic or hematogenous dissemination: how does a metastatic tumor cell decide? *Cell Cycle,* 5**,** 812-7.

WOOD, R. J. & HULETT, M. D. 2008. Cell surface-expressed cation-independent mannose 6-phosphate receptor (CD222) binds enzymatically active heparanase independently of mannose 6-phosphate to promote extracellular matrix degradation. *J Biol Chem,* 283**,** 4165-76.

WRIGHT, M. B., BORTOLINI, M., TADAYYON, M. & BOPST, M. 2014. Minireview: Challenges and opportunities in development of PPAR agonists. *Mol Endocrinol,* 28**,** 1756-68.

WU, B. W., LI, D. F., KE, Z. F., MA, D., LI, Y. J., GANG, D., ZHENG, Z. G., ZHANG, K. J. & ZHANG, Y. H. 2010a. Expression characteristics of heparanase in colon carcinoma and its close relationship with cyclooxygenase-2 and angiogenesis. *Hepatogastroenterology,* 57**,** 1510-4.

WU, D., ASIEDU, M. & WEI, Q. 2009. Myosin-interacting guanine exchange factor (MyoGEF) regulates the invasion activity of MDA-MB-231 breast cancer cells through activation of RhoA and RhoC. *Oncogene,* 28**,** 2219-2230.

WU, L., VIOLA, C. M., BRZOZOWSKI, A. M. & DAVIES, G. J. 2015. Structural characterization of human heparanase reveals insights into substrate recognition. *Nat Struct Mol Biol,* 22**,** 1016-22.

WU, W., PAN, C., MENG, K., ZHAO, L., DU, L., LIU, Q. & LIN, R. 2010b. Hypoxia activates heparanase expression in an NF-kappaB dependent manner. *Oncol Rep,* 23**,** 255-61.

XIANG, Y. Y., LADEDA, V. & FILMUS, J. 2001. Glypican-3 expression is silenced in human breast cancer. *Oncogene,* 20**,** 7408-12.

XIAO, Y., KLEEFF, J., SHI, X., BÜCHLER, M. W. & FRIESS, H. 2003. Heparanase expression in hepatocellular carcinoma and the cirrhotic liver. *Hepatology Research,* 26**,** 192-198.

XIE, Y., MUSTAFA, A., YERZHAN, A., MERZHAKUPOVA, D., YERLAN, P., N ORAKOV, A., WANG, X., HUANG, Y. & MIAO, L. 2017. Nuclear matrix metalloproteinases: functions resemble the evolution from the intracellular to the extracellular compartment. *Cell Death Discovery,* 3**,** 17036.

XIE, Y., WOLFF, D. W., WEI, T., WANG, B., DENG, C., KIRUI, J. K., JIANG, H., QIN, J., ABEL, P. W. & TU, Y. 2009. Breast Cancer Migration and Invasion Depend on Proteasome Degradation of Regulator of G-Protein Signaling 4. *Cancer Research,* 69**,** 5743.

XIONG, A., KUNDU, S., FORSBERG, M., XIONG, Y., BERGSTROM, T., PAAVILAINEN, T., KJELLEN, L., LI, J. P. & FORSBERG-NILSSON, K. 2017. Heparanase confers

a growth advantage to differentiating murine embryonic stem cells, and enhances oligodendrocyte formation. *Matrix Biol,* 62**,** 92-104.

XIONG, J., BALCIOGLU, H. E. & DANEN, E. H. 2013. Integrin signaling in control of tumor growth and progression. *Int J Biochem Cell Biol,* 45**,** 1012-5.

XIU, B., LIN, Y., GROTE, D. M., ZIESMER, S. C., GUSTAFSON, M. P., MAAS, M. L., ZHANG, Z., DIETZ, A. B., PORRATA, L. F., NOVAK, A. J., LIANG, A. B., YANG, Z. Z. & ANSELL, S. M. 2015. IL-10 induces the development of immunosuppressive CD14+HLA-DRlow/− monocytes in B-cell non-Hodgkin lymphoma. *Blood Cancer Journal,* 5**,** e328.

XU, D. & ESKO, J. D. 2014. Demystifying heparan sulfate-protein interactions. *Annu Rev Biochem,* 83**,** 129-57.

XU, X. & DAI, Y. 2010. Heparin: an intervenor in cell communication. *Journal of cellular and molecular medicine,* 14**,** 175-180.

XU, X., QUIROS, R. M., MAXHIMER, J. B., JIANG, P., MARCINEK, R., AIN, K. B., PLATT, J. L., SHEN, J., GATTUSO, P. & PRINZ, R. A. 2003. Inverse correlation between heparan sulfate composition and heparanase-1 gene expression in thyroid papillary carcinomas: a potential role in tumor metastasis. *Clin Cancer Res,* 9**,** 5968-79.

XU, Y.-J., MIAO, H.-Q., PAN, W., NAVARRO, E. C., TONRA, J. R., MITELMAN, S., CAMARA, M. M., DEEVI, D. S., KISELYOV, A. S., KUSSIE, P., WONG, W. C. & LIU, H. 2006. N-(4-{[4-(1H-Benzoimidazol-2-yl)-arylamino]-methyl}-phenyl)-benzamide derivatives as small molecule heparanase inhibitors. *Bioorganic & Medicinal Chemistry Letters,* 16**,** 404-408.

XUE, H., LI, J., XIE, H. & WANG, Y. 2018. Review of Drug Repositioning Approaches and Resources. *International journal of biological sciences,* 14**,** 1232-1244.

YABE, T., MCSHERRY, C., BACH, F. H., FISCH, P., SCHALL, R. P., SONDEL, P. M. & HOUCHINS, J. P. 1993. A multigene family on human chromosome 12 encodes natural killer-cell lectins. *Immunogenetics,* 37**,** 455-60.

YAHALOM, J., ELDOR, A., FUKS, Z. & VLODAVSKY, I. 1984. Degradation of sulfated proteoglycans in the subendothelial extracellular matrix by human platelet heparitinase. *J Clin Invest,* 74**,** 1842-9.

YANG, J. & LIU, Y. 2001. Dissection of Key Events in Tubular Epithelial to Myofibroblast Transition and Its Implications in Renal Interstitial Fibrosis. *The American Journal of Pathology,* 159**,** 1465-1475.

YANG, N. & FRIEDL, A. 2016. Syndecan-1-Induced ECM Fiber Alignment Requires Integrin alphavbeta3 and Syndecan-1 Ectodomain and Heparan Sulfate Chains. *PLoS One,* 11**,** e0150132.

YANG, N., MOSHER, R., SEO, S., BEEBE, D. & FRIEDL, A. 2011. Syndecan-1 in Breast Cancer Stroma Fibroblasts Regulates Extracellular Matrix Fiber Organization and Carcinoma Cell Motility. *The American Journal of Pathology,* 178**,** 325-335.

YANG, Y. 2015. Cancer immunotherapy: harnessing the immune system to battle cancer. *J Clin Invest,* 125**,** 3335-7.

YANG, Y., MACLEOD, V., BENDRE, M., HUANG, Y., THEUS, A. M., MIAO, H.-Q., KUSSIE, P., YACCOBY, S., EPSTEIN, J., SUVA, L. J., KELLY, T. & SANDERSON, R. D. 2005. Heparanase promotes the spontaneous metastasis of myeloma cells to bone. *Blood,* 105**,** 1303.

YANG, Y., RITCHIE, J. P., SWAIN, T., NAGGI, A., TORRI, G., CASU, B., PISANO, C., CARMINATI, P., VLODAVSKY, I. & SANDERSON, R. D. 2008. The Heparanase Inhibitor SST0001 Is a Potent Inhibitor of Myeloma Growth In Vivo. *Blood,* 112**,** 246-246.

YATES, L. R., KNAPPSKOG, S., WEDGE, D., FARMERY, J. H. R., GONZALEZ, S., MARTINCORENA, I., ALEXANDROV, L. B., VAN LOO, P., HAUGLAND, H. K., LILLENG, P. K., GUNDEM, G., GERSTUNG, M., PAPPAEMMANUIL, E., GAZINSKA, P., BHOSLE, S. G., JONES, D., RAINE, K., MUDIE, L., LATIMER, C., SAWYER, E., DESMEDT, C., SOTIRIOU, C., STRATTON, M. R., SIEUWERTS, A. M., LYNCH, A. G., MARTENS, J. W., RICHARDSON, A. L., TUTT, A., LONNING, P. E. & CAMPBELL, P. J. 2017. Genomic Evolution of Breast Cancer Metastasis and Relapse. *Cancer Cell,* 32**,** 169-184 e7.

YEO, S. K. & GUAN, J. L. 2017. Breast Cancer: Multiple Subtypes within a Tumor? *Trends Cancer,* 3**,** 753-760.

YIN, M., MACKLEY, H. B., DRABICK, J. J. & HARVEY, H. A. 2016. Primary female breast sarcoma: clinicopathological features, treatment and prognosis. *Scientific Reports,* 6**,** 31497.

YIN, X., JOHNS, S. C., LAWRENCE, R., XU, D., REDDI, K., BISHOP, J. R., VARNER, J. A. & FUSTER, M. M. 2011. Lymphatic endothelial heparan sulfate deficiency results in altered growth responses to vascular endothelial growth factor-C (VEGF-C). *J Biol Chem,* 286**,** 14952-62.

YU, G., GUNAY, N. S., LINHARDT, R. J., TOIDA, T., FAREED, J., HOPPENSTEADT, D. A., SHADID, H., FERRO, V., LI, C., FEWINGS, K., PALERMO, M. C. & PODGER, D. 2002. Preparation and anticoagulant activity of the phosphosulfomannan PI-88. *European Journal of Medicinal Chemistry,* 37**,** 783-791.

YU, H., MUNOZ, E. M., EDENS, R. E. & LINHARDT, R. J. 2005. Kinetic studies on the interactions of heparin and complement proteins using surface plasmon resonance. *Biochim Biophys Acta,* 1726**,** 168-76.

YU, L., CHEN, Y. & TOOZE, S. A. 2018. Autophagy pathway: Cellular and molecular mechanisms. *Autophagy,* 14**,** 207-215.

YU, Y., LV, Q., ZHANG, B., LAN, F. & DAI, Y. 2016. Adjuvant therapy with heparin in patients with lung cancer without indication for anticoagulants: A systematic review of the literature with meta-analysis. *J Cancer Res Ther,* 12**,** 37-42.

YUE, T. L., BAO, W., JUCKER, B. M., GU, J. L., ROMANIC, A. M., BROWN, P. J., CUI, J., THUDIUM, D. T., BOYCE, R., BURNS-KURTIS, C. L., MIRABILE, R. C., ARAVINDHAN, K. & OHLSTEIN, E. H. 2003. Activation of peroxisome proliferator-activated receptor-alpha protects the heart from ischemia/reperfusion injury. *Circulation,* 108**,** 2393-9.

ZACHARAKIS, N., CHINNASAMY, H., BLACK, M., XU, H., LU, Y.-C., ZHENG, Z., PASETTO, A., LANGHAN, M., SHELTON, T., PRICKETT, T., GARTNER, J., JIA, L., TREBSKA-MCGOWAN, K., SOMERVILLE, R. P., ROBBINS, P. F., ROSENBERG, S. A., GOFF, S. L. & FELDMAN, S. A. 2018. Immune recognition of somatic mutations leading to complete durable regression in metastatic breast cancer. *Nature Medicine,* 24**,** 724-730.

ZAKO, M., DONG, J., GOLDBERGER, O., BERNFIELD, M., GALLAGHER, J. T. & DEAKIN, J. A. 2003. Syndecan-1 and -4 synthesized simultaneously by mouse mammary gland epithelial cells bear heparan sulfate chains that are apparently structurally indistinguishable. *J Biol Chem,* 278**,** 13561-9.

ZAYNAGETDINOV, R., SHERRILL, T. P., GLEAVES, L. A., MCLOED, A. G., SAXON, J. A., HABERMANN, A. C., CONNELLY, L., DULEK, D., PEEBLES, R. S., JR., FINGLETON, B., YULL, F. E., STATHOPOULOS, G. T. & BLACKWELL, T. S. 2015. Interleukin-5 facilitates lung metastasis by modulating the immune microenvironment. *Cancer Res,* 75**,** 1624-1634.

ZCHARIA, E., JIA, J., ZHANG, X., BARAZ, L., LINDAHL, U., PERETZ, T., VLODAVSKY, I. & LI, J. P. 2009. Newly generated heparanase knock-out mice unravel co-regulation of heparanase and matrix metalloproteinases. *PLoS One,* 4**,** e5181.

ZCHARIA, E., METZGER, S., CHAJEK-SHAUL, T., AINGORN, H., ELKIN, M., FRIEDMANN, Y., WEINSTEIN, T., LI, J. P., LINDAHL, U. & VLODAVSKY, I. 2004. Transgenic expression of mammalian heparanase uncovers physiological functions of heparan sulfate in tissue morphogenesis, vascularization, and feeding behavior. *FASEB J,* 18**,** 252-63.

ZENG, C., CHEN, L., YANG, Z. & SUN, S. 2014. The close correlation between heparanase and COX-2 expression in lymphangiogenesis of cervical cancer. *Med Oncol,* 31**,** 314.

ZENG, C., KE, Z. F., LUO, W. R., YAO, Y. H., HU, X. R., JIE, W., YIN, J. B. & SUN, S. J. 2013. Heparanase overexpression participates in tumor growth of cervical cancer in vitro and in vivo. *Med Oncol,* 30**,** 403.

ZETSER, A., BASHENKO, Y., EDOVITSKY, E., LEVY-ADAM, F., VLODAVSKY, I. & ILAN, N. 2006. Heparanase induces vascular endothelial growth factor expression: correlation with p38 phosphorylation levels and Src activation. *Cancer Res,* 66**,** 1455-63.

ZETSER, A., BASHENKO, Y., MIAO, H. Q., VLODAVSKY, I. & ILAN, N. 2003. Heparanase affects adhesive and tumorigenic potential of human glioma cells. *Cancer Res,* 63**,** 7733-41.

ZHANG, D., WANG, F., LAL, N., CHIU, A. P., WAN, A., JIA, J., BIERENDE, D., FLIBOTTE, S., SINHA, S., ASADI, A., HU, X., TAGHIZADEH, F., PULINILKUNNIL, T., NISLOW, C., VLODAVSKY, I., JOHNSON, J. D., KIEFFER, T. J., HUSSEIN, B. & RODRIGUES, B. 2017a. Heparanase Overexpression Induces Glucagon Resistance and Protects Animals From Chemically Induced Diabetes. *Diabetes,* 66**,** 45-57.

ZHANG, H., WONG, C. C. L., WEI, H., GILKES, D. M., KORANGATH, P., CHATURVEDI, P., SCHITO, L., CHEN, J., KRISHNAMACHARY, B., WINNARD, P. T., JR., RAMAN, V., ZHEN, L., MITZNER, W. A., SUKUMAR, S. & SEMENZA, G. L. 2012. HIF-1-dependent expression of angiopoietin-like 4 and L1CAM mediates vascular metastasis of hypoxic breast cancer cells to the lungs. *Oncogene,* 31**,** 1757-1770.

ZHANG, H. F., CHEN, Y., WU, C., WU, Z. Y., TWEARDY, D. J., ALSHAREEF, A., LIAO, L. D., XUE, Y. J., WU, J. Y., CHEN, B., XU, X. E., GOPAL, K., GUPTA, N., LI, E. M., XU, L. Y. & LAI, R. 2016a. The Opposing Function of STAT3 as an Oncoprotein and Tumor Suppressor Is Dictated by the Expression Status of STAT3beta in Esophageal Squamous Cell Carcinoma. *Clin Cancer Res,* 22**,** 691-703.

ZHANG, H. F. & LAI, R. 2014. STAT3 in Cancer-Friend or Foe? *Cancers (Basel),* 6**,** 1408-40.

ZHANG, J., BASHER, F. & WU, J. D. 2015a. NKG2D Ligands in Tumor Immunity: Two Sides of a Coin. *Frontiers in immunology,* 6**,** 97-97.

ZHANG, J., YANG, J., CAI, Y., JIN, N., WANG, H. & YU, T. 2015b. Multiple antigenic polypeptide composed of heparanase Bcell epitopes shrinks human hepatocellular carcinoma in mice. *Oncol Rep,* 33**,** 1248-56.

ZHANG, L., NGO, J. A., WETZEL, M. D. & MARCHETTI, D. 2015c. Heparanase mediates a novel mechanism in lapatinib-resistant brain metastatic breast cancer. *Neoplasia,* 17**,** 101-13.

ZHANG, L., NGO, J. A., WETZEL, M. D. & MARCHETTI, D. 2015d. Heparanase mediates a novel mechanism in lapatinib-resistant brain metastatic breast cancer()(). *Neoplasia (New York, N.Y.),* 17**,** 101-113.

ZHANG, L., RIDGWAY, L. D., WETZEL, M. A., NGO, J., YIN, W., KUMAR, D., GOODMAN, J. C., GROVES, M. D. & MARCHETTI, D. 2013a. The identification and characterization of breast cancer CTCs competent for brain metastasis. *Science translational medicine,* 5**,** 10.1126/scitranslmed.3005109.

ZHANG, L., RIDGWAY, L. D., WETZEL, M. D., NGO, J., YIN, W., KUMAR, D., GOODMAN, J. C., GROVES, M. D. & MARCHETTI, D. 2013b. The identification and characterization of breast cancer CTCs competent for brain metastasis. *Sci Transl Med,* 5**,** 180ra48.

ZHANG, L., SULLIVAN, P., SUYAMA, J. & MARCHETTI, D. 2010. Epidermal growth factor-induced heparanase nucleolar localization augments DNA topoisomerase I activity in brain metastatic breast cancer. *Mol Cancer Res,* 8**,** 278-90.

ZHANG, L., SULLIVAN, P. S., GOODMAN, J. C., GUNARATNE, P. H. & MARCHETTI, D. 2011. MicroRNA-1258 Suppresses Breast Cancer Brain Metastasis by Targeting Heparanase. *Cancer Research*.

ZHANG, N., LOU, W., JI, F., QIU, L., TSANG, B. K. & DI, W. 2016b. Low molecular weight heparin and cancer survival: clinical trials and experimental mechanisms. *J Cancer Res Clin Oncol,* 142**,** 1807-16.

ZHANG, Q., MING, J., LI, Y., ZHANG, S., LI, B., QIU, X. & WANG, E. 2009. Heparanase expression correlates with angiogenesis and lymphangiogenesis in human lung cancer. *Zhongguo Fei Ai Za Zhi,* 12**,** 864-7.

ZHANG, Q., YU, C., PENG, S., XU, H., WRIGHT, E., ZHANG, X., HUO, X., CHENG, E., PHAM, T. H., ASANUMA, K., HATANPAA, K. J., REZAI, D., WANG, D. H., SARODE, V., MELTON, S., GENTA, R. M., SPECHLER, S. J. & SOUZA, R. F. 2014a. Autocrine VEGF signaling promotes proliferation of neoplastic Barrett's epithelial cells through a PLC-dependent pathway. *Gastroenterology,* 146**,** 461-72 e6.

ZHANG, X., WANG, B. & LI, J.-P. 2014b. Implications of heparan sulfate and heparanase in neuroinflammation. *Matrix Biology,* 35**,** 174-181.

ZHANG, X., WANG, F. & SHENG, J. 2016c. "Coding" and "Decoding": hypothesis for the regulatory mechanism involved in heparan sulfate biosynthesis. *Carbohydr Res,* 428**,** 1-7.

ZHANG, X. H., HUANG, D. P., GUO, G. L., CHEN, G. R., ZHANG, H. X., WAN, L. & CHEN, S. Y. 2008. Coexpression of VEGF-C and COX-2 and its association with lymphangiogenesis in human breast cancer. *BMC Cancer,* 8**,** 4.

ZHANG, Y., SUN, X., NAN, N., CAO, K. X., MA, C., YANG, G. W., YU, M. W., YANG, L., LI, J. P., WANG, X. M. & ZHANG, G. L. 2017b. Elemene inhibits the migration and invasion of 4T1 murine breast cancer cells via heparanase. *Mol Med Rep,* 16**,** 794-800.

ZHANG, Y., ZHANG, G.-L., SUN, X., CAO, K.-X., SHANG, Y.-W., GONG, M.-X., MA, C., NAN, N., LI, J.-P., YU, M.-W., YANG, G.-W. & WANG, X.-M. 2017c. Gubenyiliu II Inhibits Breast Tumor Growth and Metastasis Associated with Decreased Heparanase Expression and Phosphorylation of ERK and AKT Pathways. *Molecules (Basel, Switzerland),* 22**,** 787.

ZHANG, Z. H., CHEN, Y., ZHAO, H. J., XIE, C. Y., DING, J. & HOU, Y. T. 2007. Silencing of heparanase by siRNA inhibits tumor metastasis and angiogenesis of human breast cancer in vitro and in vivo. *Cancer Biol Ther,* 6**,** 587-95.

ZHAO, H., LIU, H., CHEN, Y., XIN, X., LI, J., HOU, Y., ZHANG, Z., ZHANG, X., XIE, C., GENG, M. & DING, J. 2006. Oligomannurarate sulfate, a novel heparanase

inhibitor simultaneously targeting basic fibroblast growth factor, combats tumor angiogenesis and metastasis. *Cancer Research,* 66**,** 8779-8787.

ZHAO, W., WANG, X. S., NIU, H. T., WANG, L. L., HAN, B. M. & XIA, S. J. 2009. Clinical relevance of heparanase mRNA expression in bladder cancer and its usefulness as a detection marker in voided urine. *Mol Med Rep,* 2**,** 327-31.

ZHENG, W., SUN, W. & SIMEONOV, A. 2018. Drug repurposing screens and synergistic drug-combinations for infectious diseases. *British journal of pharmacology,* 175**,** 181-191.

ZHONG, Z., WEN, Z. & DARNELL, J. E., JR. 1994. Stat3: a STAT family member activated by tyrosine phosphorylation in response to epidermal growth factor and interleukin-6. *Science,* 264**,** 95-8.

ZHOU, A. Y., ICHASO, N., ADAMAREK, A., ZILA, V., FORSTOVA, J., DIBB, N. J. & DILWORTH, S. M. 2011a. Polyomavirus Middle T-Antigen Is a Transmembrane Protein That Binds Signaling Proteins in Discrete Subcellular Membrane Sites. *Journal of Virology,* 85**,** 3046-3054.

ZHOU, H., ROY, S., COCHRAN, E., ZOUAOUI, R., CHU, C. L., DUFFNER, J., ZHAO, G., SMITH, S., GALCHEVA-GARGOVA, Z., KARLGREN, J., DUSSAULT, N., KWAN, R. Y., MOY, E., BARNES, M., LONG, A., HONAN, C., QI, Y. W., SHRIVER, Z., GANGULY, T., SCHULTES, B., VENKATARAMAN, G. & KISHIMOTO, T. K. 2011b. M402, a novel heparan sulfate mimetic, targets multiple pathways implicated in tumor progression and metastasis. *PLoS One,* 6**,** e21106.

ZOU, W., WOLCHOK, J. D. & CHEN, L. 2016. PD-L1 (B7-H1) and PD-1 pathway blockade for cancer therapy: Mechanisms, response biomarkers, and combinations. *Sci Transl Med,* 8**,** 328rv4.